HW

REPORT DOCUMENTATION PAGE

AFRL-SR-AR-TR-06-0323

PLEASE DO NOT RETURN YOUR FORM TO THE ABOVE ADDRESS.

1. REPORT DATE *(DD-MM-YYYY)*	2. REPORT TYPE	3. DATES COVERED *(From - To)*
01-04-2006	Final	June 2002 - December 2005

4. TITLE AND SUBTITLE

Quantum Computing using superconducting qubits

5a. CONTRACT NUMBER

F49620-02-1-0334

5b. GRANT NUMBER

F006790

5c. PROGRAM ELEMENT NUMBER

6. AUTHOR(S)

Nori, Franco

5d. PROJECT NUMBER

5e. TASK NUMBER

5f. WORK UNIT NUMBER

7. PERFORMING ORGANIZATION NAME(S) AND ADDRESS(ES)

Physics Department
University of Michigan
Ann Arbor, MI 48109-1040

8. PERFORMING ORGANIZATION REPORT NUMBER

9. SPONSORING/MONITORING AGENCY NAME(S) AND ADDRESS(ES)

AFOSR
875 N Randolph St
Arlington VA 22203
Dr Harold Weinstock

10. SPONSOR/MONITOR'S ACRONYM(S)

11. SPONSOR/MONITOR'S REPORT NUMBER(S)

12. DISTRIBUTION/AVAILABILITY STATEMENT

Distribution Statement A: unlimited

13. SUPPLEMENTARY NOTES

14. ABSTRACT

We have performed research on several areas of control, with particular emphasis on quantum information processing, quantum computing, superconducting qubits, and related topics (e.g., controlling the motion of flux lines, since their motion produces dissipation, introducing noise in the device).

15. SUBJECT TERMS

superconductivity, qubits, quantum information processing, controlling the quantum mechanical state of small devices, controlling the motion of flux quanta, magnetic flux effects on superconductors.

16. SECURITY CLASSIFICATION OF:			17. LIMITATION OF ABSTRACT	18. NUMBER OF PAGES	19a. NAME OF RESPONSIBLE PERSON
a. REPORT	b. ABSTRACT	c. THIS PAGE			19b. TELEPHONE NUMBER *(Include area code)*

INSTRUCTIONS FOR COMPLETING SF 298

1. REPORT DATE. Full publication date, including day, month, if available. Must cite at least the year and be Year 2000 compliant, e.g. 30-06-1998; xx-06-1998; xx-xx-1998.

2. REPORT TYPE. State the type of report, such as final, technical, interim, memorandum, master's thesis, progress, quarterly, research, special, group study, etc.

3. DATES COVERED. Indicate the time during which the work was performed and the report was written, e.g., Jun 1997 - Jun 1998; 1-10 Jun 1996; May - Nov 1998; Nov 1998.

4. TITLE. Enter title and subtitle with volume number and part number, if applicable. On classified documents, enter the title classification in parentheses.

5a. CONTRACT NUMBER. Enter all contract numbers as they appear in the report, e.g. F33615-86-C-5169.

5b. GRANT NUMBER. Enter all grant numbers as they appear in the report, e.g. AFOSR-82-1234.

5c. PROGRAM ELEMENT NUMBER. Enter all program element numbers as they appear in the report, e.g. 61101A.

5d. PROJECT NUMBER. Enter all project numbers as they appear in the report, e.g. 1F665702D1257; ILIR.

5e. TASK NUMBER. Enter all task numbers as they appear in the report, e.g. 05; RF0330201; T4112.

5f. WORK UNIT NUMBER. Enter all work unit numbers as they appear in the report, e.g. 001; AFAPL30480105.

6. AUTHOR(S). Enter name(s) of person(s) responsible for writing the report, performing the research, or credited with the content of the report. The form of entry is the last name, first name, middle initial, and additional qualifiers separated by commas, e.g. Smith, Richard, J, Jr.

7. PERFORMING ORGANIZATION NAME(S) AND ADDRESS(ES). Self-explanatory.

8. PERFORMING ORGANIZATION REPORT NUMBER. Enter all unique alphanumeric report numbers assigned by the performing organization, e.g. BRL-1234; AFWL-TR-85-4017-Vol-21-PT-2.

9. SPONSORING/MONITORING AGENCY NAME(S) AND ADDRESS(ES). Enter the name and address of the organization(s) financially responsible for and monitoring the work.

10. SPONSOR/MONITOR'S ACRONYM(S). Enter, if available, e.g. BRL, ARDEC, NADC.

11. SPONSOR/MONITOR'S REPORT NUMBER(S). Enter report number as assigned by the sponsoring/ monitoring agency, if available, e.g. BRL-TR-829; -215.

12. DISTRIBUTION/AVAILABILITY STATEMENT. Use agency-mandated availability statements to indicate the public availability or distribution limitations of the report. If additional limitations/ restrictions or special markings are indicated, follow agency authorization procedures, e.g. RD/FRD, PROPIN, ITAR, etc. Include copyright information.

13. SUPPLEMENTARY NOTES. Enter information not included elsewhere such as: prepared in cooperation with; translation of; report supersedes; old edition number, etc.

14. ABSTRACT. A brief (approximately 200 words) factual summary of the most significant information.

15. SUBJECT TERMS. Key words or phrases identifying major concepts in the report.

16. SECURITY CLASSIFICATION. Enter security classification in accordance with security classification regulations, e.g. U, C, S, etc. If this form contains classified information, stamp classification level on the top and bottom of this page.

17. LIMITATION OF ABSTRACT. This block must be completed to assign a distribution limitation to the abstract. Enter UU (Unclassified Unlimited) or SAR (Same as Report). An entry in this block is necessary if the abstract is to be limited.

Final report for the AFOSR (2002-2005)

Principal Investigator: Franco Nori

Physics Department

University of Michigan

Ann Arbor, MI 48109-1040

Final report for the AFOSR (2002-2005)

Principal Investigator: Franco Nori

Summary of Research Activities in our group

We perform theoretical studies of complex dynamics in materials. We use physically-motivated models to make predictions which can be tested experimentally and are useful to better understand the observed phenomena. We are currently working on several projects, including: quantum computing (superconducting Josephson-junction qubits, scalable quantum circuitry, improved designs for the control, coherent oscillations, and readout), vortex dynamics in superconductors, new fluxtronics devices, complex collective phenomena, and nano-magnetism. We are also working on biologically-inspired solid-state devices that can control the motion of quanta. Collective transport of interacting particles has been a frequent unifying theme on many of our projects.

Most of our work focuses on one underlying physical phenomenon: *superconductivity*. This work is done in close interaction with several experimental groups. A much smaller part of our work focuses on *magnetism*. We provide theoretical support to several experimental groups.

The main goal of most of our research is to explore novel ways of *control* and manipulation at small length scales (from mm to nm). A fraction of our work focuses on *motion-control* (e.g., controlling the motion of small particles in colloids, or flux quanta in superconductors, or generating THz radiation from moving vortices), while most of our research focuses mostly on (quantum mechanical) *state-control* (e.g., controlling the quantum state of a qubit).

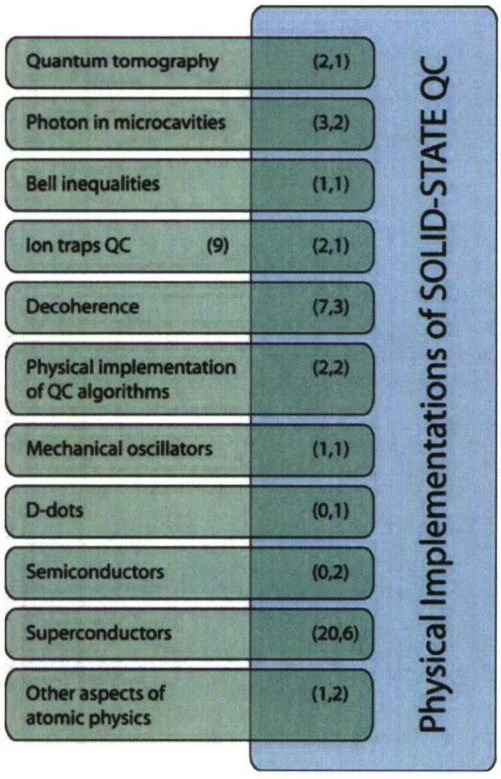

The issue of "control", both *motion-control* and *quantum-state-control*, is important to the future of nanoscience. How can the motion of tiny particles and of quanta be best controlled? How can the quantum mechanical state of a small device, acting as a two-level system, be best manipulated? These are crucial questions, with potentially applications to new technologies. We have pioneered several areas related to "control" and manipulation at the microscopic scale. For instance, in the area of quantum computing, the topics we have worked are summarized on the left. The (X,Y) numbers in parentheses on the left diagram refer to X completed projects so far (either published or submitted) and Y projects to be completed in the future. All of these are projects related to this grant. The number (9) refers to projects prior to this grant, not counted in the list at the end.

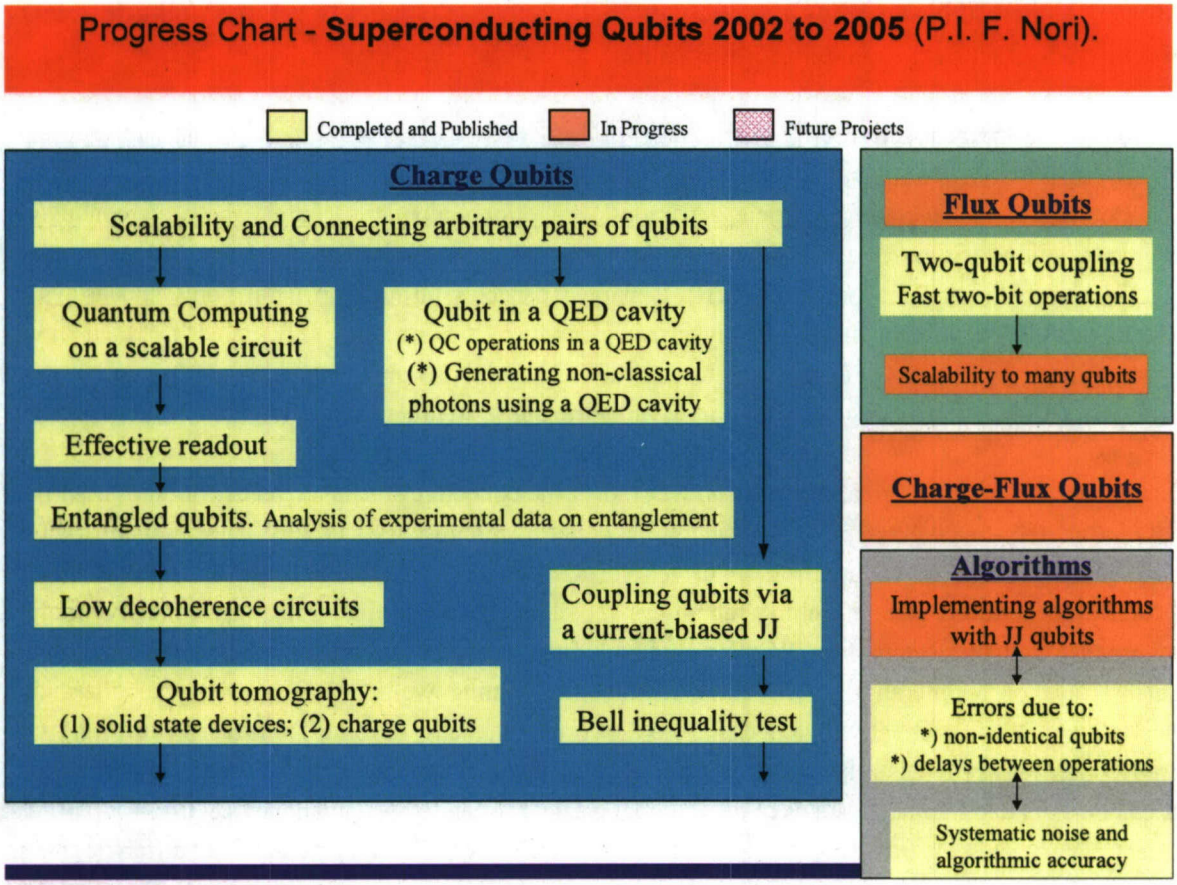

Summary:

We pioneered the area of *particle-motion control* with interacting particles, and we still hold a prominent position in this field. Our work in this area has been featured, e.g., in Physics Today and by the press in several continents. For instance, we contributed to the Einstein celebration special issues on Brownian motion to: the German Physical Society (the centenary issue of the Annalen der Physik, with just nine articles), the American Physical Society, and the British Institute of Physics. In the past few years, this area we pioneered has become a hot topic, attracting top experimental groups on vortex dynamics. For instance, the opening sessions of the (Sept. 2005) international conference on vortex physics were devoted to vortex motion control, and our work was prominent in all those presentations. Our other work on the general area of "collective transport of interacting particles" (especially vortices) still attracts considerable attention (including plenary talks at international conferences). Lately, we began working on the dynamics of Josephson vortices exploring new ways to (1) generate, (2) filter, and (3) detect THz radiation. Our very recent work on this area is also attracting interest from several groups.

In the area of *control of the quantum-mechanical state of two-level systems (i.e., qubits)* we have focused on *superconducting (SC) qubits* and related topics. For instance, in 2001, we pioneered the idea of placing a charge qubit inside a microcavity, years before the 2004 Yale experiments. We also did the first systematic studies of: (1) solid state quantum tomography, (2) Bell inequalities in SC qubits, (3) photon generation using qubits inside cavities, (4) quantum electromechanics of buckling nanotubes, etc. The color chart above summarizes our work in the area of *quantum computing.*

Sub-theme: Controlling the motion of small particles and flux quanta (analytics and numerics)
Researchers: S. Savel'ev, F. Marchesoni, B.Y. Zhu, P. Hanggi, F. Nori

(1) Summary of Research Activities

Initially inspired by biological motors, new types of nanodevices have recently been proposed for particle motion control, including particle separation, smoothing atomic surfaces, and superconducting vortex manipulation. Some of these devices have been realized experimentally to manipulate vortices, particles in asymmetric silicon pores, as well as charged particles through artificial pores and arrays of optical tweezers. The manipulation of tiny particles, which are strongly influenced by their noisy environment, has required novel approaches to control their motion. If small particles are driven by an ac external force (or by a fluctuating force) on an asymmetric substrate, their ac motion can be rectified, thus providing useful work.

Using analytical and numerical approaches, we studied the collective stochastic rectification of ac-driven vortices due to the "ratchet effect" produced by asymmetric pinning sites [1,2,3]. The regular structure studied in [1] produces a dc voltage from ac driven vortices for any value of the magnetic field. Moreover, using two interpenetrating square pinning sublattices [2] allows a precise control of the collective motion of the vortices, including stepmotors. We also studied [1] the transport of vortices in superconductors with triangular arrays of boomerang- or V-shaped asymmetric pinning wells, when applying an alternating electrical current. We numerically obtained, for the first time, magnetic "lensing" of fluxons (Left fig.). Our proposed vortex lens provides a near threefold increase of the vortex density at its "focus" regions. These results can be extended to other systems (e.g., colloidal particles or electrons in nanodevices).

Recent experiments on transport of K and Rb ions in an ion channel and particles of different size in asymmetric silicon pores pose the question of how directed motion of two or more species affect one another. Other experimentally accessible binary systems include two-size species of particles moving through silicon nanopores or two species of vortices in strongly anisotropic layered superconductors.

We studied (both analytically and via numerical simulations) the motion of two interacting species of small particles, coupled differently to their environment [3,4]. We find three ways of controlling the particle motion of one (passive) B species by means of another (active) A species: (i) dragging the target particles B by driving the auxiliary particles A, (ii) rectifying the motion of the B species on the asymmetric potential created by the A-B interactions (see the right fig.), and (iii) dynamically modifying (pulsating) this potential by controlling the motion of the A particles. This allows easy control of the magnitude and direction of the velocity of the target particles by changing either the frequency, phase and/or amplitude of the applied ac drive(s). Our findings could be potentially used for vortex motion control, for separating tiny particles with different masses, charges, interactions, etc, and for delivering target particles or small molecules, which weakly interact with cell membranes, into cells (e.g., drug delivery), among many other applications in nano-scale solid state devices.

(2) Future Plan

We also plan to obtain the crucial figure of merit characterizing the performance of different experimentally realizable devices. This area of research (pioneered by our group) is very hot now, because several devices for controlling vortex motion, particle motion in ion channels, optical and magnetic tweezers, and artificial micro-pores are now in the stage of experimental realization. Indeed, some of our proposals have been already experimentally realized.

(3) Figures

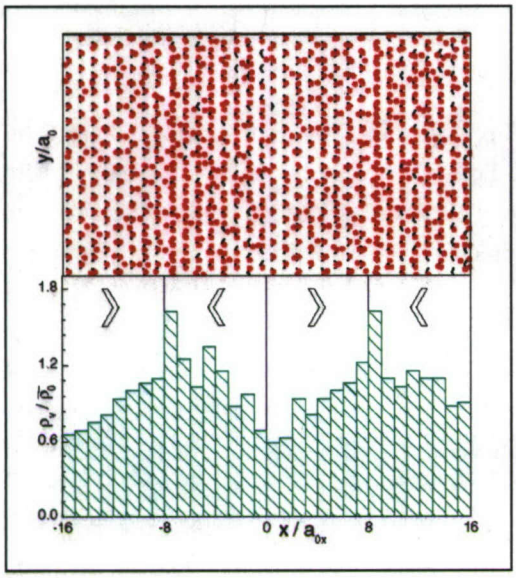

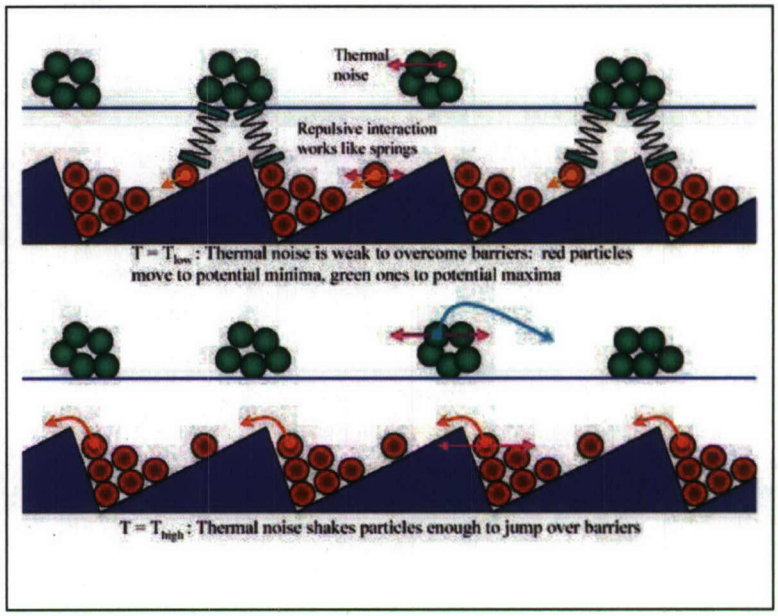

Top view of "magnetic lenses" for vortices (shown in red).
Flux density profiles for a sample with pins shaped as > and <.

(4) Representative publications

[1] B.Y. Zhu, F. Marchesoni, and F. Nori, "Controlling the Motion of Magnetic Flux Quanta", Phys. Rev. Lett. 92, 180602 (2004); "Biologically inspired devices for easily controlling the motion of magnetic flux quanta", Physica E 18, 318 (2003).

[2] B.Y. Zhu, F. Marchesoni, V.V. Moshchalkov, and F. Nori, "Controllable step motors and rectifiers of magnetic flux quanta using periodic arrays of asymmetric pinning defects", Phys. Rev. B 68, 014514 (2003); "Easily-controllable collective stepmotor of magnetic flux quanta" Physica C388-389, 665 (2003); "Controllable stepmotors and rectifiers of magnetic flux quanta", Physica C404, 260 (2004).

[3] S. Savel'ev, F. Marchesoni, and F. Nori, "Controlling Transport in Mixtures of Interacting Particles using Brownian Motors", Phys. Rev. Lett. 91, 010601 (2003); "Manipulating Small Particles in Mixtures far from Equilibrium", Phys. Rev. Lett. 92, 160602 (2004); "Stochastic transport of interacting particles in periodically driven ratchets", Phys. Rev. E 70, 061107 (2004); "Interacting particles on a rocked ratchet: Rectification by condensation", Phys. Rev. E 71, 011107 (2005).

[4] S. Savel'ev, F. Marchesoni, P. Hänggi, and F. Nori, "Nonlinear signal mixing in a ratchet device ", Europhys. Lett. 67, 179 (2004); "Transport via nonlinear signal mixing in ratchet devices", Phys. Rev. E 70, 066109 (2004).

(5) Concluding remarks

We have pioneered this field from the very beginning (1999), and we are the most prominent theory group working in this area, which is now attracting growing interest. Indeed, there is a race involving several top experimental groups exploring novel ways to control vortex motion inside superconductors.

Sub-theme: Vortex motion control (collaborations with experimental groups)
Researchers: S. Savel'ev, F. Nori, Y. Togawa, K. Harada, A. Maeda, A. Tonomura

(1) Summary of Research Activities

We studied [1] a device that can easily control the motion of flux quanta in a Niobium superconducting film grown on an array of nanoscale triangular pinning potentials (Fig. 1). Even though the input ac current has zero average, the resulting net motion of the vortices can be directed along either one direction, the opposite direction, or producing zero net motion. The remarkable reversal in the direction of the rectified current is due to the interaction between the vortices trapped on the magnetic nanostructures and the interstitial vortices (Fig. 1). The applied field and input current strength can tune both the polarity and magnitude of the rectified current. All the observed features are explained and modeled theoretically considering the interactions between particles (Fig. 2). This is the first fabricated ratchet system showing strong effects due to the correlated motion of the interacting particles, responsible for its current inversion. Also, a sawtooth vortex rectifier we proposed in 1999 was experimentally studied in [2]. This is the first experimental imaging of vortex motion inside rectifiers.

All previous proposals used spatially-asymmetric potential energies in order to control its transport properties. We proposed [3] completely new types of ratchet-like systems that do *not* require spatially asymmetric potentials in the samples. As specific examples of this new general class of ratchets, we propose devices that control the motion of flux quanta in superconductors and could address a central problem in many superconducting devices, including qubits; namely, the removal of trapped magnetic flux that produces noise. In extremely anisotropic layered superconductors placed in a tilted magnetic field, there are two interpenetrating vortex lattices consisting of Josephson vortices (JVs), aligned parallel to the CuO_2 planes, and pancake vortices (PVs), oriented perpendicularly to those planes. We show that, due to the JV-PV mutual interaction and asymmetric driving, the AC motion of JVs and/or PVs can provide a net DC vortex current. This controllable vortex motion can be used for vortex pumps, diodes and lenses (Fig. 3). These proposed devices sculpt the microscopic magnetic flux profile by simply modifying the time dependence of the AC drive, without the need of samples with static pinning. Recently, the predicted lensing effect [3] has been experimentally observed [4]. We perform simulations [4] describing an experimental device to guide flux quanta in layered superconductors using a drive which is asymmetric in time instead of being asymmetric in space (i.e., the first experimental ratchet without spatial asymmetry). Moreover, considering the dragging of out-of-plane pancake vortices (PVs) by the in-plane JVs, our simulations successfully describe several experimental manipulations of the entire micromagnetic profile in layered superconductors.

Again, in our general area of research on "Collective transport of interacting particles", we found many analogies between the friction force felt by moving vortices in superconductors and charge density waves. These experiments were described [5] both analytically and numerically. Mechanical analogs were also used. Also, mechanically vibrated granular media was studied [6] in order to extend the fluctuation dissipation theorem to very dissipative non-equilibrium systems.

(2) Future Plan

We plan to continue our fruitful collaborations in this area. The field of vortex ratchets is a very exciting and dynamic one at the moment. There are several imaginative applications for devices based on the control of superconducting vortices. Probably the most topical are those which exploit the control of flux motion in flux qubits. There is also interest in finding ways to remove vortices from active (e.g., SQUIDs) and passive (e.g. filters) superconducting devices since they lead to a large amount of unwanted noise.

(3) Figures

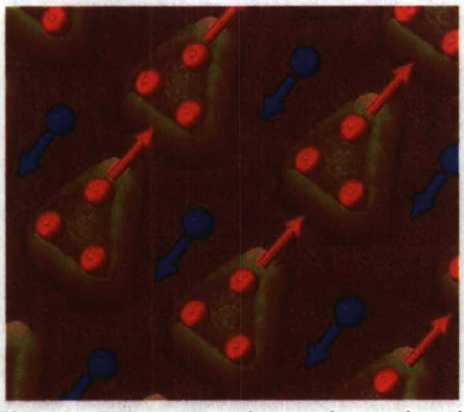

Fig. 1. Vortex motion schematics in a Nb film on nano-magnetic triangles.

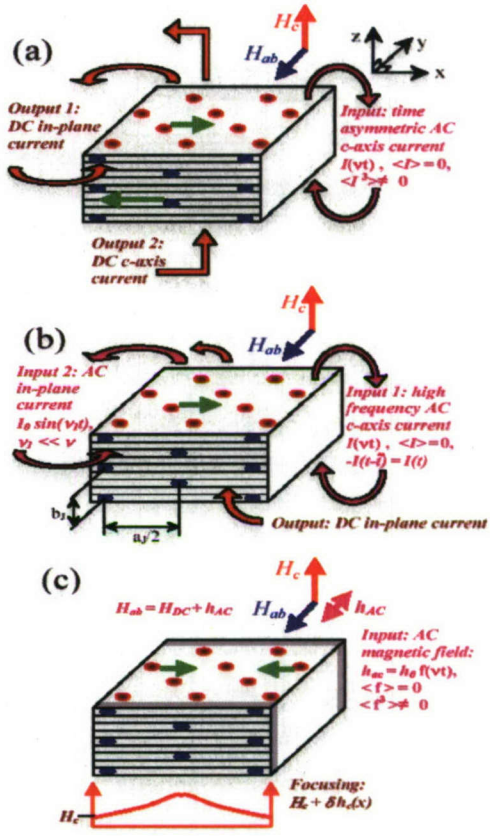

Fig. 2 Schematic diagram of three experimentally-realizable devices designed for controlling the vortex motion. These use extremely anisotropic superconductors, like Bi2212, placed in magnetic fields tilted away from the c-axis, where there are two vortex subsystems consisting of PV stacks, indicated by red circles, and JV's, shown in blue. These are the first ratchets "without a ratchet" (i.e., without anisotropic pinning).

(4) Representative publications

[1] J.E. Villegas, S. Savel'ev, F. Nori, E.M. Gonzalez, J.V. Anguita, R. Garcìa, and J. L. Vicent, A superconducting reversible rectifier that controls the motion of magnetic flux quanta, Science 302, 1188 (2003). Also a Perspective.

[2] Y. Togawa, K. Harada, T. Akashi, H. Kasai, T. Matsuda, F. Nori, A. Maeda, A. Tonomura, "Direct Observation of Rectified Motion of Vortices in a Niobium Superconductor", Phys. Rev. Lett. 95, 087002 (2005)

[3] S. Savel'ev, F. Nori, Experimentally realizable devices for controlling the motion of magnetic flux quanta in anisotropic superconductors, Nature Materials 1, 179 (2002).

[4] D. Cole, S.J. Bending, S. Savel'ev, A. Grigorenko, T. Tamegai, F. Nori, Ratchet without spatial asymmetry: Controlling the motion of magnetic flux quanta using time-asymmetric drives, preprint.

[5] A. Maeda, Y. Inoue, H. Kitano, S. Savel'ev, S. Okayasu, I. Tsukada, F. Nori , Nanoscale Friction: Kinetic Friction of Magnetic Flux Quanta and Charge Density Waves, Phys. Rev. Lett. 94, 077001 (2005)

[6] G. D'Anna, P. Mayor, A. Barrat, V. Loreto, F. Nori, Observing Brownian motion in vibration-fluidized granular matter, Nature 424, 909 (2003). Also the cover of that issue, and a News and Views.

(5) Concluding remarks

This very recent work is attracting considerable attention from the research community, has motivated experiments from top groups, has been published in top journals, and has been featured by the press worldwide.

Sub-theme: Using layered superconductors to generate, filter, and detect THz radiation
Researchers: S. Savel'ev, A. Rakhmanov, V. Yampol'skii, F. Nori

(1) Summary of Research Activities

The recent growing interest in terahertz (THz) science and technology is due to its many important applications in physics, astronomy, chemistry, biology and medicine, including THz imaging, spectroscopy, tomography, medical diagnosis, health monitoring, environmental control, as well as chemical and biological identification. A grand challenge is to generate and control electromagnetic waves in $Bi_2Sr_2CaCu_2O_{8+d}$ and other layered superconducting compounds because of its Terahertz frequency range. Considering recent advantages in sample fabrication, we propose several experimentally realizable devices for generating [1] continuous and pulsed THz radiation in a tunable frequency range as well as for filtering [2] and detecting [3] THz radiation.

For electromagnetic waves in any conducting media, the electric field E is very weak with respect to the magnetic field H: $E << H$. Also, for in-plane radiation: $E << H$. Thus, only a small fraction (about E/H) of the radiation can leave the sample. This is the so-called "impedance mismatch" problem [1] that has severely limited progress in this field for years. Now, we are also considering c-axis short-wavelength out-of-plane radiation [1]. This radiation has a strong enough in-plane electric field $E_{||}$ to overcome the superconducting-vacuum interface. Indeed, $E_{||}$ and the magnetic field both are of the same order of magnitude, similar to the one for waves propagating in the vacuum. This solves the important impedance mismatch problem [1]. The out-of-plane radiation can be emitted, for instance, by a fast moving Josephson vortex moving in a periodically modulated Bi221 samples. So we propose [1] to use modulated Bi2212 samples to generate out-of-plane THz radiation which can leave the sample without a severe impedance mismatch problem.

Another proposal [2] is potentially useful for controllable THz filters. The Josephson vortex (JV) lattice is a periodic array that scatters electromagnetic waves in the THz frequency range. We show [2] that JV lattices can produce a photonic band gap structure (*tunable THz photonic crystal*) with easily tunable forbidden zones controlled by the in-plane magnetic field. The scattering of electromagnetic waves by JVs results in a strong magnetic-field dependence of the reflection and transparency. Fully transparent or fully reflected frequency windows can be conveniently tuned by the in-plane magnetic field. [2]

Our suggested design for THz detectors [3] employs the predicted (in [3]) surface Josephson (J.) plasma wave, which can propagate along the superconductor-vacuum surface when the wave frequency is below the J. plasma frequency. We derive [3] that the incident THz wave can resonantly excite the surface wave at certain angles between the incident wave and the sample surface. This results in a strong increase of absorption of THz wave in the sample and resonant peak of the sample resistance. The position of the peak allows the determination of both the frequency and direction of the incident THz wave [3].

(2) Future Plan

We plan to considerably extend our very recent, and still preliminary, work in this area. This also nicely matches FRS future plans to expand activities studying THz science. We also plan to study different types of radiation, including the very promising "transition radiation", generated by relatively slow Josephson vortices moving through a modulated sample.

(3) Figures

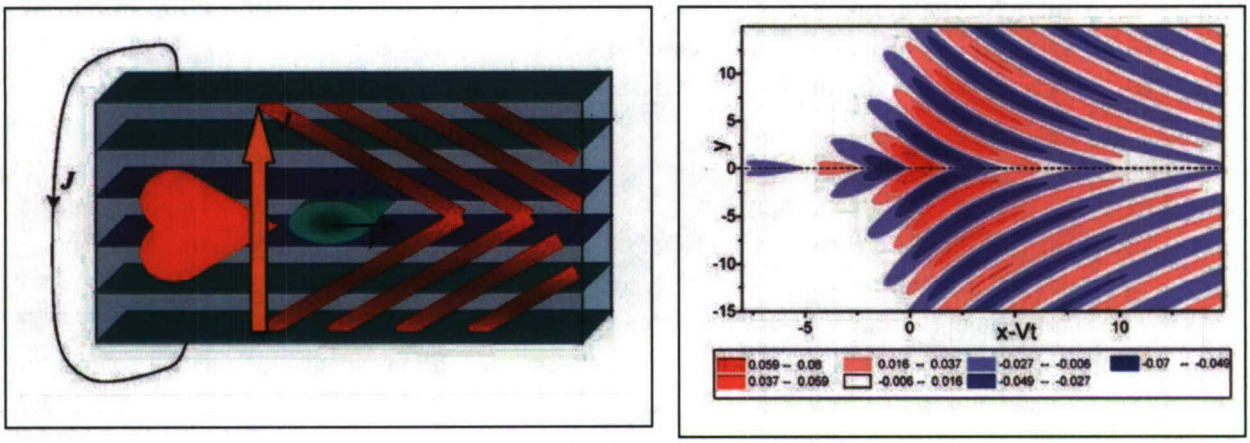

Top: a Josephson vortex (JV) producing radiation.

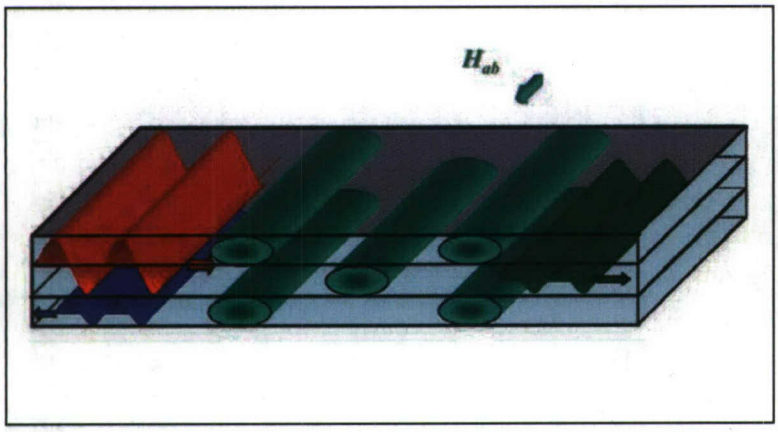

Left panel: The array of green cylinders (Josephson vortices) inside the sample, forming a so-called photonic crystal, span the width of the sample. These vortices scatter the incident electromagnetic waves, shown in red. Only red waves with certain frequencies can propagate through the crystal, resulting in the outgoing transmitted wave shown in green. The rest bounce back, shown as the reflected blue waves.

(4) Representative publications

[1] S. Savel'ev, V. Yampol'skii, A. Rakhmanov, F. Nori, Generation of tunable terahertz out-of-plane radiation using Josephson vortices in modulated layered superconductors, Phys. Rev. B 72, 144515 (2005). cond-mat/0508715

[2] S. Savel'ev, A.L. Rakhmanov, F. Nori, Using Josephson Vortex Lattices to Control Terahertz Radiation: Tunable Transparency and Terahertz Photonic Crystals, Phys. Rev. Lett. 94, 157004 (2005)

[3] S. Savel'ev, V. Yampol'skii, F. Nori, Surface Josephson plasma waves in layered superconductors, published in cond-mat/0508716. Phys. Rev. Lett. 95, 187002 (2005)

[4] S. Savel'ev, V. Yampol'skii, A. Rakhmanov, F. Nori, Nonlinear optical effects with JJ vortices, Nature Physics, in press, August 2006.

(5) Concluding remarks

This work is very recent. In spite of this: (1) it has received good evaluations from referees used by top journals; (2) it has been featured in the press; (3) it has received several invited and plenary talks; more importantly, (4) several experimental groups are now beginning work in order to implement our proposals (as always, experimental results will take time).

Sub-theme: Controlling Physical Properties of Superconducting and Magnetic Systems: increasing critical currents, nonlinear instabilities in superconductors, manipulating magnetic nano-disks, and magnetic-domain motion control

Researchers: S. Savel'ev, A. Rakhmanov, V. Misko, F. Nori

(1) Summary of Research Activities

Recent achievements in nano-technology now allow the fabrication of different arrays of small magnetic dots of various shapes and different interdot spacings. Such dot arrays are potentially useful for memory elements, magnetic field sensors, and logic devices, among other applications.

Using the rigid magnetic vortex model, we develop [1] a substantially modified Landau theory approach for analytically studying phase transitions between different spin arrangements in circular submicron magnetic dots subject to an in-plane externally-applied magnetic field. We introduce a novel order parameter: the inverse distance between the center of the circular dot and the vortex core. This order parameter is suitable for describing closed spin configurations such as curved or bent-spin structures and magnetic vortices. Depending on the radius and thickness of the dot as well as the exchange coupling, there are five different regimes for the magnetization reversal process when decreasing the in-plane magnetic field. The magnetization-reversal regimes obtained here cover practically all possible magnetization reversal processes. Moreover, we have derived the change of the dynamical response of the spins near the phase transitions and obtained a "critical slowing down" at the second order phase transition from the high-field parallel-spin state to the curved (C-shaped) spin phase. We predict a transition between the vortex and the parallel-spin state by quickly changing the magnetic field—providing the possibility to control the magnetic state of dots by changing either the value of the external magnetic field and/or its sweep rate. We study an illuminating mechanical analog (buckling instability) of the transition between the parallel-spin state and the curved spin state (i.e., a magnetic buckling transition). In analogy to the magnetic-disk case, we also develop a modified Landau theory for studying mechanical buckling instabilities of a compressed elastic rod embedded in an elastic medium. We show that the transition to a buckled state can be either first or second order depending on the ratio of the elasticity of the rod and the elasticity of the external medium. We derive the critical slowing down for the second-order mechanical buckling transition.

Magnetic domain walls (MDWs) can move when driven by an applied magnetic field. This motion is important for numerous devices, including magnetic recording read/write heads, transformers and magnetic sensors. A magnetic film, with a sawtooth profile, localizes MDWs in discrete positions at the narrowest parts of the film. We propose [2] a controllable way to move these domain walls between these discrete locations by applying magnetic field pulses. In our proposal, each applied magnetic pulse can produce an increment or step-motion for an MDW. This could be used as a shift register. A similarly patterned magnetic film attached to a large magnetic element at one end of the film operates as an XOR logic gate. The asymmetric sawtooth profile can be used as a ratchet resulting in either oscillating or running MDW motion, when driven by an ac magnetic field. Near a threshold drive (bistable point) separating these two dynamical regimes (oscillating and running MDW), a weak signal encoded in very weak oscillations of the external magnetic field drastically changes the velocity spectrum, greatly amplifying the mixing harmonics [3]. This effect can be used either to amplify or shift the frequency of a weak signal [3].

We study [4] the critical depinning current J_c versus the applied magnetic flux Φ, for quasiperiodic (QP) one-dimensional (1D) chains and 2D arrays of pinning centers placed on the nodes of a five-fold Penrose lattice. In 2D QP pinning arrays, we predict analytically and numerically the main features of $J_c(\Phi)$, and demonstrate that the Penrose lattice of pinning sites provides an enormous enhancement of $J_c(\Phi)$, even compared to triangular and random pinning site arrays [4]. This huge increase in J_c

could be useful for applications.

We consider [5] magnetic flux moving in superconductors with periodic pinning arrays. We show that sample heating by moving vortices produces negative differential resistivity (NDR) of both N- and S-type in the voltage-current characteristic (VI-curve). The uniform flux flow state is unstable in the NDR region of the VI-curve [5]. Domain structures appear during the NDR part of the VI-curve of an N-type, while a filamentary instability is observed for the NDR of an S-type. The simultaneous existence of the NDR of both types gives rise to the appearance of self-organized two-dimensional dynamical structures.

(2) Future Plan

We are considering the control of chirality on magnetic nanodisks. We are planning to simulate critical slowing down in magnetic disks. Also operation of several linked magnetic logical devices will be considered. We plan to help experimentalists to achieve an important goal: to strongly increase the critical current Jc(Φ), by using samples with quasiperiodic arrays of defects.

(3) Figures

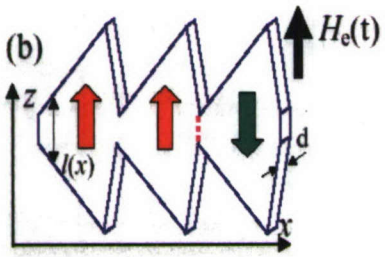

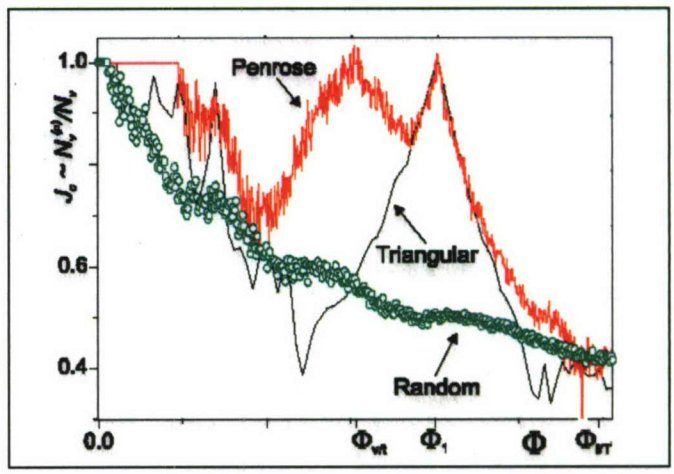

(4) Representative publications

[1] S. Savel'ev, F. Nori, "Magnetic and mechanical buckling: Modified Landau theory approach to study phase transitions in micromagnetic disks and compressed rods", Phys. Rev. B 70, 214415 (2004).

[2] S. Savel'ev, A. Rakhmanov, F. Nori, "Experimentally realizable devices for domain wall motion control", New Journal of Physics 7, 82 (2005).

[3] S. Savel'ev, A. Rakhmanov, F. Nori, "Nonlinear amplifier and frequency shifter using a tunable periodic drive", Phys. Rev E 72, 056136 (2005).

[4] V. Misko, S. Savel'ev, F. Nori, "Critical currents in quasiperiodic pinning arrays: One-dimensional chains and Penrose lattices", Phys. Rev. Lett. 95, 177007 (2005). Also published in cond-mat/0502480, and its long version published in PRB (2006)..

[5] V. Misko, S. Savel'ev, F. Nori, "Non-uniform self-organized dynamical states in superconductors with periodic pinning", Phys. Rev. Lett. 96, 127004 (2006).

(5) Concluding remarks

These results are very recent. In spite of this, several experimental groups have expressed interest in testing these proposals. Two have already started experiments based on these proposals.

Sub-theme: Superconducting qubits in microcavities
Researchers: J.Q You, Y.X. Liu, L.F. Wei, and F. Nori

(1) Summary of Research Activities

In [1] we investigate the quantum dynamics of a Cooper-pair box with a superconducting loop in the presence of a nonclassical microwave field. We demonstrate the existence of Rabi oscillations for both single- and multiphoton processes and, moreover, we propose a new quantum computing scheme (including one-bit and conditional two-bit gates) based on Josephson qubits coupled through microwaves.

Based on the interaction between the radiation field and a superconductor, we propose [2] a way to engineer quantum states using a SQUID charge qubit inside a microcavity. This device can act as a deterministic single-photon source as well as generate any Fock states and an arbitrary superposition of Fock states for the cavity field. The controllable interaction between the cavity field and the qubit can be realized by the tunable gate voltage and classical magnetic field applied to the SQUID.

In [3] we propose how to generate macroscopic quantum superposition states using a microwave cavity containing a superconducting charge qubit. Based on the measurement of charge states, we show that the superpositions of two macroscopically distinguishable coherent states of a single-mode cavity field can be generated by a controllable interaction between a cavity field and a charge qubit. After such superpositions of the cavity field are created, the interaction can be switched off by the classical magnetic field, and there is no information transfer between the cavity field and the charge qubit. We also discuss the generation of the superpositions of two squeezed coherent states.

In [4] we propose a method to create superpositions of two macroscopic quantum states of a single-mode microwave cavity field interacting with a superconducting charge qubit. The decoherence of such superpositions can be determined by measuring either the Wigner function of the cavity field or the charge qubit states. Then the quality factor Q of the cavity can be inferred from the decoherence of the superposed states. The proposed method is experimentally realizable within current technology even when the Q value is relatively low, and the interaction between the qubit and the cavity field is weak.

In [5] we analyze the optical selection rules of the microwave-assisted transitions in a flux qubit superconducting quantum circuit (SQC). We show that the parities of the states relevant to the superconducting phase in the SQC are well defined when the reduced external magnetic flux f=f/2; then the selection rules are the same as the ones for the electric-dipole transitions in usual atoms. When f is shifted away from 0.5, the symmetry of the potential of the artificial "atom" is broken, and a so-called Δ-type "cyclic" three-level atom is formed, where one- and two-photon processes can coexist. We study how the population of these three states can be selectively transferred by adiabatically controlling the electromagnetic field pulses. Different from Λ-type atoms, the adiabatic population transfer in our three-level Δ atom can be controlled not only by the amplitudes but also by the phases of the pulses.

In [6] we began studying biological circuitry, instead of only quantum circuitry. The goal there was to help find correlations within a very large network or circuit.

(2) Future Plan

This is a very exciting area of research that we pioneered early on in 2001, and the Yale experiments have confirmed (in 2004) that this was a very fruitful direction. This approach is now attracting considerable attention.

(3) Figure

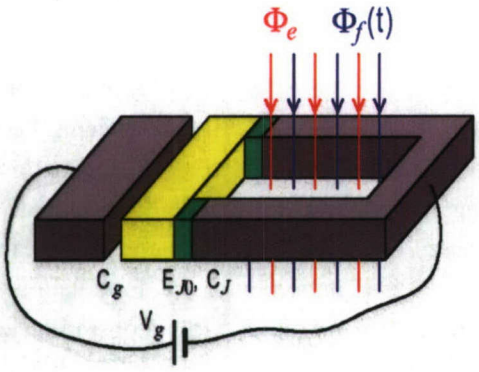

Cavity quantum electrodynamics (QED) for a Cooper-pair box with a SQUID loop, where the (yellow) charge box is coupled to a segment of a superconducting ring via two identical Josephson junctions, shown in green above, and a voltage V_g is applied to the charge box through a gate capacitor C_g. In addition to a static magnetic flux Φ_e, as denoted by the solid (red) lines with arrows, applied through the SQUID loop to control the effective Josephson coupling energy, a time-dependent microwave field $\Phi_f(t)$ in a quantum cavity, schematically shown above by the dashed (blue) lines with arrows, also threads through the SQUID loop.

(4) Representative publications

[1] J.Q. You and F. Nori, Quantum information processing with superconducting qubits in a microwave field, Phys. Rev. B 68, 064509 (2003)

[2] Y.-X. Liu, L.F. Wei, and F. Nori, Generation of nonclassical photon states using a superconducting qubit in a microcavity, Europhys. Lett. 67 , 941 (2004)

[3] Y.-X. Liu, L.F. Wei, and F. Nori, Preparation of macroscopic quantum superposition states of a cavity field via coupling to a superconducting charge qubit, Phys. Rev. A 71, 063820 (2005)

[4] Y.-X. Liu, L.F. Wei, and F. Nori, Measuring the quality factor of a microwave cavity using superconduting qubit devices, Phys. Rev. A 71, 063820 (2005)

[5] Y.-X. Liu, J. Q. You, L.F. Wei, C. P. Sun, and F. Nori, Optical Selection Rules and Phase-Dependent Adiabatic State Control in a Superconducting Quantum Circuit, Phys. Rev. Lett. 95, 087001 (2005)

[6] P. Carninci et al, The transcriptional landscape of the mammalian genome, Science 309, 1559 (2005).

(5) Concluding remarks

In the summer of 2001, we submitted to PRL one of the earliest, if not the first, proposal on QC using qubits inside a cavity. The PRL referees admitted that our work was very original, but they felt that it would never be implemented. Eventually, our manuscript was published in PRB, in 2003. Over a year later, in the Fall of 2004, the Yale group published experiments proving that SC qubits inside cavities could have Rabi oscillations. These results, which we anticipated in 2001 and sent in our preprint to Yale in 2002, are now attracting considerable attention. Since then, we have been studying ways to generate several types of non-classical photon states using a SC qubit in a microcavity, and other related proposals. The latter are very recent proposals (2005) that will be relevant to future experimental studies.

Sub-theme: Superconducting charge qubits: coupling, scalability, control, entanglement generation.
Researchers: J.Q You, Y.X. Liu, L.F. Wei, J.S. Tsai, and F. Nori

(1) Summary of Research Activities

A goal of quantum information technology is to control the quantum state of a system, including its preparation, manipulation, and measurement. However, scalability to many qubits and controlled connectivity between any selected qubits are two of the major stumbling blocks to achieve quantum computing (QC). In [1] we propose an experimental method, using Josephson charge qubits, to efficiently solve these two central problems. The proposed QC architecture is *scalable* since any two charge qubits can be effectively coupled by an experimentally accessible inductance. More importantly, we formulate an *efficient* and *realizable* QC scheme that requires *only one* (instead of two or more) two-bit operation to implement conditional gates.

In [2] we present an experimentally implementable method to couple Josephson charge qubits and to generate and detect macroscopic entangled states. A large-junction superconducting quantum interference device is used in the qubit circuit for both coupling qubits and to implement the readout. Also, we explicitly show how to achieve a microwave-assisted macroscopic entanglement in the coupled-qubit system.

Josephson qubits (JQs) without direct interaction can be effectively coupled by sequentially connecting them to an information bus: a current-biased large Josephson junction treated as an oscillator with adjustable frequency [3]. The coupling between any qubit and the bus can be controlled by modulating the magnetic flux applied to that qubit. This tunable and selective coupling provides two-qubit entangled states for implementing elementary quantum logic operations, and for experimentally testing Bell's inequality.

In [4] we propose an effective scheme for manipulating quantum information stored in a superconducting nanocircuit. The Josephson qubits are coupled via their separate interactions with an information bus, a large current-biased Josephson junction treated as an oscillator with adjustable frequency. The bus is sequentially coupled to only one qubit at a time. Distant Josephson qubits without any direct interaction can be indirectly coupled with each other by independently interacting with the bus sequentially, via exciting/deexciting vibrational quanta in the bus. This is a superconducting analog of the successful ion trap experiments on quantum computing. Our approach differs from previous schemes that simultaneously coupled two qubits to the bus, as opposed to their sequential coupling considered here. The significant quantum logic gates can be realized by using these tunable and selective couplings. The decoherence properties of the proposed quantum system are analyzed within the Bloch-Redfield formalism. Numerical estimations of certain important experimental parameters are provided.

In superconducting circuits with interbit untunable (e.g., capacitive) couplings, ideal local quantum operations cannot be exactly performed on individual Josephson qubits. In [5] we propose an effective dynamical decoupling approach to overcome the "fixed-interaction" difficulty for effectively implementing elemental logical gates for quantum computation. The proposed single-qubit operations and local measurements should allow testing Bell's inequality with a pair of capacitively-coupled Josephson qubits. This provides a powerful approach, besides spectral-analysis [Nature 421, 823 (2003); Science 300, 1548 (2003)], to verify the existence of macroscopic quantum entanglement between two fixed-coupling Josephson qubits.

(2) Future Plan

We plan to extend these studies to flux and phase qubits, as well as to SC qubits inside cavities.

(3) Figure

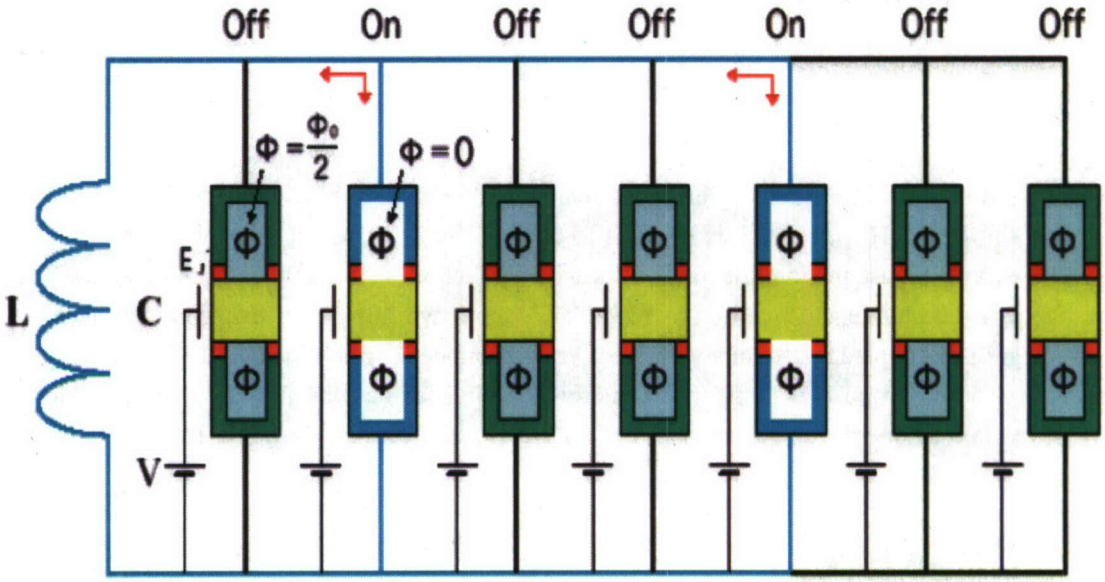

Schematic diagram of the proposed scalable and switchable quantum computer. Here we explicitly show how two charge qubits (not necessarily neighbors) can be coupled by the inductance L, where the cyan SQUIDs are switched on by setting the fluxes through the cyan SQUID loops zero, and the green SQUIDs are turned off by choosing the fluxes through the green SQUID loops as $\Phi_0/2$. This applies to the case when any selected charge qubits are coupled by the common inductance.

(4) Representative publications

[1] J.Q. You, J.S. Tsai, and F. Nori, Scalable Quantum Computing with Josephson Charge Qubits, Phys. Rev. Lett. 89, 197902 (2002)

[2] J.Q. You, J.S. Tsai, and F. Nori, Controllable manipulation and entanglement of macroscopic quantum states in coupled charge qubits, Phys. Rev. B 68, 024510 (2003)

[3] L.F. Wei, Y.-X Liu, F. Nori, Coupling Josephson qubits via a current-biased information bus, Europhys. Lett. 67, 1004 (2004)

[4] L.F. Wei, Y.-X. Liu, and F. Nori, Quantum computation with Josephson qubits using a current-biased information bus, Phys. Rev. B 71, 134506 (2005)

[5] L.F. Wei, Y.-X. Liu, and F. Nori, Testing Bell's inequality in a constantly coupled Josephson circuit by effective single-qubit operations, Phys. Rev. B 72, 104516 (2005). Also published in quant-ph/0408089.

(5) Concluding remarks

These are very novel proposals on the issues of coupling, scalability, operations, etc. in quantum circuits. Most of these are quite recent (2004 and 2005).

Sub-theme: Superconducting qubits: flux qubits, decoherence reduction, quantum tomography.
Researchers: J.Q You, Y.X. Liu, L.F. Wei, Y. Nakamura, and F. Nori

(1) Summary of Research Activities

A central problem for implementing efficient quantum computing is how to realize fast operations (both one- and two-bit ones). However, this is difficult to achieve for a collection of qubits, especially for those separated far away, because the interbit coupling is usually much weaker than the intrabit coupling. In [1] we present an experimentally feasible method to effectively couple two flux qubits via a common inductance and treat both single and coupled flux qubits with more realistic models, which include the loop inductance. The main advantage of our proposal is that a strong interbit coupling can be achieved using a small inductance, so that two-bit as fast as one-bit operations can be easily realized. We also show the flux dependence of the transitions between states for the coupled flux qubits.

Charge fluctuations from gate bias and background traps severely limit the performance of a charge qubit realized in a Cooper-pair box (CPB). In [2] we present an experimentally realizable method to control the dephasing effects of these charge fluctuations using two strongly capacitively coupled CPBs. This coupled-box system has a low-decoherence subspace of two states and we calculate the dephasing of these states using a master equation approach. Our results show that the inter-box Coulomb correlation can significantly suppress decoherence of this two-level system, making it a promising candidate as a logical qubit, encoded using two CPBs.

In [3] we propose a method for the tomographic reconstruction of qubit states for a general class of solid-state systems in which the Hamiltonians are represented by spin operators, e.g., with Heisenberg-, XXZ-, or XY-type exchange interactions. We analyze the implementation of the projective operator measurements, or spin measurements, on qubit states. All the qubit states for the spin Hamiltonians can be reconstructed by using experimental data.

In [4] we propose an approach to reconstruct any superconducting charge qubit state by using quantum state tomography. This procedure requires a series of measurements on a large enough number of identically prepared copies of the quantum system. The experimental feasibility of this procedure is explained and the time scales for different quantum operations are estimated according to experimentally accessible parameters. Based on the state tomography, we also investigate the possibility of the process tomography.

(2) Future Plan

We plan to expand on the projects listed above. Most of our previous work has been in charge qubits. We plan to continue work for other types of qubits, including flux-charge, flux, and phase qubits.

(3) Figure

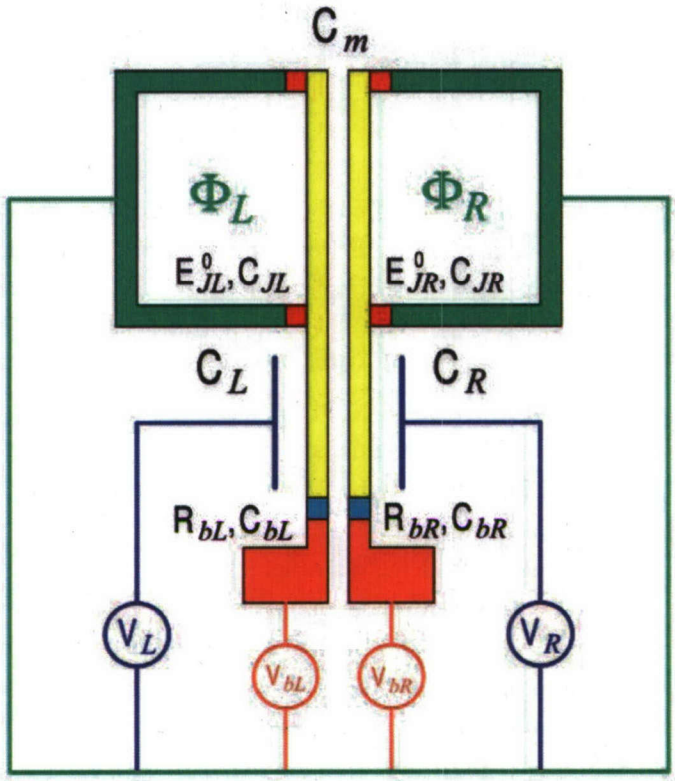

Strongly coupled Cooper-pair boxes used for reducing decoherence. A bias voltage V_i is applied to the ith charge box through a gate capacitance C_i, and a symmetric dc-SQUID is coupled to the box. Also, each box is connected to a detector via a probe junction (or a less invasive point contact). The two boxes are closely-spaced long superconducting islands with sufficiently large mutual capacitance C_m, and the barrier between them is strong enough to prohibit the inter-box Cooper-pair tunneling.

(4) Representative publications

[1] J.Q. You, Y. Nakamura, and F. Nori, Fast two-bit operations in inductively coupled flux qubits, Phys. Rev. B 71, 024532 (2005)

[2] J.Q. You, X. Hu, and F. Nori, Correlation-induced suppression of decoherence in capacitively coupled Cooper-pair boxes, Phys. Rev. B 72, 144529 (2005). Also published in cond-mat/0407423

[3] Y.-X. Liu, L.F. Wei, and F. Nori, Qubit tomography for solid-state systems, Europhys. Lett. 67, 874-880 (2004).

[4] Y.-X. Liu, L. F. Wei, and F. Nori, Tomographic measurements on superconducting qubit states , Phys. Rev. B 72, 014547 (2005)

[5] J.Q. You, J.S. Tsai, and F. Nori, Hybridized solid-state qubit in the charge-flux regime, Phys. Rev. B 72, in press (2005)

(5) Concluding remarks

First proposal on solid-state quantum tomography, an area which we are pioneering. Very novel proposals on coupling, scalability, operations, etc. These are very recent results (mostly published during 2005) and experiments on these will be done in the future (some groups already started).

Sub-theme: Quantum electromechanics, quantum transducers, EPR states, quantum algorithms, controllable couplings among qubits.
Researchers: L.F. Wei, Y.X. Liu, S. Savel'ev, J.S. Tsai, and F. Nori

(1) Summary of Research Activities

Analyzing recent experimental results, we find [1] similar behaviors and a deep analogy between three-junction superconducting qubits and suspended carbon nanotubes. When these different systems are ac-driven near their resonances, the resonance single-peak, observed at weak driving, splits into two sub-peaks when the driving increases. This unusual behavior can be explained by considering quantum tunneling in a double well potential for both systems. Inspired by these experiments, we propose a mechanical qubit based on buckling nanobars--a NEMS so small as to be quantum coherent. To establish buckling nanobars as legitimate candidates for qubits, we calculate the effective buckling potential that produces the two-level system and identify the tunnel coupling between the two local states. We propose different designs of nanomechanical qubits (fig. 1) and describe how they can be manipulated. Also, we outline possible decoherence channels and detection schemes. A comparison between nanobars and well studied superconducting qubits suggests several future experiments on quantum electromechanics.

In [2] we propose an experimentally realizable method to control the coupling between flux qubits, so far an important open problem. In our proposal, the bias fluxes are always fixed for the two inductively-coupled qubits. The detuning of these two qubits can be initially chosen to be sufficiently large that their coupling is almost negligible, and then each qubit can be treated independently. When an external field is applied to one of the qubits, a well-chosen frequency of the external field can be used to compensate the detuning and couple the qubits. This proposed method avoids fast changes of the transition frequencies of the qubits or bias magnetic flux through the qubit loops, and also offers a remarkable way to implement any logic gate as well as tomographically measure flux qubit states.

In [3] we propose an efficient approach to prepare Einstein-Podolsky-Rosen (EPR) pairs in currently-existing Josephson nanocircuits with capacitive-couplings. In these fixed-coupling circuits, two-qubit logic gates could be easily implemented while, strictly speaking, single-qubit gates cannot be easily realized. For a known two-qubit state, conditional single-qubit operations could still be designed to evolve only the selected qubit and keep the other qubit unchanged; the rotations of the selected qubit depend on the state of the other qubit. These conditional single-qubit operations allow to deterministically generate the well-known Einstein-Podolsky-Rosen pairs, represented by EPR-Bell (or Bell) states, at a macroscopic level. Quantum-state tomography is further proposed to experimentally confirm the generation of these states.

During the unavoidable delays between operations in a quantum algorithm, coherent errors will accumulate from the dynamical phases of the superposed wave functions. In [4] we explore the sensitivity of Shor's quantum factoring algorithm to such errors. Our results clearly show a severe sensitivity of Shor's factorization algorithm to the presence of delay times between successive unitary transformations. A particularly simple phase-matching approach is proposed in this paper to avoid or suppress these coherent errors when using Shor's algorithm to factorize integers. The robustness of this phase-matching condition is evaluated analytically and numerically.

(2) Future Plan

We plan to expand on the most promising projects listed above. These are very recent, and we are still exploring options about what topics to expand on, within the group of papers listed below.

(3) Figures

System	SC charge QB	SC flux QB	Nano-bar QB
States	| excess charge > : $\|0\rangle$ and $\|1\rangle$	| current direction > : $\|\circlearrowleft\rangle$ and $\|\circlearrowright\rangle$	| buckling direction > : $\|R\rangle$ and $\|L\rangle$
Hamiltonian	$H = \epsilon\,\sigma_z + \hbar\,\Delta_t\,\sigma_x$		
Tunneling Δ_t and energy splitting controlled by	Gate voltage V_g (normalized: n_g)	Magnetic flux: Φ (normalized: $f = \Phi/\Phi_0$)	Transverse force $f_\perp$ (induced, e.g., by a transverse electric field $E_\perp$)
Tunneling controlled by	Josephson energy: $\mathcal{E}_J(\Phi)$	Josephson energy: $\mathcal{E}_J$	Either • Longitudinal force (induced by pressure or electrical field $f_\parallel$) • or its gradient $E_\parallel$ Longitudinal force and its gradient control $\partial_x f_\parallel$ barrier height and its curvature
Coupling between qubits	Electrical (e.g., capacitive or inductive coupling)	Magnetic	Electrical (dipolar)
Decoherence sources include	Charge fluctuations	Flux fluctuations	1. Charge fluctuations 2. Phonon-phonon interactions
Read-out	Electrical (e.g., SET or JJ)	Magnetic (SQUID)	Either electric or optical, or mechanical

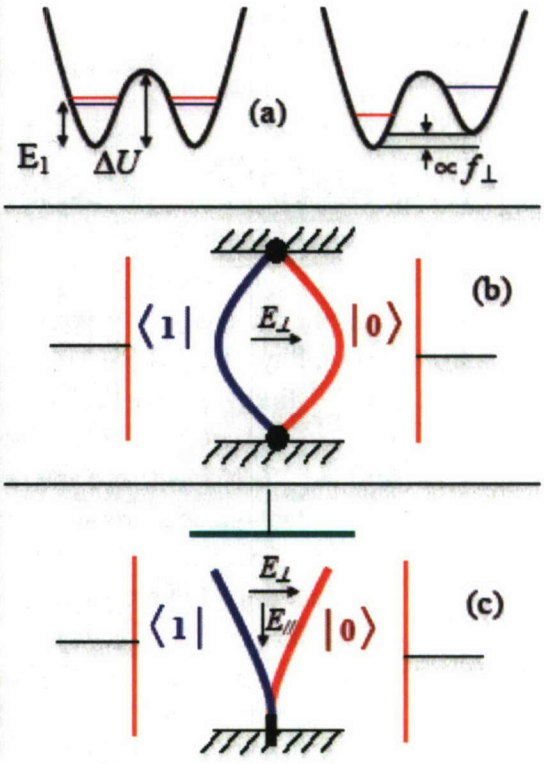

Comparison of Josephson-junction superconducting (JJ SC) charge, JJ SC flux and nano-bar qubits.

(4) Representative publications

[1] S. Savel'ev. X. Hu, A. Kasumov, F. Nori, Quantum electromechanics: Quantum tunneling near resonance and qubits from buckling nanobars, published in cond-mat/0412521. Featured in Scientific Am., page 28, April 2005.

[2] Y-X. Liu, L. F. Wei, J. S. Tsai, F. Nori, Controllable coupling between flux qubits, published in cond-mat/0507496

[3] C.P. Sun, L.F. Wei, Y.X Liu, F. Nori, Quantum transducers: Integrating Transmission Lines and Nanomechanical Resonators via Charge Qubits, published in quant-ph/0504056

[4] L.F. Wei, Y.-X. Liu, M.J. Storcz, F. Nori, Macroscopic Einstein-Podolsky-Rosen pairs in superconducting circuits. Published in quant-ph/0508027.

[5] L.F. Wei, X. Li, X. Hu, and F. Nori, Effects of dynamical phases in Shor's factoring algorithm with operational delays, Phys. Rev. A 71, 022317 (2005)

(5) Concluding remarks

First proposal on quantum electromechanics (quantum tunneling near resonance and qubits from buckling nanobars). This work has been featured, e.g., by the United Press International, Scientific American (in about eight translations). First proposal on (1) quantum transducers, (2) macroscopic EPR pairs in SC circuits, and (3) the effects of dynamical phases in Shor's factoring algorithm with operational delays.

Research Achievements
A. Publications
[Original Papers]

1. J.Q. You, J.S. Tsai, and F. Nori "Scalable quantum computing with Josephson charge qubits", Phys. Rev. Lett. 89, 197902 (2002)
2. F. Nori and Y.L. Lin, "Quantum interference in superconducting wire networks and Josephson junction arrays: An analytical approach based on multiple-loop Aharonov-Bohm Feynman path-integrals", Phys. Rev. B 65, 214504 (2002)
3. S Savel'ev, J. Mirkovic, and K. Kadowaki, "Elasticity of combined pancake and Josephson vortex lattice", Physica C 378/381, 580-583 (2002)
4. S. Savel'ev and F. Nori, "Experimentally realizable devices for controlling the motion of magnetic flux quanta in anisotropic superconductors", Nat. Mater. 1, 179-184 (2002)
5. J. Mirkovic, S. Savel'ev, E. Sugahara, K. Kadowaki, "Anisotropy of vortex-liquid and vortex-solid phases in single crystals of $Bi_2Sr_2CaCu_2O_{8+d}$: Violation of the scaling law", Phys. Rev. B 66, 132505 (2002)
6. S. Savel'ev, J. Mirkovic, and K. Kadowaki, "Influence of force-free current on vortex lattice melting transition", Physica C 378/381, 495-498 (2002)
7. J. Mirkovic, S. Savel'ev, E. Sugahara, K. Kadowaki, "Melting transition in single crystals of Bi2 Bi2Sr2CaCu2O8+d studied by the *c*-axis and in-plane resistivity measurements in parallel magnetic fields", Physica C 378/381, 428-432 (2002)
8. J. Mirkovic, S. Savel'ev, E. Sugahara, K. Kadowaki, "Dimensionality of vortex solid and liquid phases in single crystals of $Bi_2Sr_2CaCu_2O_{8+d}$ studied by the resistivity measurements", Physica C 378/381, 491-494 (2002)
9. S. Savel'ev, F. Marchesoni, and F. Nori, "Controlling the collective motion of interacting particles: analytical study via the nonlinear Fokker–Planck equation", Physica C 388/389, 661-662 (2003)
10. S. Savel'ev, C. Cattuto, F. Nori, "Force-free current-induced reentrant melting of the vortex lattice in superconductors", Phys. Rev. B 67, 180509 (2003)
11. J.Q. You, J.S. Tsai, and F. Nori, "Experimentally realizable scalable quantum computing using superconducting qubits", Physica E 18, 35-36 (2003)
12. B.Y. Zhu, F. Marchesoni, V.V. Moshchalkov, and F. Nori, "Controllable step motors and rectifiers of magnetic flux quanta using periodic arrays of asymmetric pinning defects", Phys. Rev. B 68, 064509 (2003)
13. J.W. Wambaugh, F. Marchesoni, F. Nori, "Shear and loading in channels: Oscillatory shearing and edge currents of superconducting vortices", Phys. Rev. B 67, 144515 (2003)
14. S. Savel'ev, F. Marchesoni, F. Nori, "Controlling transport in mixtures of interacting particles using Brownian motors", Phys. Rev. Lett. 91, 010601 (2003)
15. B.Y. Zhu, F. Marchesoni, and F. Nori, "Biologically inspired devices for easily controlling the motion of magnetic flux quanta", Physica E 18, 318-319 (2003)
16. B.Y. Zhu, L. Van Look, V.V. Moshchalkov, F. Marchesoni, F. Nori, "Vortex dynamics in superconductors with an array of triangular blind antidots", Physica E 18, 322-324 (2003)
17. J.Q. You and F. Nori, "Cooper-pair-box qubits in a quantum electrodynamic cavity", Physica E

18, 33-34 (2003)
18. F. Marchesoni, B.Y. Zhu, F. Nori, "Anomalous interstitial dynamics, Stokes' drift, and current inversion in AC-driven vortex lattices in superconductors with arrays of asymmetric double-well traps", Physica A 325, 78-91 (2003)
19. J.Q. You and F. Nori, "Quantum information processing with superconducting qubits in a microwave field", Phys. Rev. B 68, 064509 (2003)
20. J.Q. You, J.S. Tsai, and F. Nori, "Controllable manipulation and entanglement of macroscopic quantum states in coupled charge qubits", Phys. Rev. B 68, 024510 (2003)
21. L.F. Wei and F. Nori, "An efficient single-step scheme for manipulating quantum information of two trapped ions beyond the Lamb-Dicke limit", Phys. Lett. A 320, 131-139 (2003)
22. Y. Pashkin, T. Tilma, D.V. Averin, O. Astafiev, T. Yamamoto, Y. Nakamura, F. Nori and J.S. Tsai, "Entanglement of two coupled charge qubits", Int. J. of Quantum Info. 1, 421-426 (2003)
23. J.E. Villegas, S. Savel'ev, F. Nori, E.M. Gonzalez, J.V. Anquita, R. Garcia, and J.L. Vicent, "A superconducting reversible rectifier that controls the motion of magnetic flux quanta", Science 302, 1188-1191 (2003)
24. G. D'Anna, P. Mayor, A. Barrat, V. Loreto, and F. Nori, "Observing Brownian motion in vibration-fluidized granular matter", Nature 424, 909-912 (2003)
25. J.Q. You, J.S. Tsai, and F. Nori, "Quantum computing with many superconducting qubits", New Directions in Mesoscopic Physics, edited by R. Fazio, V.F. Gantmakher, and Y. Imry, Kluwer Academic, Dordrecht, pp. 351-360 (2003)
26. S. Savel'ev, J. Mirkovic, and F. Nori, "Fluctuations in the Josephson-Pancake combined vortex lattice", Physica C 388, 653-654 (2003)
27. S. Savel'ev, J. Mirkovic, K. Kadowaki, and F. Nori, "Vortex lattice melting in very anisotropic superconductors influenced by the force-free current", Physica C 388, 685-686 (2003)
28. J. Mirkovic, S. Savel'ev, and K. Kadowaki, "Suppression of surface barriers in single crystals of $Bi_2Sr_2CaCu_2O_{8+d}$ near ab-plane studied by c-axis and in-plane resistivity measurements", Physica C 388, 757-758 (2003)
29. J. Mirkovic, S. Savel'ev, S. Hayama, E. Sugahara, and K. Kadowaki, "Vortex Phases in Single Crystals of $Bi_2Sr_2CaCu_2O_{8+d}$ near ab-plane studies by c-axis and in-plane resistivity measurements", Physica C 388, 757-758 (2003)
30. Y.X. Liu, L.F. Wei and F. Nori, "Quantum tomography for solid-state qubits", Europhysics Lett. 67, 874-880 (2004)
31. L.F. Wei, Y.X. Liu, and F. Nori, "Coupling Josephson qubits via a current-biased information bus", Europhysics Lett. 67, 1004-1010 (2004)
32. Y.X. Liu, L.F. Wei and F. Nori, "Generation of nonclassical photon states using a superconducting qubit in a microcavity", Europhysics Lett. 67, 941-947 (2004)
33. Y.X. Liu, S. Ozdemir, A. Miranowicz, and N. Imoto, "Kraus representation of a damped harmonic oscillator and its application", Phys. Rev. A 70, 063801 (2004)
34. S. Savel'ev, F. Marchesoni, and F. Nori, "Manipulating small particles in mixtures far from equilibrium", Phys. Rev. Lett. 92, 160602 (2004)
35. B.Y. Zhu, F. Marchesoni, and F. Nori, "Controlling the motion of magnetic flux quanta", Phys. Rev. Lett. 92, 180602 (2004)
36. R. Wordenweber, P. Dymashevski, and V. Misko, "Guidance of vortices and the vortex ratchet effect in high-Tc superconducting thin films obtained by arrangement of antidots", Phys. Rev. B 69, 184504 (2004)

37. B.Y. Zhu, F. Marchesoni, V.V. Moshchalkov, and F. Nori, "Easily-controllable collective stepmotor of magnetic flux quanta", Physica C 388/389, 260-265 (2004)
38. S. Savel'ev, F. Marchesoni, P. Hanggi, and F. Nori, "Nonlinear signal mixing in a ratchet device", Europhys. Lett. 67, 179-185 (2004)
39. S. Savel'ev, F. Marchesoni, P. Hanggi, and F. Nori, "Transport via nonlinear signal mixing in ratchet devices" Phys. Rev. E 70, 066109 (2004)
40. S. Savel'ev, and F. Nori, "Magnetic and mechanical buckling: Modified Landau theory approach to study phase transitions in micromagnetic disks and compressed rods", Phys. Rev. B 70, 214415 1-19 (2004)
41. S. Savel'ev, F. Marchesoni, and F. Nori, "Stochastic transport of interacting particles in periodically driven ratchets", Phys. Rev. E 70, 161007 (2004)
42. L.F. Wei, and F. Nori, "Quantum phase estimation algorithms with delays: Effects of dynamical phases", J. Phys. A 37, 4607-4617 (2004)
43. S. Savel'ev, F. Marchesoni, P. Hanggi, and F. Nori, "Signal mixing in a ratchet device: commensurability and current control", The European Physical Journal B 40, 00208, 403-408 (2004)
44. C. Cattuto and U. Marini Bettolo Marconi, "Ordering phenomena in cooling granular mixtures", Phys. Rev. Lett. 92, 174502 (2004)
45. L.F. Wei, and F. Nori, "Coherently manipulating two-qubit quantum information using a pair of simultaneous laser pulses", Europhys. Lett. 65, (2004)
46. L.F. Wei, Y.X. Liu, and F. Nori, "Engineering quantum pure states of a trapped cold ion beyond the Lamb-Dicke limit", Phys. Rev. A 70, 063801 (2004)
47. B.Y. Zhu, F. Marchesoni, and F. Nori, "Controllable stepmotors and rectifiers of magnetic flux quanta", Physica C 404, 260-265 (2004)
48. N. Mitarai and H. Nakanishi, "Bagnold scaling, density plateau, and kinetic theory analysis of dense granular flow", Phys. Rev. Lett. 94, 128001 (2005)
49. S. Savel'ev, F. Marchesoni, and F. Nori, " Interacting particles on a rocked ratchet: rectification by condensation", Phys. Rev. E 71, 011107 (2005)
50. J.Q. You, Y. Nakamura, and F. Nori "Fast two-bit operations in inductively coupled flux qubits", Phys. Rev. B 71, 024532 (2005)
51. L.F. Wei, Y.X. Liu, X. Hu, and F. Nori, "Effects of dynamical phases in Shor's factoring algorithm with operational delays", Phys. Rev. A 71, 022317 (2005)
52. A. Maeda, Y. Inoue, H. Kitano, S. Savel'ev, S. Okayasu, I. Tsukada, and F. Nori, "Nanoscale friction: kinetic friction of magnetic flux quanta and charge density waves", Phys. Rev. Lett. 94, 128001 (2005)
53. S. Savel'ev, A. Rakhmanov, F. Nori, "Experimentally realizable devices for domain wall motion control", New J. of Phys. 7, Art. No. 82 (2005)
54. Y.X. Liu, L.F. Wei, and F. Nori, "Tomographic measurements of superconducting qubit states", Phys. Rev. B 72, 014547 (2005)
55. Y.X. Liu, L.F. Wei, and F. Nori, "Preparation of macroscopic quantum superposition states of a cavity field via coupling to a superconducting charge qubit", Phys. Rev. A 71, 063820 (2005)
56. S. Savel'ev, V. Misko, F. Marchesoni, and F. Nori "Separating particles according to their physical properties: Transverse drift of underdamped and overdamped interacting particles diffusing through two-dimensional ratchets", Phys. Rev. B 71, 214303 (2005)
57. Y.X. Liu, J.Q. You, L.F. Wei, C.P. Sun, and F. Nori, "Optical Selection Rules and Phase-Dependent Adiabatic State Control in a Superconducting Quantum Circuit", Phys. Rev.

Lett. 95, 087001 (2005)

58. S. Savel'ev, A. Rakhmanov, and F. Nori, "Using Josephson Vortex Lattices to Control Terahertz Radiation: Tunable Transparency and Terahertz Photonic Crystals", Phys. Rev. Lett. 94, 157004 (2005)
59. L.F. Wei, Y.X. Liu, and F. Nori, "Quantum computation with Josephson qubits using a current-biased information bus", Phys. Rev. B 71, 134506 (2005)
60. Y. Togawa, K. Harada, T. Akashi, H. Kasai, T. Matsuda, F. Nori, A. Maeda, A. Tonomura, "Direct observation of rectified motion of vortices in a Niobium Superconductor", Phys. Rev. Lett. 95, 087002 (2005)
61. Y. Pashkin, T. Yamamoto, O. Astafiev, Y. Nakamura, D.V. Averin, T. Tilma, F. Nori, J.S. Tsai, "Coherent manipulation of couples Josephson charge qubits", Physica C 426-431 (2005) 1552-1560
62. Y.X. Liu, L.F. Wei, and F. Nori, "Measuring the quality factor of a microwave cavity using superconducting qubit devices", Phys. Rev. A 72, 033818 (2005)
63. L.F. Wei, Y.X. Liu, and F. Nori, "Testing Bell's inequality in a constantly coupled Josephson circuit by effective single-qubit operations", Phys. Rev. B 72, 104516 (2005)
64. P. Carninci, et al., "The transcriptional landscape of the mammalian genome", Science 309, Issue 5740, 1559-1563 (2005)
65. V. Misko, S. Savel'ev, F. Marchesoni, and F. Nori, "Separating particles according to their physical properties: Transverse drift of over-damped interacting particles through two-dimensional ratchets", Physica C 426/431, 147-152 (2005)
66. J.Q. You, X. Hu, and F. Nori, "Correlation-induced suppression of decoherence in capacitively coupled Cooper-pair boxes", Phys. Rev. B, in press (2005)
67. S. Savel'ev, V. Yampol'skii, A. Rakhmanov, and F. Nori, "Generation of tunable terahertz out-of-plane radiation using Josephson vortices in modulated layered superconductors", Phys. Rev. B, in press (2005)
68. J.Q. You, J.S. Tsai, and F. Nori, "Hybridized solid-state qubit in the charge-flux regime", Phys. Rev. B, in press (2005)
69. S. Savel'ev, V. Yampol'skii, and F. Nori, "Surface Josephson plasma waves in layered superconductors", Phys. Rev. Lett., in press (2005)
70. V. Misko, S. Savel'ev, and F. Nori, "Critical currents in quasiperiodic pinning arrays: One-dimensional chains and Penrose lattices", Phys. Rev. Lett. 95, in press (2005)

[Review]

1. P. Hanggi, F. Marchesoni, and F. Nori, "Brownian motors", Annalen der Physik (Leipzig) 14, 51-70 (2005)
2. S. Savel'ev, and F. Nori, "Controlling the motion of ineracting particles: homogeneous systems and binary mixtures", Chaos 15, 026112 (2005)
3. F. Nori and S. Savel'ev, "Controlling vortex motion and vortex kinetic friction", Physica C, in press (2005)

B. Oral Presentations
[International Conferences]

1. F. Nori, "Biologically-inspired devices for controlling the motion of flux-quanta", Research Workshop on Statostoca; Mechanics of Plastic Deformation, Trieste, Italy (2002)
2. J.Q. You, F. Nori, and J.S. Tsai, "Macroscopic quantum-mechanical machines: Superconducting quantum bits and logic gates", CAS Symp. on Advanced Materials, (The Chinese Academy of Sciences), Sheng Yang, China (2002)
3. J.Q. You, "Coherent dynamics and quantum information processing in Josephson charge devices", Nano Science and Technology-Novel Structures and Phenomena, (Croucher Advanced Studay Institute), Hong Kong, China (2002)
4. B.Y. Zhu, F. Marchesoni, and F. Nori, "Biologically-inspired devices for easily controlling the motion of magnetic flux quanta" 15th Int. Symp. on Superconductivity (ISS 2002), (International Superconductivity Technology Center (ISTEC)), Yokohama (2002)
5. C. Cattuto, S. Savel'ev, and F. Nori, "Reentrant vortex melting induced by force-free current", 15th Int. Symp. on Superconductivity (ISS 2002), ISTEC, Yokohama (2002)
6. S. Savel'ev and F. Nori, "Crossing lattice vortex pump" 15th Int. Symp. on Superconductivity (ISS 2002), (ISTEC), Yokohama (2002)
7. J.Q. You, F. Nori, and J.S. Tsai, "Scalable quantum computation with superconducting charge qubits", The 10th JST International Symposium on Quantum Computing: Nano-Science & Technology for Implementation of Quantum Computers, Tokyo (2002)
8. F. Nori, "Biologically-inspired devices for controlling the motion of flux-quanta", Annual APS March Meeting 2002, Indianapolis, USA (2002)
9. F. Nori, "Vortex dynamics in superconductors", Applied Physics Seminar, (Stanford University), Stanford, USA (2002)
10. F. Nori, and J.Q. You, "Superconducting qubits inside a QED cavity", Quantum Computing Program Review (QCPR), Nashville, USA (2002)
11. F. Nori, and J.Q. You, "Scalable quantum computing with superconducting charge qubits", Quantum Computing Program Review (QCPR), Nashville, USA (2002)
12. F. Nori, "Scalability in superconducting circuitry", Quantum Computing Program Review, Nashville, USA (2002)
13. F. Nori, "Scalable superconducting qubits", Quantum Computing Program Review, Nashville, USA (2002)
14. S. Savel'ev, F. Marchesoni, and F. Nori, "Resonances in a SQUID ratchet driven by two frequencies", Stochastic Systems: From Randomness to Complexity, NATO-Advanced Research Workshop, EPS/PESC-Exploratory Workshop, Erice, Italy (2002)
15. F. Nori, "Quantum computing with superconducting qubits", New Directions in Mesoscopic Physics (Towards Nanoscience), (NATO-Advanced Study Institute), Erice, Italy (2002)
16. F. Nori, "Biologically-inspired devices for controlling the motion of flux-quanta", Stochastic Systems: From Randomness to Complexity, NATO-Advanced Research Workshop, EPS/PESC-Exploratory Workshop, Erice, Italy (2002)
17. S. Savel'ev, and F. Nori, "Experimentally realizable devices for controlling the motion of magnetic flux quanta in anisotropic superconductors", Stochastic Systems: From Randomness to Complexity, NATO-Advanced Research Workshop, EPS/PESC-Exploratory Workshop, Erice,

Italy (2002)

18. B.Y. Zhu, L. Van Look, V.V. Moshchalkov, F. Marchesoni, and F. Nori, "Vortex dynamics in superconductors with an array of triangular blind antidots", Stochastic Systems: From Randomness to Complexity, NATO-Advanced Research Workshop, EPS/PESC-Exploratory Workshop, Erice, Italy (2002)
19. B.Y. Zhu, F. Marchesoni, and F. Nori, "Biologically inspired devices for easily controlling the motion of magnetic flux quanta", Stochastic Systems: From Randomness to Complexity, NATO-Advanced Research Workshop, EPS/PESC-Exploratory Workshop, Erice, Italy (2002)
20. J.Q. You, J.S. Tsai, and F. Nori, "Scalable quantum computing with Josephson charge qubits", Stochastic Systems: From Randomness to Complexity, NATO-Advanced Research Workshop, EPS/PESC-Exploratory Workshop, Erice, Italy (2002)
21. J.Q. You, and F. Nori, "Quantum information processing with superconducting qubits in a microwave field", Stochastic Systems: From Randomness to Complexity, NATO-Advanced Research Workshop, EPS/PESC-Exploratory Workshop, Erice, Italy (2002)
22. B.Y. Zhu, F. Marchesoni, V.V. Moshchalkov, and F. Nori, "Controllable step motors and rectifiers of magnetic flux quanta using periodic arrays of asymmetric pinning defects", Stochastic Systems: From Randomness to Complexity, NATO-Advanced Research Workshop, EPS/PESC-Exploratory Workshop, Erice, Italy (2002)
23. S. Savel'ev, C. Cattuto, and F. Nori, "Force-free current-induced reentrant melting of the vortex lattice in superconductors", Stochastic Systems: From Randomness to Complexity, NATO-Advanced Research Workshop, EPS/PESC-Exploratory Workshop, Erice, Italy (2002)
24. F. Nori, "Biologically-inspired devices for controlling the motion of flux-quanta", Stochastic Systems: From Randomness to Complexity, NATO-Advanced Research Workshop, EPS/PESC-Exploratory Workshop, Erice, Italy (2002)
25. F. Nori, "Quantum computing with superconducting qubits", New Directions in Mesoscopic Physics (Towards Nanoscience), (NATO- Advanced Study Institute), Erice, Italy (2002)
26. F. Nori, "Using vortex pumps to control the motion of flux-quanta in superconductors", 23rd International Conference on Low Temperature Physics (LT23), Hiroshima (2002)
27. S. Savel'ev, F. Marchesoni, and F. Nori, "Controlling the motion of interacting particles: Analytical study via the nonlinear Fokker-Planck equation", 23rd International Conference on Low Temperature Physics (LT23), Hiroshima (2002)
28. S. Savel'ev, J. Mirkovic, and F. Nori, "Vortex fluctuations in the crossing lattice structure", 23rd International Conference on Low Temperature Physics (LT23), Hiroshima (2002)
29. S. Savel'ev, J. Mirkovic, K. Kadowaki, "Vortex lattice melting transition under the influence of the c-axis current", 23rd International Conference on Low Temperature Physics (LT23), Hiroshima (2002)
30. B.Y. Zhu, "Driven vortex dynamics in superconductors with asymmetric pinning sites", 23rd International Conference on Low Temperature Physics (LT23), Hiroshima (2002)
31. J.Q. You, and F. Nori, "Quantum information processing with Cooper-pair-box qubits in a microwave field", 23rd International Conference on Low Temperature Physics (LT23), Hiroshima (2002)
32. J.Q. You, "Scalable quantum computation with superconducting charge-flux qubits", 23rd International Conference on Low Temperature Physics (LT23), Hiroshima (2002)
33. F. Nori, "Biologically-inspired devices for controlling the motion of flux-quanta", 23rd International Conference on Low Temperature Physics (LT23), Hiroshima (2002)

34. F. Nori, "Vortex pumps to control the motion of flux quanta", The 7th International Conference on Materials and Mechanism of Superconductity and High Temperature Superconductors (M2S-HTSC-VII), Rio de Janeiro, Brazil (2003)
35. J.Q. You, J.S. Tsai, and F. Nori, "Scalable quantum computing with Josephson charge qubits", The 16th International Symposium on Superconductivity (ISS 2003), Tsukuba (2003)
36. S. Savel'ev, and F. Nori, "Dynamical phase transition in driven crossing vortex lattices in highly anisotropic superconductors "The 16th International Symposium on Superconductivity (ISS 2003), Tsukuba (2003)
37. J.Q. You, J.S. Tsai, and F. Nori, "Controllable manipulation and entanglement of macroscopic quantum states in coupled charge qubits", The 16th International Symposium on Superconductivity (ISS 2003), Tsukuba (2003)
38. S. Savel'ev, F. Marchesoni, and F. Nori, "Resonances in a SQUID ratchet driven by two frequencies", The 16th International Symposium on Superconductivity (ISS 2003), Tsukuba (2003)
39. J.Q. You, J.S. Tsai, and F. Nori, "Quantum information processing with superconducting qubits in a microwave field", The 16th International Symposium on Superconductivity (ISS 2003) Tsukuba (2003)
40. Y.X. Liu, L.F. Wei, and F. Nori "Tomographic measurements on charge qubit states", The 16th International Symposium on Superconductivity (ISS 2003) Tsukuba (2003)
41. B.Y. Zhu, F. Marchesoni, V.V. Moshchalkov, and F. Nori, "Transporting flux quanta in triangular pinning arrays", The 16th International Symposium on Superconductivity (ISS 2003), Tsukuba (2003)
42. C. Cattuto, S. Savel'ev, and F. Nori, "Melting phase diagram for Bi2Sr2CaCu2O8+d derived from the thermal fluctuations of the Josephson and pancake vortex lattices", The 16th International Symposium on Superconductivity (ISS 2003), Tsukuba (2003)
43. L.F. Wei, Y.X. Liu, and F. Nori "Coherently manipulating Josephson qubits coupled by an information bus", The 16th International Symposium on Superconductivity (ISS 2003) Tsukuba (2003)
44. J.Q. You, "Scalable quantum computing with superconducting qubits", 8th International Symposium on Advanced Physical Fields (APF8): Advanced Materials for Quantum Computing, (National Institute for Materials Science (NIMS)), Tsukuba (2003)
45. S. Savel'ev, "Devices for controlling the motion of magnetic flux quanta in layered superconductors", The 11th International Workshop on Critical Currents in Superconductors (IWCC 2003), Nihon University, Tokyo (2003)
46. C. Cattuto, "Controlling the vortex lattice melting via force-free current", The 11th International Workshop on Critical Currents in Superconductors (IWCC 2003), Nihon University, Tokyo (2003)
47. B.Y. Zhu, "Controlling the motion of magnetic flux quanta by asymmetric V-shaped pinning lattices", The 11th International Workshop on Critical Currents in Superconductors (IWCC 2003), Nihon University, Tokyo (2003)
48. S. Savel'ev, F. Marchesoni, and F. Nori, "Resonances in a SQUID ratchet driven by two frequencies", 3rd European Conference on Vortex Matter in Superconductors, (European Science Foundation), Crete, Greece (2003)
49. S. Savel'ev, and F. Nori, "Experimentally realizable devices for controlling the motion of magnetic flux quanta in anisotropic superconductors", 3rd European Conference on Vortex Matter in Superconductors, (ESF) Crete, Greece (2003)

50. B.Y. Zhu, L. Van Look, V.V. Moshchalkov, F. Marchesoni, and F. Nori, "Vortex dynamics in superconductors with an array of triangular blind antidots", 3rd European Conference on Vortex Matter in Superconductors, (ESF), Crete, Greece (2003)
51. B.Y. Zhu, F. Marchesoni, and F. Nori, "Biologically inspired devices for easily controlling the motion of magnetic flux quanta", 3rd European Conference on Vortex Matter in Superconductors, (ESF), Crete, Greece (2003)
52. B.Y. Zhu, F. Marchesoni, V.V. Moshchalkov, and F. Nori, "Controllable step motors and rectifiers of magnetic flux quanta using periodic arrays of asymmetric pinning defects", 3rd European Conference on Vortex Matter in Superconductors, (ESF), Crete, Greece (2003)
53. S. Savel'ev, C. Cattuto, and F. Nori, "Force-free current-induced reentrant melting of the vortex lattice in superconductors", 3rd European Conference on Vortex Matter in Superconductors, (ESF), Crete, Greece (2003)
54. J.Q. You, and F. Nori, "Quantum information processing with superconducting qubits in a microwave field ", 3rd European Conference on Vortex Matter in Superconductors, (ESF), Crete, Greece (2003)
55. J.Q. You, J.S. Tsai, and F. Nori, "Scalable quantum computing with Josephson charge qubits", 3rd European Conference on Vortex Matter in Superconductors, (ESF), Crete, Greece (2003)
56. F. Nori, "Controlling the motion of magnetic flux quanta in superconductors", 3rd European Conference on Vortex Matter in Superconductors, (ESF), Crete, Greece (2003)
57. S. Savel'ev, and F. Nori, "Experimentally realizable devices for controlling the motion of magnetic flux quanta in anisotropic superconductors", The Joint 9th International Workshop on Vortex Dynamics and Vortex Matter (ESF), Oleron Island, France (2003)
58. B.Y. Zhu, F. Marchesoni, V.V. Moshchalkov, and F. Nori, "Controllable stepmotors and rectifiers of magnetic flux quanta", The Joint 9th International Workshop on Vortex Dynamics and Vortex Matter (ESF), Oleron Island, France (2003)
59. S. Savel'ev, J. Mirkovic, K. Kadowaki, and F. Nori, "Fluctuations in the Josephson-Pancake combined vortex lattice ", The Joint 9th International Workshop on Vortex Dynamics and Vortex Matter (ESF), Oleron Island, France (2003)
60. S. Savel'ev, "Vortex pumps for crossing lattices in very anisotropic superconductors", The Joint 9th International Workshop on Vortex Dynamics and Vortex Matter (ESF), Oleron Island, France (2003)
61. B.Y. Zhu, L. Van Look, F. Marchesoni, V.V. Moshchalkov, and F. Nori, "Vortex dynamics in superconductors with a triangular array of triangular blind antidots", The Joint 9th International Workshop on Vortex Dynamics and Vortex Matter (ESF), Oleron Island, France (2003)
62. S. Savel'ev, F. Nori, and C. Cattuto, "Vortex lattice melting in very anisotropic superconductors influenced by the force-free current", The Joint 9th International Workshop on Vortex Dynamics and Vortex Matter (ESF), Oleron Island, France (2003)
63. F. Nori, B.Y. Zhu, V.V. Moshchalkov, and F. Marchesoni, "Vortex pumps and lenses to control the motion of flux quanta", The Joint 9th International Workshop on Vortex Dynamics and Vortex Matter (ESF), Oleron Island, France (2003)
64. F. Nori, "Controlling the motion of magnetic flux quanta in superconductors", The Joint 9th International Workshop on Vortex Dynamics and Vortex Matter (ESF), Oleron Island, France (2003)
65. Y. Pashkin, O. Astafiev, T. Yamamoto, Y. Nakamura, D.V. Averin, T. Tilma, F. Nori and J.S. Tsai, "Solid-state Josephson charge qubits", Joint Workshop on Superconductivity, Osaka (2004)

66. Y. Pashkin, O. Astafiev, T. Yamamoto, Y. Nakamura, D.V. Averin, T. Tilma, F. Nori and J.S. Tsai, "Coherent dynamics of two coupled superconducting charge qubits", International Symposium "Quantum Informatics – 2004", Moscow, Russia (2004)
67. Y. Pashkin, O. Astafiev, T. Yamamoto, Y. Nakamura, D.V. Averin, T. Tilma, F. Nori and J.S. Tsai, "Quantum coherence and entanglement of two coupled superconducting charge qubits", 4th International Workshop on Macroscopic Quantum Coherence and Computing, Napoli, Italy (2004)
68. J.Q. You, Y, Nakamura, and F. Nori, "Fast two-bit operations in inductively coupled flux qubits", ERATO Conference on Quantum Information Science 2004 (EQIS'04), Tokyo (2004)
69. Y.X. Liu, L.F. Wei, and F. Nori, "Generation of nonclassical photon states using a superconducting qubit in a microcavity", ERATO Conference on Quantum Information Science 2004 (EQIS'04), Tokyo (2004)
70. J.Q. You, and F. Nori, "Quantum information processing with superconducting qubits in a microwave field", ERATO Conference on Quantum Information Science 2004 (EQIS'04), Tokyo (2004)
71. T. Tilma, Y. Pashkin, O. Astafiev, T. Yamamoto, Y. Nakamura, J.S. Tsai, and F. Nori, "Entanglement dynamics in two coupled charge qubits", ERATO Conference on Quantum Information Science 2004 (EQIS'04), Tokyo (2004)
72. L.F. Wei, Y.X. Liu, and F. Nori, "Testing of Bell's inequality with coupled Josephson qubits", ERATO Conference on Quantum Information Science 2004 (EQIS'04), Tokyo (2004)
73. L.F. Wei, Y.X. Liu, and F. Nori, "Coupling Josephson qubits via a current-biased information bus", ERATO Conference on Quantum Information Science 2004 (EQIS'04), Tokyo (2004)
74. J.Q. You, J.S. Tsai, and F. Nori, "Scalable quantum computing with Josephson charge qubits", ERATO Conference on Quantum Information Science 2004 (EQIS'04), Tokyo (2004)
75. Y.X. Liu, L.F. Wei, and F. Nori, "Tomographic measurements on charge qubits", ERATO Conference on Quantum Information Science 2004 (EQIS'04), Tokyo (2004)
76. F. Nori, "Controlling the motion of magnetic flux quanta in superconductors", Physics and Astronomy Colloq. Series: 2004 Spring, (Michigan State University), East Lansing, USA (2004)
77. F. Nori, "Controlling the motion of particles in mixtures and the motion of magnetic flux quanta in superconductors", 34th Winter Colloquium on the Physics of Quantum Electrics, Snowbird, USA (2004)
78. V. Misko, S. Savel'ev, F. Marchesoni, and F. Nori, "Transverse rectification of vortices in superconductors with arrays of triangular pins", 17th International Symposium on Superconductivity (ISS 2004), Niigata (2004)
79. Y. Pashkin, O. Astafiev, T. Yamamoto, Y. Nakamura, D.V. Averin, T.E. Tilma, F. Nori and J.S. Tsai, "Coherent manipulation of coupled Josephson qubits", 17th International Symposium on Superconductivity (ISS 2004), (ISTEC), Niigata, (2004)
80. F. Nori, J. Villegas, S. Savel'ev, E. Gonzalez, J. Anguita, R. Garcia, and J. Vicent, "A superconducting reversible vortex diode for controlling the motion of magnetic flux quanta", 17th International Symposium on Superconductivity (ISS 2004), Niigata (2004)
81. S. Savel'ev, and F. Nori, "Magnetic bucking: Modified landau theory approach to study phase transitions in micromagnetic disks", 17th International Symposium on Superconductivity (ISS 2004), Niigata (2004)
82. T. Bersano-Begey, "Reverse engineering/inference of gene networks from Fantom data", FANTOM International Consortium on Deciphering the Logic of the Transcriptome (FANTOM

3), (RIKEN), Yokohama (2004)

83. B.Y. Zhu, F. Marchesoni, V.V. Moshchalkov, and F. Nori, "Controllable step motors and rectifiers of magnetic flux quanta using periodic arrays of asymmetric pinning defects", International Symposium on Mesoscopic Superconductivity and Spintronics: In the Light of Quantum Computation (MS+S2004), Atsugi (2004)
84. J.Q. You, J.S. Tsai, and F. Nori, "Macroscopic quantum entanglement in coupled charge qubits", International Symposium on Mesoscopic Superconductivity and Spintronics: In the Light of Quantum Computation (MS+S2004), Atsugi (2004)
85. S. Savel'ev, F. Marchesoni, and F. Nori, "Resonances in a SQUID ratchet driven by two frequencies", International Symposium on Mesoscopic Superconductivity and Spintronics: In the Light of Quantum Computation (MS+S2004), Atsugi (2004)
86. S. Savel'ev, C. Cattuto, and F. Nori, "Force-free current-induced reentrant melting of the vortex lattice in superconductors", International Symposium on Mesoscopic Superconductivity and Spintronics: In the Light of Quantum Computation (MS+S2004), Atsugi (2004)
87. S. Savel'ev, "Experimentally realizable devices for controlling the motion of magnetic flux quanta in anisotropic superconductors", International Symposium on Mesoscopic Superconductivity and Spintronics: In the Light of Quantum Computation (MS+S2004), Atsugi (2004)
88. V. Misko, "Stability of vortex-antuvortex molecules in mesoscopic superconducting triangles", International Symposium on Mesoscopic Superconductivity and Spintronics: In the Light of Quantum Computation (MS+S2004), Atsugi (2004)
89. F. Nori, "A superconducting reversible vortex diode that controls the motion of magnetic flux quanta", International Symposium on Mesoscopic Superconductivity and Spintronics: In the Light of Quantum Computation (MS+S2004), Atsugi (2004)
90. V. Misko, "Guidance of vortices and vortex ratchet effect in high-Tc superconducting thin films with special arrangements of antidots", International Symposium on Mesoscopic Superconductivity and Spintronics: In the Light of Quantum Computation (MS+S2004), Atsugi (2004)
91. Y.X. Liu, L.F. Wei, and F. Nori, "Generation of nonclassical photon states using a superconducting qubit in a microcavity", International Symposium on Mesoscopic Superconductivity and Spintronics: In the Light of Quantum Computation (MS+S2004), Atsugi (2004)
92. L.F. Wei, Y.X. Liu, and F. Nori, "Testing bell's inequality with a superconducting nanocircuit", International Symposium on Mesoscopic Superconductivity and Spintronics: In the Light of Quantum Computation (MS+S2004), Atsugi (2004)
93. J.Q. You, Y. Nakamura, and F. Nori, "Long-range inductive coupling between flux qubits", International Symposium on Mesoscopic Superconductivity and Spintronics: In the Light of Quantum Computation (MS+S2004), Atsugi (2004)
94. F. Nori, "Circuitry with superconducting qubits", Quantum Computing Program Review, Florida, USA (2004)
95. F. Nori, "Terahertz generation and vortex motion control in superconductors", 2005 APS March Meeting, Los Angeles, USA (2005)
96. X. Hu, J.Q. You, and F. Nori, "Correlation-induced suppression of decoherence in capacitively coupled Cooper-pair boxes", 2005 APS March Meeting, Los Angeles, USA (2005)
97. S. Savel'ev, and F. Nori, "Magnetic and mechanical buckling: Modified Landau theory

approach to studay phase transitions in micromagnetic disks and compressed rods", 10th International Vortex State Studies Workshop (IVW-10), Mumbai, India, (2005)

98. V. Misko, S. Savel'ev, F. Marchesoni, and F. Nori, "Separating particles according to their physical properties: Transverse drift of over-damped interacting particles through two-dimensional ratchets", 10th International Vortex State Studies Workshop (IVW-10), Mumbai, India (2005)
99. A. Maeda, Y. Inoue, H. Kitano, S. Savel'ev, S. Okayasu, I. Tsukada, and F. Nori, "Nano-scale friction : kinetic friction of magnetic flux quanta and charge-density waves", 10th International Vortex State Studies Workshop (IVW-10), Mumbai, India (2005)
100. R. Wordenweber, P. Dymashevski, and V. Misko, "Guidance of vortices and vortex ratchet effect high-Tc superconducting thin films with special arrangements of antidots", 10th International Vortex State Studies Workshop (IVW-10), Mumbai, India (2005)
101. J. Villegas, E. Gonzalez, M. Gonzalez, J. Anguita, S. Savel'ev, F. Nori, and J. Vicent, "Vortex lattice dynamics on ratchet potentials", 10th International Vortex State Studies Workshop (IVW-10), Mumbai, India (2005)
102. S. Savel'ev, and F. Nori, "Controlling vortex motion in superconductors", The 3rd International Symposium on Nanotechnology (JAPAN NANO 2005), MEXT, Tokyo (2005)
103. J.E. Villegas, S. Savel'ev, F. Nori, E. Gonzalez, J. Anguita, R. Garcia, and J. Vicent "Controlling vortex motion in superconductors", International Nanotechnology Exhibition & Conference (Nano tech 2005), Tokyo (2005)
104. Y.X. Liu, J.Q. You, L.F. Wei, C.P. Sun, and F. Nori, "Selection rules of superconducting flux qubits", International Conference on Nanoelectronics, Nanostructures and Carrier Interactions (NNCI2005) (NTT Basic Research Laboratories and Solution Oriented Research for Science and Technology (SPRST)), Atsugi, Japan (2005)
105. Y.X. Liu, S. Ozdemir, A. Miranovicz, and N. Imoto, "A study on the effects of damping on qubits using Kraus Representation", International Conference on Nanoelectronics, Nanostructures and Carrier Interactions (NNCI2005) (NTT and SPRST), Atsugi, Japan (2005)
106. S. Savel'ev, X. Hu, and F. Nori, "Quantum electromechanics: Qubits from buckling nanobars", International Conference on Nanoelectronics, Nanostructures and Carrier Interactions (NNCI2005), Atsugi, Japan (2005)
107. F. Nori, "(1) Controlling vortex motion, (2) Vortex kinetic friction, and (3) Critical currents in quasiperiodic pinning arrays", IV International Conference on Vortex Matter in Nanostructured Superconductors (VORTEX IV), (JSPS, ESF), Crete, Greece (2005)
108. S. Savel'ev, A. Rakhmanov, and F. Nori, "Using Josephson vortex lattices to control THz radiation: tunable THz photonic crystals", IV International Conference on Vortex Matter in Nanostructured Superconductors (VORTEX IV), (JSPS, ESF), Crete, Greece (2005)
109. V. Misko, S. Savel'ev, and F. Nori, "Critical currents in quasiperiodic pinning arrays: One-dimensional chains and Penrose lattices", IV International Conference on Vortex Matter in Nanostructured Superconductors (VORTEX IV), (JSPS, ESF), Crete, Greece (2005)
110. S.J. Bending, D. Cole, S. Savel'ev, F. Nori, T. Tamegai, "Vortex ratchets in hightly anisotropic superconductors", IV International Conference on Vortex Matter in Nanostructured Superconductors (VORTEX IV), (JSPS, ESF), Crete, Greece (2005)
111. R. Wordenweber, E. Hollmann, B. Rosewig, V. Yurchenko, T.J. Johansen, V.R. Misko, O.Plyushchay, "Vortex manipulation in microstructured high-Tc films up to high frequencies", IV International Conference on Vortex Matter in Nanostructured Superconductors (VORTEX

IV), (JSPS, ESF), Crete, Greece (2005)

112. Y.X. Liu, J.Q. You, L.F. Wei, C.P. Sun, and F. Nori, "Pulse phase-depenent adiabatic state control in flux qubit circuit", The 8th International Symposium on Foundations of Quantum Mechanics in the Light of New Technology (ISQM-Tokyo'05), Hatoyama, Japan (2005)
113. S. Savel'ev, X. Hu, and F. Nori, "Quantum electromechanics: qubits from buckling nanobars", The 8th International Symposium on Foundations of Quantum Mechanics in the Light of New Technology (ISQM-Tokyo'05), Hatoyama, Japan (2005)
114. V. Misko, S. Savel'ev, and F. Nori, "Controlling the motion of flux quanta using quasiperiodic pinning arrays: Enhancement of the critical currents in one-dimensional chains and Penrose lattices", The 8th International Symposium on Foundations of Quantum Mechanics in the Light of New Technology (ISQM-Tokyo'05), Hatoyama, Japan (2005)
115. S. Savel'ev, A. Rakhmanov, and F. Nori, "Using Josephson vortex lattices to control THz radiation: tunable THz photonic crystals", The 8th International Symposium on Foundations of Quantum Mechanics in the Light of New Technology (ISQM-Tokyo'05), Hatoyama, Japan (2005)
116 F. Nori, "Superconducting Qubits", International Conference on recent challenges in novel quantum systems (NQS2005), Camerino, Italy (2005)
117. J.Q. You, Y. Nakamura, and F. Nori, "Fast two-bit operations in inductively coupled flux qubits", International Conference on recent challenges in novel quantum systems (NQS2005), Camerino, Italy (2005)
118. J. Villegas, S. Savel'ev, F. Nori, E. Gonzalez, J. Anguita, R. Garcia, and J. Vicent "A superconducting reversible rectifier that controls the motion of magnetic flux quanta", International Conference on recent challenges in novel quantum systems (NQS2005), Camerino, Italy (2005)
119. J.Q. You, and F. Nori, "Quantum information processing with superconducting qubits in a microwave field", International Conference on recent challenges in novel quantum systems (NQS2005), Camerino, Italy (2005)
120. F. Nori, "Superconducting qubits", The Frontiers of Science within Nanoscience, workshop at Boston University, Boston, USA (2005)
121. F. Nori, "Superconducting qubits", Quantum Computing Program Review, Tampa, USA (2005)

[Presentations at conferences in Japan]

1. F. Nori, "Theoretical studies of magnetic flux bundle dynamics in superconductors", 理研におけるナノサイエンスの展開：単量子操作研究グループの発足を記念して，東京 (2002)
2. B.Y. Zhu, "Biologically-inspired devices to control the motion of flux quanta", 東北大学金属材料研究所研究会「超伝導体における渦糸状態の物理：統一的理解に向けて」，仙台，(2002)
3. F. Nori, "Vortex dynamics in Kagome lattice", Seminar at Advanced Research Laboratory, Hitachi, Ltd., Hatoyama (2002)
4. F. Nori, "Localized melting in vortex structures", Seminar at Advanced Research Laboratory, Hitachi, Ltd., Hatoyama (2002)
5. J.Q. You, "Controllable manipulation of macroscopic quantum states in coupled charge qubits", Seminar at NEC Fundamental Research Laboratories, Tsukuba (2002)
6. F. Nori, "Controlling the motion of magnetic flux quanta in superconductors", CREST First NANOFAB Workshop: Theoretical developments of Nanosuperconductors and its applications,

Kyoto (2003)

7. J.Q. You, J.S. Tsai, and F. Nori, "Scalable quantum computing with Josephson charge qubits", CREST First NANOFAB Workshop: Theoretical developments of Nanosuperconductors and its applications, Kyoto (2003)
8. T. Tilma, Y. Pashkin, D. Averin, Y. Nakamura, J.S. Tsai, and F. Nori, "Entanglement in multi-qubit superconducting circuits", CREST First NANOFAB Workshop: Theoretical developments of Nanosuperconductors and its applications, Kyoto (2003)
9. S. Savel'ev, "Vortex pumps for crossing lattices in very anisotropic superconductors", CREST First NANOFAB Workshop: Theoretical developments of Nanosuperconductors and its applications, Kyoto (2003)
10. S. Savel'ev, C. Cattuto, and F. Nori, "Force-free current-induced reentrant melting of the vortex lattice in superconductors", CREST First NANOFAB Workshop: Theoretical developments of Nanosuperconductors and its applications, Kyoto (2003)
11. S. Savel'ev, F. Marchesoni, and F. Nori, "Resonances in a SQUID ratchet driven by two frequencies", CREST First NANOFAB Workshop: Theoretical developments of Nanosuperconductors and its applications, Kyoto (2003)
12. B.Y. Zhu, L. Van Look, V.V. Moshchalkov, F. Marchesoni, and F. Nori, "Vortex dynamics in superconductors with an array of triangular blind antidots", CREST First NANOFAB Workshop: Theoretical developments of Nanosuperconductors and its applications, Kyoto (2003)
13. B.Y. Zhu, F. Marchesoni, and F. Nori, "Biologically inspired devices for easily controlling the motion of magnetic flux quanta", CREST First NANOFAB Workshop: Theoretical developments of Nanosuperconductors and its applications, Kyoto (2003)
14. B.Y. Zhu, F. Marchesoni, V.V. Moshchalkov, and F. Nori, "Controllable step motors and rectifiers of magnetic flux quanta using periodic arrays of asymmetric pinning defects", CREST First NANOFAB Workshop: Theoretical developments of Nanosuperconductors and its applications, Kyoto (2003)
15. J.Q. You, and F. Nori, "Quantum information processing with superconducting qubits in a microwave field", CREST First NANOFAB Workshop: Theoretical developments of Nanosuperconductors and its applications, Kyoto (2003)
16. Y. Pashkin, T. Tilma, D.V. Averin, O. Astafiev, T. Yamamoto, Y. Nakamura, F. Nori and J.S. Tsai, "Time evolution of entanglement in coupled Josephson junction qubits", CREST First NANOFAB Workshop: Theoretical developments of Nanosuperconductors and its applications, Kyoto (2003)
17. S. Savel'ev, and F. Nori, "Experimentally realizable devices for controlling the motion of magnetic flux quanta in anisotropic superconductors". CREST First NANOFAB Workshop: Theoretical developments of Nanosuperconductors and its applications, Kyoto (2003)
18. F. Nori, "Controlling the motion of vortices in superconductors and quantum computing using superconducting qubits", 第 17 回佐々木学術シンポジウム, 東京大学物性研究所, Tokyo (2004)
19. N. Mitarai, H. Nakanishi, 「高密度な粉体斜面流の密度プロファイル」, 日本物理学会 2004 年秋季大会, (青森, 高知) (2004)
20. F. Nori, and S. Savel'ev, "(I) Controlling vortex motion in superconductors and (II) Kinetic friction of magnetic flux quanta and charge density waves", Joint Workshop on Superconductivity (NFS2004/VPJ12), (JST), Osaka (2004)
21. S. Savel'ev, and F. Nori, "(I) Magnetic and mechanical buckiling: Modified Landau theory

approach to studay phase transitions in micro-magnetic disks and compressed rods, and (II) Quantum electromechanics: Qubits from buckling nanobars", Joint Workshop on Superconductivity (NFS2004/VPJ12), (JST), Osaka (2004)

22. N. Mitarai, H. Nakanishi, 「高密度な粉体斜面流の密度プロファイル」, 京都大学数理解析研究所「複雑流体の構造形成と崩壊の数理」研究集会, 京都 (2004)

C. Awards received during 2002-2005

1. Franco Nori, "Fellow of APS (American Physical Society)", American Physical Society, March 2003
2. Franco Nori, "Fellow of the Institute of Physics", Institute of Physics (IOP), U.K., July 2003
3. Sergey Savel'ev, "Best Presentation Award", Tata Institute of Fundamental Research, Jan. 2005
4. Misko Vyacheslav, "Best Presentation Award", Tata Institute of Fundamental Research, Jan. 2005

D. Press Releases

2002: Our publication:
"Scalable Quantum Computing with Josephson junction Qubits", J.Q.
You, J.S. Tsai, and F. Nori, in "Physical Review Letters" 89, 179 (November 2002) (available on line from http://link.aps.org/abstract/PRL/v89/e197902) has been featured in several places, including:

The December 11 to 18, 2002, issue of the "Technology Review News", Page 1. Available at http://www.trnmag.com/. It features our results, and also four other stories for that week.

The article, titled "Design links quantum bits", is in
http://www.trnmag.com/Stories/2002/121102/Design_links_quantum_bits_121102.html
and it is relatively long (for a news piece).

November 22, 2002: United Business Media's "Electrical Engineering Times", described as "The Industry Source for Engineers and Technical Managers Worldwide", has an article describing our results (titled: "Superconducting junctions eyed for quantum computing" and available at http://www.eetimes.com/story/OEG20021122S0013).

"Electronics Weekly", November 06, 2002, News; Pg. 5, on our results on "Quantum qubits".

October 23, 2002. "Paper Discusses Circuitry for Quantum Computing", in "Supercomputing online". Available at http://www.supercomputingonline.com/article.php?sid=2756

Our work motivated the long article "Thoughtful about uploading", Bill Tammeus, Kansas City Star, November 2, 2002.

October 2002: Featured in "Innovations Report", "Forum für Wissenschaft, Industrie und Wirtschaft,

a technical news site in Germany.
http://www.innovations-report.com/berichte/ansicht_ctyp1.php3?id=13910

October 23, 2002, featured in "Ascribe - The Public Interest Newswire".

October 24, 2002, featured in "NewsWise", that covers new science and technology developments.

The December 2002 issue of "Science and Technology Trends" (number 21, Dec. 2002) has a one-page article featuring our November 2002 PRL results. This is a publication of the "Science and Technology Foresight Center" of the National Institute of Science and Technology Policy (NISTEP). The latter is part of the Ministry of Education, Culture, Science and Technology. Japan.

It is available on-line in English at
http://www-personal.engin.umich.edu/¥~nori/scalable/Science_Trends_Japan-b.pdf

and in Japanese in
http://www.nistep.go.jp/achiev/ftx/jpn/stfc/stt021j/0212_02_topics/200212_topics.html#tp_info_01
in http://www.nistep.go.jp/index-j.html

The summary is in
http://www.nistep.go.jp/achiev/ftx/jpn/stfc/stt021j/0212_01_outline/200212_outline.html

Press coverage also appeared in
http://www.umich.edu/~newsinfo/Releases/2002/Oct02/r102302a.html
news-wire web page in the USA

http://www.ascribe.org/cgi-bin/d?asid=20021023.083538

another news wire info

http://www.newswise.com/articles/2002/10/SCALABLE.UMI.html?sc=wire

Newspaper articles overseas include the following ones:

"Japan Industry News" of the "Japan Industrial Journal", page 2, Thursday, October 24, 2002.

"Daily Industrial Newspaper" (the Nikkan Kogyo Shinbun), page 4, Thursday, October 24, 2002.

"Nikkei" (this important newspaper is the Japanese version of the "Wall Street Journal"), Friday, October 25, 2002.

"Science News" (in Japan), November 8, 2002.

2003. The "NEDO Kaigai Report" (published biweekly and featuring news articles and

summaries as well as other information related to science and technology). It is published by the Information Center of the New Energy and Industrial Technology Development Organization (NEDO), a semi-governmental organization affiliated with Japan's Ministry of Economy, Trade and Industry.

==========

2002: Our publication "Experimentally-realizable devices for controlling the motion of magnetic flux quanta in anisotropic superconductors", S. Savelev and F. Nori, published in "Nature Materials" 1, 179 (November 2002), has been:

Listed on the cover of the November issue of "Nature Materials".

also featured in a pedagogical two-pages "News and Views", "Nature Materials" 1, 143 (2002), titled: "Controlling the Motion of Quanta".

"Nikkei" (this important newspaper is the Japanese version of the "Wall Street Journal"), Monday, January 6, 2003. An article on Page 23 describing these results.

November 6, 2002. "Stories of modern science, from UPI", by Ellen Beck. (UPI = United Press International).

November 13, 2002. "Electronics Weekly", Pg. 6. "US and Japanese scientists control magnetic flux quanta".

The UM press release in
http://www.umich.edu/~newsinfo/Releases/2002/Nov02/r110402c.html

was covered by news agencies and newswire services, including:

"Innovations Report", "Forum fur Wissenschaft, Industrie und Wirtschaft", a technical news site in Germany;
http://www.innovations-report.com/berichte/ansicht_ctyp1.php3?id=13910

"AScribe, The Public Interest Newswire";

"NewsWise" that covers new science and technology developments.

==========

2002: Our work on ``Biologically-inspired solid-state devices for the control of the motion of quanta" is nicely highlighted in the "Molecular Motors" first feature article of the November, 2002, Physics Today, page 38.

http://www.physicstoday.org/vol-55/iss-11/p33.shtml?jsessionid=2714771041499442571

also available in PDF (without need to register on-line) at

http://www.physik.uni-augsburg.de/theo1/hanggi/309.pdf

2003: Our work "Observing Brownian motion in vibro-fluidized granular matter", by G. D'Anna, P. Mayor, A. Barrat, V. Loreto, F. Nori, "Nature" 424, 909-912 (August 21, 2003), available on-line at http://www.nature.com/nature/links/030821/030821-1.html
has been featured in (the list below is very incomplete):

The Cover Story of Nature (August 21st 2003 issue of Nature). The text accompanying the cover photo was: "Against the Grain. Brownian motion in a non-equilibrium system".

A companion "News and Views" in that issue of Nature.

"Science Letter", September 15, 2003. http://www.NewsRX.net

Several TV programs. Three examples (of about five minutes each totally devoted to our work) were broadcasted in Europe (one on the German "Fokus" (by "MTW: Menschen Technik Wissenschaft"), a different program in Italian, and a quite different one in French.
Also in radio programs (e.g., Radio Swiss International).

Featured (in all languages of the European Union) in the High-Tech News of "Euronews".

Long Newspaper articles include "Il Secolo XIX", Agosto 27, 2003, page 31, (in Italian) in the section on ``Research and Science". Also, "it Sole 24 Ore", Settembre 11, 2003, the most important Italian newspaper on finances and the economy.

Featured in the long article: "Nel Mondo dei Granelli di Sabbia", "Scienza e Conoscenza", 9-12-2003.

the article was in
http://www.mosac.com/fisica/news/leggi.php?codice=191.

News coverage in French include the following three newspapers: L`Hebdo, Le Temps, 24 Heures.

News coverage in German include the following four newspapers: Tages-Anzeiger, Neue Z¥"urcher Zeitung, St. Galler Tagblatt Gesamtausgabe, Basler Zeitung}.

Interviewed by the newspaper Nikkei, Japan.

The University of Michigan press release in

http://www.umich.edu/news/index.html?Releases/2003/Aug03/r082003

http://ipumich.temppublish.com/cgi-bin/print.cgi?Releases/2003/Aug03/r082003

was covered by news agencies and newswire services, including:

"The Resource for Science Information" (BrightSurf.com).
http://www.brightsurf.com/news/aug_03/EDU_news_082503_c.php.

One of the few ``Today's Science News" for August, 25, 2003.

"Innovations Report" (Forum fur Wissenschaft, Industrie und Wirtschaft, Germany). August, 25, 2003.
http://www.innovationsreport.de/html/berichte/physik_astronomie/bericht-20770.html

"Global Technology Market Place" (GlobalTechnoScan.com). Weekly Magazine on New Technology. Issue 27th Aug to 2nd Sept. 2003.

http://www.globaltechnoscan.com/27thAug-2ndSep03/granular_materials.htm

"EurekAlert! Public News". A Service of the American Association for the Advancement of Science, with support from the US Department of Energy and the US National Institutes of Health. Eurekalert.org is described as the premier web site for science
news since 1996. Public release date: 22-Aug-2003.

http://www.eurekalert.org/pub_releases/2003-08/uom-gmn082203.php

"Science News". 8/22/2003.
http://sciguy.com/News/Article.asp?ArticleID=5410

"Headline News". NewsHub.com. 22-Aug-2003. http://NewsHub.com

"Knowledge Science". http://www.kenkyu40.net/index.php

"Health News" (HealthNews.ws) 8/24/2003. http://www.healthnews.ws/index.aspx?id=394

World Wide News Headliner.

The EPFL press release is in

http://news.swiss-science.ch/news/news-docs/sabled.pdf (in German)
http://news.swiss-science.ch/news/news-docs/sable.pdf (in French)

2003: Our work on vortex dynamics in superconductors was featured in part of a television program, prepared by the Danish Broadcast Corporation, about the study of superconducting materials.

==========

2003: Our recent publication "Controlling Transport in Mixtures of Interacting Particles using Brownian Motors", by S. Savel'ev, F. Marchesoni, and F. Nori, Phys. Rev. Lett. 91, 10601 (2003), available on-line at http://link.aps.org/abstract/PRL/v91/e010601, has been featured in:

for several weeks as the top-listed research news in the front page of the University of Michigan web site (www.umich.edu). This web site gets a lot of traffic everyday. The
actual press release is in
http://www.umich.edu/news/Releases/2003/Jun03/r061903.html.

A very non-technical and brief graphical summary is in
http://www.umich.edu/news/Releases/2003/May03/img/ratchets.jpg

"Newswise/Science News" also appeared in "Small Times magazine"
(presenting technological advances in nano-science). http://www.smalltimes.com

http://www.smalltimes.com/document_display.cfm?document_id=6259

"Le Scienze", the Italian version of Scientific American, among other science news outlets.

featured in the article "Conveyor Belt on a nanometer scale", published in "Machine Design", No. 19. Vol. 75, Pg. 35; October 9, 2003.

2003: Our recent publication "Reversible Rectifier that Controls the Motion of Magnetic Flux Quanta in Superconductors", by J.E. Villegas, S. Savel'ev, F. Nori, E.M. Gonzalez, J.V. Anguita, R. Garcia, and J.L. Vicent, "Science", 302, 1188 (2003) has been featured in several venues including:

an "Enhanced Perspectives" in Science 302, 1159 (2003). It is available on-line at http://www.sciencemag.org/cgi/content/full/302/5648/1159 .
This is the only "Enhanced Perspectives" of that issue of " Science", with dozens of links with further information on the subject, and one of three "Enhanced Perspectives" covering all of physics for 2003.

prominently featured in the page "This week in Science" of that issue of "Science" (Nov. 14, 2003).

High-Tc Update (November 2003).
http://www.iitap.iastate.edu/htcu/notabene.html (November 2003)

Newspapers in Europe (e.g., El Pais, Madrid), Japan, and the USA.

Spain Nano-technology Network:
http://www.nanospain.net/nanospain$_{}$papers$_{}$g.htm

Nanopic site:

http://www.nanopicoftheday.org/2005Pics/January2005/25MagFluxRectifier.htm

==========

2005: Our work on mechanical qubits (by S. Savel'ev, X. Hu, and F. Nori) has been featured in several venues including:

Scientific American, April 2005, page 28. "Qubit Twist: Bending Nanotubes as Mechanical Quantum Bits."
http://www-personal.engin.umich.edu/~nori/Sci-am-mechanical-qubits.pdf

United Press International (UPI). "Nano World: Nano for quantum computers".
http://www.upi.com/view.cfm?StoryID=20050317-124226-2271r

==========

2005: Our recent publication "Using Josephson Vortex Lattices to Control THz Radiation: Tunable Transparency and THz Photonic Crystals", by S. Savel'ev, A.L. Rakhmanov, and F. Nori, Physical Review Letters 94, 157004 (2003), has been featured in several venues including:
PhysicsOrg.com: The latest Physics and Technology News.
http://www.physorg.com/printnews.php?newsid=3767

Daily Science News, http://www.sciencenewsdaily.org/story-3767.html
Also at SciCentral ("Gateway to the best scientific research news sources"),
Air Force News (http://afpet.ft-belvoir.af.mil/topnews.asp),
Broad Education (http://broad-education.com/news-18670.html), and PhysicsNews.com.

PhysicsLink.com. Physics and Astronomy online. http://www.physlink.com/index.cfm ¥¥
http://www.physlink.com/News/042205ThzPhotonicCrystal.cfm ¥¥

The UM press release is in
http://www.umich.edu/news/index.html?Releases/2005/Apr05/r041805a

Quantum Information Processing Research Projects (from 2002 to July 2004) in Prof. F. Nori's Research Group

Mostly superconducting qubits using Josephson junctions
(and a few other related projects on algorithm performance
implementation, quantum computation with ion traps, etc.)

Fast two-bit operations in inductively coupled flux qubits

J. Q. You,[1,2,*] Y. Nakamura,[1,3,4,†] and Franco Nori[1,5,‡]

[1] *Frontier Research System, The Institute of Physical and Chemical Research (RIKEN), Wako-shi 351-0198, Japan*
[2] *National Laboratory for Surface Physics and Department of Physics, Fudan University, Shanghai 200433, China*
[3] *NEC Fundamental and Environmental Research Laboratories, Tsukuba, Ibaraki 305-8051, Japan*
[4] *CREST, Japan Science and Technology Agency (JST), Kawaguchi, Saitama 332-0012, Japan*
[5] *Center for Theoretical Physics, Physics Department, Center for the Study of Complex Systems, University of Michigan, Ann Arbor, MI 48109-1120, USA*

(Dated: August 3, 2004)

A central problem for implementing efficient quantum computing is how to realize fast operations (both one- and two-bit ones). However, this is difficult to achieve for a collection of qubits, especially for those separated far away, because the interbit coupling is usually much weaker than the intrabit coupling. Here we present an experimentally feasible method to effectively couple two flux qubits via a common inductance and treat both single and coupled flux qubits with more realistic models which include the loop inductance. The main advantage of our proposal is that a strong interbit coupling can be achieved using a small inductance, so that two-bit operations as fast as one-bit ones can be easily realized. We also show the flux dependence of the transitions between states for the coupled flux qubits.

PACS numbers: 74.50.+r, 03.67.Lx, 85.25.Cp

I. INTRODUCTION

Josephson-junction circuits can exhibit quantum behaviors. Among qubits based on Josephson-junction circuits, the charge qubit realized in a Cooper-pair box can demonstrate quantum oscillations.[1] An improved version of this circuit has showed quantum oscillations with a high quality factor.[2] In addition to charge qubits, flux qubits achieved in a superconducting loop with one[3] or three Josephson junctions[4] have been studied and some of these have shown quantum dynamics.[5] The phase qubit consists of a large-area current-biased Josephson junction.[6]

Capacitive couplings of two superconducting qubits (both charge-[7] and phase-types[8]) were attained recently in experiments, and quantum entanglement was observed in these systems. Also, controllable interbit couplings of charge qubits were proposed using a variable electrostatic transformer,[9] a current-biased Josephson junction[10] and a tunable dc-SQUID.[11] These interbit couplings can link nearest neighboring qubits. Actually, there are quantum-computing protocols (e.g., adiabatic quantum computing[12]) that only demand nearest-neighbor couplings. However, for more general quantum-computing protocols, it is desirable to achieve strong enough couplings among non-neighboring qubits as well. When charge qubits are coupled by LC-oscillator modes[13] or by an inductance,[14] long-ranged interbit couplings can be realized, but a very large value of the inductance is needed. An alternative way of coupling charge qubits was proposed using a Josephson junction.[15,16,17] Moreover, the charge qubit can be very sensitive to the background charge fluctuations, which generate noise that severely limits the performance of charge-qubit devices and, unfortunately, is difficult to reduce.

In this paper, we present an experimentally feasible method to effectively couple two flux qubits. In contrast with the charge qubit, the flux qubit is *insensitive* to the charge noise. In this qubit, the major noise is due to the fluctuations of the magnetic fluxes. Estimations show that the flux qubit can have a relatively high quality factor.[18] Here we include the effect of the loop inductance in a three-junction flux qubit and couple two flux qubits via a common inductance. Because the critical current of each Josephson junction in the flux qubit is larger than that in the charge qubit, we can produce a *strong* interbit coupling using an inductance as small as 20 pH (corresponding to a loop of approximately 16 μm and comparable to the loop inductance of the single flux qubit currently achieved in experiments), and thereby two-bit operations as fast as one-bit ones can be easily achieved, improving the efficiency of quantum computing. Moreover, we show a novel flux dependence of the state transitions in two coupled flux qubits. We find that, except for some specific values of the external flux, the forbidden transitions in the two coupled flux qubits become allowed when the parameters of the two qubits change from being initially equal to each other and then making these different.

Coupling two flux qubits by a mutual inductance was proposed in Refs. 19,20,21 and was recently realized in experiments.[22,23] Here we treat both single and coupled flux qubits using more realistic models which include the loop inductance. We numerically solve the Schrödinger equation to obtain the energy levels and the eigenstates of the flux-qubit systems. This numerical method allows us to extend our study to the larger inductance regime.

The paper is organized as follows. In Sec. II, we study a single flux qubit containing loop inductance. It is shown that the system can still be used to achieve a qubit even for a larger loop inductance of $L \sim 1$ nH. Section III focuses on two flux qubits coupled by a common induc-

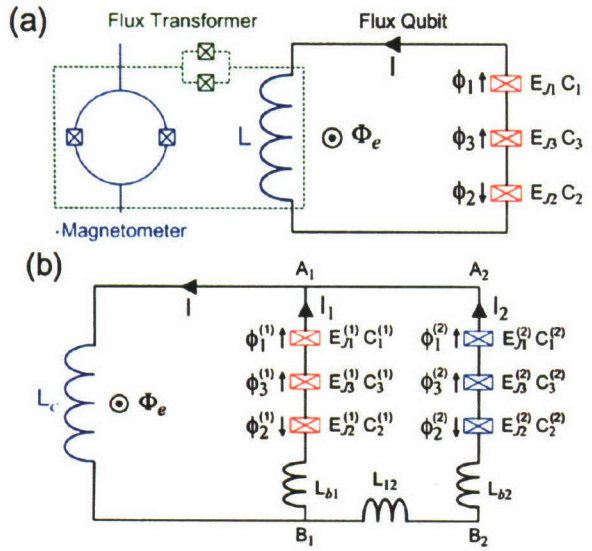

FIG. 1: (a) A flux qubit, where an external magnetic flux Φ_e pierces the superconducting loop that contains three Josephson junctions and an inductance L. The Josephson energies and capacitances of the junctions are $E_{J1} = E_{J2} = E_J$, $C_1 = C_2 = C$, $E_{J3} = \alpha E_J$, and $C_3 = \alpha C$. Here we choose $\alpha = 0.8$ and $E_J = 35E_c$, where $E_c = e^2/2C$. (b) Two flux qubits coupled by a common inductance L_c, where the external flux Φ_e is applied within the left loop $A_1L_cB_1A_1$. The parameters of each flux qubit are $E_{J1}^{(i)} = E_{J2}^{(i)} = E_J^{(i)}$, $C_1^{(i)} = C_2^{(i)} = C^{(i)}$, $E_{J3}^{(i)} = \alpha_i E_J^{(i)}$, and $C_3^{(i)} = \alpha_i C^{(i)}$, with $i = 1, 2$. Here we choose $\alpha_i = 0.8$ and $E_J^{(i)} = 35E_c^{(i)}$, where $E_c^{(i)} = e^2/2C^{(i)}$. To implement a readout of the flux-qubit states, a switchable superconducting flux transformer is employed to couple the dc-SQUID magnetometer with the inductance L in (a) or L_c in (b) during the quantum measurement. However, this coupling is switched off in the absence of a readout.

tance. In Sec. IV, we study the state transitions induced by the microwave field. Section V deals with the circulating supercurrents and quantum measurement. Finally, the discussion and conclusion are given in Sec. VI.

II. SINGLE FLUX QUBIT

We first consider a single flux qubit in the absence of a quantum measurement, where the dc-SQUID magnetometer for measuring quantum states of the flux qubit is decoupled from the qubit. As shown in Fig. 1(a), the flux qubit consists of a superconducting loop with three Josephson junctions and the total inductance of the whole loop is L. Fluxoid quantization around the loop imposes a constraint on the phase drops across the three junctions:

$$\phi_1 - \phi_2 + \phi_3 + 2\pi f' = 0, \tag{1}$$

where

$$f' = f + \frac{IL}{\Phi_0}. \tag{2}$$

Here, $\Phi_0 = h/2e$ is the flux quantum, $f = \Phi_e/\Phi_0$ represents the reduced magnetic flux, and

$$I = I_0 \sin\phi_1, \tag{3}$$

with $I_0 = 2\pi E_J/\Phi_0$, is the circulating supercurrent. When the loop inductance is included, the Hamiltonian of the single flux qubit is

$$H = \frac{P_p^2}{2M_p} + \frac{P_m^2}{2M_m} + U(\phi_p, \phi_m), \tag{4}$$

with the potential energy given by

$$U(\phi_p, \phi_m) = E_J[2 + \alpha - 2\cos\phi_p \cos\phi_m - \alpha\cos(2\pi f' + 2\phi_m)] + \frac{1}{2}LI^2. \tag{5}$$

Here $P_k = -i\hbar\partial/\partial\phi_k$ (with $k = p$ and m), $M_p = (\Phi_0/2\pi)^2 2C$, $M_m = M_p(1 + 2\alpha)$, and

$$\phi_p = (\phi_1 + \phi_2)/2, \quad \phi_m = (\phi_1 - \phi_2)/2. \tag{6}$$

Also, the supercurrent I can be rewritten as

$$I = I_0 \sin(\phi_p + \phi_m). \tag{7}$$

The Hamiltonian (4) is reduced to Eq. (12) in Ref. 19 when $L \to 0$.

Figure 2 presents the contour plots of the periodic potential $U(\phi_p, \phi_m)$ for $f = 0.5$ and $\alpha = 0.8$. The numerical results show that the minima of the potential *preserve* the two-dimensional centered cubic lattice even for a large loop inductance. For inductance ratio

$$\beta_L \equiv L/L_J \tag{8}$$

from zero to one (where $L_J = \Phi_0/2\pi I_0$ is the Josephson inductance of the junction), a well defined double-well potential structure exists at each lattice point even though at higher energies the well shapes are modified by the loop inductance L. This double-well structure is required for achieving a two-level system. As shown in Fig. 3, the lowest two levels of the single-qubit system are not significantly affected by the variation of β_L because the corresponding two eigenstates are mainly contributed by the weakly β_L-dependent ground state in each well. However, since varying L significantly modifies the well shapes at higher energies, the excited states within or above the wells (which, as seen in Fig. 3, dominantly contribute to the eigenstates corresponding to the third and higher levels) become pronouncedly β_L-dependent. Indeed, Figure 3 shows that the top three levels are sensitive to the variation of β_L. Moreover, with the loop inductance increasing to $\beta_L = 4$ [see Fig. 2(c)], a more

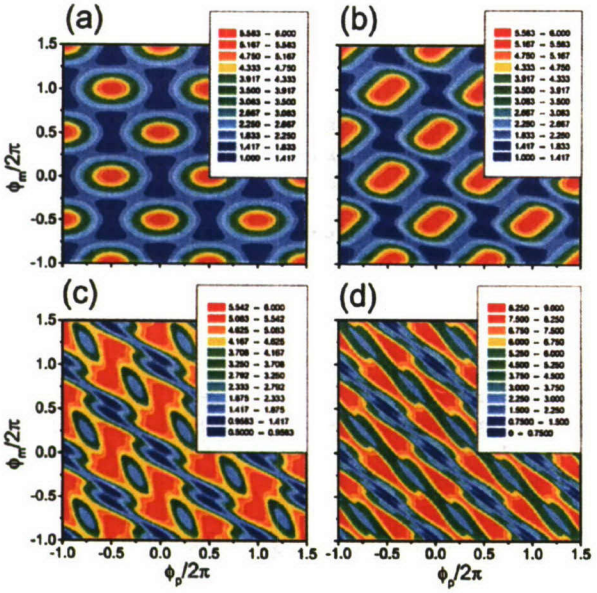

FIG. 2: Contour plots of the potential energy $U(\phi_p, \phi_m)$, in units of E_J, for $\alpha = 0.8$ and $f = 0.5$. Here $\beta_L \equiv 2\pi I_0 L/\Phi_0 =$ (a) 0, (b) 1, (c) 4, and (d) 10. Notice that the well defined double-well potential structure vanishes in (d), and thus the flux qubit breaks down.

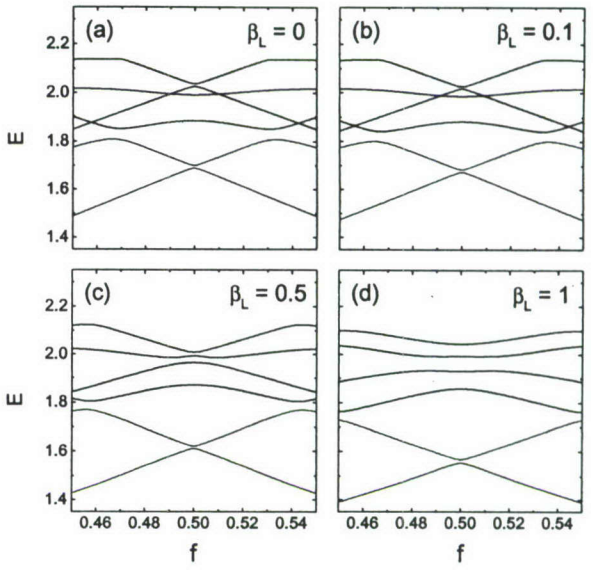

FIG. 3: Energy levels of a single flux qubit versus reduced flux f for different values of β, where only the levels of the states $|i\rangle$, $i = 0$ to 5, are shown. Here the energy E is in units of E_J.

distorted double-well structure appears at each lattice point, and a local energy minimum develops along the diagonal direction between every two adjoining double-well structures. These newly-developed local minima will affect the two-level system achieved for the qubit. When the loop inductance increases even more to $\beta_L = 10$ [see Fig. 2(d)], the periodic potential is even more distorted. In this case, the well defined double-well potential structure vanishes, and thus the flux qubit breaks down.

The energy spectrum and the eigenstates are determined by

$$H\Psi(\phi_p, \phi_m) = E\Psi(\phi_p, \phi_m). \tag{9}$$

Figure 3 shows the dependence of the energy levels on the magnetic flux for $\beta_L \leq 1$. Here we choose $E_J = 35E_c$, where the charging energy E_c is defined as $E_c = e^2/2C$. These parameters are close to those used in a recently fabricated flux-qubit device.[5] Around $f = 0.5$, in sharp contrast with the higher energy levels, the energy difference

$$\Delta = \varepsilon_1 - \varepsilon_0 \tag{10}$$

between the lowest two levels is *not* sensitive to the variation of β_L. In Fig. 4, we show the energy separation of the two lowest levels, Δ, as a function of β_L. We find the interesting result that $\Delta(\beta_L)$ is almost flat at $f = 0.5$ ($0.011 < \Delta(\beta_L)/E_J < 0.0135$) when $0 \leq \beta_L \leq 0.85$. These features indicate that, even with a large loop inductance of $\beta_L = 1$, in the vicinity of $f = 0.5$ the two lowest eigenstates (denoted by $|0\rangle$ and $|1\rangle$ for the ground and the first excited states, respectively) remain to be suitable basis states for a flux qubit. Within the subspace of qubit states spanned by $|0\rangle$ and $|1\rangle$, the Hamiltonian is reduced to

$$H = \varepsilon_1|1\rangle\langle 1| + \varepsilon_0|0\rangle\langle 0|. \tag{11}$$

If the average energy $(\varepsilon_1 + \varepsilon_0)/2$ is chosen to be the new zero-point energy of the flux qubit, the Hamiltonian can be further expressed as

$$H = \frac{1}{2}\Delta\rho_z, \tag{12}$$

where $\rho_z = |1\rangle\langle 1| - |0\rangle\langle 0|$. In Ref. 24, the effects of the loop inductance in a flux qubit are considered using a perturbation approach, where the Hamiltonian is expanded into three parts: an inductance-free Hamiltonian, an inductance-related harmonic oscillator term, and a small correction term. This perturbation method is valid for $\beta_L \ll 1$ since the correction term is proportional to the loop inductance of the flux qubit. Instead of using the perturbation approach, we numerically solve Eq. (9) to obtain the eigenvalues and eigenstates of the system. This numerical method allows us to extend our study to the regime of $\beta_L \sim 1$, where the lowest two eigenstates of the system can still be used for achieving a qubit. Using the experimental value[5] $I_0 \sim 0.5\ \mu$A, this regime corresponds to a loop inductance of $L \sim 1$ nH.

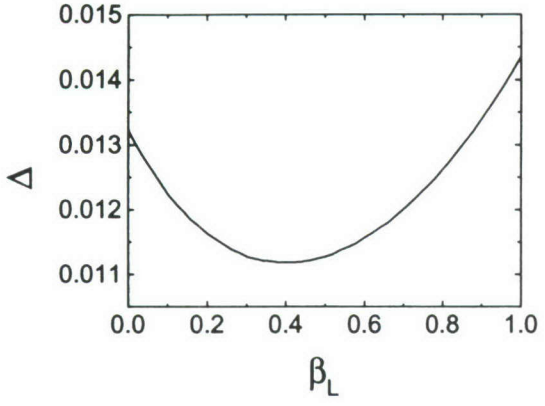

FIG. 4: Energy difference Δ between qubit states $|1\rangle$ and $|0\rangle$ as a function of β for $f = 0.5$. Here Δ is in units of E_J.

III. COUPLED FLUX QUBITS

To couple two flux qubits, we use a *common* inductance L_c shared by these two qubits [see Fig. 1(b)]. Here the external flux Φ_e is applied within the loop $A_1L_cB_1A_1$. Also, the circuit is designed in such a way that the mutual inductance between loops $A_1L_cB_1A_1$ and $A_1B_1B_2A_2A_1$ may be ignored. This is achieved when only a small fraction of the flux generated by one loop passes through the other. (If this were not to be the case, the interbit coupling can still be achieved by the common inductance L_c, but the interaction Hamiltonian takes a more complicated form.) Phase drops through the three Josephson junctions of the ith flux qubit are constrained by

$$\phi_1^{(i)} - \phi_2^{(i)} + \phi_3^{(i)} + 2\pi\left[f + (I_iL_i + I_jL_c)/\Phi_0\right] = 0, \quad (13)$$

where $i, j = 1, 2$ $(i \neq j)$, $L_1 = L_c + L_{b1}$, and $L_2 = L_c + L_{12} + L_{b2}$. The total supercurrent through L_c is

$$I = I_1 + I_2, \quad (14)$$

where

$$I_i = I_{0i}\sin(\phi_{pi} + \phi_{mi}), \quad (15)$$

with $I_{0i} = 2\pi E_J^{(i)}/\Phi_0$, $\phi_{pi} = (\phi_1^{(i)} + \phi_2^{(i)})/2$, and $\phi_{mi} = (\phi_1^{(i)} - \phi_2^{(i)})/2$.

The Hamiltonian of the two coupled flux qubits can be written as

$$H = H_1 + H_2 + H_I. \quad (16)$$

Here H_i is the Hamiltonian of the ith isolated flux qubit, with loop inductance L_i and circulating supercurrent I_i, which has the form in Eq. (4) but with f' replaced by

$$f_i' = f + \frac{I_iL_i}{\Phi_0}. \quad (17)$$

Also, E_J, C and α are replaced by $E_J^{(i)}$, $C^{(i)}$ and α_i. The interaction Hamiltonian is

$$H_I = L_cI_1I_2 - \sum_{i=1}^{2}\alpha_iE_J^{(i)}\Pi_i, \quad (18)$$

where

$$\Pi_i = \cos(\gamma_i + 2\pi I_jL_c/\Phi_0) - \cos\gamma_i, \quad (19)$$

with

$$\gamma_i = 2\pi f_i' + 2\phi_{mi}, \quad (20)$$

and $i \neq j$.

The supercurrent I_i flows through each of the three Josephson junctions in the ith flux qubit, so I_i can also be written as

$$\begin{aligned} I_i &= \alpha_iI_{0i}\sin\phi_3^{(i)} \\ &= -\alpha_iI_{0i}\sin\left\{2\pi(f_i' + I_jL_c/\Phi_0) + 2\phi_{mi}\right\}, \end{aligned} \quad (21)$$

where $i, j = 1, 2$ and $i \neq j$. Taking advantage of this relation for I_i, one can expand the interaction Hamiltonian (18) as

$$H_I = -\lambda L_cI_1I_2 - \sum_{i=1}^{2}\alpha_iE_J^{(i)}\xi_i, \quad (22)$$

where

$$\lambda = 1 + \sum_{i=1}^{2}\left[\frac{1}{3}\beta_{Li}^2\left(\frac{I_i}{I_{0i}}\right)^2 + \frac{2}{15}\beta_{Li}^4\left(\frac{I_i}{I_{0i}}\right)^4 + \ldots\right], \quad (23)$$

and

$$\begin{aligned} \xi_i = \frac{1}{2}&\cos(2\pi f_i' + 2\phi_{mi}) \\ &\times\left[\beta_{Lj}^2\left(\frac{I_j}{I_{0j}}\right)^2 + \frac{5}{12}\beta_{Lj}^4\left(\frac{I_j}{I_{0j}}\right)^4 + \ldots\right], \end{aligned} \quad (24)$$

with $\beta_{Li} \equiv 2\pi I_{0i}L_c/\Phi_0 < \pi/2$. The term $-\lambda L_cI_1I_2$ in H_I produces an interbit coupling between flux qubits 1 and 2, while $\alpha_iE_J^{(i)}\xi_i$ slightly modifies the energy levels of the ith flux qubit.

When $\beta_{Li} \equiv 2\pi I_{0i}L_c/\Phi_0 \ll 1$, H_I is approximated by

$$H_I = -L_cI_1I_2 \quad (25)$$

because $\alpha_iE_J^{(i)}\Pi_i \approx L_cI_1I_2$ in this case. Within the qubit-state subspace of the ith isolated flux qubit, H_i is reduced to

$$H_i = \frac{1}{2}\Delta_i\rho_z^{(i)}, \quad (26)$$

where $\rho_z^{(i)} = |1_i\rangle\langle 1_i| - |0_i\rangle\langle 0_i|$. In the vicinity of $f = 0.5$, because the supercurrents I_i at states $|1_i\rangle$ and $|0_i\rangle$

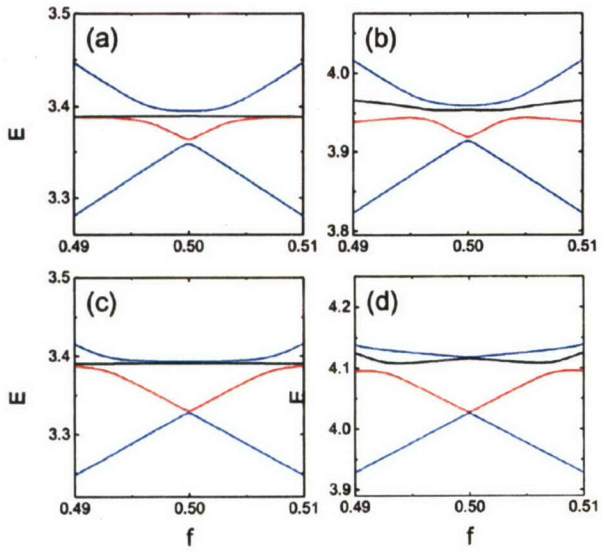

FIG. 5: Energy levels of two coupled flux qubits versus reduced flux f for $L_{b1}/L_c = 0.1$ and $(L_{12} + L_{b2})/L_c = 0.2$. The parameters $\beta_{Li} \equiv 2\pi I_{0i} L_c/\Phi_0$ are (a) $\beta_{L1} = \beta_{L2} = 0.03$, (b) $\beta_{L1} = 0.03$, $\beta_{L2} = 0.04$, (c) $\beta_{L1} = \beta_{L2} = 0.07$, and (d) $\beta_{L1} = 0.07$, $\beta_{L2} = 0.1$. Here the energy E is in units of $E_J^{(1)}$.

have equal magnitudes but opposite directions, I_i can be written as

$$I_i = a_i \rho_z^{(i)} + b_i |1_i\rangle\langle 0_i| + b_i^* |0_i\rangle\langle 1_i|, \tag{27}$$

where $a_i = \langle 1_i|I_i|1_i\rangle$, and $b_i = \langle 1_i|I_i|0_i\rangle$. Because the supercurrent I_i at state $|1_i\rangle$ (i.e., a_i) is proportional to the slope of the energy level that corresponds to state $|1_i\rangle$ with respect to f (see, e.g., Ref. 19), it falls to zero at the *symmetric* point, $f = 0.5$, where the level becomes flat. Also, our numerical results show that b_i becomes a real number at $f = 0.5$. Thus, we can rewrite I_i at $f = 0.5$ as

$$I_i = b_i \rho_x^{(i)}, \tag{28}$$

with $\rho_x^{(i)} = |1_i\rangle\langle 0_i| + |0_i\rangle\langle 1_i|$. For $\beta_{Li} \ll 1$, the Hamiltonian at $f = 0.5$ can be cast to

$$H = \sum_{i=1}^{2} \frac{1}{2} \Delta_i \rho_z^{(i)} - \chi \rho_x^{(1)} \rho_x^{(2)}, \tag{29}$$

with

$$\chi = L_c b_1 b_2. \tag{30}$$

It is clear that the interbit coupling persists at $f = 0.5$.

Figure 5 shows the energy spectrum of the two coupled flux qubits around $f = 0.5$. In order to realize fast two-bit operations while keeping the leakage from the qubit states to other higher energy states small, we choose the interbit coupling strength to be comparable to the energy difference, at $f = 0.5$, between the basis states $|1_i\rangle$ and $|0_i\rangle$ of each qubit. As shown in Figs. 5(a) and 5(b), the energy spectrum remains similar in the vicinity of $f = 0.5$ when the two flux qubits have different values of parameters. Furthermore, the two higher energy levels, ϵ_3 and ϵ_4, in the first four energy levels (i.e., ϵ_k with $k = 1$ to 4) of the two coupled flux qubits are flat in a relatively broad range around $f = 0.5$; this flat region is *much broader* than the corresponding flat-energy-level range of the single flux qubit around $f = 0.5$. The flux-independent level ϵ_3 in Fig. 5(a) corresponds to a singlet eigenstate, while other three levels correspond to triplet eigenstates. As expected, the transitions between this singlet state and other three triplet states are not allowed by the microwave perturbation [cf. Fig. 6(a)]. Similar spectral results were also obtained by Storcz and Wilhelm[21] and by Majer *et al.*[22] using simpler model Hamiltonians for two coupled flux qubits. However, because a different setup is used for coupling two qubits, the four energy levels are flipped in Ref. 22. As in Ref. 21, since $\chi > 0$, the interbit coupling is *ferromagnetic*, in sharp contrast with the antiferromagnetic coupling obtained in Ref. 22, where the corresponding coupling parameter χ is negative. When the interbit coupling increases further, the flat region for both levels ϵ_3 and ϵ_4 widens for two qubits having identical parameters [see Fig. 5(c)], but ϵ_3 and ϵ_4 become much different in this region when the two qubits are not identical [see Fig. 5(d)]. Moreover, it can be seen that the gap between levels ϵ_1 and ϵ_2 and that bewteen ϵ_3 and ϵ_4 become narrow at $f = 0.5$ with the interbit coupling increasing.

In the case of Fig. 5(a), because $2\pi I_{0i} L_c/\Phi_0 = 0.03$, the common inductance is $L_c \approx 20$ pH if the critical currents I_{0i} are equal to the experimental value[5] $I_0 \sim 0.5$ μA. Such a small inductance is experimentally realizable, e.g., using a loop of diameter $d \approx 16$ μm. Also, our numerical calculations show that $b_i \approx 0.66 I_0$ at $f = 0.5$. The interbit coupling is thus of the order $\chi = L_c b_1 b_2 \approx 0.013 E_J$, which is equal to the energy difference Δ at $f = 0.5$ of the single flux qubit with $\beta_L = 0.03$. Therefore, *the corresponding two-bit operation is as fast as the one-bit operation.* Moreover, at $f = 0.5$, the first four energy levels, ϵ_k, $k = 1$ to 4, of the coupled flux qubits can be approximated by

$$\begin{aligned} \epsilon_1 &= -\frac{1}{2} E_A, \quad \epsilon_3 = \frac{1}{2} E_B, \\ \epsilon_2 &= -\frac{1}{2} E_B, \quad \epsilon_4 = \frac{1}{2} E_A, \end{aligned} \tag{31}$$

where

$$\begin{aligned} E_A &= [(\Delta_1 + \Delta_2)^2 + 4\chi^2]^{1/2}, \\ E_B &= [(\Delta_1 - \Delta_2)^2 + 4\chi^2]^{1/2}. \end{aligned} \tag{32}$$

The gap between levels ϵ_2 and ϵ_3 is E_B, which increases with χ. The gap between levels ϵ_1 and ϵ_2 and that between ϵ_3 and ϵ_4 are given by $E_A - E_B$. Figures 5(a) and 5(b) correspond to $\chi \approx \Delta_1$; in Fig. 5(a) where $\Delta_1 = \Delta_2 = \Delta$, the two equal gaps, $E_A - E_B$, at $f = 0.5$

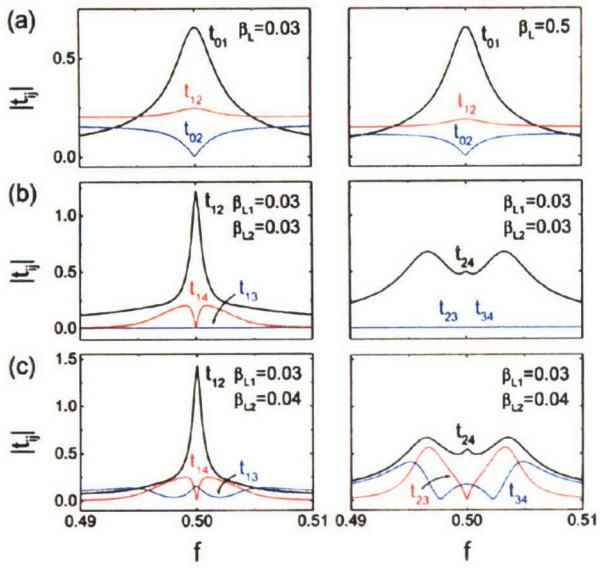

FIG. 6: (a) Moduli of the transition matrix elements t_{ij} between single-qubit states $|i\rangle$ and $|j\rangle$ versus reduced flux f. (b) and (c) Moduli of the transition matrix elements between coupled-qubit states $|\epsilon_i\rangle$ and $|\epsilon_j\rangle$ versus f for $L_{b1}/L_c = 0.1$ and $(L_{12}+L_{b2})/L_c = 0.2$. Here $|t_{ij}|$ is in units of $I_0\Phi_X$ in (a) and $I_{01}\Phi_X$ in (b) and (c).

are $(\sqrt{2}-1)\Delta$. When χ further increases, the value of $E_A - E_B$ decreases; namely, the two equal gaps become narrow [cf. Figs. 5(c) and 5(d)].

IV. STATE TRANSITIONS

When a microwave field with an appropriate frequency ω is applied through the superconducting loop of the single flux qubit, a transition between two states occurs. Now, the total flux within the loop is $\Phi_e + \Phi_f$, where

$$\Phi_f = \Phi_X \cos(\omega t + \theta) \tag{33}$$

is the microwave-field-induced flux through the loop. For a weak microwave field, the single flux qubit experiences a time-dependent perturbation

$$H'(t) = -I\Phi_X \cos(\omega t + \theta), \tag{34}$$

and the transition matrix element t_{ij} between states $|i\rangle$ and $|j\rangle$ is given by $\langle i|I\Phi_X|j\rangle$. Similarly, when the microwave field is applied through the left loop $A_1L_cB_1A_1$ of the coupled flux qubits, the transition matrix element t_{ij} between the coupled-qubit states $|\epsilon_i\rangle$ and $|\epsilon_j\rangle$ is then $\langle\epsilon_i|I\Phi_X|\epsilon_j\rangle$.

Figure 6(a) presents the flux dependence of $|t_{ij}|$ for transitions $|0\rangle \to |1\rangle$, $|0\rangle \to |2\rangle$, and $|1\rangle \to |2\rangle$ in a single flux qubit. Because of the symmetry of the wave functions, $|t_{02}| = 0$ at $f = 0.5$, and thus the transition $|0\rangle \to |2\rangle$ is forbidden. Also, it can be seen that $|t_{01}|$ is not sensitive to the variation of β_L, while $|t_{02}|$ and $|t_{12}|$ are suppressed by increasing β_L. This observation is consistent with the energy spectrum in Fig. 3, where the gap between the lowest two levels 0 and 1 is not significantly changed, but the gap between levels 1 and 2 increases with β_L. In Figs. 6(b) and 6(c), we show the flux dependence of $|t_{ij}|$ for all possible transitions in the coupled flux qubits. When the two flux qubits have the same parameters, the transitions $|\epsilon_1\rangle \to |\epsilon_3\rangle$, $|\epsilon_2\rangle \to |\epsilon_3\rangle$, and $|\epsilon_3\rangle \to |\epsilon_4\rangle$ are *forbidden* because $|t_{ij}| = 0$ [see Fig. 6(b)]. However, they are *allowed* (except for some specific values of f) when the parameters of the two flux qubits are different [see Fig. 6(c)]. At $f = 0.5$ in particular, $|t_{12}|$ has the largest value, while $|t_{24}|$ has a smaller value and others are either zero or much smaller.

For a single flux qubit with $\beta_L = 0.03$, the energy difference Δ between states $|1\rangle$ and $|0\rangle$ is $0.01291E_J$ at $f = 0.5$. Using an experimental value[5] for the critical current $I_0 \sim 0.5$ μA, we obtain $E_J \sim 1.03$ meV. The energy difference of $0.01291E_J$ corresponds to a gap of $\nu \approx 3.2$ GHz. The one-bit operation can be implemented using a resonant microwave field. For a weak driving field, the Rabi frequency Ω_{01} is given by $|t_{01}|/\hbar$. The typical switching time is π/Ω_{01} when the states $|0\rangle$ and $|1\rangle$ *flip*. For instance, because $|t_{01}| \approx 0.66I_0\Phi_X$ at $f = 0.5$, the switching time is about 3 ns for $I_0\Phi_X \sim 1$ μeV. If the leakage from these two states to others is small, one can realize a fast one-bit operation, e.g., with a switching time $\pi/\Omega_{01} \sim 10\nu^{-1}$ (≈ 3 ns), by increasing the microwave-field intensity. Let the energy difference between states $|0\rangle$ ($|1\rangle$) and $|1\rangle$ ($|2\rangle$) be $\hbar\omega_{01}$ ($\hbar\omega_{12}$). When the field is tuned to be *resonant* with the transition $|0\rangle \to |1\rangle$, the ratio of the transition probabilities between $|1\rangle \to |2\rangle$ and $|0\rangle \to |1\rangle$ can be estimated as

$$\frac{\rho_{12}}{\rho_{01}} = \left(\frac{\Omega_{12}}{\Omega}\right)^2 \frac{\sin^2(\Omega\tau/2)}{\sin^2(\Omega_{01}\tau/2)}, \tag{35}$$

where

$$\Omega = [\Omega_{12}^2 + (\omega_{12} - \omega_{01})^2]^{1/2}, \tag{36}$$

$\Omega_{12} = |t_{12}|/\hbar$, and τ is the duration of the microwave-field pulse. When $\tau = \pi/\Omega_{01} \sim 10\nu^{-1}$, using the numerical results $\hbar\omega_{01} = 0.01291E_J$, $\hbar\omega_{12} = 0.18763E_J$, and $|t_{12}/t_{01}| \approx 0.38$ at $f = 0.5$, we have

$$\frac{\rho_{12}}{\rho_{01}} \approx 1.5 \times 10^{-6}. \tag{37}$$

This implies that the leakage to other states is small for a fast one-bit operation implemented via a microwave field.

Corresponding to Fig. 5(a), $|\epsilon_1\rangle$ and $|\epsilon_2\rangle$ at $f = 0.5$ are approximated by

$$|\epsilon_1\rangle = \frac{1}{\sqrt{\eta^2+1}}(\eta|00\rangle + |11\rangle),$$
$$|\epsilon_2\rangle = \frac{1}{\sqrt{2}}(|01\rangle + |10\rangle), \tag{38}$$

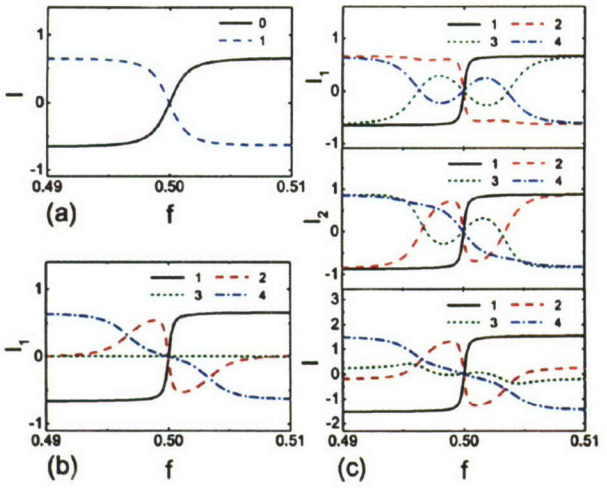

FIG. 7: (a) Supercurrents I versus reduced flux f at eigenstates $|0\rangle$ and $|1\rangle$ of a single flux qubit for $\beta_L = 0.03$. (b) Supercurrents I_1 versus f at eigenstates $|\epsilon_k\rangle$, $k = 1$ to 4, of two coupled flux qubits for $\beta_{L1} = \beta_{L2} = 0.03$. (c) Supercurrents I_1, I_2, and I versus f at eigenstates $|\epsilon_k\rangle$, $k = 1$ to 4, of two coupled flux qubits for $\beta_{L1} = 0.03$ and $\beta_{L2} = 0.04$. Here we choose $L_{b1}/L_c = 0.1$ and $(L_{12}+L_{b2})/L_c = 0.2$ for the coupled flux qubits. The supercurrents are in units of I_0 in (a) and I_{01} in (b) and (c).

with

$$\eta = \frac{\Delta + (\Delta^2 + \chi^2)^{1/2}}{\chi}. \tag{39}$$

Initially preparing the system at the (entangled) ground state $|\epsilon_1\rangle$, one can produce the *maximally entangled* state $|\epsilon_2\rangle$ using a microwave-field pulse of duration $\tau = \pi/\Omega_{12}$, where the Rabi frequency Ω_{12} is given by $|t_{12}|/\hbar$ for a weak driving field. At $f = 0.5$, we have $\hbar\omega_{12} = 0.00528E_J$, $\hbar\omega_{24} = 0.03124E_J$, and $|t_{24}/t_{12}| \approx 0.41$. When the microwave field is in resonance with the transition $|\epsilon_1\rangle \to |\epsilon_2\rangle$ at $f = 0.5$,

$$\frac{\rho_{24}}{\rho_{12}} \approx 4.4 \times 10^{-6} \tag{40}$$

for $\tau = \pi/\Omega_{12} \sim 20\pi/\omega_{12}$. This implies that a fast two-bit operation can also be implemented using a microwave field.

V. SUPERCURRENTS AND QUANTUM MEASUREMENT

The circulating supercurrents flowing through the inductance L or L_c are different for different eigenstates. This property can be used for implementing a readout of the qubit states. For a single flux qubit, around $f = 0.5$, the supercurrents I at eigenstates $|0\rangle$ and $|1\rangle$ (i.e., $\langle 0|I|0\rangle$ and $\langle 1|I|1\rangle$) have equal magnitudes but opposite directions [see Fig. 7(a)]. During quantum measurement, one can switch on the flux transformer to couple the inductance L with a dc-SQUID magnetometer [cf. Fig. 1(a)] to distinguish the two eigenstates of the qubit because at these two states the supercurrents I through L generate two different fluxes in the SQUID loop of the magnetometer. In general, if the single flux qubit is at the superposition state $c_1|1\rangle + c_0|0\rangle$, the measurement will show that the qubit has probability $|c_i|^2$ at the eigenstate $|i\rangle$, where $i = 0, 1$. For the two coupled flux qubits, the supercurrents through the common inductance L_c take different values at its four eigenstates.

Similar to the single flux qubit, a switchable flux transformer can be used to couple L_c and the SQUID loop of the magnetometer for reading out the coupled-qubit states because the supercurrents I at different eigenstates contribute different fluxes in the SQUID loop of the magnetometer. The supercurrents I_1 at the four eigenstates of the coupled qubits are shown in Fig. 7(b) for two flux qubits having identical parameters. Since $I_1 = I_2$ in this case, the total supercurrent I is $2I_1$. When the parameters of the two flux qubits become *different*, the total supercurrents I look *similar* to those in Fig. 7(b), but I_1 and I_2 (which flow through the Josephson junctions of the qubits) change *drastically* [cf. Fig. 7(c)]. Also, it can be seen that at the eigenstates of the system the circulating supercurrents in both single and coupled flux qubits fall to zero at $f = 0.5$. To read out the qubit states, one can shift the system away from this point.

VI. DISCUSSION AND CONCLUSION

For the charge qubits coupled by LC-oscillator modes[13] or by an inductance,[14] the inductances proposed to be used are ~ 3.6 μH or ~ 30 nH, respectively, for a two-bit operation ten times slower than the typical one-bit operation. An inductance for coupling charge qubits similar to that in Ref. 13, particularly, has a value much larger than L_c (≈ 20 pH) for coupling flux qubits. It is difficult to fabricate in a small size without introducing a strong coupling with the environment. Because two-bit operations are much slower than one-bit ones in the inductively coupled *charge* qubits, an efficient scheme is thus required to minimize the number of two-bit (as opposed to one-bit) operations to obtain a conditional gate.[14] However, for inductively coupled *flux* qubits, the above limitation in using two-bit operations for constructing a conditional gate is removed since two-bit operations can be as fast as one-bit ones. In this case, *any* schemes for constructing conditional gates become *efficient* by minimizing the number of operations that are used (either one- or two-bit). Note that the common inductance of $L_c \approx 20$ pH can produce a strong interbit coupling. As a result, two-bit operations as fast as one-bit ones can be achieved. This common inductance is comparable to the loop inductance, $L \sim 10$ pH, of the single flux qubit currently realized in experiments.

To couple several flux qubits, the inductances of all

loops involved could be small, comparable to the loop inductance of a single flux qubit currently realized in experiments. This is the case we studied in the present paper, where two coupled flux qubits are considered. If a number of flux qubits are coupled, the inductances of some loops will become larger, but the common or shared inductance for producing the interbit coupling can still be chosen small (about 20 pH). If the circuits except for the line $A_1L_cB_1$ (corresponding to the common or shared inductance) could be screened from the environment (that is a big challenge for experimentalists for sure), the main noise would be due to the small common or shared inductance.

In conclusion, we have proposed an experimentally realizable method for inductively coupled flux qubits that can achieve two-bit operations performing as fast as one-bit ones. We treat both single and coupled flux qubits with more realistic models including the loop inductance. Moreover, we show that the coupled flux qubits have novel flux-dependent behaviors in the transitions between states. We find that the forbidden transitions in the coupled two flux qubits become allowed (except for some specific values of the external flux) when the parameters of the two qubits change from being initially equal to each other and then making these different.

Acknowledgments

We thank J.S. Tsai, T. Yamamoto, Yu. Pashkin, O. Astafiev, Y.X. Liu, L.F. Wei, T. Tilma, F. Wilhelm, Q. Niu, and S.C. Bernstein for discussions and comments. This work was supported in part by the National Security Agency (NSA) and Advanced Research and Development Activity (ARDA) under Air Force Office of Research (AFOSR) contract number F49620-02-1-0334, and by the National Science Foundation grant No. EIA-0130383. J.Q.Y. was also supported by the National Natural Science Foundation of China grant No. 10174075 and the Special Funds for Major State Basic Research of China grant No. G2001CB3095.

---

* Email: jqyou@fudan.edu.cn
† Email: yasunobu@frl.cl.nec.co.jp
‡ Email: nori@umich.edu

[1] Y. Nakamura, Yu. A. Pashkin, and J.S. Tsai, Nature (London) **398**, 786 (1999).
[2] D. Vion, A. Aassime, A. Cottet, P. Joyez, H. Pothier, C. Urbina, D. Esteve, and M.H. Devoret, Science **296**, 886 (2002).
[3] J.R. Friedman, V. Patel, W. Chen, S.K. Tolpygo, and J.E. Lukens, Nature (London) **406**, 43 (2000).
[4] J.E. Mooij, T.P. Orlando, L. Levitov, L. Tian, C.H. van der Wal, and S. Lloyd, Science **285**, 1036 (1999); C.H. van der Wal, A.C.J. ter Haar, F.K. Wilhelm, R.N. Schouten, C.J.P.M. Harmans, T.P. Orlando, S. Lloyd, and J.E. Mooij, *ibid.* **290**, 773 (2000).
[5] I. Chiorescu, Y. Nakamura, C.J.P.M. Harmans, and J.E. Mooij, Science **299**, 1869 (2003).
[6] Y. Yu, S.Y. Han, X. Chu, S.I. Chu, and Z. Wang, Science **296**, 889 (2002); J.M. Martinis, S. Nam, J. Aumentado, and C. Urbina, Phys. Rev. Lett. **89**, 117901 (2002).
[7] Yu. A. Pashkin, T. Yamamoto, O. Astafiev, Y. Nakamura, D.V. Averin, and J.S. Tsai, Nature (London) **421**, 823 (2003); T. Yamamoto, Yu. A. Pashkin, O. Astafiev, Y. Nakamura, and J.S. Tsai, *ibid.* **425**, 941 (2003).
[8] A.J. Berkley, H. Xu, R.C. Ramos, M.A. Gubrud, F.W. Strauch, P.R. Johnson, J.R. Anderson, A.J. Dragt, C.J. Lobb, and F.C. Wellstood, Science **300**, 1548 (2003).
[9] D.V. Averin and C. Bruder, Phys. Rev. Lett. **91**, 057003 (2003).
[10] A. Blais, A. Maassen van den Brink, and A.M. Zagoskin, Phys. Rev. Lett. **90**, 127901 (2003).
[11] J. Siewert and R. Fazio, Phys. Rev. Lett. **87**, 257905 (2001).
[12] W.M. Kaminsky and S. Lloyd, quant-ph/0211152.
[13] Yu. Makhlin, G. Schön, and A. Shnirman, Nature (London) **398**, 305 (1999).
[14] J.Q. You, J.S. Tsai, and F. Nori, Phys. Rev. Lett. **89**, 197902 (2002). A longer version of it is available in cond-mat/0306203; see also *New Directions in Mesoscopic Physics*, edited by R. Fazio, V.F. Gantmakher, and Y. Imry (Kluwer Academic Publishers, 2003), 351.
[15] J.Q. You, J.S. Tsai, and F. Nori, Phys. Rev. B 68, 024510 (2003).
[16] J. Lantz, M. Wallquist, V.S. Shumeiko, and G. Wendin, cond-mat/0403285.
[17] Y.D. Wang, P. Zhang, D.L. Zhou, and C.P. Sun, cond-mat/0307043.
[18] C.H. van der Wal, F.K. Wilhelm, C.J.P.M. Harmans, and J.E. Mooij, Eur. Phys. J. B **31**, 111 (2003); L. Tian, S. Lloyd, and T.P. Orlando, Phys. Rev. B **65**, 144516 (2002).
[19] T.P. Orlando, J.E. Mooij, L. Tian, C.H. van der Wal, L.S. Levitov, S. Lloyd, and J.J. Mazo, Phys. Rev. B **60**, 15398 (1999).
[20] M.J. Storcz and F.K. Wilhelm, Appl. Phys. Lett. **83**, 2387 (2003).
[21] M.J. Storcz and F.K. Wilhelm, Phys. Rev. A **67**, 042319 (2003).
[22] J.B. Majer, F.G. Paauw, A.C.J. ter Haar, C.J.P.M. Harmans, and J.E. Mooij, cond-mat/0308192; J.B. Majer, *Superconducting Quantum Circuits* (PhD Thesis, TU Delft, 2002), Chap. 5.
[23] A. Izmalkov, M. Grajcar, E. Il'ichev, Th. Wagner, H.-G. Meyer, A.Yu. Smirnov, M.H.S. Amin, A. Maassen van den Brink, A.M. Zagoskin, cond-mat/0312332.
[24] D.S. Crankshaw and T.P. Orlando, IEEE Trans. Appl. Supercond. **11**, 1006 (2001)

Correlation-induced suppression of decoherence in macroscopic quantum states

J. Q. You,[1,2,*] Xuedong Hu,[1,3,†] and Franco Nori[1,4,‡]

[1] *Frontier Research System, The Institute of Physical and Chemical Research (RIKEN), Wako-shi 351-0198, Japan*
[2] *Department of Physics and National Laboratory for Surface Physics, Fudan University, Shanghai 200433, China*
[3] *Department of Physics, University at Buffalo, SUNY, Buffalo, NY 14260-1500, USA*
[4] *Center for Theoretical Physics, Physics Department, Center for the Study of Complex Systems, The University of Michigan, Ann Arbor, MI 48109-1120, USA*

(Dated: August 2, 2004)

Charge fluctuations from gate bias and background traps severely limit the performance of a charge qubit realized in a Cooper-pair box (CPB). Here we present an experimentally realizable method to control the dephasing effects of these charge fluctuations using two strongly capacitively coupled CPBs. This coupled-box system has a low-decoherence subspace of two states and we calculate the dephasing of these states using a master equation approach. Our results show that the inter-box Coulomb correlation can significantly suppress decoherence of this two-level system, making it a promising candidate as a logical qubit, encoded using two CPBs.

PACS numbers: 03.67.Pp, 74.50.+r

Advances in nanotechnology have led to the successful fabrication of ever smaller solid-state devices, whose behaviors are increasingly quantum mechanical. In particular, various superconducting nanocircuits have been proposed as quantum bits (qubits) for a quantum computer [1, 2, 3, 4]. In the meantime, it has long been recognized that background charge fluctuations can severely limit the performance of microelectronic devices, particularly those based on the manipulation of electrical charge, such as single electron transistors [5] and superconducting Cooper-pair boxes (CPBs) [6, 7, 8]. The struggle to suppress or even eliminate noise from charge fluctuations in superconducting devices has been a prolonged battle with limited success. Here, instead of focusing on perfecting materials, we propose an alternative experimentally-realizable method to suppress the effects of these charge fluctuations using two strongly (capacitively) coupled CPBs. We demonstrate how the inter-box Coulomb correlation can help generate a two-state subspace with reduced decoherence for the coupled CPBs, and then outline a scheme to manipulate and characterize the encoded qubits.

Cooper-pair boxes are one of the prominent candidates for qubits in a quantum computer. Recent experiments [9] have revealed quantum coherent oscillations in two CPBs coupled capacitively and demonstrated the feasibility of a conditional gate as well as creating macroscopic entangled states. An efficient scalable quantum-computing scheme [10] has also been proposed based on charge qubits. It has been shown [8] that while operating at the degeneracy point (where the two lowest charge states have the same energy in the absence of Josephson coupling), the charge-qubit states are quite coherent with a decoherence time of $\tau \approx 500$ ns. When the charge-qubit system is operated away from the degeneracy point, it experiences strong dephasing by the charge fluctuations, and the decoherence time of the system is greatly reduced [6, 8]. Clearly, effective suppression of the charge noise is of essential importance for the practical implementation of scalable quantum computing.

Two different CPBs generally experience uncorrelated charge fluctuations as they are most strongly affected by their own gate bias and the nearest fluctuating charge traps. However, if two boxes are strongly coupled capacitively, the fluctuations affecting one box will affect the other through the Coulomb coupling. In the limit of extremely strong inter-box coupling (corresponding to an infinite mutual capacitance between two CPBs), the two boxes would experience an identical charge environment, so that, in principle, a decoherence-free subspace [11] could be established for coupled-box states. However, in reality this limit involves more than just the two lowest energy states, making the coupled boxes unsuitable as two-level systems. Thus, can we still achieve decoherence-suppressed logical qubit encoding in capacitively coupled boxes? Below we show that there indeed exists an intermediate parameter regime where a strong inter-box Coulomb correlation can induce a significant suppression of decoherence in certain two-box states, so that considerable benefit can be reaped by encoding a logical qubit in terms of these states.

Characterization of two coupled CPBs. — The proposed circuit consists of two capacitively coupled CPBs (see Fig. 1). Each CPB is individually biased by an applied gate voltage V_i and coupled to the leads by a symmetric dc-SQUID. The dc-SQUID is pierced by a magnetic flux Φ_i, which provides a tunable effective coupling $E_{Ji}(\Phi_i) = 2E_{Ji}^0 \cos(\pi\Phi_i/\Phi_0)$, where $\Phi_0 = h/2e$ is the flux quantum. The Hamiltonian of the system is

$$H_S = \sum_i [E_{ci}(n_i - n_{xi})^2 - E_{Ji}(\Phi_i)\cos\varphi_i] + E_m(n_L - n_{xL})(n_R - n_{xR}), \quad (1)$$

with $i = L, R$ for left and right. Here the charging energy

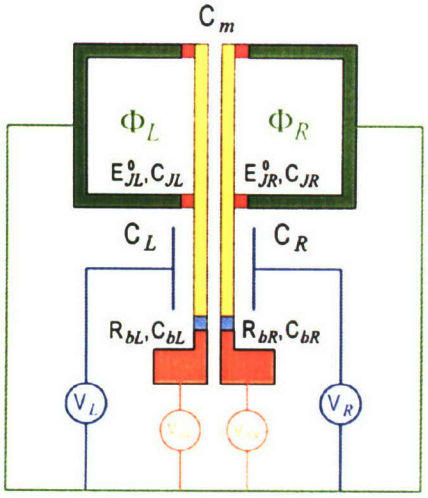

FIG. 1: Strongly coupled Cooper-pair boxes. A bias voltage V_i is applied to the ith charge box through a gate capacitance C_i, and a symmetric dc-SQUID (with Josephson coupling energy E_{Ji}^0 and capacitance C_{Ji} for each junction) is coupled to the box. Also, each box is connected to a detector via a probe junction (or a less invasive point contact). When a measurement is performed, the probe junction is biased with an appropriate voltage V_{bi}. The two boxes are closely-spaced long superconducting islands with sufficiently large mutual capacitance C_m, and the barrier between them is strong enough to prohibit the inter-box Cooper-pair tunneling.

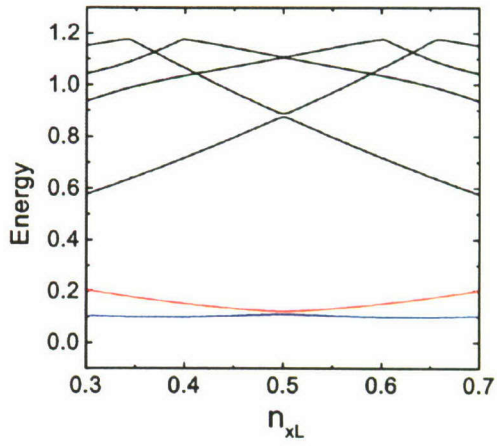

FIG. 2: Dependence of the energy levels of the coupled-box system on the reduced offset charge n_{xL} for $n_{xR} = 0.5$. Here we choose $\Delta E_i = E_{ci}/4$, and $E_{Ji} = E_{ci}/10$, with $i = L, R$. The two lowest levels remain nearly unchanged in a wide region around the degeneracy point $(n_{xL}, n_{xR}) = (\frac{1}{2}, \frac{1}{2})$.

E_{ci} of the ith superconducting island and the mutual capacitive coupling E_m are given by [12] $E_{ci} = 2e^2 C_{\Sigma j}/\Lambda$, and $E_m = 4e^2 C_m/\Lambda$, with $\Lambda = C_{\Sigma i} C_{\Sigma j} - C_m^2$, where $C_{\Sigma i} = C_m + C_i + C_{Ji}$ is the total capacitance of the ith island. The offset charge is $2en_{xi} = Q_{Vi} + Q_{0i}$, where Q_{0i} is the background charge, and $Q_{Vi} = C_i V_i + C_{bi} V_{bi}$ is induced by both the gate voltage V_i and the probe voltage V_{bi}. The average phase drop φ_i across the two Josephson junctions in the dc-SQUID is conjugate to the number of the Cooper pairs n_i on the box. Both CPBs operate in the charging regime $E_{ci} \gg E_{Ji}$ and at low temperatures $k_B T \ll E_{ci}$. The states of the two coupled boxes can thus be expanded on the basis of the charge eigenstates $|n_L n_R\rangle \equiv |n_L\rangle |n_R\rangle$.

When the two CPBs are strongly coupled, the total Hamiltonian can be rewritten in terms of the total charge on the coupled boxes and the charge difference across the boxes (assuming for simplicity $C_{\Sigma L} = C_{\Sigma R} = C_\Sigma$ so that $E_{cL} = E_{cR} = E_c$):

$$H_S = \left(E_c - \frac{\Delta E}{2}\right)(n_L + n_R - n_{xL} - n_{xR})^2 + \frac{\Delta E}{2}(n_L - n_R - n_{xL} + n_{xR})^2 , \quad (2)$$

where $\Delta E = 2e^2/(C_m + C_\Sigma)$. Notice that E_c is essentially determined by junction and gate capacitances, representing the charging energy of individual Josephson junctions, while ΔE represents the charging energy of the large capacitor C_m. Around the double degeneracy point of $(n_{xL}, n_{xR}) = (\frac{1}{2}, \frac{1}{2})$, the two lowest energy states, $|\pm\rangle$, of this coupled-box system have a splitting of $E_J^2/2(E_c - \Delta E)$.

At the degeneracy point $(n_{xL}, n_{xR}) = (\frac{1}{2}, \frac{1}{2})$, the lowest two states are $|\pm\rangle = (|01\rangle \pm |10\rangle)/\sqrt{2}$, which are degenerate because the states $|01\rangle$ and $|10\rangle$ have the same energies. When the tunable Josephson couplings are switched on, the degeneracy is removed and the states $|\pm\rangle$ are given by $|\pm\rangle = (|01\rangle \pm |10\rangle)/\sqrt{2} + |\delta\psi_\pm\rangle$, where $|\delta\psi_\pm\rangle = O(E_J(\Phi_i)/E_m)[\alpha_\pm(|00\rangle \pm |11\rangle) + \cdots]$. These two states, and the corresponding energy levels (see Fig. 2), remain nearly unchanged in a wide region around the degeneracy point. At the degeneracy point, the Josephson coupling cannot lead to a direct transition between these two states since one is symmetric while the other antisymmetric, so that the relaxation of the excited state $|-\rangle$ to $|+\rangle$ is prohibited. As long as the system does not stray too far from the degeneracy point, we expect that the relaxation should still be much slower than pure dephasing. Furthermore, the symmetry in these states implies that they are also well insulated from pure dephasing due to charge noise, as we will show below. It is thus quite natural to adopt these two coupled-box states $|\pm\rangle$ to achieve a logical qubit. Below we calculate the dephasing properties of the $|\pm\rangle$ states and discuss how they can be coherently manipulated.

Correlation-induced coherence-preserving subspace. — To clarify the origin of the correlated environments for the two coupled CPBs, we study the fluctuations [13] of

the reduced offset charge from n_{xi}, which could originate from the gate voltage V_i, probe voltage V_{bi}, and background charge Q_{0i}. Below we examine how the Coulomb correlation can help suppress the effects of this noise in the two-island subspace of $|\pm\rangle$ states.

We can use a simple two-level system language to describe each of the boxes around the degeneracy point $(n_{xL}, n_{xR}) = (\frac{1}{2}, \frac{1}{2})$, and rewrite the Hamiltonian in terms of the Pauli matrices:

$$H_S = \sum_i H_i + \frac{1}{4} E_m \sigma_{zL} \sigma_{zR}, \tag{3}$$

$$H_i = [\varepsilon_i(n_{xi}) + \varepsilon_m(n_{xj})]\sigma_{zi} - \frac{1}{2} E_{Ji}(\Phi_i)\sigma_{xi},$$

where $\varepsilon_i(n_{xi}) = E_{ci}(n_{xi} - \frac{1}{2})$, $\varepsilon_m(n_{xj}) = \frac{1}{2}E_m(n_{xj} - \frac{1}{2})$, $|\uparrow\rangle_i \equiv |0\rangle_i$, $|\downarrow\rangle_i \equiv |1\rangle_i$, and $i, j = L, R$ $(i \neq j)$. The higher energy states do not affect the coherence properties of $|\pm\rangle$ at the level of approximation of our calculation.

The interaction Hamiltonian between the CPB system and the environment is

$$H_I = \sum_i (E_{ci}\delta n_{xi} + \frac{1}{2} E_m \delta n_{xj})\sigma_{zi}, \tag{4}$$

with $i, j = L, R$, and $i \neq j$. Though each CPB is directly coupled to a different environment by itself, the inter-island Coulomb interaction ensures that the environment is partly shared between the two islands, causing the CPBs to experience two correlated noises. When each of the two environments is modeled by a thermal bath of simple harmonic oscillators described by the annihilation (creation) operator b_{ji} $(b_{ji}^\dagger)$, the Hamiltonian of the whole system, including the two baths, is

$$\begin{aligned} H &= H_S + H_B + H_I, \\ H_B &= \sum_n (\hbar\omega_{nL} b_{nL}^\dagger b_{nL} + \hbar\omega_{nR} b_{nR}^\dagger b_{nR}), \\ H_I &= \frac{1}{2}\sum_i \left(\sigma_{zi} + \frac{E_m}{2E_{ci}}\sigma_{zj}\right) X^{(i)}, \end{aligned} \tag{5}$$

with $i, j = L, R$ $(i \neq j)$. Here, the bath operator $X^{(i)} = 2E_{ci}\delta n_{xi}$ is given by $X^{(i)} = \sum_n \lambda_{ni} x_n^{(i)} \equiv \sum_n \hbar K_n^{(i)}(b_{ni}^\dagger + b_{ni})$, with $K_n^{(i)} = \lambda_{ni}/\sqrt{2m_{ni}\hbar\omega_{ni}}$.

With the two CPBs experiencing correlated environments, the system has unusual dephasing properties that can be exploited to enhance the decoherence time. Here the master equation approach is used to derive the decoherence time of the system. As shown in [14], the reduced density operator, $\rho(t)$, of the system in the interaction picture is approximately governed by

$$\begin{aligned} \dot{\rho}(t) = &-\frac{i}{\hbar\tau}\int_0^\tau d\tau' \, \mathrm{Tr}_B[H_I(\tau')P(t)] \\ &-\frac{1}{\hbar^2\tau}\int_0^\tau d\tau' \int_0^{\tau'} d\tau'' \, \mathrm{Tr}_B[H_I(\tau')H_I(\tau'')P(t) \\ &-H_I(\tau')P(t)H_I(\tau'')] + \mathrm{H.c.}, \end{aligned} \tag{6}$$

where $H_I(t) = e^{i(H_S+H_B)t/\hbar} H_I e^{-i(H_S+H_B)t/\hbar}$ is the interaction Hamiltonian in the interaction picture, and $P(t) = \rho(t)\rho_B(H_B)$, with $\rho_B(H_B) = e^{-\beta H_B}/\mathrm{Tr}_B[e^{-\beta H_B}]$ being a time-independent bath density operator in thermal equilibrium at temperature T. Here we focus on the pure dephasing case with $E_{Ji}(\Phi_i) = 0$, which can be solved analytically. In the subspace with basis states $|b\rangle \equiv |01\rangle$ and $|c\rangle \equiv |10\rangle$, the states of the two coupled CPBs have novel decoherence properties. It can be derived that the reduced density matrix elements ρ_{bc} and ρ_{cb} (thus ρ_{+-} and ρ_{-+}) obey: $\rho_{bc}, \rho_{cb}, \rho_{+-}, \rho_{-+} \sim e^{-t/\tau}$, where the decoherence time τ of the coupled-box system is given by

$$\frac{1}{\tau} = \sum_{i=L,R} \left(1 - \frac{E_m}{2E_{ci}}\right)^2 J_i(\Omega)N(\Omega)|_{\Omega\to 0}, \tag{7}$$

with $J_i(\Omega) = \pi\sum_n [K_n^{(i)}]^2 \delta(\Omega - \omega_{ni})$ being the spectral density function of each bath, and $N(\Omega) = \coth(\hbar\Omega/2k_BT)$. For a symmetric case $E_{cL} = E_{cR} = E_c$, so that $\Delta E = E_c - \frac{1}{2}E_m$, we obtain

$$\frac{1}{\tau} = \left(\frac{\Delta E}{E_c}\right)^2 \sum_{i=L,R} J_i(\Omega)N(\Omega)|_{\Omega\to 0}, \tag{8}$$

In the limit of strong inter-box coupling, $\Delta E \ll E_c$, pure dephasing can then be strongly suppressed. For example, if we choose $\Delta E = E_c/4$, the prefactor takes the value $1/16$, so that the dephasing time becomes more than one order of magnitude longer than when the boxes are only weakly coupled. This is in strong contrast to the corresponding single CPB expression for pure dephasing $1/\tau = J(\Omega)N(\Omega)|_{\Omega\to 0}$, which is purely determined by the bath spectral density function J.

Preparation and measurement of the coherence-preserving states. — Now that we have obtained a decoherence-suppressed subspace for two strongly coupled CPBs, the question now becomes how to prepare and measure these states.

Coherence-preserving quantum states can be prepared as follows. First, consider an initial point on the n_{xL}–n_{xR} plane that is away from the degeneracy point $(\frac{1}{2}, \frac{1}{2})$. The lowest state of the system is $|00\rangle$ at this point. Then, shifting the point adiabatically (e.g., along the $n_{xL} = n_{xR}$ direction) to the region around the degeneracy point, we arrive at the coherence-preserving ground state $|+\rangle$. Finally, using a two-frequency microwave to interact with the system for a period of time (basically a Raman process), as in the trapped ion case [15], one can obtain any superposition of $|\pm\rangle$ states, so that an arbitrary single qubit operation is feasible. Readout of the logical-qubit states can be achieved through various approaches. For instance, one can rotate the logical qubit states to the charge eigenstates $|01\rangle$ and $|10\rangle$. Then simple charge detection using either single electron transistors or other charge probes can determine the state of the

coupled CPBs. Let us consider the specific case of employing probe junctions [9]. When appropriate bias voltages V_{bi} are applied to the probe junctions, the measured current I_i through the ith probe junction is proportional to the probability for the ith box to have a Cooper pair in it.

Discussion. — Decoherence in two coupled qubits [16, 17] and during a conditional gate [18] has attracted much attention recently. It has also been shown that a decoherence-free subspace exists for two physical qubits coupled to the same bath [17]. Very recently, Zhou *et al.* [19] proposed an encoded qubit using a pair of closely spaced CPBs sharing a common lead, and the two boxes were assumed to couple to an identical bath. In their proposed setup, fluctuations originating from the gate voltage may be identical because of the common lead. However, the often very important background charge fluctuations cannot be so since these fluctuations originate from local charge traps near each box. Indeed, as shown in Eq. (4), their proposed identical bath could only be achieved in the limiting case of $E_{ci} = \frac{1}{2}E_m$. Unfortunately, in this limiting case, the two-level-system description for each individual CPB breaks down for the paired boxes, thus the proposed single-bath scenario can never be achieved. As shown in our study of the coupled CPBs [20], though the ideal single-bath case cannot be realized to obtain a decoherence-free subspace, we can employ the strong inter-box coupling to achieve a coherence-preserving logical qubit where the correlated baths suppress the decoherence in the coupled CPBs.

In conclusion, we have shown that in two strongly capacitively coupled CPBs, the charge fluctuations experienced by the two boxes are strongly correlated. This inter-box Coulomb correlation can create a two-box subspace of two states in which pure dephasing is strongly suppressed due to the correlation, while relaxation is also suppressed because first order transitions are prohibited. Therefore, we have demonstrated that these two coupled CPBs can be used to encode a logical qubit that possesses superior coherence properties. We also discussed how such logical qubits can be manipulated and measured.

We thank J.S. Tsai, H. Fu, and T. Tilma for discussions. This work was supported in part by the NSA and ARDA under AFOSR contract No. F49620-02-1-0334, and by the NSF grant No. EIA-0130383. J.Q.Y. was also supported by the National Natural Science Foundation of China grant No. 10174075 and the Special Funds for Major State Basic Research of China grant No. G2001CB3095.

---

* Email address: jqyou@fudan.edu.cn
† Email address: xhu@buffalo.edu
‡ Email address: nori@umich.edu

[1] Yu. Makhlin, G. Schön, and A. Shnirman, Rev. Mod. Phys. **73**, 357 (2001).
[2] J.E. Mooij *et al.*, Science **285**, 1036 (1999).
[3] J.R. Friedman *et al.*, Nature **406**, 43 (2000).
[4] Y. Yu *et al.*, Science **296**, 889 (2002); J.M. Martinis *et al.*, Phys. Rev. Lett. **89**, 117901 (2002); A.J. Berkley *et al.*, Science **300**, 1548 (2003).
[5] A.B. Zorin *et al.*, Phys. Rev. B **53**, 13682 (1996).
[6] Y. Nakamura *et al.*, Phys. Rev. Lett. **88**, 047901 (2002).
[7] E. Paladino *et al.*, Phys. Rev. Lett. **88**, 228304 (2002).
[8] D. Vion *et al.*, Science **296**, 886 (2002).
[9] Yu.A. Pashkin *et al.*, Nature **421**, 823 (2003); T. Yamamoto *et al.*, Nature **425**, 941 (2003).
[10] J.Q. You, J.S. Tsai, and F. Nori, Phys. Rev. Lett. **89**, 197902 (2002); cond-mat/0306203.
[11] P. Zanardi and M. Rasetti, Phys. Rev. Lett. **79**, 3306 (1997); D.A. Lidar, I.L. Chuang, and K.B. Whaley, *ibid.* **81**, 2594 (1998); L.-M. Duan and G.-C. Guo, Phys. Rev. A **57**, 737 (1998).
[12] F. Marquardt and C. Bruder, Phys. Rev. B **63**, 054514 (2001).
[13] In addition to the fluctuations from gate and probe voltages as well as the background charge fluctuations, the fluxes through the dc-SQUID loops and the applied microwaves for quantum operations will also produce decoherence. However, the flux noise is much weaker than the dominant background charge fluctuations in producing decoherence. Indeed, it is even weaker than the gate voltage noise in the charging regime. The microwaves used for gate operations can be applied to the logical qubit via the gate capacitances, thus their noise only produce gate voltage fluctuations, which can also be suppressed using the encoded logical qubit presented here.
[14] P. Meystre and M. Sargent III, *Elements of Quantum Optics*, third edition, Ch. 15 (Springer, Berlin, 1999).
[15] J.I. Cirac and P. Zoller, Phys. Rev. Lett. **74**, 4091 (1995).
[16] M. Governale, M. Grifoni, and G. Schön, Chem. Phys. **268**, 273 (2001).
[17] M.J. Storcz and F.K. Wilhelm, Phys. Rev. A **67**, 042319 (2003).
[18] M. Thorwart and P. Hänggi, Phys. Rev. A **65**, 012309 (2001).
[19] X. Zhou *et al.*, Phys. Rev. A **69**, 030301(R) (2004).
[20] J.Q. You, X. Hu, and F. Nori, DML-FRS preprint 2002.

Scalable Quantum Computing with Josephson Charge Qubits

J. Q. You,[1] J. S. Tsai,[1,2] and Franco Nori[1,3,*]

[1]*Frontier Research System, The Institute of Physical and Chemical Research (RIKEN), Wako-shi 351-0198, Japan*
[2]*NEC Fundamental Research Laboratories, Tsukuba, Ibaraki 305-8051, Japan*
[3]*Center for Theoretical Physics, Physics Department, Center for the Study of Complex Systems, The University of Michigan, Ann Arbor, Michigan 48109-1120*

(Received 11 March 2002; published 21 October 2002)

A goal of quantum information technology is to control the quantum state of a system, including its preparation, manipulation, and measurement. However, scalability to many qubits and controlled connectivity between any selected qubits are two of the major stumbling blocks to achieve quantum computing (QC). Here we propose an experimental method, using Josephson charge qubits, to efficiently solve these two central problems. The proposed QC architecture is *scalable* since any two charge qubits can be effectively coupled by an experimentally accessible inductance. More importantly, we formulate an *efficient* and *realizable* QC scheme that requires *only one* (instead of two or more) two-bit operation to implement conditional gates.

DOI: 10.1103/PhysRevLett.89.197902 PACS numbers: 03.67.Lx, 74.50.+r, 85.25.Cp

The macroscopic quantum effects in low-capacitance Josephson-junction circuits have recently been used to realize qubits for quantum information processing, and these qubits are expected to be scalable to large-scale circuits using modern microfabrication techniques. Josephson-qubit devices [1] are based on the charge and phase degrees of freedom. The charge qubit is achieved in a Cooper-pair box [2], where two dominant charge states are coupled through coherent Cooper-pair tunneling [3], while the phase qubit is based on two different flux states in a small superconducting-quantum-interference-device (SQUID) loop [4,5]. Experimentally, the energy-level splitting and the related properties of state superpositions were observed via Cooper-pair tunneling in the Josephson charge device [6,7] and by spectroscopic measurements for the Josephson phase device [8,9]. Moreover, coherent oscillations were demonstrated in a Josephson charge device prepared in a superposition of two charge states [2]. These striking experimental observations reveal that the Josephson charge and phase devices are suitable for solid-state qubits in quantum information processing. The next immediate challenge would include implementing a *two-bit coupling* and then *scaling up* the architecture to many qubits. Here, we focus on the Josephson charge qubit realized in a Cooper-pair box and propose a new quantum-computing (QC) scheme based on scalable charge-qubit structures.

A straightforward way of coupling Josephson charge qubits is to use the Coulomb interactions between charges on different islands of the charge qubits (e.g., to connect two Cooper-pair boxes via a capacitor). A two-bit operation [10], similar to the controlled-NOT gate, was derived using this interbit coupling, but it is hard to switch the coupling on and off [1] in this scheme as well as to make the system scalable because only neighboring qubits can be coupled. A scalable way of coupling Josephson charge qubits was proposed [1,3] in terms of the oscillator modes in an LC circuit formed by an inductance and the qubit capacitors. In this design, the interbit coupling is switchable and any two charge qubits can be coupled. However, there is no efficient (i.e., using one two-bit operation) QC scheme for this design [1,3] to achieve conditional gates such as the controlled-phase-shift and controlled-NOT gates. Moreover, the calculated interbit coupling terms [1,3] apply only to the case when two conditions are met: (i) the eigenfrequency ω_{LC} of the LC circuit is much faster than the quantum manipulation frequencies (*which limits the allowed number N of the qubits in the circuit* because ω_{LC} scales with $1/\sqrt{N}$) and (ii) the phase conjugate to the total charge on the qubit capacitors fluctuates weakly. These two limitations do not apply to our approach. In our proposal, a common inductance (but no LC circuit) is used to couple all Josephson charge qubits. In our scheme, both dc and ac supercurrents can flow through the inductance, while in [1,3] only ac supercurrents can flow through the inductance and it is the LC-oscillator mode that couples the charge qubits. These yield different interbit couplings (e.g., $\sigma_y\sigma_y$ type [1,3] as opposed to $\sigma_x\sigma_x$ in our scheme). To have a *controllable interbit coupling,* we employ two dc SQUIDs to connect each Cooper-pair box. Our proposed QC architecture is scalable in the sense that *any* two charge qubits (*not* necessarily neighbors) can be effectively coupled by an experimentally accessible inductance. More importantly, we formulate an efficient QC scheme that requires *only one* (instead of two or more) two-bit operation to implement conditional gates. To our knowledge, this is the first efficient scalable QC scheme for this type of architecture.

The proposed quantum computer consists of N Cooper-pair boxes coupled by a common superconducting inductance L (see Fig. 1). For the kth Cooper-pair box, a superconducting island with charge $Q_k = 2en_k$ is weakly coupled by two symmetric dc SQUIDs and biased by an

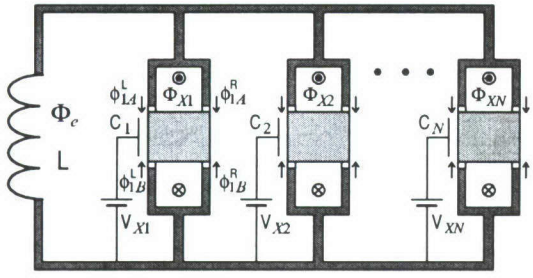

FIG. 1. Schematic diagram of the proposed scalable and switchable quantum computer. All Josephson charge-qubit structures are coupled by a common superconducting inductance. Here, each Cooper-pair box is operated both in the charging regime $E_{ck} \gg E^0_{Jk}$ and at low temperatures $k_BT \ll E_{ck}$. Moreover, the superconducting gap is larger than E_{ck}, so that quasiparticle tunneling is prohibited in the system.

applied voltage V_{Xk} through a gate capacitance C_k. The two symmetric dc SQUIDs are assumed to be identical and all Josephson junctions in them have Josephson coupling energy E^0_{Jk} and capacitance C_{Jk}. Each SQUID pierced by a magnetic flux Φ_{Xk} provides an effective coupling energy given by $-E_{Jk}(\Phi_{Xk})\cos\phi_{kA(B)}$, with $E_{Jk}(\Phi_{Xk}) = 2E^0_{Jk}\cos(\pi\Phi_{Xk}/\Phi_0)$, and $\Phi_0 = h/2e$ is the flux quantum. The effective phase drop $\phi_{kA(B)}$, with subscript $A(B)$ labeling the SQUID above (below) the island, equals the average value, $[\phi^L_{kA(B)} + \phi^R_{kA(B)}]/2$, of the phase drops across the two Josephson junctions in the dc SQUID, where the superscript L (R) denotes the left (right) Josephson junction. Since the size of the loop is usually very small ($\sim 1\ \mu$m), above we have ignored the self-inductance effects of each SQUID loop. The Hamiltonian of the system is $H = \sum_{k=1}^N H_k + \frac{1}{2}LI^2$, with H_k given by $H_k = E_{ck}(n_k - n_{Xk})^2 - E_{Jk}(\Phi_{Xk}) \times (\cos\phi_{kA} + \cos\phi_{kB})$. Here, $E_{ck} = 2e^2/(C_k + 4C_{Jk})$ is the charging energy of the superconducting island and $I = \sum_{k=1}^N I_k$ is the total persistent current through the superconducting inductance, as contributed by all coupled Cooper-pair boxes. The offset charge $2en_{Xk} = C_kV_{Xk}$ is induced by the gate voltage V_{Xk}. The phase drops ϕ^L_{kA} and ϕ^L_{kB} are related to the total flux $\Phi = \Phi_e + LI$ through the inductance L by the constraint $\phi^L_{kB} - \phi^L_{kA} = 2\pi\Phi/\Phi_0$, where Φ_e is the externally applied magnetic flux threading the inductance L. Without loss of generality and in order to implement QC more conveniently, the magnetic fluxes through the two SQUID loops of each Cooper-pair box are designed to have the *same* values but *opposite* directions; this simplifies the form of the Hamiltonian. (If this were not to be the case, the interbit coupling can still be realized, but the Hamiltonian of the qubit circuits takes a more complicated form.) Because this pair of fluxes *cancels* each other in any loop enclosing them, then $\phi^L_{kB} - \phi^L_{kA} = \phi^R_{kB} - \phi^R_{kA}$. This gives rise to the constraint $\phi_{kB} - \phi_{kA} = 2\pi\Phi/\Phi_0$ for the average phase drops across the Josephson junctions in the SQUIDs. The common superconducting inductance L plays the role of coupling Cooper-pair boxes. The coupling of selected Cooper-pair boxes can be implemented by switching on the SQUIDs connected to the chosen Cooper-pair boxes, and the persistent currents through the inductance L are composed of contributions from all the coupled Cooper-pair boxes.

One- and two-bit circuits.—For any given Cooper-pair box, say i, when $\Phi_{Xk} = \frac{1}{2}\Phi_0$ and $V_{Xk} = (2n_k + 1)e/C_k$ for all boxes except $k = i$, the inductance L connects only the ith Cooper-pair box to form a superconducting loop [see Fig. 2(a)]. The Hamiltonian of the system can be reduced to [11]

$$H = \varepsilon_i(V_{Xi})\,\sigma_z^{(i)} - \overline{E}_{Ji}(\Phi_{Xi}, \Phi_e, L)\sigma_x^{(i)}, \qquad (1)$$

where $\varepsilon_k(V_{Xk})$ is controllable via the gate voltage V_{Xi}, while the intrabit coupling $\overline{E}_{Jk}(\Phi_{Xi}, \Phi_e, L)$ can be controlled by both the applied external flux Φ_e through the common inductance, and the local flux Φ_{Xi} through the two SQUID loops of the ith Cooper-pair box. The intrabit coupling $\overline{E}_{Ji}$ in (1) is different from that in [1,3] because a very different contribution by L is considered. To couple *any* two Cooper-pair boxes, say i and j, we choose $\Phi_{Xk} = \frac{1}{2}\Phi_0$ and $V_{Xk} = (2n_k + 1)e/C_k$ for all boxes except $k = i$ and j. As shown in Fig. 2(b), the inductance L is shared by the Cooper-pair boxes i and j to form superconducting loops. The reduced Hamiltonian of the system is given by [13]

$$H = \sum_{k=i,j}[\varepsilon_k(V_{Xk})\,\sigma_z^{(k)} - \overline{E}_{Jk}\sigma_x^{(k)}] + \Pi_{ij}\sigma_x^{(i)}\sigma_x^{(j)}. \qquad (2)$$

Here the interbit coupling Π_{ij} is controlled by both the external flux Φ_e through the inductance L, and the local fluxes, Φ_{Xi} and Φ_{Xj}, through the SQUID loops.

Quantum computing.—The quantum system evolves according to $U(t) = \exp(-iHt/\hbar)$. Initially, we choose $\Phi_{Xk} = \frac{1}{2}\Phi_0$ and $V_{Xk} = (2n_k + 1)e/C_k$ for all boxes in Fig. 1, so that the Hamiltonian of the system is $H = 0$ and no time evolution occurs. Afterwards, we *switch* certain fluxes Φ_{Xk} and/or gate voltages V_{Xk} away from the above initial values for certain periods of times, to implement logic gates required for QC. For any two Cooper-pair boxes, say i and j, when fluxes Φ_{Xi} and Φ_{Xj} are switched away from the initial value $\Phi_0/2$ for a given period of time τ, the Hamiltonian of the system becomes $H = -\overline{E}_{Ji}\sigma_x^{(i)} - \overline{E}_{Jj}\sigma_x^{(j)} + \Pi_{ij}\sigma_x^{(i)}\sigma_x^{(j)}$. This anisotropic Hamiltonian is Ising-like [14], with its anisotropic direction and the "magnetic" field along the x axis. When the parameters are suitably chosen so that $\overline{E}_{Ji} = \overline{E}_{Jj} = \Pi_{ij} = -\pi\hbar/4\tau$ for the switching time τ, we obtain a controlled-phase-shift gate, $U'_{\rm CPS} = e^{i\pi/4}U_{2b} = \exp\{i\frac{\pi}{4}[1 - \sigma_x^{(i)} - \sigma_x^{(j)} + \sigma_x^{(i)}\sigma_x^{(j)}]\}$, which does not alter the two-bit states $|+\rangle_i|+\rangle_j$, $|+\rangle_i|-\rangle_j$, and $|-\rangle_i|+\rangle_j$ but transforms $|-\rangle_i|-\rangle_j$ to $-|-\rangle_i|-\rangle_j$. Here, the phase factor $e^{i\pi/4}$ corresponds to an overall energy shift of the Hamiltonian, and $|\pm\rangle$ are defined by $|\pm\rangle = (|\uparrow\rangle \pm |\downarrow\rangle)/\sqrt{2}$.

To obtain the controlled-phase-shift gate $U_{\rm CPS}$ for the basis states $|\uparrow\rangle_i|\uparrow\rangle_j$, $|\uparrow\rangle_i|\downarrow\rangle_j$, $|\downarrow\rangle_i|\uparrow\rangle_j$, and $|\downarrow\rangle_i|\downarrow\rangle_j$, one

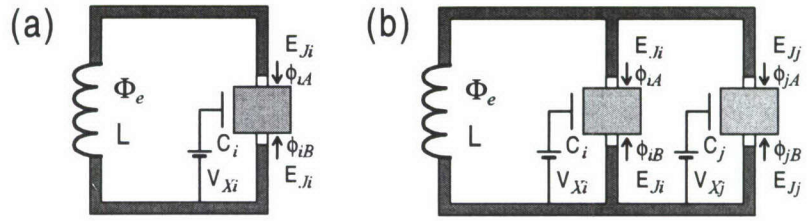

FIG. 2. (a) One-bit circuit with a Cooper-pair box connected to the inductance. (b) Two-bit structure where two Cooper-pair boxes are commonly connected to the inductance. Here, each SQUID connecting the superconducting island is represented by an effective Josephson junction.

needs to combine $U'_{\rm CPS}$ with suitable one-bit rotations. For any Cooper-pair box, say i, one can shift flux Φ_{Xi} and/or gate voltage V_{Xi} for a given switching time τ to derive one-bit rotations. A universal set of one-bit gates $U_z^{(i)}(\alpha) = e^{i\alpha\sigma_z^{(i)}}$, and $U_x^{(i)}(\beta) = e^{i\beta\sigma_x^{(i)}}$, where $\alpha = -\varepsilon_i(V_{Xi})\tau/\hbar$ and $\beta = \overline{E}_{Ji}\tau/\hbar$, can be defined by choosing $\overline{E}_{Ji} = 0$ and $\varepsilon_i(V_{Xi}) = 0$ (which can be done with suitable choices of Φ_{Xi} and V_{Xi}) in the one-bit Hamiltonian (1), respectively. Any one-bit rotation can be derived in terms of these two types of one-bit gates. For instance, the Hadamard gate is given by $\mathcal{H}_i = e^{-i\pi/2}U_z^{(i)}(\frac{\pi}{4})U_x^{(i)}(\frac{\pi}{4})U_z^{(i)}(\frac{\pi}{4})$. Using $\mathcal{H}_i$, we derive the controlled-phase-shift gate $U_{\rm CPS}$: $U_{\rm CPS} = \mathcal{H}_j^\dagger\mathcal{H}_i^\dagger U'_{\rm CPS}\mathcal{H}_i\mathcal{H}_j$. The one-bit rotation $V_j = e^{i\pi\sigma_y^{(j)}/4}$ is given by $V_j = U_z^{(j)}(-\frac{\pi}{4})U_x^{(j)}(\frac{\pi}{4})U_z^{(j)}(\frac{\pi}{4})$. Combining V_j with $U_{\rm CPS}$, we obtain the controlled-NOT gate, $U_{\rm CNOT} = V_j^\dagger U_{\rm CPS}V_j$, which transforms the basis states as $|\uparrow\rangle_i|\uparrow\rangle_j \to |\uparrow\rangle_i|\uparrow\rangle_j$, $|\uparrow\rangle_i|\downarrow\rangle_j \to |\uparrow\rangle_i|\downarrow\rangle_j$, $|\downarrow\rangle_i|\uparrow\rangle_j \to |\downarrow\rangle_i|\downarrow\rangle_j$, and $|\downarrow\rangle_i|\downarrow\rangle_j \to |\downarrow\rangle_i|\uparrow\rangle_j$. A sequence of such conditional two-bit gates supplemented with one-bit rotations constitute a universal element for QC [15]. Usually, a two-bit operation is much slower than a one-bit operation. Our designs for conditional gates $U_{\rm CPS}$ and $U_{\rm CNOT}$ are *efficient* since *only one* (instead of two or more) two-bit operation $U'_{\rm CPS}$ is used.

Persistent currents and entanglement.—The one-bit circuit modeled by Hamiltonian (1) has two eigenvalues $E_\pm^{(i)} = \pm E_i$, with $E_i = [\varepsilon_i^2(V_{Xi}) + \overline{E}_{Ji}^2]^{1/2}$. The corresponding eigenstates are $|\psi_+^{(i)}\rangle = \cos\xi_i|\uparrow\rangle_i - \sin\xi_i|\downarrow\rangle_i$, and $|\psi_-^{(i)}\rangle = \sin\xi_i|\uparrow\rangle_i + \cos\xi_i|\downarrow\rangle_i$, where $\xi_i = \frac{1}{2}\tan^{-1}(\overline{E}_{Ji}/\varepsilon_i)$. At these two eigenstates, the persistent currents through the inductance L are given by $\langle\psi_\pm^{(i)}|I|\psi_\pm^{(i)}\rangle = \pm(\overline{E}_{Ji}I_{ci}/E_i)\sin(\pi\Phi_e/\Phi_0) + (\pi LI_{ci}^2/2\Phi_0)\sin(2\pi\Phi_e/\Phi_0)$, where the expansion in I is retained up to the linear term in η_i. When a dc SQUID magnetometer is inductively coupled to the inductance L, these two supercurrents generate different fluxes through the SQUID loop of the magnetometer and the quantum-state information of the one-bit structure can be obtained from the measurements. To perform sensitive measurements with weak dephasing, one could use the underdamped dc SQUID magnetometer designed previously for the Josephson phase qubit [4,8].

For the two-bit structure described by Eq. (2), the Hamiltonian has four eigenstates and the supercurrents through inductance L take different values at these states. The fluxes produced by the supercurrents through L can also be detected by the dc SQUID magnetometer. For instance, when $\varepsilon_k(V_{Xk}) = 0$ and $\overline{E}_{Jk} > 0$ for $k = i$ and j, the four eigenstates of the two-bit structure are

$$|1\rangle = \tfrac{1}{2}(|\uparrow\rangle_i|\uparrow\rangle_j - |\uparrow\rangle_i|\downarrow\rangle_j - |\downarrow\rangle_i|\uparrow\rangle_j + |\downarrow\rangle_i|\downarrow\rangle_j),$$

$$|2\rangle = \tfrac{1}{2}(|\uparrow\rangle_i|\uparrow\rangle_j + |\uparrow\rangle_i|\downarrow\rangle_j - |\downarrow\rangle_i|\uparrow\rangle_j - |\downarrow\rangle_i|\downarrow\rangle_j),$$

$$|3\rangle = \tfrac{1}{2}(|\uparrow\rangle_i|\uparrow\rangle_j - |\uparrow\rangle_i|\downarrow\rangle_j + |\downarrow\rangle_i|\uparrow\rangle_j - |\downarrow\rangle_i|\downarrow\rangle_j),$$

$$|4\rangle = \tfrac{1}{2}(|\uparrow\rangle_i|\uparrow\rangle_j + |\uparrow\rangle_i|\downarrow\rangle_j + |\downarrow\rangle_i|\uparrow\rangle_j + |\downarrow\rangle_i|\downarrow\rangle_j).$$

When expansions in I_i and I_j are retained up to the linear terms in η_i and η_j, the corresponding supercurrents through inductance L are $\langle k|I|k\rangle = I_k\sin(\pi\Phi_e/\Phi_0) + (\pi LI_k^2/2\Phi_0)\sin(2\pi\Phi_e/\Phi_0)$ for $k = 1$ to 4, where $I_1 = -(I_{ci} + I_{cj})$, $I_2 = I_{cj} - I_{ci}$, $I_3 = I_{ci} - I_{cj}$, and $I_4 = I_{ci} + I_{cj}$. These supercurrents produce different fluxes threading the SQUID loop of the magnetometer and can be distinguished by dc SQUID measurements. If the two-bit system is prepared at the maximally entangled Bell states $|\Psi^{(\pm)}\rangle = (|\uparrow\rangle_i|\downarrow\rangle_j \pm |\downarrow\rangle_i|\uparrow\rangle_j)/\sqrt{2}$, the supercurrents through L are given by $\langle\Psi^{(\pm)}|I|\Psi^{(\pm)}\rangle = (\pi L/2\Phi_0)(I_{ci} \pm I_{cj})^2\sin(2\pi\Phi_e/\Phi_0)$. These two states should be distinguishable by detecting the fluxes (generated by the supercurrents) through the SQUID loop of the magnetometer.

Discussion.—The typical switching time $\tau^{(1)}$ during a one-bit operation is of the order $\hbar/E_J^0$. For the experimental value of $E_J^0 \sim 100$ mK, there is $\tau^{(1)} \sim 0.1$ ns. The switching time $\tau^{(2)}$ for the two-bit operation is typically of the order $(\hbar/L)(\Phi_0/\pi E_J^0)^2$. Choosing $E_J^0 \sim 100$ mK and $\tau^{(2)} \sim 10\tau^{(1)}$ (i.e., 10 times slower than the one-bit rotation), we have $L \sim 30$ nH in our proposal, which is experimentally accessible. A small-size inductance with this value can be made with Josephson junctions. Our expansion parameter η is of the order $\pi^2LE_J^0/\Phi_0^2 \sim 0.1$. Our inductance L is related with the inductance L' in [1,3] by $L' = (C_J/C_{qb})^2L$. Let us now consider the case when $\tau^{(2)} \sim 10\tau^{(1)}$. For the earlier design [3], $C_J \sim 11C_{qb}$ since $C_g/C_J \sim 0.1$, which requires the inductance ~ 3.6 μH. Such a large inductance is difficult to fabricate at nanometer scales. In the improved design [1], $C_J \sim 2C_{qb}$,

greatly reducing the inductance to ~120 nH. This inductance is about 4 times larger than the one used in our scheme.

All charge qubits suffer decoherence due to the fluctuations of voltage sources and fluxes. Reference [1] shows that the gate voltage fluctuations play the dominant role in producing decoherence. The estimated dephasing time is $\tau_\varphi \sim 10^{-4}$ s, allowing in principle 10^6 coherent single-bit manipulations. When a probe junction is used for measurements, the experimental observations of coherent oscillations in the Josephson charge qubits show that the phase coherence time is only about 2 ns [2,16]. In this experimental setup, background charge fluctuations and the probe-junction measurement may be two of the major factors in producing decoherences. Though the charge fluctuations are important only in the low-frequency region and can be reduced by the echo technique [16] and by shifting the gate voltage to the degeneracy point, an effective technique for suppressing charge fluctuations still needs to be explored. As for the measurement, it has also been a challenge to design effective detecting devices.

In conclusion, we propose a *scalable* quantum computer with Josephson charge qubits. We employ a common inductance to couple all charge qubits and design *switchable interbit couplings* using two dc SQUIDs to connect the island in each Cooper-pair box. The proposed QC architectures are scalable since any two charge qubits can be effectively coupled by an experimentally accessible inductance. Furthermore, we formulate an efficient QC scheme in which *only one* two-bit operation is used in the conditional transformations such as controlled-phase-shift and controlled-NOT gates.

We thank Yu. Pashkin for useful discussions. We acknowledge support from the U.S. ARDA, AFOSR, and the U.S. National Science Foundation Grant No. EIA-0130383.

*Corresponding author.
Electronic address: nori@umich.edu

[1] See, e.g., Y. Makhlin, G. Schön, and A. Shnirman, Rev. Mod. Phys. **73**, 357 (2001), and references therein.

[2] Y. Nakamura, Yu. A. Pashkin, and J. S. Tsai, Nature (London) **398**, 786 (1999).

[3] Y. Makhlin, G. Schön, and A. Shnirman, Nature (London) **398**, 305 (1999).

[4] J. E. Mooij *et al.*, Science **285**, 1036 (1999).

[5] T. P. Orlando *et al.*, Phys. Rev. B **60**, 15 398 (1999).

[6] Y. Nakamura, C. D. Chen, and J. S. Tsai, Phys. Rev. Lett. **79**, 2328 (1997).

[7] V. Bouchiat *et al.*, Phys. Scr. **T76**, 165 (1998).

[8] C. H. van der Wal *et al.*, Science **290**, 773 (2000).

[9] J. R. Friedman *et al.*, Nature (London) **406**, 43 (2000).

[10] F. Plastina, R. Fazio, and G. M. Palma, Phys. Rev. B **64**, 113306 (2001).

[11] The Hamiltonian of the one-bit circuit shown in Fig. 2(a) is $H = H_i + \frac{1}{2}LI_i^2$, with $H_i = E_{ci}(n_i - n_{Xi})^2 - 2E_{Ji}(\Phi_{Xi})\cos(\pi\Phi/\Phi_0)\cos\varphi_i$. Here, the phase $\varphi_i = (\phi_{iA} + \phi_{iB})/2$ is canonically conjugate with the number of the extra Cooper pairs on the island and the persistent circulating current I_i in the superconducting loop is given by $I_i = 2I_{ci}\cos\varphi_i \sin(\pi\Phi_e/\Phi_0 + \pi LI_i/\Phi_0)$, where $I_{ci} = -\pi E_{Ji}(\Phi_{Xi})/\Phi_0$. In the spin-$\frac{1}{2}$ representation, based on charge states $|\uparrow\rangle_i = |n_i\rangle$ and $|\downarrow\rangle_i = |n_i + 1\rangle$, the reduced Hamiltonian of the system becomes Eq. (1), where $\varepsilon_i(V_{Xi}) = \frac{1}{2}E_{ci}[C_iV_{Xi}/e - (2n_i + 1)]$, and $\overline{E}_{Ji}(\Phi_{Xi}, \Phi_e, L) = E_{Ji}(\Phi_{Xi})(\gamma_i + \eta_i\alpha_i\beta_i)$. Here α_i, β_i, and γ_i are power series of the expansion parameter $\eta_i = \pi LI_{ci}/\Phi_0$, which is ~0.1 in our case (see the discussion part above). These have the same expressions as α, β, and γ in Ref. [12], with I_c and Φ_X there replaced by I_{ci} and Φ_e. Retained up to second-order terms in the expansion parameter, $\overline{E}_{Ji}(\Phi_{Xi}, \Phi_e, L) = E_{Ji}(\Phi_{Xi})\cos(\pi\Phi_e/\Phi_0)\xi$, with $\xi = 1 - \frac{1}{2}\eta_i^2\sin^2(\pi\Phi_e/\Phi_0)$.

[12] J. Q. You, C.-H. Lam, and H. Z. Zheng, Phys. Rev. B **63**, 180501(R) (2001).

[13] The Hamiltonian of the two-bit circuit given in Fig. 2(b) is $H = H_i + H_j + \frac{1}{2}L(I_i + I_j)^2$, where $I_i = 2I_{ci}\cos\varphi_i \sin[\pi\Phi_e/\Phi_0 + \pi L(I_i + I_j)/\Phi_0]$ is the persistent circulating current contributed by the Cooper-pair box i. Interchanging i and j in I_i gives the circulating current I_j contributed by the Cooper-pair box j. In the spin-$\frac{1}{2}$ representation, the Hamiltonian of the system reduces to Eq. (2), where the intrabit coupling $\overline{E}_{Jk}$ and the interbit coupling Π_{ij} are also power series, which have the same expressions as in Ref. [12], but with L_i, L_j, and M_{ij} replaced by L; Φ_{Xi} and Φ_{Xj} replaced by Φ_e; and E_{Jk}^0 replaced by $E_{Jk}(\Phi_{Xk})$. Up to second-order terms, $\overline{E}_{Ji}(\Phi_{Xi}, \Phi_e, L) = E_{Ji}(\Phi_{Xi})\cos(\pi\Phi_e/\Phi_0)\xi$, with $\xi = 1 - \frac{1}{2}(\eta_i^2 + 3\eta_j^2)\sin^2(\pi\Phi_e/\Phi_0)$, and $\Pi_{ij} = -LI_{ci}I_{cj}\sin^2(\pi\Phi_e/\Phi_0)$. When the two qubits are far apart, the inductance of the wires connecting them might not be neglected. However, the reduced two-bit Hamiltonian is still given by Eq. (2), but with $\overline{E}_{Jk}$ and Π_{ij} slightly modified. In deriving the interbit coupling Π_{ij}, here we ignore the collective LC-oscillator mode associated with the total charge q accumulated on the gate capacitors of the arrays of Cooper-pair boxes [1]. When it is taken into account, a term $(q - \sum_k 2en_k\chi_k)^2/2C_\Sigma$, with $C_\Sigma = \sum_k 2C_J(C_k + 2C_J)/(C_k + 4C_J)$ and $\chi_k = C_k/(C_k + 4C_J)$, needs to be included in the Hamiltonian. Fast collective oscillations in the LC circuit then yield an effective coupling between qubits i and j, and the effective coupling strength $|\Lambda_{ij}|$ is $\sim\chi_i\chi_j|\Pi_{ij}|$. For typical values of $C_k/C_J \sim 0.1$, there is $\chi_k \sim 0.025$. Thus, we have $|\Lambda_{ij}| \sim 6 \times 10^{-4}|\Pi_{ij}|$, implying that neglecting the LC-oscillator effect here is quite reasonable.

[14] G. Burkard *et al.*, Phys. Rev. B **60**, 11 404 (1999).

[15] S. Lloyd, Phys. Rev. Lett. **75**, 346 (1995); D. Deutsch, A. Barenco, and A. Ekert, Proc. R. Soc. London A **449**, 669 (1995).

[16] Recent measurement shows that the oscillations survive up to 5 ns; see Y. Nakamura, Yu. A. Pashkin, T. Yamamoto, and J. S. Tsai, Phys. Rev. Lett. **88**, 047901 (2002).

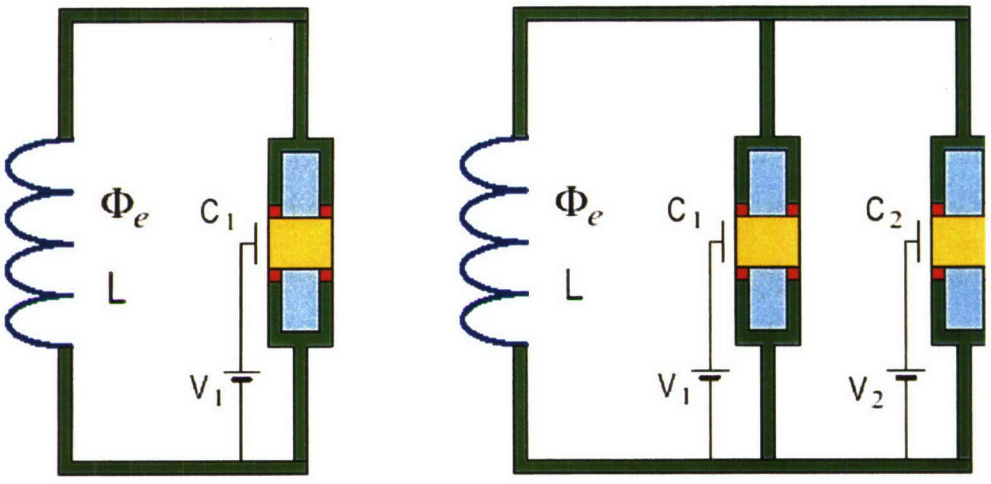

Figure 1. This is a schematic diagram of two micro-circuits, one with one qubit (left) and the other with two coupled qubits (right). Using a plumbing analogy, with an electrical charge taking the place of water, the yellow box is like a reservoir, storing charge (actually, storing pairs of superconducting electrons). This charge can be pushed in and out of the box using a pump (the voltage, V1) that moves the charge through the "valves" or "faucets" (the red boxes, known as Josephson junctions) and into the superconducting wires acting as "pipes." The blue magnetic field controls the strength of the red barriers, and thus can control the flow of electrons in and out of the yellow charge box.

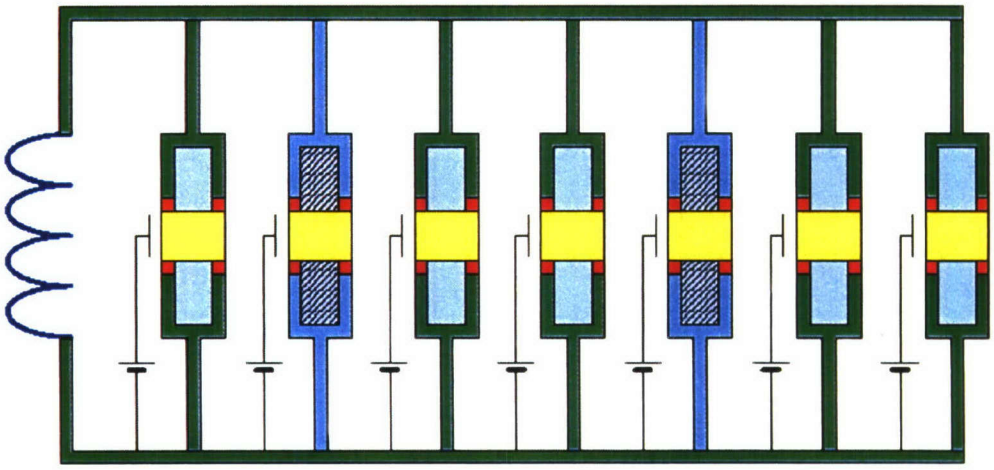

Figure 2. This is a schematic diagram of a micro-circuit with seven qubits. The applied magnetic field (shown in blue) can be chosen to have two specific values. One value closes the red "faucets" of each yellow charge storage box. The other value selects two qubits by opening the corresponding red valves, so electronic charge can come in and out (controlled by the voltages that act as "charge pumps"). Thus, two qubits, from the total of seven, are coupled with each other. This idea can be extended to an arbitrary number of qubits.

Quantum computing with many superconducting qubits

J. Q. You[1], J. S. Tsai[1,2] and Franco Nori[1,3,*]
[1] *Frontier Research System, The Institute of Physical and Chemical Research (RIKEN), Wako-shi 351-0198, Japan*
[2] *NEC Fundamental Research Laboratories, Tsukuba, Ibaraki 305-8051, Japan*[†]
[3] *Center for Theoretical Physics, Physics Department, Center for the Study of Complex Systems, The University of Michigan, Ann Arbor, MI 48109-1120, USA*[†]

Abstract. Two of the major obstacles to achieve quantum computing (QC) are (i) scalability to many qubits and (ii) controlled connectivity between any selected qubits. Using Josephson charge qubits, here we propose an experimentally realizable method to efficiently solve these two central problems. Since any two charge qubits can be effectively coupled by an experimentally accessible inductance, the proposed QC architecture is *scalable*. In addition, we formulate an efficient and realizable QC scheme that requires *only one* (instead of two or more) two-bit operation to implement conditional gates.

Introduction

Josephson-qubit devices [1] are based on the charge and phase degrees of freedom. The charge qubit is achieved in a Cooper-pair box [2], where two dominant charge states are coupled through coherent Cooper-pair tunneling [3]. Using Cooper-pair tunneling in Josephson charge devices [4, 5] and via spectroscopic measurements for the Josephson phase device [6, 7], it has been possible to experimentally observe energy-level splitting and related properties for state superpositions. In addition, using Josephson charge devices prepared in a superposition of two charge states [2], coherent oscillations were observed. While operating at the degeneracy point, the charge-qubit states are highly coherent [8] ($Q = 2.5 \times 10^4$), with a decoherence time of $\tau \sim 500$ ns. These important experimental results indicate that the Josephson charge and phase devices are potentially useful for solid-state qubits in quantum information processing. Important open problems would now include implementing a *two-bit coupling* and then *scaling up* the architecture to many qubits. Here, we propose a new quantum-computing (QC) scheme based on scalable charge-qubit structures. We focus on the Josephson charge qubit realized in a Cooper-pair box.

* Corresponding author (e-mail address: nori@umich.edu)
† Permanent address.

COUPLING QUBITS

The Coulomb interaction between charges on different islands of the charge qubits would seem to provide a natural way of coupling Josephson charge qubits (e.g., to connect two Cooper-pair boxes via a capacitor). Using this type of capacitive interbit coupling, a two-bit operation [9] similar to the controlled-NOT gate was derived. However, as pointed out in [1], it is difficult in this scheme to switch on and off the coupling. Also, it is hard to make the system scalable because only neighboring qubits can interact. Moreover, implementations of quantum algorithms such as the Deutsch and Bernstein-Vazirani algorithms were studied using a system of Josephson charge qubits [10], where it was proposed that the nearest-neighbor charge qubits would be coupled by tunable dc SQUIDs. In the semiconductor literature, scalability often refers to reducing the size of the device (packing more components). In QC, scalability refers to increasing the number of qubits coupled with each other.

A suggestion for a scalable coupling of Josephson charge qubits was proposed [1, 3] using oscillator modes in a LC circuit formed by an inductance and the qubit capacitors. In this proposal, the interbit coupling can be switched and any two charge qubits could be coupled. Nevertheless, there is no efficient (that is, using one two-bit operation) QC scheme for this proposal [1, 3] in order to achieve conditional gates—e.g., the controlled-phase-shift and controlled-NOT gates. In addition, the calculated interbit coupling terms [1, 3] only apply to the case when the following two conditions are met:
(i) The quantum manipulation frequencies, which are fixed experimentally, are required to be much smaller than the eigenfrequency ω_{LC} of the LC circuit. This condition *limits* the allowed number N of the qubits in the circuit because ω_{LC} scales with $1/\sqrt{N}$. In other words, the circuits in [1, 3] are not really scalable.
(ii) The phase conjugate to the total charge on the qubit capacitors fluctuates weakly.

IMPROVED AND SCALABLE COUPLING BETWEEN ANY SELECTED QUBITS

The limitations listed above do not apply to our approach. In our scheme, a common inductance, but no LC circuit, is used to couple all Josephson charge qubits. In our proposal, both dc and ac supercurrents can flow through the inductance, while in [1, 3] only ac supercurrents can flow through the inductance and it is the LC-oscillator mode that couples the charge qubits. These yield different interbit couplings (e.g., $\sigma_y\sigma_y$ type [1, 3] as opposed to $\sigma_x\sigma_x$ in our proposal).

We employ two dc SQUIDs to connect each Cooper-pair box in order to achieve a *controllable interbit coupling*. Our proposed QC architecture is scalable in the sense that *any* two charge qubits (*not* necessarily neighbors)

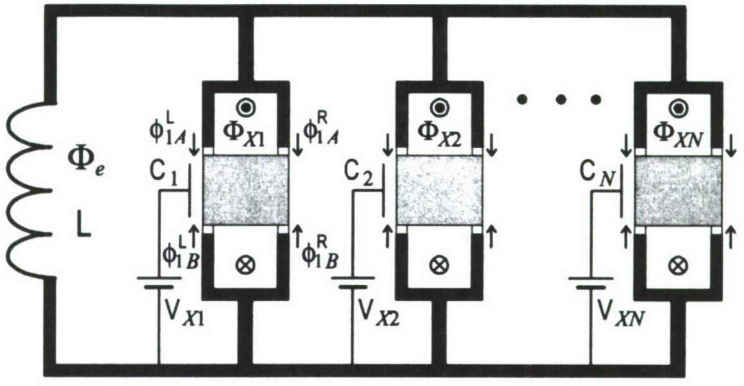

Figure 1. Schematic diagram of the proposed scalable and switchable quantum computer. Here, each Cooper-pair box is operated in the charging regime, $E_{ck} \gg E^0_{Jk}$, and at low temperatures $k_B T \ll E_{ck}$. Also, the superconducting gap is larger than E_{ck}, so that quasiparticle tunneling is strongly suppressed. All Josephson charge-qubit structures are coupled by a common superconducting inductance.

can be effectively coupled by an experimentally accessible inductance. We also formulate [11] an efficient QC scheme that requires only one (instead of two or more) two-bit operation to implement conditional gates.

This Erice summer-school presentation is based on our work in [11]. Additional work on decoherence and noise-related issues appears in, e.g., [12, 13]. Also, work more focused on entanglement and readout issues appears in [14]. Other interesting studies on charge qubits can be found in [15] for the adiabatic controlled-NOT gate, in [16] for geometric phases, and in [17, 18, 19, 20] for the dynamics of a Josephson charge qubit coupled to a quantum resonator.

Proposed scalable and switchable quantum computer

Figure 1 shows a proposed QC circuit consisting of N Cooper-pair boxes coupled by a common superconducting inductance L. For the kth Cooper-pair box, a superconducting island with charge $Q_k = 2en_k$ is weakly coupled by two symmetric dc SQUIDs and biased, through a gate capacitance C_k, by an applied voltage V_{Xk}. The two symmetric dc SQUIDs are assumed to be equal and all Josephson junctions in them have Josephson coupling energy E^0_{Jk} and capacitance C_{Jk}. The effective coupling energy is given by the SQUIDs, each one enclosing a magnetic flux Φ_{Xk}. Each SQUID provides a tunable coupling

$-E_{Jk}(\Phi_{Xk})\cos\phi_{kA(B)}$, with

$$E_{Jk}(\Phi_{Xk}) = 2E_{Jk}^{0}\cos(\pi\Phi_{Xk}/\Phi_0), \tag{1}$$

and $\Phi_0 = h/2e$ is the flux quantum. The effective phase drop $\phi_{kA(B)}$, with subscript $A(B)$ labelling the SQUID above (below) the island, equals the average value, $[\phi_{kA(B)}^{L}+\phi_{kA(B)}^{R}]/2$, of the phase drops across the two Josephson junctions in the dc SQUID, where the superscript L (R) denotes the left (right) Josephson junction. Above we have neglected the self-inductance effects of each SQUID loop because the size of the loop is usually very small ($\sim 1\ \mu$m). The Hamiltonian of the system then becomes

$$H = \sum_{k=1}^{N} H_k + \frac{1}{2}LI^2, \tag{2}$$

with H_k given by

$$H_k = E_{ck}(n_k - n_{Xk})^2 - E_{Jk}(\Phi_{Xk})(\cos\phi_{kA} + \cos\phi_{kB}). \tag{3}$$

Here

$$E_{ck} = 2e^2/(C_k + 4C_{Jk}) \tag{4}$$

is the charging energy of the superconducting island and $I = \sum_{k=1}^{N} I_k$ is the total persistent current through the superconducting inductance, as contributed by all coupled Cooper-pair boxes. The offset charge $2en_{Xk} = C_kV_{Xk}$ is induced by the gate voltage V_{Xk}. The phase drops ϕ_{kA}^{L} and ϕ_{kB}^{L} are related to the total flux

$$\Phi = \Phi_e + LI \tag{5}$$

through the inductance L by the constraint

$$\phi_{kB}^{L} - \phi_{kA}^{L} = 2\pi\Phi/\Phi_0, \tag{6}$$

where Φ_e is the externally applied magnetic flux threading the inductance L. In order to obtain a simpler expression for the interbit coupling, and without loss of generality, the magnetic fluxes through the two SQUID loops of each Cooper-pair box are designed to have the *same* values but *opposite* directions. If this were not to be the case, the interbit coupling can still be realized, but the Hamiltonian of the qubit circuits would just take a more complicated form. Because this pair of fluxes cancel each other in any loop enclosing them, then

$$\phi_{kB}^{L} - \phi_{kA}^{L} = \phi_{kB}^{R} - \phi_{kA}^{R}. \tag{7}$$

This imposes the constraint

$$\phi_{kB} - \phi_{kA} = 2\pi\Phi/\Phi_0 \tag{8}$$

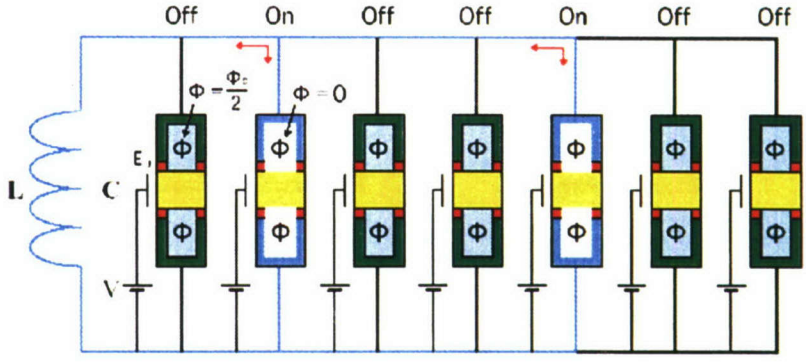

Figure 2. Simplified diagram of the circuit shown in Fig. 1. Here we explicitly show how two charge qubits (not necessarily neighbors) can be coupled by the inductance L, where the cyan SQUIDs are switched on by setting the fluxes through the cyan SQUID loops zero, and the green SQUIDs are turned off by choosing the fluxes through the green SQUID loops as $\Phi_0/2$. This applies to the case when any selected charge qubits are coupled by the common inductance [21].

for the average phase drops across the Josephson junctions in the SQUIDs. The common superconducting inductance L provides the coupling among Cooper-pair boxes. The coupling of selected Cooper-pair boxes can be implemented by switching "on" the SQUIDs connected to the chosen Cooper-pair boxes. In this case, the persistent currents through the inductance L have contributions from all the coupled Cooper-pair boxes. The essential features of our proposal can be best understood via the very simplified diagram shown in Fig. 2.

ONE-BIT CIRCUIT

As seen in Fig. 3(a), for any given Cooper-pair box, say i, when

$$\Phi_{Xk} = \frac{1}{2}\Phi_0, \quad V_{Xk} = (2n_k + 1)e/C_k$$

for all boxes except $k = i$, the inductance L only connects the ith Cooper-pair box to form a superconducting loop. The Hamiltonian of the system can be reduced to [11]

$$H = \varepsilon_i(V_{Xi})\,\sigma_z^{(i)} - \overline{E}_{Ji}(\Phi_{Xi}, \Phi_e, L)\,\sigma_x^{(i)}, \tag{9}$$

where

$$\varepsilon_i(V_{Xi}) = \frac{1}{2}E_{ci}[C_i V_{Xi}/e - (2n_i + 1)] \tag{10}$$

is controllable via the gate voltage V_{Xi}, while the intrabit coupling $\overline{E}_{Ji}$ can be controlled by both the applied external flux Φ_e through the common inductance, and the local flux Φ_{Xi} through the two SQUID loops of the ith

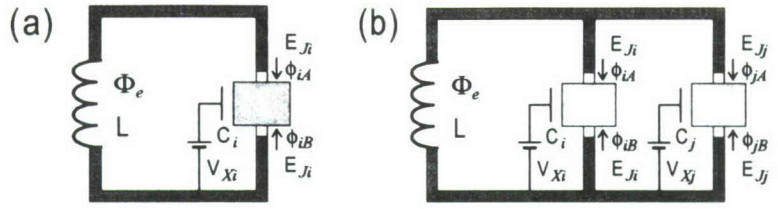

Figure 3. (a) One-bit circuit with a Cooper-pair box connected to the inductance. (b) Two-bit structure where two Cooper-pair boxes are commonly connected to the inductance. Here, each SQUID connecting the superconducting island is represented by an effective Josephson junction.

Cooper-pair box. Retained up to second-order terms in the expansion parameter

$$\eta_i = \pi L I_{ci}/\Phi_0, \tag{11}$$

where

$$I_{ci} = -\pi E_{Ji}(\Phi_{Xi})/\Phi_0, \tag{12}$$

we obtain

$$\overline{E}_{Ji}(\Phi_{Xi}, \Phi_e, L) = E_{Ji}(\Phi_{Xi}) \cos(\pi\Phi_e/\Phi_0)\, \xi, \tag{13}$$

with

$$\xi = 1 - \frac{1}{2}\eta_i^2 \sin^2(\pi\Phi_e/\Phi_0). \tag{14}$$

The intrabit coupling $\overline{E}_{Ji}$ in (9) is different from that in [1, 3] because a very different contribution by L is considered.

TWO-BIT CIRCUIT

To couple *any* two Cooper-pair boxes, say i and j, we choose

$$\Phi_{Xk} = \frac{1}{2}\Phi_0, \quad V_{Xk} = (2n_k + 1)e/C_k$$

for all boxes except $k = i$ and j. As shown in Fig. 3(b), the inductance L is shared by the Cooper-pair boxes i and j to form superconducting loops. The reduced Hamiltonian of the system is given by [11]

$$H = \sum_{k=i,j} [\varepsilon_k(V_{Xk})\, \sigma_z^{(k)} - \overline{E}_{Jk}\, \sigma_x^{(k)}] + \Pi_{ij}\, \sigma_x^{(i)} \sigma_x^{(j)}. \tag{15}$$

Up to second-order terms,

$$\overline{E}_{Ji}(\Phi_{Xi}, \Phi_e, L) = E_{Ji}(\Phi_{Xi}) \cos(\pi\Phi_e/\Phi_0)\, \xi, \tag{16}$$

with

$$\xi = 1 - \frac{1}{2}(\eta_i^2 + 3\eta_j^2)\sin^2(\pi\Phi_e/\Phi_0), \tag{17}$$

and

$$\Pi_{ij} = -LI_{ci}I_{cj}\sin^2(\pi\Phi_e/\Phi_0). \tag{18}$$

Here the interbit coupling Π_{ij} is controlled by both the external flux Φ_e through the inductance L, and the local fluxes, Φ_{Xi} and Φ_{Xj}, through the SQUID loops.

Using these two types of circuits, we can derive the required one- and two-bit operations for QC. Specifically, the conditional gates such as the controlled-phase-shift and controlled-NOT gates can be obtained using one-bit rotations and only one basic two-bit operation. For details, see Ref. [11]. A sequence of such conditional gates supplemented with one-bit rotations constitute a universal element for QC [22, 23]. Usually, a two-bit operation is much slower than a one-bit operation. Our designs for conditional gates $U_{\rm CPS}$ and $U_{\rm CNOT}$ are *efficient* since *only one* (instead of two or more) basic two-bit operation is used.

Persistent currents and entanglement

The one-bit circuit modeled by Hamiltonian (9) has two eigenvalues $E_{\pm}^{(i)} = \pm E_i$, with

$$E_i = [\varepsilon_i^2(V_{Xi}) + \overline{E}_{Ji}^2]^{1/2}. \tag{19}$$

The corresponding eigenstates are

$$\begin{aligned} |\psi_+^{(i)}\rangle &= \cos\xi_i|\uparrow\rangle_i - \sin\xi_i|\downarrow\rangle_i, \\ |\psi_-^{(i)}\rangle &= \sin\xi_i|\uparrow\rangle_i + \cos\xi_i|\downarrow\rangle_i, \end{aligned} \tag{20}$$

where

$$\xi_i = \frac{1}{2}\tan^{-1}(\overline{E}_{Ji}/\varepsilon_i). \tag{21}$$

At these two eigenstates, the persistent currents through the inductance L are given by

$$\langle\psi_{\pm}^{(i)}|I|\psi_{\pm}^{(i)}\rangle = \pm\left(\frac{\overline{E}_{Ji}I_{ci}}{E_i}\right)\sin\left(\frac{\pi\Phi_e}{\Phi_0}\right) + \left(\frac{\pi LI_{ci}^2}{2\Phi_0}\right)\sin\left(\frac{2\pi\Phi_e}{\Phi_0}\right), \tag{22}$$

up to the linear term in η_i. In the case when a dc SQUID magnetometer is inductively coupled to the inductance L, these two supercurrents generate different fluxes through the SQUID loop of the magnetometer and the quantum-state information of the one-bit structure can be obtained from the

measurements. In order to perform sensitive measurements with weak dephasing, one could use the underdamped dc SQUID magnetometer designed previously for the Josephson phase qubit [6].

For the two-bit circuit described by Eq. (15), the Hamiltonian has four eigenstates and the supercurrents through inductance L take different values for these four states. The fluxes produced by the supercurrents through L can also be detected by the dc SQUID magnetometer. For example, when $\varepsilon_k(V_{Xk}) = 0$ and $\overline{E}_{Jk} > 0$ for $k = i$ and j, the four eigenstates of the two-bit circuit are

$$\begin{aligned}
|1\rangle &= \frac{1}{2}\left(|\uparrow\rangle_i|\uparrow\rangle_j - |\uparrow\rangle_i|\downarrow\rangle_j - |\downarrow\rangle_i|\uparrow\rangle_j + |\downarrow\rangle_i|\downarrow\rangle_j\right), \\
|2\rangle &= \frac{1}{2}\left(|\uparrow\rangle_i|\uparrow\rangle_j + |\uparrow\rangle_i|\downarrow\rangle_j - |\downarrow\rangle_i|\uparrow\rangle_j - |\downarrow\rangle_i|\downarrow\rangle_j\right), \\
|3\rangle &= \frac{1}{2}\left(|\uparrow\rangle_i|\uparrow\rangle_j - |\uparrow\rangle_i|\downarrow\rangle_j + |\downarrow\rangle_i|\uparrow\rangle_j - |\downarrow\rangle_i|\downarrow\rangle_j\right), \\
|4\rangle &= \frac{1}{2}\left(|\uparrow\rangle_i|\uparrow\rangle_j + |\uparrow\rangle_i|\downarrow\rangle_j + |\downarrow\rangle_i|\uparrow\rangle_j + |\downarrow\rangle_i|\downarrow\rangle_j\right). \qquad (23)
\end{aligned}$$

Retained up to linear terms in η_i and η_j, the corresponding supercurrents through the inductance L are

$$\langle k|I|k\rangle = \mathcal{I}_k \sin\left(\frac{\pi\Phi_e}{\Phi_0}\right) + \frac{\pi L\mathcal{I}_k^2}{2\Phi_0}\sin\left(\frac{2\pi\Phi_e}{\Phi_0}\right) \qquad (24)$$

for $k = 1$ to 4, where

$$\begin{aligned}
\mathcal{I}_1 &= -(I_{ci} + I_{cj}), \qquad \mathcal{I}_2 = I_{cj} - I_{ci}, \\
\mathcal{I}_3 &= I_{ci} - I_{cj}, \qquad \mathcal{I}_4 = I_{ci} + I_{cj}. \qquad (25)
\end{aligned}$$

These supercurrents produce different fluxes threading the SQUID loop of the magnetometer and can be distinguished by dc SQUID measurements. When the two-bit system is prepared at the maximally entangled Bell states

$$|\Psi^{(\pm)}\rangle = \frac{1}{\sqrt{2}}(|\uparrow\rangle_i|\downarrow\rangle_j \pm |\downarrow\rangle_i|\uparrow\rangle_j), \qquad (26)$$

the supercurrents through L are given by

$$\langle\Psi^{(\pm)}|I|\Psi^{(\pm)}\rangle = \frac{\pi L}{2\Phi_0}(I_{ci} \pm I_{cj})^2 \sin\left(\frac{2\pi\Phi_e}{\Phi_0}\right). \qquad (27)$$

These two states should be distinguishable by measuring the fluxes, generated by the supercurrents, through the SQUID loop of the magnetometer.

Estimates of the inductance for optimal coupling

The typical switching time $\tau^{(1)}$ during a one-bit operation is of the order of $\hbar/E_J^0$. Using the experimental value $E_J^0 \sim 100$ mK, then $\tau^{(1)} \sim 0.1$ ns. The switching time $\tau^{(2)}$ for the two-bit operation is typically of the order

$$\tau^{(2)} \sim (\hbar/L)(\Phi_0/\pi E_J^0)^2.$$

Choosing $E_J^0 \sim 100$ mK and $\tau^{(2)} \sim 10\tau^{(1)}$ (i.e., ten times slower than the one-bit rotation), we have

$$L \sim 30 \text{ nH}$$

in our proposal. This number for L is experimentally realizable. A small-size inductance with this value can be made with Josephson junctions. Our expansion parameter η is of the order

$$\eta \sim \pi^2 L E_J^0/\Phi_0^2 \sim 0.1.$$

Our inductance L is related with the inductance L' in [1, 3] by

$$L' = (C_J/C_{qb})^2 L. \tag{28}$$

Let us now consider the case when $\tau^{(2)} \sim 10\tau^{(1)}$. For the earlier design [3], $C_J \sim 11C_{qb}$ since $C_g/C_J \sim 0.1$, which requires an inductance $L' \sim 3.6$ μH. Such a large inductance is problematic to fabricate at nanometer scales. In the improved design [1], $C_J \sim 2C_{qb}$, greatly reducing the inductance to $L' \sim$ 120 nH. This inductance is about four times larger than the one used in our scheme, making it somewhat more difficult to realize than our proposed L.

Conclusion

We propose a *scalable* quantum information processor with Josephson charge qubits. We use a common inductance to couple all charge qubits and design *switchable* interbit couplings using two dc SQUIDs to connect the island in each Cooper-pair box. The proposed circuits are scalable in the sense that any two charge qubits can be effectively coupled by an experimentally accessible inductance. In addition, we formulate [11] an efficient QC scheme in which only one two-bit operation is used in the conditional transformations, including controlled-phase-shift and controlled-NOT gates.

Acknowledgments

We thank Yu. Pashkin, B. Plourde and Xuedong Hu for useful discussions. This work is supported in part by ARDA, the AFOSR, and the US National Science Foundation grant No. EIA-0130383.

References

1. See, e.g., Y. Makhlin, G. Schön, and A. Shnirman, Rev. Mod. Phys. **73**, 357 (2001), and references therein.
2. Y. Nakamura, Yu. A. Pashkin, and J.S. Tsai, Nature (London) **398**, 786 (1999).
3. Y. Makhlin, G. Schön, and A. Shnirman, Nature (London) **398**, 305 (1999).
4. Y. Nakamura, C.D. Chen, and J.S. Tsai, Phys. Rev. Lett. **79**, 2328 (1997).
5. V. Bouchiat, D. Vion, P. Joyez, D. Esteve, and M.H. Devoret, Phys. Scripta **T76**, 165 (1998).
6. C.H. van der Wal, A.C.J. ter Haar, F.K. Wilhelm, R.N. Schouten, C.J.P.M. Harmans, T.P. Orlando, S. Lloyd, and J.E. Mooij, Science **290**, 773 (2000).
7. J.R. Friedman, V. Patel, W. Chen, S.K. Tolpygo, and J.E. Lukens, Nature (London) **406**, 43 (2000).
8. D. Vion, A. Aassime, A. Cottet, P. Joyez, H. Pothier, C. Urbina, D. Esteve, and M.H. Devoret, Science **296**, 886 (2002).
9. F. Plastina, R. Fazio, and G.M. Palma, Phys. Rev. B **64**, 113306 (2001).
10. J. Siewert and R. Fazio, Phys. Rev. Lett. **87**, 257905 (2001).
11. J.Q. You, J.S. Tsai, and F. Nori, Phys. Rev. Lett. **89**, 197902 (2002).
12. E. Paladino, L. Faoro, G. Falci, and R. Fazio, Phys. Rev. Lett. **88**, 228304 (2002).
13. J.Q. You, X. Hu, and F. Nori, preprint.
14. J.Q. You, J.S. Tsai, and F. Nori, preprint.
15. D.V. Averin, Solid State Commun. **105**, 659 (1998).
16. G. Falci, R. Fazio, G.M. Palma, J. Siewert, and V. Vedral, Nature (London) **407**, 355 (2000).
17. O. Buisson and F.W.J. Hekking, cond-mat/0008275; also in *Macroscopic Quantum Coherence and Quantum Computing* (Kluwer Academic, Dordrecht, 2000), p. 137.
18. F. Marquardt and C. Bruder, Phys. Rev. B **63**, 054514 (2001).
19. A.D. Armour, M.P. Blencowe, and K.C. Schwab, Phys. Rev. Lett. **88**, 148301 (2002).
20. J.Q. You and F. Nori, preprint.
21. Additional schematic color diagrams for the proposed circuitry appear in http://www-personal.engin.umich.edu/~nori/scalable/scalableQC_figs.pdf
22. S. Lloyd, Phys. Rev. Lett. **75**, 346 (1995).
23. D. Deutsch, A. Barenco, and A. Ekert, Proc. R. Soc. London, Ser. A **449**, 669 (1995).

Controllable manipulation and entanglement of macroscopic quantum states in coupled charge qubits

J. Q. You,[1] J. S. Tsai,[1,2] and Franco Nori[1,3,*]

[1]*Frontier Research System, The Institute of Physical and Chemical Research (RIKEN), Wako-shi 351-0198, Japan*

[2]*NEC Fundamental Research Laboratories, Tsukuba, Ibaraki 305-8051, Japan*

[3]*Center for Theoretical Physics, Physics Department, Center for the Study of Complex Systems, The University of Michigan, Ann Arbor, Michigan 48109-1120, USA*

(Received 25 February 2003; published 22 July 2003)

We present an experimentally implementable method to couple Josephson charge qubits and to generate and detect macroscopic entangled states. A large-junction superconducting quantum interference device is used in the qubit circuit for both coupling qubits and implementing the readout. Also, we explicitly show how to achieve a microwave-assisted macroscopic entanglement in the coupled-qubit system.

DOI: 10.1103/PhysRevB.68.024510 PACS number(s): 85.25.−j, 03.65.Ud, 03.67.Lx

I. INTRODUCTION

Quantum-mechanical systems can exploit the fundamental properties of superposition and entanglement to process information in an efficient and powerful way that no classical device can do. Recently, Josephson-junction circuits have received renewed attention because these may be used as qubits in a quantum computer.[1] Based on the charge and phase degrees of freedom in Josephson-junction devices, charge[2,3] and phase qubits[4–6] have been developed. Also, a type of solid-state qubit can be realized in a large-area current-biased Josephson junction.[7,8]

Experimentally, coherent oscillations were demonstrated in a Josephson charge qubit prepared in a superposition of two charge states.[2] More recent experimental measurements[9] showed that the charge qubit at suitable working points can have a sufficiently high quality of coherence ($Q_\varphi \approx 2.5 \times 10^4$), corresponding to a decoherence time $T_\varphi \approx 500$ ns. Current-biased Josephson junctions can also have long decoherence times[7,8] and Q_φ can reach 10^4. These exciting experimental advancements demonstrate the potential of Josephson qubits for manufacturing macroscopic quantum-mechanical machines. Towards the practical implementation of a solid-state quantum computer, the next important step would be the coupling of two qubits and then scaling up the architecture to many qubits.

In this work, we present an experimentally implementable method to couple two Josephson charge qubits and to generate and detect macroscopic quantum entangled states in this charge-qubit system. Motivated by very recent experimental results,[9] we employ a superconducting quantum interference device (SQUID) with *two* large Josephson junctions to implement the readout. The generation of the macroscopic entanglement is assisted by applying a microwave field to each charge qubit. The key advantage of our design is that the SQUID can also produce an experimentally feasible and controllable coupling between the two charge qubits. As verified in a single qubit,[9] the coupled charge qubits may be well decoupled from the readout system when the measurement is not implemented. Moreover, our design can be readily extended to coupled multiple[10] qubits as well as any selected pairs (not necessarily neighbors).

The paper is organized as follows. In Sec. II, the controllable coupling between two charge qubits is proposed using a large Josephson junction or a large-junction dc SQUID. Also, we demonstrate how this interbit coupling can be conveniently used to generate the controlled-phase-shift gate. In Sec. III, we study the microwave-assisted macroscopic quantum entanglement in the coupled charge qubits, where the microwave fields are coupled to the qubits via gate capacitances. Section IV focuses on the readout of the quantum states in the coupled-qubit system. Finally, the discussion and conclusion are given in Sec. V.

A. Other qubit coupling schemes

A different type of interbit coupling from the one studied here was proposed using the Coulomb interaction between charges on the islands of the charge qubits.[11] As pointed out in Ref. 1, the interbit coupling in this scheme is not switchable and also it is hard to make the system scalable because only neighboring qubits can be coupled. Implementations of quantum algorithms such as the Deutsch and Bernstein-Vazirani algorithms were studied using a system of Josephson charge qubits,[12] where it was proposed that the nearest-neighbor superconducting islands would be coupled by tunable dc SQUIDs. In Ref. 13, a pair of charge qubits were proposed to be capacitively coupled to a current-biased Josephson junction where, by varying the bias current, the junction can be tuned in and out of resonance with the qubits coupled to it.

Another different type of interbit coupling was proposed[1,3] in terms of the oscillator modes in an LC circuit. In contrast, we use a large junction or a large-junction dc SQUID (but *no* LC circuit) to couple the charge qubits. In our scheme, *both* dc and ac supercurrents can flow through the charge-qubit circuit, while in Refs. 1 and 3 *only* ac supercurrents can flow through the circuit. These yield different interbit couplings (e.g., the $\sigma_y\sigma_y$ type[1,3] as opposed to $\sigma_x\sigma_x$ in our proposal). As revealed in Ref. 10, the $\sigma_x\sigma_x$ type interbit coupling can be conveniently used to formulate an efficient quantum computing scheme.

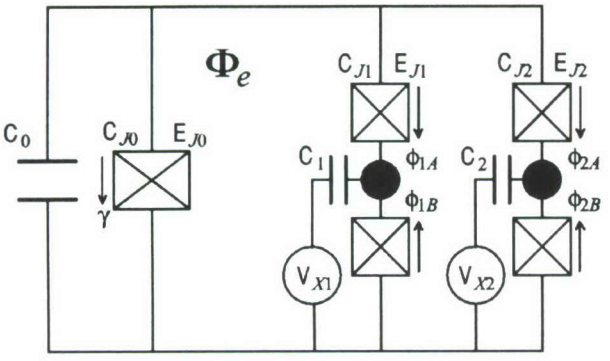

FIG. 1. Schematic diagram of two charge qubits coupled by a large Josephson junction (denoted by a square with an X inside) of coupling energy E_{J0} and capacitance C_{J0}. To make the effective charging energy of the large Josephson junction as small as required, a large capacitance C_0 is placed close to and in parallel with it. Each filled circle denotes a superconducting island, the Cooper-pair box, which is biased by a voltage V_{Xi} via the gate capacitance C_i and coupled to the bulk superconductors by two identical small Josephson junctions (each with a coupling energy E_{Ji} and a capacitance C_{Ji}). Here the arrow near each Josephson junction denotes the chosen direction for the positive phase drop across the corresponding junction.

Moreover, the calculated interbit-coupling terms in Refs. 1 and 3 only apply to the case in which the following two conditions are met:

(i) The eigenfrequency ω_{LC} of the LC circuit is much faster than the quantum manipulation frequencies. This condition *limits* the allowed number N of the qubits in the circuit because ω_{LC} scales with $1/\sqrt{N}$. In other words, this implies that the circuits in Refs. 1 and 3 are not really scalable.

(ii) The phase conjugate to the total charge on the qubit capacitors fluctuates weakly. Our interbit-coupling approach discussed below is free from these two limitations.

II. CONTROLLABLE COUPLING OF CHARGE QUBITS

A. Coupling qubits with a large junction

We first use a large Josephson junction to couple two charge qubits (see Fig. 1). Each qubit is realized by a Cooper-pair box, where a superconducting island with excess charge $\hat{Q}_i = 2e\hat{n}_i$ ($i=1,2$) is weakly coupled to the bulk superconductors via two identical small junctions (with Josephson coupling energy E_{Ji} and capacitance C_{Ji}) and biased by an applied voltage V_{Xi} through a gate capacitance C_i. The large Josephson junction on the left has a coupling energy E_{J0} (much larger than E_{Ji}) and a capacitance C_{J0}. As in the single-qubit case,[9] close to the large Josephson junction, we also place a large capacitance C_0 in parallel with it, so that the effective charging energy of the large Josephson junction can be ignored (even though the capacitance of the large junction might not be large enough). Moreover, we assume that the inductance of the qubit circuit (i.e., the two Cooper-pair boxes with the nearby junctions, and the superconducting lines connecting these two qubits with the large Josephson junction) is much smaller than the Josephson inductance of the large junction. The Hamiltonian of the system can be written as

$$H=\sum_{i=1}^{2}\left[E_{ci}(\hat{n}_i-n_{Xi})^2-E_{Ji}(\cos\hat{\phi}_{iA}+\cos\hat{\phi}_{iB})\right] - E_{J0}\cos\hat{\gamma}, \tag{1}$$

where

$$E_{ci}=\frac{2e^2}{C_i+2C_{Ji}} \tag{2}$$

is the charging energy of the superconducting island and $n_{Xi}=C_iV_{Xi}/2e$ is the reduced offset charge (in units of $2e$) induced by the gate voltage. Flux quantization around loops containing the phase drops of the involved junctions gives the constraint

$$\hat{\phi}_{iA}-\hat{\phi}_{iB}-\hat{\gamma}+\frac{2\pi\Phi_e}{\Phi_0}=0, \quad i=1,2, \tag{3}$$

which gives

$$\hat{\phi}_{iA}=\hat{\phi}_i-\left(\frac{\pi\Phi_e}{\Phi_0}-\frac{1}{2}\hat{\gamma}\right),$$

$$\hat{\phi}_{iB}=\hat{\phi}_i+\left(\frac{\pi\Phi_e}{\Phi_0}-\frac{1}{2}\hat{\gamma}\right), \tag{4}$$

where the average phase drop $\hat{\phi}_i=(\hat{\phi}_{iA}+\hat{\phi}_{iB})/2$ is canonically conjugate to the number, $\hat{n}_i$, of the excess Cooper pairs on the ith superconducting island:

$$[\hat{\phi}_j,\ \hat{n}_j]=i, \quad j=1,2.$$

Here $\hat{\phi}_{iA}$ and $\hat{\phi}_{iB}$ ($i=1,2$) are the phase drops across the small Josephson junctions above (A) and below (B) the ith Cooper-pair box.

The Hamiltonian (1) can be rewritten as

$$H=\sum_{i=1}^{2}\left[E_{ci}(\hat{n}_i-n_{Xi})^2-2E_{Ji}\cos\left(\frac{\pi\Phi_e}{\Phi_0}-\frac{1}{2}\hat{\gamma}\right)\cos\hat{\phi}\right] - E_{J0}\cos\hat{\gamma}. \tag{5}$$

The externally applied flux Φ_e threads the area between the large Josephson junction and the left Cooper-pair box. It induces circulating supercurrents in the qubit circuit. The total circulating supercurrent $\hat{I}$ has contributions from the two charge qubits:

$$\hat{I}=\hat{I}_1+\hat{I}_2, \tag{6}$$

where

$$\hat{I}_i=2I_{ci}\sin\left(\frac{\pi\Phi_e}{\Phi_0}-\frac{1}{2}\hat{\gamma}\right)\cos\hat{\phi}_i, \tag{7}$$

with $I_{ci}=\pi E_{Ji}/\Phi_0$. This total supercurrent flows through the large Josephson junction and it can also be written as

$$\hat{I}=I_0\sin\hat{\gamma}, \tag{8}$$

with $I_0=2\pi E_{J0}/\Phi_0$. From Eqs. (6)–(8) it follows that

$$I_0 \sin\hat{\gamma} = 2\sin\left(\frac{\pi\Phi_e}{\Phi_0} - \frac{1}{2}\hat{\gamma}\right)(I_{c1}\cos\hat{\phi}_1 + I_{c2}\cos\hat{\phi}_2). \tag{9}$$

When the coupling energy $E_{Ji}=\Phi_0 I_{ci}/\pi$ of each Josephson junction connected to the charge box is much smaller than that of the large Josephson junction in the circuit, the phase drop $\hat{\gamma}$ across the large junction will be small. Expanding the operator functions of $\hat{\gamma}$ in Eq. (9) into a series and retaining the terms up to second order of the parameters

$$\eta_i = \frac{I_{ci}}{I_0} \ (<1), \quad i=1,2, \tag{10}$$

we have

$$\hat{\gamma} = 2\sin\left(\frac{\pi\Phi_e}{\Phi_0}\right)(\eta_1\cos\hat{\phi}_1 + \eta_2\cos\hat{\phi}_2) - \sin\left(\frac{2\pi\Phi_e}{\Phi_0}\right)(\eta_1\cos\hat{\phi}_1 + \eta_2\cos\hat{\phi}_2)^2. \tag{11}$$

It is clear that the phase drop $\hat{\gamma}$ across the large Josephson junction is controllable via the applied flux Φ_e.

For Hamiltonian (5), we also expand the operator functions of $\hat{\gamma}$ into a series and retain the terms up to second order of η_i. Moreover, we consider the charging regime with E_{ci} much larger than E_{Ji}. Also, we assume that the temperature is low enough ($k_B T \ll E_{ci}$) and the superconducting gap is larger than E_{ci}, so that quasiparticle tunneling is strongly suppressed. In this case, only the lowest two charge states are important for each qubit operating around the degeneracy point $V_{Xi}=(2n_i+1)e/C_i$. In the spin-$\frac{1}{2}$ representation based on the charge states $|n_i\rangle \equiv |\uparrow\rangle_i$, and $|n_i+1\rangle \equiv |\downarrow\rangle_i$ of each Cooper-pair box, the Hamiltonian of the system can be reduced to

$$H = \sum_{i=1}^{2}[\varepsilon_i(V_{Xi})\sigma_z^{(i)} - \bar{E}_{Ji}\sigma_x^{(i)}] - \chi\sigma_x^{(1)}\sigma_x^{(2)}, \tag{12}$$

with

$$\varepsilon_i(V_{Xi}) = \frac{1}{2}E_{ci}\left[\frac{C_i V_{Xi}}{e} - (2n_i+1)\right] \tag{13}$$

and

$$\bar{E}_{Ji} = E_{Ji}\cos\left(\frac{\pi\Phi_e}{\Phi_0}\right)\xi_i, \tag{14}$$

where

$$\xi_i = 1 - \frac{3}{8}(\eta_i^2 + 3\eta_j^2)\sin^2\left(\frac{\pi\Phi_e}{\Phi_0}\right), \tag{15}$$

and $i,j=1,2$ $(i\neq j)$. The interbit coupling χ is given by

$$\chi = L_J I_{c1} I_{c2}\sin^2\left(\frac{\pi\Phi_e}{\Phi_0}\right), \tag{16}$$

where the large Josephson junction acts as an *effective* inductance of value

$$L_J = \frac{\Phi_0}{2\pi I_0}. \tag{17}$$

It is clear that the interbit coupling is switched off at $\Phi_e = 0$. It is well known that a large Josephson junction can act as an inductance (e.g., Ref. 1). Here we explicitly show a specific way that it can be used to couple qubits.

Retaining up to second-order terms in the expansion parameters η_i, the total circulating current $\hat{I}$ can be written as

$$\hat{I} = 2\sin\left(\frac{\pi\Phi_e}{\Phi_0}\right)(I_{c1}\cos\hat{\phi}_1 + I_{c2}\cos\hat{\phi}_2) - \frac{1}{I_0}\sin\left(\frac{2\pi\Phi_e}{\Phi_0}\right)(I_{c1}\cos\hat{\phi}_1 + I_{c2}\cos\hat{\phi}_2)^2. \tag{18}$$

In the spin-$\frac{1}{2}$ representation, it is given by

$$\hat{I} = \sin\left(\frac{\pi\Phi_e}{\Phi_0}\right)[I_{c1}\sigma_x^{(1)} + I_{c2}\sigma_x^{(2)}] - \frac{1}{4I_0}\sin\left(\frac{2\pi\Phi_e}{\Phi_0}\right)[I_{c1}^2 + I_{c2}^2 + 2I_{c1}I_{c2}\sigma_x^{(1)}\sigma_x^{(2)}], \tag{19}$$

which depends on the states of the charge-qubit system.

B. Coupling qubits with a SQUID

There are somewhat conflicting requirements imposed on this circuit. To obtain a large value for the effective Josephson inductance $L_J=\Phi_0/2\pi I_0$, a relatively small I_0 is needed, so that a large interbit coupling can be achieved. However, when the large Josephson junction is also employed for a readout, it is desirable to use a large I_0. This permits a larger range of I_b, so that a higher resolution in distinguishing qubit states can be achieved in the quantum measurement based on the switching of the supercurrent through the large junction.

These two opposite requirements can be conveniently solved if the leftmost large Josephson junction in Fig. 1 is replaced by a symmetric dc SQUID with two sufficiently large junctions (see Fig. 2). Instead of Φ_e inside the circuit loop between E_{J0} and the first qubit (as in Fig. 1), we now apply a flux Φ_s inside the large-junction dc SQUID loop (see Fig. 2). This SQUID can be used both for coupling the two charge qubits and implementing the readout. When the readout is not active ($I_b=0$), we can choose a suitable flux Φ_s inside the SQUID loop to generate a larger interbit coupling. For $I_b=0$, the reduced Hamiltonian of the coupled-qubit system and the total circulating current I have the same forms as in Eqs. (12) and (19), but with Φ_e and I_0 replaced by $\frac{1}{2}\Phi_s$ and

$$I_0 = 2I_0^s\cos\left(\frac{\pi\Phi_s}{\Phi_0}\right), \tag{20}$$

where $I_0^s = 2\pi E_{J0}^s/\Phi_0$. When the readout is active (see Sec. IV), Φ_s is chosen as zero to obtain a larger effective Josephson coupling energy.

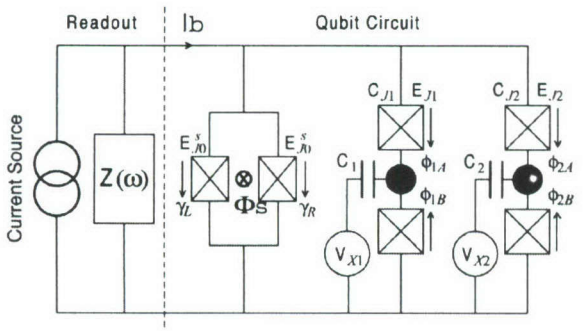

FIG. 2. Schematic diagram of the coupled-qubit circuit with a biased-current source of impedance $Z(\omega)$. The dc SQUID, with two junctions of large E^s_{J0}, plays the role of both coupling the charge qubits and implementing the readout. Here the large capacitance C_0 placed close to and in parallel with the dc SQUID is included in the impedance $Z(\omega)$.

C. Controlled-phase-shift gate

When the system works at the degeneracy points with $\varepsilon_i(V_{Xi})=0$, the Hamiltonian becomes

$$H=-\bar{E}_{J1}\sigma_x^{(1)}-\bar{E}_{J2}\sigma_x^{(2)}-\chi\sigma_x^{(1)}\sigma_x^{(2)}. \tag{21}$$

For instance, when $\bar{E}_{Ji}>0$, $i=1,2$, its four eigenvalues are

$$\bar{E}_{J1}+\bar{E}_{J2}-\chi,$$

$$\bar{E}_{J1}-\bar{E}_{J2}+\chi,$$

$$\bar{E}_{J2}-\bar{E}_{J1}+\chi,$$

$$-\bar{E}_{J1}-\bar{E}_{J2}-\chi. \tag{22}$$

The corresponding eigenstates are $|e_1,e_2\rangle$, $|e_1,g_2\rangle$, $|g_1,e_2\rangle$, and $|g_1,g_2\rangle$, where

$$|e_i\rangle=\frac{1}{\sqrt{2}}(|\uparrow\rangle_i-|\downarrow\rangle_i),$$

$$|g_i\rangle=\frac{1}{\sqrt{2}}(|\uparrow\rangle_i+|\downarrow\rangle_i). \tag{23}$$

Because they are also the eigenstates of the two uncoupled charge qubits, when prepared initially at an eigenstate, the system does not evolve to an entangled state even in the presence of interbit coupling. As shown below, one can take advantage of this property to implement the measurement. In addition, this property can be used to construct efficient conditional gates. For instance, if

$$\bar{E}_{J1}=\bar{E}_{J2}=\chi, \tag{24}$$

the controlled-phase-shift (CPS) gate is given by

$$U_{\mathrm{CPS}}(\tau)=e^{i\chi\tau/\hbar}U, \tag{25}$$

with

$$U=e^{-iH\tau/\hbar}=\exp\{i(\chi\tau/\hbar)[\sigma_x^{(1)}+\sigma_x^{(2)}+\sigma_x^{(1)}\sigma_x^{(2)}]\}, \tag{26}$$

at $\tau=\pi\hbar/4\chi$. This gate transforms the basis states $|e_1,e_2\rangle$, $|e_1,g_2\rangle$, $|g_1,e_2\rangle$, and $|g_1,g_2\rangle$ as

$$\begin{pmatrix}|e_1,e_2\rangle\\|e_1,g_2\rangle\\|g_1,e_2\rangle\\|g_1,g_2\rangle\end{pmatrix}\rightarrow\begin{pmatrix}1&0&0&0\\0&1&0&0\\0&0&1&0\\0&0&0&-1\end{pmatrix}\begin{pmatrix}|e_1,e_2\rangle\\|e_1,g_2\rangle\\|g_1,e_2\rangle\\|g_1,g_2\rangle\end{pmatrix}. \tag{27}$$

The generation of this conditional two-bit gate is efficient because the condition (24) can be realized in one step via changing the gate voltages V_{Xi}, $i=1,2$, and the flux Φ_s simultaneously. Also, the architecture is scalable because multiple charge qubits can be coupled by connecting them in parallel with the large-junction SQUID. If the two Josephson junctions in each Cooper-pair box are replaced by small-junction dc SQUIDs, any selected pairs of charge qubits (not necessarily neighbors) can be coupled.[10]

III. MICROWAVE-ASSISTED MACROSCOPIC ENTANGLEMENT

When a microwave field is applied to the Josephson charge qubit, Rabi oscillations occur in the system.[14] These oscillations can also be demonstrated by coupling a quantum resonator to the charge qubit.[15] Here we apply the microwave field to the Cooper-pair box via the gate capacitance, as in Refs. 9 and 14, but each charge qubit is driven by a different microwave field.[16] In this situation, n_{Xi} in Eq. (1) is replaced by

$$n_{Xi}+\hat{n}_{ACi}=n_{Xi}+\left(\frac{C_i d_i}{2e}\right)\hat{\mathcal{E}}_{ACi}. \tag{28}$$

Here d_i is the thickness of the gate capacitor and

$$\hat{\mathcal{E}}_{ACi}=\mathcal{E}_{\lambda i}\,a_i+\mathcal{E}^*_{\lambda i}\,a_i^\dagger \tag{29}$$

is the microwave electric field in the gate capacitor of the ith Cooper-pair box, where a_i is the annihilation operator of the microwave mode. Because the microwave wavelength is much larger than d_i, $\mathcal{E}_{\lambda i}$ can be considered constant in the gate capacitor. In the charging regime, the Hamiltonian of the system (including the microwave fields) can be written as

$$H=\sum_{i=1}^{2}[\varepsilon_i(V_{Xi})\sigma_z^{(i)}-\bar{E}_{Ji}\sigma_x^{(i)}+\hbar\omega_{\lambda i}\,a_i a_i^\dagger + \sigma_z^{(i)}(K_i\,a_i+K_i^*\,a_i^\dagger)]-\chi\,\sigma_x^{(1)}\sigma_x^{(2)}, \tag{30}$$

where

$$K_i=\left(\frac{E_{ci}C_i d_i}{2e}\right)\mathcal{E}_{\lambda i}. \tag{31}$$

Here, we also consider the system working at the degeneracy points $\varepsilon_i(V_{Xi})=0$, $i=1,2$. When $\hbar\omega_{\lambda i}\approx 2|\bar{E}_{Ji}|$ and under the rotating-wave approximation, the Hamiltonian is cast to

$$H=\sum_{i=1}^{2}\left[-\bar{E}_{Ji}\sigma_x^{(i)}+\hbar\omega_{\lambda i}a_i a_i^{\dagger}+(K_i|e_i\rangle\langle g_i|a_i+\text{H.c.})\right]$$

$$-\chi\sigma_x^{(1)}\sigma_x^{(2)}. \tag{32}$$

Without interbit coupling, each Josephson charge qubit exhibits Rabi oscillations between states $|e_i,l_i\rangle$ and $|g_i,l_i+1\rangle$, where $|l_i\rangle$ is a photon state with l_i photons. For the resonant case with $\hbar\omega_{\lambda i}=2|\bar{E}_{Ji}|$, the eigenvalues of each charge-qubit system are given by

$$\epsilon_{\pm}^{(i)} = E_{0i} \pm \frac{1}{2}\hbar\Omega_i, \tag{33}$$

where

$$E_{0i}=\hbar\omega_{\lambda i}(l_i+1), \tag{34}$$

and

$$\Omega_i=\frac{2}{\hbar}|K_i|\sqrt{l_i+1} \tag{35}$$

is the Rabi frequency. Though entanglement occurs between each charge qubit and the nonclassical microwave field, the two qubits do not entangle with each other since the system evolves as

$$|\Psi(t)\rangle=|\psi_1(t)\rangle|\psi_2(t)\rangle, \tag{36}$$

where

$$|\psi_i(t)\rangle=\sin(\Omega_i t)|e_i,l_i\rangle+\cos(\Omega_i t)|g_i,l_i+1\rangle \tag{37}$$

if the system is initially prepared at state $|g_1,g_2,l_1+1,l_2+1\rangle$. However, in the presence of microwave fields, when the interbit coupling is switched on, the coupled-qubit system exhibits complicated quantum oscillations and it will evolve to the entangled state. For instance, in the resonant situation, the eigenvalues are given by

$$\begin{aligned}\varepsilon_{1,4} &= E_{01}+E_{02}\pm\hbar\Lambda_1,\\ \varepsilon_{2,3} &= E_{01}+E_{02}\pm\hbar\Lambda_2,\end{aligned} \tag{38}$$

where

$$\Lambda_{1,2}=[(\Omega_1\pm\Omega_2)^2+(\chi/\hbar)^2]^{1/2}. \tag{39}$$

The state of the coupled-qubit system evolves as

$$\begin{aligned}|\Psi(t)\rangle=&C_1(t)|e_1,e_2,l_1,l_2\rangle+C_2(t)|e_1,g_2,l_1,l_2+1\rangle\\ &+C_3(t)|g_1,e_2,l_1+1,l_2\rangle\\ &+C_4(t)|g_1,g_2,l_1+1,l_2+1\rangle.\end{aligned} \tag{40}$$

For the system prepared initially at $|g_1,g_2,l_1+1,l_2+1\rangle$,

$$\begin{aligned}C_1(t)&=\frac{1}{2}\{R_2(t)-R_1(t)+i(\chi/\hbar)[S_2(t)-S_1(t)]\},\\ C_2(t)&=\frac{1}{2}[(\Omega_1+\Omega_2)S_1(t)+(\Omega_1-\Omega_2)S_2(t)],\\ C_3(t)&=\frac{1}{2}[(\Omega_1+\Omega_2)S_1(t)-(\Omega_1-\Omega_2)S_2t)],\\ C_4(t)&=\frac{1}{2}\{R_1(t)+R_2(t)+i(\chi/\hbar)[S_1(t)+S_2(t)]\},\end{aligned} \tag{41}$$

where

$$R_i(t)=\cos(\Lambda_i t), \quad S_i(t)=\frac{\sin(\Lambda_i t)}{\Lambda_i}. \tag{42}$$

For a two-level system interacting with a single-mode field, the Rabi oscillations can be explained using either quantum or semiclassical theory, where the single-mode field is described quantum mechanically or treated as a classical field.[17] Here the quantum oscillations of coupled charge qubits (namely, the Rabi oscillations in coupled two-level systems) are studied using quantum theory, where the microwave field coupled to each qubit is quantized. This also applies to the classical-field case, in which the quantum oscillations are still described by Eq. (40), but $|e_1,e_2,l_1,l_2\rangle$, $|e_1,g_2,l_1,l_2+1\rangle$, $|g_1,e_2,l_1+1,l_2\rangle$, and $|g_1,g_2,l_1+1,l_2+1\rangle$ are replaced by $|e_1,e_2\rangle$, $|e_1,g_2\rangle$, $|g_1,e_2\rangle$, and $|g_1,g_2\rangle$.

Figure 3 shows the occupation probability $|C_1(t)|^2$ as a function of time t. For instance, when $|C_1(t)|^2\simeq 1$, both charge qubits are in their excited states. It can be seen that $|C_1(t)|^2$ looks very different when the interbit coupling is switched on or off. The macroscopic entanglement between the two coupled qubits can be explicitly shown at $\Omega_1=\Omega_2$ $(=\Omega)$. In this case, when $t_{\text{ent}}=n\pi\hbar/W\chi$, with $n=1,2,3,\ldots$, and

$$W=[(2\hbar\Omega/\chi)^2+1]^{1/2}. \tag{43}$$

$|\Psi(t)\rangle$ becomes

$$\begin{aligned}|\Psi(t_{\text{ent}})\rangle=&C_1(t_{\text{ent}})|e_1,e_2,l_1,l_2\rangle\\ &+C_4(t_{\text{ent}})|g_1,g_2,l_1+1,l_2+1\rangle,\end{aligned} \tag{44}$$

where

$$\begin{aligned}C_1(t_{\text{ent}})&=\frac{1}{2}[-\cos(n\pi)+\exp(in\pi/W)],\\ C_4(t_{\text{ent}})&=\frac{1}{2}[\cos(n\pi)+\exp(in\pi/W)].\end{aligned} \tag{45}$$

The peaks away from either zero or 1 shown in Fig. 3(a) correspond to this kind of entangled state. Furthermore, if suitable values of W are taken, the maximally entangled state with $|C_1|^2=|C_4|^2=\frac{1}{2}$ can be derived. This state is a macroscopic Schrödinger-cat state of the two charge qubits. For instance, if $\hbar\Omega/\chi=\sqrt{3}/2$, the coupled-qubit system evolves to the maximally entangled state at the times given by

$$t_{\text{ent}}^{(\max)}=(2l+1)\pi\hbar/2\chi, \quad l=0,1,2,\ldots. \tag{46}$$

This entangled state corresponds to the half-probability peaks in Fig. 3(c).

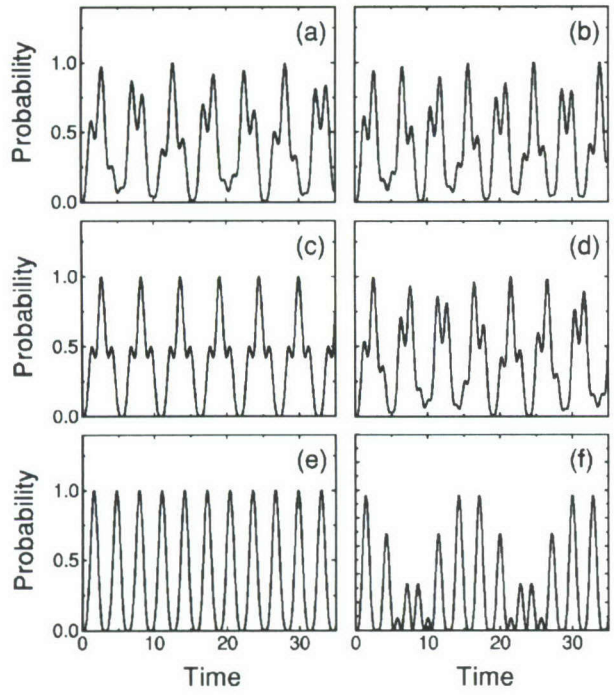

FIG. 3. Occupation probability $|C_1(t)|^2$ as a function of time. (a) $\Omega_2=\Omega_1, \chi/\hbar=\Omega_1$; (b) $\Omega_2=1.2\Omega_1, \chi/\hbar=\Omega_1$; (c) $\Omega_2=\Omega_1, \chi/\hbar=\sqrt{3}\Omega_1/2$; (d) $\Omega_2=1.2\Omega_1, \chi/\hbar=\sqrt{3}\Omega_1/2$; (e) $\Omega_2=\Omega_1, \chi=0$; (f) $\Omega_2=1.2\Omega_1, \chi=0$. The time is in units of Ω_1^{-1}.

IV. QUANTUM MEASUREMENT

To implement a readout, we bias a current pulse I_b to the qubit circuit (see Fig. 2), as in the single-qubit case.[9] Now, a term $-\Phi_0 I_b \hat{\delta}/2\pi$, with

$$\hat{\delta}=\frac{1}{4}\left[\hat{\gamma}_L+\hat{\gamma}_R+\sum_{i=1,2}(\hat{\phi}_{iA}-\hat{\phi}_{iB})\right], \tag{47}$$

should be added to the Hamiltonian (1), where $\hat{\delta}$ is the average phase drop of the total qubit circuit and it can be written as

$$\hat{\delta}=\hat{\gamma}-\frac{\pi\Phi_s}{2\Phi_0}, \tag{48}$$

with $\hat{\gamma}=\frac{1}{2}(\hat{\gamma}_L+\hat{\gamma}_R)$. Here we set the flux Φ_s equal to zero to have a larger effective Josephson coupling energy. In the spin-$\frac{1}{2}$ representation based on charge states, the Hamiltonian of the system is also reduced to Eq. (12). The interbit coupling is here induced by the bias current and given by

$$\chi=L_J I_{c1} I_{c2}\sin^2(\gamma_0/2), \tag{49}$$

where the effective inductance is

$$L_J=\frac{\Phi_0}{2\pi I_0\cos\gamma_0}, \tag{50}$$

and

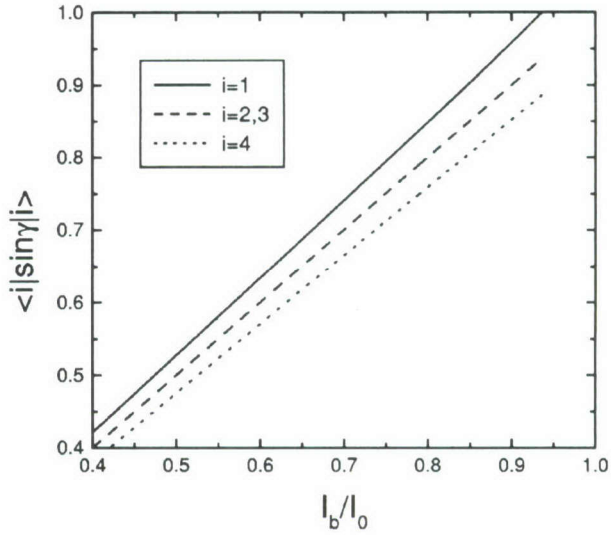

FIG. 4. Eigenstate dependence of the supercurrent through the SQUID as a function of the bias current I_b. Here, $E_{J1}=E_{J2}=\frac{1}{5}E_{J0}^s$, $|1\rangle=|e_1,e_2\rangle$, $|2\rangle=|e_1,g_2\rangle$, $|3\rangle=|g_1,e_2\rangle$, and $|4\rangle=|g_1,g_2\rangle$.

$$\gamma_0=\sin^{-1}(I_b/I_0), \tag{51}$$

with $I_0=4\pi E_{J0}^s/\Phi_0$, and $I_b<I_0$. The intrabit couplings are

$$\bar{E}_{Ji}=E_{Ji}\cos(\gamma_0/2)\ \xi_i, \tag{52}$$

where

$$\xi_i=1-\alpha(\eta_i^2+3\eta_j^2)\sin^2(\gamma_0/2), \tag{53}$$

with

$$\alpha=\frac{2+\cos\gamma_0}{8\cos^3\gamma_0}, \tag{54}$$

and $i,j=1,2$ $(i\neq j)$. The supercurrent through the SQUID,

$$I_0\sin\hat{\gamma}=I_b-\sin(\gamma_0/2)[I_{c1}\sigma_X^{(1)}+I_{c2}\sigma_X^{(2)}]+\frac{1}{4I_0}\tan\gamma_0[I_{c1}^2+I_{c2}^2+2I_{c1}I_{c2}\sigma_X^{(1)}\sigma_X^{(2)}], \tag{55}$$

has contributions from both the bias current and the current from the Josephson charge qubits.

At the working points with $\varepsilon_i(V_{Xi})=0$, the eigenstates of the system are also $|e_1,e_2\rangle$, $|e_1,g_2\rangle$, $|g_1,e_2\rangle$, and $|g_1,g_2\rangle$. In Fig. 4, we show the dependence of the supercurrents through the SQUID on the eigenstates of the charge-qubit system. The supercurrents through the SQUID increase with the bias current and the difference between the supercurrents at different (nondegenerate) eigenstates widens. For the measurement setup shown in Fig. 2, the supercurrent through the SQUID is the largest at the eigenstate $|e_1,e_2\rangle$ and it first reaches the maximal value I_0 (namely, the critical current) when the bias current I_b approaches a value I_{SW} near I_0.

Around this value, the supercurrent through the SQUID switches, with a very large probability P_1, from the zero-voltage state to the dissipative nonzero-voltage state in the quasiparticle-current branch and the measurement on the voltage is carried out. However, due to environmental noise as well as thermal and quantum fluctuations, the switching actually occurs before the supercurrent through the SQUID reaches I_0. At $I_b \sim I_{SW}$, the supercurrents through the SQUID will also switch to the nonzero voltage state at other eigenstates, but the switching probabilities are small. In the ideal case, if the difference between the large switching probability P_1 and the small ones is close to 1, then, in principle, a single-shot readout would be achieveable. As shown in Ref. 9, the Josephson-junction switching experiment can provide sufficient accuracy to discriminate the state $|e_1,e_2\rangle$ from others.

The operation and readout of the macroscopic entanglement of the coupled-qubit system can be implemented by simultaneously applying a pulsed microwave field (with the same duration τ) to each charge qubit. The sequence would be:

(i) before the microwave fields are applied, the flux Φ_s through the SQUID is set equal to zero and no interbit coupling exists;

(ii) the flux Φ_s is switched on to a certain nonzero value exactly at the start of the microwave pulse and off at the end of the microwave pulse. Within the microwave pulse duration τ, the evolution of the system is described by Eq. (40);

(iii) a pulsed bias current I_b is applied to perform a measurement after the microwave pulse.

During the measurement, the quantum state of the charge-qubit system collapses to the eigenstate $|e_1,e_2\rangle$ with probability $|C_1(\tau)|^2$. This probability is proportional to the switching probability P_1 of the SQUID. Because of relaxation, the envelope of the measured switching probability P_1 decays exponentially with time. This is used to obtain the relaxation time.[2,9] Ramsey fringes of the probability P_1 can be used[9] to determine the decoherence time of the coupled-qubit system. For each given microwave pulse duration τ, through repeated measurements, one can determine the occupation probability $|C_1(\tau)|^2$ and thus deduce the information about the macroscopic entanglement between the coupled charge qubits [see Figs. 3(a) and 3(c)].

V. DISCUSSION AND CONCLUSION

Finally, we estimate some important parameters using available quantities for the single charge qubit. Here we consider the maximally entangled case shown in Fig. 3(c), in which $\Omega_1=\Omega_2=\Omega$, and

$$\frac{\chi}{\hbar}=\frac{\sqrt{3}}{2}\Omega.$$

Taking $2\pi/\Omega \simeq 0.22\mu$s, as derived from the Rabi oscillation of the measured switching probability,[9] we have $\chi/\hbar \approx 0.25$ GHz. Reference 9 also gives $E_J/\hbar \approx 16.5$ GHz. Choosing

$$E_{J0}^s \approx 5E_{Ji} \approx 5E_J,$$

and using the relation for χ, we obtain $\Phi_s \approx 0.35\Phi_0$. For $\Phi_s=0$, the expansion parameters are

$$\eta_i=\frac{I_{0i}}{I_0}\approx 0.05$$

for $E_{J0}^s \approx 5E_{Ji}$. When $\Phi_s \approx 0.35\Phi_0$, they become $\eta_i \approx 0.14$. The results are sufficiently accurate when $\bar{E}_{Ji}$ and χ are retained up to second- and higher-order terms in the expansion parameters η_i. When Φ_s approaches $\Phi_0/2$, the interbit coupling strengthens. The reduced Hamiltonian of the system also has the same form as Eq. (12), but higher-order terms in the expansion parameters should be included to obtain accurate results.

Here we consider the charging regime with $E_{ci} \gg E_{Ji}$ in order to obtain analytical results. We expect that the interbit coupling can still be realized in the regime with $E_{ci} \sim E_{Ji}$, i.e., the regime used by the Saclay group in the experiment on a single Josephson qubit.[9] In this latter regime, the results can only be obtained numerically, but a relatively long decoherence time would be expected for the coupled-qubit system to work at the degeneracy points because at these points the states are more stable against the variations of both the offset charges and the flux Φ_e or Φ_s.

Very recently, quantum oscillations were experimentally observed in two coupled charge qubits.[18] Also, a novel method for the controllable coupling of charge qubits was proposed using a variable electrostatic transformer.[19] In contrast with our interbit coupling scheme, these studies involve capacitively-coupled (as opposed to inductively-coupled) charge qubits. The main advantage of this inductive coupling among qubits is that it allows a controllable link between any selected qubits, not necessarily nearest neighbors.

In conclusion, we employ a large-junction SQUID to couple Josephson charge qubits and implement a readout. This architecture is readily scalable to multiple qubits. When the system works at the degeneracy points, where the dephasing effects are suppressed, it is shown that the macroscopic entanglement can be generated with the assistance of microwave fields. Also, we show the quantum measurement of the macroscopic entanglement.

ACKNOWLEDGMENTS

We thank X. Hu and B. Plourde for useful comments. We acknowledge support from the U.S. ARDA, AFOSR, and the U.S. National Science Foundation Grant No. EIA-0130383.

*Corresponding author. Email address: nori@umich.edu

[1] See, e.g., Y. Makhlin, G. Schön, and A. Shnirman, Rev. Mod. Phys. **73**, 357 (2001), and references therein.

[2] Y. Nakamura, Yu. A. Pashkin, and J. S. Tsai, Nature (London) **398**, 786 (1999).

[3] Y. Makhlin, G. Schön, and A. Shnirman, Nature (London) **398**, 305 (1999).

[4] J. E. Mooij, T. P. Orlando, L. Levitov, L. Tian, C. H. van der Wal,

and S. Lloyd, Science **285**, 1036 (1999); T. P. Orlando, J. E. Mooij, L. Tian, C. H. van der Wal, L. S. Levitov, S. Lloyd, and J. J. Mazo, Phys. Rev. B **60**, 15 398 (1999).

[5] C. H. van der Wal, A. C. J. ter Haar, F. K. Wilhelm, R. N. Schouten, C. J. P. M. Harmans, T. P. Orlando, S. Lloyd, and J. E. Mooij, Science **290**, 773 (2000).

[6] J. R. Friedman, V. Patel, W. Chen, S. K. Tolpygo, and J. E. Lukens, Nature (London) **406**, 43 (2000).

[7] Y. Yu, S. Han, X. Chu, S.-I. Chu, and Z. Wang, Science **296**, 889 (2002).

[8] J. M. Martinis, S. Nam, J. Aumentado, and C. Urbina, Phys. Rev. Lett. **89**, 117901 (2002).

[9] D. Vion, A. Aassime, A. Cottet, P. Joyez, H. Pothier, C. Urbina, D. Esteve, and M. H. Devoret, Science **296**, 886 (2002); A. Cottet, D. Vion, A. Aassime, P. Joyez, D. Esteve, and M. H. Devoret, Physica C **367**, 197 (2002).

[10] J. Q. You, J. S. Tsai, and F. Nori, Phys. Rev. Lett. **89**, 197902 (2002). A longer version of this work is available online in cond-mat/0306208.

[11] F. Plastina, R. Fazio, and G. M. Palma, Phys. Rev. B **64**, 113306 (2001).

[12] J. Siewert and R. Fazio, Phys. Rev. Lett. **87**, 257905 (2001).

[13] A. Blais, A. Maassen van den Brink, and A. M. Zagoskin, Phys. Rev. Lett. **90**, 127901 (2003).

[14] Y. Nakamura, Yu. A. Pashkin, and J. S. Tsai, Phys. Rev. Lett. **88**, 047901 (2002).

[15] A. D. Armour, M. P. Blencowe, and K. C. Schwab, Phys. Rev. Lett. **88**, 148301 (2002); O. Buisson and F. W. J. Hekking, in *Macroscopic Quantum Coherence and Quantum Computing* (Kluwer Academic, Dordrecht, 2001), pp. 137–145; F. W. J. Hekking, O. Buisson, F. Balestro, and M. G. Vergniory, cond-mat/0201284 (unpublished); F. Marquardt and C. Bruder, Phys. Rev. B **63**, 054514 (2001).

[16] J. Q. You and F. Nori, cond-mat/0306207, Phys. Rev. B (to be published) studied the quantum dynamics of a Cooper-pair box with a nonclassical microwave *magnetic* field going through the superconducting loop, instead of a microwave voltage (electric) oscillation applied to the gate capacitance.

[17] M. O. Scully and M. S. Zubairy, *Quantum Optics* (Cambridge University, Cambridge, England, 1997), Chaps. 5 and 6.

[18] Yu. A. Pashkin, T. Yamamoto, O. Astafiev, Y. Nakamura, D. V. Averin, and J. S. Tsai, Nature (London) **421**, 823 (2003).

[19] D. V. Averin and C. Bruder, cond-mat/0304166 (unpublished).

Quantum information processing with superconducting qubits in a microwave field

J. Q. You[1,2,3] and Franco Nori[1,2,*]

[1]*Frontier Research System, The Institute of Physical and Chemical Research (RIKEN), Wako-shi 351-0198, Japan*

[2]*Center for Theoretical Physics, Physics Department, Center for the Study of Complex Systems, The University of Michigan, Ann Arbor, Michigan 48109-1120, USA*

[3]*National Laboratory for Superlattices and Microstructures, Institute of Semiconductors, Chinese Academy of Sciences, Beijing 100083, China*

(Received 16 June 2003; published 22 August 2003)

We investigate the quantum dynamics of a Cooper-pair box with a superconducting loop in the presence of a nonclassical microwave field. We demonstrate the existence of Rabi oscillations for both single- and multi-photon processes and, moreover, we propose a new quantum computing scheme (including one-bit and conditional two-bit gates) based on Josephson qubits coupled through microwaves.

DOI: 10.1103/PhysRevB.68.064509 PACS number(s): 74.50.+r, 03.67.Lx, 85.25.Cp

I. INTRODUCTION

A. Background

Quantum computing deals with the processing of information according to the laws of quantum mechanics. Within the last few years, it has attracted considerable attention because quantum computers are expected to be capable of performing certain tasks which no classical computers can do in practical time scales. Early proposals for quantum computers were mainly based on quantum optical systems, such as those utilizing laser-cooled trapped ions,[1,2] photon or atoms in quantum electrodynamical (QED) cavities,[3,4] and nuclear magnetic resonance.[5] These systems are well isolated from their environment and satisfy the low-decoherence criterion for implementing quantum computing. Moreover, due to quantum error correction algorithms,[5] now decoherence[6] is not regarded as an insurmountable barrier to quantum computing. Because scalability of quantum computer architectures to many qubits is of central importance for realizing quantum computers of practical use, considerable efforts have recently been devoted to solid-state qubits. Proposed solid-state architectures include those using electron spins in quantum dots,[7–9] electrons on helium,[10] and Josephson-junction (JJ) charge (see, e.g., Refs. 11–13 and 15) and JJ flux (see, e.g., Refs. 14 and 15) devices. These qubit systems have the advantage of relatively long coherent times and are expected to be scalable to large-scale networks using modern microfabrication techniques.

The Josephson charge qubit is achieved in a Cooper-pair box,[11] which is a small superconducting island weakly coupled to a bulk superconductor, while the Josephson flux qubit is based on two different flux states in a small superconducting-quantum-interference-device (SQUID) loop.[14,15] Cooper-pair tunneling and energy-level splitting associated with the superpositions of charge states were experimentally demonstrated in a Cooper-pair box,[16,17] and recently the eigenenergies and the related properties of the superpositions of different flux states were observed in SQUID loops by spectroscopic measurements.[18] In particular, Nakamura *et al.*[19] demonstrated the quantum coherent oscillations of a Josephson charge qubit prepared in a superposition of two charge states. In addition, Vion *et al.*[20] extended coherent oscillations to the charge-flux regime and Chiorescu *et al.*[21] studied the quantum dynamics of the flux qubit. Moreover, two charge qubits were capacitively coupled by Pashkin *et al.*[22] and coherent oscillations were also observed in this coupled-qubit system. Furthermore, other superconducting devices (e.g., Refs. 23 and 24) have also exhibited coherent oscillations. In addition, several other types of studies (see, for instance, Refs. 25 and 26) have been made on superconducting qubits.

B. This work

In this paper, we show that the coupled system of a Cooper-pair box and a cavity photon mode undergoes Rabi oscillations and propose a different quantum computing scheme based on Josephson charge qubits.[27] The microwave-controlled approach proposed in our paper has the significant advantage that *any* two qubits (*not* necessarily neighbors) can be effectively coupled through photons in the cavity. In addition to the advantages of a superconducting device exhibiting quantum coherent effects in a macroscopic scale as well as the controllable feature of the Josephson charge qubit by *both* gate voltage *and* external flux, the motivation for this scheme is fourfold:

(i) The experimental measurements[16] showed that the energy difference between the two eigenstates in a Cooper-pair box lies in the microwave region and the eigenstates can be effectively interacted by the microwave field.

(ii) A single photon can be readily prepared in a *high-Q* QED cavity using the Rabi precession in the microwave domain.[28] Moreover, using a QED cavity, Ref. 29 produced a reliable source of photon number states on demand. In addition, the cavity in Ref. 29 was tuned to ~ 21 GHz, which is close to the 20 GHz microwave frequency used in a very recent experiment[30] on the Josephson charge qubit. Furthermore, the Q value of the cavity is 4×10^{10} (giving a very large photon lifetime of 0.3 sec).

(iii) Our quantum computer proposal should be scalable to 10^6–10^8 charge qubits in a microwave cavity, since the dimension of a Cooper-pair box is $\sim 10-1\,\mu$m.

(iv) The QED cavity has the advantage that *any* two qubits (*not* necessarily neighbors) can be effectively coupled through photons in the cavity.

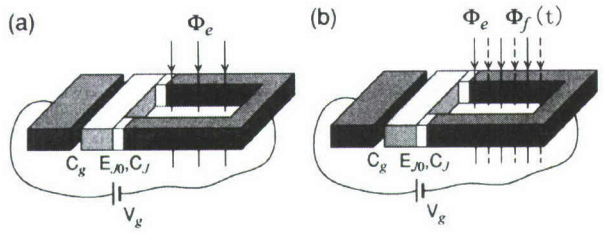

FIG. 1. Cooper-pair box with a SQUID loop, where the charge box is coupled to a segment of a superconducting ring via two identical Josephson junctions, shown in white above, and a voltage V_g is applied to the charge box through a gate capacitor C_g (on the left side of the above diagram). (a) A static magnetic flux Φ_e, as denoted by the solid lines with arrows, pierces the SQUID loop to control the effective Josephson coupling energy. (b) In addition to Φ_e, a microwave field $\Phi_f(t)$, schematically shown above by the dashed lines with arrows, is also applied through the SQUID loop.

Also, we study multiphoton processes in the Josephson charge qubit since, in contrast to the usual Jaynes-Cummings model (see, e.g., Chap. 10 in Ref. 31), the Hamiltonian includes higher-order interactions between the two-level system and the nonclassical microwave field. As shown by the very recent experiment on Rabi oscillations in a Cooper-pair box,[30] these higher-order interactions may be important in the Josephson charge-qubit system.

Note that the driving microwave field is typically generated using an *electrical* voltage acting on the charge qubit via a gate capacitor. Here, the microwave field is applied as a *magnetic* flux piercing the SQUID loop of the qubit in order to perform the unitary transformations needed for quantum computing.

The dynamics of a Josephson charge qubit coupled to a quantum resonator was studied in Ref. 32. In contrast to our study here, the model in Ref. 32 involves: (a) only one qubit, (b) only the Rabi oscillation with a single excitation quantum of the resonator (as opposed to one or more photons), and (c) *no* quantum computing scheme.

II. CHARGE QUBIT IN A CAVITY

A. Cooper-pair box with a SQUID loop

We study the Cooper-pair box with a SQUID loop.[11,15,19] In this structure, the superconducting island with Cooper-pair charge $Q=2ne$ is coupled to a segment of a superconducting ring via two Josephson junctions (each with capacitance C_J and Josephson coupling energy E_{J0}). Also, a voltage V_g is coupled to the superconducting island through a gate capacitor C_g; the gate voltage V_g is externally controlled and used to induce offset charges on the island. A schematic illustration of this single-qubit structure is given in Fig. 1(a). The Hamiltonian of the system is

$$H=4E_c\left(n-\frac{C_gV_g}{2e}\right)^2-E_J(\Phi)\cos\varphi, \tag{1}$$

where

$$E_c=\frac{e^2}{2(C_g+2C_J)} \tag{2}$$

is the single-particle charging energy of the island and

$$E_J(\Phi)=2E_{J0}\cos\left(\frac{\pi\Phi}{\Phi_0}\right) \tag{3}$$

is the effective Josephson coupling. The number n of the extra Cooper pairs on the island and average phase drop

$$\varphi=\frac{1}{2}(\varphi_1+\varphi_2)$$

are canonically conjugate variables. The gauge-invariant phase drops φ_1 and φ_2 across the junctions are related to the total flux Φ through the SQUID loop by the constraint

$$\varphi_2-\varphi_1=2\pi\frac{\Phi}{\Phi_0}, \tag{4}$$

where $\Phi_0=h/2e$ is the flux quantum.

This structure is characterized by two energy scales, i.e., the charging energy E_c and the coupling energy E_{J0} of the Josephson junction. In the charging regime $E_c\gg E_{J0}$ and at low temperatures $k_BT\ll E_c$, the charge states $|n\rangle$ and $|n+1\rangle$ become dominant as the *controllable* gate voltage is adjusted to $V_g\sim(2n+1)e/C_g$. Here, the superconducting gap is assumed to be larger than E_c, so that quasiparticle tunneling is greatly reduced in the system.

Here we ignore self-inductance effects on the single-qubit structure.[33] Now Φ reduces to the classical variable Φ_e, where Φ_e is the flux generated by the applied *static* magnetic field. In the spin-$\frac{1}{2}$ representation with charge states $|\uparrow\rangle=|n\rangle$ and $|\downarrow\rangle=|n+1\rangle$, the reduced two-state Hamiltonian is given by[11,15]

$$H=\varepsilon(V_g)\,\sigma_z-\frac{1}{2}E_J(\Phi_e)\sigma_x, \tag{5}$$

where

$$\varepsilon(V_g)=2E_c\left[\frac{C_gV_g}{e}-(2n+1)\right]. \tag{6}$$

This single-qubit Hamiltonian has two eigenvalues

$$E_{\pm}=\pm\frac{1}{2}E, \tag{7}$$

with

$$E=[4\varepsilon^2(V_g)+E_J^2(\Phi_e)]^{1/2}, \tag{8}$$

and eigenstates

$$|e\rangle=\cos\xi\ |\uparrow\rangle-\sin\xi\ |\downarrow\rangle,$$

$$|g\rangle=\sin\xi\ |\uparrow\rangle+\cos\xi\ |\downarrow\rangle, \tag{9}$$

with

$$\xi=\frac{1}{2}\tan^{-1}\left(\frac{E_J}{2\varepsilon}\right). \tag{10}$$

Using these eigenstates as new basis, the Hamiltonian takes the diagonal form

$$H=\frac{1}{2}E\rho_z, \tag{11}$$

where

$$\rho_z=|e\rangle\langle e|-|g\rangle\langle g|. \tag{12}$$

Here we employ $\{|e\rangle,|g\rangle\}$ to represent the qubit.

B. Interaction of the charge qubit with a microwave field

When a *nonclassical* microwave field is applied, the total flux Φ is a quantum variable

$$\Phi=\Phi_e+\Phi_f(t), \tag{13}$$

where Φ_f is the microwave-field-induced flux through the SQUID loop [see Fig. 1(b)]. Here we assume that a single-qubit structure is embedded in a QED microwave cavity with only a single-photon mode λ. Generally, the vector potential of the nonclassical microwave field is written as

$$\begin{aligned}\mathbf{A}(\mathbf{r})&=\mathbf{u}_\lambda(\mathbf{r})a+\mathbf{u}_\lambda^*(\mathbf{r})a^\dagger\\&=|\mathbf{u}_\lambda(\mathbf{r})|(e^{-i\theta}a+e^{i\theta}a^\dagger)\hat{\mathbf{A}},\end{aligned} \tag{14}$$

where $a^\dagger(a)$ is the creation (annihilation) operator of the cavity mode. Thus the flux Φ_f is given by

$$\Phi_f=|\Phi_\lambda|(e^{-i\theta}a+e^{i\theta}a^\dagger), \tag{15}$$

with

$$\Phi_\lambda=\oint \mathbf{u}_\lambda\cdot d\mathbf{l}, \tag{16}$$

where the contour integration is over the SQUID loop. Here, θ is the phase of the mode function $\mathbf{u}_\lambda(\mathbf{r})$ and its value depends on the chosen microwave field (see, e.g., Chap. 2 in Ref. 31). For instance, if a planar cavity is used and the SQUID loop of the charge qubit is perpendicular to the cavity mirrors, one has $\theta=0$.

We shift the gate voltage V_g (and/or vary Φ_e) to bring the single-qubit system into resonance with k photons:

$$E\approx k\hbar\omega_\lambda, \qquad k=1,2,3,\ldots. \tag{17}$$

Expanding the functions $\cos(\pi\Phi_f/\Phi_0)$ and $\sin(\pi\Phi_f/\Phi_0)$ into series of operators and employing the standard rotating wave approximation, we derive the total Hamiltonian of the system in this situation (with the photon Hamiltonian included),

$$H=\frac{1}{2}E\rho_z+\hbar\omega_\lambda\left(a^\dagger a+\frac{1}{2}\right)+H_{Ik}, \tag{18}$$

$$H_{Ik}=\rho_z f(a^\dagger a)+[e^{-ik\theta}|e\rangle\langle g|a^k g^{(k)}(a^\dagger a)+\text{H.c.}].$$

Here

$$f(a^\dagger a)=-E_{J0}\sin(2\xi)\cos\left(\frac{\pi\Phi_e}{\Phi_0}\right)F(a^\dagger a), \tag{19}$$

with

$$\begin{aligned}F(a^\dagger a)=&\frac{1}{2!}\phi^2(2a^\dagger a+1)-\frac{3}{4!}\phi^4[2(a^\dagger a)^2+2a^\dagger a+1]\\&+\frac{5}{6!}\phi^6[4(a^\dagger a)^3+6(a^\dagger a)^2+8a^\dagger a+3]-\ldots,\end{aligned} \tag{20}$$

where $\phi=\pi|\Phi_\lambda|/\Phi_0$, and

$$\begin{aligned}g^{(2m-1)}(a^\dagger a)&=E_{J0}\cos(2\xi)\sin\left(\frac{\pi\Phi_e}{\Phi_0}\right)G^{(2m-1)}(a^\dagger a),\\g^{(2m)}(a^\dagger a)&=E_{J0}\cos(2\xi)\cos\left(\frac{\pi\Phi_e}{\Phi_0}\right)G^{(2m)}(a^\dagger a),\end{aligned} \tag{21}$$

with $m=1,2,3,\ldots$, and

$$\begin{aligned}G^{(1)}(a^\dagger a)&=\phi-\frac{1}{2!}\phi^3a^\dagger a+\frac{1}{4!}\phi^5[2(a^\dagger a)^2+1]-\ldots,\\G^{(2)}(a^\dagger a)&=\frac{1}{2!}\phi^2-\frac{2}{4!}\phi^4(2a^\dagger a-1)\\&\quad+\frac{15}{6!}\phi^6[(a^\dagger a)^2-a^\dagger a+1]-\ldots,\\G^{(3)}(a^\dagger a)&=-\frac{1}{3!}\phi^3+\frac{5}{5!}\phi^5(a^\dagger a-1)-\ldots,\\G^{(4)}(a^\dagger a)&=-\frac{1}{4!}\phi^4+\frac{3}{6!}\phi^6(2a^\dagger a-3)-\ldots,\\&\ldots,\end{aligned} \tag{22}$$

where $g^{(k)}(a^\dagger a)$ is the k-photon-mediated coupling between the charge qubit and the microwave field. This Hamiltonian (18) is a generalization of the Jaynes-Cummings model to a solid-state system. Here multiphoton processes[34] are involved for $k>1$, in contrast with the usual Jaynes-Cummings model for an atomic two-level system interacting with a single-photon mode, where only one photon is exchanged between the two-level system and the external field.[31]

III. RABI OSCILLATIONS IN MULTIPHOTON PROCESS

The eigenvalues of the total Hamiltonian (18) are

$$\begin{aligned}\mathcal{E}_\pm(l,k)=&\hbar\omega_\lambda\left[l+\frac{1}{2}(k+1)\right]+\frac{1}{2}[f(l)-f(l+k)]\\&\pm\frac{\hbar}{2}\sqrt{\delta_{l,k}^2+\Omega_{l,k}^2},\end{aligned} \tag{23}$$

and the corresponding eigenstates, namely, the dressed states are given by

$$|+,l\rangle = e^{-ik\theta}\cos\eta\ |e,l\rangle + \sin\eta\ |g,l+k\rangle,$$

$$|-,l\rangle = -\sin\eta\ |e,l\rangle + e^{ik\theta}\cos\eta\ |g,l+k\rangle, \quad (24)$$

where

$$\Omega_{l,k} = 2g^{(k)}(l+k)[(l+1)(l+2)\cdots(l+k)]^{1/2}/\hbar \quad (25)$$

is the Rabi frequency,

$$\delta_{l,k} = (E/\hbar - k\omega_\lambda) + [f(l)+f(l+k)]/\hbar, \quad (26)$$

and

$$\eta = \frac{1}{2}\tan^{-1}\left(\frac{\Omega_{l,k}}{\delta_{l,k}}\right). \quad (27)$$

Here, k is the number of photons emitted or absorbed by the charge qubit when the qubit transits between the excited state $|e\rangle$ and the ground state $|g\rangle$, and l is the number of photons in the cavity when the qubit state is $|e\rangle$.

When the system is initially at the state $|e,l\rangle$, after a period of time t, the probabilities for the system to be at states $|g,l+k\rangle$ and $|e,l\rangle$ are

$$|\langle g,l+k|\psi(t)\rangle|^2 = \frac{\Omega_{l,k}^2}{\delta_{l,k}^2+\Omega_{l,k}^2}\sin^2\left[\frac{1}{2}(\delta_{l,k}^2+\Omega_{l,k}^2)^{1/2}t\right], \quad (28)$$

and

$$|\langle e,l|\psi(t)\rangle|^2 = 1 - |\langle g,l+k|\psi(t)\rangle|^2. \quad (29)$$

Thus the probabilities are oscillating with frequency

$$\Omega_{\text{Rabi}} = (\delta_{l,k}^2+\Omega_{l,k}^2)^{1/2}. \quad (30)$$

This is the *Rabi oscillation with k photons* involved in the state transition; when $k=1$, it reduces to the usual single-photon Rabi oscillation.

Very recently, Nakamura *et al.*[30] investigated the temporal behavior of a Cooper-pair box driven by a strong microwave field and observed the Rabi oscillations with *multiphoton* exchanges between the two-level system and the microwave field. Different to the case studied here, the microwave field was employed there to drive the gate voltage to oscillate. Here, in order to implement quantum computing, we consider the Cooper-pair box with a SQUID loop and use the microwave field to change the flux through the loop.

A. Analogies between Rabi oscillations and the AC Josephson effect

Rabi oscillations have been observed a long time ago in atomic physics. It is a relatively new development to observe Rabi oscillations in a condensed-matter system. Since the Josephson effect can be used for this purpose, it is instructive to point out analogies and differences between Rabi oscillations and the Josephson effect.

(i) Both Rabi oscillations and the AC Josephson effect involve interactions of the photons with electrons (for Rabi oscillations) or a junction (for AC Josephson effect); (ii) the radiation must be tuned creating two-level transitions; (iii) the junction behaves like an atom undergoing transitions between the quantum states of each side of the junction as it absorbs and emits radiation.

However, the Rabi oscillation is a strong-coupling effect[31] and produces long-lived coherent superpositions.

IV. QUANTUM COMPUTING

Let us consider more than one single charge qubit in the QED cavity, and the cavity initially prepared at the zero-photon state $|0\rangle$. We first show the implementation of a controlled-phase-shift operation. Here a single photon process, $k=1$, is used to implement quantum computing.

(i) For all Josephson charge qubits, let

$$\Phi_e = \frac{1}{2}\Phi_0,$$

then $\cos(\pi\Phi_e/\Phi_0)=0$, which yields

$$f(a^\dagger a) = 0.$$

Furthermore, the gate voltage for a control qubit, say A, is adjusted to have the qubit on resonance with the cavity mode ($E=\hbar\omega_\lambda$) for a period of time (where single photon is involved in the state transition), while all other qubits are kept off-resonant. The interaction Hamiltonian (in the interaction picture with $H_0=\frac{1}{2}E\rho_z$) is given by

$$H_{\text{int}} = e^{-i\theta}|e\rangle_A\langle g|\ ag^{(1)}(a^\dagger a) + \text{H.c.}, \quad (31)$$

and the evolution of qubit A is described by

$$U_A(\theta,t) = \exp(-iH_{\text{int}}t/\hbar). \quad (32)$$

This unitary operation does not affect state $|g\rangle_A|0\rangle$, but transforms $|g\rangle_A|1\rangle$ and $|e\rangle_A|0\rangle$ as

$$|g\rangle_A|1\rangle \to \cos(\alpha t)|g\rangle_A|1\rangle - ie^{-i\theta}\sin(\alpha t)|e\rangle_A|0\rangle,$$

$$|e\rangle_A|0\rangle \to \cos(\alpha t)|e\rangle_A|0\rangle - ie^{i\theta}\sin(\alpha t)|g\rangle_A|1\rangle, \quad (33)$$

where $\alpha = g^{(1)}(1)/\hbar$. To obtain the controlled-phase-shift gate, we need the unitary operation with $\theta=0$ and interaction time $t_1=\pi/2\alpha$, which gives

$$|g\rangle_A|1\rangle \to -i|e\rangle_A|0\rangle,$$

$$|e\rangle_A|0\rangle \to -i|g\rangle_A|1\rangle. \quad (34)$$

This operation swaps the qubit state and the state of the QED cavity. A similar swapping transformation was previously used for the quantum computing with laser-cooled trapped ions.[1]

(ii) While all qubits are kept off-resonant with the cavity mode and the flux Φ_e is originally set to $\Phi_e=\frac{1}{2}\Phi_0$ for each qubit, we change Φ_e to zero for only the target qubit, say B. In this case, the evolution of the target qubit B is described in the interaction picture by

$$U_B(t)=\exp(-iH_{\rm int}t/\hbar), \tag{35}$$

where the Hamiltonian is

$$H_{\rm int}=(|e\rangle_B\langle e|-|g\rangle_B\langle g|)f(a^\dagger a). \tag{36}$$

This Hamiltonian can be used to produce *conditional* phase shifts in terms of the photon state of the QED cavity.[3] Applying this unitary operation to qubit B for a period of time $t_2=\pi\hbar/2|f(1)-f(0)|$, we have[35]

$$\begin{aligned}
|g\rangle_B|0\rangle &\rightarrow e^{i\beta}|g\rangle_B|0\rangle,\\
|e\rangle_B|0\rangle &\rightarrow e^{-i\beta}|e\rangle_B|0\rangle,\\
|g\rangle_B|1\rangle &\rightarrow ie^{i\beta}|g\rangle_B|1\rangle,\\
|e\rangle_B|1\rangle &\rightarrow -ie^{-i\beta}|e\rangle_B|1\rangle,
\end{aligned} \tag{37}$$

where $\beta=\pi f(0)/2|f(1)-f(0)|$.

(iii) Qubit A is again brought into resonance for $t_3=\pi/2\alpha$ with $\theta=0$, as in step (i). Afterwards, a controlled two-bit gate is derived as a controlled-phase-shift gate combined with two one-bit phase gates. In order to obtain the controlled-phase-shift gate U_{AB}, which transforms $|g\rangle_A|g\rangle_B$, $|g\rangle_A|e\rangle_B$, $|e\rangle_A|g\rangle_B$, and $|e\rangle_A|e\rangle_B$ as

$$\begin{pmatrix} |g\rangle_A|g\rangle_B\\ |g\rangle_A|e\rangle_B\\ |e\rangle_A|g\rangle_B\\ |e\rangle_A|e\rangle_B \end{pmatrix} \rightarrow \begin{pmatrix} 1&0&0&0\\ 0&1&0&0\\ 0&0&1&0\\ 0&0&0&-1 \end{pmatrix} \begin{pmatrix} |g\rangle_A|g\rangle_B\\ |g\rangle_A|e\rangle_B\\ |e\rangle_A|g\rangle_B\\ |e\rangle_A|e\rangle_B \end{pmatrix}, \tag{38}$$

one needs to further apply successively the unitary operation given in step (ii) to the control and target qubits with interaction times $t_4=3\pi\hbar/4|f(0)|$ and $t_5=(2\pi-|\beta|)\hbar/|f(0)|$, respectively.

In analogy with atomic two-level systems,[1,3] one can use an appropriate *classical microwave field*[36] to produce *one-bit rotations* for the Josephson charge qubits. When the classical microwave field is on resonance with the target qubit B, the interaction Hamiltonian becomes

$$H_{\rm int}=\frac{\hbar\Omega}{2}[e^{-i\nu}|e\rangle_B\langle g|+\text{H.c.}], \tag{39}$$

with

$$\hbar\Omega=2E_{J0}\cos(2\xi)\sin\left(\frac{\pi\Phi_e}{\Phi_0}\right)\left(\frac{\pi|\Phi_f|}{\Phi_0}\right), \tag{40}$$

where the value of the phase ν depends on the chosen microwave field (see, e.g., Chap. 2 in Ref. 31) and Φ_f is the flux through the SQUID loop produced by the classical microwave field. For the interaction time $t_6=\pi/2\Omega$, the unitary operation

$$V_B(\nu,t_6)=\exp(-iH_{\rm int}t_6/\hbar) \tag{41}$$

transforms $|g\rangle_B$ and $|e\rangle_B$ as

$$\begin{aligned}
|g\rangle_B &\rightarrow \frac{1}{\sqrt{2}}(|g\rangle_B-ie^{i\nu}|e\rangle_B),\\
|e\rangle_B &\rightarrow \frac{1}{\sqrt{2}}(|e\rangle_B-ie^{-i\nu}|g\rangle_B).
\end{aligned} \tag{42}$$

In terms of this one-bit rotation, the controlled-phase-shift gate U_{AB} can be converted to the controlled-NOT gate,[1]

$$C_{AB}=V_B\left(-\frac{\pi}{2},\frac{\pi}{2\Omega}\right)U_{AB}\;V_B\left(\frac{\pi}{2},\frac{\pi}{2\Omega}\right). \tag{43}$$

A sequence of such gates supplemented by one-bit rotations can serve as a universal element for quantum computing.[37]

V. DISCUSSION AND CONCLUSION

For microwaves of wavelength $\lambda\sim 1$ cm, the volume of a planar cavity is ~ 1 cm^3. For SQUID loop dimension ~ 10–$1\,\mu$m, then 10^3–10^4 charge qubits may be constructed along the cavity direction. Furthermore, for a two-dimensional (2D) array of qubits, 10^6–10^8 charge qubits could be placed within the cavity.[38] This number of qubits is large enough for a quantum computer. For practical quantum information processing, one needs to improve the experimental setup to have a QED cavity with a high enough Q value so as to implement more quantum operations within the long photon lifetime of the cavity. Alternatively, one can also increase the number of permitted quantum operations within the given photon lifetime of the cavity by strengthening the coupling between the charge qubit and the microwave field. Because the typical interaction energy between the charge qubit and the microwave field is propositional to Φ_λ, the qubit-photon coupling can be strengthened by increasing the area enclosed by the SQUID loop and the field intensity (e.g., by putting a high-μ material inside the SQUID loop).

In the conditional gates discussed above, the two charge qubits are coupled through photons in the QED cavity. Our approach is scalable, but similar to the coupling scheme using an LC-oscillator mode,[11,15] only a pair of charge qubits at a time can be coupled. In order to implement parallel operations on different pairs of qubits, one can make use of a multimode QED cavity or more than one cavity, where *different cavity modes couple different pairs of qubits simultaneously*. Moreover, our approach might have potential applications in quantum communications using both the qubit-photon coupling (to convert quantum information between charge qubits and photons) and the photons, acting as flying qubits, to transfer quantum information between remotely separated charge-qubit systems.

In conclusion, we have studied the dynamics of the Cooper-pair box with a SQUID loop in the presence of a nonclassical microwave field. Rabi oscillations in the multiphoton process are demonstrated, which involve multiple photons in the transition between the two-level system and the microwave field. Also, we propose a scheme for quantum computing, which is realized by Josephson charge qubits coupled through photons in the QED cavity.

ACKNOWLEDGMENTS

We thank X. Hu, B. Plourde, C. Monroe, and C. Kurdak for useful comments. This work was supported in part by the U.S. National Security Agency (NSA) and Advanced Research and Development Activity (ARDA) under Air Force Office of Research (AFOSR) Contract No. F49620-02-1-0334, and by the U.S. National Science Foundation Grant No. EIA-0130383. J.Q.Y. was also supported by the National Natural Science Foundation of China, Grant No. 10174075.

*Corresponding author. Email address: nori@umich.edu

[1] J.I. Cirac and P. Zoller, Phys. Rev. Lett. **74**, 4091 (1995).

[2] C. Monroe, D.M. Meekhof, B.E. King, W.M. Itano, and D.J. Wineland, Phys. Rev. Lett. **75**, 4714 (1995).

[3] T. Sleator and H. Weinfurter, Phys. Rev. Lett. **74**, 4087 (1995).

[4] Q.A. Turchette, C.J. Hood, W. Lange, H. Mabuchi, and H.J. Kimble, Phys. Rev. Lett. **75**, 4710 (1995).

[5] M.A. Nielsen and I.L. Chuang, *Quantum Computation and Quantum Information* (Cambridge University Press, Cambridge, England, 2000).

[6] See, e.g., M. Thorwart and P. Hänggi, Phys. Rev. A **65**, 012309 (2001); J. Shao and P. Hänggi, Phys. Rev. Lett. **81**, 5710 (1998).

[7] D. Loss and D.P. DiVincenzo, Phys. Rev. A **57**, 120 (1998); X. Hu and S. Das Sarma, *ibid.* **61**, 062301 (2000), and references therein.

[8] A. Imamoğlu, D.D. Awschalom, G. Burkard, D.P. DiVincenzo, D. Loss, M. Sherwin, and A. Small, Phys. Rev. Lett. **83**, 4204 (1999); M.S. Sherwin, A. Imamoğlu, and T. Montroy, Phys. Rev. A **60**, 3508 (1999).

[9] X. Hu, R. de Sousa, and S. Das Sarma, Phys. Rev. Lett. **86**, 918 (2001).

[10] P.M. Platzman and M.I. Dykman, Science **284**, 1967 (1999).

[11] A. Shnirman, G. Schön, and Z. Hermon, Phys. Rev. Lett. **79**, 2371 (1997); Y. Makhlin, G. Schön, and A. Shnirman, Nature (London) **398**, 305 (1999).

[12] D.V. Averin, Solid State Commun. **105**, 659 (1998).

[13] G. Falci, R. Fazio, G.M. Palma, J. Siewert, and V. Vedral, Nature (London) **407**, 355 (2000); A. Blais and A.-M.S. Tremblay, Phys. Rev. A **67**, 012308 (2003); L. Faoro, J. Siewert, and R. Fazio, Phys. Rev. Lett. **90**, 028301 (2003).

[14] J.E. Mooij, T.P. Orlando, L. Levitov, L. Tian, C.H. van der Wal, and S. Lloyd, Science **285**, 1036 (1999); T.P. Orlando, J.E. Mooij, L. Tian, C.H. van der Wal, L.S. Levitov, S. Lloyd, and J.J. Mazo, Phys. Rev. B **60**, 15 398 (1999).

[15] For a review on both Josephson charge and flux qubits, see Y. Makhlin, G. Schön, and A. Shnirman, Rev. Mod. Phys. **73**, 357 (2001).

[16] Y. Nakamura, C.D. Chen, and J.S. Tsai, Phys. Rev. Lett. **79**, 2328 (1997).

[17] V. Bouchiat, D. Vion, P. Joyez, D. Esteve, and M.H. Devoret, Phys. Scr. **T76**, 165 (1998).

[18] C.H. van der Wal, A.C.J. ter Haar, F.K. Wilhelm, R.N. Schouten, C.J.P.M. Harmans, T.P. Orlando, S. Loyd, and J.E. Mooij, Science **290**, 773 (2000); J.R. Friedman, V. Patel, W. Chen, S.K. Tolpygo, and J.E. Lukens, Nature (London) **406**, 43 (2000).

[19] Y. Nakamura, Yu. A. Pashkin, and J.S. Tsai, Nature (London) **398**, 786 (1999).

[20] D. Vion, A. Aassime, A. Cottet, P. Joyez, H. Pothier, C. Urbina, D. Esteve, and M.H. Devoret, Science **296**, 886 (2002).

[21] I. Chiorescu, Y. Nakamura, C.J.P.M. Harmans, and J.E. Mooij, Science **299**, 1869 (2003).

[22] Yu. A. Pashkin, T. Yamamoto, O. Astafiev, Y. Nakamura, D.V. Averin, and J.S. Tsai, Nature (London) **421**, 823 (2003).

[23] Y. Yu, S. Han, X. Chu, S. Chu, and Z. Wang, Science **296**, 889 (2002).

[24] J.M. Martinis, S. Nam, J. Aumentado, and C. Urbina, Phys. Rev. Lett. **89**, 117901 (2002).

[25] A.A. Clerk, S.M. Girvin, A.K. Nguyen, and A.D. Stone, Phys. Rev. Lett. **89**, 176804 (2002); J. Siewert and R. Fazio, *ibid.* **87**, 257905 (2001); O. Buisson, F. Balestro, J.P. Pekola, and F.W.J. Hekking, *ibid.* **90**, 238304 (2003); A. Blais, A. Maassen van den Brink, and A.M. Zagoskin, *ibid.* **90**, 127901 (2003); E. Bibow, P. Lafarge, and L.P. Lévy, *ibid.* **88**, 017003 (2002); E. Paladino, L. Faoro, G. Falci, and R. Fazio, *ibid.* **88**, 228304 (2002); L. Tian, S. Lloyd, and T.P. Orlando, Phys. Rev. B **65**, 144516 (2002); G. Blatter, V.B. Geshkenbein, and L.B. Ioffe, *ibid.* **63**, 174511 (2001); J.M. Martinis, S. Nam, J. Aumentado, K.M. Lang, and C. Urbina, *ibid.* **67**, 094510 (2003); P.R. Johnson, F.W. Strauch, A.J. Dragt, R.C. Ramos, C.J. Lobb, J.R. Anderson, and F.C. Wellstood, *ibid.* **67**, 020509 (2003); Z. Zhou, S.-I. Chu, and S. Han, *ibid.* **66**, 054527 (2002); S. Oh, *ibid.* **65**, 144526 (2002); E. Almaas and D. Stroud, *ibid.* **65**, 134502 (2002); V. Schöllmann, P. Agren, D.B. Haviland, T.H. Hansson, and A. Karlhede, *ibid.* **65**, 020505 (2002); M.C. Goorden and F.K. Wilhelm, *ibid.* **68**, 012508 (2003); T.L. Robertson, B.L.T. Plourde, A. Garcia-Martinez, P.A. Reichardt, B. Chesca, R. Kleiner, Y. Makhlin, G. Schön, A. Shnirman, F.K. Wilhelm, D.J. Van Harlingen, and J. Clarke, *ibid.* (to be published); J. Clarke, T.L. Robertson, B.L.T. Plourde, A. Garcia-Martinez, P.A. Reichardt, D. J. Van Harlingen, B. Chesca, R. Kleiner, Yu. Makhlin, G. Schön, A. Schnirman, and F.K. Wilhelm, Phys. Scr. **T102**, 173 (2002); C.-P. Yang, S.-I. Chu, and S. Han, Phys. Rev. A **67**, 042311 (2003); D.V. Averin and C. Bruder, Phys. Rev. Lett. **91**, 057003 (2003); M.J. Storcz and F.K. Wilhelm, cond-mat/0306317 (unpublished); M.J. Storcz and F.K. Wilhelm, Phys. Rev. A **67**, 042319 (2003).

[26] A scalable superconducting qubit structure is proposed in J.Q. You, J.S. Tsai, and F. Nori, Phys. Rev. Lett. **89**, 197902 (2002). A longer version of it is available in cond-mat/0306208 (unpublished). Entanglement of states in a circuit with superconducting qubits and improved readout is described in J.Q. You, J.S. Tsai, and F. Nori, Phys. Rev. B **68**, 024510 (2003).

[27] While here we focus on charge qubits, similar ideas also apply to *flux* qubits.

[28] X. Maître, E. Hagley, G. Nogues, C. Wunderlich, P. Goy, M. Brune, J.M. Raimond, and S. Haroche, Phys. Rev. Lett. **79**, 769 (1997).

[29] S. Brattke, B.T.H. Varcoe, and H. Walther, Phys. Rev. Lett. **86**, 3534 (2001).

[30] Y. Nakamura, Yu. A. Pashkin, and J.S. Tsai, Phys. Rev. Lett. **87**, 246601 (2001).

[31] See, e.g., D.F. Walls and G.J. Milburn, *Quantum Optics* (Springer, Berlin, 1994).

[32] A.D. Armour, M.P. Blencowe, and K.C. Schwab, Phys. Rev. Lett. **88**, 148301 (2002); O. Buisson and F.W.J. Hekking, cond-mat/0008275, in *Macroscopic Quantum Coherence and Quantum Computing* (Kluwer Academic, Dordrecht, in press), pp. 137–145; F. Marquardt and C. Bruder, Phys. Rev. B **63**, 054514 (2001).

[33] This is the case usually investigated (see Refs. 11–15). Self-inductance is taken into account in J.Q. You, C.-H. Lam, and H.Z. Zheng, Phys. Rev. B **63**, 180501(R) (2001).

[34] For an experimental multiphonon generalization of the Jaynes-Cummings model, see, e.g., D.M. Meekhof, C. Monroe, B.E. King, W.M. Itano, and D.J. Wineland, Phys. Rev. Lett. **76**, 1796 (1996).

[35] This is similar to the conditional quantum-phase gate realized in a QED cavity for two photon qubits (Ref. 4). Like the controlled-NOT gate, this conditional two-bit gate is also universal for quantum computing (Refs. 4 and 37). One can entangle charge qubits and photons using this conditional quantum-phase gate (supplemented with one-bit rotations) and employ photons as flying qubits to implement quantum communications, e.g., quantum teleportation.

[36] One can irradiate the classical microwave field on a charge qubit to realize the coupling between the charge qubit and the classical field. Also, the classical microwave field can be adjusted to be off-resonant with the QED cavity so as to eliminate its influence on the cavity mode.

[37] S. Lloyd, Phys. Rev. Lett. **75**, 346 (1995); D. Deutsch, A. Barenco, and A. Ekert, Proc. R. Soc. London, Ser. A **449**, 669 (1995).

[38] A 2D array would require local gate voltages $V_g(i,j)$ and local fluxes $\Phi_e(i,j)$ (e.g., with coils).

Generation of nonclassical photon states using a superconducting qubit in a microcavity

Yu-xi Liu,[1] L.F. Wei,[1,2] and Franco Nori[1,3]

[1] *Frontier Research System, The Institute of Physical and Chemical Research (RIKEN), Wako-shi 351-0198, Japan*
[2] *Institute of Quantum optics and Quantum information, Department of Physics, Shanghai Jiaotong University, Shanghai 200030, P.R. China*
[3] *Center for Theoretical Physics, Physics Department, Center for the Study of Complex Systems, The University of Michigan, Ann Arbor, Michigan 48109-1120*

(Dated: July 12, 2004)

Based on the interaction between the radiation field and a superconductor, we propose a way to engineer quantum states using a SQUID charge qubit inside a microcavity. This device can act as a deterministic single photon source as well as generate any Fock states and an arbitrary superposition of Fock states for the cavity field. The controllable interaction between the cavity field and the qubit can be realized by the tunable gate voltage and classical magnetic field applied to the SQUID.

PACS numbers: 42.50.Dv, 74.50.+r, 42.50.Ct

The generation of quantum states of the radiation field has been a topic of growing interest in recent years. This is because of possible applications in quantum communication and information processing, such as quantum networks, secure quantum communications, and quantum cryptography [1]. Based on the interaction between the radiation field and atoms, many theoretical schemes have been proposed for the generation of Fock states [2, 3] and their arbitrary superpositions [4, 5]. Experiments have generated single-photon states in quantum dots [6], atoms inside a microcavity [7], and other systems [8]. A superposition of the vacuum and one-photon states can also be experimentally created by truncating an input coherent state or using cavity quantum electrodynamics [9]. However, how to generate an arbitrary photon state by virtue of the interaction between the radiation field and solid state quantum devices seems to be unknown both theoretically and experimentally. Recent progress in superconducting quantum devices (e.g., [10, 11]) makes it possible to do quantum state engineering experiments in these systems, and also there have been proposals on superconducting qubits interacting with the nonclassical electromagnetic field [12, 13, 14, 15, 16, 17].

Here, we present an experimentally feasible scheme to generate quantum states of a single-mode cavity field in the microwave regime by using the photon transition between the ground and first excited states of a macroscopic two-level system formed by a superconducting quantum interference device (SQUID). This artificial two-level "atom" can be easily controlled by an applied gate voltage V_g and the flux Φ_c generated by the classical magnetic field through the SQUID (e.g., [14, 18]). The process of generating photon states in this device includes three main steps: (i) The artificial atom operates at the degeneracy point by choosing appropriate values for $V_{\rm g}$ and $\Phi_{\rm c}$. There is no interaction between the quantized cavity field and "atom" at this stage. (ii) Afterwards new $V_{\rm g}$ and Φ_c are selected such that the cavity field interacts resonantly with the "atom" and evolves during a designated time. (iii) The above two steps can be repeated until a desired state is obtained. Finally, the flux Φ_c can be adjusted to a special value, then the interaction is switched off, and the desired photon state appears in the cavity. This process is similar to that of a micromaser [2] and it is described below.

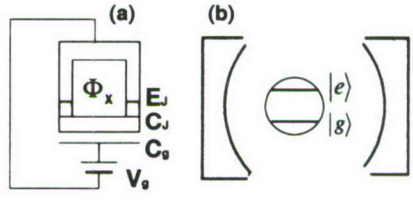

FIG. 1: (a) A charge qubit formed by a SQUID device, equivalent to a controllable macroscopic two-level system, is placed into a superconducting microwave cavity in (b). The coupling between the quantized cavity field and qubit system is realized via the magnetic flux Φ_X through the SQUID.

Model.— The macroscopic two-level system studied here is shown in Fig. 1 (a). A SQUID-type superconducting box with $n_{\rm c}$ excess Cooper-pair charges is connected to a superconducting loop via two identical Josephson junctions with capacitors $C_{\rm J}$ and coupling energies $E_{\rm J}$. A controllable gate voltage $V_{\rm g}$ is coupled to the box via a gate capacitor $C_{\rm g}$. We assume that the superconducting energy gap Δ is the largest energy. Then, at low temperatures, the quasi-particle tunneling is suppressed and no quasi-particle excitation can be found on the island. Only Cooper pairs coherently tunnel in the superconducting junctions. The above assumptions are consistent with most experiments on charge qubits. Then the standard Hamiltonian [18] is

$$H_{\rm qb} = 4E_{\rm ch}(n_c - n_{\rm g})^2 - 2E_{\rm J}\cos\left(\frac{\pi\Phi_X}{\Phi_0}\right)\cos\Theta, \quad (1)$$

where Φ_X is the total flux through the SQUID loop and Φ_0 the flux quantum. Thus, the superconducting loop is used to control the Josephson coupling energy by adjusting the flux through this loop. Below, we show that it can also switch on and off the qubit-field interaction. The dimensionless gate charge, $n_{\rm g} = C_{\rm g}V_{\rm g}/2e$, is controlled by $V_{\rm g}$. The

single-electron charging energy is $E_{\rm ch} = e^2/2(C_{\rm g} + 2C_{\rm J})$. $\Theta = (\phi_1 + \phi_2)/2$ is the quantum mechanical conjugate of the number operator $n_{\rm c}$ of the Cooper pairs on the box, where ϕ_i $(i = 1, 2)$ is the phase difference for each junction. The superconducting box is assumed to work in the charging regime with condition $k_B T \ll E_{\rm J} \ll E_{\rm ch} \ll \Delta$ where T and k_B are temperature and Boltzmann constant respectively. If the gate voltages is near a degeneracy point $n_{\rm g} = 1/2$, the superconducting box is a charge qubit [18], which is a controllable two-level system characterized by the two lowest charge states $|g\rangle$ (for $n_{\rm c} = 0$) and $|e\rangle$ (for $n_{\rm c} = 1$). However, if the quasiparticle excitation cannot be completely suppressed, a continuum of low-lying quasi-particle states will be present, and the Hamiltonian (1) cannot be reduced to a system with two energy levels even when the gate voltage is near the degeneracy point [19].

Now we further consider that the qubit is placed in a single-mode microwave superconducting cavity, depicted in Fig. 1(b), the flux Φ_X through the SQUID can be expressed as [12, 13, 14] $\Phi_X = \Phi_{\rm c} + \Phi_{\rm q}$ where the flux Φ_c and $\Phi_q = \eta\, a + \eta^*\, a^\dagger$ are generated by a classical applied magnetic field and the quantized cavity field, respectively. Here $\eta = \int_S \mathbf{u}(\mathbf{r}) \cdot d\mathbf{s}$ and $\mathbf{u}(\mathbf{r})$ is the mode function of the cavity field, with annihilation (creation) operators a $(a^\dagger)$, and S is the surface defined by the contour of the SQUID. Considering the above, we obtain

$$H = \hbar\omega a^\dagger a + E_z \sigma_z \qquad (2)$$
$$- E_{\rm J}(\sigma_+ + \sigma_-)\cos\left[\frac{\pi}{\Phi_0}\left(\Phi_{\rm c} I + \eta\, a + \eta^*\, a^\dagger\right)\right]$$

where the first two terms represent the free Hamiltonians of the cavity field with frequency $\omega = 4E_{\rm ch}/\hbar$ and the qubit with the energy $E_z = -2E_{\rm ch}(1 - 2n_{\rm g})$, I is the identity operator. The third term is the nonlinear photon-qubit interaction which is switchable by the flux Φ_c. The charge excited state $|e\rangle$ and ground state $|g\rangle$ correspond to the eigenstates $|\downarrow\rangle$ and $|\uparrow\rangle$ of the spin operator σ_z, respectively. The cosine in Eq. (2) can be further decomposed into classical and quantized parts, and the quantized parts $\sin[\pi(\eta\, a + H.c.)/\Phi_0]$ and $\cos[\pi(\eta\, a + H.c.)/\Phi_0]$ can be further expanded as a power series in a $(a^\dagger)$. Here, the single photon transition between the states $|e, n\rangle$ and $|g, n+1\rangle$ satisfies the condition $(\pi|\eta|/\Phi_0)\sqrt{n+1} \ll 1$, where n is the number of photons; therefore all higher orders of $\pi|\eta|/\Phi_0$ can be neglected and only a single-photon transition is kept in the expansion of Eq. (2). Using the notation for trapped ion systems (e.g., [20]), the first red (blue) sideband excitations $\beta a\sigma_+ + H.c.$ $(\beta a\sigma_- + H.c.)$ for interactions of the cavity field and the qubit [13], with photon-qubit coupling constant $\beta = (\pi\eta E_{\rm J}/\Phi_0)\sin(\pi\Phi_{\rm c}/\Phi_0)$, can be obtained by adjusting the gate voltages V_g and the flux Φ_c. They correspond to $2E_z = \hbar\omega$ $(2E_z = -\hbar\omega)$ and dimensionless gate charge $n_{\rm g} = 1$ $(n_{\rm g} = 0)$. Also $\xi(\sigma_+ + \sigma_-)$ with $\xi = E_{\rm J}\cos(\pi\Phi_{\rm c}/\Phi_0)$ is called the carrier [13], which corresponds to $n_{\rm g} = 1/2$. The Hamiltonian (2), with the above assumptions, is our model.

Preparation process.— We choose $|0, g\rangle$ as our initial state, where the cavity field is in the vacuum state $|0\rangle$ and the qubit is in the ground state $|g\rangle$. The goal is to prepare an arbitrary pure state of the cavity field

$$|\psi\rangle = \sum_{n=0}^{N} c_n |n, g\rangle = |g\rangle \otimes \sum_{n=0}^{N} c_n |n\rangle \qquad (3)$$

where $|n\rangle$ denotes the Fock states of the cavity field with excitation number $n = 0, 1, 2, \cdots$. A Fock state $|m\rangle$ with m photons is a special case of Eq. (3) with conditions $c_n = 0$ for all $n \neq m$ with $0 < m \leq N$.

Thermal photons in the cavity have to be suppressed in order to obtain the vacuum state $|0\rangle$. In the microwave region $0.1 \sim 15$ cm, the mean number of thermal photons $\langle n_{\rm th}\rangle$ satisfies $3.0 \times 10^{-208} \leq \langle n_{\rm th}\rangle \leq 0.043$ at $T = 30$ mK, and $1.7 \times 10^{-104} \leq \langle n_{\rm th}\rangle \leq 0.26$ at $T = 60$ mK. These temperatures can be obtained experimentally (e.g., in [11, 21]).

After the system is initialized, two different processes are required to engineer the state of the cavity field. The first process involves rotating the qubit state, but keeping the cavity field state unchanged. This stage can be experimentally realized by tuning the gate voltage and classical magnetic field such that $n_{\rm g} = 1/2$ and $\Phi_{\rm c} = 0$; then the time evolution operator $U_{\rm C}(t)$ of the qubit in the interaction picture is

$$U_{\rm C}(t) = \cos(\Omega_1 t) I + i\sin(\Omega_1 t)(|g\rangle\langle e| + |e\rangle\langle g|) \qquad (4)$$

where $\Omega_1 = E_{\rm J}/\hbar$. The subscript "C" in $U_{\rm C}(t)$ denotes the carrier process, which can superpose two levels of the qubit, and it can also flip the ground state $|g\rangle$ or excited state $|e\rangle$ to each other, after a time $t = \pi(2p-1)/2\Omega_1$, with positive integer p.

The second process is the first red (blue) sideband excitation, which can be realized by tuning the gate voltage and classical magnetic field such that $n_{\rm g} = 1$ $(n_{\rm g} = 0)$ and $\Phi_c = \Phi_0/2$. Thus, in the interaction picture, the time evolution operators $U_{\rm R}(t)$ for the red ($U_{\rm B}(t)$ for the blue) of the cavity field and qubit can be expressed [22] as

$$\begin{aligned} U_{\rm R}(t) &= R_{ee}(t)|e\rangle\langle e| + R_{gg}(t)|g\rangle\langle g| \\ &- iR_{ge}(t)|g\rangle\langle e| - iR_{eg}(t)|e\rangle\langle g| \end{aligned} \qquad (5)$$

or

$$\begin{aligned} U_{\rm B}(t) &= R_{gg}(t)|e\rangle\langle e| + R_{ee}(t)|g\rangle\langle g| \\ &- iR_{ge}(t)|e\rangle\langle g| - iR_{eg}(t)|g\rangle\langle e| \end{aligned} \qquad (6)$$

with $R_{eg}(t) = \left[e^{i\theta}\sin\left(|\Omega_2|t\sqrt{aa^\dagger}\right)/\sqrt{aa^\dagger}\right] a$, $R_{ge}(t) = B_{eg}^\dagger(t)$, $R_{ee}(t) = \cos\left(|\Omega_2|t\sqrt{aa^\dagger}\right)$, and $R_{gg}(t) = \cos\left(|\Omega_2|t\sqrt{a^\dagger a}\right)$, where we have assumed that $\Omega_2 = \pi\eta E_{\rm J}/\hbar\Phi_0 = |\Omega_2|e^{i\theta}$, in which the phase θ depends on the mode function of the cavity field $u(\mathbf{r})$. The red sideband excitation described by operator $U_R(t)$ can entangle $|g, n+1\rangle$ with $|e, n\rangle$, or flip $|g, n+1\rangle$ to $|e, n\rangle$ and vice versa, by

choosing the duration of the interaction between the cavity field and the qubit. From Eq. (5), it is easy to verify that the emission probability P_g of the upper level for the qubit is $P_g = \sin^2(|\Omega_2|t\sqrt{n+1})$. We find that $P_g = 1$ when $|\Omega_2|t\sqrt{n+1} = \pi(2k-1)/2$, with positive integer k. So when $t = \pi(2k-1)/(2|\Omega_2|\sqrt{n+1})$, there are $n+1$ photons in the cavity and the qubit is in its ground state. The first blue sideband excitation, denoted by $U_{\rm B}(t)$, can entangle state $|e, n+1\rangle$ with state $|g, n\rangle$, or flip $|e, n+1\rangle$ to $|g, n\rangle$ and vice versa. Below we use the carrier and the first red sideband excitation, represented by $U_{\rm C}(t)$ and $U_{\rm R}(t)$, as an example showing the generation of an arbitrary quantum state of the cavity field.

Using the quantum operations $U_{\rm C}(t)$ and $U_{\rm R}(t)$ in Eqs. (4) and (5), the single photon state $|1\rangle$ can be generated from the initial vacuum state $|0\rangle$. That is, we can first flip the ground state of the qubit to the excited state when the condition $\Omega_1 t_1 = \pi/2$ is satisfied for the carrier $U_{\rm C}(t_1)$, then we turn on the first red sideband excitation $U_{\rm R}(t_2)$ and let the photon-qubit system evolve a time t_2 satisfying the condition $|\Omega_2|t_2 = \pi/2$. Finally, we adjust the classical magnetic field such that $\Phi_{\rm c} = 0$; thus the interaction between the cavity field and qubit vanishes, and a single-photon state exists in the cavity, that is,

$$|1\rangle \otimes |g\rangle = U_{\rm R}(t_2|)\, U_{\rm C}(t_1)\, |0\rangle \otimes |g\rangle. \tag{7}$$

Also any Fock state $|m\rangle$ can be easily created from the vacuum state $|0\rangle$ by alternatively turning on and off the quantum operations in Eqs. (4-5) to excite the qubit and emit photons during the time interval T. The latter is divided by $2m$ subintervals $\tau_1, \tau_2, \cdots, \tau_{2l-1}, \tau_{2l} \cdots, \tau_{2m-1}, \tau_{2m}$ which satisfy conditions $|\Omega_1|\tau_{2l-1} = \pi/2$ and $|\Omega_2|\tau_{2l}\sqrt{l+1} = \pi/2$ where $l = 1, \cdots, m$. This process can be described as

$$|m\rangle \otimes |g\rangle = U_{\rm R}(\tau_{2m}) U_C(\tau_{2m-1}) \cdots U_{\rm R}(\tau_2) U_C(\tau_1) |0\rangle \otimes |g\rangle. \tag{8}$$

Finally, the classical magnetic field is changed such that $\Phi_{\rm c} = \Phi_0$, and an n-photon state is provided in the cavity.

Our next goal is to prepare superpositions of different Fock states (e.g., $\alpha_1|0\rangle + \alpha_2|1\rangle$) for the vacuum $|0\rangle$ and single photon $|1\rangle$ states. This very important state can be deterministically generated by two steps, $U_{\rm C}(t_1')$ and $U_{\rm R}(t_2')$, with $t_2' = \pi/2|\Omega_2|$; that is

$$(\alpha_1|0\rangle + \alpha_2|1\rangle) \otimes |g\rangle = U_{\rm R}(t_2') U_{\rm C}(t_1') |0\rangle \otimes |g\rangle \tag{9}$$

where the operation time t_1' determines the weights of the coefficients of the superposition $\alpha_1 = \cos(\Omega_1 t_1')$ and $\alpha_2 = e^{-i\theta}\sin(\Omega_1 t_1')$. If the condition $t_1' = \pi/4\Omega_1$ is satisfied, then we have a superposition $(|0\rangle + e^{-i\theta}|1\rangle)/\sqrt{2}$ with equal probabilities for each component and the relative phase between them can be further specified by the phase of the mode of the cavity field.

An arbitrary target state (3) can be generated from the initial state by alternatively switching on and off the carrier and first red sideband excitation during the time T', which can be divided into $2n$ subintervals $\tau_1', \cdots, \tau_{2n}'$. That is, the target state can be deterministically generated as follows

$$|\psi\rangle = \sum_{n=0}^{N} c_n |n, g\rangle = U(T')|0, g\rangle, \tag{10}$$

where $U(T')$ is determined by a sequence of time evolution operators associated with chosen time subintervals as $U(T') = U_{\rm R}(\tau_{2n}') U_{\rm C}(\tau_{2n-1}') \cdots U_{\rm R}(\tau_2') U_{\rm C}(\tau_1')$. Therefore, the coefficients c_n are

$$c_n = \langle g, n| U_{\rm R}(\tau_{2n}') U_{\rm C}(\tau_{2n-1}') \cdots U_{\rm R}(\tau_2') U_{\rm C}(\tau_1')|0, g\rangle. \tag{11}$$

Reference [4] has explicitly discussed how to adjust the rescaled times to obtain the expected state by solving the inverse evolution of Eq. (10). Ideally, any state of the cavity field can be created according to our proposal by adjusting the gate voltage, classical magnetic field, and duration of the photon-qubit interaction. It is very easy to check that the state (3) can also be created by the carrier and blue sideband excitation whose time evolutions $U_{\rm C}(t)$ and $U_{\rm B}(t)$ are described by Eqs. (4) and (6).

Environmental effects.— We now discuss the environmental effects on the prepared states, which are actually limited by the following time scales: the relaxation time T_1, the preparation time τ_e of the excited state, and the dephasing time T_2 of the qubit, the lifetime τ_p of the photon and an effective interaction time $\tau_c^{(n)}$ which corresponds to the transition from $|n, e\rangle$ and $|n+1, g\rangle$. If $T_1,\ \tau_p \gg \tau_e,\ \tau_c^{(n)}$, then the Fock states can be prepared. If the condition $T_1,\ T_2,\ \tau_p \gg \tau_e,\ \tau_c^{(n)}$ is satisfied, then the superposition can also be obtained.

Now let us estimate the photon number of the obtainable Fock state in a full-wave cavity. In microwave experiments, it is possible to obtain very high-Q superconducting cavities, with Q values around 3×10^8 to 5×10^{10} [2, 23], which correspond to the lifetimes of the microwave region from $0.001 \leq \tau_p \leq 0.15$ s to $0.167 \leq \tau_p \leq 25$ s. The parameters of the charge qubit [24] without the cavity are $2E_{\rm J}/h = 13.0$ GHz (so the operation time corresponding to a completely excited qubit is about $\tau_e \approx 3.8 \times 10^{-11}$ s). The lifetime of the excited-state for the qubit $T_1 = 1.3 \times 10^{-6}$ s, i.e. $\tau_e \ll T_1$. For an estimate of the interaction coupling between the cavity field and the qubit, we assume that the cavity mode function is taken as a standing-wave form such as $B_x = -i\sqrt{\hbar\omega/\varepsilon_0 V c^2}(a - a^\dagger)\cos(kz)$, with polarization along the normal direction of the surface area of the SQUID, located at an antinode of the standing-wave mode; then the interaction between the cavity field and the qubit reaches its maximum and the interaction strength can be expressed as $|\beta| = \pi|\eta|E_{\rm J}/\Phi_0 = (\pi S E_{\rm J}/c\Phi_0)\sqrt{\hbar\omega/\varepsilon_0 V}$. For example, if the wavelength of the cavity mode is taken as $\lambda_1 = 0.1$ cm, then $\pi|\eta|/\Phi_0 \approx 7.38 \times 10^{-5} \ll 1$, where the dimension of the SQUID is taken as 10 μm and the mode function $u(\mathbf{r})$ is assumed to be independent of the integral area because the dimension of the SQUID, 10 μm, is much less than 0.1 cm, for the wavelength of the cavity mode. In this case,

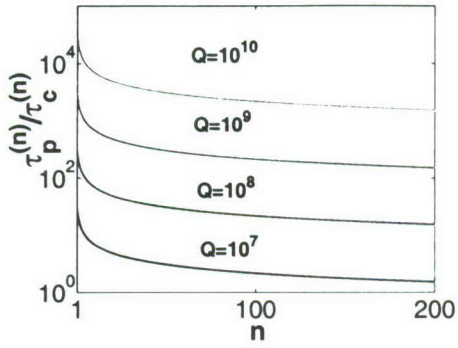

FIG. 2: Ratio $\tau_p^{(n)}/\tau_c^{(n)}$, versus photon number $n \geq 1$, of the lifetime $\tau_p^{(n)}$ of the photon number state $|n\rangle$ and the effective operation time $\tau_c^{(n)}$. The latter corresponds to the transition from $|n, e\rangle$ to $|n+1, g\rangle$ for a 10μm $\times 10\mu$m SQUID in the full-wave cavity.

$\tau_c^{(0)} \approx 5.0 \times 10^{-7}$s, which is less than one order of magnitude of the excited lifetime T_1. This means that the qubit in its excited state can emit a photon before it relaxes to its ground state. But if we take the dimension of the SQUID as 1 μm, the coupling between the cavity field and the qubit is two orders of magnitude smaller than for the 10 μm SQUID, and then the interaction time is $5.0 \times 10^{-5} > T_1$. Therefore, in this case, the qubit relaxes to the ground state before the photon can be emitted from the qubit, and thus it is difficult to obtain a photon state. In Fig. (2), we plot the ratio $\tau_p^{(n)}/\tau_c^{(n)}$ between the lifetime [25] $\tau_p^{(n)} = \tau_p/n$ (here, $\tau_p^{(1)} = \tau_p$) of the Fock state $|n\rangle$ for the zero-temperature environment and the effective operation time $\tau_p^{(n)}$ of transitions from state $|n, e\rangle$ to $|n+1, g\rangle$ for different values of Q and for $\lambda = 0.1$ cm. Fig. 2 shows that the photon number of the prepared Fock states can reach 10^2 in the above mentioned high-Q cavity. But if the Q values are less than 10^7, it might be difficult to prepare a photon state with our estimated coupling. We also find that a longer microwave in the full-wave cavity corresponds to a longer $\tau_c^{(n)}$ for a fixed Q, which means that it is easy to create photon states for shorter microwaves. For example, if the wavelength is taken as $\lambda = 1$ cm, then the coupling between the qubit-photon in the full-wave cavity might not be strong enough for generating Fock states within the currently known experimental data for T_1. So for longer microwaves, we can make a smaller cavity and place the qubit where the qubit-photon interaction is maximum.

If we want to prepare a superposition of different Fock states of the cavity field, we need to consider T_2, which is of the order of a few ns (e.g., 5 ns in [11]). Then the survival time of the entangled state between the cavity field and qubit, which is required for the preparation of the superposition of the Fock states, maybe be very short. With the improvement of read-out techniques, a longer dephasing time can make our proposal far more realizable.

Discussions.— We propose a scheme for deterministically generating nonclassical photon states via the interaction of photons and a charge qubit. Indeed, the Fock state can be prepared with current technology. The superposition would be easier to obtain by increasing the dephasing time T_2 and the qubit-photon coupling strength. Our discussions above are based on experimental values for T_1 and T_2 without the cavity; the decoherence may become shorter when the SQUID is placed inside the cavity. Further, in order to obtain a stronger coupling, the following steps would help to increase the qubit-field coupling strength: i) decrease the volume V of the cavity; ii) increase the area S of the SQUID; iii) increase the Josephson coupling energy E_J under the condition $E_J \ll E_{ch}$. We can also put a high permeability μ material inside the SQUID loop [14], then the qubit-field coupling strength can increase to $\mu|\beta|$, because the relative permeability in ferromagnetic materials can be 10^2 to 10^6, and might partly compensate some of the decoherence effects due to the μ material itself. Increasing the SQUID dimension and decreasing the cavity volume will reduce the maximum allowed number of SQUIDs inside the cavity making it unadvantageous for quantum computing. However, one qubit is enough for the generation of nonclassical photon states, our goal here. We note that Girvin *et al.* [17] proposed a different system in which the coupling of the photon-qubit can reach 10^8 Hz, corresponding to $\tau_c^{(0)} \sim 10^{-9}$ s. We are considering how to generate nonclassical photon states by using such a system. This scheme might not be easy to generalize in a straightforward manner to the flux qubit case. This because the interaction between the flux-qubit and the cavity field cannot be switched on and off in the same way for the charge qubit. However in some modified manner, it should be possible to generalize this scheme.

We thank X. Hu helpful comments. This work was supported in part by the US NSA and ARDA under AFOSR contract No. F49620-02-1-0334, and by the NSF grant No. EIA-0130383.

[1] M.N. Nielsen and I.L. Chuang, *Quantum Computation and Quantum Information* (Cambridge University Press 2000).

[2] J. Krause, *et al.*, Phys. Rev. A **36**, 4547 (1987); *ibid.* **39**, 1915 (1989).

[3] W. Leonski, *et al.*, Phys. Rev. A **49**, R20 (1994); W. Leonski, *ibid.* **54**, 3369 (1996); M. Brune, *et al.*, Phys. Rev. Lett. **65**, 976 (1990); M. J. Holland, *et al.*, *ibid.* **67**, 1716 (1991).

[4] C.K. Law, *et al.*, Phys. Rev. Lett. **76**, 1055 (1996).

[5] K. Vogel, *et al.*, Phys. Rev. Lett. **71**, 1816 (1993); A.S. Parkins, *et al.*, *ibid.* **71**, 3095 (1993); Phys. Rev. A **51**, 1578 (1995); D.T. Pegg, *et al.*, Phys. Rev. Lett. **81**, 1604 (1998).

[6] P. Michler, *et al.*, Science **290**, 2282 (2000); J. Kim, *et al.*, Nature **397**, 500 (1999); P. Michler, *et al.*, *ibid.* **406**, 968 (2000).

[7] C.J. Hood, *et al.*, Science **287**, 1447 (2000); B.T.H. Varcoe, *et al.*, Nature **403**, 743 (2000); P.W.H. Pinkse, *et al.*, *ibid.* **404**, 365 (2000); P. Bertet, *et al.*, Phys. Rev. Lett. **88**, 143601 (2002); A. Kuhn, *et al.*, *ibid.* **89**, 067901 (2002).

[8] B. Lounis *et al.*, Nature **407**, 491 (2000); C.K. Hong, *et al.*, Phys. Rev. Lett. **56**, 58 (1986); C. Brunel, *et al.*, *ibid.* **83**, 2722 (1999); C. Kurtsiefer, *et al.*, *ibid.* **85**, 290 (2000); C. Santori, *et al.*, *ibid.* **86**, 1502 (2001).

[9] A.I. Lvovsky, *et al.*, Phys. Rev. Lett. **88**, 250401 (2002); X.

Maitre, *ibid.* **79**, 769 (1997).
[10] J.E. Mooij, *et al.*, Science **285**, 1036 (1999); C.H. van der Wal, *et al.*, *ibid.* **290**, 773 (2000); S. Han, *et al.*, *ibid.* **293**, 1457 (2001); D. Vion, *et al.*, *ibid.* **296**, 886 (2002); Y. Yu, *et al*, *ibid.* **296**, 889 (2002); I. Chiorescu, *et al.*, *ibid.* **299**, 1869 (2003); A.J. Berkley, *et al.*, *ibid.* **300**, 1548 (2003); J.R. Friedman, *et al.*, Nature **406**, 43 (2000).
[11] Y. Nakamura, *et al.*, Nature **398**, 786 (1999); Y.A. Pashkin, *et al.*, *ibid.* **421**, 823 (2003).
[12] W.A. Al-Saidi, *et al.*, Phys. Rev. B **65**, 224512 (2002).
[13] S.L. Zhu, *et.al*, Phys. Rev. A **68**, 034303 (2003).
[14] J.Q. You and F. Nori, Phys. Rev. B **68**, 064509 (2003).
[15] J.Q. You, *et. al*, Phys. Rev. B **68**, 024510 (2003).
[16] C.P. Yang, *et.al*, Phys. Rev. A **67**, 042311 (2003)
[17] S.M. Girvin, *et al.*, cond-mat/0310670.
[18] Y. Makhlin, *et al.*, Rev. Mod. Phys. **73**, 357 (2001).
[19] D.V. Averin and Y.V. Nazarov, Phys. Rev. Lett. **69**, 1993 (1992); M. Tinkham, *Introduction to Superconductivity* (McGraw-Hill, New York, 1996).
[20] D.M. Meekhof, *et al.*, Phys. Rev. Lett. **76**, 1796 (1996); A. Ben-Kish, *et al.*, *ibid.* **90**, 037902 (2003); B. Kneer, *et al.*, Phys. Rev. A **57**, 2096 (1998); L.F. Wei, *et al.*, quant-ph/0308079.
[21] Y. Nakamura, *et al.*, Phys. Rev. Lett. **87**, 246601 (2001); *ibid.* **88**, 047901 (2002).
[22] S. Stenholm, Phys. Rep. **6**, 1(1973).
[23] S. Brattke, *et al.*, Phys. Rev. Lett. **86**, 3534 (2001); J. M. Raimond, *et al.*, Rev. Mod. Phys. **73**, 565 (2001).
[24] K.W. Lehnert, *et al.*, Phys. Rev. Lett. **90**, 027002 (2003).
[25] V. Perinova and A. Luks, Phys. Rev. A **41**, 414 (1990).

Preparation of Schrödinger cat states of a cavity field via coupling to a SQUID-based charge qubit

Yu-xi Liu,[1] L.F. Wei,[1,2] and Franco Nori[1,3]

[1] *Frontier Research System, The Institute of Physical and Chemical Research (RIKEN), Wako-shi 351-0198*
[2] *Institute of Quantum Optics and Quantum Information, Department of Physics, Shanghai Jiaotong University, Shanghai 200030, P.R. China*
[3] *Center for Theoretical Physics, Physics Department, Center for the Study of Complex Systems, The University of Michigan, Ann Arbor, Michigan 48109-1120*

(Dated: June 15, 2004)

Based on the measurement of charge states, we show that the superpositions of two macroscopically distinguishable coherent states (Schrödinger cat states) of a single-mode cavity field can be generated by a controllable interaction between a cavity field and a SQUID-based charge qubit. After such cat states of the cavity field are created, the interaction can be switched off by the classical magnetic field through the SQUID, and there is no information transfer between the cavity field and the charge qubit. We also discuss the generation of superpositions of two squeezed coherent states.

I. INTRODUCTION

The principle of linear superposition is central to quantum mechanics. However, it is difficult to create and observe superposed states because the fragile coherence of these states can be easily spoiled by the environment. Typical examples are the Schrödinger cat states (SCSs), which are superpositions of two macroscopically distinguishable states. Many theoretical schemes [1] have been proposed to generate SCSs in optical systems. Also, much experimental progress has been made to demonstrate different kinds of SCSs: in superconducting systems (e.g. Ref. [2]), laser trapped ions [3], optical systems constructed by Rydberg atoms, and superconducting cavity in the microwave regime [4]. The SCSs, which are formed by two optical coherent states, e.g. in Ref. [5], have been investigated for applications in quantum information processing [5, 6, 7]. These states can also be used as a robust qubit encoding for a single bosonic mode subject to amplitude damping. They can also be used to study both the measurement process and decoherence by coupling the system to the external environment [5, 6, 7]. Thus, generating and measuring cat states is not only important to understand fundamental physics, but also to explore potential applications.

Superconducting quantum devices [8, 9, 10, 12, 21] allow to perform quantum state engineering including the demonstration of SCSs. Theoretical schemes to generate SCSs that are different from the above experiments [2] have also been proposed [13, 14, 15] in superconducting quantum devices. For example, the scheme in Ref. [13] generates a SCS of Bloch states for the current of a Josephson junction. Marquardt and Bruder [14] proposed ways to create superpositions of two coherent states for a harmonic oscillator approximated by a large superconducting island capacitively coupled to a smaller Cooper-pair box. Armour *et al.* [15] proposed a similar scheme as in Ref. [14] but using a micromechanical resonator as the harmonic oscillator. A review paper on micromechanical resonators [16] can be found in Ref. [17]. In Ref. [18], a scheme was proposed to generate macroscopic quantum superpositions and squeezed states for a superconducting quantum interference device (SQUID) ring modelled as an oscillator. Since then, several proposals have been made which focus on superconducting qubits interacting with the nonclassical electromagnetic field [19, 20, 21, 22, 23, 24].

Optical SCSs allow a fast and convenient optical transmission of the quantum information which is stored in charge qubits. Compared with the harmonic system [14, 15] formed by the large superconducting junction and the micromechanical resonator, optical qubits can easily fly relatively long distances between superconducting charge qubits. Moreover, the qubit formed by SCSs enables a more efficient error correction than that formed by the single photon and vacuum states, and the generation and detection of coherent light are easy to implement.

In contrast to [14, 15], here we aim at generating SCSs formed by two optical coherent states of a single-mode microwave cavity field which interacts with a SQUID-based charge qubit. The generation of such states has been studied theoretically [25] and demonstrated in optical cavity QED experiments [4]. However, in these cases: i) several operations are needed because atoms must pass through three cavities, and ii) the interaction times are tuned by the controlling velocity of the atoms flying through the cavity. In our proposal, we need only one cavity, and interaction times are controlled by changing the external magnetic field.

Although our scheme is similar to that proposed in Ref. [15], the interaction between the box and the resonator in Ref. [15] is not switchable. Due to the fixed coupling in Ref. [15], the transfer of information between the micromechanical resonator and the box still exists even after the SCS is produced. In our proposal, the interaction between the cavity field and the SQUID can be switched off by a classical magnetic field after the SCS is generated. Furthermore, three operations, with different approximations made in every operation, are required in Ref. [15]. In addition, in order to minimize the environmental effect on the prepared state, the number of operations and instruments should be as small as possible; *one* operation is enough to generate SCS. Thus our proposed scheme offers significant advantages over the pioneering proposals in Refs. [14] and [15].

II. MODEL

We consider a SQUID-type qubit superconducting box with n excess Cooper-pair charges connected to a superconducting loop via two identical Josephson junctions with capacitors C_J and coupling energies E_J. A controllable gate voltage V_g is coupled to the box via the gate capacitor C_g with dimensionless gate charge $n_g = C_g V_g/2e$. The qubit is assumed to work in the charge regime with $k_B T \ll E_J \ll E_C \ll \Lambda$, where k_B, T, E_C, and Λ are the Boltzmann constant, temperature, charge and superconducting gap energies, respectively. We consider a gate voltage range near a degeneracy point $n_g = 1/2$, where only two charge states, called $n = 0$ and $n = 1$, play a leading role. The other charge states with a much higher energy can be neglected, which implies that the superconducting box can be reduced to a two-level system or qubit [26]. This superconducting two-level system can be represented by a spin-$\frac{1}{2}$ notation such that the charge states $n = 0$ and $n = 1$ correspond to eigenstates $|\uparrow\rangle$ and $|\downarrow\rangle$ of the spin operator σ_z, respectively. If such a qubit is placed into a single-mode superconducting cavity, the Hamiltonian can be written as [21, 27]

$$H = \hbar\omega a^\dagger a + E_z\sigma_z - E_J\sigma_x \cos\frac{\pi}{\Phi_0}\left(\Phi_c I + \eta\, a + \eta^*\, a^\dagger\right), \quad (1)$$

where the first term represents the free Hamiltonian of the cavity field with frequency ω, and $E_z = -2E_{\rm ch}(1 - 2n_g)$ with the single-electron charging energy $E_{ch} = e^2/(C_g + 2C_J)$. Here Φ_0 is the flux quantum, Φ_c is the flux generated by the classical magnetic field through the SQUID, and I is the identity operator. The last term in Eq. (1) is the nonlinear photon-qubit interaction. The parameter η has units of magnetic flux and its absolute value represents the strength of the quantum flux inside the cavity. We will later on assume this "quantum magnetic flux" η to be small, becoming our perturbation parameter. The parameter η can be written as

$$\eta = \int_S \mathbf{u}(\mathbf{r}) \cdot d\mathbf{s}, \quad (2)$$

where $\mathbf{u}(\mathbf{r})$ is the mode function of the cavity field, with annihilation (creation) operators a ($a^\dagger$), and S is the surface defined by the contour of the SQUID. For convenience, hereafter, we denote $|\downarrow\rangle$ and $|\uparrow\rangle$ by $|e\rangle$ and $|g\rangle$, respectively. The cosine in Eq. (1) can be decomposed into classical and quantized parts; Eq. (1) can then be expressed as

$$\begin{aligned} H &= \hbar\omega a^\dagger a - E_J\sigma_x \cos\left(\frac{\pi\Phi_c}{\Phi_0}\right)\cos\frac{\pi}{\Phi_0}\left(\eta\, a + \eta^*\, a^\dagger\right) \\ &+ E_z\sigma_z + E_J\sigma_x \sin\left(\frac{\pi\Phi_c}{\Phi_0}\right)\sin\frac{\pi}{\Phi_0}\left(\eta\, a + \eta^*\, a^\dagger\right). \quad (3) \end{aligned}$$

The factors $\sin[\pi(\eta\, a + H.c.)/\Phi_0]$ and $\cos[\pi(\eta\, a + H.c.)/\Phi_0]$ can be further expanded as a power series in a ($a^\dagger$). For the single photon transition between the states $|e, n\rangle$ and $|g, n+1\rangle$, if the condition

$$\frac{\pi|\eta|}{\Phi_0}\sqrt{n+1} \ll 1 \quad (4)$$

is satisfied, all higher orders of $\pi|\eta|/\Phi_0$ can be neglected in the expansion of Eq. (3). To estimate the interaction coupling between the cavity field and the qubit, we assume that the mode function of the cavity field is a standing-wave

$$B_x = -i\sqrt{\frac{\hbar\omega}{\varepsilon_0 V c^2}}(a - a^\dagger)\cos(kz),$$

where V, ε_0, c, and k are the volume of the cavity, permittivity of the vacuum, light speed and wave vector of the cavity mode, respectively. The magnetic field is assumed to propagate along the z direction. The SQUID is placed in the middle of the cavity and the polarization of the magnetic field is assumed along the normal direction of the surface area of the SQUID. If the mode function $u(\mathbf{r})$ is assumed to be independent of the integral area (because the dimension of the SQUID, such as 10 μm, is much less than the microwave wavelength of the cavity mode), then

$$|\eta| = S\sqrt{\frac{h}{\varepsilon_0 c\lambda V}}\cos(kz),$$

which shows that the parameter $|\eta|$ depends on the area S and the position z of the SQUID, the wavelength λ of cavity field, and the volume V of the cavity. It is obvious that a larger S for the SQUID corresponds to a larger $|\eta|$. If the dimension of the cavity is equal to a full wavelength, then the interaction between the cavity field and the qubit reaches its maximum, and

$$3.28 \times 10^{-9} \le \pi|\eta|/\Phi_0 \le 7.38 \times 10^{-5} \ll 1 \quad (5)$$

in the microwave region with 15 cm $\ge \lambda \ge$ 0.1 cm. The linear dimension of the SQUID is taken as 10 μm, and the mode function $u(\mathbf{r})$ is assumed to be independent of the integral area because the dimension of the SQUID, 10 μm, is much less than the microwave wavelength λ of the cavity mode. For a half- or quarter-wavelength cavity, the condition $\pi|\eta|/\Phi_0 \ll 1$ can also be satisfied. Therefore, the approximation in Eq. (4) can be safely made in the microwave regime, and then Eq. (3) can be further simplified (up to first order in $\xi = \pi\eta/\Phi_0$) as

$$\begin{aligned} H_1 &= \hbar\omega a^\dagger a + E_z\sigma_z - E_J\sigma_x \cos\left(\frac{\pi\Phi_c}{\Phi_0}\right) \\ &+ E_J\sigma_x \sin\left(\frac{\pi\Phi_c}{\Phi_0}\right)\left(\xi\, a + \xi^*\, a^\dagger\right), \quad (6) \end{aligned}$$

where ξ is a dimensionless complex number with its absolute value equal to the dimensionless quantum magnetic flux, and it is defined by

$$\xi = \frac{\pi}{\Phi_0}\int_S \mathbf{u}(\mathbf{r}) \cdot d\mathbf{s} = \frac{\pi}{\Phi_0}\eta. \quad (7)$$

III. GENERATION OF CAT STATES

We assume that the qubit is initially in the ground state $|g\rangle$, and the cavity field is in the vacuum state $|0\rangle$. Now let us

adjust the gate voltage V_g and classical magnetic field such that $n_g = 1/2$ and $\Phi_c = \Phi_0/2$, and then let the whole system evolve a time interval τ. The state of the qubit-photon system evolves into

$$|\psi(\tau)\rangle = \exp\{-i[\omega a^\dagger a + \sigma_x(\Omega a + \Omega^* a^\dagger)]\tau\}|0\rangle|g\rangle$$
$$= \frac{1}{2}[(|\alpha\rangle + |-\alpha\rangle)|g\rangle + (|\alpha\rangle - |-\alpha\rangle)|e\rangle], \quad (8)$$

where the complex Rabi frequency $\Omega = \xi E_J$, and $|\pm\alpha\rangle$ denotes coherent state

$$|\pm\alpha\rangle \equiv e^{-|\alpha|^2/2}\sum_{n=0}^{\infty}\frac{(\pm\alpha)^n}{\sqrt{n!}}|n\rangle \quad (9)$$

with

$$\alpha = \frac{\xi E_J}{\hbar\omega}(e^{-i\omega\tau} - 1).$$

In the derivation of Eq. (8), we use the formula $\exp[\theta(\beta_1 a + \beta_2 a^\dagger a + \beta_3 a^\dagger)] = \exp[f_1 a^\dagger]\exp[f_2 a^\dagger a]\exp[f_3 a]\exp[f_4]$ with the relations $f_1 = \beta_3(e^{(\beta_2\theta)} - 1)/\beta_2$, $f_2 = \exp(\beta_2\theta)$, $f_3 = \beta_1(e^{(\beta_2\theta)} - 1)/\beta_2$, and $f_4 = \beta_1\beta_3(e^{(\beta_2\theta)} - \beta_2 - 1)/\beta_2^2$. After the time interval τ, we impose $\Phi_c = 0$ by adjusting the classical magnetic field, thus the interaction between the charge qubit and the cavity field is *switched off* (e.g., the last term in Eq. (6) vanishes). Eq. (8) shows that an entanglement of the qubit and the cat states can be prepared for an evolution time $\tau \neq 2m\pi$ with the integer number m. If the condition $e^{-i\omega\tau} \neq 1$ is satisfied in Eq. (8), the SCSs of the cavity field

$$|\text{cat}\rangle_\pm = \frac{1}{\sqrt{2 \pm e^{-2|\alpha|^2}}}(|\alpha\rangle \pm |-\alpha\rangle) \quad (10)$$

can be obtained by measuring the charge state $|e\rangle$ or $|g\rangle$, by using, for example, a single-electron transistor (SET).

If we initially inject a coherent light $|\alpha'\rangle$, then by using the same method as in the derivation of Eq. (8), we can also obtain the time-dependent cat states formed by two different optical coherent states $|\alpha_\pm\rangle$ with the evolution time τ_1:

$$|\varphi(\tau_1)\rangle = \frac{1}{2}[(|\alpha_+\rangle + |\alpha_-\rangle)|g\rangle + (|\alpha_+\rangle - |\alpha_-\rangle)|e\rangle], \quad (11)$$

where

$$\alpha_\pm = \alpha' e^{(-i\omega\tau_1)} \pm \kappa[1 - e^{(-i\omega\tau_1)}]$$

with

$$\kappa = \frac{\xi^* E_J}{\hbar\omega}.$$

After a time interval τ_1, we can switch off the interactions between the charge qubit and the cavity field by setting $\Phi_c = 0$ and $n_g = 1/2$. Measuring the charge states, we can obtain the cat states denoted by $|\text{SCS}\rangle$

$$|\text{SCS}\rangle = N_\pm^{-1}(|\alpha_+\rangle \pm |\alpha_-\rangle)$$

with normalized constant

$$N_\pm = \sqrt{2 \pm (\langle\alpha_+|\alpha_-\rangle + \langle\alpha_-|\alpha_+\rangle)},$$

where $\langle\alpha_\mp|\alpha_\pm\rangle$ can be easily obtained [30] by the above expression of $\alpha_\pm$, for example,

$$\langle\alpha_+|\alpha_-\rangle = \exp\{-4\kappa^2[1 - \cos(\omega\tau_1)] - i2\kappa\alpha'\sin(\omega\tau_1)\},$$

here we assume that the injected coherent field has a real amplitude α'. In Eq. (11), we entangle two different superpositions of coherent states with the ground and excited states of the qubit. We can also entangle two different coherent states $|\alpha_\pm\rangle$ with the qubit states by applying a classical flux such that $\Phi_c = \Phi_0$. Then with the time evolution $t = \pi/4E_J$, we have

$$|\psi(\tau_1)\rangle = \frac{1}{2}(|\alpha_-\rangle|g\rangle + |\alpha_+\rangle|e\rangle). \quad (12)$$

From a theoretical point of view, if we can keep the expansion terms in Eq. (3) up to second order in $\xi = \pi\eta/\Phi_0$, we can also *prepare a superposition of two squeezed coherent states, which could be used to encode an optical qubit* [29]. To obtain this superposition of two squeezed coherent states, we can set $n_g = 1/2$ and $\Phi_c = 0$, and derive the Hamiltonian from Eq. (3) to get (up to second order in ξ)

$$H_2 = (\hbar\omega - |\xi|^2 E_J\sigma_x)a^\dagger a - E_J\left(1 + \frac{|\xi|^2}{2}\right)\sigma_x$$
$$- E_J\sigma_x\left(\frac{\xi^2}{2}a^2 + \frac{\xi^{*2}}{2}a^{\dagger 2}\right). \quad (13)$$

If the system is initially in the coherent state $|\gamma\rangle$, and if the charge qubit is in the ground state $|g\rangle$, we can entangle qubit states with superpositions of two different squeezed coherent states with an evolution time t as

$$|\psi(t)\rangle = \frac{1}{2}\left[e^{-i\theta t}|\gamma, -i\frac{\xi^{*2}E_J}{\hbar}t\rangle + e^{i\theta t}|\gamma, i\frac{\xi^{*2}E_J}{\hbar}t\rangle\right]|g\rangle$$
$$+\frac{1}{2}\left[e^{-i\theta t}|\gamma, -i\frac{\xi^{*2}E_J}{\hbar}t\rangle - e^{i\theta t}|\gamma, i\frac{\xi^{*2}E_J}{\hbar}t\rangle\right]|e\rangle, \quad (14)$$

where

$$\theta = E_J\left(1 + \frac{|\xi|^2}{2}\right), \quad (15a)$$

$$|\gamma, \mp i\frac{\xi^{*2}E_J}{\hbar}t\rangle = U_\pm(t)|\gamma\rangle, \quad (15b)$$

and

$$U_\pm(t) = \exp\left\{-it\left(\omega \mp \frac{|\xi|^2 E_J}{\hbar}\right)a^\dagger a\right\}$$
$$\times \exp\left\{\mp i\frac{E_J}{\hbar}\left(\frac{\xi^2}{2}a^2 + \frac{\xi^{*2}}{2}a^{\dagger 2}\right)t\right\}. \quad (15c)$$

Here, $|\gamma, \mp i\xi^{*2}E_J t/\hbar\rangle$ denote squeezed coherent states, and the degree of squeezing [31, 32] is determined by the time-dependent parameter $|\xi|^2 E_J t/\hbar$. A superposition of two squeezed coherent states can be obtained by the measurement on the charge qubit. However, we should note that if we keep to first order in $|\xi| = \pi|\eta|/\Phi_0$ the expansions of Eq. (3), the interaction between the cavity field and the charge qubit is switchable (e.g., the last term in Eq. (6) vanishes for $\Phi_c = 0$). But if we keep terms up to second order in $|\xi|$ for the expansions of Eq. (3), then the qubit-field coupling is not switchable.

IV. DISCUSSIONS

The analytical expressions in Eqs. (8), (11), and (14) show how to prepare two macroscopically distinguishable states by measuring the charge states. However, similarly to the optical cavity QED [25], prepared superpositions of states are limited by the following physical quantities: the Rabi frequency $|\Omega| = |\xi| E_J$ (which determines the quantum operation time t_q of two charge qubit states through the cavity field), the lifetime t_d of the cavity field, the lifetime T_1 and dephasing time T_2 of the charge qubit, as well as the measurement time τ_m on the charge qubit.

We now estimate the Rabi frequency $|\Omega|$ in the microwave regime for a standing-wave field in the cavity. A SQUID with a typical linear dimension of about $10\,\mu$m is assumed to be placed in the middle of the cavity. In the microwave regime with different ratios of $E_{\rm ch}/E_{\rm J}$, we provide a numerical estimate of $|\Omega|/h$ for $\omega = 2E_{ch}/\hbar$ in a full-wavelength cavity, shown in Fig. 1(a), and a quarter-wavelength cavity, shown in Fig. 1(b). The results reveal that a shorter wavelength of cavity field corresponds to a larger Rabi frequency $|\Omega|$. For example, in the full-wavelength cavity, $|\Omega|/h$ with microwave length 0.1 cm is of the order of 10^6 Hz, and yet it is about 10 Hz for a microwave wavelength of 15 cm. In both cases, the transition times from $|0\rangle|e\rangle$ to $|1\rangle|g\rangle$ are about 10^{-6} s and 0.1 s respectively, where $|0\rangle$ ($|1\rangle$) is the vacuum (single-photon) state. The experiment for this scheme should be easier for shorter wavelengths than for long wavelengths. For a fixed wavelength, the effect of the ratios $E_{\rm ch}/E_{\rm J}$ on the coupling between the cavity field and the charge qubit is not so large. However, decreasing the volume V of the cavity can efficiently increase the coupling.

In order to obtain a cat state, the readout time τ_m of the charge qubit should be less than the dephasing time T_2 of the charge qubit (because the relaxation time T_1 of the charge qubit is longer than its dephasing time T_2) and the lifetime time t_d of the cavity field. For example, in Ref. [15] with a set of given parameters, the estimated time, $\tau_m = 4$ ns, is less than $T_2 = 5$ ns [9]. For a good cavity [33], the quality factor Q can reach very high values, such as $Q = 3 \times 10^8$, and then the lifetimes of the microwave field would be in the range $0.001\ {\rm s} \leq t_d \leq 0.15\ {\rm s}$, which implies $t_m \ll t_d$. So the readout is possible within current technology. It is easier to prepare a cat state in such a system even when the coupling between the charge qubit and the cavity field is weak because, in principle, two different coherent states could be obtained with a very short time t_q such that $t_q \ll T_2$.

V. CONCLUSIONS

In conclusion, we have analyzed the generation of Schrödinger cat states of a single-mode microwave field by coupling it to a controllable SQUID-type charge qubit. Based on our scheme, the SCS can be generated by using one quantum operation together with the quantum measurement on the charge qubit. After the SCS is created, the coupling between the charge qubit and the cavity field can be switched off if the coupling constant $|\xi| = \pi|\eta|/\Phi_0 \ll 1$ because, in such a condition, all interaction terms of higher order in $\xi = \pi\eta/\Phi_0$ are negligible. This results in a switchable qubit-field interaction.

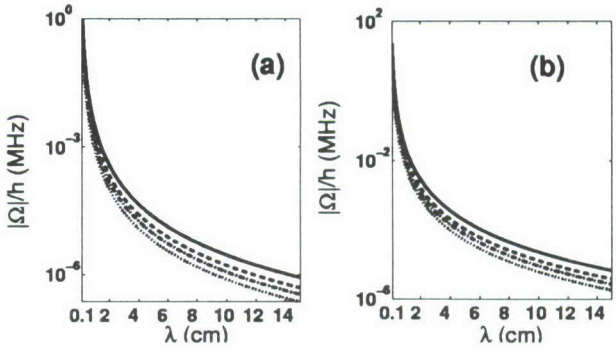

FIG. 1: Rabi frequency $|\Omega|$ versus the microwave wavelength λ for a full-wavelength cavity (a) and a quarter-wavelength cavity (b) with ratios $E_{\rm ch}/E_{\rm J} = 4$ (top solid line), 7 (dashed line), 10 (dashed-dotted line), 15 (bottom dotted line), respectively.

We have also proposed a scheme to generate superpositions of two squeezed coherent states if we can keep the expansion terms in Eq. (3) up to second order in $\xi = \pi\eta/\Phi_0$. However, in this case the interaction between the cavity field and the charge qubit cannot be switched off. By using the same method employed for trapped ions [34], we can measure the decay rate of the SCS and obtain the change of the Q value due to the presence of the SQUID.

Also, the generated SCSs can be used as a source of optical qubits. Our suggestion is that the first experiment for generating nonclassical states via the interaction with the charge qubit should be the generation of superpositions of two macroscopically distinct coherent states. It needs only one quantum operation, and the condition for the coupling between the cavity field and the charge qubit can be slightly relaxed. This proposal should be experimentally accessible in the near future.

VI. ACKNOWLEDGMENTS

We acknowledge comments on the manuscript from X. Hu and S. C. Bernstein. This work was supported in part by the National Security Agency (NSA), Advanced Research and Development Activity (ARDA) under Air Force Office of Research (AFOSR) contract number F49620-02-1-0334, and by the National Science Foundation grant No. EIA-0130383.

[1] see, e.g., B. Yurke and D. Stoler, Phys. Rev. Lett. **57**, 13 (1986); B. Yurke, W. Schleich, and D.F. Walls, Phys. Rev. A **42**, 1703 (1990); V. Buzek, H. Moya-Cessa, P. L. Knight, S. J. D. Phoenix, *ibid.* **45**, 8190 (1992); G. J. Milburn, *ibid.* **33**, 647 (1986); T. Ogawa, M. Ueda, and N. Imoto, *ibid.* **43**, 6458 (1991); A. Miranowicz, R. Tanas, and S. Kielich, Quantum Opt. **2**, 253 (1990).

[2] C.H. van der Wal, A.C.J. ter Haar, F.K. Wilhelm, R.N. Schouten, C.J.P.M. Harmans, T.P. Orlando, S. Lloyd, J. E. Mooij, Science **290**, 773 (2000); S. Han, Y. Yu, X. Chu, S. Chu, and Z. Wang, *ibid.* **293** 1457 (2001); J.R. Friedman, V. Patel, W. Chen, S.K. Tolpygo, and J. E. Lukens, Nature **406**, 43 (2000);

[3] C. Monroe, D.M. Meekhof, B.E. King, D.J. Wineland, Science **272**, 1131 (1996).

[4] M. Brune, E. Hagley, J. Dreyer, X. Matre, A. Maali, C. Wunderlich, J.M. Raimond, and S. Haroche, Phys. Rev. Lett. **77**, 4887 (1996); J.M. Raimond, M. Brune, and S. Haroche, Phys. Rev. Lett. **79**, 1964 (1997).

[5] T.C. Ralph, A. Gilchrist, G.J. Milburn, W.J. Munro, and S. Glancy, Phys. Rev. A **68**, 042319 (2003).

[6] P.T. Cohrane, G.J. Milburn, and W.J. Munro, Phys. Rev. A **59**, 2631 (1999); S.J. van Enk and O. Hirota, *ibid.* **64**, 022313 (2001); H. Jeong, M.S. Kim, and J. Lee, *ibid.* **64**, 052308 (2001).

[7] Yu-xi Liu, S.K. Özdemir, M. Koashi, and N. Imoto, Phys. Rev. A **65**, 042326 (2002); Yu-xi Liu, A. Miranowicz, M. Koashi, and N. Imoto, *ibid.* A **66**, 062309 (2002).

[8] J.E. Mooij, T.P. Orlando, L. Levitov, L. Tian, C.H. van der Wal, and S. Lloyd, Science **285**, 1036 (1999); Y. Yu, S. Han, Xi Chu, S.I. Chu, and Z. Wang, *ibid.* **296**, 889 (2002); I. Chiorescu, Y. Nakamura, C.J.P.M. Harmans, and J.E. Mooij, *ibid.* **299**, 1869 (2003); A.J. Berkley, H. Xu, R.C. Ramos, M.A. Gubrud, F.W. Strauch, P.R. Johnson, J.R. Anderson, A.J. Dragt, C.J. Lobb, and F.C. Wellstood, *ibid.* **300**, 1548 (2003).

[9] Y. Nakamura, Y.A. Pashkin, and J.S. Tsai, Nature **398**, 786 (1999); Y.A. Pashkin, T. Yamamoto, O. Astafiev, Y. Nakamura, D.V. Averin, and J.S. Tsai, *ibid.* **421**, 823 (2003).

[10] D. Vion, A. Aassime, A. Cottet, P. Joyez, H. Pothier, C. Urbina, D. Esteve, M.H. Devoret, Science **296**, 886 (2002).

[11] J.Q. You, J.S. Tsai, and F. Nori, Phys. Rev. Lett. **89**, 197902 (2002). A longer version of it is available in cond-mat/0306203; see also *New Directions in Mesoscopic Physics*, edited by R. Fazio, V.F. Gantmakher, and Y. Imry (Kluwer Academic Publishers, 2003), 351.

[12] L.F. Wei, Y.X. Liu, and F. Nori, cond-mat/0402678.

[13] C.C. Gerry, Phys. Rev. B **57**, 7474 (1998).

[14] F. Marquardt and C. Bruder, Phys. Rev. B **63**, 054514 (2001).

[15] A.D. Armour, M.P. Blencowe, and K.C. Schwab, Phys. Rev. Lett. **88**, 148301 (2002).

[16] M.D. Lahaye, O. Buu, B. Camarota, and K.C. Schwab, Science, **304**, 74 (2004); E.K. Irish and K.C. Schwab, Phys. Rev. B **68**, 155311 (2003); A. Hopkips, K. Jacobs, S. Habib, and K. Schwab, Phys. Rev. B **68**, 235328 (2003)

[17] M. Blencowe, Phys. Rep. **395**, 159 (2004).

[18] M.J. Everitt, T.D. Clark, P.B. Stiffell, A. Vourdas, J.F. Ralph, R.J. Prance, H. Prance, Phys. Rev. A **69**, 043804 (2004).

[19] W.A. Al-Saidi and D. Stroud, Phys. Rev. B **65**, 224512 (2002).

[20] S.L. Zhu, Z.D. Wang, and K. Yang, Phys. Rev. A **68**, 034303 (2003).

[21] J.Q. You and F. Nori, Phys. Rev. B **68**, 064509 (2003); J.Q. You, J.S. Tsai, and Franco Nori, *ibid.* **68**, 024510 (2003).

[22] A. Vourdas, Phys. Rev. B **49**, 12040 (1994); C.P. Yang, S.I. Chu, and S. Han, Phys. Rev. A **67**, 042311 (2003).

[23] Y.B. Gao, C. Li, and C.P. Sun, quant-ph/0402172.

[24] S.M. Girvin, R.S. Huang, A. Blais, A. Wallraff, and R.J. Schoelkopf, cond-mat/0310670.

[25] L. Davidovich, M. Brune, J. M. Raimond, and S. Haroche, Phys. Rev. A **53**, 1295 (1996); M.C. de Oliveira, M.H.Y. Moussa, and S.S. Mizrahi, *ibid.* **61**, 063809 (2000).

[26] Y. Makhlin, G. Schön, and A. Shnirman, Rev. Mod. Phys. **73**, 357(2001); Y. Makhlin, G. Schön, and A. Shnirman, Nature, **398**, 305 (1999).

[27] Yu-xi Liu, L.F. Wei, and F. Nori, quant-ph/0402189.

[28] E. Knill, R. laflamme, and G.J. Milburn, Nature, **409**, 46 (2001); J.I. Cirac, P. Zoller, H.J. Kimble, and H. Mabuchi, Phys. Rev. Lett. **78**, 3221 (1997).

[29] D. Gottesman, A. Kitaev, and J. Preskill, Phys. Rev. A **64**, 012310 (2001).

[30] M.O. Scully and M.S. Zubairy, *Quantum optics* (Cambridge University Press, Cambridge, 1997).

[31] D. Stoler, Phys. Rev. D **1**, 3217 (1970); H.P. Yuan, Phys. Rev. A **13**, 2226 (1976); C.M. Caves, Phys. Rev. D **23**, 1693 (1981).

[32] A. Yariv, *Quantum electronics* (John Wiley & Sons, New York, 1988).

[33] J. Krause, M.O.Scully, and H. Walther, Phys. Rev. A **36**, 4547 (1987); J. Krause, M.O.Scully, T. Walther, and H. Walther, *ibid.* **39**, 1915 (1989); S. Brattke, B.T.H. Varcoe, and H. Walther, Phys. Rev. Lett. **86**, 3534 (2001); J.M. Raimond, M. Brune, and S. Haroche, Rev. Mod. Phys. **73**, 565 (2001).

[34] Q.A. Turchette, C.J. Myatt, B.E. King, C.A. Sackett, D. Kielpinski, W.M. Itano, C. Monroe, and D.J. Wineland, Phys. Rev. A **62**, 053807 (2000).

International Journal of Quantum Information
Vol. 1, No. 4 (2003) 1–6

World Scientific
www.worldscientific.com

ENTANGLEMENT OF TWO COUPLED CHARGE QUBITS

YU. A. PASHKIN*,¶, T. TILMA*,§, D. V. AVERIN†, O. ASTAFIEV*, T. YAMAMOTO*,‡, Y. NAKAMURA*,‡, F. NORI*,§ and J. S. TSAI*,‡

The Institute of Physical and Chemical Research (RIKEN), 2-1 Hirosawa, Wako, Saitama 305-0198, Japan

†*Department of Physics and Astronomy, Stony Brook University, SUNY Stony Brook, NY 11794, USA*

‡*NEC Fundamental Research Laboratories, 34 Miyukigaoka, Tsukuba, Ibaraki 305-8501, Japan*

§*Department of Physics and Astronomy, University of Michigan, Ann Arbor, MI 48109-1120, USA*

Received 31 October 2003

We have analyzed the entanglement of a system of two coupled charge qubits. We calculate the amount of entanglement using several different approaches. We show that in the ideal case the system remains entangled most of the time and the amount of entanglement reaches almost unity, i.e. the system becomes maximally entangled at certain instances.

Keywords: quantum computation; quantum bits; entanglement.

1. Introduction

Entanglement is a peculiar, yet natural, nonclassical correlation that is possible between separated quantum systems. Although entanglement has been known for many years as a purely theoretical subject, it turned into a practical issue recently after it was realized that it plays a crucial role in quantum computation and quantum comunication.

Entanglement of two quantum systems can be understood by using the following example. Let us consider two single qubits A and B whose states can be presented as a superposition of the basis states: $|\psi_A\rangle = a_1|0\rangle_1 + a_2|1\rangle_1$ and $|\psi_B\rangle = b_1|0\rangle_2 + b_2|1\rangle_2$, where $|0\rangle_{1(2)}$ and $|1\rangle_{1(2)}$ are the basis states of the first (second) qubits and $a_{1,2}$ and $b_{1,2}$ are the corresponding amplitudes. In the unentangled case, the state $|\psi\rangle$ of a composite two-qubit system can be described as a product of two single-qubit states:

$$|\psi\rangle = |\psi_A\rangle|\psi_B\rangle = c_1|00\rangle + c_2|10\rangle + c_3|01\rangle + c_4|11\rangle \quad (1)$$

¶Permanent address: P. N. Lebedev Physical Institute Moscow 117924, Russia.

where c_i $(i = 1, 2, 3, 4)$ are the amplitudes of the two-qubit states that are the product of the corresponding amplitudes of the single-qubit states (e.g. $c_1 = a_1 b_1$, etc). Here we use the following notations: $|00\rangle = |0\rangle_1|0\rangle_2$, $|10\rangle = |1\rangle_1|0\rangle_2$, $|01\rangle = |0\rangle_1|1\rangle_2$ and $|11\rangle = |1\rangle_1|1\rangle_2$. There exist certain two-qubit states for which $|\psi\rangle \neq |\psi_A\rangle|\psi_B\rangle$. For example, the state $|\psi\rangle = 1/\sqrt{2}(|00\rangle + |11\rangle)$ cannot be reduced to a product of two single-qubit states described by Eq. (1). Such a state is called an entangled state.

For practical purposes, one needs to quantify entanglement. A few measures of entanglement have been introduced: *negativity*, *concurrence*, *entanglement of formation* and *entropy of entanglement*.

Here we consider a system of two coupled charge qubits and calculate the time evolution of entanglement using these criteria.

2. Measures of Entanglement

Let us note first that there is a simple qualitative test for entanglement provided by Peres[1] and Horodecki.[2] For 2×2 systems like the one we consider here, the necessary and sufficient condition for entanglement is the negativity of the partial transposition of a state of the system. That is, if the partially transposed density matrix[a]

$$\rho = \sum_i p_i |\psi_i\rangle\langle\psi_i|$$

has negative eigenvalues then the system is entangled, if the eigenvalues are zero or positive then the system is unentangled.

Based on the qualitative partial transpose approach, a quantitative entanglement measure, called *negativity*, can be introduced:[3]

$$N(\rho) = \max(0, -2\lambda_{\min}), \tag{2}$$

where $\lambda_{\min}$ is the smallest eigenvalue of the partial transpose of the state ρ.

The concept of *concurrence* originates from Ref. 4 and is defined for a pair of qubits as[5]

$$C(\rho) = \max(0, \lambda_1 - \lambda_2 - \lambda_3 - \lambda_4), \tag{3}$$

where the λ_i's are the square roots of the eigenvalues of $\rho\tilde{\rho}$ in descending order. Here $\tilde{\rho}$ is the result of applying the spin-flip operation to ρ: $\tilde{\rho} = (\sigma_y \otimes \sigma_y)\rho^*(\sigma_y \otimes \sigma_y)$, where ρ^* is a complex conjugate of ρ.

For a pure state $|\psi\rangle$ of a composite system (see Eq. (1)), the concurrence can be expressed as[6] $C(\psi) = 2|c_1 c_4 - c_2 c_3|$.

[a] (p_i are the state probabilities satisfying the normalization condition $\sum_i p_i = 1$).

For a pair of qubits, there exists an explicit formula for the *entanglement of formation* E_f based on the concept of concurrence. For a pure state ρ, the entanglement of formation is related to concurrence as[6]

$$E_f = \mathcal{E}(C(\rho)), \tag{4}$$

where the function $\mathcal{E}$ is defined by

$$\mathcal{E}(C) = h\left(\frac{1+\sqrt{1-C^2}}{2}\right); \tag{5}$$

$$h(x) = -x\log_2 x - (1-x)\log_2(1-x). \tag{6}$$

This definition can be further extended to the more general case of mixed states.[7]

The simplest case of an entangled system is a pair of qubits in a pure but nonfactorizable state. In this case the entanglement can be defined via the von Neuman *entropy* of either qubit A or B:[8]

$$E_e = -\mathrm{Tr}\rho_A \log_2 \rho_A = -\mathrm{Tr}\rho_B \log_2 \rho_B\,, \tag{7}$$

where $\rho_A = |\psi_A\rangle\langle\psi_A|$ and $\rho_B = |\psi_B\rangle\langle\psi_B|$ are the density matrices of subsystem A and B, respectively. For such a sytem, the entanglement of formation defined in Eq. (4) coincides with the entropy of entanglement.

3. Circuit and Model

We consider a system of two coupled charge qubits.[9] Each qubit is a Cooper-pair box whose charge states are quantized when the charging energy of the box $E_{c1,2} = (2e)^2/2C_{1,2}$ exceeds the Josephson energy $E_{J1,2}$ of its coupling to a reservoir. Here $C_{1,2}$ is the total capacitance of the corresponding Cooper-pair box and $2e$ is the Cooper-pair charge. The qubits are coupled by an on-chip capacitor giving a mutual coupling energy E_m. At low temeperature and in a proper voltage range, each qubit is reduced to a two-level system and, under condition $E_{J1,2} \sim E_m$, the whole system can be described by the two-qubit Hamiltonian

$$H = \sum_{n_1,n_2=0}^{1} E_{n_1n_2}|n_1n_2\rangle\langle n_1n_2| - \frac{E_{J1}}{2}\sum_{n_2=0}^{1}(|0\rangle\langle 1| + |1\rangle\langle 0|)\otimes|n_2\rangle\langle n_2|$$

$$-\frac{E_{J2}}{2}\sum_{n_1=0}^{1}|n_1\rangle\langle n_1|\otimes(|0\rangle\langle 1| + |1\rangle\langle 0|) \tag{8}$$

where

$$E_{n_1n_2} = E_{c1}(n_{g_1} - n_1) + E_{c2}(n_{g_2} - n_2) + E_m(n_{g_1} - n_1)(n_{g_2} - n_2)$$

are the electrostatic energies corresponding to different charge configurations, n_{g_1} and n_{g2}, are the normalized gate-induced charges on the corresponding qubit. The system has double degeneracy of electrostatic energies at $n_{g1} = n_{g2} = 0.5$:

$E_{00} = E_{11}$ and $E_{10} = E_{01}$. If the system is driven nonadiabatically from the $|00\rangle$ state to this point, it evolves coherently as was demonstrated in Ref. 9. The values of electrostatic energies at the double degeneracy point as well as Josephson energies were determined from the independent measurements: $E_{00} = E_{11} \approx 70.9$ GHz, $E_{10} = E_{01} \approx 63.6$ GHz and $E_{J1} = E_{J2} \approx 9.1$ GHz. Josephson energies were made equal by applying an external magnetic field to suppress E_{J1} from its maximum value of 13.4 GHz at zero magnetic field.

Then we calculate the evolution of entanglement using the criteria described above.

4. Results and Discussion

We consider an ideal case of a pure bipartite system. The evolution of the system starts from the $|00\rangle$ state, $\rho_0 = |00\rangle\langle 00|$. Neglecting decoherence, we calculate the time dependence of the density matrix using the Hamiltonian given in Eq. (8):

$$\rho(t) = U^{TC} \rho_0 U \,, \tag{9}$$

where $U = \exp(-iHt/\hbar)$ and U^{TC} is a transpose conjugate of U. Then we use $\rho(t)$ to check the Peres–Horodecki criteria and to calculate the amount of entanglement using Eqs. (2)–(4) and (7).

The result of the Peres–Horodecki test is shown in Fig. 1. It is clear that most of the time the product of eigenvalues is negative,[10] therefore our system passes the test. We then proceed with the calculation of the amount of entanglement.

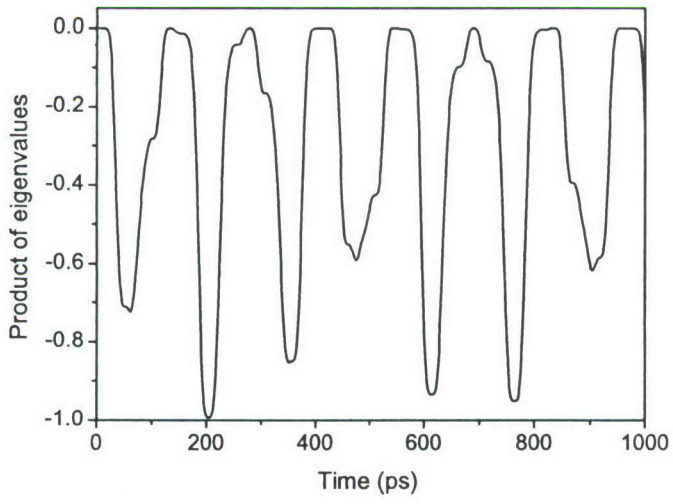

Fig. 1. Peres–Horodecki test for a coupled qubit system. Here the product has been normalized to the interval [0, 1].

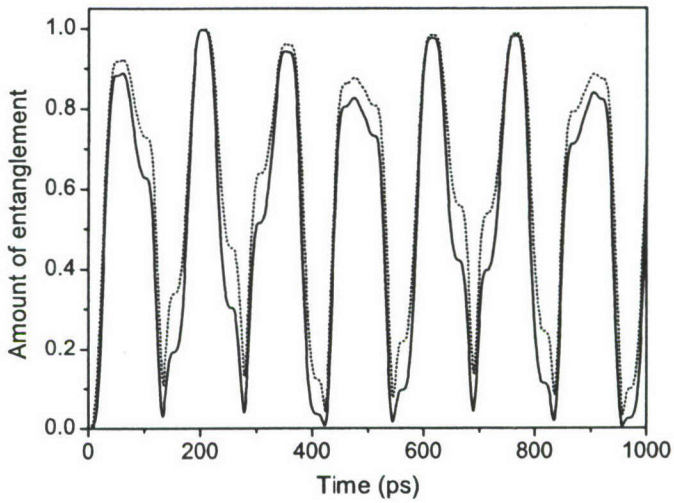

Fig. 2. Amount of entanglement in a system of two coupled charge qubits calculated by negativity, concurrence, entanglement of formation and entropy of entanglement. Dotted line — negativity and concurrence; solid line — entanglement of formation and entropy of entanglement.

Dependence of the amount of entanglement on time is presented in Fig. 2. All four criteria have been used, however, only two curves are seen in Fig. 2. This is due to the fact that for the considered case of pure states different approaches give similar results. For example, negativity coincides with concurrence and entanglement of formation coincides with the entropy of entanglement. Note that the results in Fig. 2 are consistent: despite small difference in absolute value the amout of entanglement basically coinsides and reaches maxima and minima at the same time instances. The results in Fig. 2 are also consistent with the results in Fig. 1. Amount of entanglement in Fig. 2 reaches maximum values when the product of eigenvalues in Fig. 1 reaches minimum values and vice versa.

Comparing the time evolution of the amount of entanglement with the time evolution of the state probabilities ρ_{00}, ρ_{10}, etc., we can conclude that the amount of entanglement reaches maximum values when the probabilities ρ_{00} and ρ_{11} are close to 1/2 while the probabilities of the states $|10\rangle$ and $|01\rangle$ almost vanish. On the other hand, the amount of entanglement is close to zero, when the probability of only one state, $|00\rangle$ or $|11\rangle$, approaches unity while the rest three being almost zero.

We stress finally that entanglement of two qubits is a result of their interaction described by the $E_m(n_{g_1}-n_1)(n_{g_2}-n_2)$ term in the Hamiltonian given in Eq. (8). If we switch off the interaction, i.e. set E_m equal to zero, then entanglement vanishes. With the non-zero interaction between the qubits, entanglement oscillates with the same frequencies as do other quantities of the system like state probabilities.

5. Conclusions

Our results show that the ideal coupled two-qubit system remains entangled most of the time during its coherent evolution. The amount of entanglement oscillates between zero (completely unentangled qubits) and unity (maximally entangled qubits). This is an optimistic scenario for entanglement because we considered only pure states and neglected decoherence. Still these results are basically true at least for the first $100, \ldots, 200$ picoseconds when decoherence is weak. In a more realistic approach, one should consider mixed states and take into account decoherence and real pulse shape.

Acknowledgements

We thank S. Lloyd for fruitful discussions.

References

1. A. Peres, *Phys. Rev. Lett.* **77**, 1413 (1996).
2. M. Horodecki, P. Horodecki and R. Horodecki, *Phys. Lett.* **A223**, 1 (1996).
3. G. Vidal and R. F. Werner, *Phys. Rev.* **A65**, 032314 (2002).
4. S. Hill and W. K. Wootters, *Phys. Rev. Lett.* **78**, 5022 (1997).
5. W. K. Wootters, *Phys. Rev. Lett.* **80**, 2245 (1998).
6. W. K. Wootters, *Quant. Inform. Comp.* **1**, 27 (2001).
7. H. H. Bennett, D. P. DiVincenzo, J. A. Smolin and W. K. Wootters, *Phys. Rev.* **A54**, 3824 (1996).
8. H. H. Bennett, H. J. Bernstein, S. Popescu and B. Schumacher, *Phys. Rev.* **A53**, 2046 (1996).
9. Yu. A. Pashkin, T. Yamamoto, O. Astafiev, Y. Nakamura, D. V. Averin and J. S. Tsai, *Nature* **421**, 823 (2003).
10. T. Tilma, M. Byrd and E. C. G. Sudarshan, *J. Phys. A.: Math. and Gen.* **35**, 10445 (2002).

Entanglement dynamics in two coupled charge qubits

T. Tilma,[1 2] * Yu. A. Pashkin, [3 4] † O. Astafiev, [3]
T. Yamamoto, [3] Y. Nakamura, [3] J. S. Tsai, [3] and F. Nori [1 2]

[1] *The Institute of Physical and Chemical Research, Wako-shi, Saitama-ken 350-0198 Japan*
[2] *Center for Theoretical Physics, Department of Physics, University of Michigan, Ann Arbor, Michigan 48109 USA*
[3] *NEC Fundamental Research Laboratories, Tsukuba-shi, Ibaraki-ken 305-8501 Japan*
[4] *P. N. Lebedev Physical Institute, Moscow 117924, Russia*

Abstract. We have analyzed the entanglement of two capacitively coupled Josephson-junction qubits under various pulse-induced regimes. Using Wootters concurrence we calculate the amount of entanglement produced. We show that, under specific pulse shapes, the qubits remain entangled most of the time and that the amount of entanglement reaches almost unity, i.e., the qubits are effectively maximally entangled, at certain instances.

Keywords: Implementation of Quantum Computation, Entanglement and Entanglement Measures

1 Introduction

Entanglement is a peculiar, yet natural, non-classical correlation that is possible between separated quantum systems. Although entanglement has been known for many years as a purely theoretical subject, it recently turned into a practical issue after it was realized that it plays a crucial role in quantum computation and quantum communication. For practical purposes then, one needs to quantify the entanglement in such systems; in this case, two capacitively-coupled, superconducting, charge qubits. To do this, we have chosen Wootters concurrence [1] as the practical, quantitative measure of entanglement between our two qubits, and have calculated its time evolution under various voltage pulse shapes.

2 Concurrence

The concurrence, $C(\phi)$, of a pair of qubits is defined as [1]

$$C(\phi) = \max(0, \lambda_1 - \lambda_2 - \lambda_3 - \lambda_4), \qquad (1)$$

where the λ_i's are the square roots of the eigenvalues of $\phi = \rho\tilde{\rho}$ in descending order. Here $\tilde{\rho}$ is the result of applying the spin-flip operation to ρ: $\tilde{\rho} = (\sigma_y \otimes \sigma_y)\rho^*(\sigma_y \otimes \sigma_y)$, where ρ^* is the complex conjugate of ρ. For a pure state $|\psi\rangle = c_1|00\rangle + c_2|10\rangle + c_3|01\rangle + c_4|11\rangle$, such as that found in our composite system, the concurrence, $C(\psi)$ can be expressed as [5]: $C(\psi) = 2|c_1c_4 - c_2c_3|$.

3 Circuit and model

In this work, we consider a system of two coupled charge qubits [6]. Each qubit is a Cooper-pair box whose charge states are quantized when the charging energy of the box $E_{c1(2)} = (2e)^2/2C_{1(2)}$ exceeds the Josephson energy $E_{J1(2)}$ of its coupling to a reservoir. Here $C_{1(2)}$ is the total capacitance of the corresponding Cooper-pair box and $2e$ is the Cooper-pair charge. The qubits are coupled by an on-chip capacitor giving a mutual coupling energy E_m. At low temperatures and in the proper voltage range, each qubit behaves as a two-level system, and under the condition $E_{J1(2)} \sim E_m$ the whole system can be described by the following, two qubit, Hamiltonian

$$\begin{aligned} H = & \sum_{n_1,n_2=0}^{1} E_{n_1n_2} |n_1n_2\rangle\langle n_1n_2| \\ & - \frac{E_{J1}}{2} \sum_{n_2=0}^{1} (|0\rangle\langle 1| + |1\rangle\langle 0|) \otimes |n_2\rangle\langle n_2| \\ & - \frac{E_{J2}}{2} \sum_{n_1=0}^{1} |n_1\rangle\langle n_1| \otimes (|0\rangle\langle 1| + |1\rangle\langle 0|) \end{aligned} \qquad (2)$$

where $E_{n_1n_2} = E_{c1}(n_{g_1} - n_1) + E_{c2}(n_{g_2} - n_2) + E_m(n_{g_1} - n_1)(n_{g_2} - n_2)$ are the electrostatic energies corresponding to different charge configurations, and n_{g_1} and n_{g2} are the normalized, gate-induced charges on the corresponding qubit. The system has a double degeneracy of electrostatic energies at $n_{g1} = n_{g2} = 0.5$: $E_{00} = E_{11}$ and $E_{10} = E_{01}$. If the system is driven from the $|00\rangle$ state to this point, it evolves coherently as was demonstrated in Ref. [6]. The values of the electrostatic energies at the double degeneracy point as well as Josephson energies were determined from independent measurements to be [6]: $E_{00} = E_{11} \approx 70.9$ GHz, $E_{10} = E_{01} \approx 63.6$ GHz and $E_{J1} = E_{J2} \approx 9.1$ GHz. The Josephson energies were made equal by applying an external magnetic field to suppress E_{J1} from its maximum value of 13.4 GHz at zero magnetic field.

4 Numerical simulations

As the model indicates, n_{g1} and n_{g2}, are the normalized, gate-induced charges on qubits 1 and 2 respectively. Now, one can calculate the time evolution of the system by first setting n_{g1} and n_{g2} to specific values (in this case 0.5) and, ignoring decoherence [7], use

$$\rho(t) = U\rho_0U^\dagger, \qquad (3)$$

where $U = \exp\left(-\frac{iHt}{\hbar}\right)$ and $U^\dagger$ is the transpose conjugate of U. Alternatively, one can assume that n_{g1} and n_{g2} are also time-dependent functions, hereafter referred to as

*tilma@riken.jp
†pashkin@frl.cl.nec.co.jp

"pulses" and use

$$\rho(t)' = \frac{\partial \rho(t)}{\partial t} = i[H,\rho] + \frac{1}{2}[K(\alpha)\rho, K(\alpha)^\dagger] + \frac{1}{2}[K(\alpha), \rho K(\alpha)^\dagger] \quad (4)$$

where

$$\sum_{\alpha=1}^{N} K(\alpha)K(\alpha)^\dagger = 1 \quad (5)$$

and the $K(\alpha)$'s are the standard Choi-Krauss operators used to describe dissipative effects [8].

5 Results and discussion

We considered the ideal case of a pure bipartite system. The evolution of the system starts from the $|00\rangle$ state, $\rho_0 = |00\rangle\langle 00|$. First neglecting decoherence, we calculated the time dependence of the density matrix via the Hamiltonian given in (2) and equation (4) using three specific pulse shapes: square, trapezoidal, and hyperbolic with the latter two having various rise and fall times. Then we used $\rho(t)'$ to calculate the average concurrence while the system was at $n_{g1} = 0.5$ and $n_{g2} = 0.5$, the degeneracy point, and the final state of the system after the pulse was concluded. The result of the simulations for each pulse shows that *both* the rise time *and* the pulse shape affects the instantaneous and overall concurrence of the system at the degeneracy point.

The square and trapezoidal pulses, with rise times less than a few tens of picoseconds, yield large amplitude oscillations in the concurrence, with periods of maximal and minimal entanglement. Oscillation amplitudes decrease as the rise time increases from tens of picoseconds to hundreds of picoseconds, but they are still quite pronounced. In contrast, the hyperbolic tangent pulse yields a much more suppressed oscillatory behavior in the concurrence; the minimal and maximal values are pushed up and down, respectively, towards what could be considered a "mid-range" entangled state. This behavior becomes more pronounced at comparable rise times in the hundreds of picoseconds with the trapezoidal pulse shape.

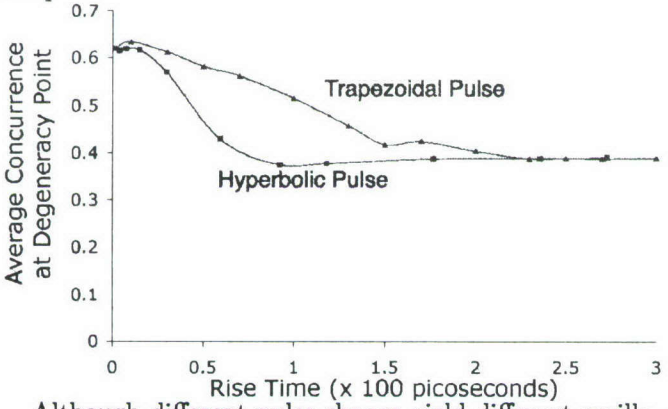

Although different pulse shapes yield different oscillatory behavior in the concurrence, both trapezoidal and hyperbolic pulses yield similar average concurrence values, at the degeneracy point, in the very short and long pulse rise/fall time regimes; as the previous figure shows. However, between 10 picoseconds and 150 picoseconds, the trapezoidal pulse shape shows much higher average concurrence values than the corresponding hyperbolic pulse shape. Thus, in this regime, the pulse shape makes a significant impact on the operational usefulness of this system.

As has been shown in Ref. [9], the quicker the system moves to the degeneracy point, the greater the overall fidelity of the corresponding quantum operation. Our calculations not only confirm this, but also show that, when selecting the gate-voltage pulse shape to use, one must choose between the following two physical regimes:

- long-term, steady (read: low-amplitude oscillations) concurrence values but reduced-fidelity (the system remains at a "mid-level" entangled state for a long period) when slowly driven to the degeneracy point, or
- long-term, unsteady (read: high-amplitude oscillations) concurrence values but high-fidelity (the system can be used to do quantum operations, such as a CNOT gate, while the system is in a "near-maximally" entangled state for a short period) when rapidly driven to $n_{g1} = n_{g2} = 0.5$.

The inter-qubit coupling strength as well as pulse shaping can also lead to other difficulties, as has been pointed out, for example, in Ref. [10] and Ref. [11].

References

[1] S. Hill and W. K. Wootters. *Phys. Rev. Lett.*, 78:5022, 1997.

[2] A. Peres. *Phys. Rev. Lett.*, 77:1413, 1996.

[3] M. Horodecki, P. Horodecki and R. Horodecki. *Phys. Lett.*, A(223):1, 1996.

[4] T. Tilma, M. Byrd, and E. C. G. Sudarshan. *J. Phys. A: Math. and Gen.*, 35:10445, 2002.

[5] W. K. Wootters. *Phys. Rev. Lett.*, 80:2245, 1998.

[6] Yu. A. Pashkin, T. Yamamoto, O. Astafiev, Y. Nakamura, D. V. Averin and J. S. Tsai. *Nature*, 421:823, 2003.

[7] Yu. A. Pashkin, T. Tilma, D. V. Averin, O. Astafiev, T. Yamamoto, Y. Nakamura, F. Nori, and J. S. Tsai. *Int. J. of Quant. Inf.*, 1:1, 2003.

[8] M. D. Choi. *Can. J. Math.*, 24:520, 1972. See also K. Kraus, *States Effects and Operators: Fundamental Notions of Quantum Theory*, Springer Verlag, 1983.

[9] T. Yamamoto, Yu. A. Pashkin, O. Astafiev, Y. Nakamura, and J. S. Tsai. *Nature*, 425:941, 2003.

[10] S. Oh. *Phys. Rev. B.*, 65:144526, 2002.

[11] X. Hu and S. Das Sarma. *Phys. Rev. A.*, 66:012312, 2002.

Quantum tomography for solid state qubits

Yu-xi Liu,[1] L.F. Wei,[1,2] and Franco Nori[1,3]

[1] *Frontier Research System, The Institute of Physical and Chemical Research (RIKEN), Wako-shi 351-0198*
[2] *Institute of Quantum Optics and Quantum Information, Department of Physics, Shanghai Jiaotong University, Shanghai 200030, P.R. China*
[3] *Center for Theoretical Physics, Physics Department, Center for the Study of Complex Systems, The University of Michigan, Ann Arbor, Michigan 48109-1120*

(Dated: August 3, 2004)

We propose a method for the tomographic reconstruction of qubit states for a general class of solid state systems in which the Hamiltonians are represented by spin operators, e.g., with Heisenberg-, XXZ-, or XY-type exchange interactions. We analyze the implementation of the projective operator measurements, or spin measurements, on qubit states. All the qubit states for the spin Hamiltonians can be reconstructed by using experimental data.

PACS numbers: 03.65.Ta, 03.65.Wj

Quantum information processing requires the effective measurement of quantum states. However, a single quantum measurement can only obtain partial information of a quantum state. The reconstruction of a quantum state requires measuring a complete set of observables on an ensemble of identically prepared copies of the system. This method called quantum state tomography [1], is very important because any unknown state can be ascertained by tomographic measurements. Moreover, the full description of qubit states can increase the accuracy of quantum operations. Tomographic measurements have been experimentally implemented for, e.g., the nuclear spin state of an NMR system [2], the electromagnetic field and photon state [3], the vibration state of molecules [4], the motional quantum state of a trapped atom [5], and atomic wave packets [6].

Experimental investigations on solid state qubits are very promising, especially in superconducting [7, 8] and quantum dot structures [9]. These recent achievements make it necessary to experimentally determine quantum states in solid state systems. Although there are many theoretical studies on tomography (e.g., references [10] and references therein), to our knowledge, these are not specific to solid state systems. Here, we focus on this question for quantum computing models using standard spin representations for solid state qubits. Our proposal is related to tomographic measurements using NMR. The measurements of the density matrix in NMR experiments are obtained from the NMR spectrum of the linear combination of "product operators", i.e. products of the angular momentum operators [11]. However, experiments in solid state systems usually involve the local single-qubit projective operator measurement (POM) or spin measurement. So, we study the method of tomographic reconstruction of solid state qubits by POM or spin measurement for a number of promising solid-state quantum computing models [12, 13, 14, 15, 16, 17, 18, 19]. We will investigate how the multi-qubit correlation measurements can be realized by virtue of an appropriate two-qubit operation combined with single qubit operations.

State and measurements. — Using the density matrix form, an n-qubit state ρ can be expressed as

$$\rho = \frac{1}{2^n} \sum_{l_1,\cdots,l_n=0,x,y,z} r_{l_1\cdots l_n}\ \sigma_{l_1} \otimes \sigma_{l_2} \otimes \cdots \otimes \sigma_{l_n}, \quad (1)$$

where $r_{l_1\cdots l_n}$ are 4^n real parameters, $\sigma_{l_m=x,y,z}$ and $\sigma_{l_m=0}$ $(0 \le m \le n)$ are the Pauli spin and identity operators of the mth qubit respectively. We adopt the convention $|0\rangle = |\uparrow\rangle$ and $|1\rangle = |\downarrow\rangle$ to denote the computational basis states of each qubit. The normalization condition $\mathrm{Tr}\rho = 1$ makes $r_{0,\cdots,0} = 1$ which means that ρ can be specified by $(4^n - 1)$ real parameters. These parameters correspond to the expectation values of the measurements given by the operators $\sigma_{j_1} \otimes \cdots \otimes \sigma_{j_n}$; that is, $\mathrm{Tr}\{\rho(\sigma_{j_1} \otimes \cdots \otimes \sigma_{j_n})\} = r_{l_1\cdots l_n}\delta_{j_1 l_1}\cdots\delta_{j_n l_n}$, where $l_1, \cdots, l_n$ are not simultaneously taken as zero. If there are $n - m$ identity operators among $\sigma_{l_1} \otimes \cdots \otimes \sigma_{l_n}$, the measurement is really done by the m qubits and it can be abbreviated by the tensor product of only the m Pauli operators, which is denoted hereafter by $\sigma_{1 l_1} \otimes \cdots \otimes \sigma_{m l_m}$. The $(4^n - 1)$ measurements required to reconstruct the n-qubit state can be decomposed into a summation from the single-qubit to n-qubit measurements as $\sum_{j=1}^{n} 3^j \binom{n}{j}$; where $3^j\binom{n}{j}$ is the number of j-qubit measurements and $\binom{n}{j}$ is the binomial coefficient.

To reconstruct the n-qubit state ρ, we need to determine all of its expanded coefficients $\{r_{l_1,\cdots,l_n}\}$. In solid state systems, the correlated multi-qubit measurement is not realizable now, and the experimental readout is often done via single-qubit POM (e.g., Refs. [12, 13, 14, 15]) or single spin measurement (e.g., Refs. [16, 17]). Without loss of generality, we assume that the POM is denoted by $|1\rangle\langle 1|$ and the spin measurement is presented by σ_x or σ_y. Below, we will discuss how to determine the $(4^n - 1)$ coefficients of an n-qubit state by using experimental data of the POM and then generalize it to the spin case. Our goal is to build a correspondence between above the measurements and actual measurements done via $|1\rangle\langle 1|$.

Single-qubit measurements.— The single-qubit measurements σ_{lz} $(l = 1, 2, \cdots, n)$ can be done by the projectors $(|1\rangle\langle 1|)_l$ due to the equivalence $\sigma_{lz} = \sigma_{l0} - 2(|1\rangle\langle 1|)_l$, with

identity operators σ_{l0}. Thus the POM experiments can directly determine n coefficients via n outcomes of the measurements $(|1\rangle\langle 1|)_l$. The measurements corresponding to the remaining $(4^n - n - 1)$ coefficients cannot be directly performed because of limitations of current experiment. In order to obtain these coefficients, a sequence of quantum operations W is needed such that each coefficient can be transformed to a position that is measurable by a POM experiment. The probability p of the lth single-qubit measurement $(|1\rangle\langle 1|)_l$ on the operated state ρ can be expressed as

$$p = \mathrm{Tr}\{W\rho W^\dagger (|1\rangle\langle 1|)_l\} = \mathrm{Tr}\{\rho W^\dagger (|1\rangle\langle 1|)_l W\}, \quad (2)$$

which means that the experimental POM $(|1\rangle\langle 1|)_l$ on the state $W\rho W^\dagger$ can be equivalently described as $W^\dagger(|1\rangle\langle 1|)_l W = \left[\frac{1}{2} - \frac{1}{2}W^\dagger\sigma_{lz}W\right]$ on the original state ρ. Because the POM experiment is equivalent to $W^\dagger\sigma_{lz}W$, we can call it an equivalent m-qubit measurement of $(|1\rangle\langle 1|)_l$, if the largest number of Pauli operators in the operator product expansion of $W^\dagger\sigma_{lz}W$ is an m-qubit. Thus the $(4^n - n - 1)$ coefficients can be obtained by the single-qubit projection $(|1\rangle\langle 1|)_l$ on the state ρ with appropriate operations W implemented by the dynamical evolution of the system with experimentally controllable parameters.

For all universal quantum computing proposals, the most general Hamiltonian of the system can be described as

$$H = \sum_{l=1}^{n} \sum_{\alpha=x,y,z} \varepsilon_{l\,\alpha}\, \sigma_{l\,\alpha} + \sum_{1=l<m}^{n} \sum_{\alpha,\beta=x,y,x} J_{l\,m}^{\alpha\beta}\, \sigma_{l\,\alpha} \otimes \sigma_{m\,\beta}, \quad (3)$$

where $\{\varepsilon_{l\,\alpha}\}$ and $\{J_{l\,m}^{\alpha\beta}\}$ are controllable and tunable system-specific one-qubit and exchange coupling parameters, which are required by the universality of quantum computing [20], $\sigma_{l\,\alpha=x,y,z}$ denote the Pauli operators of the lth qubit. Without loss of generality, all parameters are assumed to be positive real numbers.

In order to obtain each coefficient corresponding to single-qubit measurements σ_{lx} or σ_{ly}, all single-qubit operations need to be performed separately by controlling the one-qubit parameters $\varepsilon_{l\,\alpha}$ while turning off all interactions in the Hamiltonian (3), that is, $J_{l\,m}^{\alpha\beta} = 0$. For n single-qubit measurements $\{\sigma_{ly}\}$, each σ_{ly} can be equivalently obtained by $(|1\rangle\langle 1|)_l$, after the lth qubit is rotated $\pi/2$ about the x axis, the latter expressed as $X_l = \exp\{-i\pi\sigma_{lx}/4\}$. This rotation can be realized within the evolution time $t = \hbar\pi/4\varepsilon_{lx}$, after the one-qubit parameters ε_{ly} and ε_{lz} are adjusted to zero. Other n single-qubit measurements $\{\sigma_{lx}\}$ can also be obtained by measuring $(|1\rangle\langle 1|)_l$ on the state, within the evolution time $t = \hbar\pi/4\varepsilon_{ly}$, after ε_{lx} and ε_{lz} are set to zero. This quantum operation is equivalent to a $\pi/2$ rotation of the lth qubit about the y axis, which is denoted by $Y_l = \exp\{-i\pi\sigma_{ly}/4\}$. However, not all of the three one-qubit parameters ε_{lx}, ε_{ly} and ε_{lz} appear in the Hamiltonian of most physical systems. For example, the parameter ε_{ly} is always zero in the charge qubit system [12]. For this case, to obtain the rotation angle θ about the y axis we need to alternatively turn on and off the single-qubit quantum operations: (1) $\overline{X}_l = \exp\{-i\varepsilon_{lx}\sigma_{lx}t_1/\hbar\}$, with the operation time $t_1 = 3\hbar\pi/4\varepsilon_{lx}$; (2) $Z_l(\theta) = \exp\{-i\theta\sigma_{lz}/2\}$, with $\theta = \varepsilon_{lz}t_2/\hbar$; and (3) $X_l = \exp\{-i\varepsilon_{lx}\sigma_{lx}t_3/\hbar\}$, with $t_3 = \hbar\pi/4\varepsilon_{lx}$. These can be expressed as $Y_l(\theta) = X_l Z_l(\theta)\overline{X}_l = \exp\{-i\theta\sigma_{1y}/2\}$. Especially, we denote the rotation $\pi/2$ about the z axis by $Z_l = \exp\{-i\pi\sigma_{lz}/4\}$. In principle, if the lth qubit system has only two controllable one-qubit parameters ε_α and ε_β, then the rotation angle $\epsilon_{\alpha\beta\gamma}\theta$ about the axis γ can be obtained by first doing a rotation of $\pi/4$ about the axis α, then a rotation of θ about the axis β, and finally a rotation by $-\pi/4$ about the axis α; that is, $\exp\{-i\epsilon_{\alpha\beta\gamma}\theta\sigma_\gamma/2\} = e^{-i\pi\sigma_\alpha/4}e^{-i\theta\sigma_\beta/2}e^{i\pi\sigma_\alpha/4}$, where α, β, γ can be x, y, or z and the Levi-Civita tensor $\epsilon_{\alpha\beta\gamma}$ is equal to $+1$ and -1 for the even and odd permutation of its indices, respectively. To reconstruct a single-qubit state, three single-qubit measurements σ_α $(\alpha = x, y\, z)$ are sufficient to obtain r_z, which determines the probabilities of finding 0 and 1, as well as r_x and r_y which determine the relative phase of $|0\rangle$ and $|1\rangle$.

TABLE I: Quantum operation and two-qubit measurements.

XY model		Heisenberg model	
EM	Operations	Equivalent measurement (EM)	Operations
$\sigma_{1y} + \sigma_{1x}\sigma_{1x}$	$X_1U_1Y_1$	$\sigma_{1z} + \sigma_{2z} + \sigma_{1y}\sigma_{2x} - \sigma_{1x}\sigma_{2y}$	U_2
$-\sigma_{1z} + \sigma_{1x}\sigma_{2y}$	$Y_1U_1Y_1$	$\sigma_{1y} + \sigma_{2z} - \sigma_{1z}\sigma_{2x} - \sigma_{1x}\sigma_{2y}$	U_2X_1
$-\sigma_{1z} - \sigma_{1x}\sigma_{2z}$	$Y_1U_1Y_1X_2$	$\sigma_{2z} - \sigma_{1x} + \sigma_{1y}\sigma_{2x} - \sigma_{1z}\sigma_{2y}$	U_2Y_1
$-\sigma_{1z} - \sigma_{1y}\sigma_{2x}$	$X_1U_1X_1$	$\sigma_{1z} + \sigma_{2z} + \sigma_{1x}\sigma_{2x} + \sigma_{1y}\sigma_{2y}$	U_2Z_1
$-\sigma_{1x} - \sigma_{1y}\sigma_{2y}$	$Y_1U_1X_1$	$\sigma_{1z} - \sigma_{2x} + \sigma_{1y}\sigma_{2z} - \sigma_{1x}\sigma_{2y}$	U_2Y_2
$-\sigma_{1x} + \sigma_{1y}\sigma_{2z}$	$Y_1U_1X_1X_2$	$-\sigma_{1x} - \sigma_{2x} - \sigma_{1z}\sigma_{2y} + \sigma_{1y}\sigma_{2z}$	Y_1U_2
$\sigma_{1y} - \sigma_{1z}\sigma_{2x}$	X_1U_1	$\sigma_{1y} + \sigma_{2y} - \sigma_{1z}\sigma_{2x} + \sigma_{1x}\sigma_{2z}$	X_1U_2
$-\sigma_{1x} - \sigma_{1z}\sigma_{2y}$	Y_1U_1	$\sigma_{1y} + \sigma_{2z} + \sigma_{1z}\sigma_{2y} - \sigma_{1x}\sigma_{2x}$	$U_2X_1Z_2$
$-\sigma_{1x} + \sigma_{1z}\sigma_{2z}$	$Y_1U_1X_2$	$\sigma_{1z} - \sigma_{2x} + \sigma_{1x}\sigma_{2z} + \sigma_{1y}\sigma_{2y}$	$U_2Z_1Y_2$

Two-qubit measurements.— The above discussions show that all the single-qubit measurements can be experimentally implemented by POMs $(|1\rangle\langle 1|)_l$ on the given state with or without single-qubit quantum operations. However, the implementation of multiple-qubit measurements needs non-local two-qubit operations. The basic two-qubit operation can be derived from the time-evolution operator $U_{12}(t)$ of a pair of coupled qubits, labelled by 1 and 2, whose Hamiltonian H_{12} can be obtained from Eq. (3) with $n = 2$. Without loss of generality, we assume: (i) $\varepsilon_{1\alpha} = \varepsilon_{2\alpha} = \varepsilon_\alpha$; and (ii) $J_{lm}^{\alpha\beta} = J_{lm}^{\alpha}\delta_{\alpha\beta}$ in the Hamiltonian (3), because by applying local unitary operations, e.g., [21], the Hamiltonian (3) can always be transformed into a diagonal form—which is actually used for a number of promising solid-state quantum computing models [12, 13, 14, 15, 16, 17, 18, 19]. Then in the basis $\{|0_1, 0_2\rangle, |0_1, 1_2\rangle, |1_1, 0_2\rangle, |1_1, 1_2\rangle\}$, the time-evolution operator $U_{12}(t)$ is

$$U_{12}(t) = \exp\{-iH_{12}t/\hbar\} = \sum_{g=1}^{4} e^{-iE_g t/\hbar}|\psi_g\rangle\langle\psi_g| \quad (4)$$

where $|\psi_g\rangle$ $(g = 1, 2, 3, 4)$ are four eigenvectors of the Hamiltonian H_{12}. The corresponding eigenvalues $E_1 =$

$-J_{12}^x - J_{12}^y - J_{12}^z$, E_2, E_3 and E_4 are given [22] by the solutions of the cubic equation of the parameter E. Here, we only focus on two typical Hamiltonians which play an important role in the process of two-qubit operation for the most representative solid state quantum computing models. One is that all of the one-qubit parameters are switchable, for example, quantum dots in cavities [23]. However, due to technical constraints and difficulties, it was found [24] that not all the one-qubit parameters are switchable in the two-qubit operation, for instance, for spin-coupled quantum dots [14], donor-atom nuclear or electron spins [18], and quantum Hall systems [19], two one-qubit parameters such as ε_x and ε_y are switchable, but ε_z is fixed. The basic two-qubit operation with fixed ε_z is

$$
\begin{aligned}
U_{12}(t) &= \frac{1}{2}(e^{i\phi}\cos\gamma + e^{-i\phi}\cos\beta)I + i\frac{(1-a^2)c}{2}e^{-i\phi} \\
&\times \sin\beta(\sigma_{1z}+\sigma_{2z}) + \frac{1}{2}(e^{-i\phi}\cos\beta - e^{i\phi}\cos\gamma)\ \sigma_{1z}\otimes\sigma_{2z} \\
&-i\frac{1}{2}(e^{i\phi}\sin\gamma + 2ac\,e^{-i\phi}\sin\beta)\ \sigma_{1x}\otimes\sigma_{2x} \\
&-i\frac{1}{2}(e^{i\phi}\sin\gamma - 2ac\,e^{-i\phi}\sin\beta)\ \sigma_{1y}\otimes\sigma_{2y} \qquad (5)
\end{aligned}
$$

where $\gamma = \frac{t}{\hbar}(J_{12}^x + J_{12}^y)$, $\beta = \frac{t}{\hbar}\sqrt{4\varepsilon_z^2 + (J_{12}^x - J_{12}^y)^2}$, $\phi = \frac{t}{\hbar}J_{12}^z$, $a = 2b + \sqrt{4b^2+1}$, with $b = \varepsilon_z/(J_{12}^x - J_{12}^y)$, and $c = 1/(1+a^2)$. We also assume in Eq. (5) that the parameters satisfy conditions $[2J_{12}^z \pm (J_{12}^x + J_{12}^y)]^2 \neq 4\varepsilon_z^2 + (J_{12}^x - J_{12}^y)^2$ and $2J_{12}^z \pm \sqrt{4\varepsilon_z^2 + (J_{12}^x - J_{12}^y)^2} \neq (J_{12}^x + J_{12}^y)^2$.

Examples of two-qubit measurements.— Using Eq. (5), we can obtain the two-qubit operations by choosing system-specific parameters. For example, the two-qubit operation with fixed ε_z for the Heisenberg model, XXZ model, and the XY model can be obtained from Eq. (5) by setting parameters $J_{mn}^x = J_{mn}^y = J_{mn}^z$, $J_{mn}^x = J_{mn}^y \neq J_{mn}^z$ and $J_{mn}^x = J_{mn}^y, J_{mn}^z = 0$, respectively. If all one-qubit parameters are switchable, then the two-qubit operation can be obtained from Eq. (5) by only setting $\varepsilon_z = 0$. Other effective spin quantum computing models presented up to now can be reduced by single-qubit operations to Eq. (5). For instance, i) the two-qubit operations of the superconducting charge qubit [12] can be reduced to Eq. (5) with $J_{12}^x = J_{12}^z = 0$ by a conjugation-by-$(\pi/4)(\sigma_{1y}+\sigma_{2y})$ [25] on the Hamiltonian; ii) the two-qubit operation for the models in Refs. [17] and [26] can be reduced to Eq. (5) with $J_{12}^x = J_{12}^y = 0$ and model [12] by the conjugation-by-$(\pi/4)(\sigma_{1y}+\sigma_{2y})$ and conjugation-by-$(\pi/4)(\sigma_{1x}+\sigma_{2x})$ on the Hamiltonian of the system. Combining the basic two-qubit operations $U_{12}(t)$ with the single-qubit operations, we can obtain any desired two-qubit operation by choosing the evolution time t and the system-specific parameters $\{\varepsilon_\alpha, J_{12}^\alpha : \alpha = x, y, z\}$.

Now, let us consider the XY exchange coupling system with switchable one-qubit parameters as an example to answer how to obtain the expectation values of two-qubit measurements. If we want to obtain, for example, the expectation value r_{zy} of $\sigma_{1z}\otimes\sigma_{2y}$ in such system, we can first switch off all the one-qubit parameters $\varepsilon_{l\,\alpha}$, then let the two-qubit system evolve during the time $\tau = \hbar\pi/8J_{12}^x$ with the evolution operator $U_{12}(\tau)$, then switch off the exchange coupling and only make the first qubit have a $\pi/2$ rotation $Y_1 = \exp\{-i\pi\sigma_{1y}/4\}$ around the y axis, that is

$$
\rho \xrightarrow{U_{12}(\tau)} U_{12}(\tau)\rho U_{12}^\dagger(\tau) \xrightarrow{Y_1} Y_1 U_{12}(\tau)\rho U_{12}^\dagger(\tau) Y_1^\dagger = \widetilde{\rho}. \qquad (6)
$$

Afterwards we make the measurement $(|1\rangle\langle 1|)_1$ on the rotated state $\widetilde{\rho}$ obtaining the probability $p = \mathrm{Tr}[\widetilde{\rho}(|1\rangle\langle 1|)_1] = (\sqrt{2} + r_{x0} + r_{zx})/2\sqrt{2}$, corresponding to the equivalent two-qubit measurement $-\sigma_{1x} - \sigma_{1z}\otimes\sigma_{2x}$. Because r_{x0} has been obtained by the equivalent single-qubit measurement σ_{1x}, r_{zx} is completely determined by the above result. Eight other values of equivalent two-qubit measurements for this pair can also be obtained by projecting $(|1\rangle\langle 1|)_1$ on the measured state with the quantum operations summarized in Table I. Each measured value is related to the expectation values of a single-qubit and a two-qubit measurements. For a two-qubit state in this system, the above 9 two-qubit and 6 single-qubit measurements are enough to obtain 15 unknown parameters $r_{l_1 l_2}$ $(l_1, l_2 = 0, x, y, z)$ where l_1, l_2 are not simultaneously taken as zero. The 16 matrix elements of the two-qubit state are obtained by combining the 15 parameters $r_{l_1 l_2}$ with the normalization condition and finally the two-qubit state can be completely reconstructed.

The implementation of equivalent two-qubit measurements with a well-chosen two-qubit operation for a pair of coupled two-qubit system plays a significant role in the reconstruction of a state. For the XY and Heisenberg models with switchable one-qubit parameters, the equivalent measurements $\sqrt{2}W^\dagger\sigma_{1z}W$ and $2W^\dagger\sigma_{1z}W$, to obtain the expectation values of 9 two-qubit measurements, are summarized in table I, where the non-local two-qubit operation operators U_1 and U_2 for the XY and Heisenberg models are chosen by Eq. (5) with the system specific parameters and the evolution time $\tau = \hbar\pi/8J_{12}^x$ as

$$
\begin{aligned}
2\sqrt{2}U_1 &= \left(\sqrt{2}+1\right)I + \left(\sqrt{2}-1\right)\sigma_z^1\otimes\sigma_z^2 \\
&- i\sigma_y^1\otimes\sigma_y^2 - i\sigma_x^1\otimes\sigma_x^2, \qquad (7) \\
2\sqrt{2}U_2 &= (2-i)\,I - i\sigma_z^1\otimes\sigma_z^2 - i\sigma_y^1\otimes\sigma_y^2 \\
&- i\sigma_x^1\otimes\sigma_x^2. \qquad (8)
\end{aligned}
$$

The reconstructions of the qubit states in these models with fixed ε_z are the same with switchable one-qubit parameters, if the ratios $\varepsilon_z/J_{12}^x = 4m/(2n-1)$ $(m, n = 1, 2, \cdots)$ are appropriately chosen and the operation time is $\tau = (n\hbar\pi)/(2\varepsilon_z)$.

We also find that the tomographic measurement steps for most systems can be reduced to the same steps needed for the XY model. For example, i) by choosing appropriate values of J_{12}^z, J_{12}^x (J_{12}^z, J_{12}^x, and ε_z) and operation time τ for the XXZ model with the switchable one-qubit parameters (fixed ε_z) such that $J_{12}^z\tau/\hbar = 2n\pi$, $J_{12}^x\tau/\hbar = (2m-1)\pi/8$ ($J_{12}^z\tau/\hbar = 2n\pi$, $J_{12}^x\tau/\hbar = (2m-1)\pi/8$, $\varepsilon_z\tau/\hbar = l\pi/2$) with $l, m, n = 1, 2\cdots$, then we can obtain the same two-qubit operation as for the XY model and the qubit state can

be reconstructed by using the same steps as the XY model, ii) the qubit state of the superconducting charge qubit model can also be reconstructed by using the same steps as the XY model when the parameters and evolution time are appropriately chosen [27], iii) the qubit states in the systems modelled in Refs [17] and [26] can also be reconstructed by using the same steps used for the XY model.

It should be emphasized that the different qubit measurements on the quantum state with fixed quantum operations produce different results and the quantum operations are not unique to obtain each expectation value of the measurement. In table I, we only discuss the procedure for the first qubit POM, if we can make all single-qubit measurements, then the operation steps to obtain some of the expectation values of the multiple-qubit measurements can be decreased. For example, if we can experimentally perform the second qubit projection $(|1\rangle\langle 1|)_2$ in the XY model, the expectation value of $\sigma_{1y} \otimes \sigma_{2z}$ can be obtained by using two steps of operations $U_{12}(\tau)$ and Y_2, that is $U_{12}^{\dagger}(\tau) Y_2^{\dagger}\, \sigma_{2z}\, Y_2 U_{12}(\tau) = -(\sigma_{2x} + \sigma_{1y} \otimes \sigma_{2z})/\sqrt{2}$. But four steps are needed for the first qubit measurement. The price paid is that noise may be increased because the system is in contact with more probes.

Multi-qubit measurements.—These measurements can also be obtained by designing step-by-step single- and two-qubit operations. In principle, to obtain the expectation value of an l-qubit $(2 < l \leq n)$ measurement, we need at least $l-1$ two-qubit operations for different pairs of the l-qubit. For example, let us obtain the expectation value r_{zzx} corresponding to the three-qubit measurement $\sigma_{1z} \otimes \sigma_{2z} \otimes \sigma_{3x}$ for the XY interaction system with switchable one-qubit parameters. We can replace the first qubit by the third qubit in the two-qubit operation $U_{12}(\tau)$ and perform an operation $U_{23}(\tau)$ on the second and third qubits, followed by another operation $U_{12}(\tau)$ on the first and second qubits, followed by a $\pi/2$ rotation Y_1 about the y axis for the first qubit, followed finally by the measurement $(|1\rangle\langle 1|)_1$. That is, an equivalent three-qubit measurement can be obtained as

$$U_{23}^{\dagger}(\tau) U_{12}^{\dagger}(\tau) Y_1^{\dagger} \sigma_{1z} Y_1 U_{12}(\tau) U_{23}(\tau)$$
$$= -\frac{1}{2\sqrt{2}}\sigma_{1x} - \frac{1}{4}\sigma_{1z} \otimes \sigma_{2y} + \frac{1}{4}\sigma_{1z} \otimes \sigma_{2z} \otimes \sigma_{3x}, \quad (9)$$

where the assumption of exchange couplings are the same for all qubit pairs used. The probability of measuring $(|1\rangle\langle 1|)_1$ on the above rotated three-qubit state is $p' = (2\sqrt{2} + 2r_{x00} + \sqrt{2}r_{zy0} - \sqrt{2}r_{zzx})/4\sqrt{2}$. Then r_{zzx} can be determined by the p, r_{x00}, and r_{zy0}, the latter two parameters have been obtained by single- and two-qubit measurements. We can also obtain other probabilities of the equivalent three-qubit measurements related to the expectation values of the three-qubit measurements by projecting $(|1\rangle\langle 1|)_l$ on the final operated state. For a three-qubit state, we can solve the equations for all probabilities of equivalent one-, two-, and three-qubit measurements to obtain expectation values of all measurements, finally all matrix elements of a three-qubit state are obtained by these expectation values, and the state is reconstructed. Any n-qubit measurement can be obtained in a similar way to the three-qubit measurement, then the n-qubit state can also be reconstructed.

Discussion.— In summary, we have proposed a scheme for tomographic reconstruction of qubit states for a class of promising solid-state quantum computing models. We find that elemental logic gates, such as CNOT gate, control phase gate, etc. are not necessary in this process. An appropriate non-local two-qubit operation is enough to realize this purpose. The generalization of the above discussion to the spin measurement [16, 17] is straightforward because of the equivalence between $|1\rangle\langle 1| = \frac{1}{2}(\sigma_0 - \sigma_z)$ and σ_x (σ_y) by a $\pi/2$ $(-\pi/2)$ rotation about the y (x) axes. Using present technology, our proposal is experimentally feasible in these solid state qubit systems. Ideally, the reconstructed qubit state ρ should satisfy the properties of the normalization, positivity, and Hermiticity. However, we always deal with a limited amount of experimental data, which are also affected by noise and imperfect quantum measurements. To overcome problems due to unavoidable statistical errors, we can use the maximum-likelihood estimation of the density matrix [28] to obtain a more accurate reconstructed qubit.

We thank J. Q. You, X. Hu, J. S. Tsai, and Q. Niu for helpful discussions. This work was supported in part by the NSA and ARDA under AFOSR contract No. F49620-02-1-0334, and by the NSF grant No. EIA-0130383.

[1] W. Band and J.L. Park, Am. J. Phys. **47**, 188 (1979); G.M. D'Ariano, Phys. Lett. A **268**, 151 (2000); G.M. D'Ariano, *et al.*, *ibid.* **276**, 25 (2000).

[2] I.L. Chuang, *et al.*, Proc. R. Soc. Lond. A **454**, 447 (1998); C. Miquel, *et al.*, Nature **418**, 59 (2002); G. Teklemariam, *et al.*, Phys. Rev. Lett. **86**, 5845 (2001).

[3] D.T. Smithey, *et al.*, Phys. Rev. Lett. **70**, 1244 (1993); S. Schiller, *et al.*, *ibid.* **77**, 2933 (1996); A.G. White, *et al.*, *ibid.* **83**, 3103 (1999); P.G. Kwiat, *et al.*, Nature **409**, 1014 (2001); T. Yamamoto, *et al.*, *ibid.* **421**, 343 (2003).

[4] T.J. Dunn, *et al.*, Phys. Rev. Lett. **74**, 884 (1995).

[5] D. Leibfried, *et al.*, Phys. Rev. Lett. **77**, 4281 (1996)

[6] C. Kurtsiefer, *et al.*, Nature **386**, 150 (1997).

[7] J.R. Friedman, *et al.*, Nature **406**, 43 (2000); J.E. Mooij, *et al.*, Science **285**, 1036 (1999); C.H. van der Wal, *et al.*, *ibid.* **290**, 773 (2000); S. Han, *et al.*, *ibid.* **293**, 1457 (2001); D. Vion, *et al.*, *ibid.* **296**, 886 (2002); Y. Yu, *et al.*, *ibid.* **296**, 889 (2002); I. Chiorescu, *et al.*, *ibid.* **299**, 1869 (2003).

[8] Y. Nakamura, *et al.*, Nature **398**, 786 (1999); Y.A. Pashkin, *et al.*, *ibid.* **421**, 823 (2003).

[9] G. Chen, *et al.*, Science **289**, 1906 (2000); M. Bayer, *et al.*, *ibid.* **291**, 451 (2001).

[10] R. Walser, *et al.*, Phys. Rev. Lett. **77**, 2658 (1996); S. Weigert, *ibid.* **84**, 802 (2000); M. Beck, *ibid.* **84**, 5748 (2000); G.M. D'Ariano, *et al.*, *ibid.* **86**, 4195 (2001); G. Klose, *et al.*, *ibid.* **86**, 4721 (2001); U. Leonhardt, Phys. Rev. A **53**, 2998 (1996); D.F.V. James, *et al.*, *ibid.* **64**, 052312 (2001); G.M. D'Ariano *et al.*, quant-ph/0302028.

[11] G. Teklemariam, *et al.*, Phys. Rev. Lett. **86**, 5845 (2001).

[12] Y. Makhlin, *et al.*, Rev. Mod. Phys. **73**, 357 (2001).

[13] A. Shnirman *et al.*, Phys. Rev. B **57**, 15400 (1998).

[14] D. Loss *et al.*, Phys. Rev. A **57**, 120 (1998); X. Hu, *et al.*, *ibid.* **61**, 062301 (2000); X. Hu, *et al.*, Phys. Rev. Lett. **86**, 918 (2001).
[15] W.G. van der Wiel, *et al.*, Rev. Mod. Phys. **75**, 1 (2003).
[16] A.B. Zorin, Physica C **368**, 284 (2002).
[17] J.Q. You, *et al.*, Phys. Rev. Lett. **89**, 197902 (2002); Phys. Rev. B **68**, 024510 (2003).
[18] B. E. Kane, Nature **393**, 133 (1998).
[19] D. Mozyrsky, *et al.*, Phys. Rev. Lett. **86**, 5112 (2001).
[20] D. P. DiVincenzo, Phys. Rev. A **51**, 1015 (1995); S. Lloyd, Phys. Rev. Lett. **75**, 346 (1995).
[21] W. Dür, *et al.*, Phys. Rev. Lett. **87**, 137901 (2001); J. I. Cirac, *et al.*, *ibid.* **86**, 544 (2001).
[22] $(E+J_{12}^z-J_{12}^x-J_{12}^y)[(E-J_{12}^z)^2-4\varepsilon_z^2+(J_{12}^x-J_{12}^y)^2]+4(\varepsilon_x^2+\varepsilon_y^2)(J_{12}^z-E)-4(\varepsilon_x^2-\varepsilon_y^2)(J_{12}^x-J_{12}^y)=0$
[23] A. Imamoglu, *et al.*, Phys. Rev. Lett. **83**, 4204 (1999).
[24] D. A. Lidar, *et al.*, Phys. Rev. Lett. **88**, 017905 (2002); L. A. Wu, *et al.*, *ibid.* **89**, 127901 (2002).
[25] D. A. Lidar, *et al.*, Phys. Rev. A **63**, 022307 (2001).
[26] V. W. Scarola, *et al.*, cond-mat/0304225.
[27] Yu-xi Liu, L.F. Wei, and F. Nori, unpublished.
[28] Z. Hradil, Phys. Rev. A **55**, R1561 (1999); M. F. Sacchi, *et al.*, *ibid.* **63**, 054104 (2001); D. F. James, *et al.*, *ibid.* **64**, 052312 (2001).

Tomographic measurements on superconducting qubit states

Yu-xi Liu,[1] L.F. Wei,[1,2] and Franco Nori[1,3]

[1] *Frontier Research System, The Institute of Physical and Chemical Research (RIKEN), Wako-shi 351-0198, Japan*
[2] *Institute of Quantum Optics and Quantum Information, Department of Physics, Shanghai Jiaotong University, Shanghai 200030, P.R. China*
[3] *Center for Theoretical Physics, Physics Department, Center for the Study of Complex Systems, The University of Michigan, Ann Arbor, Michigan 48109-1120, USA*

(Dated: August 3, 2004)

We propose an approach to reconstruct any superconducting charge qubit state by using quantum *state* tomography. This procedure requires a series of measurements on a large enough number of identically prepared copies of the quantum system. The experimental feasibility of this procedure is explained and the time scales for different quantum operations are estimated based on experimentally accessible parameters. The state tomography allows the characterization of a quantum "black box" connected to an unknown external reservoir. This "black box" transfers any known input state to an unknown output state. The determination of the quantum transfer function for this 'black box" is called quantum *process* tomography. This procedure needs to input a large enough number of different known states into the "black box", then to make tomographic measurements on output states, finally to obtain the quantum transfer function, which determines the "black box".

PACS numbers: 03.65.Wj, 74.50.+r, 03.67.-a, 85.25.Cp

I. INTRODUCTION

The generation of superpositions of macroscopic quantum states in superconducting devices [1, 2, 3, 4, 5] have motivated further research on quantum information processing in these systems. Two types of superconducting qubits based on Josephson junction devices have been proposed and experimentally demonstrated. One involves two Cooper-pair charge states in a small superconducting island connected to a circuit by a Josephson tunnel junction and a gate capacitor (see, e.g., [2, 3, 6]). An alternative approach is based on the phase states of a Josephson junction or the flux states in a ring superconducting structure [4, 5, 7]. Further, experimental observations on quantum oscillations and the demonstration of conditional gate operations in two coupled charge qubits [3] are necessary first steps towards future realizations of quantum information processors.

A crucial step in quantum information processing is the measurement of the output quantum states. However, a quantum state cannot be ascertained by a single quantum measurement. This is because quantum states may comprise many complementary features which cannot be measured simultaneously and precisely due to uncertainty relations. However, all complementary aspects can in principle be observed by a series of measurements on a large enough number of identically prepared copies of the quantum system. Then we can reconstruct a quantum state from such a complete set of measurements of system observables (i.e., the quorum [8]). Such a procedure is called "reconstruction of quantum states" or Quantum State Tomography (QST).

Quantum state tomography is not only important for quantum computation, which requires the verification of the accuracy of quantum operations, but it is also important for fundamental physics. Many theoretical studies for tomographic reconstruction of quantum states have been done, e.g. references [9, 10, 11]. Experimentally, tomography has been investigated for a variety of systems, including: the vibrational state of molecules [12], the motional quantum state of a trapped atom [13, 14], two-photon states [15] and the electromagnetic field [16]. The quantum states of multiple spin-$\frac{1}{2}$ nuclei have also been measured in the high-temperature regime using NMR techniques [17, 18, 19].

For continuous variable cases (e.g., the molecular vibrational mode [12], motional quantum states of a trapped ion [13, 14], a single-mode [16] of the electromagnetic field), the quantum states can be known by the tomographic measurement of their Wigner function. For the discrete variable case (e.g., in NMR systems), the measurements on the density matrix in NMR experiments are realized by the NMR spectrum of the linear combinations of "product operators", i.e. products of the usual angular momentum operators [19].

To our knowledge, there is no adequate theoretical analysis or experimental demonstration for the reconstruction of qubit states in solid state systems, besides our recent work in Ref. [20]. There, we considered a very general class of spin Hamiltonians used to model generic solid state systems [20]. Here, the emphasis is not on a general model but on specific system: superconducting qubits. Recent technical progress makes it possible to realize quantum control in superconducting quantum devices and ascertain either the charge [2, 3] or the flux [4] qubit states. Further, practical experiments on quantum computing require us to know the full information of the quantum state, so the reconstruction of quantum states in solid state systems is a very important issue.

In this paper, we analyze how to reconstruct charge qubit states using superconducting circuits. Although our analysis of the tomographic reconstruction of charge qubit states might seem somewhat similar to the one used for NMR systems [17, 18, 19], there are significant differences on how to realize the state tomography in Josephson junction (JJ) charge qubits. A question we will focus on is the following: is it possible to do QST with current experimental capability on JJ qubits? In view of the limitation of the relaxation and decoherence times, it is also necessary to estimate quantum operation

times required for reconstructing charge qubit state. In particular, it is not trivial to find an appropriate two-qubit operation to realize all two and multiple qubit measurements.

Here, we theoretically analyze in detail the necessary experimental steps for the tomographic reconstruction of dc-SQUID-controlled charge qubit states. This analysis can be easily generalized to other proposals of controllable superconducting qubits (e.g., flux qubits). In Sec. II, the reconstruction of single-qubit states is described in detail. The time scales of operations for measurements of all three unknown matrix elements are also estimated by using currently accessible experimental parameters. The basic idea of this section on single-qubit rotation is known to QST optics specialists, but here we specify a detailed description of the steps needed for the experimental realization of the tomographic reconstruction for charge qubit states. This should be helpful to solid state experimentalists who are not specialists on quantum state tomography in quantum optics. In Sec. III, all operations required to reconstruct two-qubit states are given, the time scales for the first and second qubit measurements are estimated using experimentally accessible parameters. In Sec. IV, using an example, we generalize our two-qubit tomography to the multiple-qubit case. Finally in Sec. V, we discuss the "process tomography" of singe-qubit charge systems based the "state tomography". Sections III, IV, and V contain our most important results. The conclusions and further discussions are given in sections VI and VII, respectively.

II. RECONSTRUCTION OF SINGLE-QUBIT STATES

A. Theoretical model and single-qubit states

We consider a controllable dc-SQUID system which consists of a small superconducting island with n excess Cooper-pair charges, connected by two nominally-identical ultra-small Josephson junctions; each having capacitance C_J^0 and Josephson coupling energy E_J^0. A control gate voltage V_g is coupled to the Cooper-pair island by a gate capacitance C_g. The qubit is assumed to work in the charge regime, e.g., the single-electron charging energy $E_C = e^2/2(C_g + 2C_J^0)$ and Josephson coupling energy E_J^0 satisfy the condition $E_C \gg E_J$. If the applied gate voltage range V_g is near a value $V_g = e/C_g$, only two charge states, denoted by $n = 0$ and $n = 1$, play a key role, then this charged box is reduced to a two-level system (qubit) whose dynamical evolution is governed by the Hamiltonian [6, 22]

$$H = -\frac{1}{2}\delta E_{\rm ch}(n_{\rm g})\,\sigma_z - \frac{1}{2}E_{\rm J}(\Phi_x)\,\sigma_x, \qquad (1)$$

where we adopt the convention of charge states $|0\rangle = |\uparrow\rangle$ and $|1\rangle = |\downarrow\rangle$. The charge energy $\delta E_{\rm ch}(n_{\rm g}) = 4\,E_{\rm C}(1-2n_{\rm g})$ with $n_{\rm g} = C_{\rm g}V_{\rm g}/2e$ can be controlled by the gate voltage $V_{\rm g}$. The Josephson coupling energy $E_{\rm J}(\Phi_x) = 2\,E_{\rm J}^0\cos(\pi\Phi_x/\Phi_0)$ is adjustable by the external flux Φ_x, and $\Phi_0 = hc/2e$ is the flux quantum. Our goal here is to determine any single charge qubit state by the controllable dynamical operation governed by the Hamiltonian (1).

Any single-qubit state (mixed or pure) can be represented by a density matrix operator in a basis $\{|0\rangle = |\uparrow\rangle, |1\rangle = |\downarrow\rangle\}$ as

$$\rho = \begin{pmatrix} \rho_{00} & \rho_{01} \\ \rho_{10} & \rho_{11} \end{pmatrix} = \frac{1}{2}\sum_{k=0,x,y,z} r_k\,\sigma_k, \qquad (2a)$$

or

$$\rho = \rho_{00}\,|0\rangle\langle 0| + \rho_{01}\,|0\rangle\langle 1| + \rho_{10}\,|1\rangle\langle 0| + \rho_{11}\,|1\rangle\langle 1|, \qquad (2b)$$

where $\sigma_{k=x,y,z}$ are Pauli operators and $\sigma_{k=0}$ is an identity operator. Four real parameters r_k $(k = 0, x, y, z)$ can be expressed as

$$r_0 = \rho_{00} + \rho_{11}, \qquad r_x = \rho_{01} + \rho_{10},$$
$$r_y = i(\rho_{01} - \rho_{10}), \qquad r_z = \rho_{00} - \rho_{11}.$$

The normalization condition $\rho_{00} + \rho_{11} = 1$ ensures that the qubit (2) can actually be determined by three real parameters r_x, r_y, r_z corresponding [21] to a Bloch vector $\vec{r}$, which satisfies the condition $|\vec{r}| \leq 1$ (see Fig.1(a)). The state ρ is pure if and only if $|\vec{r}| = 1$. When the state ρ is pure, the Bloch vector $\vec{r}$ defines a point on the unit three-dimensional sphere.

These three coefficients r_k $(k = x, y, z)$ can be obtained from measurements of σ_x, σ_y, σ_z. The correspondence between these three measurements and the coefficients r_k is given by

$$r_k = {\rm Tr}(\rho\,\sigma_k),$$

due to the relation ${\rm Tr}(\sigma_i\sigma_j) = 2\delta_{ij}$, where δ_{ij} is the Kronecker delta.

B. Quantum operations and measurements on single-qubit states

In principle, the state of the charge qubit can be read by a single-electron transistor (SET) [2, 3, 22] coupled capacitively to a charge qubit. Here we consider the ideal case in which the SET is coupled to the qubit only during the measurement. When the SET is coupled to the qubit, the dissipative current I flowing through the SET is proportional to the probability of a projective operator measurement $|1\rangle\langle 1|$ on the qubit state, which has actually been applied by the experiment [2, 3]. The $|1\rangle\langle 1|$ measurement is equivalent to a σ_z measurement on the state ρ,

$$p_1 = {\rm Tr}(\rho\,|1\rangle\langle 1|) = \frac{1}{2}[1 - {\rm Tr}(\rho\,\sigma_z)] = \rho_{11}$$

due to the relation

$$|1\rangle\langle 1| = \frac{1}{2}(\sigma_0 - \sigma_z).$$

The parameters r_0 and r_z can be determined by the result of the measurement $|1\rangle\langle 1|$, together with the normalization condition.

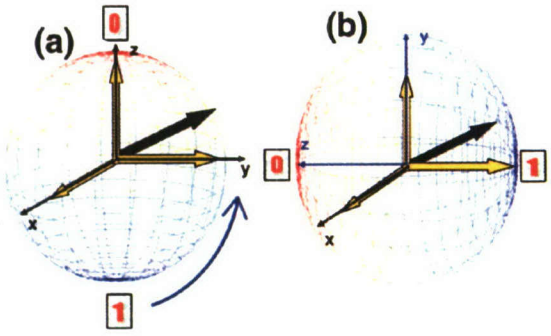

FIG. 1: (Color on line) The black Bloch vector indicates a qubit state; the (yellow arrows) r_x, r_y and r_z represent the three components of the Bloch vector along the x, y and z axes. The 0 and 1 in the north and south poles of the Bloch sphere denote the measured states $|0\rangle$ and $|1\rangle$, respectively. The measurement instrument is attached to a pole (e.g., "1") of the sphere. A $-\pi/2$ rotation of the qubit state along the x direction is equivalent to a $\pi/2$ rotation of the measuring instrument along the x direction.

We can also relate the two other measurement operators, σ_x and σ_y, to the operator $|1\rangle\langle 1|$ (essentially σ_z), which is the measurement experimentally realized in the charge qubits. This is because the current I flowing through the SET is sensitive to the charge state $|1\rangle$, so the single qubit operations have to be performed so that the desired parameter r_x or r_y is transformed to the measured diagonal positions.

Now, we describe the steps to measure r_x or r_y. Let us first choose the external flux $\Phi_x = 0$ and suddenly drive the qubit to the degeneracy point for a time

$$t_x = \frac{\hbar\pi}{2\,E_{\rm J}(0)} = \frac{\hbar\pi}{4\,E_{\rm J}^0}$$

such that the qubit state can be rotated $-\pi/2$ along the x direction, here $E_{\rm J}(0) = E_{\rm J}(\Phi_x = 0)$.

The probability p_2 of the measurement $|1\rangle\langle 1|$ on the rotated state is

$$\begin{aligned} p_2 &= {\rm Tr}\left(R_x(t_x)\ \rho\ R_x^\dagger(t_x)\,|1\rangle\langle 1|\right) \\ &= {\rm Tr}\left(\exp\left\{i\frac{\pi}{4}\sigma_x\right\}\ \rho\ \exp\left\{-i\frac{\pi}{4}\sigma_x\right\}|1\rangle\langle 1|\right) \\ &= {\rm Tr}\left(\rho\ \exp\left\{-i\frac{\pi}{4}\sigma_x\right\}|1\rangle\langle 1|\ \exp\left\{i\frac{\pi}{4}\sigma_x\right\}\right) \\ &= \frac{1}{2}\,(1+r_y), \end{aligned} \tag{3}$$

where $R_x(t_x) = \exp\{iE_J(0)\sigma_x t_x/2\hbar\}$, Eq. (3) means that the measurement $|1\rangle\langle 1|$ on the state rotated $-\pi/2$ along the x direction is equivalent to the measurement σ_y, and the rotation $-\pi/2$ of the qubit is equivalent to an inverse rotation of the measuring instrument, see Fig. 1.

In order to make the third measurement σ_x, the qubit state needs now to be rotated $-\pi/2$ (or $\pi/2$) along the y direction. This can be done (e.g., $-\pi/2$ rotation) as follows:

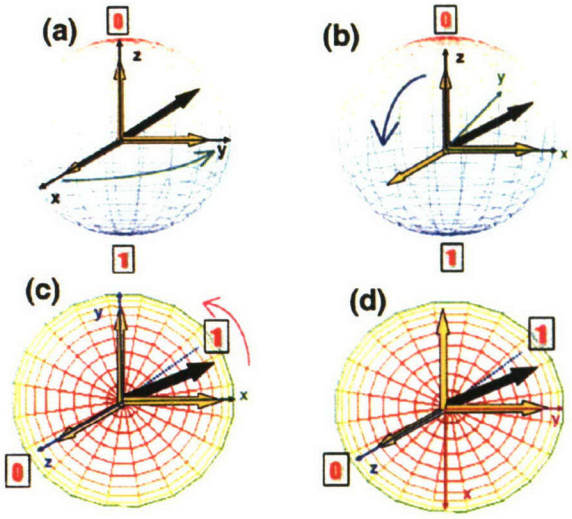

FIG. 2: (Color on line) The Bloch vector is the same as Fig. 1. A $-\pi/2$ rotation of the qubit along the y direction is equivalently realized by the rotation $\pi/2$ of the measuring instrument along the z direction (from (a) to (b)), then a $\pi/2$ rotation along the x direction (from (b) to (c)), and a $3\pi/2$ rotation along z direction (from (c) to (d)).

(i) Set $\Phi_x = \Phi_0/2$ and $n_{\rm g} = 0$; let the system evolve a time $t_{z,1} = \hbar\pi/8E_{\rm C}$ such that a rotation of $-\pi/2$ along the z direction is realized.

(ii) After the time $t_{z,1}$, set $\Phi_x = 0$ and $n_{\rm g} = 1/2$ and let the system evolve a time period $t_{x,1} = \hbar\pi/2E_{\rm J}(0) = \hbar\pi/4E_{\rm J}^0$ such that the system rotates $-\pi/2$ along the x direction.

(iii) Set $\Phi_x = 0$ and $n_{\rm g} = 1/2$ again and let the system evolve a time $t_{z,2} = 3\hbar\pi/8E_{\rm C}$ and a rotation $-3\pi/2$ along the z direction is obtained.

Combining the above three steps, shown in Fig. 2, a $-\pi/2$ rotation of the qubit along the y direction is realized.

(iv) After the above rotations, a measurement $|1\rangle\langle 1|$ on this rotated state must be made, which is equivalent to measuring σ_x. Then, the measured probability becomes

$$\begin{aligned} p_3 &= {\rm Tr}(\,R_{z,x,z}\,\rho\,R_{z,x,z}^\dagger\,|1\rangle\langle 1|\,) \\ &= {\rm Tr}\left(\exp\left\{i\frac{\pi}{4}\sigma_y\right\}\rho\exp\left\{-i\frac{\pi}{4}\sigma_y\right\}|1\rangle\langle 1|\right) \\ &= \frac{1}{2}\,(1+r_x) \end{aligned}$$

with $R_{z,x,z} = R_z(t_{z,1})R_x(t_{x,1})R_z(t_{z,2})$, and

$$R_z(t_{z,1}) = \exp\left\{i\frac{2E_C}{\hbar}\sigma_z t_{z,1}\right\} = \exp\left\{i\frac{\pi}{4}\sigma_z\right\},$$
$$R_x(t_{x,1}) = \exp\left\{i\frac{E_J^0}{\hbar}\sigma_x t_{x,1}\right\} = \exp\left\{i\frac{\pi}{4}\sigma_x\right\},$$
$$R_z(t_{z,2}) = \exp\left\{i\frac{2E_C}{\hbar}\sigma_z t_{z,2}\right\} = \exp\left\{i\frac{3\pi}{4}\sigma_z\right\}.$$

We explained how to measure the single qubit states by single qubit operations and measuring $|1\rangle\langle 1|$. Below, we give an example that shows a reconstructed single-qubit state can be graphically represented, and we further give estimates of the operation times to obtain each of the matrix elements of single-qubit states.

C. An example

The three measurement results (p_1, p_2, p_3) can be used to obtain four coefficients (r_0, r_x, r_y, r_z) that define a single-qubit state. A single-qubit state can be reconstructed following the steps presented above and an example is described here. If we obtain $r_x = 1$, $r_y = \sqrt{3}$, $r_z = 1$ by the three experimentally measured probabilities (p_1, p_2 and p_3) on a quantum ensemble of an unknown charge qubit state ρ, then

$$\rho_{00} = \rho_{11} = \frac{1}{2},$$
$$\rho_{01} = \frac{1}{4}\left(1 - i\sqrt{3}\right),$$
$$\rho_{10} = \frac{1}{4}\left(1 + i\sqrt{3}\right).$$

Thus, the reconstructed state ρ can be written as

$$\rho = \frac{1}{2}\left(|0\rangle\langle 0| + |1\rangle\langle 1|\right) + \frac{1}{4}\left[\left(1 + i\sqrt{3}\right)|1\rangle\langle 0|\right] + \frac{1}{4}\left[\left(1 - i\sqrt{3}\right)|0\rangle\langle 1|\right]$$

whose real $\rho_{ij}^{(R)}$ and imaginary $\rho_{ij}^{(I)}$ parts are graphically represented in Fig. 3.

D. Operation time estimates

The coherent operations required for the tomographic measurements are limited by the decoherence time T_2. Now let us explore whether the single-qubit state can be reconstructed with the current experiments. To estimate the corresponding time scales for quantum operations to obtain the measurements of σ_y and σ_x, we first take the suggested parameters from Ref. [22], that is, $E_J^0 = 100$ mK (about 8.6 μeV or 2.08 GHz) and $E_C = 1$ K (about 86 μeV or 20.8 GHz). Here, we use temperature units for energies as in reference [22]. Thus the approximate time scales of one-qubit operations to obtain r_y and r_x are

$$t_x \approx 5.9 \times 10^{-11} \text{ s}$$

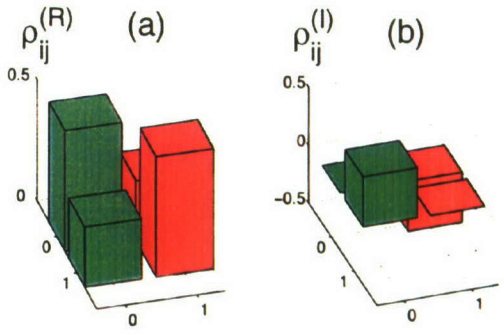

FIG. 3: Graphical representation of the density matrix ρ for single-qubit states, see the example explained in section II. The real $\rho_{ij}^{(R)}$ and imaginary $\rho_{ij}^{(I)}$ parts of the density matrix elements $\rho_{ij} = \langle i|\rho|j\rangle$ (i, $j = 0, 1$) are plotted in (a) and (b), respectively.

and

$$t_y = t_{z,1} + t_{x,1} + t_{z,2} \approx 7.1 \times 10^{-11} \text{ s}.$$

These time scales, required to reconstruct the single-qubit states, are within the measured values [2, 3] of the decoherence time T_2 (of the order of magnitude of ns) of single-qubit charge states.

Now let us consider another set of experimental values. For example, if the Josephson and charge energies are taken (second paper in Ref. [3]) as $2E_J^0 = 45\mu$eV (about 520 mK or 10.9 GHz) and $4E_C = 580\mu$eV (about 6.73 K or 140 GHz), then the time scales required to reconstruct single-qubit states are about $t_x \approx 2.3 \times 10^{-11}$s and $t_y \approx 3.0 \times 10^{-11}$s, which are within the decoherence time $T_2 = 5$ ns obtained by that experiment [3].

If we take the Josephson and charge energies from in Ref. [23], that is, $2E_J^0/h = 13.0$ GHz (about 625 mK or 53.7 μeV) and $4E_C/h = 149.1$ GHz (about 7.16 K or 618 μeV), then the time scales required to reconstruct single-qubit states are about $t_x \approx 1.9 \times 10^{-11}$s and $t_y \approx 2.6 \times 10^{-11}$s, which are also less than one order of magnitude of the decoherence time $T_2 = 325$ ps measured by that experiment [23].

III. RECONSTRUCTION OF TWO-QUBIT STATES

A. Theoretical model and two-qubit states

In this section, we focus on the reconstruction of two-qubit charge states. Our task is to find a non-local two-qubit operation and use this operation to realize all necessary two-qubit measurements on two-qubit states. Here we consider a model proposed by Makhlin et al. [6], where two charge qubits are coupled in parallel to a common inductor with inductance L. The Hamiltonian [6] is

$$H = -\frac{1}{2}\sum_{l=1}^{2}\left[\delta E_{\rm ch}(n_{l,g})\,\sigma_{lz} + E_J(\Phi_{lx})\,\sigma_{lx}\right] - E_{\rm int}(\Phi_{1x}, \Phi_{2x})\,\sigma_{1y}\otimes\sigma_{2y}, \quad (4)$$

where it is assumed that both qubits are identical, so the charge energies $\delta E_{\rm ch}(n_{l,{\rm g}})$ and Josephson coupling energies $E_{\rm J}(\Phi_{lx})$ take the same form as in Eq. (1), but now $\delta E_{\rm ch}(n_{l,{\rm g}})$ and $E_{\rm J}(\Phi_{lx})$ for each qubit can be separately controlled by the gate voltages and external fluxes. The interaction energy $E_{\rm int}$ for two coupled qubits can be written as

$$E_{\rm int}(\Phi_{1x},\Phi_{2x}) = \frac{E_{\rm J}(\Phi_{1x})E_{\rm J}(\Phi_{2x})}{E_{\rm L}}$$

with

$$E_{\rm L} = \left(\frac{C_{\rm J}^0}{C_{\rm qb}}\right)^2 \left(\frac{\Phi_0^2}{\pi^2 L}\right)$$

and $C_{\rm qb}^{-1} = (2C_{\rm J}^0)^{-1} + C_{\rm g}^{-1}$. Thus, the interaction between the two qubits can be controlled by two external fluxes Φ_{lx} applied to each qubit.

Any two-qubit state ρ_1 can be characterized by a density matrix operator

$$\rho_1 = \frac{1}{4}\sum_{i,j=0,x,y,z} r_{i,j}\,\sigma_{1i}\otimes\sigma_{2j} \qquad (5)$$

where the 16 parameters $r_{i,j}$ are real numbers. The normalization property of the quantum state requires that $r_{0,0} = 1$, so the state ρ_1 in Eq. (5) can in principle be reconstructed [24] by 15 measurements described by the operators $\sigma_{1i}\otimes\sigma_{2j}$, where all i and j are not simultaneously taken to be 0. If one of σ_{1i} ($i = 0,\ x,\ y,\ z$) or σ_{2j} ($i = 0,\ x,\ y,\ z$) is an identity operator among the measurement operators $\sigma_{1i}\otimes\sigma_{2j}$, we call such a measurement a single-qubit measurement and only write out the non-identity Pauli operator in the following expressions. For example, the operator $\sigma_{1x}\otimes\sigma_{20}$ is called σ_x measurement of the first qubit, and abbreviated by σ_{1x}. Compared with the reconstruction of a single-qubit state, we cannot obtain all 15 measurements by only using single-qubit operations. The two-qubit operations must be applied according the general theory of quantum computation [25].

B. Quantum operations and measurements on two-qubit states

Now, we discuss how to reconstruct two-qubit states from the experimental measurements $(|1\rangle\langle 1|)_l$ ($l = 1,\ 2$). Single charge qubit operations can be realized by controlling the gate voltage and Josephson couplings. However the two-qubit operations need to couple a pair of interacting charge qubits. The realization of the coupling of two charge qubits have to simultaneously turn on the Josephson couplings of the two charge qubits in Eq. (4), then σ_{lx} terms have to be included in the two-qubit operation. However the charge energies for two qubits can be switched off by applying gate voltages such that $n_{l,{\rm g}} = 1/2$ ($l = 1,\ 2$), so a two-qubit operation can be governed by a simpler Hamiltonian

$$H' = -\frac{1}{2}\sum_{l=1,2} E_{\rm J}(\Phi_{lx})\,\sigma_{lx} - E_{\rm int}(\Phi_{1x},\Phi_{2x})\,\sigma_{1y}\otimes\sigma_{2y}, \quad (6)$$

where charging energies are set to zero, $\delta E_{\rm ch}(n_{l,{\rm g}}) = 0$ ($l = 1,\ 2$), with $n_{1,{\rm g}} = n_{2,{\rm g}} = 1/2$, and the external magnetic fields are chosen such that

$$\Phi_{1x} = \Phi_{2x} \neq \frac{\pi}{2}(2q+1)\Phi_0$$

with the positive integer number q. The coupling $E_{\rm int}(\Phi_{1x},\Phi_{2x})$ can be controlled by the external fluxes Φ_{1x} and Φ_{2x}.

The basic two-qubit operation can be given by the time-evolution operator $U(t) = \exp\{-iH't/\hbar\}$, which can be written by using the Pauli operators as

$$\begin{aligned} U(t) &= \frac{1}{2}\left(\cos\phi' + \cos\theta'\right) I + i n_z \frac{\sin\theta'}{2}\left(\sigma_{1x}+\sigma_{2x}\right) \\ &+ i\frac{\sin\phi' - n_x\sin\theta'}{2}\,\sigma_{1z}\otimes\sigma_{2z} \\ &+ i\frac{\sin\phi' + n_x\sin\theta'}{2}\,\sigma_{1y}\otimes\sigma_{2y} \\ &- \frac{\cos\phi' - \cos\theta'}{2}\,\sigma_{1x}\otimes\sigma_{2x}, \end{aligned} \qquad (7)$$

where

$$\begin{aligned} \phi' &= \frac{t}{\hbar}E_{\rm int}(\Phi_{1x},\Phi_{2x}), \quad n_z = \frac{a}{\sqrt{1+a^2}}, \\ n_x &= \frac{1}{\sqrt{1+a^2}}, \quad a = \frac{E_{\rm J}}{E_{\rm int}(\Phi_{1x},\Phi_{2x})}, \\ \theta' &= \frac{2}{\hbar}E_{\rm int}(\Phi_{1x},\Phi_{2x})\sqrt{1+a^2}\,. \end{aligned}$$

Since the two external fluxes satisfy the condition $\Phi_{1x} = \Phi_{2x}$, we let $E_{\rm J}(\Phi_{1x}) = E_{\rm J}(\Phi_{2x}) = E_{\rm J}$ in the expression Eq. (7) for the two-qubit operation. The physical meaning of the angles θ' and ϕ' becomes clearer by virtue of the "conjugation-by-$\frac{\pi}{4}\Sigma$" operation [26] on the time evolution operator $U(t)$, which is defined as

$$U'(t) = \exp\left\{i\frac{\pi}{4}(\sigma_{1y}+\sigma_{2y})\right\} U(t) \exp\left\{-i\frac{\pi}{4}(\sigma_{1y}+\sigma_{2y})\right\},$$

here, $\Sigma = \sigma_{1y} + \sigma_{2y}$. In the conjugate representation, the time evolution $U'(t)$ corresponds to rotations [27] around the y axis by an angle ϕ' and the $(n_x, 0, n_z)$ axis by an angle θ'. By choosing the duration t and tuning the values of $E_{\rm J}$ and $E_{\rm int}(\Phi_{1x},\Phi_{2x})$, we can obtain any desired two-qubit operation.

From Eq. (5), it is known that six single-qubit measurements $\{\sigma_{1i},\sigma_{2j}\}$ with $i,j = x,y,z$ and nine two-qubit measurements $\{\sigma_{1i}\otimes\sigma_{2j}\}$ with $i,j = x,y,z$ are enough to obtain fifteen parameters $r_{i,j}$ of the two-qubit state $\rho_1 = \frac{1}{4}\sum_{i,j=0,x,y,z} r_{i,j}\,\sigma_{1i}\otimes\sigma_{2j}$. However, experiments now perform the single-qubit measurements $(|1\rangle\langle 1|)_l = \frac{1}{2}(\sigma_{l0} - \sigma_{lz})$ ($l = 1,\ 2$) on a given state ρ_1. Moreover, two single-qubit measurements σ_{1z} and σ_{2z} can be implemented by the direct measurements $(|1\rangle\langle 1|)_1$ and $(|1\rangle\langle 1|)_2$ on the given state ρ_1. Other four single-qubit measurements (corresponding to σ_{1x}, σ_{2x}, σ_{1y}, σ_{2y}) need single-qubit operations.

The single-qubit operations corresponding to these two kinds of measurements σ_{lx} and σ_{ly} on two-qubit states are the same as measuring σ_x and σ_y on single-qubit states. However, in the single qubit operations, we need to switch off the interaction of the two qubits. For example, in order to obtain the measurement σ_{1y}, we need to switch off the interaction between the two-qubit system by setting the applied external flux $\Phi_{2x} = \pi/2$, and setting the first subsystem at the degeneracy point and evolving a time $t = \hbar\pi/4E_J^0$. Finally, we make a measurement $(|1\rangle\langle 1|)_1$ on the rotated state, then the coefficient $r_{y,0}$ can be obtained by this measured result. The other three measurements can also be obtained by taking single-qubit operations similar to σ_{1y}.

The single-qubit measurements have been obtained by the measurements $(|1\rangle\langle 1|)_l (l = 1, 2)$ on given states by using appropriate single-qubit operations as described above. In order to find out how to obtain the two-qubit measurements via $(|1\rangle\langle 1|)_l$, let us consider the measurements $(|1\rangle\langle 1|)_l$ on the given state ρ_1 performed by a sequence W of single-qubit and two-qubit operations. The corresponding measured probability p can be expressed as

$$p = \mathrm{Tr}\left[W\,\rho_1\,W^\dagger(|1\rangle\langle 1|)_l\right] = \frac{1}{2} - \frac{1}{2}\mathrm{Tr}\left[\rho_1\,W^\dagger\sigma_{lz}W\right], \quad (8)$$

where we show that the measurement $(|1\rangle\langle 1|)_l$ on the rotated state $W\rho_1\,W^\dagger$ may be interpreted as an equivalent measurement $W^\dagger\sigma_{lz}W$ with $(l = 1, 2)$ on the state ρ_1. So our task now is to find an appropriate two-qubit operation and apply this two-qubit and single-qubit operations to the measured state ρ_1, such that we can equivalently obtain the desired two-qubit measurement.

Here, the required two-qubit operation $U(\tau)$ can be obtained by choosing the evolution time τ, the Josephson coupling energies E_J, and E_L in Eq. (7) such that $\phi' = (2m - 1)\pi/4$ and $\theta' = n\pi$ where m, n are positive integers. The above conditions can be satisfied if the ratio

$$\frac{E_\mathrm{L}}{E_\mathrm{J}} = \sqrt{\left(\frac{4n}{2m-1}\right)^2 - 1},$$

and the evolution time τ is chosen as

$$\tau = \frac{\hbar\pi}{4E_\mathrm{J}}\sqrt{(4n)^2 - (2m-1)^2}.$$

If we choose the integers m and n to minimize the ratio $E_\mathrm{L}/E_\mathrm{J}$, then $E_\mathrm{L}/E_\mathrm{J} = \sqrt{15} \cong 3.87$ when $\theta' = \pi$ and $\phi' = \pi/4$; so the two-qubit operation time τ is chosen as $\tau = \hbar\pi\sqrt{15}/4E_\mathrm{J}$. Thus Eq. (7) is specified by the time evolution operator

$$\begin{aligned} U(\tau) &= \frac{1}{2\sqrt{2}}\left[\left(1-\sqrt{2}\right) I - \left(1+\sqrt{2}\right)\,\sigma_{1x}\otimes\sigma_{2x}\right. \\ &+ \left. i\sigma_{1y}\otimes\sigma_{2y} + i\sigma_{1z}\otimes\sigma_{2z}\right]. \end{aligned} \quad (9)$$

Combined with other single qubit rotations, $U(\tau)$ can be used to obtain all the desired coefficients $r_{i,j}$ corresponding to the two-qubit measurements $\sigma_{1i}\otimes\sigma_{2j}$, with $i, j = x, y, z$.

Let us further discuss how to obtain a desired coefficient, for example, $r_{y,y}$ corresponding to the two-qubit measurement $\sigma_{1y}\otimes\sigma_{2y}$. We can take the following steps:

(i) We switch off the interaction between the first and second qubits by applying an external flux $\Phi_{2x} = \pi/2$, which means $E_\mathrm{J}(\Phi_{2x}) = 0$. Now we only manipulate the first qubit such that a rotation $\pi/2$ about the z axis, defined as $Z_1 = \exp[i\pi\sigma_{1z}/4]$, is performed; this single-qubit operation is described in Section II.

(ii) Following the single-qubit rotation Z_1 of the first qubit, the gate voltages are applied such that $n_{1,g} = n_{2,g} = 1/2$, which means that the two qubits work at the degeneracy points. Simultaneously, we turn on and adjust the external fluxes so that the external fluxes Φ_{lx}, energies E_L and E_J in the two-qubit operation described by the Hamiltonian (6) satisfy the conditions $\Phi_{1x} = \Phi_{2x} \neq \pi(2q+1)/2$ with positive integer q and $E_\mathrm{L}/E_\mathrm{J} = \sqrt{15} \cong 3.87$. Afterwards, we let the system evolve a time $\tau = \hbar\pi\sqrt{15}/4E_\mathrm{J}$; which means that a two-qubit rotation $U(\tau)$ has been performed.

The operation sequence $W = U(\tau)Z_1$ described above changes state ρ_1 into

$$\widetilde{\rho} = U(\tau)\,Z_1\,\rho_1\,Z_1^\dagger\,U^\dagger(\tau).$$

(iii) Finally, when a single-qubit measurement $(|1\rangle\langle 1|)_1$ is performed on the state $\widetilde{\rho}$, a two-qubit measurement equivalent to $\sigma_{1z}\otimes\sigma_{2y}$ is implemented:

$$Z_1^\dagger\,U^\dagger(\tau)\,(|1\rangle\langle 1|)_1\,U(\tau)\,Z_1 = \frac{1}{2} + \frac{1}{2\sqrt{2}}\left(\sigma_{1z} + \sigma_{1y}\otimes\sigma_{2y}\right).$$

The corresponding measurement probability $\widetilde{p}$ can be given as

$$\begin{aligned} \widetilde{p} &= \mathrm{Tr}\left\{U(\tau)\,Z_1\,\rho_1\,Z_1^\dagger\,U^\dagger(\tau)(|1\rangle\langle 1|)_1\right\} \\ &= \frac{1}{2} + \frac{1}{2\sqrt{2}}\mathrm{Tr}\left[\rho_1\left(\sigma_{1z} + \sigma_{1y}\otimes\sigma_{2y}\right)\right] \\ &= \frac{1}{2} + \frac{1}{2\sqrt{2}}(r_{z,0} + r_{y,y}). \end{aligned} \quad (10)$$

Because the coefficient $r_{z,0} = \mathrm{Tr}(\rho_1\,\sigma_{1z})$, corresponding to the operator $\sigma_{1z}\otimes\sigma_{20}$, has been given by the single-qubit measurement σ_{1z}, then the coefficient $r_{y,y} = \mathrm{Tr}(\rho_1\,\sigma_{1y}\otimes\sigma_{2y})$ is obtained via $\widetilde{p}$ and $r_{z,0}$.

In table I, we have summarized nine equivalent two-qubit measurements described by $-\sqrt{2}\,W^\dagger\sigma_{1z}W$ on the original state ρ_1, which are obtained by the first qubit measurement $(|1\rangle\langle 1|)_1$ on the rotated state $W\rho_1 W^\dagger$ for a sequence W of operations with appropriately-chosen single-qubit and two-qubit operations. We can use the results corresponding to these nine equivalent two-qubit measurements together with the other six single-qubit measurements to obtain all the coefficients corresponding to the two-qubit measurements, and then obtain any two qubit state.

We can also obtain coefficients r_{ij} $(i, j \neq 0)$ corresponding to all two-qubit measurements by using the second qubit measurement $(|1\rangle\langle 1|)_2$. For example, if we make a measurement $(|1\rangle\langle 1|)_2$ on the rotated state $\widetilde{\rho}$ considered above, we

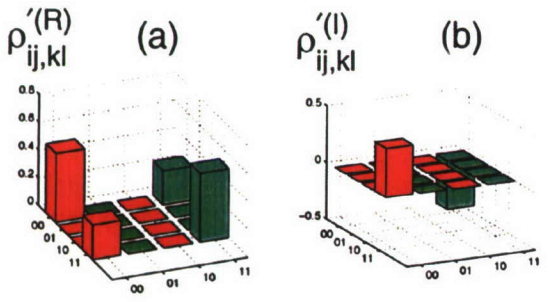

FIG. 4: Graphical representation of the density matrix ρ' for the two-qubit state described in the example given in section III. The real $\rho'^{(R)}_{ij,kl}$ and imaginary $\rho'^{(I)}_{ij,kl}$ parts of the density matrix elements for the two-qubit state ρ' in the basis $|00\rangle$, $|01\rangle$, $|10\rangle$, $|11\rangle$ are plotted in (a) and (b) respectively.

obtain another equivalent two-qubit measurement, which is expressed as

$$Z_1^\dagger U^\dagger(\tau)\,(|1\rangle\langle 1|)_2\,U(\tau)\,Z_1 = \frac{1}{2} + \frac{1}{2\sqrt{2}}(\sigma_{2z} - \sigma_{1x}\otimes\sigma_{2x}).$$

Using this measurement, combined with the single-qubit measurement σ_{2z}, we can obtain the coefficient $r_{x,x}$ corresponding to the two-qubit measurement $\sigma_{1x}\otimes\sigma_{2x}$. Nine equivalent two-qubit measurements realized by the second qubit $(|1\rangle\langle 1|)_2$ have also been summarized in Table II. Comparing tables I and II shows that different operations and steps are required in order to obtain the same coefficient for different measurements. For example, in order to obtain $r_{x,z}$, two operation steps are needed for the first qubit measurement $(|1\rangle\langle 1|)_1$, but it needs four steps for the second qubit measurement $(|1\rangle\langle 1|)_2$.

C. An example

We can also give another schematic example for a reconstructed two-qubit state. For instance, according to the operations steps discussed above for the reconstruction of any two-qubit state, if we obtain $r_{x,x} = 1/8$, $r_{x,y} = r_{y,x} = \sqrt{3}/8$, $r_{z,z} = 1/4$ and $r_{y,y} = -1/8$ from the sixteen measured probabilities on an ensemble of identically prepared copies of a two-qubit system with unknown state ρ', then we can reconstruct this unknown state as

$$\begin{aligned}\rho' &= \frac{1}{2}[|00\rangle\langle 00| + |11\rangle\langle 11|] + \frac{1}{2}\left(1 - i\sqrt{3}\right)|00\rangle\langle 11| \\ &+ \frac{1}{2}\left(1 + i\sqrt{3}\right)|11\rangle\langle 00|,\end{aligned}$$

which is graphically shown in Fig. (4) with the real $\rho'^{(R)}_{ij,kl}$ and imaginary $\rho'^{(I)}_{ij,kl}$ parts of the reconstructed state ρ', where i, j, k, l can take the values 0 or 1.

D. Operation time estimates

We can also estimate the operation time required to reconstruct two-qubit states for the Josephson and charge energies [22] $E_J^0 = 100$ mK and $E_C = 1$ K. We assume that the ratio $E_L/E_J = \sqrt{15} \cong 3.87$ is obtained by adjusting the external flux Φ_{lx} ($l = 1, 2$) such that $\Phi_{lx} = 0$, which means the ratio between E_L and E_J^0 should satisfy the condition $E_L/E_J^0 = 2\sqrt{15} \cong 7.74$ when the circuits are fabricated. In such case, the realization of the two-qubit operation in Eq. (9) requires a time $\tau \approx 2.32 \times 10^{-10}$ s. Our previous estimates for the times to perform $\pi/2$ rotations about the x and z axes are 5.9×10^{-11} s and 3.0×10^{-12} s, respectively. Then, using tables I and II, we can estimate the total operation time required for obtaining the coefficients of the two-qubit measurements corresponding to the first or second qubit measurements, respectively. We find that the required operation times for the two-qubit measurements are less than 0.4 ns for the two-qubit measurements. The decoherence time T_2 (e.g., the decoherence time of charge qubit is about 5 ns in reference [2]) experimentally obtained shows that it is possible to reconstruct two-qubit states within the current measurement technology.

At present, completely controllable multi-qubit superconducting circuits are not experimentally achievable. Here, let us consider the operation time estimates based on another promising controllable theoretical model [28]. According to calculations [20] of tomographic measurements for a class of representative quantum computing models of solid state systems, the two-qubit operation required for the realization of the multi-qubit measurements in this circuit can be easily obtained. That is, if the ratio between the Josephson energy E_J^0 and the two-qubit coupling energy χ is $E_J^0 = 2\chi$, when the circuit is fabricated, then a two-qubit operation $\widetilde{U}(\tau') = -i\sigma_{1x}\otimes\sigma_{2x}$ can be obtained with the evolution time $\tau' \approx 1.2 \times 10^{-10}$ s when the Josephson energy is taken as $E_J^0 = 100$ mK. Here, we assume that the two charge qubits are identical and the Josephson energies are maximum when two-qubit operation is performed If the charging energy is taken as $E_C = 1$ K, then $\pi/2$ rotations around the z and x axes need times 3.0×10^{-12} s and 5.9×10^{-11} s, respectively. The operations to get each of the sixteen (single- and two-qubit) measurements can also be obtained for this model by using an approach similar to the one described above, the estimated operation times to obtain all coefficients of the two-qubit measurements are less than 0.3 ns, which is also within the experimentally obtained decoherence time $T_2 = 5$ ns.

IV. RECONSTRUCTION OF MULTIPLE QUBIT STATES

In the above two sections, we focused on the reconstruction of the single and two qubits states. In this section, we discuss the reconstruction of any n-qubit state. In the multiple qubit charge circuit, the dynamical evolution is governed by

TABLE I: Equivalent two-qubit measurements $-\sqrt{2}\,W^\dagger\,\sigma_{1z}\,W$ obtained by measuring $(|1\rangle\langle 1|)_1$ on the state $W\rho_1\,W^\dagger$ with a sequence of appropriately-chosen quantum operations W.

Two-qubit measurement	Quantum operation[a] W	Equivalent two-qubit measurement
$\sigma_{1x}\otimes\sigma_{2y}$	$U(\tau)$	$\sigma_{1z}+\sigma_{1x}\otimes\sigma_{2y}$
$\sigma_{1x}\otimes\sigma_{2z}$	$X_1U(\tau)$	$-\sigma_{1y}+\sigma_{1x}\otimes\sigma_{2z}$
$\sigma_{1x}\otimes\sigma_{2x}$	$U(\tau)Z_2$	$\sigma_{1z}-\sigma_{1x}\otimes\sigma_{2x}$
$\sigma_{1y}\otimes\sigma_{2y}$	$U(\tau)Z_1$	$\sigma_{1z}+\sigma_{1y}\otimes\sigma_{2y}$
$\sigma_{1y}\otimes\sigma_{2z}$	$X_1U(\tau)Z_1$	$\sigma_{1x}+\sigma_{1y}\otimes\sigma_{2z}$
$\sigma_{1y}\otimes\sigma_{2x}$	$U(\tau)Z_1Z_2$	$\sigma_{1z}-\sigma_{1y}\otimes\sigma_{2x}$
$\sigma_{1z}\otimes\sigma_{2y}$	$U(\tau)Z_1X_1$	$-\sigma_{1y}+\sigma_{1z}\otimes\sigma_{2y}$
$\sigma_{1z}\otimes\sigma_{2z}$	$X_1U(\tau)Z_1X_1$	$\sigma_{1x}+\sigma_{1z}\otimes\sigma_{2z}$
$\sigma_{1z}\otimes\sigma_{2x}$	$U(\tau)Z_1Z_2X_1$	$-\sigma_{1y}-\sigma_{1z}\otimes\sigma_{2x}$

[a] X_l and Z_l denote single qubit rotations $\pi/2$ of lth qubit about the x and z axes, respectively, and $\tau=\hbar\pi\sqrt{15}/4E_{\rm J}$.

TABLE II: Equivalent two-qubit measurements $-\sqrt{2}\,W^\dagger\,\sigma_{2z}W$ obtained by measuring $(|1\rangle\langle 1|)_2$ on the state $W\,\rho_1\,W^\dagger$ with a sequence of appropriately-chosen quantum operations W.

Two-qubit measurement	Quantum operation W	Equivalent quantum measurement
$\sigma_{1x}\otimes\sigma_{2x}$	$U(\tau)Z_1$	$\sigma_{2z}-\sigma_{1x}\otimes\sigma_{2x}$
$\sigma_{1y}\otimes\sigma_{2x}$	$U(\tau)$	$\sigma_{2z}+\sigma_{1y}\otimes\sigma_{2x}$
$\sigma_{1z}\otimes\sigma_{2x}$	$U(\tau)X_1$	$-\sigma_{2y}+\sigma_{1z}\otimes\sigma_{2x}$
$\sigma_{1x}\otimes\sigma_{2y}$	$U(\tau)Z_1Z_2$	$\sigma_{2z}-\sigma_{1x}\otimes\sigma_{2y}$
$\sigma_{1y}\otimes\sigma_{2y}$	$U(\tau)Z_2$	$\sigma_{2z}+\sigma_{1y}\otimes\sigma_{2y}$
$\sigma_{1z}\otimes\sigma_{2y}$	$U(\tau)X_1Z_2$	$\sigma_{2x}+\sigma_{1z}\otimes\sigma_{2y}$
$\sigma_{1x}\otimes\sigma_{2z}$	$U(\tau)Z_1Z_2X_2$	$-\sigma_{2y}-\sigma_{1x}\otimes\sigma_{2z}$
$\sigma_{1y}\otimes\sigma_{2z}$	$U(\tau)Z_2X_2$	$-\sigma_{2y}+\sigma_{1y}\otimes\sigma_{2z}$
$\sigma_{1z}\otimes\sigma_{2z}$	$U(\tau)X_1Z_2X_2$	$\sigma_{2x}+\sigma_{1z}\otimes\sigma_{2z}$

the Hamiltonian [6]

$$H = -\frac{1}{2}\sum_{l=1}^{n}[\delta E_{\rm ch}(n_{l,g})\,\sigma_{lz}+E_{\rm J}(\Phi_{lx})\,\sigma_{lx}] - \sum_{l<k}E_{\rm int}(\Phi_{lx},\Phi_{kx})\,\sigma_{ly}\otimes\sigma_{ky}, \quad (11)$$

where $\delta E_{\rm ch}(n_{l,g}) = 4E_{\rm C}(1-2n_{l,g})$, $E_{\rm J}(\Phi_{lx}) = 2E_{\rm J}^0\cos(\pi\Phi_{lx}/\Phi_0)$, and $E_{\rm int}(\Phi_{lx},\Phi_{kx})$ take the same form as in Eq. (4). We also assume $E_{\rm L}/2E_{\rm J}^0=\sqrt{15}\cong 3.87$ and the single-qubits are nominally identical. By virtue of the controllable Hamiltonian (11), in principle we can use $(n-1)$ two-qubit operations together with some single-qubit operations to reconstruct any n-qubit state, which can also be described by the density matrix operator

$$\rho_2=\frac{1}{2^n}\sum_{l_1,l_2,\cdots,l_n=0,x,y,z} r_{l_1,l_2,\cdots,l_n}\,\sigma_{l_1}\otimes\sigma_{l_2}\cdots\otimes\sigma_{l_n}$$

with 2^n real parameters $r_{l_1,l_2,\cdots,l_n}$ corresponding to the measurements $\sigma_{l_1}\otimes\sigma_{l_2}\cdots\otimes\sigma_{l_n}$. But, here, we only show how to obtain a coefficient corresponding to a three-qubit measurement. The generalization to obtain coefficients of multiple qubit measurements is straightforward.

In order to determine a three-qubit state, we need to make, single-qubit, two-qubit, and three-qubit measurements. It is known that all coefficients corresponding to single-qubit and two-qubit measurements can be obtained by using the same operations and measurements $(|1\rangle\langle 1|)_{l=1,2,3}$ as in section I and II. When we make two-qubit operations on, for example, the first and second qubits, the interaction of the third qubit with these two qubits is switched off by the applied flux $\Phi_{3x}=\pi/2$. Now let us show how to obtain the coefficients corresponding to the three-qubit measurements. For example, for the coefficient $r_{x,z,y}$ of the measurement $\sigma_{1x}\otimes\sigma_{2z}\otimes\sigma_{3y}$, we should make the following sequence of quantum operations:

(i) Switch off the interaction of the third qubit with the first and second qubits by applying the flux $\Phi_{3x}=\pi/2$. Then make a two-qubit operation $U_{12}(\tau)$, with the same form as Eq. (9). We use the subscript "12" to denote two-qubit operations on the first and second qubits.

(ii) Switch off the interaction between the first and second qubits by setting $\Phi_{2x}=\pi/2$, and making a $\pi/2$ rotation about the z axis for the first qubit.

(iii) Make another two-qubit rotation $U_{13}(\tau)$ on the first and third qubits by adjusting the external fluxes such that $\Phi_{1x}=\Phi_{3x}=0$. The two-qubit operation $U_{13}(\tau)$ takes the same form as Eq. (9), but the subscript "2" of the Pauli operators in Eq. (9) is replaced by the subscript "3". This process can be described as

$$\rho_2 \xrightarrow{U_{12}(\tau)} U_{12}(\tau)\,\rho_2\,U_{12}^\dagger(\tau)\xrightarrow{Z_1} Z_1\,U_{12}(\tau)\,\rho_2\,U_{12}^\dagger(\tau)\,Z_1^\dagger \xrightarrow{U_{13}} U_{13}\,Z_1\,U_{12}(\tau)\,\rho_2\,U_{12}^\dagger(\tau)\,Z_1^\dagger\,U_{13}^\dagger. \quad (12)$$

(iv) Finally, make a measurement $(|1\rangle\langle 1|)_1$ on the above rotated state, and obtain the equivalent measurement

$$U_{12}^\dagger(\tau)\,Z_1^\dagger\,U_{13}^\dagger\,(|1\rangle\langle 1|)_1\,U_{13}\,Z_1\,U_{12}=\frac{1}{2}-\frac{1}{4}\sigma_{1z}+ +\frac{1}{4}(\sigma_{1x}\otimes\sigma_{2y}+\sigma_{1y}\otimes\sigma_{3y}-\sigma_{1x}\otimes\sigma_{2z}\otimes\sigma_{3y}), \quad (13)$$

and corresponding measurement result p'' is

$$p''=\frac{1}{2}-\frac{r_{z,0,0}+r_{x,y,0}+r_{y,0,y}-r_{x,z,y}}{4}. \quad (14)$$

Finally, we can obtain the coefficient $r_{x,y,z}$ based on p'' and the single and two qubit measurement results $r_{z,0,0}$, $r_{x,y,0}$ and $r_{y,0,y}$, which can be obtained by using the same way described in sections II and III. Other coefficients corresponding to three-qubit measurements can also be obtained by using a similar procedure. According to the estimated time for reconstructing the two-qubit states, we believe that it is

also possible to reconstruct the three-qubit states using current technology. Any multiple-qubit can also be reconstructed by sequentially designing the single-qubit and two-qubit operations. The generalization to multiple-qubit is an extension of the procedure that we outlined above.

V. QUANTUM PROCESS TOMOGRAPHY

It is worth briefly reviewing that, based on qubit *state* tomography, the noisy channel (usually denoted as the "black box") of the controllable charge qubits can also be determined. This experimental determination of the dynamics of a "black box" is called quantum *process* tomography [30], which can be described as follows: i) many known quantum pure states of the system under investigation are input into the "black box", which is an unknown quantum channel, for example, an arbitrary environment; ii) after a certain time, the output states evolve into unknown states; iii) by using the state tomography, we can ascertain these unknown states; vi) finally, an unknown quantum channel is determined by the data obtained for the tomographic measurements on these states. Experimentally, N^2 pure states need to be prepared in order to determine the noisy channel of the studied qubits, which live in N dimensional space [30].

We have shown that single-qubit *state* tomography is experimentally accessible. In order to perform quantum *process* tomography for a single charge qubit. Four kinds of different charge states $|0\rangle$, $|1\rangle$, $(|0\rangle + |1\rangle)/\sqrt{2}$, and $(|0\rangle + i|1\rangle)/\sqrt{2}$ need to be experimentally prepared. These states can be generated in a SQUID-based charge qubit with current experiments [2, 3, 23]. Thus, the *process* tomography of a single charge qubit is achievable using current technology. With further developments of this technique, the *process* tomography of multiple charge qubits could also be realized when data from multi-qubit state tomography is obtainable.

VI. CONCLUSIONS

In conclusion, we discuss how to reconstruct charge qubit states by using controllable superconducting quantum devices. Detailed operations for reconstructing single- and two-qubit states are presented. Any n-qubit state can also be reconstructed by using $n-1$ two-qubit operations similar to Eq. (9) for different qubit pairs and combining these with required single-qubit operations. Thus the non-local two-qubit operation Eq. (9) plays a key role in the reconstruction of the multiple-qubit states. However, this two-qubit operation is not unique for achieving our purpose. We should note that operations to obtain a fixed coefficient corresponding to multiple-qubit measurements are not unique. The measurements $(|1\rangle\langle 1|)_l$ $(l = 1, 2, \ldots, n)$ on the given state with fixed operations W are different for each qubit l, because W is not symmetric when exchanging l. Our proposal can also be generalized to other superconducting computing circuits with the coupling mediated by photons or a tunable oscillator, e.g., Ref. [29, 31].

We find that the longest operation times to obtain the coefficient of single-qubit and two-qubit states are of the order of 0.01 ns and 0.4 ns, respectively, which is less than the decoherence time [2] $T_2 = 5$ ns. Thus, in principle, the single-qubit and two-qubit states could be reconstructed with current experimental capabilities. We should also note that larger values of the charge energy $E_{\rm ch}$, the Josephson energy $E_{\rm J}^0$, and coupling energy $E_{\rm int}(\Phi_{lx}, \Phi_{kx})$ can make the operation times shorter. Thus these larger values should be realized in order to facilitate the tomographic reconstruction.

Quantum oscillations and conditional gate operations have been demonstrated in two coupled charge qubits with the interactions [3] always turned on. Completely controllable two-qubit charge systems have not been realized yet. Because the unswitchable two-qubit interaction makes single-qubit operations impossible, our proposed scheme cannot be readily used to the experimental reconstruction of multiple-qubit charge states when the two-qubit interactions are always turned on. However, controllable coupled two charge qubits, allowing on and off switching of the interaction between qubits, might be realizable in the future [32]. Then our proposal will become realizable. However, how to reconstruct the superconducting charge qubit states with the two-qubit couplings always turned on will be presented elsewhere by using a different scheme.

VII. DISCUSSIONS

Finally, it should be pointed out that: here we discuss an ideal case without environmental effects on the circuit. In practice, errors are unavoidable due to environmental effects and limited statistical data. In order to reconstruct a reasonable qubit state, the maximum likelihood estimation of density matrices can be employed [33] to minimize experimental errors.

When the tomography is processed, the external flux applied to the SQUID needs to be very quickly changed. For instance, the duration for changing $\Phi_0/2$ within a SQUID loop should at least be less than the decoherence time. Thus a pulse field magnetometer with a rapid sweep rate may be required in this experiment. If the sweep rate [34] of the pulse field magnetometer reaches, e.g. 10^8 Oe/s, then the time to change $\Phi_0/2$ in the loop needs about 0.25 ns for a SQUID area of 20×20 $(\mu\text{m})^2$.

We also notice that the number of rotation for the measured density matrix elements to a preferable direction (e.g. y instead of z) grows exponentially with the number of qubits. How to solve this problem is still an open question.

VIII. ACKNOWLEDGMENTS

We thank X. Hu, J.Q. You, Y.A. Pashkin, O. Astafiev, and J.S. Tsai for their helpful comments and discussions. This work was supported in part by the National Security Agency (NSA) and Advanced Research and Development Activity (ARDA) under Air Force Office of Research (AFOSR) contract number F49620-02-1-0334, and by the National Science

Foundation grant No. EIA-0130383.

[1] J.R. Friedman, V. Patel, W. Chen, S.K. Tolpygo and J.E. Lukens, Nature **406**, 43 (2000); C.H. van der Wal, A.C.J. ter Haar, F.K. Wilhelm, R.N. Schouten, C.J.M. Harmans, T.P. Orlando, S. Lloyd, and J.E. Mooij, Science **290**, 773 (2000); D. Vion, *et al.*, Science **296**, 886 (2002).

[2] Y. Nakamura, Y.A. Pashkin, and J.S. Tsai, Nature **398**, 786 (1999); O. Astafiev, Y.A. Pashkin, T. Yamamoto, Y. Nakamura, and J. S. Tsai, Phys. Rev. B **69**, 180507(R) (2004).

[3] Y.A. Pashkin, T. Yamamoto, O. Astafiev, Y. Nakamura, D.V. Averin, and J.S. Tsai, Nature **421**, 823 (2003); T. Yamamoto, Y.A. Pashkin, O. Astafiev, Y. Nakamura, and J.S. Tsai, Nature **425**, 941 (2003).

[4] J.E. Mooij, T.P. Orlando, L. Levitov, L. Tian, C.H. van der Wal, S. Lloyd, Science **285**, 1036 (1999); I. Chiorescu, Y. Nakamura, C.J.P.M. Harmans, and J.E. Mooij, Science **299**, 1869 (2003).

[5] S. Han, Y. Yu, X. Chu, S. Chu, and Z. Wang, Science **293**, 1457 (2001); Y. Yu, S. Han, X. Chu, S. Chu, and Z. Wang, *ibid.* **296**, 889 (2002).

[6] Y. Makhlin, G. Schön, and A. Shnirman, Nature **398**, 305 (1999).

[7] L. B. Ioffe, V.B. Geshkenbein, M.V. Feigel'man, A.L. Fauchère, and G. Blatter, Nature **398**, 679 (1999)

[8] W. Band and J.L. Park, Am. J. Phys. **47**, 188 (1979); Found. Phys. **1**, 133 (1970); 339 (1971); G.M. D'Ariano, Phys. Lett. A **268**, 151 (2000); G.M. D'Ariano, L. Maccone and M.G.A. Paris, *ibid.* **276**, 25 (2000).

[9] U. Leonhardt, Phys. Rev. Lett. **74**, 4101 (1995); S. Weigert, *ibid.* **84**, 802 (2000); M. Beck, *ibid.* **84**, 5748 (2000); G. Klose, G. Smith, and P.S. Jessen, *ibid.* **86**, 4721 (2001); O. Steuernagel and J.A. Vaccaro, *ibid.* **75**, 3201 (1995); G. M. D'Ariano and P. Lo Presti, *ibid.* **86**, 4195 (2001); U. Leonhardt, Phys. Rev. A **53**, 2998 (1996); D.F.V. James, P.G. Kwait, W.J. Munro, and A.G. White, *ibid.* **64**; 052312 (2001).

[10] G.L. Long, H.Y. Yan, and Y. Sun, J. Opt. B **3** 376 (2001); L. Xiao and G.L. Long, Phys. Rev. A **66**, 052320 (2002); R. Das, T.S. Mahesh, and A. Kumar, Phys. Rev. A **67**, 062304 (2003); Chem. Phys. Lett. **369**, 8 (2003); J.S. Lee, Phys. Lett. A **305**, 349 (2002).

[11] G. M. D'Ariano, M.G.A. Paris, and M. F. Sacchi, Adv. in Imaging and Electron Phys. **128**, 205 (2003).

[12] T.J. Dunn, I.A. Walmsley, and S. Mukamel, Phys. Rev. Lett. **74**, 884 (1995).

[13] D. Leibfried, D.M. Meekhof, B.E. King, C. Monroe, W.M. Itano, and D.J. Wineland, Phys. Rev. Lett. **77**, 4281 (1996)

[14] C. Kurtsiefer, T. Pfau, and J. Mlynek, Nature **386**, 150 (1997).

[15] D.F.V. James, P.H. Eberhard, and P.G. Kwiat, Phys. Rev. Lett. **83**, 3103 (1999); T. Yamamoto, M. Koashi, S.K. Özdemir, and N. Imoto, Nature **421**, 343 (2003).

[16] D.T. Smithey, M. Beck, M.G. Raymer, and A. Faridani, Phys. Rev. Leet. **70**, 1244 (1993); A.I. Lvovsky, H. Hansen, T. Aichele, O. Benson, J. Mlynek, and S. Schiller, Phys. Rev. Lett. **87**, 050402 (2001); S.A. Babichev, J. Appel, and A.I. Lvovsky, Phys. Rev. Lett. **92**, 193601 (2004).

[17] I.L. Chuang, N. Gershenfeld, M.G. Kubinec, D.W. Leung, Proc. R. Soc. Lond. A **454**, 447 (1998); I.L. Chuang, N. Gershenfeld, and M. Kubinec, Phys. Rev. Lett. **80**, 3408 (1998).

[18] C. Miquel, J.P. Paz, M. Saraceno, E. Knill, R. Laflamme, and C. Negrevergne, Nature **418**, 59 (2002).

[19] Y. Sharf, D.G. Cory, S.S. Somaroo, T.F. Havel, E. Knill, R. Laflamme, and W.H. Zurek, Molecular Phys. **98**, 1347 (2000); T.F. Havel, D.G. Cory, S. Lloyd, N. Boulant, E.M. Fortunato, M.A. Pravia, G. Teklemariam, Y.S. Weinstein, A. Bhattacharyya, and J. Hou, Am. J. Phys. **70**, 345 (2002); G. Teklemariam, E.M. Fortunato, M.A. Pravia, T.F. Havel, and D.G. Cory, Phys. Rev. Lett. **86**, 5845 (2001).

[20] Yu-xi Liu, L.F. Wei, and F. Nori, quant-ph/0402179.

[21] M.A. Nielsen and I.L. Chuang, *Quantum computation and quatum information* (Cambridge University press, Cambridge, 2000).

[22] Y. Makhlin, G. Schön, A. Shnirman, Rev. Mod. Phys. **73**, 357 (2001).

[23] K.W. Lehnert, K. Bladh, L.F. Spietz, G. Gunnarsson, D.I. Schuster, P. Delsing, and R.J. Schoelkopf, Phys. Rev. Lett. **90**, 027002 (2003).

[24] If we make a measurement $\sigma_{1i} \otimes \sigma_{2j}$ on multi-qubit state ρ, then the measurement probability $p = \mathrm{Tr}(\rho\sigma_{1i} \otimes \sigma_{2j}) = \frac{1}{4}\sum_{i',j'=0}^{3} r_{i',j'}\mathrm{Tr}(\sigma_{1i'}\sigma_{1i})\mathrm{Tr}(\sigma_{2j'}\sigma_{2j}) = r_{i,j}\delta_{ii'}\delta_{jj'}$.

[25] D.P. DiVincenzo, Phys. Rev. A **51**, 1015 (1995).

[26] D.A. Lidar, D. Bacon, J. Kempe, and K.B. Whaley, Phys. Rev. A **63**, 022307 (2001); D.A. Lidar and L.-A. Wu, Phys. Rev. Lett. **88**, 017905 (2002).

[27] S. Oh, Phys. Rev. B **65**, 144526 (2002).

[28] J.Q. You, J.S. Tsai, and F. Nori, Phys. Rev. Lett. **89**, 197902 (2002). A longer version of this is available in cond-mat/0306203; see also *New Directions in Mesoscopic Physics*, edited by R. Fazio, V.F. Gantmakher, and Y. Imry (Kluwer Academic Publishers, 2003), page 351.

[29] J.Q. You, J.S. Tsai, and F. Nori, Phys. Rev. B 68, 024510 (2003); Physica E 18, 35 (2003).

[30] I. L. Chuang and M. A. Nielsen, J. Mod. Opt. **44**, 2455 (1997).

[31] L.F. Wei, Yu-xi Liu, and F. Nori, cond-mat/0402678.

[32] D.V. Averin and C. Bruder, Phys. Rev. Lett. **91**, 057003 (2003).

[33] Z. Hradil, Phys. Rev. A **55**, R1561 (1999); M. F. Sacchi, *et al.*, *ibid.* **63**, 054104 (2001); D. F. James, *et al.*, *ibid.* **64**, 052312 (2001).

[34] H. Uwazumi, T. Shimatsu, and Y. Kuboki, J. of Appl. Phys. **91**, 7095 (2002).

Coupling Josephson qubits via a current-biased information bus

L.F. Wei,[1,2] Yu-xi Liu,[1] and Franco Nori[1,3]

[1] *Frontier Research System, The Institute of Physical and Chemical Research (RIKEN), Wako-shi, Saitama, 351-0198, Japan*
[2] *Institute of Quantum Optics and Quantum Information, Department of Physics, Shanghai Jiaotong University, Shanghai 200030, P.R. China*
[3] *Center for Theoretical Physics, Physics Department, CSCS, The University of Michigan, Ann Arbor, Michigan 48109-1120*

(Dated: August 3, 2004)

Josephson qubits without direct interaction can be effectively coupled by sequentially connecting them to an information bus: a current-biased large Josephson junction treated as an oscillator with adjustable frequency. The coupling between any qubit and the bus can be controlled by modulating the magnetic flux applied to that qubit. This tunable and selective coupling provides two-qubit entangled states for implementing elementary quantum logic operations, and for experimentally testing Bell's inequality.

PACS. 74.50.+r - Proximity effects, weak links, tunneling phenomena, and Josephson effects.
PACS. 03.67.Lx - Quantum computation.
PACS. 03.65.Ud - Entanglement and quantum nonlocality (e.g. EPR paradox, Bell's inequalities, GHZ states, etc.).

Superconducting circuits with Josephson junctions offer one of the most promising candidates for realizing quantum computation [1, 2, 3, 4, 5, 6, 7, 8, 9, 10, 11, 12, 13, 14, 15, 16]. These superconducting qubits can be either charge- [2], flux- [3], mixed- [4], current-biased Josephson-junction (CBJJ) qubits [5, 6], and others. Much attention is now devoted to realizing controlled couplings between superconducting qubits and implementing quantum logic operations (see, e.g., [7, 8, 9, 10, 11]). Two qubits, i and j, can be connected by a common inductor or capacitor, with Ising-type couplings $\sigma_\alpha^{(i)} \otimes \sigma_\alpha^{(j)}$ ($\alpha = x, y, \text{or } z$). However, in general, (1) the capacitive coupling [8, 12] between qubits is not tunable (and thus adjusting the physical parameters for realizing two-qubit operation is not easy), and (2) a large inductance is required in [7] to achieve a reasonably high interaction strength and speed for two-qubit operations [10]. Alternatively, other schemes (see, e.g., [11, 13, 14]) use sequential interactions of individual qubits with an information bus. These provide some advantages: allow faster two-qubit operations, may possess longer decoherence times, and are scalable. These schemes are similar to the techniques used for trapped ions [17], where the ions are entangled by exciting and de-exciting quanta (data bus) of their shared collective vibrational modes.

Compared to the externally-connected LC-resonator used in Ref. [13] and the cavity QED mode proposed in Ref. [14], a large (e.g., 10 μm) CBJJ [6, 15] is more suitable as an information bus, because its eigenfrequency can be controlled by adjusting the applied bias current. In fact, such data bus to couple distant qubits has been proposed in [11]. However, there all non-resonant interactions between the qubits and the bus were ignored. This is problematic because these near-resonance interactions must be considered, otherwise, the desired coupling/decoupling between the chosen qubit and the bus cannot be implemented because a perfect resonance condition is not always achievable. Also, modulating the bias current to selectively couple different qubits changes the physical characteristics (e.g., eigenfrequency) of the bus, and thus may yield additional errors during the communication between qubits. Finally, an effective method still lacks for refocusing the dynamical-phase shifts of the qubits to realize the desired quantum operations.

Here, we propose an effective scheme for coupling any pair of superconducting qubits without direct interaction between them by letting these be sequentially connected to a large CBJJ that acts as a data bus. The qubit in Ref. [12] is a CBJJ, while here we consider charge qubits. Here, a large CBJJ acts only as the information bus between the qubits. Also, in contrast to Ref. [11], in the present circuit any chosen qubit can be coupled to and decouple from the bus by switching on and off its Josephson energy. The bias current applied to the bus is fixed during the operations, and the dynamical-phase shifts of the qubits can be conveniently refocused by properly setting the free-evolution times of the bus. Therefore, an entanglement between distant qubits can be created in a controllable way for realizing quantum computation, and also for testing Bell's inequality. Its experimental realizability is also briefly discussed.

Model.— Without loss of generality, we consider the simplest network sketched in Fig. 1. It can be easily modified to include arbitrary qubits. Each qubit consists of a gate electrode of capacitance C_g and a single-Cooper-pair box with two ultrasmall identical Josephson junctions of capacitance c_J and Josephson energy ε_J, forming a superconducting quantum interference device (SQUID) ring threaded by a flux Φ and with a gate voltage V. The superconducting phase difference across the kth qubit is represented by ϕ_k, $k = 1, 2$. The large CBJJ has capacitance C_b, phase drop ϕ_b, Josephson energy E_b, and a bias current I_b. The qubit is assumed to work in the charge regime with $k_B T \ll E_J \ll E_C \ll \Lambda$, wherein quasi-particle tunnelling or excitations are effec-

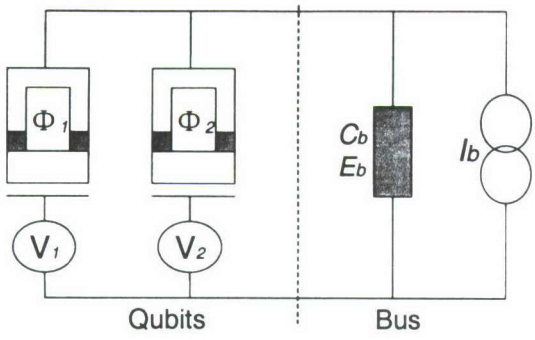

FIG. 1: A pair of SQUID-based charge qubits, located on the left of the dashed line, coupled to a large CBJJ on the right, which acts as an information bus. The circuit is divided into two parts, the qubits and the bus. The dashed line only indicates a separation between these. The controllable gate voltage V_k ($k = 1, 2$) and external flux Φ_k are used to manipulate the qubits and their interactions with the bus. The bus current remains fixed during the operations.

tively suppressed. Here, k_B, T, Λ, E_C, and E_J are the Boltzmann constant, temperature, superconducting gap, charging and Josephson coupling energies of the qubit, respectively. The present mechanism of quantum manipulation is significantly different from Refs. [7, 10, 11], although the circuits appear to be similar. The Hamiltonian for the circuit in Fig. 1 is

$$\hat{H} = \sum_{k=1}^{2}\left\{\frac{4e^2}{2C_k}\left[\hat{n}_k - n_g^{(k)}\right]^2 - E_J^{(k)}\cos\left[\hat{\phi}_k - \frac{C_g^{(k)}}{C_k}\hat{\phi}_b\right]\right\} + \frac{\hat{Q}_b^2}{2\tilde{C}_b} - E_b\cos\hat{\phi}_b - \frac{\Phi_0 I_b}{2\pi}\hat{\phi}_b, \quad (1)$$

with $[\hat{\phi}_k, \hat{n}_k] = i$. Here, $\hat{Q}_b = 2\pi\hat{p}_b/\Phi_0$ is the operator of charges on the CBJJ and $[\hat{\phi}_b, \hat{p}_b] = i\hbar$. $C_J^{(k)} = 2c_J^{(k)}$, $E_J^{(k)} = 2\varepsilon_J^{(k)}\cos(\pi\Phi_k/\Phi_0), C_k = C_g^{(k)} + C_J^{(k)}$, $n_g^{(k)} = C_g^{(k)}V_k/(2e)$, and $\tilde{C}_b = C_b + \sum_{k=1}^{2} C_J^{(k)}C_g^{(k)}/C_k$. $\Phi_0 = h/(2e)$ and n_k are the flux quantum and the excess number of Cooper pairs in the superconducting box of the kth qubit, respectively. When the applied gate voltage V_k is set near the degeneracy points ($n_g^{(k)} = (l+1/2)$, $l = 0, 1, 2, ...$), then only the two lowest-energy charge states, $|n_k = 0\rangle = |\uparrow_k\rangle$ and $|n_k = 1\rangle = |\downarrow_k\rangle$, play a role. The large CBJJ works in the phase regime and describes the motion of a "particle" with mass $m = \tilde{C}_b(\Phi_0/2\pi)^2$ in a potential $U(\phi_b) = -E_b(\cos\phi_b + I_b\phi_b/I_c)$ with $I_c = 2\pi E_b/\Phi_0$. For $I_b < I_c$, there exist a series of minima of $U(\phi_b)$. Near these points, $U(\phi_b)$ approximates a harmonic oscillator potential with characteristic frequency $\omega_b = \sqrt{8E_C^{(b)}E_b/\hbar^2}\left[1 - (I_b/I_c)^2\right]^{1/4}$, $E_C^{(b)} = e^2/(2\tilde{C}_b)$. The approximate number of metastable quantum bound states [15] is $N_s = 2^{3/4}\sqrt{E_b/E_C^{(b)}}(1 - I_b/I_c)^{5/4}$. For a low bias current, the dynamics of the CBJJ can be safely restricted [6] to the Hilbert space spanned by the two lowest states of this data bus: $|0_b\rangle$ and $|1_b\rangle$.

The eigenenergy $\hbar\omega_{LC}$ of the bus used in [7] is much higher than that of the qubits. Therefore, adiabatically eliminating such a bus yields a direct interbit coupling. However, the energy scale of our proposed data bus (i.e., the CBJJ oscillator) is $\omega_b/2\pi \sim 10$ GHz [6], which is of the same order of the Josephson energy (e.g., $E_J/h \sim 13$ GHz [2]). Therefore, the quanta in the present bus can be excited or de-excited when the qubit is operated. The Hamiltonian (1) clearly shows that the coupling between the chosen kth qubit and the bus can be turned on and off [18], when the threaded flux Φ_k differs from or equals to $(l' + 1/2)\Phi_0$, $l' = 0, 1, 2, ...$ For simplicity, hereafter we let $l, l' = 0$. Two qubits can be indirectly coupled by independently interacting with the bus sequentially when exciting/de-exciting the vibrational quanta of the bus. Under the usual rotating-wave approximation, the dynamics for such a coupling mechanism can be described by the following effective Hamiltonian

$$\hat{H}_{kb} = \hat{H}_k + \hat{H}_b + i\lambda_k\left[\hat{\sigma}_+^{(k)}\hat{a} - \hat{\sigma}_-^{(k)}\hat{a}^\dagger\right], \quad (2)$$

$$\hat{H}_k = \frac{E_J^{(k)}}{2}\hat{\sigma}_z^{(k)} - \frac{\delta E_C^{(k)}}{2}\hat{\sigma}_x^{(k)}, \quad \hat{H}_b = \hbar\omega_b\left(\hat{n} + \frac{1}{2}\right),$$

with $\hat{a} = \left[\sqrt{\tilde{C}_b\omega_b/\hbar}\left(\frac{\Phi_0}{2\pi}\right)\hat{\phi}_b + i\left(\frac{2\pi}{\Phi_0}\right)\hat{p}_b/\sqrt{\hbar\omega_b\tilde{C}_b}\right]/\sqrt{2}$ and $\hat{n} = \hat{a}^\dagger\hat{a}$ being the Boson operators of the bus. Here, $\delta E_C^{(k)} = 2e^2(1 - 2n_g^{(k)})/C_k$, $\lambda_k = \zeta_k\cos(\pi\Phi_k/\Phi_0)$, $\zeta_k = \varepsilon_J^{(k)}C_g^{(k)}\pi\sqrt{2\hbar}/(C_k\Phi_0\sqrt{\tilde{C}_b\omega_b})$. The pseudospin operators: $\hat{\sigma}_z^{(k)} = |1_k\rangle\langle 1_k| - |0_k\rangle\langle 0_k|$, $\hat{\sigma}_+^{(k)} = |1_k\rangle\langle 0_k|$, and $\hat{\sigma}_-^{(k)} = |0_k\rangle\langle 1_k|$ are defined in the subspace spanned by the logic states: $|0_k\rangle = (|\downarrow_k\rangle + |\uparrow_k\rangle)/\sqrt{2}$ and $|1_k\rangle = (|\downarrow_k\rangle - |\uparrow_k\rangle)/\sqrt{2}$. Only the single-quantum transition process, approximated to first-order in $\hat{\phi}_b$, is considered during the expansion of the cosine-term of the Hamiltonian (1), as the fluctuation of ϕ_b is very weak. In fact, $C_g^{(k)}\sqrt{\langle\phi_b^2\rangle}/C_k \lesssim 10^{-2} \ll 1$, for typical experimental parameters [2, 6, 8]: $C_b \sim 6\,\mathrm{pF}, \omega_b/2\pi \sim 10$ GHz, and $C_g^{(k)}/C_J^{(k)} \sim 10^{-2}$. Once the bias current I_b is properly set up beforehand, various dynamical evolutions can be induced by selecting the applied flux Φ_k and the gate voltage V_k. Considering two extreme cases, the strongest coupling ($\Phi_k = 0$) and the decoupling ($\Phi_k = \Phi_0/2$), several typical realizable evolutions deduced from the Hamiltonian (2) are given in table I. There, $\hbar\Delta_k = \varepsilon_k - \hbar\omega_b$, $\varepsilon_k = \sqrt{[2\varepsilon_J^{(k)}]^2 + [\delta E_C^{(k)}]^2}$.

Quantum gates.— The physical characteristic (e.g., the eigenfrequency) of the bus in the present circuit does not need to be changed, once it is set up beforehand. It still undergoes a free evolution $\hat{U}_0(t)$ ruled by a non-zero $\hat{H}_b$ during the operational delay, i.e., the time interval when the qubits do not evolve because their Hamiltonians are temporarily set to zero (when $\Phi_k = \Phi_0/2$, $V_k = e/C_g^{(k)}$).

Controllable Parameters	Evolutions
$V_k = e/C_g^{(k)}$, $\Phi_k = \Phi_0/2$	$\hat{U}_0(t)$
$V_k \neq e/C_g^{(k)}$, $\Phi_k = \Phi_0/2$	$\hat{U}_1^{(k)}(t)$
$V_k = e/C_g^{(k)}$, $\Phi_k = 0$, $\hbar\omega_b = 2\varepsilon_J^{(k)}$	$\hat{U}_2^{(k)}(t)$
$V_k \neq e/C_g^{(k)}$, $\Phi_k = 0$, $2\zeta_k\sqrt{n+1} \ll \hbar\Delta_k$	$\hat{U}_3^{(k)}(t)$

TABLE I: Typical settings of the controllable experimental parameters (V_k and Φ_k) and the corresponding time evolutions $\hat{U}_j(t)$ of the qubit-bus system. Here, $C_g^{(k)}$ and $2\varepsilon_J^{(k)}$ are the gate capacitance and the maximal Josephson energy of the kth SQUID-based charge qubit. ζ_k is the maximum strength of the coupling between the kth qubit with energy ε_k and the bus of frequency ω_b. The detuning between the qubit and the bus energies is $\hbar\Delta_k = \varepsilon_k - \hbar\omega_b$. $n = 0, 1$ is occupation number for the number state $|n\rangle$ of the bus. The various time-evolution operators are: $\hat{U}_0(t) = \exp(-it\hat{H}_b/\hbar), \hat{U}_1^{(k)}(t) = \exp[-it\delta E_C^{(k)}\hat{\sigma}_x^{(k)}/(2\hbar)] \otimes \hat{U}_0(t), \hat{U}_2^{(k)} = \hat{A}(t)\cos\hat{\lambda}_n|0_k\rangle\langle 0_k| - (\sin\hat{\lambda}_n)\hat{a}/\sqrt{\hat{n}+1}|0_k\rangle\langle 1_k| + \hat{a}^\dagger \sin\hat{\xi}_n/\sqrt{\hat{n}}|1_k\rangle\langle 0_k| + \cos\hat{\xi}_n|0_k\rangle\langle 0_k|$, and $\hat{U}_3^{(k)}(t) = \hat{A}(t)\exp\{-it\zeta_k^2[|1_k\rangle\langle 1_k|(\hat{n}+1) - |0_k\rangle\langle 0_k|\hat{n}]/(\hbar\Delta_k)\}$, with $\hat{A}(t) = \exp[-it(2\hat{H}_b + E_J^{(k)}\hat{\sigma}_z^{(k)})/(2\hbar)]$, $\hat{\lambda}_n = 2\zeta_k t\sqrt{\hat{n}+1}/\hbar$, and $\hat{\xi}_n = 2\zeta_k t\sqrt{\hat{n}}/\hbar$.

Before and after the desired operations, the bus should remain in its ground state $|0_b\rangle$. In principle, the time-evolutions listed in table I are sufficient to implement any desired operation for manipulating the quantum information stored in the present circuit. In fact, any single-qubit rotation, including the typical Hadamard gate: $\hat{H}_g^{(k)} = [\hat{\sigma}_z^{(k)} + \hat{\sigma}_+^{(k)} + \hat{\sigma}_-^{(k)}]/\sqrt{2}$, on the kth qubit can be easily realized by selectively using $\hat{U}_1^{(k)}(t)$ and $\hat{U}_3^{(k)}(t)$. Any single-qubit operation is not influenced by the free evolution of the bus during the time delay between successive operations.

In order to realize two-qubit gates, we must be able to couple distant qubits via their sequential interactions to the bus. We set the bias current I_b such that $\hbar\omega_b = 2\varepsilon_J^{(1)}$ and then perform a three-step process. First, we couple the first (control) qubit to the bus by switching off its applied flux Φ_1 and produce the evolution $\hat{U}_2^{(1)}(t_1)$. After a duration t_1 determined by $\sin(2\zeta_1 t_1/\hbar) = -1$, the control qubit is decoupled from the bus. This process implements the evolutions: $|0_b\rangle|0_1\rangle \to |0_b\rangle|0_1\rangle$ and $|0_b\rangle|1_1\rangle \to e^{-i\omega_b t_1}|1_b\rangle|0_1\rangle$. Next, we let the second (target) qubit work at a non-degenerate point ($V_2 \neq e/C_g^{(2)}$) and couple it to the bus by switching off its applied flux Φ_2. After a duration t_2 determined by

$$\sin\left(\frac{\zeta_2^2 t_2}{\hbar^2\Delta_2}\right) = \cos\left(\frac{\varepsilon_2 t_2}{2\hbar} + \frac{\zeta_2^2 t_2}{2\hbar^2\Delta_2}\right) = 1, \qquad (3)$$

the target qubit is backed to its degenerate point ($V_2 = e/C_g^{(2)}$) and decoupled from the bus. This sequence of operations generate the evolutions:

$$\begin{cases} |0_b\rangle|0_2\rangle \to e^{-i\xi}|0_b\rangle|0_2\rangle, \ |0_b\rangle|1_2\rangle \to e^{-i\xi}|0_b\rangle|1_2\rangle, \\ |1_b\rangle|0_2\rangle \to i\,e^{-i(\xi+\omega_b t_g)}(\cos\eta_2|1_b\rangle|0_2\rangle + \sin\eta_2|1_b\rangle|1_2\rangle), \\ |1_b\rangle|1_2\rangle \to i\,e^{-i(\xi+\omega_b t_g)}(\sin\eta_2|1_b\rangle|0_2\rangle - \cos\eta_2|1_b\rangle|1_2\rangle), \end{cases}$$

with $\xi = \omega_b(\tau_1 + t_2 + \tau_2)/2 + \zeta_i^2 t_2/(2\hbar^2\Delta_2)$, and $t_g = \sum_{s=1}^{3} t_s + \sum_{s=1}^{2}\tau_s$. Finally, we couple again the control qubit to the bus and perform the evolution $\hat{U}_2^{(1)}(t_3)$ with $\sin(2\zeta_1 t_3/\hbar) = 1$, yielding evolutions: $|0_b\rangle|0_1\rangle \to |0_b\rangle|0_1\rangle$ and $|1_b\rangle|0_1\rangle \to e^{-i\omega_b t_3}|0_b\rangle|1_1\rangle$. In practice, the free evolutions $\hat{U}_0(\tau_1)$ and $\hat{U}_0(\tau_2)$ exist during the time delays between the first (second) and second (third) pulses. If the delays are further set accurately such that the total duration t_g satisfies the condition $\sin\omega_b t_g = 1$, then the above three-step process with two delays yields a quantum operation $\hat{U}(t_g) = \hat{U}_2^{(1)}(t_3)\hat{U}_0(\tau_2)\hat{U}_3^{(2)}(t_2)\hat{U}_0(\tau_1)\hat{U}_2^{(1)}(t_1) = \exp(-i\xi)|0_b\rangle\langle 0_b| \otimes \hat{U}_d^{(12)}(\beta_2)$, with

$$\hat{U}_d^{(12)}(\beta_2) = \begin{pmatrix} 1 & 0 & 0 & 0 \\ 0 & 1 & 0 & 0 \\ 0 & 0 & \cos\beta_2 & \sin\beta_2 \\ 0 & 0 & \sin\beta_2 & -\cos\beta_2 \end{pmatrix} \qquad (4)$$

being a universal two-qubit gate. Here, $\cos\beta_2 = 2\varepsilon_J^{(2)}/\varepsilon_2$. This gate can produce entanglement between qubits and also realize any quantum computation, accompanied by single-qubit rotations.

Testing Bell's inequality.— Entanglement is a key ingredient for computational speedup in quantum computation. Historically, Bell's inequalities were seen as an entanglement test: its violation implies that entanglement must exist. For a two-qubit entangled state $|\psi_e\rangle$, the Clauser, Horne, Shimony and Holt (CHSH) form of Bell's inequality : $f(|\psi_e\rangle) \leq 2$ is usually tested by experimentally measuring the CHSH function $f(|\psi_e\rangle) = |E(\theta_1,\theta_2) + E(\theta_1',\theta_2) + E(\theta_1,\theta_2') - E(\theta_1',\theta_2')|$. Here, θ_k are controllable classical variables and $E(\theta_1,\theta_2)$ is the correlation for the outcomes of separately projected measurements of two qubits. A number of experimental tests [20] of Bell's inequality have already been performed by using entangled photons and atoms. We now show that a desired entangled state can be created in a repeatable way and thus Bell's inequality can also be tested experimentally by using this circuit.

We begin with an initial state $|\psi_0\rangle = |0_b\rangle|\downarrow_1\rangle|\downarrow_2\rangle = |0_b\rangle \otimes (|0_1\rangle + |1_1\rangle) \otimes (|0_2 + |1_2\rangle)/2$ with two qubits decoupled from the bus but working at their non-degenerate points (i.e., $V_k \neq e/C_g^{(k)}$). After applying a Hadamard gate $\hat{H}_g^{(2)}$ to the second qubit, the system evolves to the state $|\psi_1\rangle = |0_b\rangle \otimes (|0_1\rangle + |1_1\rangle) \otimes |1_2\rangle/\sqrt{2}$. The desired two-qubit entangled state is then generated as

$$|\psi_d^{(12)}(\theta_1,\theta_2,\beta_2)\rangle = \hat{U}_1^{(1)}(\theta_1)\hat{U}_1^{(2)}(\theta_2)\hat{U}_d^{(12)}(\beta_2)|\psi_1\rangle, \quad (5)$$

with $\hat{U}_1^{(k)}(\theta_k) = \exp\left[i\theta_k\hat{\sigma}_x^{(k)}/2\right]$, $\theta_k = \delta E_C^{(k)} t_k/\hbar$. The corresponding correlation function is $E(\theta_1,\theta_2,\beta_2) =$

$\langle\psi_d^{(12)}(\theta_1,\theta_2,\beta_2)|\hat{\sigma}_z^{(1)} \otimes \hat{\sigma}_z^{(2)}|\psi_d^{(12)}(\theta_1,\theta_2,\beta_2)\rangle = \sin\beta_2(\sin\theta_1\sin\theta_2 - \sin\beta_2\cos\theta_1\cos\theta_2)$. For certain chosen sets of angles: $\theta_k = \{-\pi/8, 3\pi/8\}$, the CHSH function becomes

$$f(|\psi_d^{(12)}(\beta_2)\rangle) = \sqrt{2}\,|\sin\beta_2(\sin\beta_2 + 1)|. \quad (6)$$

It is easy to numerically check that Bell's inequality, $f(|\psi_d^{(12)}(\beta_2)\rangle) \leq 2$, is violated when $E_J^{(2)}/\delta E_C^{(2)} < 0.776$, which can be easily satisfied for this charge-qubit system.

Experimentally, the above procedure can be repeated many times at each of the four sets of angles and thus the correlation function $E(\theta_1,\theta_2,\beta_2) = [N_{\rm same}(\theta_1,\theta_2) - N_{\rm diff}(\theta_1,\theta_2)]/N_{\rm tot}$, with $N_{\rm same}(\theta_1,\theta_2)$ ($N_{\rm diff}(\theta_1,\theta_2)$) being the number of events with two qubits being found in the same (different) logic states and $N_{\rm tot} = N_{\rm same}(\theta_1,\theta_2) + N_{\rm diff}(\theta_1,\theta_2)$ being the total experimental times for the same θ_1 and θ_2. Finally, Bell's inequality can be tested by calculating the experimental CHSH function: $f(|\psi_d^{(12)}(\beta_2)\rangle) = |E(\theta_1,\theta_2,\beta_2) + E(\theta_1',\theta_2,\beta_2) + E(\theta_1,\theta_2',\beta_2) - E(\theta_1',\theta_2',\beta_2)|$.

Discussion.— Two types of noise, fluctuations of the applied gate voltage V_k and bias current I_b, must be considered in the present qubit-bus system. For simplicity, these two environmental noises are treated as two separate Boson baths with Ohmic spectral densities and assumed to be weakly coupled to the qubit and CBJJ, respectively. The Hamiltonian of the kth qubit coupling to the bus, containing these fluctuations, can be written as

$$\hat{H} = \hat{H}_{kb} + \sum_{j=1,2}\sum_{\omega_j}\hbar\omega_j\hat{a}_{\omega_j}^\dagger\hat{a}_{\omega_j} - \frac{eC_g^{(k)}}{C_k}\hat{\sigma}_z^{(k)}(\hat{R}_1 + \hat{R}_1^\dagger) - \sqrt{\frac{\hbar}{2\tilde{C}_b\omega_b}}\left(\hat{a}^\dagger\hat{R}_2 + \hat{a}\hat{R}_2^\dagger\right),\ \hat{R}_j = \sum_{\omega_j} g_{\omega_j}\hat{a}_{\omega_j}. \quad (7)$$

Here, $\hat{a}_{\omega_j}$ is the Boson operator of the jth bath and g_{ω_j} its coupling strength. The relaxation and decoherence rates of our qubit-bus system can also be calculated by using the well established Bloch-Redfield formalism [16]. Under the usual secular approximation, the relaxation and decoherence rates are characterized [21] by two dimensionless coupling parameters, $\alpha_V = (C_g^{(k)}/C_k)^2 R_V/R_K$ and $\alpha_I = {\rm Re}(Y_I)/(\tilde{C}_b\omega_b)$, which describe the couplings of the voltage fluctuations to the qubit and the bias-current fluctuations to the bus, respectively. Here, $R_K = h/e^2 \approx 25.8$ kΩ is the quantum of resistance, R_V is the Ohmic resistor of the voltage, and ${\rm Re}(Y_I)$ is the dissipative part of the admittance of the current bias. If the qubit decouples from the bus, α_V (α_I) characterizes the decoherence and relaxation of the qubit (bus). It has been estimated in Ref. [1] that the dissipation for a single SQUID-based charge qubit is sufficiently weak ($\alpha_V \approx 10^{-6}$), which allows, in principle, for 10^6 coherent single-qubit manipulations. However, for a single CBJJ the dimensionless parameter α_I only reaches 10^{-3} for typical experimental parameters [6]: $1/{\rm Re}(Y_I) \sim 100\ \Omega$, $C_b \sim 6$ pF, $\omega_b/2\pi \sim 10$ GHz. This implies that the quantum coherence of the present qubit-bus system is mainly limited by the bias-current fluctuations. Fortunately, the impedance of the above CBJJ can be engineered to be $1/{\rm Re}(Y_I) \sim 560$ kΩ [6]. This lets α_I reach up to 10^{-5} and allow about 10^5 coherent manipulations of the qubit-bus system.

In summary, we have proposed a scheme for coupling two SQUID-based charge qubits by sequentially using their interactions with a common large Josephson junction biased by a fixed current. Each interaction is tunable by controlling the external flux applied to the chosen SQUID-based charge qubit. The proposed circuit allows the possibility of implementing elementary quantum logic operations, including arbitrary single-qubit gates and universal two-qubit gates. The created two-qubit entangled states can be used to test Bell's inequality.

Acknowledgments

We acknowledge useful discussions with Drs. J.Q. You, J.S. Tsai, and X. Hu, and the support of the US NSA and ARDA under AFOSR contract No. F49620-02-1-0334, and the NSF grant No. EIA-0130383.

[1] Y. Makhlin, G. Schön and A. Shnirman, Rev. Mod. Phys. **73**, 357 (2001).
[2] Y. Nakamura, Yu.A. Pashkin, and J.S. Tsai, Nature **398**, 786 (1999); K.W. Lehner *et al.*, Phys. Rev. Lett. **90**, 027002 (2003).
[3] J.E. Mooij *et al.*, Science **285**, 1036 (1999); **290**, 773 (2000); E. Il'ichev *et. al.*, Phys. Rev. Lett. **91**, 097906 (2003).
[4] D. Vion *et al.*, Science **296**, 886 (2002).
[5] Y. Yu *et al.*, Science **296**, 889 (2002).
[6] J.M. Martinis *et al.*, Phys. Rev. Lett. **89**, 117901 (2002).
[7] Y. Makhlin, G. Schön and A. Shnirman, Nature **398**, 305 (1999).
[8] Yu.A. Pashkin *et al.*, Nature **421**, 823 (2003); T. Yamamoto *et al.*, Nature **425**, 941 (2003).
[9] D.V. Averin and C. Bruder, Phys. Rev. Lett. **91**, 057003 (2003).
[10] J.Q. You, J.S. Tsai, and F. Nori, Phys. Rev. Lett. **89**, 197902 (2002); Phys. Rev. B **68**, 024510 (2003).
[11] A. Blais, A.M. van den Brink, and A.M. Zagoskin, Phys. Rev. Lett. **90**, 127901 (2003).
[12] A.J. Berkley *et al.*, Science **300**, 1548 (2003); F.W. Strauch *et al.*, Phys. Rev. Lett. **91**, 167005 (2003).
[13] F. Plastina and G. Falci, Phys. Rev. B **67**, 224514 (2003).
[14] S.L. Zhu, Z.D. Wang, and K. Yang, Phys. Rev. A **68**, 034303 (2003); C.-P. Yang and S.-I Chu, *ibid.* **67**, 042311

(2003); J.Q. You and F. Nori, Phys. Rev. B **68**, 064509 (2003).

[15] J. Clarke *et al.*, Science **239**, 992 (1988); J.M. Martinis, M.H. Devoret, and J. Clarke, Phys. Rev. B **35**, 4682(1987).

[16] M. Storcz and F.K. Wilhelm, Phys. Rev. A **67**, 042319 (2003); E. Paladino *et al.*, Phys. Rev. Lett. **88**, 228304 (2002); U. Weiss, *Quantum Dissipative systems*, 2nd ed. (World Scientific, Singapore, 1999).

[17] J.I. Cirac and P. Zoller, Phys. Rev. Lett. **74**, 4091 (1995); L.F. Wei, S.Y. Liu, and X.L. Lei, Phys. Rev. A **65**, 062316 (2002); Opt. Comm. **208**, 131 (2002).

[18] Indeed, such a possibility requires that the Josephson energies of two junctions in a SQUID-loop to be equal or have a very small relative difference $|\delta\varepsilon_J/\varepsilon_J|$ in their coupling energies. Experimentally [19], this has been reached with $|\delta\varepsilon_J/\varepsilon_J| \sim 1\%$. This implies that another interaction term $\delta H \approx \delta\varepsilon_J \sin(\pi\Phi_k/\Phi_0)\sin\left[\hat{\phi}_k - C_g^{(k)}\hat{\phi}_b/C_k\right]$, due to the different critical currents of the two junctions, can be safely neglected and thus the system can be described by the Hamiltonian (1).

[19] See, e.g., R. Rouse, S. Han, and J.E. Lukens, Phys. Rev. Lett. **75**, 1614 (1995).

[20] M.A. Rowe *et al.*, Nature **409**, 791 (2001); G. Weihs *et al.*, Phys. Rev. Lett. **81**, 5039 (1998).

[21] Only a few lower-energy eigenstates of $\hat{H}_{kb}$, i.e., the ground state $|g\rangle=|-_k,0_b\rangle$ and the first doublet, $|u\rangle=\cos\chi_k|+_k,0_b\rangle-i\sin\chi_k|-_k,1_b\rangle$ and $|v\rangle=-i\sin\chi_k|+_k,0_b\rangle+\cos\chi_k|-_k,1_b\rangle$, are involved in our calculations. Their corresponding eigenvalues are $\hbar\omega_g$, $\hbar\omega_u$, and $\hbar\omega_v$, respectively. Here, $|\pm_k\rangle$ ($|0_b\rangle,|1_b\rangle$) are the eigenstates of $\hat{H}_k$ ($\hat{H}_b$), and $\cos\chi_k=\sqrt{(\rho_k-\delta_k)/(2\rho_k)}$, $\rho_k=\sqrt{\delta_k^2+4\lambda_k^2}$, $\delta_k=\varepsilon_k-\hbar\omega_b$. This simplifies the calculation of the rates of decoherence and relaxation. For example, the decoherence rate of the superposition of states $|u\rangle$ and $|v\rangle$ can be estimated as $\gamma_{uv} \sim \alpha_V A_V + \alpha_I A_I$, with $A_V=B_1\sin^2\alpha_k + B_2\cos^2\alpha_k$, $A_I=\Omega_{ug}\sin^2\chi_k + \Omega_{vg}\cos^2\chi_k$, $B_1=4\cos^2(2\chi_k)(2k_BT)/\hbar+2\Omega_{vu}\sin^2(2\chi_k)$, and $B_2 = \Omega_{ug}\cos^2\chi_k + \Omega_{vg}\sin^2\chi_k$. Also, $\Omega_{ug} = \omega_{ug}\coth[\hbar\omega_{ug}/(2k_bT)]$, $\Omega_{vg} = \omega_{vg}\coth[\hbar\omega_{vg}/(2k_bT)]$, $\Omega_{vu}=\omega_{vu}\coth[\hbar\omega_{vu}/(2k_bT)]$ and $\omega_{vu}=\omega_v-\omega_u$, etc. Specifically, for the decoupling case with $\sin\chi_k = 0$, the qubit and bus independently dephase with the rate $\gamma_{+-} \sim \alpha_V\{4\sin^2\alpha_k 2k_BT/\hbar + \omega_{+-}\cos^2\alpha_k\coth[\hbar\omega_{+-}/(2k_bT)]\}$ and $\gamma_{10} \sim \alpha_I\omega_b\coth[\hbar\omega_b/(2k_BT)]$.

Quantum computation with Josephson-qubits by using a current-biased information bus

L.F. Wei,[1,2] Yu-xi Liu,[1] and Franco Nori[1,3]

[1] *Frontier Research System, The Institute of Physical and Chemical Research (RIKEN), Wako-shi, Saitama, 351-0198, Japan*
[2] *Institute of Quantum Optics and Quantum Information, Department of Physics, Shanghai Jiaotong University, Shanghai 200030, P.R. China*
[3] *Center for Theoretical Physics, Physics Department, Center for the Study of Complex Systems, The University of Michigan, Ann Arbor, Michigan 48109-1120*

(Dated: July 28, 2004)

We propose an effective scheme for manipulating quantum information stored in a superconducting nanocircuit. The Josephson qubits are coupled via their separate interactions with an information bus, a large current-biased Josephson junction treated as an oscillator with adjustable frequency. The bus is sequentially coupled to only one qubit at a time. Distant Josephson qubits without any direct interaction can be indirectly coupled with each other by independently interacting with the bus sequentially, via exciting/de-exciting vibrational quanta in the bus. This is a superconducting analog of the successful ion trap experiments on quantum computing. Our approach differs from previous schemes that simultaneously coupled two qubits to the bus, as opposed to their sequential coupling considered here. The significant quantum logic gates can be realized by using these tunable and selective couplings. The decoherence properties of the proposed quantum system are analyzed within the Bloch-Redfield formalism. Numerical estimations of certain important experimental parameters are provided.

PACS numbers: 03.67.Lx, 74.50.+r, 85.25.Cp

I. INTRODUCTION.

The coherent manipulation of quantum states for realizing certain potential applications, e.g, quantum computation and quantum communication, is attracting considerable interest [1]. In principle, any two-state quantum system works as a qubit, the fundamental unit of quantum information. However, only a few real physical systems have worked as qubits, because of requirements of a long coherent time and operability. Among various physical realizations, such as ions traps (see, e.g., [2, 3, 4]), QED cavities (see, e.g., [5, 6]), quantum dots (see, e.g., [7, 8]) and NMR (see, e.g., [9, 10]) etc., superconductors with Josephson junctions offer one of the most promising platforms for realizing quantum computation (see, e.g., [11, 12, 13, 14, 15, 16, 17, 18, 19, 20, 21, 22, 24, 25, 26, 27, 28, 29, 30, 31]). The nonlinearity of Josephson junctions can be used to produce controllable qubits. Also, circuits with Josephson junctions combine the intrinsic coherence of the macroscopic quantum state and the possibility to control its quantum dynamics by using voltage and magnetic flux pulses. In addition, present-day technologies of integration allow scaling to large and complex circuits. Recent experiments have demonstrated quantum coherent dynamics in the time domain in both single-qubit (see, e.g., [12, 13, 14]) and two-qubit Josephson systems [15].

There are two basic types of Josephson systems used to implement qubits: charge qubits [12] and flux qubits [13], depending on the ratio of two characteristic energies: the charging energy E_C and the Josephson energy E_J. The charge qubit is a Cooper-pair box with a small Josephson coupling energy, $E_J \ll E_C$, and a well defined number of Cooper pairs is well defined. The flux qubit operates in another extreme limit, where $E_J \gg E_C$ and the phase is well defined. A "quantronium" circuit operating in the intermediate regime of the former two has also been proposed [14]. Voltage-biased superconducting quantum interference devices (SQUIDs), which work in the charge regime and with controllable Josephson energies, form the SQUID-based charge qubits that we will consider in this work. Our results can be extended to flux and flux-charge qubits.

The key ingredient for computational speedup in quantum computation is entanglement, a property that does not exist in classical physics. Thus, manipulating coupled qubits plays a central role in quantum information processing (QIP). Heisenberg-type qubit-couplings are common for the usual solid state QIP systems, e.g., the real spin states of the electrons in quantum dots [7, 8]. However, the interbit couplings for Josephson junctions involve Ising-type interactions, as superconducting qubits with two macroscopic quantum states provide pseudo-spin-1/2 states. Recently, either the current-current interaction, by connecting to a common inductor, or the charge-charge coupling, via sharing a common capacitor, have been proposed to directly couple two Josephson charge qubits: the ith and jth ones. These interactions implement $\sigma_z^{(i)} \otimes \sigma_z^{(j)}$–type [15, 16], $\sigma_y^{(i)} \otimes \sigma_y^{(j)}$–type [17], and the $\sigma_x^{(i)} \otimes \sigma_x^{(j)}$–type [18] Ising couplings, respectively. Compared to the single-qubit operations, the two-qubit operations based on these second-order interactions are more sensitive to the environment. Thus, quantum decoherence can be more problematic. In addition, capacitive coupling between qubits is not easily tunable [15]. Thus adjusting the physical parameters for realizing two-qubit operation is not easy. In order to ensure that the quanta of the relevant LC oscillator is not excited during the desired quantum operations, the time scales of manipulation in the inductively coupled circuit should be much slower than the eigenfrequency of the LC-circuit [17].

Alternatively, the Josephson qubits may also be coupled together by sequentially interacting with a data bus, instead of simultaneously. This is similar to the techniques used for trapped ions [2, 3], wherein the trapped ions are entangled by exciting and de-exciting quanta of their shared center-of-mass vibrational mode (i.e., the data bus). This scheme allows for

faster two-qubit operations and possesses longer decoherent times. In fact, an externally connected LC-resonator [19] and a cavity QED mode [20] were chosen as alternative data buses. However, it is not always easy to control all the physical properties, such as the eigenfrequencies and decoherence, of these data buses.

A large (e.g., up to 10μm) current-biased Josephson junction (CBJJ) [21] is very suitable to act as information bus for coupling Josephson qubits. This because: i) the CBJJ is an easily fabricated device [22] and may provide more effective immunities to both charge and flux noise; ii) due to its large junction capacitance, the CBJJ can enable to be capacitively coupled over relatively long distances; iii) the quantum properties, e.g., quantum transitions between the junction energy levels, of the current-biased Josephson junction are well established [23, 24]; and iv) its eigenfrequency can be controlled by adjusting the applied bias-current. In fact, a CBJJ itself can be an experimentally realizable qubit, as demonstrated by the recent observations of Rabi oscillations in them [25, 26]. Two logic states of such a qubit are encoded by the two lowest zero-voltage metastable quantum energy levels of the CBJJ. The decoherent properties of this CBJJ-qubit were discussed in detail in [27]. Experimentally, the entangled macroscopic quantum states in two CBJJ-qubits coupled by a capacitor were created [28]. Also, by numerical integration of the time-dependent Schrödinger equation, a full dynamical simulation of two-qubit quantum logic gates between two capacitively coupled CBJJ-qubits was given in [29].

In this paper, we propose a convenient scheme to selectively couple two Josephson charge-qubits. Here, a large CBJJ acts only as the information bus for transferring the quantum information between the qubits. Thus, hereafter the CBJJ will not be a qubit, as in [21, 25, 26, 27, 28, 29]. Two chosen distant SQUID-based charge qubits can be indirectly coupled by sequentially interacting these with the bus. This coupling method provides a repeatable way to generate entangled states, and thus can implement elementary quantum logic gates between arbitrarily selected qubits. Our proposal shares some features with the circuits proposed in [17, 18, 19, 21], but also has significant differences. Our proposal might be more amenable to experimental verification.

The outline of the paper is as follows. In Sec. II we propose a superconducting nanocircuit with a CBJJ acting as the data bus, and investigate its elemental quantum dynamics. The bus is biased by a *dc* current and is assumed to interact with only one qubit at a time. There is no direct interaction between qubits. Therefore, the elemental operations in this circuit consist of: i) the free evolution of the single qubit, ii) the free evolution of the bus, and iii) the coherent dynamics for a single qubit coupled to the bus. In Sec. III we show how to realize the elemental logic gates in the proposed nanocircuit: the single-qubit rotations by properly switching on/off the applied gate voltage and external flux, and the two-qubit operations by letting them couple sequentially to the bus. The vibrational quanta of the bus is excited/absorded during the qubit-bus interactions. In Sec. IV we analyze the decoherent properties of the present qubit-bus interaction within the Bloch-Redfield formalism [32], and give some numerical estimates for experimental implementations. Conclusions and some discussions are given in Sec. V.

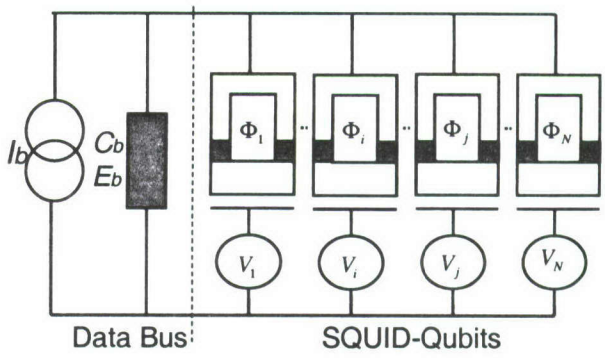

FIG. 1: SQUID-based charge qubits coupled via a large CBJJ.

II. A SUPERCONDUCTING NANOCIRCUIT AND ITS ELEMENTARY QUANTUM EVOLUTIONS.

The circuit considered here is sketched in Fig. 1. It consists of N voltage-biased SQUIDs connected to a large CBJJ. The kth ($k = 1, 2, ..., N$) qubit consists of a gate electrode of capacitance C_{g_k} and a single-Cooper-pair box with two ultrasmall Josephson junctions of capacitance $C^0_{J_k}$ and Josephson energy $E^0_{J_k}$, forming a DC-SQUID ring. The inductances of these DC-SQUID rings are assumed to be very small and can be neglected. The SQUIDs work in the charge regime with $k_BT \ll E_J \ll E_C \ll \Delta$, in order to suppress quasiparticle tunneling or excitation. Here, k_B, Δ, E_C, T, and E_J are the Boltzmann constant, the superconducting gap, charging energy, temperature, and the Josephson coupling energy, respectively.

The connected large CBJJ biased by a dc current works in the *phase regime* with $E_J \gg E_C$. It acts as a tunable anharmonic LC-resonator with a nonuniform level spacing and works as a data bus for transferring quantum information between the chosen qubits. The mechanism for manipulating quantum information in the present approach is different from that in [17, 18, 19, 21], although the circuit proposed here might seem similar to those there. The differences are:

(1) a large CBJJ, instead of LC-oscillator [17, 18, 19] formed by the externally connected inductance L and the capacitances in circuit, works as the data bus;

(2) we modulate the applied external flux, instead of the bias-current [21], to realize the perfect coupling/decoupling between the chosen qubit and the bus; and especially

(3) the free evolution of the bus during the operational delays will be utilized for the first time to control the dynamical phases for implementing the expected quantum gates.

The Hamiltonian for the present circuit can be written as

$$\hat{H} = \sum_{k=1}^{N} \left[\frac{2e^2}{C_k} \left(\hat{n}_k - n_{g_k} \right)^2 - E_{J_k} \cos \left(\hat{\theta}_k - \frac{C_{g_k}}{C_k} \hat{\theta}_b \right) \right] + \hat{H}_r, \quad (1)$$

with

$$\hat{H}_r = \frac{(2\pi\hat{p}_b/\Phi_0)^2}{2\tilde{C}_b} - E_b\cos\hat{\theta}_b - \frac{\Phi_0 I_b}{2\pi}\hat{\theta}_b. \qquad (2)$$

Here, $n_{g_k} = C_{g_k}V_k/(2e)$, $C_k = C_{g_k} + C_{J_k}$, $C_{J_k} = 2C^0_{J_k}$, $\tilde{C}_b = C_b + \sum_{k=1}^{N} C_{J_k}C_{g_k}/C_k$, $E_{J_k} = 2E^0_{J_k}\cos(\pi\Phi_k/\Phi_0)$, and $\theta_k = (\theta_{k_2} + \theta_{k_1})/2$ with θ_{k_1} and θ_{k_2} being the phase drops across two small Josephson junctions in the kth qubit, respectively. Also, C_{g_k}, Φ_0, Φ_k, and V_k are the gate capacitance, flux quantum, external flux, and gate voltage applied to the kth qubit, respectively. Correspondingly, C_b, θ_b, E_b, and I_b are the capacitance, phase drops, Josephson energy, and the bias-current of the large CBJJ, respectively. Above, the number operator $\hat{n}_k$ of excess Cooper-pair charges in the superconducting island and the phase operator $\hat{\theta}_k$ of the order parameter of the kth charge qubit are a pair of canonical variables and satisfy the commutation relation:

$$[\hat{\theta}_k, \hat{n}_k] = i.$$

The operators θ_b and $\hat{p}_b$ are another pair of canonical variables and satisfy the commutation relation:

$$[\hat{\theta}_b, \hat{p}_b] = i\hbar,$$

with $2\pi p_b/\Phi_0 = 2n_b e$ representing the charge difference across the CBJJ.

The CBJJ works in the phase regime. Thus, $E_{C_b} = e^2/(2\tilde{C}_b) \ll E_b$ and the quantum motion ruled by the Hamiltonian $\hat{H}_r$ equals to that of a particle with mass $m = \tilde{C}_b(\Phi_0/2\pi)^2$ in a potential $U(\theta_b) = -E_b(\cos\theta_b + I_b\theta_b/I_r)$, $I_r = 2\pi E_b/\Phi_0$. For the biased case $I_b < I_r$, there exists a series of minima of $U(\theta_b)$, where $\partial U(\theta_b)/\partial\theta_b = 0$, $\partial^2 U(\theta_b)/\partial\theta_b^2 > 0$. Near these points, $U(\theta_b)$ approximates to a harmonic oscillator potential with a characteristic frequency

$$\omega_b = \sqrt{\frac{2\pi I_r}{\tilde{C}_b\Phi_0}}\left[1 - \left(\frac{I_b}{I_r}\right)^2\right]^{1/4},$$

depending on the applied bias-current I_b. Correspondingly, the Hamiltonian $\hat{H}_r$ reduces to

$$\hat{H}_b = \left(\hat{a}^\dagger\hat{a} + \frac{1}{2}\right)\hbar\omega_b, \qquad (3)$$

with

$$\hat{a} = \frac{1}{\sqrt{2}}\left[\left(\frac{\Phi_0}{2\pi}\right)\sqrt{\frac{\tilde{C}_b\omega_b}{\hbar}}\,\hat{\theta}_b + i\left(\frac{2\pi}{\Phi_0}\right)\frac{\hat{p}_b}{\sqrt{\hbar\omega_b\tilde{C}_b}}\right],$$

and

$$\hat{a}^\dagger = \frac{1}{\sqrt{2}}\left[\left(\frac{\Phi_0}{2\pi}\right)\sqrt{\frac{\tilde{C}_b\omega_b}{\hbar}}\,\hat{\theta}_b - i\left(\frac{2\pi}{\Phi_0}\right)\frac{\hat{p}_b}{\sqrt{\hbar\omega_b\tilde{C}_b}}\right].$$

The approximate number of quantum metastable bound states [33] of the quantum oscillator is $N_s = 2^{3/4}\sqrt{E_b/E_{C_b}}(1 - I_b/I_r)^{5/4}$.

The energy scale of the quantum oscillator (3) is $\omega_b/(2\pi) \sim 10\,\mathrm{GHz}$ [25], which is of the same order of the Josephson energy in the SQUID. Therefore, the oscillating quantum of the information bus will be really excited, even if only one of the qubits is operated quantum mechanically. This is different from the case considered in [17], wherein the LC-oscillator shared by all charge qubits are not really excited, as the eigenfrequency of the LC-circuit is much higher than the typical frequencies of the qubits dynamics. For operational convenience, we assume that the bus is coupled to only one qubit at a time. The coupling between any one of the qubits (e.g., the kth one) and the bus can, in principle, be controlled by adjusting the applied external flux (e.g., Φ_k). In this case, any direct interaction does not exist between the qubits, and the dynamics of the CBJJ can be safely restricted to the Hilbert space spanned by the two Fock states: $|0_b\rangle$ and $|1_b\rangle$, which are the lowest two energy eigenstates of the harmonic oscillator of Eq. (3). Furthermore, we assume that the applied gate voltage of any chosen (kth) qubit works near its degeneracy point with $n_{g_k} = 1/2$, and thus only two charge states: $|n_k = 0\rangle = |\uparrow_k\rangle$ and $|n_k = 1\rangle = |\downarrow_k\rangle$, play a role during the quantum operation. All other charge states with a higher energies can be safely ignored. Therefore, the Hamiltonian

$$\hat{H}_{kb} = \hat{H}_k + \hat{H}_b + \lambda_k\left(\hat{a}^\dagger + \hat{a}\right)\sigma_y^{(k)}, \qquad (4)$$

with

$$\hat{H}_k = \left[\frac{\delta E_{C_k}}{2}\,\sigma_z^{(k)} - \frac{E_{J_k}}{2}\,\sigma_x^{(k)}\right], \qquad (5)$$

describes the interaction between any one of the qubits (e.g., the kth one) and the bus, and provides the basic dynamics for the present network. Here, $\delta E_{C_k} = 2e^2(1-2n_{g_k})/C_k$, $\lambda_k = C_{g_k}(2\pi/\Phi_0)\sqrt{\hbar/(2\tilde{C}_b\omega_b)}/(2C_k)$, and the pseudospin operators are defined by:

$$\begin{cases} \sigma_x^{(k)} = |\uparrow_k\rangle\langle\downarrow_k| + |\downarrow_k\rangle\langle\uparrow_k|, \\ \sigma_y^{(k)} = -i|\uparrow_k\rangle\langle\downarrow_k| + i|\downarrow_k\rangle\langle\uparrow_k|, \\ \sigma_z^{(k)} = |\uparrow_k\rangle\langle\uparrow_k| - |\downarrow_k\rangle\langle\downarrow_k|. \end{cases}$$

Above, when the first cosine-term in Hamiltonian (2) was expanded, only the single-quantum transition process approximated to the first-order of $\hat{\theta}_b$ was considered. The higher order nonlinearities have been neglected as their effects are very weak. In fact, for the lower number states of the bus, we have $C_{g_k}\sqrt{\langle\theta_b^2\rangle}/C_k \lesssim 10^{-2}$, for the typical experimental parameters [11, 15, 24, 27]: $C_b \sim 1pF$, $\omega_b/2\pi \sim 10\,\mathrm{GHz}$, and $C_{g_k}/C_{J_k} \sim 10^{-2}$.

Notice that the coupling strength λ_k between the qubit and the bus is tunable by controlling the flux Φ_k, applied to the selected qubit, and the bias-current I_b, applied to the information bus. For example, such a coupling can be simply turn off by setting the flux Φ_k as $\Phi_0/2$. This allows various elemental operations for quantum manipulations to be realizable in a

controllable way. In the logic basis $\{|0_k\rangle, |1_k\rangle\}$, defined by

$$|0_k\rangle = \frac{|\downarrow_k\rangle + |\uparrow_k\rangle}{\sqrt{2}}, \ |1_k\rangle = \frac{|\downarrow_k\rangle - |\uparrow_k\rangle}{\sqrt{2}},$$

and under the usual rotating-wave approximation, the above Hamiltonian (4) can be rewritten as

$$\begin{aligned}\hat{H}_{kb} &= \left[\frac{E_{J_k}}{2}\tilde{\sigma}_z^{(k)} - \frac{\delta E_{C_k}}{2}\tilde{\sigma}_x^{(k)}\right] + \hbar\omega_b\left(\hat{a}^\dagger\hat{a} + \frac{1}{2}\right) \\ &+ i\lambda_k\left[\hat{a}\tilde{\sigma}_+^{(k)} - \hat{a}^\dagger\tilde{\sigma}_-^{(k)}\right],\end{aligned} \tag{6}$$

with

$$\begin{cases}\tilde{\sigma}_x^{(k)} = |1_k\rangle\langle 0_k| + |0_k\rangle\langle 1_k|, \\ \tilde{\sigma}_y^{(k)} = -i|1_k\rangle\langle 0_k| + i|0_k\rangle\langle 1_k|, \\ \tilde{\sigma}_z^{(k)} = |1_k\rangle\langle 1_k| - |0_k\rangle\langle 0_k|,\end{cases}$$

and $\tilde{\sigma}_\pm^{(k)} = (\tilde{\sigma}_x^{(k)} \pm \tilde{\sigma}_y^{(k)})/2$. Here, the logic states $|0_k\rangle$ and $|1_k\rangle$ correspond to the clockwise and anticlockwise persistent circulating currents in the kth SQUID-loop, respectively.

We now discuss the quantum dynamics of the above Josephson network. Without loss of generality, we assume in what follows that the bias-current I_b applied to the CBJJ doesn't change, once it is set up properly beforehand. The quantum evolutions of the system are then controlled by other external parameters: the fluxes applied to the qubits and the voltages across the gate capacitances of the qubits. Depending on the different settings of the controllable external parameters, different Hamiltonians can be induced from Eq. (6) and thus different time-evolutions are obtained. Obviously, during any operational delay τ with $\Phi_{X_i} = \Phi_0/2$ and $V_k = e/C_{g_i}$, the ith qubit remains in its idle state because the Hamiltonian vanishes (i.e., $H_0^{(i)} = 0$) as $E_{J_i} = 0$, $n_{g_i} = 0$. However, the data bus still undergoes a free time-evolution:

$$\hat{U}_0(t) = \exp\left(\frac{-it}{\hbar}\hat{H}_b\right). \tag{7}$$

This evolution is useful for controlling the dynamical phase of the qubits to exactly realize certain quantum operations. For the other cases, the dynamical evolutions of the chosen qubit depend on the different settings of the experimental parameters.

1) For the case where $\Phi_k = \Phi_0/2$ and $V_k \neq e/C_{g_k}$, the ith qubit and the bus separately evolve with the Hamiltonians $\hat{H}_1^{(k)} = -\delta E_{C_k}\tilde{\sigma}_x^{(k)}/2$ and $\hat{H}_b$ determined by Eq. (3), respectively. The relevant time-evolution operator of the whole system reads

$$\hat{U}_1^{(k)}(t) = \exp\left(\frac{-it}{\hbar}\hat{H}_1^{(k)}\right) \otimes \exp\left(\frac{-it}{\hbar}\hat{H}_b\right). \tag{8}$$

2) If the kth qubit works at its degenerate point and couples to the bus, i.e., $V_k = e/C_{g_k}$ and $\Phi_k \neq \Phi_0/2$, then we have the Hamiltonian

$$\tilde{\hat{H}}_{kb} = E_{J_i}\tilde{\sigma}_z^{(k)}/2 + \hat{H}_b + i\lambda_k\left[\hat{a}\tilde{\sigma}_+^{(k)} - \hat{a}^\dagger\tilde{\sigma}_-^{(k)}\right] \tag{9}$$

from (6). The corresponding dynamical evolutions are

$$\begin{cases}|0_b\rangle|0_k\rangle \xrightarrow{\tilde{\hat{U}}_{kb}} e^{i\Delta_k t/2}|0_b\rangle|0_i\rangle, \ \tilde{\hat{U}}_{kb} = \exp(-i\tilde{\hat{H}}_{kb}t), \ \Delta_k = E_{J_k}/\hbar - \omega_b, \\ |0_b\rangle|1_k\rangle \xrightarrow{\tilde{\hat{U}}_{kb}} e^{-i\omega_b t}\left\{\left[\cos\left(\frac{\Omega_k}{2}t\right) - i\frac{\Delta_k}{\Omega_k}\sin\left(\frac{\Omega_k}{2}t\right)\right]|0_b\rangle|1_k\rangle - \frac{2\lambda_k}{\hbar\Omega_k}\sin\left(\frac{\Omega_k}{2}t\right)|1_b\rangle|0_k\rangle\right\}, \\ |1_b\rangle|0_k\rangle \xrightarrow{\tilde{\hat{U}}_{kb}} e^{-i\omega_b t}\left\{\left[\cos\left(\frac{\Omega_k}{2}t\right) + i\frac{\Delta_k}{\Omega_k}\sin\left(\frac{\Omega_k}{2}t\right)\right]|1_b\rangle|0_k\rangle + \frac{2\lambda_k}{\hbar\Omega_k}\sin\left(\frac{\Omega_k}{2}t\right)|0_b\rangle|1_k\rangle\right\},\end{cases} \tag{10}$$

with $\Omega_k = \sqrt{\Delta_k^2 + (2\lambda_k/\hbar)^2}$.

Specifically, we have the time-evolution operator

$$\hat{U}_2^{(k)}(t) = \hat{A}(t)\begin{pmatrix}\cos\left(\frac{2\lambda_k t}{\hbar}\sqrt{\hat{n}+1}\right) & -\frac{1}{\sqrt{\hat{n}+1}}\sin\left(\frac{2\lambda_k t}{\hbar}\sqrt{\hat{n}+1}\right)\hat{a} \\ \frac{\hat{a}^\dagger}{\sqrt{\hat{n}}}\sin\left(\frac{2\lambda_k t}{\hbar}\sqrt{\hat{n}}\right) & \cos\left(\frac{2\lambda_k t}{\hbar}\sqrt{\hat{n}}\right)\end{pmatrix}, \tag{11}$$

with

$$\hat{A}(t) = \exp\left[-it\left(\frac{\hat{H}_b}{\hbar} + \frac{E_{J_k}\tilde{\sigma}_z^{(k)}}{2\hbar}\right)\right],$$

for the resonant case: $\Delta_k = 0$. This reduces Eq. (10) to the time evolutions:

$$\begin{cases} |0_b\rangle|0_k\rangle \xrightarrow{\hat{U}_2^{(k)}(t)} |0_b\rangle|0_k\rangle, \\ |0_b\rangle|1_k\rangle \xrightarrow{\hat{U}_2^{(k)}(t)} e^{-i\omega_b t}\left[\cos\left(\frac{\lambda_k t}{\hbar}\right)|0_b\rangle|1_k\rangle - \sin\left(\frac{\lambda_k t}{\hbar}\right)|1_b\rangle|0_k\rangle\right], \\ |1_b\rangle|0_k\rangle \xrightarrow{\hat{U}_2^{(k)}(t)} e^{-i\omega_b t}\left[\cos\left(\frac{\lambda_k t}{\hbar}\right)|1_b\rangle|0_k\rangle + \sin\left(\frac{\lambda_k t}{\hbar}\right)|0_b\rangle|1_k\rangle\right]. \end{cases}$$

For another extreme case, i.e., the system works in the dispersive regime (far from the resonant point): $2\lambda_k/(\hbar|\Delta_k|) \ll 1$, we have the time evolution operator

$$\tilde{\hat{U}}_2^{(k)}(t) = \hat{A}(t)\exp\left(-i\frac{\tilde{\hat{H}}'_{kb}t}{\hbar}\right), \tag{12}$$

with

$$\tilde{\hat{H}}'_{kb} = \lambda_k^2(|1_k\rangle\langle 1_k|\hat{a}\hat{a}^\dagger - |0_k\rangle\langle 0_k|\hat{a}^\dagger\hat{a})/(\hbar\Delta_k).$$

It reduces to the following time evolutions:

$$\begin{cases} |0_b\rangle|0_k\rangle \xrightarrow{\tilde{U}_2^{(k)}(t)} \exp\left(it\frac{\Delta_i}{2}\right)|0_b\rangle|0_i\rangle, \\ |0_b\rangle|1_k\rangle \xrightarrow{\tilde{U}_2^{(k)}(t)} \exp\left[-it\left(\omega_b + \frac{\Delta_i}{2} + \frac{\lambda_k^2}{\hbar^2\Delta_k}\right)\right]|0_b\rangle|1_k\rangle, \\ |1_b\rangle|0_k\rangle \xrightarrow{\tilde{U}_2^{(k)}(t)} \exp\left[-it\left(\omega_b - \frac{\Delta_k}{2} - \frac{\lambda_k^2}{\hbar^2\Delta_k}\right)\right]|1_b\rangle|0_k\rangle, \\ |1_b\rangle|1_k\rangle \xrightarrow{\tilde{U}_2^{(k)}(t)} \exp\left[-it\left(2\omega_b + \frac{\Delta_k}{2} + \frac{2\lambda_k^2}{\hbar^2\Delta_k}\right)\right]|1_b\rangle|1_k\rangle. \end{cases}$$

3) Generally, if $\Phi_k \neq \Phi_0/2$ and $V_{g_k} \neq e/C_{g_k}$, then the Hamiltonian (6) can be rewritten as

$$\bar{\hat{H}}_{kb} = \frac{E_k}{2}\bar{\sigma}_z^{(k)} + \hat{H}_b + i\lambda_k(\hat{a}^\dagger\bar{\sigma}_-^{(k)} - \hat{a}\bar{\sigma}_+^{(k)}), \tag{13}$$

with

$$\begin{cases} \bar{\sigma}_x^{(k)} = -\sin\eta_k\,\tilde{\sigma}_z^{(k)} - \cos\eta_k\,\tilde{\sigma}_x^{(k)}, \\ \bar{\sigma}_y^{(k)} = -\tilde{\sigma}_y^{(k)}, \\ \bar{\sigma}_z^{(k)} = \cos\eta_i\,\tilde{\sigma}_z^{(k)} - \sin\eta_k\,\tilde{\sigma}_x^{(k)}, \end{cases}$$

and $\bar{\sigma}_\pm^{(k)} = (\bar{\sigma}_x^{(k)} \pm \bar{\sigma}_y^{(k)})/2$. Here, $\cos\eta_k = E_{J_k}/E_k$, and $E_k = \sqrt{(\delta E_{C_k})^2 + E_{J_k}^2}$. If the bias-current I_b and the flux Φ_k are set properly beforehand such that $E_{J_k} \sim \hbar\omega_b \ll \delta E_{C_k}$, then the detuning $\hbar\bar{\Delta}_k = E_k - \hbar\omega_b$ is very large (compared to the coupling strength $\lambda_k \lesssim 10^{-1}E_{J_k}$). Therefore, the time-evolution operator of the system can be approximated as

$$\bar{\hat{U}}_3^{(k)}(t) = \hat{B}(t)\exp\left\{-i\frac{\lambda_k^2 t}{\hbar^2\bar{\Delta}_k}\left[\bar{\sigma}_z^{(k)}\left(\hat{a}^\dagger\hat{a} + \frac{1}{2}\right) + \frac{1}{2}\right]\right\} \tag{14}$$

with

$$\hat{B}(t) = \exp\left[-it\left(\frac{\hat{H}_b}{\hbar} + \frac{E_k\bar{\sigma}_z^{(k)}}{2\hbar}\right)\right].$$

This implies the following evolutions

$$
\begin{cases}
|0_b\rangle|0_k\rangle \xrightarrow{\bar{U}_3^{(k)}(t)} e^{-i\zeta_k t}\left\{[\cos(\xi_k t)+i\cos\eta_k\sin(\xi_k t)]\,|0_b\rangle|0_k\rangle + i\sin\eta_k\sin(\xi_k t)\,|0_b\rangle|1_k\rangle\right\}, \\
|0_b\rangle|1_k\rangle \xrightarrow{\bar{U}_3^{(k)}(t)} e^{-i\zeta_k t}\left\{[\cos(\xi_k t)-i\cos\eta_k\sin(\xi_k t)]\,|0_b\rangle|1_k\rangle + i\sin\eta_k\sin(\xi_k t)\,|0_b\rangle|0_k\rangle\right\}, \\
|1_b\rangle|0_k\rangle \xrightarrow{\bar{U}_3^{(k)}(t)} e^{-i(\zeta_k+\omega_b)t}\left\{[\cos(\xi'_k t)+i\cos\eta_k\sin(\xi'_k t)]\,|1_b\rangle|0_k\rangle + i\sin\eta_k\sin(\xi'_k t)\,|1_b\rangle|1_k\rangle\right\}, \\
|1_b\rangle|1_k\rangle \xrightarrow{\bar{U}_3^{(k)}(t)} e^{-i(\zeta_k+\omega_b)t}\left\{i\sin\eta_k\sin(\xi'_k t)\,|1_b\rangle|0_k\rangle + [\cos(\xi'_k t)-i\cos\eta_i\sin(\xi'_k t)]\,|1_b\rangle|1_k\rangle\right\},
\end{cases}
$$

with

$$\zeta_k = \omega_b/2 + \lambda_k^2/(2\hbar^2\bar{\Delta}_k)\,, \xi_k = E_k/(2\hbar) + \lambda_k^2/(2\hbar^2\bar{\Delta}_k),$$

and

$$\xi'_k = \xi_k + \lambda_k^2/(\hbar^2\bar{\Delta}_i).$$

In what follows we shall show that any process for manipulating the quantum information stored in the present circuit can be effectively implemented by selectively using the above elementary time-evolutions: $\hat{U}_0(t)$, $\hat{U}_1^{(k)}(t)$, $\hat{U}_2^{(k)}(t)$, $\tilde{\hat{U}}_2^{(k)}(t)$, and $\bar{\hat{U}}_3^{(k)}(t)$.

III. QUANTUM MANIPULATIONS OF THE SUPERCONDUCTING NANOCIRCUIT.

It is well known that any valid quantum transformation can be decomposed into a sequence of elementary one- and two-qubit quantum gates. The set of these gates is universal, and any quantum computing circuit comprises only gates from this set. Several schemes [17, 18, 29] have been proposed for implementing one of the universal two-qubit gates with Josephson qubits by using the direct interactions between them. By making use of the data bus interacting sequentially with the selective qubits, Blais *et al.* [21] showed that the two-qubit gate may be effectively realized. Two important problems will be solved in our indirect-coupling approach:

i) when one of two qubits is selected to couple with the data bus, how we can let the remainder qubit decouple completely from the bus; and

ii) the phase changes of the bus' and qubit's states during the operations are very complicated, how we can control these phase changes in order to precisely implement the desired quantum gate.

The scheme in [21] assumed that, when one of the two qubits is tuned to resonance with the bus, then the other qubit is hardly affected because of its different Rabi frequency. Obviously, this decoupling is not complete and thus it is not easy to assure that the bus couples only one qubit at a time. By controlling the external flux Φ_k applied to the qubits, the network proposed here provides an effective method for making the remainder qubit completely decouple from the bus. All the desired elementary operations for quantum computing can be exactly implemented by properly setting the experimentally controllable parameters, e.g., the external Φ_k, the gate voltage V_k, the bias-current I_b, and the duration t of each selected quantum evolution, etc.

Hereafter, we assume that each of the selected time-evolutions can be switched on/off very quickly.

A. single-qubit operations

First, we show how to realize the single-qubit operations on each SQUID-qubit. This will be achieved by simply turning on/off the relevant experimentally controllable parameters. For example, if $n_{g_k} \neq 1/2$ and $E_{J_k} = 0$ for a time span t, then the time-evolution $\hat{U}_1^{(k)}(t)$ in equation (8) is realized. This operation is the single-qubit rotation around the x axis:

$$\hat{R}_x^{(k)}(\varphi_k) = \begin{pmatrix} \cos\frac{\varphi_k}{2} & i\sin\frac{\varphi_k}{2} \\ i\sin\frac{\varphi_k}{2} & \cos\frac{\varphi_k}{2} \end{pmatrix}, \tag{15}$$

with $\varphi_k = \delta E_{C_k} t/\hbar$. Rotations by $\varphi_i = \pi$ and $\varphi_k = \pi/2$ produce a spin flip (i.e., a NOT-gate operation) and an equal-weight superposition of logic states, respectively.

The rotation around the z axis can be implemented by using the evolution (12). This operation is conditional and dependent on the state of the bus. If the bus is in the ground state $|0_b\rangle$, the rotation reads

$$R_z^{(k)}(\phi_k) = e^{-i\varrho_k t}\begin{pmatrix} e^{-i\phi_k} & 0 \\ 0 & e^{i\phi_k} \end{pmatrix}, \tag{16}$$

with $\varrho_k = \omega_b/2 + \lambda_k^2/(2\hbar^2\Delta_k)$, $\phi_k = E_{J_k}t/(2\hbar) + \lambda_k^2 t/(2\hbar^2\Delta_k)$. With a sequence of x- and z-rotations, any rotation on the single-qubit can be performed. For example, the Hadamard gate applied to the kth qubit:

$$\hat{H}_g = \frac{1}{\sqrt{2}}\begin{pmatrix} 1 & 1 \\ 1 & -1 \end{pmatrix},$$

can be implemented by a three-step rotation:

$$\hat{R}_z^{(k)}\left(\frac{\pi}{4}\right)\otimes\hat{R}_x^{(k)}\left(-\frac{\pi}{2}\right)\otimes\hat{R}_z^{(k)}\left(\frac{\pi}{4}\right) = -ie^{-i\kappa_i(t_1+t_3)}\hat{H}_g^{(k)}. \tag{17}$$

Here, the relevant durations t_1, t_2, and t_3 are set properly to satisfy the conditions

$$\begin{aligned}\cos\left(\frac{\delta E_{C_k} t_2}{\hbar}\right) &= -\sin\left(\frac{\delta E_{C_k} t_2}{\hbar}\right) \\ &= \sin\left[\frac{E_{J_k} t_1}{2\hbar} + \frac{(\lambda_k/\hbar)^2 t_1}{2\Delta_k}\right] \\ &= \sin\left[\frac{E_{J_k} t_3}{2\hbar} + \frac{(\lambda_k/\hbar)^2 t_3}{2\Delta_k}\right] \\ &= \frac{1}{\sqrt{2}}.\end{aligned}$$

B. two-qubit operations

Second, we show how to realize two-qubit gates by letting a pair of qubits (the kth- and jth ones) interact separately with the bus. Before the quantum operation, the chosen qubits decouple from the bus. At the end of the desired gate operation the bus should be disentangled again from the qubits, and returned to its ground state. For operational simplicity, we assume that the bus resonates with the control qubit, the kth one, i.e., $\Delta_k = 0$. We now consider the following three-step operational process:

i) Couple the control qubit to the bus (i.e., the applied external flux Φ_k is varied to Φ_0) and realize the evolution $\hat{U}_1^{(k)}(t_1)$ for the duration t_1:

$$\sin\left(\frac{\lambda_k\, t_1}{\hbar}\right) = -1. \tag{18}$$

Then, by returning the Φ_k to its initial value, i.e., $\Phi_k = \Phi_0/2$, the kth qubit can be decoupled from the bus exactly. Before the next step operation, there is an operational delay τ_1. During this delay the state of the qubits does not evolve, while the data bus still undergoes a time-evolution $\hat{U}_0(\tau_1)$.

ii) Couple the target qubit (the jth one) to the bus and realize the time-evolution $\hat{U}_3^{(j)}(t_2)$. This is achieved by letting the chosen qubit work near its degenerate point (i.e., $n_{g_j} \neq 1/2$) and switching on its Josephson energy (i.e., $\Phi_j \neq \Phi_0/2$). After the time t_2 determined by the condition

$$\cos(\xi_j t_2) = -\sin(\xi_j' t_2) = 1, \tag{19}$$

we decouple the jth qubit from the bus and let it be in the idle state by returning its gate-voltage V_j to the degenerate point ($n_{g_j} = 1/2$), and simultaneously switching off the relevant Josephson energy. During another operational delay τ_2 before the next step operation, the bus undergoes another free-evolution $\hat{U}_0(\tau_2)$.

iii) Repeat the first step and realize the evolution $\hat{U}_1^{(k)}(t_3)$ with

$$\sin\left(\frac{\lambda_k\, t_3}{\hbar}\right) = 1. \tag{20}$$

Diagrammatically, the above three-step operational process with two delays can be represented as follows:

$$\left\{\begin{array}{l}
|0_b0_k0_j\rangle \xrightarrow{\hat{U}_0(\tau_1)\hat{U}_2^{(k)}(t_1)} e^{-i\omega_b\tau_1/2}|0_b0_k0_j\rangle \xrightarrow{\hat{U}_0(\tau_2)\bar{\hat{U}}_3^{(j)}(t_2)} e^{-i\chi}|0_b0_k0_j\rangle \xrightarrow{\hat{U}_2^{(k)}(t_3)} e^{-i\chi}|0_b0_k0_j\rangle, \\
|0_b0_k1_j\rangle \xrightarrow{\hat{U}_0(\tau_1)\hat{U}_2^{(k)}(t_1)} e^{-i\omega_b\tau_1/2}|0_b0_k1_j\rangle \xrightarrow{\hat{U}_0(\tau_2)\bar{\hat{U}}_3^{(j)}(t_2)} e^{-i\chi}|0_b0_k1_j\rangle \xrightarrow{\hat{U}_2^{(k)}(t_3)} e^{-i\chi}|0_b0_k1_j\rangle, \\
|0_b1_k0_j\rangle \xrightarrow{\hat{U}_0(\tau_1)\hat{U}_2^{(k)}(t_1)} e^{-i\omega_b(t_1+3\tau_1/2)}|1_b0_k0_j\rangle \\
\qquad\qquad \xrightarrow{\hat{U}_0(\tau_2)\bar{\hat{U}}_3^{(j)}(t_2)} ie^{-i\chi-i\omega_b(t_1+t_2+\tau_1+\tau_2)}(\cos\eta_j|1_b0_k0_j\rangle + \sin\eta_j|1_b0_k1_j\rangle) \\
\qquad\qquad\qquad \xrightarrow{\hat{U}_2^{(k)}(t_3)} ie^{-i\chi-i\omega_bT}(\cos\eta_j|0_b1_k0_j\rangle + \sin\eta_j|0_b1_k1_j\rangle), \\
|0_b1_k1_j\rangle \xrightarrow{\hat{U}_0(\tau_1)\hat{U}_2^{(k)}(t_1)} e^{-i\omega_b(t_1+3\tau_1/2)}|1_b0_k1_j\rangle \\
\qquad\qquad \xrightarrow{\hat{U}_0(\tau_2)\bar{\hat{U}}_3^{(j)}(t_2)} ie^{-i\chi-i\omega_b(t_1+t_2+\tau_1+\tau_2)}(\sin\eta_j|1_b0_k0_j\rangle - \cos\eta_j|1_b0_k1_j\rangle) \\
\qquad\qquad\qquad \xrightarrow{\hat{U}_2^{(k)}(t_3)} ie^{-i\chi-i\omega_bT}(\sin\eta_j|0_b1_k0_j\rangle - \cos\eta_j|0_b1_k1_j\rangle),
\end{array}\right.$$

with $T = t_1 + t_2 + t_3 + \tau_1 + \tau_2$ being the total duration of the process, and $\chi = \zeta_j t_2 + \omega_b(\tau_1 + \tau_2)/2$. Obviously, the information bus remains in its ground state $|0_b\rangle$ after the operations. If the total duration T is satisfied as

$$\sin(\omega_b T) = 1, \tag{21}$$

the above three-step process with two delays yields a two-

qubit gate expressed by the following matrix form

$$\hat{U}_1^{(kj)}(\eta_j) = \begin{pmatrix} 1 & 0 & 0 & 0 \\ 0 & 1 & 0 & 0 \\ 0 & 0 & \cos\eta_j & \sin\eta_j \\ 0 & 0 & \sin\eta_j & -\cos\eta_j \end{pmatrix}, \tag{22}$$

which is a universal two-qubit Deutsch gate [34].

Analogously, if the second step operation $\tilde{U}_3^{(j)}(t_2)$ in the above three-step process is replaced by the operation $\tilde{U}_2^{(j)}(t_2)$, then another two-qubit operation expressed by

$$\tilde{U}_2^{(kj)}(t_2) = \begin{pmatrix} \Gamma_j & 0 & 0 & 0 \\ 0 & \Gamma_j^* & 0 & 0 \\ 0 & 0 & \Lambda_j e^{-i\omega_b T} & 0 \\ 0 & 0 & 0 & \Lambda_j^* e^{-i\omega_b T} \end{pmatrix}, \tag{23}$$

with $\Gamma_j = \exp(i\varsigma_j t_2), \Lambda_j = \exp(i\varsigma_j' t_2)$, $\varsigma_j = E_{J_j}/(2\hbar) + \lambda_j^2/(2\hbar^2\Delta_j)$, $\varsigma_j' = \varsigma_j + \lambda_j^2 t_2/(\hbar^2\Delta_j)$, can be implemented. This three-step operational process can similarly be represented diagrammatically as

$$\begin{cases} |0_b0_k0_j\rangle \xrightarrow{\hat{U}_0(\tau_1)\hat{U}_2^{(k)}(t_1)} e^{-i\omega_b\tau_1}|0_b0_k0_j\rangle \xrightarrow{\hat{U}_0(\tau_2)\tilde{U}_2^{(j)}(t_2)} \Gamma e^{-i\nu}|0_b0_k0_j\rangle \xrightarrow{\hat{U}_2^{(k)}(t_3)} \Gamma e^{-i\nu}|0_b0_k0_j\rangle, \\ |0_b0_k1_j\rangle \xrightarrow{\hat{U}_0(\tau_1)\hat{U}_2^{(k)}(t_1)} e^{-i\omega_b\tau_1}|0_b0_k1_j\rangle \xrightarrow{\hat{U}_0(\tau_2)\tilde{U}_2^{(j)}(t_2)} \Gamma^* e^{-i\nu}|0_b0_k1_j\rangle \xrightarrow{\hat{U}_2^{(k)}(t_3)} \Gamma^* e^{-i\nu}|0_b0_k1_j\rangle, \\ |0_b1_k0_j\rangle \xrightarrow{\hat{U}_0(\tau_1)\hat{U}_2^{(k)}(t_1)} e^{-i\omega_b(t_1+3\tau_1/2)}|1_b0_k0_j\rangle \xrightarrow{\hat{U}_0(\tau_2)\tilde{U}_2^{(j)}(t_2)} \Lambda e^{-i\nu-i\omega_b(t_1+t_2+\tau_1+\tau_2)}|1_b0_k0_j\rangle \\ \qquad\qquad \xrightarrow{\hat{U}_2^{(k)}(t_3)} \Lambda e^{-i\nu-i\omega_b T}|0_b1_k0_j\rangle, \\ |0_b1_k1_j\rangle \xrightarrow{\hat{U}_0(\tau_1)\hat{U}_2^{(k)}(t_1)} e^{-i\omega_b(t_1+3\tau_1/2)}|1_b0_k1_j\rangle \xrightarrow{\hat{U}_0(\tau_2)\tilde{U}_2^{(j)}(t_2)} \Lambda^* e^{-i\nu-i\omega_b(t_1+t_2+\tau_1+\tau_2)}|1_b0_k1_j\rangle \\ \qquad\qquad \xrightarrow{\hat{U}_2^{(k)}(t_3)} \Lambda^* e^{-i\nu-i\omega_b T}|0_b1_k1_j\rangle, \end{cases}$$

with $\nu = \omega_b t_2/2 + \lambda_i^2 t_2/(2\hbar^2\Delta_i) + \omega_b(\tau_1+\tau_2)/2$. Above, the durations of the first- and third-step operations have been set the same as those for realizing the two-qubit operation $\hat{U}_1^{kj}(\eta_j)$.

The two-qubit gate $\hat{U}_1^{(kj)}(\eta_j)$ (or $\hat{U}_2^{(kj)}(t_2)$) performed above forms a universal set. Any quantum manipulation can be implemented by using one of them, accompanied by arbitrary rotations of single qubits. Obviously, if the system works in the strong charge regime: $E_{J_j}/(\delta E_{C_j}) \ll 1$, and $\cos\eta_j \sim 0$, $\sin\eta_j \sim 1$, then the two-qubit gate $\hat{U}_1^{(kj)}(\eta_j)$ in (22) approximates the well-known controlled-NOT (CNOT) gate

$$\hat{U}_{CNOT}^{(kj)} = \begin{pmatrix} 1 & 0 & 0 & 0 \\ 0 & 1 & 0 & 0 \\ 0 & 0 & 0 & 1 \\ 0 & 0 & 1 & 0 \end{pmatrix}.$$

Also, if the duration t_2 of the evolution $\tilde{U}_2^{(j)}(t_2)$ and the delays τ_1, τ_2 are further set properly such that

$$\cos(\varsigma_j t_2) = \sin(\varsigma_j' t_2) = \sin(\omega_b T) = 1,$$

then the two-qubit operation $\hat{U}_2^{(kj)}$ in (23) reduces to the well-known controlled-phase (CROT) gate

$$\hat{U}_{CROT}^{(kj)} = \begin{pmatrix} 1 & 0 & 0 & 0 \\ 0 & 1 & 0 & 0 \\ 0 & 0 & 1 & 0 \\ 0 & 0 & 0 & -1 \end{pmatrix}.$$

IV. DECOHERENCE OF THE QUBIT-BUS SYSTEM DUE TO THE BIASED VOLTAGE- AND CURRENT-NOISES

An ideal quantum system preserves quantum coherence, i.e., its time evolution is determined by deterministic reversible unitary transformations. Quantum computation requires a long phase coherent time-evolution. In practice, any physical quantum system is subject to various disturbing factors which destroy phase coherence. In fact, solid-state systems are very sensitive to decoherence, as they contain a macroscopic number of degrees of freedom and interact with the environment. However, coherent quantum manipulations of the qubits are still possible if the decoherence time is finite but not too short. Hence, it is important to investigate the effects of the environmental noise on the present quantum circuit.

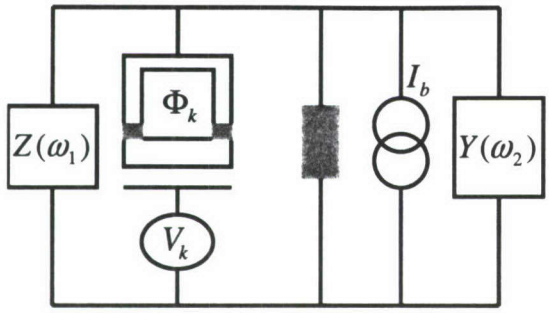

FIG. 2: Schematic diagram of a SQUID-based charge qubit with impedance $Z(\omega_1)$ coupled to a CBJJ with admittance $Y(\omega_2)$.

The typical noise sources in Josephson circuits consist of the linear fluctuations of the electromagnetic environments (e.g., circuitry and radiation noises) and the low-frequency noise due to fluctuations in various charge/current channels (e.g., the "background charge" and "critical current"). Usually, the former one behaves as Ohmic dissipation [35] and the latter one produces a $1/f$ spectrum [36]. Within the present work, we will consider the case of Ohmic dissipation due to linear fluctuations of the external circuit parameters: the bias-current I_b applied to the CBJJ and the gate voltages applied to the qubits. The effect of gate-voltage noise on a single charge qubit and that of bias-current noise on a single CBJJ has been discussed in [11, 35] and in [27], respectively. We now study these noises together (see figure 2), since the interaction between a CBJJ, acting as a bus here, and a selected (e.g., the kth) qubit takes a central role in the present scheme for quantum manipulations. Each electromagnetic environment is treated as a quantum system with many degrees of freedom and modeled by a bath of harmonic oscillators. Furthermore, each of these oscillators is assumed to be weakly coupled to the chosen system. The Hamiltonian of a chosen (kth) qubit coupling to the bus, containing the fluctuations of the applied gate voltage V_k and bias-current I_b, can be generally written as

$$\hat{H} = \bar{\hat{H}}_{kb} + \hat{H}_B + \hat{V},$$

with

$$\begin{aligned} H_B &= \sum_{j=1,2}\sum_{\omega_j}\left[\frac{p_{\omega_j}^2}{2m_{\omega_j}} + \frac{m_{\omega_j}\omega_j^2 x_{\omega_j}^2}{2}\right] \\ &= \sum_{j=1,2}\sum_{\omega_j}\left(\hat{a}_{\omega_j}^\dagger \hat{a}_{\omega_j} + \frac{1}{2}\right)\hbar\omega_j, \end{aligned} \tag{24}$$

and

$$\hat{V} = -\left[\sin\alpha_k \overline{\sigma}_z^{(k)} + \cos\alpha_k \overline{\sigma}_x^{(k)}\right](\hat{R}_1 + \hat{R}_1^\dagger) - (\hat{a}^\dagger R_2 + \hat{a}\hat{R}_2^\dagger), \tag{25}$$

being the Hamiltonians of the two baths and their interactions with the non-dissipative qubit-bus system $\bar{\hat{H}}_{kb}$, respectively. Above, $\hat{a}_{\omega_j}, \hat{a}_{\omega_j}^\dagger$ are the Boson operators of the jth bath, and

$$\hat{R}_1 = \frac{eC_{g_k}}{C_k}\sum_{\omega_1} g_{\omega_1}\hat{a}_{\omega_1}, \quad R_2 = \sqrt{\frac{\hbar}{2\widetilde{C}_b\omega_b}}\sum_{\omega_2} g_{\omega_2}\hat{a}_{\omega_2},$$

with g_{ω_j} being the coupling strength between the oscillator of frequency ω_j and the non-dissipative system. The effects of these noises can be characterized by their power spectra, which in turn depend on the corresponding "impedance" (or "inductance") and the temperature of the relevant circuits. For example, introducing the impedance $Z_t(\omega) = 1/[i\omega C_t + Z^{-1}(\omega)]$ with $Z(\omega) = R_V$ being the Ohmic resistor, the corresponding voltage between the terminals of impedance $Z_t(\omega)$ can be expressed as $\delta V = \sum_{\omega_1}\lambda_{\omega_1}x_{\omega_1}$. Thus, the spectral density of this voltage source for Ohmic dissipation can be expressed as

$$\begin{aligned} G(\omega) &= \pi\sum_{\omega_1}\frac{\lambda_{\omega_1}^2}{2m\omega_1}\delta(\omega-\omega_1) \\ &= \pi\sum_{\omega_1}|g_{\omega_1}|^2\delta(\omega-\omega_1) \sim R_V\omega. \end{aligned} \tag{26}$$

Similarly, the spectral density for the bias-current source can be approximated as

$$F(\omega) = \pi\sum_{\omega_2}|g_{\omega_2}|^2\delta(\omega-\omega_2) \sim Y_I\omega, \tag{27}$$

with Y_I being the dissipative part of the admittance of the current bias.

The well-established Bolch-Redfield formalism [32, 37] offers a systematic way to obtain a generalized master equation for the reduced density matrix of the system, weakly influenced by dissipative environments. A subtle Markov approximation is also made in this theory such that the resulting master equation is local in time. Of course, in the regime of weak bath coupling and low temperatures, this theory is numerically equivalent to a full non-Markovian path-integral approach [38]. For the present qubit-bus system and in the basis spanned by the eigenstates $\{|g\rangle, |u_n\rangle, |v_n\rangle, n = 1, 2, ...\}$ of the non-dissipative Hamiltonian $\bar{\hat{H}}_{kb}$, the Bloch-Redfield theory leads to the following master equations

$$\frac{d\sigma_{\alpha\beta}}{dt} = -i\omega_{\alpha\beta}\sigma_{\alpha\beta} + \sum_{\mu,\nu}(R_{\alpha\beta\mu\nu} + S_{\alpha\beta\mu\nu})\,\sigma_{\mu\nu}, \tag{28}$$

with

$$R_{\alpha\beta\mu\nu} = -\frac{1}{\hbar^2}\int_0^\infty d\tau \times \left[g_1(\tau)\left(\delta_{\beta\nu}\sum_\kappa A_{\alpha\kappa}A_{\kappa\mu}e^{i\omega_{\mu\kappa}\tau} - A_{\alpha\mu}A_{\nu\beta}e^{i\omega_{\mu\alpha}\tau}\right)\right.$$
$$\left. + \; g_1(-\tau)\left(\delta_{\alpha\mu}\sum_\kappa A_{\nu\kappa}A_{\kappa\beta}e^{i\omega_{\kappa\nu}\tau} - A_{\alpha\mu}A_{\nu\beta}e^{i\omega_{\beta\nu}\tau}\right)\right], \tag{29}$$

and

$$S_{\alpha\beta\mu\nu} = -\frac{1}{\hbar^2}\int_0^\infty d\tau \times \left[g_2^\dagger(\tau)\left(\delta_{\beta\nu}\sum_\kappa B_{\alpha\kappa}^\dagger B_{\kappa\mu}e^{i\omega_{\mu\kappa}\tau} - B_{\alpha\mu}B_{\nu\beta}^\dagger e^{i\omega_{\mu\alpha}\tau}\right)\right.$$
$$+ \; g_2^\dagger(-\tau)\left(\delta_{\alpha\mu}\sum_\kappa B_{\nu\kappa}^\dagger B_{\kappa\beta}e^{i\omega_{\kappa\nu}\tau} - B_{\alpha\mu}B_{\nu\beta}^\dagger e^{i\omega_{\beta\nu}\tau}\right)$$
$$+ \; g_2^-(\tau)\left(\delta_{\beta\nu}\sum_\kappa B_{\alpha\kappa}B_{\kappa\mu}^\dagger e^{i\omega_{\mu\kappa}\tau} - B_{\alpha\mu}^\dagger B_{\nu\beta}e^{i\omega_{\mu\alpha}\tau}\right)$$
$$\left. + \; g_2^-(-\tau)\left(\delta_{\alpha\mu}\sum_\kappa B_{\nu\kappa}B_{\kappa\beta}^\dagger e^{i\omega_{\beta\kappa}\tau} - B_{\alpha\mu}^\dagger B_{\nu\beta}e^{i\omega_{\beta\nu}\tau}\right)\right], \tag{30}$$

with

$$\begin{cases} g_1(\pm\tau) = \left(\frac{eC_{g_k}}{C_k}\right)^2 \sum_{\omega_1} |g_{\omega_1}|^2[\langle n(\omega_1)+1\rangle e^{\mp i\omega_1\tau} + \langle n(\omega_1)\rangle e^{\pm i\omega_1\tau}], \\ g_2^\dagger(\pm\tau) = \left(\frac{\hbar}{2\tilde{C}_b\omega_b}\right)\sum_{\omega_2}|g_{\omega_2}|^2\langle n(\omega_2)+1\rangle e^{\mp i\omega_2\tau}, \\ g_2^-(\pm\tau) = \left(\frac{\hbar}{2\tilde{C}_b\omega_b}\right)\sum_{\omega_2}|g_{\omega_2}|^2\langle n(\omega_2)\rangle e^{\mp i\omega_2\tau}. \end{cases}$$

Above, each one of the states $|\alpha\rangle, |\beta\rangle, \ldots$ can be equal to one of the eigenstates of $\bar{\hat{H}}_{kb}$. $\langle n(\omega_j)\rangle = 1/[\exp(\hbar\omega_j/k_BT) - 1]$ is the average number of thermal photons in the mode of frequency ω_j. The denotation $x_{ab} = \langle\alpha|\hat{x}|\beta\rangle$ accounts for the matrix element of operator $\hat{x}$, i.e.,

$$A_{\alpha\beta} = \langle\alpha|\hat{A}_k|\beta\rangle, \;\; \hat{A}_k = \overline{\sigma}_z^{(k)}\sin\alpha_k + \overline{\sigma}_x^{(k)}\cos\alpha_k = \sigma_z^{(k)},$$

and

$$B_{\alpha\beta} = \langle\alpha|\hat{a}|\beta\rangle, \;\; B_{\alpha\beta}^\dagger = \langle\alpha|\hat{a}^\dagger|\beta\rangle.$$

Also, $\omega_{\alpha\beta} = (E_\alpha - E_\beta)/\hbar$ with E_α (E_β) being one of eigenvalues of the non-dissipative Hamiltonian $\bar{\hat{H}}_{kb}$, corresponding to the eigenstate $|\alpha\rangle$ ($|\beta\rangle$). The spectrum of $\bar{\hat{H}}_{kb}$ includes the ground state $|g\rangle = |-_k, 0\rangle$, corresponding to the energy $E_g = -\hbar\overline{\Delta}_k/2$, and a series of dressed doubled states

$$\begin{cases} |u_n\rangle = \cos\theta_n|+_k, n\rangle - i\sin\theta_n|-_k, n+1\rangle, \\ |v_n\rangle = -i\sin\theta_n|+_k, n\rangle + \cos\theta_n|-_k, n+1\rangle \end{cases}$$

corresponding to the eigenvalues

$$E_{u_n} = \hbar\omega_b(n+1) - \frac{\rho_n}{2}, \;\; E_{v_n} = \hbar\omega_b(n+1) + \frac{\rho_n}{2},$$

with

$$\cos\theta_n = \rho_n - \hbar\overline{\Delta}_k/\sqrt{(\rho_n - \hbar\overline{\Delta}_k)^2 + 4\lambda_k^2(n+1)},$$

and

$$\rho_n = \sqrt{(\hbar\overline{\Delta}_k)^2 + 4\lambda_k^2(n+1)}.$$

Here, $|\pm_k\rangle$ and $|n\rangle$ are the eigenstates of the operators $\overline{\sigma}_z^{(k)}$ and $\hat{H}_b$ with eigenvalues ± 1 and $\hbar\omega_b(n+1/2)$, respectively.

Under the secular approximation, the evolution of the non-diagonal element $\sigma_{\alpha\beta}$ of the reduced density matrix σ is determined by

$$\frac{d}{dt}\sigma_{\alpha\beta} + \{i[\omega_{\alpha\beta} + \mathrm{Im}(R_{\alpha\beta\alpha\beta}) + \mathrm{Im}(S_{\alpha\beta\alpha\beta})] + [\mathrm{Re}(R_{\alpha\beta\alpha\beta}) + \mathrm{Re}(S_{\alpha\beta\alpha\beta})]\}\sigma_{\alpha\beta} = 0. \quad (31)$$

Here, $R_{\alpha\beta\mu\nu}$ and $S_{\alpha\beta\mu\nu}$ are calculated respectively from $R_{\alpha\beta\mu\nu}$ and $S_{\alpha\beta\mu\nu}$ by setting $\mu = \alpha$ and $\nu = \beta$. $\mathrm{Re}(x)$ and $\mathrm{Im}(x)$ represent the real- and imaginary parts of the complex number x. The formal solution of the above differential equation (31) reads

$$\sigma_{\alpha\beta}(t) = \sigma_{\alpha\beta}(0)\exp\left(-T_{\alpha\beta}^{-1}t\right)\exp\left(-i\Theta_{\alpha\beta}t\right), \quad (32)$$

with $\Theta_{\alpha\beta} = \omega_{\alpha\beta} + \mathrm{Im}(R_{\alpha\beta\alpha\beta}) + \mathrm{Im}(S_{\alpha\beta\alpha\beta})$ being the effective oscillating frequency (the original Bohr frequency $\omega_{\alpha\beta}$ plus the Lamb shift $\Delta\omega_{\alpha\beta} = \mathrm{Im}R_{\alpha\beta\alpha\beta} + \mathrm{Im}S_{\alpha\beta\alpha\beta}$), and

$$T_{\alpha\beta}^{-1} = -[\mathrm{Re}(R_{\alpha\beta\alpha\beta}) + \mathrm{Re}(S_{\alpha\beta\alpha\beta})] \quad (33)$$

describing the rate of decoherence between the states $|\alpha\rangle$ and $|\beta\rangle$.

In the present qubit-bus system operating near the resonant point: $E_k \sim \hbar\omega_b$, the decoherences relating to the lowest three energy eigenstates, i.e., $|g\rangle, |u_0\rangle = |u\rangle$, and $|v_0\rangle = |v\rangle$, are specially important for the desired quantum manipulations. The decoherences outside these three states are negligible. After a long but direct derivation, we obtain the decoherence rates of interest:

$$T_{gu}^{-1} = \alpha_V\left\{4\left(\sin\alpha_k\cos^2\theta_0\right)^2\frac{2k_BT}{\hbar} + 2\left(\cos\alpha_k\cos\theta_0\right)^2\coth\left(\frac{\hbar\omega_{ug}}{2k_BT}\right)\omega_{ug} + \left(\cos\alpha_k\sin\theta_0\right)^2\left[\coth\left(\frac{\hbar\omega_{vg}}{2k_BT}\right) - 1\right]\omega_{vg} + \left(\sin\alpha_k\sin 2\theta_0\right)^2\left[\coth\left(\frac{\hbar\omega_{vu}}{2k_BT}\right) - 1\right]\omega_{vu}\right\} + \alpha_I\sin^2\theta_0\left\{\coth\left(\frac{\hbar\omega_{ug}}{2k_BT}\right) + 1\right\}\omega_{ug}, \quad (34)$$

$$T_{gv}^{-1} = \alpha_V\left\{4\left(\sin\alpha\sin^2\theta_0\right)^2\frac{2k_BT}{\hbar} + 2\left(\cos\alpha\sin\theta_0\right)^2\coth\left(\frac{\hbar\omega_{vg}}{2k_BT}\right)\omega_{vg} + \left(\cos\alpha\cos\theta_0\right)^2\left[\coth\left(\frac{\hbar\omega_{ug}}{2k_BT}\right) - 1\right]\omega_{ug} + \left(\sin\alpha\sin 2\theta_0\right)^2\left[\coth\left(\frac{\hbar\omega_{vu}}{2k_BT}\right) + 1\right]\omega_{vu}\right\} + \alpha_I\cos^2\theta_0\left\{\coth\left(\frac{\hbar\omega_{vg}}{2k_BT}\right) + 1\right\}\omega_{vg}, \quad (35)$$

and

$$T_{uv}^{-1} = \alpha_V\left\{4\left(\sin\alpha\cos 2\theta_0\right)^2\frac{2k_BT}{\hbar} + 2\left(\sin\alpha\sin 2\theta_0\right)^2\coth\left(\frac{\hbar\omega_{vu}}{2k_BT}\right)\omega_{vu} + \left(\cos\alpha\cos\theta_0\right)^2\left[\coth\left(\frac{\hbar\omega_{ug}}{2k_BT}\right) + 1\right]\omega_{ug} + \left(\cos\alpha\sin\theta_0\right)^2\left[\coth\left(\frac{\hbar\omega_{vg}}{2k_BT}\right) + 1\right]\omega_{vg}\right\} + \alpha_I\left\{\sin^2\theta_0\left[\coth\left(\frac{\hbar\omega_{ug}}{2k_BT}\right) + 1\right]\omega_{ug} + \cos^2\theta_0\left[\coth\left(\frac{\hbar\omega_{vg}}{2k_BT}\right) + 1\right]\omega_{vg}\right\}. \quad (36)$$

Above, the various Bohr frequencies read

$$\omega_{ug} = \omega_b/2 + E_k/(2\hbar) - \sqrt{(\hbar\omega_b - E_k)^2 + 4\lambda_k^2}/(2\hbar),$$

$$\omega_{vg} = \omega_b/2 + E_k/(2\hbar) + \sqrt{(\hbar\omega_b - E_k)^2 + 4\lambda_k^2}/(2\hbar),$$

and

$$\omega_{vu} = \sqrt{(\hbar\omega_b - E_k)^2 + 4\lambda_k^2}/\hbar.$$

Two dimensionless parameters $\alpha_V = \pi R_V C_{g_k}^2/[R_K C_k^2]$, $R_K = h/e^2 \approx 25.8\ k\Omega$ and $\alpha_I = Y_I/(\widetilde{C}_b\omega_b)$ characterize the coupling strengths between the environments and the system.

Specially, if the system works far from the resonant point (with $\lambda_k \sim 0$, achieved by switching off the Josephson energy), the above results (shown in Eqs. (34-36)) reduce to those [11, 27, 35] for the case when the qubit and the bus independently decohere. Namely, T_{gu}^{-1} reduces to the rate [11]

$$T_{\uparrow\downarrow}^{-1} = 8\alpha_V k_B T/\hbar,$$

which describes the decoherence between two charge states $|\downarrow\rangle$ and $|\uparrow\rangle$ of the superconducting box with zero Josephson energy. Also, T_{gv}^{-1} reduces to the decoherent rate [27]

$$T_{01}^{-1} = \alpha_I[\coth(\hbar\omega_b/2k_BT) + 1]\omega_b,$$

between the ground and first excited states of the data bus. However, for the strongest coupling case (i.e., when the system works at the resonant point), we have $E_k = E_{J_k} = \hbar\omega_b, \cos\alpha_k = 1, \cos\theta_0 = \sin\theta_0 = 1/\sqrt{2}$, and $\coth[\hbar\omega_{ug}/(2k_BT)] - 1 \simeq \coth[\hbar\omega_{vg}/(2k_BT)] - 1 \sim 0\ (< 10^{-7}$, for the typical experimental parameters [12]: $\lambda_k \simeq 0.1E_{J_k}$, $E_{J_k} = \hbar\omega_b \simeq 50\mu eV \gg k_BT \simeq 3\mu eV)$. Thus, the minimum decoherent rates

$$\widetilde{T}_{gu}^{-1} = (\alpha_V + \alpha_I)\omega_{ug}, \tag{37}$$

$$\widetilde{T}_{gv}^{-1} = (\alpha_V + \alpha_I)\omega_{vg}, \tag{38}$$

and

$$\widetilde{T}_{uv}^{-1} = \widetilde{T}_{gu}^{-1} + \widetilde{T}_{gv}^{-1}, \tag{39}$$

are obtained for the above three dressed states, respectively.

It has been estimated in Ref. [11] that the dissipation for a single SQUID-qubit is sufficiently weak: $\alpha_V \sim 10^{-6}$ for $R_V = 50\Omega$, $C_{J_k}/C_{g_k} \sim 10^{-2}$, which allows, in principle, for 10^6 coherent single-qubit manipulations. For a single CBJJ the dimensionless parameter α_I only reaches 10^{-3} for typical experimental parameters [25]: $1/Y_I \sim 100\ \Omega$, $C_b \sim 6\ pF$, $\omega_b/2\pi \sim 10\,GHz$. This implies that the quantum coherence of the present qubit-bus system is mainly limited by the bias-current fluctuations. Fortunately, the impedance of the above CBJJ can be engineered [25] to be $1/Y_I \sim 560\ k\Omega$. This lets α_I reach up to 10^{-5} and allow about 10^5 coherent manipulations of the qubit-bus system.

V. CONCLUSIONS AND DISCUSSIONS

In summary, we have proposed an effective scheme to couple any pair of selective Josephson charge qubits by letting them sequentially couple to a common CBJJ, which can be treated as an oscillator with adjustable frequency. Two logic states of the present qubit are encoded by the clockwise and anti-clockwise persistent circuiting currents in the dc SQUID-loop. At most one qubit can be set to interact with the bus at any moment. The interaction between the selected qubit and the data bus is tunable by controlling the flux applied to the qubit and the bias-current applied to the data bus. This selective coupling provides a simple way to manipulate the quantum information stored in the connected SQUID-qubits. Indeed, any pair of selective qubits without any direct interaction can be entangled by using a three-step coupling process. Furthermore, if the total duration is set up properly, the desired two-qubit universal gates, which are very similar to the CNOT- and CROT gates, can be implemented via such three-step operational processes. During this operation, the mode of the data bus is unchanged, although its vibrational quantum is really excited/absorbed. After the desired quantum operation is performed on the chosen qubits, the data bus disentangles from the qubits and returns to its ground state.

In previous schemes, the distant Josephson qubits are coupled directly by either the charge-charge interaction, via connecting to a common capacitor, or by a current-current interaction, via sharing a common inductor. The present indirect coupling scheme offers some advantages: i) the coupling strength is tunable and thus easy to be controlled for realizing the desired quantum gate, ii) this first-order interaction is more insensitive to the environment, and thus possesses a longer decoherence time. Also, compared to previous data buses, the externally connected LC-resonator [19] and cavity QED mode [20], the present CBJJ bus might be easier to control for coupling the chosen qubit. For example, its eigenfrequency can be controlled by adjusting the applied dc bias-current. In addition, the CBJJ is easy to fabricate using current technology [22] and may provide more effective immunities to both charge and flux noise.

By considering the decoherence due to the linear fluctuations of the applied voltage V_k and current I_b, we have analyzed the experimental possibility of the present scheme within the Bloch-Redfield formalism. A simple numerical estimate showed that the quantum manipulations of the present qubit-bus system are experimentally possible, once the impedance Y_I of the CBJJ can be engineered to have a sufficient low value, i.e., $1/Y_I$ can be enlarged sufficiently (e.g., $1/Y_I \sim 560\,K\ \Omega$ [25]). Of course, this possibility, like those in previous schemes [17, 18, 19, 20, 21], is also limited by other technological difficulties, e.g., suppress the low-frequency $1/f$ noise, and fast switch on/off the external flux to couple/decouple the chosen qubit, etc.. For example, a very high sweep rate of magnetic pulse (e.g., up to $\sim 10^8$ Oe/s [39]), is required to change half of flux quantum through a SQUID-loop (with the size e.g., $50\mu m$) in a sufficiently short time (e.g., the desired ~ 40 ps). This and other obstacles pose a challenge that motivate the exploration of novel circuit designs that might minimize some of the problems that lie ahead in the future.

Acknowledgments

This work was supported in part by the National Security Agency (NSA) and Advanced Research and Development Activity (ARDA) under Air Force Office of Research (AFOSR) contract number F49620-02-1-0334, and by the National Science Foundation grant No. EIA-0130383.

[1] See, e.g., M.A. Nielsen, I.L. Chuang, *Quantum Computation and Quantum Information*, (Cambridge University Press, Cambridge, 2000); C.H. Bennett and D.P. DiVincenzo, Nature **44**, 247 (2000).

[2] J.I. Cirac and P. Zoller, Phys. Rev. Lett. **74** (1995) 4091.

[3] L.F. Wei and F. Nori, Europhys. Lett. (2004); L.F. Wei, S.Y. Liu and X.L. Lei, Phys. Rev. A **65**, 062316 (2002).

[4] D. J. Wineland, M. Barrett, J. Britton, J. Chiaverini, B. L. DeMarco, W. M. Itano, B. M. Jelenkovic, C. Langer, D. Leibfried, V. Meyer, T. Rosenband, and T. Schaetz, Phil. Trans. Royal Soc. London A **361**, 1349 (2003).

[5] T. Sleator and H. Weinfurter, Phys. Rev. Lett. **74**, 4087(1995).

[6] J. M. Raimond, M. Brune, and S. Haroche, Rev. Mod. Phys. **73**, 565 (2001).

[7] X. Hu and S. Das Sarma, Phys. Stat. Sol. (b) 238, 360-365 (2003); Phys. Rev. A **61**, 062301 (2000); X. Hu, R. de Sousa, and S. Das Sarma, Phys. Rev. Lett. **86**, 918 (2001).

[8] T.H. Stievater, X. Li, D.G. Steel, D. Gammon, D.S. Katzer, D. Park, C. Piermarocchi, and L.J. Sham, Phys. Rev. Lett. 87, 133603 (2001).

[9] N. Gershenfeld and I. Chuang, Science **275**, 350(1997).

[10] L.M.K. Vandersypen *et al*, Nature **414**, 883 (2001); Phys. Rev. Lett. **85**, 5452 (2000).

[11] Y. Makhlin, G. Schön, and A. Shnirman, Rev. Mod. Phys. **73**, 357 (2001).

[12] Y. Nakamura, Yu.A. Pashkin, and J.S. Tsai, Nature **398**, 786 (1999); K.W. Lehner *et al.*, Phys. Rev. Lett. **90**, 027002 (2003).

[13] J.E. Mooij, T.P. Orlando, L. Levitov, L. Tian, C.H. van der Wal, and S. Lloyd, Science **285**, 1036 (1999); **290**, 773 (2000); E. Il'ichev, N. Oukhanski, A. Izmalkov, Th. Wagner, M. Grajcar, H.-G. Meyer, A. Yu. Smirnov, A. M. van den Brink, M.H.S. Amin, and A.M. Zagoskin, Phys. Rev. Lett. **91**, 097906 (2003).

[14] D. Vion, A. Aassime, A. Cottet, P. Joyez, H. Pothier, C. Urbina, D. Esteve, and M.H. Devoret, Science **296**, 886 (2002).

[15] Yu.A. Pashkin, T. Yamamoto, O. Astafiev, Y. Nakamura, D.V. Averin, and J.S. Tsai, Nature **421**, 823 (2003); T. Yamamoto, Yu.A. Pashkin, O. Astafiev, Y. Nakamura, and J.S. Tsai, Nature **425**, 941 (2003).

[16] D.V. Averin and C. Bruder, Phys. Rev. Lett. **91**, 057003 (2003).

[17] Y. Makhlin, G. Schön, and A. Shnirman, Nature **398**, 305 (1999).

[18] J.Q. You, J.S. Tsai, and F. Nori, Phys. Rev. Lett. **89**, 197902 (2002). A longer version of this is available in cond-mat/0306203; see also *New Directions in Mesoscopic Physics*, edited by R. Fazio, V.F. Gantmakher, and Y. Imry (Kluwer Academic Publishers, 2003), page 351.

[19] F. Plastina and G. Falci, Phys. Rev. B **67**, 224514 (2003).

[20] J.Q. You and F. Nori, Phys. Rev. B **68**, 064509 (2003); Physica E, **18**, 33 (2003); S.L. Zhu, Z.D. Wang, and K. Yang, Phys. Rev. A **68**, 034303 (2003); C.-P. Yang and S.-I Chu, *ibid.* **67**, 042311 (2003).

[21] A. Blais, A.M. van den Brink, and A.M. Zagoskin, Phys. Rev. Lett. **90**, 127901 (2003).

[22] R.C. Ramos, M.A. Gubrud, A.J. Berkley, J.R. Anderson, C.J. Lobb, F.C. Wellstood, IEEE Trans. Appl. Supercond. **11**, 998 (2001).

[23] J. Clarke, A.N. Cleland, M.H. Devoret, D. Esteve, and J.M. Martinis, Science **239**, 992 (1988).

[24] A. Wallraff, T. Duty, A. Lukashenko, and A.V. Ustinov, Phys. Rev. Lett. **90**, 037003 (2003); P. Silvestrini, V.G. Palmieri, B. Ruggiero, and M. Russo, Phys. Rev. Lett. **79**, 3046 (1997).

[25] J.M. Martinis, S. Nam, J. Aumentado, and C. Urbina, Phys. Rev. Lett. **89**, 1179 (2002).

[26] Y. Yu, S.Y. Han, X. Chu, S.-I Chu, and Z. Wang, Science **296**, 889 (2002).

[27] J.M. Martinis, S.Nam, J. Aumentado, K.M. Lang, and C. Urbina, Phys. Rev. B **67**, 094510 (2003).

[28] A.J. Berkley, H. Xu, R.C. Ramos, M.A. Gubrud, F.W. Strauch, P.R. Johnson, J.R. Anderson, A.J. Dragt, C.J. Lobb, and F.C. Wellstood, Science **300**, 1548 (2003).

[29] F.W. Strauch, P.R. Johnson, A.J. Dragt, C.J. Lobb, J.R. Anderson, and F.C. Wellstood, Phys. Rev. Lett. **91**, 167005 (2003).

[30] H.Y. Fan, Phys. Lett. A **289**, 172 (2001).

[31] Yu-xi Liu, L.F. Wei, and F. Nori, quant-ph/0407197.

[32] P.N. Argyres and P.L. Kelley, Phys. Rev. **134**, A98 (1964).

[33] J.M. Martinis, M.H. Devoret, and J. Clarke, Phys. Rev. B**35**, 4682 (1987).

[34] A. Barenco, C.H. Bennett, R. Cleve, D.P. DiVincenzo, N. Margolus, P. Shor, T. Sleator, J.A. Smolin, and H. Weinfurter, Phys. Rev. A **52**, 3457 (1995).

[35] U. Weiss, Quantum Dissipative systems, 2nd ed., World Scientific, Singapore, 1999.

[36] E. Paladino, L. Faoro, G. Falci, and R. Fazio, Phys. Rev. Lett. **88**, 228304 (2002).

[37] M.C. Goorden and F.K. Wilhelm, Phys. Rev. B **68**, 012508 (2003).

[38] L. Hartmann, I. Goychuk, M. Grifoni, and P. Hänggi, Phys. Rev. E **61**, R4687 (2000).

[39] H. Uwazumi, T. Shimatsu, and Y. Kuboki, J. Appl. Phys. **91**, 7095 (2002).

Effects of dynamical phases in Shor's factoring algorithm with operational delays

L.F. Wei,[1,2] Xiao Li,[3,4] Xuedong Hu,[1,5] and Franco Nori[1,6]

[1] *Frontier Research System, The Institute of Physical and Chemical Research (RIKEN), Wako-shi, Saitama, 351-0198, Japan*
[2] *Institute of Quantum Optics and Quantum Information, Department of Physics, Shanghai Jiaotong University, Shanghai 200030, P.R. China*
[3] *Department of Physics, Shanghai Jiaotong University, Shanghai 200030, P.R. China*
[4] *Department of Physics, PMB 179, 104 Davey Laboratory, Penn State University, University Park, PA 16802-6300, USA*
[5] *Department of Physics, University at Buffalo, SUNY, Buffalo NY14260-1500, USA*
[6] *Center of Theoretical Physics, Physics Department, Center for the Study of Complex Systems, University of Michigan, Ann Arbor, Michigan 48109-1120, USA**

(Dated: August 4, 2004)

Ideal quantum algorithms usually assume that quantum computing is performed continuously by a sequence of unitary transformations. However, there always exist idle finite time intervals between consecutive operations in a realistic quantum computing process. During these delays, coherent "errors" will accumulate from the dynamical phases of the superposed wave functions. Here we explore the sensitivity of Shor's quantum factoring algorithm to such errors. Our results clearly show a severe sensitivity of Shor's factorization algorithm to the presence of delay times between successive unitary transformations. Specifically, in the presence of these *coherent "errors"*, the probability of obtaining the correct answer decreases exponentially with the number of qubits of the work register. A particularly simple phase-matching approach is proposed in this paper to *avoid* or suppress these *coherent errors* when using Shor's algorithm to factorize integers. The robustness of this phase-matching condition is evaluated analytically or numerically for the factorization of several integers: 4, 15, 21, and 33.

PACS numbers: 03.67.Lx

I. INTRODUCTION

Building a practical quantum information processor has attracted considerable interest during the past decade [1]. With the resources provided by quantum mechanics, such as superposition and entanglement, a quantum computer could achieve a significant speedup for certain computational tasks. The most prominent example is Shor's factoring algorithm [2, 3], which allows an exponential speedup over the known classical algorithms. The proposed quantum algorithms are constructed assuming that all quantum operations can be performed precisely. In reality, any physical realization of such a computing process must treat various errors arising from various noise and imperfections (see, e.g., [4]). Physically, these errors can be distinguished into two different kinds: incoherent and coherent errors. The incoherent errors originate from the coupling of the quantum information processor to an uncontrollable external environment, which is stochastic, and results in decoherence. Coherent errors usually arise from non-ideal quantum gates which lead to unitary but non-ideal temporal evolutions of a quantum computer. So far, most previous works (see, e.g., [5, 6, 7, 8, 9]) have been concerned with quantum errors arising from the decoherence due to interactions with the external environment and external operational imperfections. Here, we focus instead on internal ones. The coherent errors we consider here are related to the *intrinsic* dynamical evolution of the qubits *between* operations.

A quantum computing process generally consists of a sequence of quantum unitary operations. These transformations are usually applied to the superposition states so that the quantum computer evolves from an input initial state to the desired final state. If the two qubit levels have different energies, as it is usually the case, the superposition wave function of the quantum register undergoes fast coherent oscillations during the finite time delay between two consecutive operations. These oscillation, if not controlled, can spoil the correct computational results expected from the ideal quantum algorithms, where operational delays are neglected.

In principle, these coherent errors can be either (1) avoided by tuning the relevant energy splittings of the qubits to zero [10, 11]; or (2) eliminated by introducing a "natural" phase induced by using a stable continuous reference oscillation for each quantum transition in the computing process [12]. Experimentally, for example in NMR systems (see, e.g., [3, 13]), these errors were usually corrected by introducing two additional operations before and after the delay to reverse each undesired free evolution.

In this paper we perform a quantitative assessment of the effects of the dynamical phases in Shor's algorithm by realistically assuming that operational delays, between successive unitary transformations, exist throughout the computation. We explore a phase-matching approach to deal with the dynamical phase problem. We show that coherent "errors" due to these phases, acquired by the dynamical evolution of the superposed wavefunction during the operational delays, may be avoided by properly setting the *total* delay. We then carefully evaluate the robustness of such a phase-matching condition, focusing on its dependence on the number of qubits, the length of the delay, and the fluctuations in the qubit energy splitting. Our discussions are in the context of

*Permanent address

Shor's algorithm, but can be extended to other quantum algorithms, such as the phase estimation and other algorithms [14]. For simplicity and clarity, here we assume that the influence of the environmental decoherence and the gate imperfections on the computing process are negligible.

The paper is organized as follows. In Section II, we present a decomposition of Shor's algorithm and explain how we incorporate the dynamical phases into the realization of this algorithm. The usual decompositions of quantum algorithms into consecutive elementary gates are strictly limited by the short decoherence time. Here, we reconstruct the standard Shor's algorithm out of four functional unitary transformations, and only consider the operational delays between these larger building blocks. We assume that each block can be exactly performed by only one-time evolution as a multi-qubit gate (see, e.g., [15, 16]), avoiding the existing idle time inside it. It is shown that the effects of dynamical phases are not negligible, even in this primary or "coarse-grained" decomposition. In Section III, we numerically evaluate several examples to illustrate the phase-matching condition, and establish a clear relationship between this condition and the equivalence of the Schrödinger picture and the interaction picture description of a physical system. We also demonstrate the robustness of the phase-matching condition by varying the number of qubits involved, the delay duration, and distribution of qubit energy splitting. Finally, in section IV we present some conclusions and discussions from our numerical studies.

II. FOUR-BLOCK DECOMPOSITION OF SHOR'S ALGORITHM WITH OPERATIONAL DELAYS

We study the dynamical phase problem in the context of Shor's factoring algorithm. In Shor's algorithm [2], the factorization of a given number N is based on calculating the period of the function $f(x) = a^x \bmod N$ quantum mechanically for a randomly selected number a $(1 < a < N)$ coprime with N. Here $y \bmod N$ is the remainder when y is divided by N. The order r of $a \bmod N$ is the smallest integer r such that $a^r \bmod N = 1$. Once r is known, factors of N are obtained by calculating the greatest common divisor of N and $y^{r/2} \pm 1$. A quantum computer can find r efficiently by a series of quantum operations on two quantum registers W and A. One is the work register W with L qubits, in which the job of finding the order is done; while the values of the function $f(x)$ are stored in the auxiliary register A with L' qubits. The sizes of the work and auxiliary registers are chosen as the integers satisfying the inequalities $N^2 < q = 2^L < 2N^2$ and $2^{L'-1} < N < 2^{L'}$. Here q is the Hilbert space dimension of the work register.

As shown in figure 1, a realistic implementation of Shor's algorithm can be decomposed into the following unitary transformations:

1) Initialize the work register in an equal-weight superposition of all the logical states, and the auxiliary register in its logical ground state $|0\rangle_A$. Initially, each work qubit is in its logical ground state $|0\rangle$. Assuming that a Hadamard gate H is applied to each qubit in the work register at one time, the

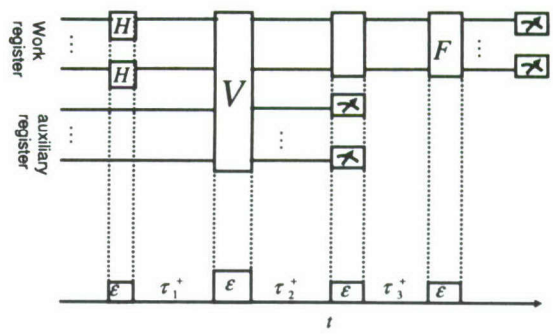

FIG. 1: Quantum circuit for implementing Shor's algorithm with time delays τ_j^+ $(j = 1, 2, 3)$ between the successive operations. Here H refers to a Hadamard gate, while F refers to a quantum Fourier transformation. Each block operation is assumed to be exactly performed in a very short time interval ϵ (so that phases accumulated during the operations are either accounted for by the operations themselves or simply neglected).

computational initial state of the system becomes:

$$|\Psi(0)\rangle = \frac{1}{\sqrt{q}} \sum_{j=0}^{q-1} |j\rangle_W \otimes |0\rangle_A .$$

Here, the subindex W stands for the work register state, and the subindex A for the auxiliary register. After a finite time delay τ_1, and right before the second unitary transformation is applied, the initial state $|\Psi(0)\rangle$ of the whole system evolves to

$$|\Psi(\tau_1)\rangle = \frac{1}{\sqrt{q}} \sum_{j=0}^{q-1} e^{-iE_j\tau_1} |j\rangle_W \otimes e^{-iE_0\tau_1} |0\rangle_A , \qquad (1)$$

with E_j being the energy of state $|j\rangle$ and $\hbar = 1$. Here, τ_m $(m = 1, 2, 3, ...)$ denotes the time interval between the $(m-1)$th and mth unitary operations. $\tau_m^+ = \tau_m + \epsilon$ with $\epsilon \ll \tau_m$ being the operational time of the mth unitary transformation, here assumed to be extremely small compared to other time scales. In other words, τ_m^+ refers to the time interval between the end of $(m-1)$th operation and the end of the mth operation. In what follows, the global dynamical phase $\exp(-iE_0\tau_1)$ will be omitted as it does not have any physical meaning.

2) Calculate the function $f_{N,a}(j) = a^j \bmod N$ and then entangle the work $\{|j\rangle_W\}$ and auxiliary registers $|f_{a,N}(s)\rangle_A$ by applying a joint operation $\hat{V}$. After another finite-time delay τ_2 before the next step (i.e., the third unitary transformation), the entangled state of the whole system becomes

$$|\Psi(\tau_1^+ + \tau_2)\rangle = \frac{1}{\sqrt{q}} \sum_{s=0}^{r-1} |\psi\rangle_W \otimes |\phi\rangle_A , \qquad (2)$$

where

$$|\phi\rangle_A = \exp[-iE_{f_{a,N}(s)}\tau_2] \; |f_{a,N}(s)\rangle_A ,$$

and

$$|\psi\rangle_W = \sum_{l=0}^{w} \exp[-iE_{(lr+s)}(\tau_1^+ + \tau_2)]\ |lr+s\rangle_W ,$$

with $w = [(q-s-1)/r]$ being the largest integer less than $(q-s-1)/r$. The dynamical phases of the qubits in the work register, before and after the joint operation $\hat{V}$, can be added directly, as this operator is diagonal in the logical basis.

3) Measure the auxiliary register $|\phi\rangle_A$ in its computational basis $\{|j\rangle_A\}$. After this operation, the state of the whole system becomes $|\Psi(\tau_1^+ + \tau_2^+)\rangle = |\psi(\tau_1^+ + \tau_2^+)\rangle_W \otimes |\phi(\tau_1^+ + \tau_2^+)\rangle_A$. In other words, the work and auxiliary registers disentangle and the work register collapses to one of its periodic states $|\psi(\tau_1^+ + \tau_2^+)\rangle_W$.

For example, if the measurement on the auxiliary register $|\phi\rangle_A$ gives a value $A_s = a^s \bmod N$, then the work register immediately becomes

$$|\psi(\tau_1^+ + \tau_2^+)\rangle_W = \frac{1}{\sqrt{w+1}} \sum_{l=0}^{w} \exp[-iE_{(lr+s)}(\tau_1^+ + \tau_2^+)]\ |lr+s\rangle_W .$$

After the third unitary transformation is applied, there is a third time delay τ_3. The state $|\psi(\tau_1^+ + \tau_2^+)\rangle_W$ now evolves to

$$|\psi(\tau_1^+ + \tau_2^+ + \tau_3)\rangle_W = \frac{1}{\sqrt{w+1}} \sum_{l=0}^{w} \exp\left[-iE_{(lr+s)}(\tau_1^+ + \tau_2^+ + \tau_3)\right]\ |lr+s\rangle_W . \tag{3}$$

Because of the collapse of the wavefunction $|\Psi(\tau_1^+ + \tau_2)\rangle$ in Eq. (2), the dynamical phases accumulated by the wavefunction $|\phi\rangle_A$ of the auxiliary register do not affect the algorithm anymore, as the relevant phase $\exp[-iE_{f_{a,N}(s)}\tau_2^+]$ becomes a global phase.

4) Perform the fourth unitary transformation: the quantum Fourier transform (F-Transformation) on the work register $|\psi\rangle_W$, so that information regarding the order r of $a \bmod N$ (i.e., the smallest integer r such that $a^r \bmod N = 1$) can be more easily extracted. After the F-Transformation the state of the work register becomes

$$|\psi(\tau)\rangle_W = \frac{1}{\sqrt{q}} \sum_{k=0}^{q-1} g(k)\,|k\rangle_W ,$$

with

$$\tau = \tau_1^+ + \tau_2^+ + \tau_3^+ ,$$

being the time after applying the fourth unitary transformation, and

$$g(k) = \frac{\exp(2\pi isk/q)}{\sqrt{w+1}} \sum_{l=0}^{w} \exp\left[-iE_{(lr+s)}\tau + 2\pi ilk\frac{l}{q}\right] .$$

After another delay time τ_4, i.e., right before applying the fifth unitary transformation, the work register evolves into

$$|\psi(\tau+\tau_4)\rangle_W = \frac{1}{\sqrt{q}} \sum_{k=0}^{q-1} g(k)\, e^{-iE_k\tau_4}\,|k\rangle_W . \tag{4}$$

5) Finally, we carry out a measurement on the work register in the computational basis $\{|j\rangle_W\}$ and derive the desired order r satisfying the condition $a^r \bmod N = 1$. This measurement yields the state $|k\rangle_W$ with probability

$$P(k) = \frac{1}{q\,(w+1)} \left| \sum_{l=0}^{w} \exp\left[-iE_{(lr+s)}\tau + 2\pi ilk\frac{r}{q}\right] \right|^2 , \tag{5}$$

which is independent of the free evolution during the last delay τ_4. Notice that here $P(k)$ only depends on the *total* effective delay time $\tau = \tau_1^+ + \tau_2^+ + \tau_3^+$, but *not* directly on the *individual* time intervals τ_m, $m = 1, 2, 3, 4$.

In this decomposition of Shor's algorithm we have included time delays only in between the various unitary operations, which were implemented by independently using various one-time evolutions [15, 16]. Note that only the delays from the initial Hadamard gates to the finishing Fourier transformation may result in physical effects. Fortunately, all the operators during these delays are either diagonal or at least not affecting the phase accumulation. Therefore, the phases in each qubit simply add up.

If each unitary transformation is itself composed of several consecutive steps, with delays between these internal steps, we assume these delays to be negligible. This condition implies that the internal time delays occurring between steps within each unitary operation should be so short that their accumulated phases are negligible. Such a condition is possibly difficult to satisfy experimentally. However, our results below show that even under such a restrictive condition the interference effects due to dynamical phases between successive unitary transformation are already too significant to be ignored.

For the ideal situation without any delay ($\tau_m \equiv 0$), the probability distribution $P(k)$ in Eq. (5) reduces to that in the original Shor's algorithm [2]. However, Eq. (5) clearly shows that the expected probabilistic distribution may be strongly modified by the interferences due to the dynamical phases of the superposition wavefunction, which would consequently lead to a lower probability for obtaining the desired final output.

III. EFFECTS OF DYNAMICAL PHASES

In order to study the effects of dynamical phases, we need to compute $P(k)$. The probability $P(k)$ in (5) can be computed if the energies $E_{(lr+s)}$ for the various states $|lr+s\rangle_W$ involved are known exactly. These will be computed below.

A. Phase-matching condition for eliminating the coherent errors due to operational delays

As a first approximation we assume that all qubits in a quantum computer system possess identical energy spectra. Such an approximation is valid for naturally identical systems like trapped ions. In this ideal case, when all the qubits have the same energy splitting between ground and excited states, different quantum states with the same number of excited qubits

will acquire the same dynamical phase. For example, the four-qubit states $|1_3 0_2 0_1 0_0\rangle$ and $|0_3 0_2 0_1 1_0\rangle$ would acquire the same dynamical phase $\exp(-i3\epsilon_0 t - i\epsilon_1 t)$ during a delay time t. Here ϵ_0 and ϵ_1 are the energies of a single qubit corresponding to the ground state $|0\rangle$ and the excited state $|1\rangle$, respectively. Under this approximation, equation (5) can be rewritten as

$$P(k) = \frac{1}{q\,(w+1)} \left| \sum_{l=0}^{w} \exp\left[2\pi i l k \frac{r}{q}\right] \exp[-i(L_l^{(1)} - L_l^{(0)})\tau\,\Delta] \right|^2, \quad \Delta = \epsilon_1 - \epsilon_0, \tag{6}$$

where Δ is the qubit energy splitting and $L_l^{(1)}$ ($L_l^{(0)}$) is the number of qubits in the logical state $|1\rangle$ ($|0\rangle$) for the number state $|lr+s\rangle_W$. Obviously, when the *total* effective delay time τ ($\tau = \tau_1^+ + \tau_2^+ + \tau_3^+$) satisfies the phase-matching condition

$$\tau\,\Delta = (\epsilon_1 - \epsilon_0)\,\tau = 2\,n\,\pi, \quad n = 1, 2, 3, \ldots, \tag{7}$$

the above probability distribution $P(k)$ reduces to that of an ideal computation process with $\tau\Delta = 0$. This implies that *the interference due to the fast evolution of the dynamical phases can be suppressed periodically* so that the correct results are obtained at the delay points indicated in (7).

Physically, this phase matching condition is related to the transformation of wavefunction from the interaction to the Schrödinger pictures. Theoretical derivations (see, e.g., [17]) for realizing quantum computation are usually in the interaction picture, in which the Hamiltonian for the qubit free-evolution does not appear, and the oscillation of the superposed wavefunction does not exist. More specifically, if a system Hamiltonian $\hat{H}$ can be written as a sum of a free oscillator part and an interaction part $\hat{H} = \hat{H}_0 + \hat{V}$, so that the time-dependent Schrödinger equation can be written as (in the so-called Schrödinger picture where operators are time-independent while states evolve with time)

$$i\hbar\frac{\partial}{\partial t}|\psi_S(t)\rangle = (\hat{H}_0 + \hat{V})|\psi_S(t)\rangle\,,$$

one can introduce the interaction picture wavefunction $|\psi_S(t)\rangle = \exp(-i\hat{H}_0 t/\hbar)|\psi_I(t)\rangle$, which satisfies

$$i\hbar\frac{\partial}{\partial t}|\psi_I(t)\rangle = \hat{V}_I|\psi_I(t)\rangle\,,$$

where $\hat{V}_I = \exp(i\hat{H}_0 t/\hbar)\hat{V}\exp(-i\hat{H}_0 t/\hbar)$. Now that $\hat{H}_0$ has been eliminated from the Schrödinger equation, it seems that dynamical phases due to the qubit free evolution would have no effect. However, at the end of a calculation, physical measurements have to be performed to read out the computational results, and these measurements are generally performed in the lab frame (the Schrödinger picture), in which the dynamical phases reappear. More specifically, the measurement of an observable $\widehat{O}$ can be expressed as $\langle\psi_S(t)|\widehat{O}|\psi_S(t)\rangle = \langle\psi_I(t)|\exp(i\hat{H}_0 t/\hbar)\widehat{O}\exp(-i\hat{H}_0 t/\hbar)|\psi_I(t)\rangle = \langle\psi_I(t)|\widehat{O}_I(t)|\psi_I(t)\rangle$. In other words, if we prefer calculating the expectation value of a time-independent operator, it has to be done in the Schrödinger picture. If $|\psi_I(\tau)\rangle = \sum_j \alpha_j\,|j\,\rangle$ is the desired final state, the Schrödinger picture final state would take the form

$$|\psi_S(\tau)\rangle = \sum_j \alpha_j\, e^{-iE_j\tau}|j\,\rangle = \sum_j \alpha_j\, e^{-i(L_j^{(1)} - L_j^{(0)})\tau\Delta}|j\,\rangle\,. \tag{8}$$

Therefore, the phase-matching condition (7) would render the phases $\exp[-i(L_j^{(1)} - L_j^{(0)})\tau\Delta] = 1$, so that it enforces the equivalence of interaction picture and Schrödinger picture states, which ensures that the coherent error arising from the free evolution during the delay can be effectively eliminated.

In what follows, we illustrate our discussion with a few instances of Shor's algorithm.

B. An analytical example for factoring a small composite number

Let us first consider the factorization of the smallest composite number 4, which uses a two-qubit work register, a two-qubit auxiliary register and $a = 3$. After going through the four steps of Shor's algorithm as discussed above, the final work register state (Eq. (4)) is

$$\begin{aligned} |\psi(\tau+\tau_4)\rangle_W &= \frac{1}{\sqrt{2}}\left\{\frac{1}{\sqrt{2}}\left(|0_1\rangle_W + e^{-i\tau_4\Delta}|1_1\rangle_W\right)\otimes\frac{1}{\sqrt{2}}\left[\zeta|0_0\rangle_W + \xi e^{-i\tau_4\Delta}|1_0\rangle_W\right]\right\} \\ &= \frac{1}{\sqrt{8}}\left[\zeta|0\rangle_W + \xi|1\rangle_W + e^{-i\tau_4\Delta}\zeta|2\rangle_W + e^{-i\tau_4\Delta}\xi|3\rangle_W\right], \end{aligned} \tag{9}$$

with $\zeta = 1 + e^{-i\tau\Delta}$, and $\xi = 1 - e^{-i\tau\Delta}$. Here, $|\alpha_k\rangle_W$ refers to the logical states (with $\alpha = 0, 1$) of the kth (with $k = 0, 1$) qubit in the work register. In other hands, $|0\rangle_W = |0_1 0_0\rangle_W$, $|1\rangle_W = |0_1 1_0\rangle$, $|2\rangle_W = |1_1 0_0\rangle$, and $|3\rangle_W = |1_1 1_0\rangle_W$.

To derive Eq. (9), the measurement on the auxiliary register is the projection $\hat{P}_A = |1\rangle_A\langle 1|_A$. Measuring the work register in the computational basis, the state (9) collapses to the expected one: either $|0\rangle_W$, or $|2\rangle_W$, with probability $p_e = |\zeta|^2 = [1 + \cos(\tau\Delta)]/4$. This implies that the desired results ($|\zeta|^2 = 1/2$) are obtained, only if the phase-matching condition (7) is satisfied. Equation (9) also shows that the dynamical phase acquired by each qubit after the Fourier transform does not result in any measurable physical effect.

C. Numerical examples for factoring a few integers

To quantitatively evaluate the effects of the dynamical phases when running Shor's algorithm, we introduce two delay-dependent functions: $p_e(k_e)$ is used to quantify the probability of obtaining the correct result k_e, and

$$P_e = \sum_{k_e} p_e(k_e) \tag{10}$$

is the probability of computing all the correct outputs. $P_e = 1$ for an ideal computation process and for practical quantum computers at the phase-matching time intervals consistent with Eq. (7). For other delays not satisfying Eq. (7) wrong results ($k \neq k_e$) can be obtained so that $P_e < 1$.

We now run the algorithm to factorize $N = 21$ with $a = 5$ using 9 work qubits. Fig. 2 shows the various outputs and the corresponding probabilities for different delay times τ: $\tau\Delta = 0$, 0.4π, π, 1.6π, and 2π. It is seen from Fig. 2 that, when the phase-matching condition (7) is satisfied, the computed results are identical to that of an ideal computation process with $\tau\Delta = 0$. Note in Fig. 2 that the maximum value of $P(k) \approx 0.2$ at the matching condition and $P(k) < 0.02$ away from it.

We plot the delay-dependent P_e in Fig. 3 for several examples: factorizing $N = 15$, 21, and 33, with $a = 13$, 5, and 5, and when using 4, 9, and 11 work qubits, respectively. As is shown in Fig. 3, the correct results are always obtained at the phase-matching time intervals given by Eq. (7). For other delay cases, especially near the delay points satisfying the condition: $\tau\Delta = (\epsilon_1 - \epsilon_0)\tau = (2n - 1)\pi$, the correct results cannot be obtained (for the case where the expected order is a power of two; see, e.g., the continuous line for $r = 4$ in Fig. 3) or may be obtained with very low probabilities P_e (for the cases where the order r cannot divide the given q exactly; see, e.g., the lines for $r = 6$, 10 in Fig. 3). Of course, the dynamical oscillations can also be suppressed by trivially setting up individual delays τ_m as $\tau\Delta_m = 2n\pi$. The key observation here is that *only the total delay time*, instead of the duration for every delay, *needs to be set up accurately to avoid the coherent dynamical phase error.*

Classically, higher precision is usually obtained by using more computational bits. However, this is not necessarily the case in practical quantum computation. Indeed, in the current example of Shor's algorithm, after taking into consideration the influence of the time delays between consecutive computational operations, the more qubits are used, the *lower* the computational efficiency is. This relationship is clearly demonstrated in Fig. 4, which shows that *the probability of obtaining any one of the correct results decreases exponentially when increasing the number of qubits of the work register.* Such a scenario is to be expected, since the number of possible outputs in the final measurement increases exponentially with the number of the work qubits, which makes the constructive interference in Eq. (5) for the probability $P(k)$ harder to achieve if $\tau\Delta$ deviates from the phase-matching condition (7). At the exact points when $(\epsilon_1 - \epsilon_0)\tau = 2n\pi$, the constructive interference of the superposition wave functions ensures that the computational accuracy is independent of the number of involved qubits.

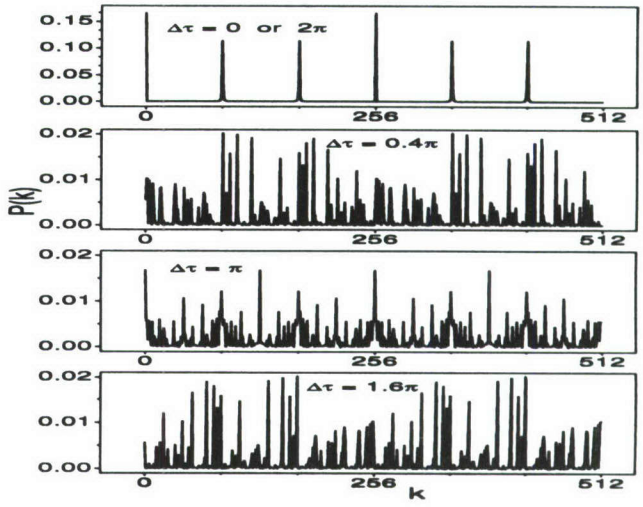

FIG. 2: The probability $P(k)$ (see Eq. (6)) of observing values of k for different values of $\tau\Delta = (\epsilon_1 - \epsilon_0)\tau = 0$, 0.4π, π, 1.6π, and 2π, given $N = 21$, $q = 512$, $a = 5$, and the expected order $r = 6$. Here, τ is the total effective delay time between unitary operations. The correct outputs are obtained when the phase-matching condition $\tau\Delta = 2\pi$ (or the ideal case $\tau\Delta = 0$) is satisfied. The probabilities of obtaining the correct outputs far from the phase-matching conditions are very low (see the second, third, and fourth panels. Note the different scales for the vertical axes). Indeed, as shown in the bottom three panels, many incorrect results are produced when the phase matching condition given by Eq. (7) is not enforced.

D. Effect of energy splitting inhomogeneity

In the calculations up to now, we have assumed that all qubits possess an identical energy splitting $\Delta = \epsilon_1 - \epsilon_0$. In reality, especially for the solid state quantum systems such as the Josephson junction qubits and quantum dot trapped spins, different qubits may have slightly *different* energy splittings due to system inhomogeneity. The logical states with the same energy in the "identical qubit" assumption (e.g., $|1_3 0_2 0_1 0_0\rangle$ and

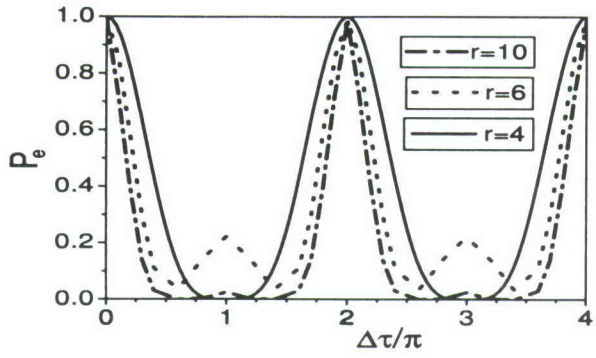

FIG. 3: The probability P_e of obtaining the correct results versus $\Delta\tau = (\epsilon_1 - \epsilon_0)\tau$ for running Shor's factoring algorithm in the presence of delays. The lines for $r = 4, 6, 10$ correspond to the cases where 4, 9, 11 work qubits, given $q = 16, 512, 2048$, are used to factorize $N = 15, 21, 33$ with $a = 13, 5, 5$, respectively. Note that the expected outputs can be obtained at phase-matching points: $\Delta\tau = 2\pi, 4\pi$.

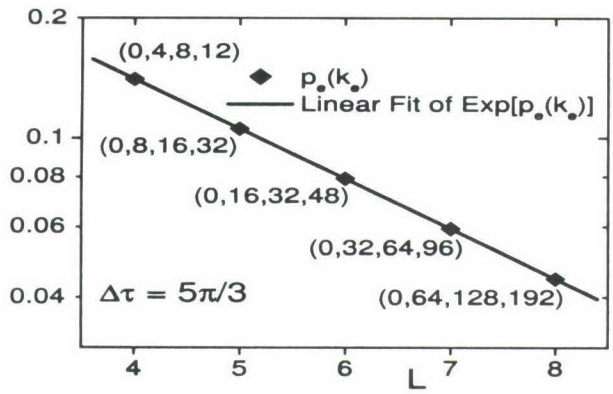

FIG. 4: The probability $p_e(k_e)$ of obtaining one of the correct results versus the number L of work qubits used to run the quantum algorithm factorizing $N = 15$ in the presence of a delay $\Delta\tau = (\epsilon_1 - \epsilon_0)\tau = 5\pi/3$. The straight line shows that this probability $p_e(k_e)$ decreases exponentially with the number L of qubits used. The points on the line show the probability of obtaining one of the correct outputs $k_e = (0, 4, 8, 12)$ for 4-qubits, (0, 8, 16, 24) for 5-qubits, (0, 16, 32, 48) for 6-qubits, (0 , 32, 64, 96) for 7-qubits, and (0, 64, 128, 192) for 8-qubits cases, respectively.

$|0_3 0_2 0_1 1_0\rangle$) may now have slightly different energies. A critical question then is how robust the phase matching condition (7) is for a system of multiple qubits with fluctuations in the qubit energy splittings. Here we provide quantitative answers to this important question by numerically simulating Shor's algorithm assuming a Gaussian distribution for the qubit energy splittings. In other words, the energy splitting Δ_j of the jth qubit is chosen randomly according to the distribution function

$$P(\Delta_j) = \frac{1}{\sqrt{2\pi}\,\sigma} \exp\left[-\frac{(\Delta_j - \langle\Delta\rangle)^2}{2\sigma^2}\right] \qquad (11)$$

around an average value $\langle\Delta\rangle$ and width σ. Figure 5 shows that the probability of obtaining correct answers decreases as

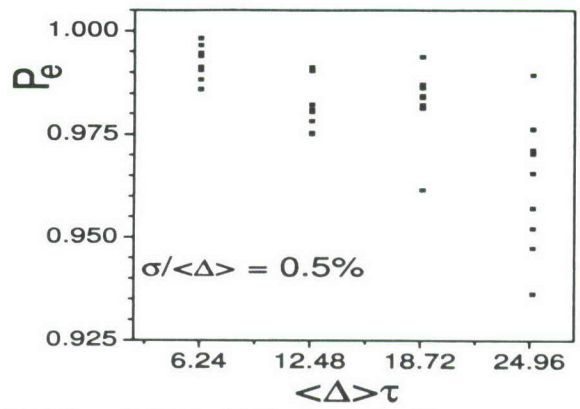

FIG. 5: The probabilities P_e (for factorizing $N = 15$ using 8 work qubits) of obtaining the correct results for different phase-matching cases: $\langle\Delta\rangle\tau = 2\pi, 4\pi, 6\pi, 8\pi$, with a common Gaussian energy splitting fluctuation with $\sigma/\langle\Delta\rangle = 0.5\%$. Note that this probability P_e is higher at the phase matching points with shorter total delay time τ.

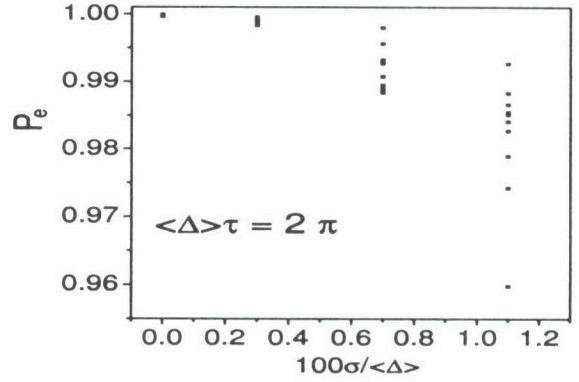

FIG. 6: The probabilities P_e (for factorizing $N = 15$ using 8 work qubits) of obtaining the correct results for different fluctuations of energy splittings: $\sigma/\langle\Delta\rangle = 0.01\%, 0.3\%, 0.7\%, 1.1\%$, with a common phase-matching point: $\langle\Delta\rangle\tau = 2\pi$. Note that the probability at the pase-matching point is still sufficiently high, even if the energy splittings of the qubits exist with certain fluctuations around the average value $\langle\Delta\rangle$.

the total time delay τ increases. Also, Fig. 6 shows the dependence of P_e on the width of the qubit energy splitting distribution σ, with the delay condition set at $\langle\Delta\rangle\tau = 2\pi$. As expected, a quantum computer runs with higher efficiencies for shorter time delays τ and for narrower distributions $P(\Delta_j)$ of energy splittings. In essence, here we study an effect similar to inhomogeneous broadening, which is not a true dephasing effect. This is consistent with our focus in this paper on the coherent errors instead of the incoherent ones.

IV. CONCLUSIONS AND DISCUSSIONS

When a real quantum computer performs a computational task, there must be unavoidable time intervals between consecutive unitary operations. During these delays, the wavefunction of a system with non-zero free Hamiltonian would

acquire relative dynamical phases, if the two states for each qubit have different energies. These dynamical phases lead to fast oscillations in the total wavefunction, and modify the desired quantum interference required by quantum algorithms, which in turn reduce the probability of obtaining correct computational results.

Here we have studied the effects of the dynamical phases in running a quantum algorithm (more specifically, Shor's factoring algorithm). We point out that a phase-matching condition can potentially help allieviate the interference problems caused by the dynamical phases, and this condition is closely related to establishing the equivalence between quantum states in the Schrödinger picture and the interaction picture through a quantum computation process. In the presence of coherent phase errors, we have demonstrated that, the probability of obtaining the correct answer decreases exponentially with increasing number of qubits of the work register. In addition, Shor's algorithm fails for the worst case scenario of $\tau\Delta = (2n-1)\pi$ if the expected order r is a power of two. We have further shown that the phase-matching condition studied here is quite robust in the presence of small fluctuations in the qubit energy splittings. Unlike the refocusing technique in NMR experiments [3], which deals with unwanted evolutions due to uncontrolled qubit interaction, we have shown here that by properly setting the *total* effective delay, the unwanted oscillations of the superposed wavefunctions due to the free Hamiltonians of the bare qubits can be effectively suppressed, thus the desired output can be obtained without additional operations. This implies that the quantum computing may be performed in an effective interaction picture, in which coherent errors arising from the free evolution of the bare qubits during the operational delay can be automatically avoided.

We emphasize that the present simplified approach only treats the delays between two sequential functional operations and neglects those inside these transforms. In fact, each functional transform, which is actually equivalent to a multi-qubit gate, can be, in principle, implemented exactly by using only one-time evolution [15, 16]. This "coarse-grained" one-step implementation implies that the evolutions relating to the various parts of the total Hamiltonian have been well controlled. Therefore, the operational delays, relating only to the free evolution ruled by the free Hamiltonian of the bare physical qubits, within each one of these larger functional building blocks are assumed to be zero. Also, the dynamical phases acquired by the superposed wavefunctions can be added up for the operational delays before and after each functional transformation. Therefore, the phase-matching condition (7) exists for the *total* delay.

The present calculation is done assuming that Shor's algorithm is accomplished in 5 lumped steps. A simple analysis can prove that, even if using an actual elementary gate array model, e.g., shown in figure 7 (for implementing the initializations by using the Hadamard gates and the quantum Fourier transformation), the proposed phase-matching conditions (in terms of the total delay time instead of individual delay times of each operational delay) for avoiding the coherent phase errors are still valid. The key is that, only two elementary non-

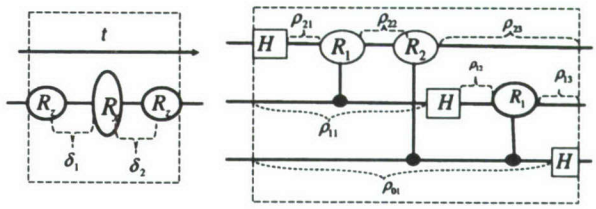

FIG. 7: Quantum circuits formed by the elementary single- and two-qubit logic gates for performing (a) Hadamard gate for one qubit, and (b) quantum Fourier transformation for three-qubit. Here, δ_l $(l = 1, 2, ...)$ and ρ_{kl} $(k = 0, 1, 2, ...)$ refer to the operational delays inside them, respectively. In the logical basis, the single-qubit gate $\hat{R}_z = \exp(i\pi\sigma_z/4)$ and the two-qubit controlled-phase gate $R_k = |00\rangle\langle 00| + |01\rangle\langle 01| + |10\rangle\langle 10| + \exp(2i\pi/2^k)|11\rangle\langle 11|$ are diagonal, while the single-qubit $\hat{R}_x = \exp(i\pi\sigma_x/4)$ is not.

diagonal operations (i.e., $\hat{R}_x$ in Hadamard gates) are applied to each qubit in the work register (see Fig. 7). The qubit is in a product state before the first non-diagonal $\hat{R}_x$ gate, while the delays after the second non-diagonal $\hat{R}_x$ in the corresponding Hadamard gate do not affect the results of projective measurement (see, e.g., Eq. (9)). Therefore, the dynamical phases acquired in different effective operational delays accumulate even when the operational delays inside the functional steps are considered.

In the present approach, we have assumed that every qubit in the work register has the same waiting time τ_j^+ for each effective operational delay. In practice, this assumption is not necessary. Indeed, in the elementary gate array model, the waiting times for different qubits would have been different. However, the phase-matching condition Eq. (7) needs only a slight modification in this case, so that it becomes a condition for each qubit [14]: $\tau_k\Delta_k = 2n_k\pi, k = 1, 2, ...; n_k = 1, 2, ..$ for each qubit. Here, Δ_k and τ_k are the energy splitting and *total* controllable effective delay of the kth qubit in the work register, respectively.

Finally, we emphasize that the results presented in this paper, through obtained using a simple model for the delays, clearly demonstrate the necessity of taking into consideration the dynamical phases of the qubits in implementing quantum algorithms.

Acknowledgments

This work was supported in part by the National Security Agency (NSA) and Advanced Research and Development Activity (ARDA) under Air Force Office of Research (AFOSR) contract number F49620-02-1-0334, and by the National Science Foundation grant No. EIA-0130383.

[1] See, e.g., M.A. Nielsen, I.L. Chuang, *Quantum Computation and Quantum Information*, (Cambridge University Press, Cambridge, September 2000); C.H. Bennett and D.P. DiVincenzo, Nature, **44**, 247 (2000); A. Ekert and R. Josza, Rev. Mod. Phys. **68**, 733 (1996); A.M. Steane, Rep. Prog. Phys. **61**, 117 (1998).

[2] P. Shor, in Proceedings of the 35th Annual Symposium on the Foundations of Computer Science, edited by Shafi Goldwasser (IEEE Computer Society Press, New York, 1994), p. 124;

[3] L.M.K. Vandersypen, M. Steffen, G. Breyta, C.S. Yannoni, M.H. Sherwood, and I.L. Chuang, Nature, **414**, 883 (2001); Phys. Rev. Lett. **85**, 5452 (2000).

[4] M. Mussinger, A. Delgado and G. Alber, New J. Phys. **2**, 191 (2000).

[5] P.W. Shor, Phys. Rev. A **52**, R2493 (1995); A.M. Steane, Phys. Rev. Lett. **77**, 793 (1996).

[6] C. Miquel, J.P. Paz, and R. Perazzo, Phys. Rev. A **54**, 2605 (1996); C.P. Sun, H. Zhan and X.F. Liu, Phys. Rev. A **58**, 1810 (1998); E. Knill, R. Laflamme and W.H. Zurek, Science, **279**, 342 (1998).

[7] See, e.g., D.A. Lidar, I.L. Chuang, and K.B. Whaley, Phys. Rev. Lett. **81**, 2594 (1998); P. Zanardi and M. Rasetti, Phys. Rev. Lett. **79**, 3306 (1997).

[8] G.L. Long, Y.S. Li, W.L. Zhang, and C.C. Tu, Phys. Rev.A **61**, 042305 (2000); J. Chin. Chem. Soc. **48**, 449 (2001). X. Hu and S. Das Sarma, Phys. Rev. A **66**, 012312 (2002).

[9] M.B. Plenio and P.L. Knight, Proc. Roy. Soc. **453**, 2017 (1997).

[10] Y. Makhlin, G. Schön and A. Shnirman, Nature, **398**, 305 (1999).

[11] M. Feng, Phys. Rev. A **63**, 052308 (2001).

[12] G.B. Berman, G.D. Doolen, and V.I. Tsifrinvovish, Phys. Rev. Lett. **84**, 1615 (2000).

[13] N. A. Gershenfeld and I. L. Chuang, Science **275**, 350 (1997); D. G. Cory, A. F. Fahmy, and T. F. Havel, Proc. Nat. Acad. Sci. **94**, 1634 (1997).

[14] L.F. Wei and F. Nori, J. Phys. A**37**, 4607 (2004).

[15] L.F. Wei and F. Nori, Eurphys. Lett. **65**(1), 1 (2004); Phys. Lett. **320**(2-3), 131 (2003).

[16] A.O. Niskanen, J.J. Vartianen, and M.M. Salomaa, Phys. Rev. Lett. **90**, 197901 (2003); X.Wang, A. Søresen, and K. Mølmer, Phys. Rev. Lett. **86**, 3907 (2001); J.F. Du, M.J. Shi, J.H. Wu, X.Y. Zhou, and R.D. Han, Phys. Rev. A **63**, 042302 (2001); F. Yamaguchi, C.P. Master and Y. Yamamoto, quant-ph/0005128.

[17] J.I. Cirac and P. Zoller, Phys. Rev. Lett. **74** (1995) 4091; L.F. Wei, S.Y. Liu and X.L. Lei, Phys. Rev. A **65**, 062316 (2002); T. Sleator and H. Weinfurter, Phys. Rev. Lett. **74**, 4087 (1995).

CE: AK

INSTITUTE OF PHYSICS PUBLISHING JOURNAL OF PHYSICS A: MATHEMATICAL AND GENERAL

J. Phys. A: Math. Gen. 37 (2004) 1–11 PII: S0305-4470(04)63429-9

Quantum phase estimation algorithms with delays: effects of dynamical phases

L F Wei[1,2] **and Franco Nori**[1,3]

[1] Frontier Research System, The Institute of Physical and Chemical Research (RIKEN), Wako-shi, Saitama, 351-0198, Japan

[2] Institute of Quantum Optics and Quantum Information, Department of Physics, Shanghai Jiaotong University, Shanghai 200030, People's Republic of China

Received 8 May 2003, in final form 27 January 2004

Published DD MMM 2004

Online at stacks.iop.org/JPhysA/37/1 (DOI: 10.1088/0305-4470/37/0/000)

Abstract

The unavoidable finite time intervals between the sequential operations needed for performing practical quantum computing can degrade the performance of quantum computers. During these delays, unwanted relative dynamical phases are produced due to the free evolution of the superposition wavefunction of the qubits. In general, these coherent 'errors' modify the desired quantum interferences and thus spoil the correct results, compared to the ideal standard quantum computing that does not consider the effects of delays between successive unitary operations. Here, we show that, in the framework of the quantum phase estimation algorithm, these coherent phase 'errors', produced by the time delays between sequential operations, can be avoided by setting up the delay times to satisfy certain matching conditions.

PACS number: 03.67.Lx

1. Introduction

Building a prototype quantum information processor has attracted considerable interest during the past decade (see, e.g., [1]). This desired device should be able to simultaneously accept many different possible inputs and subsequently evolve them into a corresponding quantum mechanical superposition of outputs. The proposed quantum algorithms are usually constructed for ideal quantum computers. In reality, any physical realization of such a computing process must treat various errors arising from various noise and imperfections (see, e.g., [1–3]). Physically, these errors can be distinguished into two different kinds: incoherent and coherent errors. The incoherent perturbations, originating from the coupling of the quantum computer to an uncontrollable external environment, result in decoherence

[3] Permanent address: Center of Theoretical Physics, Physics Department, Center for the Study of Complex Systems, University of Michigan, Ann Arbor, MI 48109-1120, USA.

and stochastic errors. Coherent errors usually arise from non-ideal quantum gates which lead to a unitary but non-ideal temporal evolution of the quantum algorithm. So far, almost all previous works (see, e.g., [4–7]) have been concerned with quantum errors arising from the decoherence due to interactions with the external environment and external operational imperfections. Here, we will not be concerned with these two types of externally induced errors, but will focus instead on intrinsic ones. The coherent errors we consider here relate to the intrinsic dynamical evolution of the qubits between operations. This has not been paid much attention until a recent work in [8], where a kind of dynamical phase error was introduced. It is well known that a practical quantum computing process usually consists of a number of sequential quantum unitary operations. These transformations operate on superposition states and evolve the quantum register from the initial states (input) into the desired final states (output). According to the Schrödinger equation, the superposition wavefunction oscillates fast during the finite-time delay between two sequential operations. In general, these oscillations modify the desired quantum interferences and thus spoil the correct computational results, expected by the ideal quantum algorithms without any operational delay.

Two different strategies have been proposed to deal with these coherent errors. One is the so-called 'avoiding error' approach proposed by Makhlin *et al* in [9]. Its key idea is to let the Hamiltonian of the bare two-level physical system be zero by properly setting up experimental parameters. Thus the system does not evolve during the delays. This requirement is restrictive and cannot be easily implemented for some physical set-ups of quantum computing e.g., for trapped ions. A modified approach to remove this stringent condition was proposed by Feng in [10], where a pair of degenerate quantum states of a pair of two-level systems are used to encode two logic states of a single qubit. During the delay these logical states acquire a common dynamical phase, which is the global phase without any physical meaning. Thus the above dynamical error can be avoided efficiently. However, this modified scheme complicates the process of encoding information. Another strategy to this problem was proposed by Berman *et al* [8]. They pointed out that the unwanted dynamical oscillations can be routinely eliminated by introducing a 'natural' phase, which can be induced by using a stable continuous reference oscillation for each quantum transition in the computing process. However, this scheme only does well for the resonant implementations of quantum computation. The additional reference pulses also complicate the quantum computing process and may result in other operational errors.

We show in this paper that, in the framework of the quantum phase estimation algorithm, the coherent phase errors, produced by the free evolutions of the superposition wavefunctions of bare two-level systems, can be avoided simply and effectively by setting up the delay time intervals appropriately. The proposed matching condition can be considered a sort of strobed operation (with strobe frequencies corresponding to each different transition energy). For simplicity, we simplify each quantum algorithm to a three-step functional process, namely, preparation, evolution and measurement. All the functional operations in this three-step process are assumed to be carried out in an infinitesimally short time duration, and thus only the delays between them, instead of the operations themselves, are considered. The effects of the environment decoherence and the operational imperfections are neglected in the present treatment.

The paper is organized as follows. In section 2, we present our general approach with the phase estimation algorithm. Section 3 gives a few special demonstrations and shows how to perform quantum order-finding and quantum counting algorithms in the presence of operational delays. Finally, we give a short summary and discussion in section 4.

2. Phase estimation algorithm with operational delays

Our discussion begins with the phase estimation algorithm [11, 12] and its finite-time implementation with some delays. The programs for some of the existing other important quantum algorithms, such as quantum factoring and counting ones, can be reformulated in terms of this problem. The goal of the phase estimation algorithm is to obtain an n-bit estimation of the eigenvalue $\exp(\mathrm{i}\phi)$ of a unitary operation $\hat{U}_T$,

$$\hat{U}_T|\phi\rangle_T = \mathrm{e}^{\mathrm{i}\phi}|\phi\rangle_T \tag{1}$$

if the corresponding eigenvector $|\phi\rangle_T$, and the devices that can perform operations $\hat{U}_T$, $\hat{U}_T^2$, $\hat{U}_T^4, \ldots,$ and $\hat{U}_T^{2^n}$, are given initially. Two quantum registers are required to perform this algorithm. One is the target register, whose quantum state is kept in the eigenstate $|\phi\rangle_T$ of the unitary operator $\hat{U}_T$. Another one, with n physical qubits and called the *index* register, is used to read the corresponding estimation results. The needed number of qubits n in the *index* register depends on the desired accuracy and on the success probability of the algorithm. The most direct application [13] of this algorithm is to find eigenvalues and eigenvectors of a local Hamiltonian $\hat{H}_T$ by determining the time-evolution unitary operator $\hat{U}_T = \exp(-\mathrm{i}\hat{H}_T t/\hbar)$. The phase estimation algorithm can be viewed as a quantum nondemolition measurement, and can also be used to generate eigenstates of the corresponding unitary operator $\hat{U}_T$ [14].

The ideal quantum algorithm usually assumes that the quantum computing process can be continuously performed by using a series of sequential operations without any time delay between them. In reality, a delay between two sequential operations always exists, introducing errors that need to be corrected. For simplicity, we reduce the phase estimation algorithm to a three-step functional process, namely, initialization, global phase shift and measurement. All the functional operations in this three-step process are assumed to be carried out exactly, and thus only the delays between them, instead of the operations themselves, are considered. Such a simplified finite-time implementation of the phase estimation algorithm is sketched in figure 1. For convenience we distinguish the physical qubit and the logic qubit in the index register. The physical qubit is just a two-level physical system and the logical qubit is the unit of binary information. Unlike the scheme in [10], wherein two physical qubits are used to encode one logical qubit, in the present work *one* physical qubit is enough to encode *one* logical qubit. The symbol $|a_j\rangle_k$ with $a = 0, 1$, $j, k = 0, 1, \ldots, n-1$ means that the kth logical qubit is encoded by the jth physical qubit. $|a_j\rangle$ is the eigenstate of the bare Hamiltonian of the jth physical qubit corresponding to the eigenvalue E_a.

The quantum phase estimation algorithm with operational delays can be divided into three distinct functional steps.

2.1. Initialization

First, we initialize the index register with n physical qubits in an equal-weight superposition of all logical states. This can be performed by applying the Hadamard transform to its ground state $|0\rangle_I = \prod_{j=n-1}^{0}|0\rangle_j$. Note that the target register holds an eigenstate $|\phi\rangle_T$ of $\hat{U}_T$ with eigenvalue $\exp(\mathrm{i}\phi)$. Hereafter, the subindex I will denote the index state, while the subindex T refers to the target state. The computational initial state of the whole system is

$$|\Psi(0)\rangle = \left\{\prod_{j=n-1}^{0}\hat{H}_j|0_j\rangle_j\right\}_I \otimes |\phi\rangle_T = \frac{1}{\sqrt{2^n}}\sum_{k=0}^{2^n-1}|k\rangle_I \otimes |\phi\rangle_T \tag{2}$$

$$\hat{H}_j = \frac{1}{\sqrt{2}}\begin{pmatrix}1 & 1\\ 1 & -1\end{pmatrix}_j$$

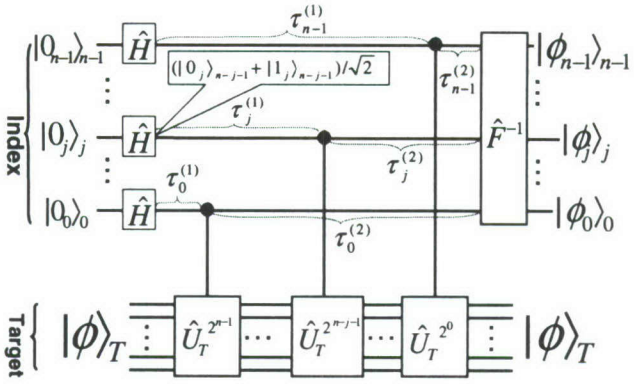

Figure 1. Quantum phase estimation with operational delays. Note that (1) there is an operational delay $\tau_j^{(m)}$ $(m = 1, 2)$ between successive quantum operations on the jth physical qubit, and (2) the jth logical qubit is changed to the $(n-j-1)$th one after the Hadamard gate $\hat{H}$ and inverse QFT $\hat{F}^{-1}$. Here, $\tau_j^{(1)}$ is time delay between the $\hat{H}$ and $\hat{U}_T^{2^{n-j-1}}$ operations, while $\tau_j^{(2)}$ is the delay between $\hat{U}_T^{2^{n-j-1}}$ and $\hat{F}^{-1}$.

where $|k\rangle_I = |a_0\rangle_{n-1}^k \otimes \cdots \otimes |a_{n-1}\rangle_0^k$ are the number states of the index register, and $\hat{H}_j$ is the Hadamard transform applied to the jth logical qubit. For convenience, in this paper the jth logical qubit is changed into the $(n-1-j)$th logical qubit when applying either the Hadamard or the (inverse) quantum Fourier transform (QFT). Of course, the order of the physical qubits is not changed.

After a finite time delay $\tau_j^{(1)}$ for the jth physical qubit, the initial state $|\Psi(0)\rangle$ of the whole system evolves into

$$\left|\Phi\left\{\tau_j^{(1)}\right\}\right\rangle = \left\{\prod_{j=n-1}^{0} \frac{1}{\sqrt{2}}\left(\exp\left(-\mathrm{i}E_j^0\tau_j^{(1)}\right)|0_j\rangle_{n-j-1} + \exp\left(-\mathrm{i}E_j^1\tau_j^{(1)}\right)|1_j\rangle_{n-j-1}\right)\right\}_I \otimes |\phi\rangle_T \tag{3}$$

with E_j^0 and E_j^1 being the eigenvalues of the Hamiltonian for the jth bare physical qubit corresponding to the eigenvectors $|0_j\rangle$ and $|1_j\rangle$, respectively.

2.2. *Global phase shift*

Second, we shift the 'global' phase in the eigenvector of the operator $\hat{U}$ into a measurable relative phase. This can be achieved by using the 'phase kick-back' technique [12]. Indeed, after applying a controlled-$\hat{U}_T^{2^j}$ operation $c-\hat{U}_j$, defined by

$$c-\hat{U}_j = |1\rangle_{j\,j}\langle 1| \otimes \hat{U}_T^{2^j} + |0\rangle_{j\,j}\langle 0| \otimes \hat{I}_T \tag{4}$$

to the jth logical qubit, the state $\left|\Phi\left\{\tau_j^{(1)}\right\}\right\rangle$ is evolved into

$$\begin{aligned}\left|\Psi\left\{\tau_j^{(1)}\right\}\right\rangle &= \prod_{j=n-1}^{0}(c-\hat{U}_j)\left|\Phi\left\{\tau_j^{(1)}\right\}\right\rangle \\ &= \frac{1}{\sqrt{2}}\left(\exp\left(-\mathrm{i}E_0^0\tau_0^{(1)}\right)|0_0\rangle_{n-1} + \exp\left(-\mathrm{i}E_0^1\tau_0^{(1)}\right)\exp(\mathrm{i}2^{n-1}\phi)|1_0\rangle_{n-1}\right) \otimes\end{aligned}$$

$$\cdots \otimes \frac{1}{\sqrt{2}}\left(\exp\left(-\mathrm{i}E^0_{n-1}\tau^{(1)}_{n-1}\right)|0_{n-1}\rangle_0 + \exp\left(-\mathrm{i}E^1_{n-1}\tau^{(1)}_{n-1}\right) \times \exp(\mathrm{i}2^0\phi)|1_{n-1}\rangle_0\right) \otimes |\phi\rangle_T. \tag{5}$$

Here $|1\rangle_{j\,j}\langle 1|$ and $|0\rangle_{j\,j}\langle 0|$ are the projectors of the jth logical qubit. $\hat{I}_T$ is the identity or unity operation. The controlled-$\hat{U}_T^{2^j}$ operator means that, if the jth logical qubit in the index register is in the state $|1\rangle_j$, the 2^j-fold iteration of $\hat{U}_T$ is applied to the target register. The 'global' phase in the eigenvector of the operator $\hat{U}_T^{2^j}$ is changed as the measurable relative phases in the states of the index qubits.

Before the next step in the operation of the algorithm there is another finite-time delay $\tau_j^{(2)}$ for the jth physical qubit. During this time interval each physical qubit of the index register evolves again freely according to the Schrödinger equation, while the target register is assumed to be still in the state $|\phi\rangle_T$. As a consequence, the state of the whole system becomes

$$|\Phi\{\tau_j\}\rangle = \tfrac{1}{\sqrt{2}}\left(\exp\left(-\mathrm{i}E^0_0\tau_0\right)|0_0\rangle_{n-1} + \exp\left(-\mathrm{i}E^1_0\tau_0\right)\exp\left(\mathrm{i}2^{n-1}\phi\right)|1_0\rangle_{n-1}\right) \otimes \cdots \otimes \tfrac{1}{\sqrt{2}}\left(\exp\left(-\mathrm{i}E^0_{n-1}\tau_{n-1}\right)|0_{n-1}\rangle_0 + \exp\left(-\mathrm{i}E^1_{n-1}\tau_{n-1}\right) \times \exp\left(\mathrm{i}2^0\phi\right)|1_{n-1}\rangle_0\right) \otimes |\phi\rangle_T \tag{6}$$

with

$$\tau_j = \tau_j^{(1)} + \tau_j^{(2)} \tag{7}$$

being the total delay before and after the controlled-$\hat{U}_T^{2^{n-j-1}}$ operation. Note that the dynamical phases of the index qubit can be added up before and after this, as controlled-$\hat{U}_T^{2^{n-j-1}}$ operator is diagonal in the basis of the $(n-j-1)$th logical qubit of the index register.

2.3. *Measurement*

Third, we finally apply the inverse quantum Fourier transform (QFT) on the index register to measure the phase in the eigenvector of the unitary operator $\hat{U}_T$. The inverse QFT, defined by the formula

$$\mathrm{QFT}^{-1} : |k\rangle \longrightarrow \hat{F}^{-1}|k\rangle = \frac{1}{\sqrt{2^n}}\sum_{y=0}^{2^n-1}\exp\left(-2\pi\mathrm{i}\frac{k\cdot l}{2^n}\right)|l\rangle \tag{8}$$

can be performed by using the sequential unitary operations $\hat{F}^{-1} = \hat{F}^\dagger = \hat{H}_0\hat{R}^\dagger_{0,1}\cdots\hat{H}_{n-2}\cdots\hat{R}^\dagger_{0,n-1}\cdots\hat{R}^\dagger_{n-2,n-1}\hat{H}_{n-1}$, to the corresponding logical qubits. Here,

$$\hat{R}^\dagger_{j-k,j} = \begin{pmatrix} 1 & 0 & 0 & 0 \\ 0 & 1 & 0 & 0 \\ 0 & 0 & 1 & 0 \\ 0 & 0 & 0 & \mathrm{e}^{-\mathrm{i}\pi/2^k} \end{pmatrix}_{j-k,j}$$

is a two-qubit controlled-phase operation. It implies that the state $|1\rangle_j$ of the target jth logical qubit will change by a phase $\exp(-\mathrm{i}\pi/2^k)$, if the control $(j-k)$th logical qubit is in the state $|1\rangle_{j-k}$. If the phase ϕ can be exactly written as a n-bit binary expansion, i.e.,

$$\phi = 2\pi(\phi_0\cdots\phi_{n-1}) = \frac{\phi_0}{2^n} + \frac{\phi_1}{2^{n-1}} + \cdots + \frac{\phi_{n-1}}{2} \qquad \phi_j = 0, 1 \quad j = 0, 1, \ldots, n-1 \tag{9}$$

then the expected final output state of the index register, after applying the inverse QFT, is the following product state

$$|\Psi\{\tau_j\}\rangle_I = |\phi_{n-1}\rangle_{n-1} \otimes \cdots |\phi_j\rangle_j \cdots \otimes |\phi_0\rangle_0. \tag{10}$$

However, the existing dynamical phase error, arising from the free evolution of the physical qubits during the delays, may spoil the desired results. For example, measuring the jth physical qubit in the computational basis $\{|0\rangle, |1\rangle\}$, we have

$$\hat{F}^{\dagger} : \left[\exp\left(-\mathrm{i}E_j^0\tau_j\right)|0_j\rangle_{n-1-j} + \exp\left(-\mathrm{i}E_j^1\tau_j\right)\exp(\mathrm{i}2^{n-1}2\pi(\phi_0\cdots\phi_{n-1-j}))|1_j\rangle_{n-1-j}\right]/\sqrt{2}$$
$$\rightarrow \exp\left(-\mathrm{i}E_j^0\tau_j\right)[(1+\exp(-\mathrm{i}\Delta_j\tau_j)\exp(\mathrm{i}\pi\phi_j))|0_j\rangle_j + (1-\exp(-\mathrm{i}\Delta_j\tau_j)$$
$$\times \exp(\mathrm{i}\pi\phi_j))|1_j\rangle_j]/\sqrt{2}. \tag{11}$$

The expected result $|\phi_j\rangle_j$ is obtained with the following probability,

$$P_{\phi_j} = \tfrac{1}{2}[1+\cos(\Delta_j\tau_j)] \qquad \Delta_j = E_j^1 - E_j^0 \tag{12}$$

while an error output state $|\phi_j \oplus 1\rangle_j$ is obtained with the probability $P_{\phi_j\oplus 1} = [1-\cos(\Delta_j\tau_j)]/2$. Here $\oplus$ refers to addition modulo 2. Note that the above probability (12) of obtaining the correct result only depends on the *total* delay time τ_j, but *not* directly on the individual time intervals $\tau_j^{(m)}$, $m = 1, 2$.

Obviously, if $\tau^{(1)} = \tau^{(2)} = 0$, i.e., for the ideal algorithm realization without any delay, one obtains the desired output $|\phi_j\rangle_j$. While for the realistic case where $\tau_j^{(1)}, \tau_j^{(2)} \neq 0$, the required quantum inference may be modified, and thus the real output may not be the expected one. A worst case scenario is produced if

$$\Delta_j\tau_j = (2l+1)\pi \qquad l = 0, 1, 2, \ldots \tag{13}$$

because the corresponding error-state output is $|\phi_j \oplus 1\rangle_j$, which is incorrect. However, if the following matching condition

$$\Delta_j\tau_j = 2(l+1)\pi \tag{14}$$

is satisfied, one obtains the desired output $|\phi_j\rangle_j$, and thus the fast oscillation of the superpositional wavefunction is suppressed in the output of the computation. Above, $\tau_j = \tau_j^{(1)} + \tau_j^{(2)}$ is the *total effective delay time* of the jth physical qubit in the algorithm. The condition in equation (14) is desirable for implementing quantum algorithms with an arbitrary number of qubits and includes as a particular case, the less general condition in [8] for the finite-time implementation of the four-qubit Shor's algorithm.

3. Example and applications

We now demonstrate the above general approach via a simple example, and show the effects of dynamical phases in finite-time implementations of a few quantum algorithms.

3.1. NOT gate eigenvalue

First, we wish to determine the eigenvalue of the Pauli operator $\hat{\sigma}_x$, or NOT gate, by running the realistic single-qubit phase estimation algorithm discussed above. Assuming that the single-qubit target register is prepared into one of the eigenstates

$$|\phi\rangle_T = |\pm\rangle_T = \frac{1}{\sqrt{2}}\begin{pmatrix}1\\ \pm 1\end{pmatrix}_T \tag{15}$$

corresponding to the eigenvalues $\mathrm{e}^{\mathrm{i}\phi}$ with $\phi = 0, \pi$, respectively. According to the above discussions, the final state of the index single-qubit register, after the single-qubit measurement just performed by Hadamard transform, can be written as

$$|\Psi(\tau)\rangle_I = \tfrac{1}{2}\{[1+\exp(-\mathrm{i}\Delta\tau+\mathrm{i}\phi)]\exp(-\mathrm{i}E^0\tau)|0\rangle_I$$
$$+ [1-\exp(-\mathrm{i}\Delta\tau+\mathrm{i}\phi)]\exp(-\mathrm{i}E^1\tau)|1\rangle_I\}. \tag{16}$$

This implies that the probability for the index register to be finally in the state $|0\rangle_I$ or $|1\rangle_I$ is

$$P_0(\tau) = \tfrac{1}{2}[1 + \cos\phi\cos(\Delta\tau) + \sin\phi\sin(\Delta\tau)] \tag{17}$$

or

$$P_1(\tau) = \tfrac{1}{2}[1 - \cos\phi\cos(\Delta\tau) + \sin\phi\sin(\Delta\tau)]. \tag{18}$$

If the target register is in the eigenstate $|+\rangle_I$ of operator $\hat{\sigma}_x$ with eigenvalue +1, i.e., $\phi = 0$, the probability of getting the expected output $|0\rangle_I$ is $P_0(\tau) = 1$, if condition (14) is satisfied. However, if condition (13) is satisfied, the index register will show the error output, i.e., $|1\rangle_I$.

3.2. Dynamical phase effects in the quantum order-finding algorithm with delays

Shor's algorithm [15] for factoring a given number N is based on calculating the period of the function $f(x) = y^x \bmod N$ for a randomly selected integer y between 1 and N. Once, the order r of $y \bmod N$ is known, factors of N are obtained by calculating the greatest common divisor of N and $y^{r/2} \pm 1$. A finite-time implementation of the order-finding algorithm can be translated to the above quantum phase estimation algorithm with delays. Here, the unitary operator whose eigenvalue we want to estimate is the unitary transformation $\hat{U}_y$, with $\hat{U}_y^r = \hat{I}$, which maps $|x\rangle$ to $|yx \bmod N\rangle$ and

$$\hat{U}_y|u_k\rangle = \exp\left(\mathrm{i}\frac{2\pi k}{r}\right)|u_k\rangle \qquad |u_k\rangle = \frac{1}{\sqrt{r}}\sum_{x=0}^{r-1}\exp\left(\frac{2\pi \mathrm{i}kx}{r}\right)|y^x \bmod N\rangle$$
$$k = 0, \ldots, r-1. \tag{19}$$

By the phase estimation algorithm, we can measure the eigenvalue $\exp(2\pi \mathrm{i}k/r)$ and consequently get the order r. However, the present target register cannot be prepared accurately in one of the eigenvectors $|u_k\rangle$, as the order r is initially unknown. It is noted that $\sum_{k=0}^{r-1}|u_k\rangle/\sqrt{r} = |1\rangle$, and $|1\rangle$ is an easy state to prepare. Thus, the algorithm may be run by initially generating a superposition of all eigenstates of the operator $\hat{U}_y$, rather than one of them accurately.

Without loss of generality, we demonstrate our discussion with the simplest meaningful instance of Shor's algorithm, i.e., the factorization of $N = 15$ with $y = 7$, which had been implemented in a recent NMR experiment [16]. In this simplest case, the order r is the power of 2, i.e., $r = 2^n$, $n = 2$, and thus the expected phase estimation algorithm can measure exactly the n-qubit eigenvalue $k/2^n : k = \sum_{j=0}^{n-1} k_j 2^j$, $k_j = 0, 1$. From the measurement eigenvalues we can obtain the order r by checking if $y^r \bmod N = 1$. Following the corresponding experimental demonstration [16], we need an index register with $n = 2$ physical qubits to measure the eigenvalues of the present unitary operator $\hat{U}_y$, and a target register with $m = 4$ physical qubits to represent the state $|1\rangle_T = \sum_{k=0}^{3}|u_k\rangle_T/2$. $|u_k\rangle_T = \sum_{x=0}^{3}\exp(-2\pi\,\mathrm{i}kx/2^2)|7^x \bmod 15\rangle_T/2$, which, in fact, is the equal-weight superposition of all the eigenvectors of the operator $\hat{U}_y : |x\rangle_T \longrightarrow |7^x \bmod 15\rangle_T$, $x = 0, 1, 2, 3$, with $\hat{U}_y|u_k\rangle_T = \exp(2\pi\,\mathrm{i}k/2^2)|u_k\rangle_T$. According to the three-step finite-time implementation of the phase estimation discussed in the last section, one can easily prove that the whole system is in the following entangled state,

$$|\Phi\{\tau_j\}\rangle = \frac{1}{2}\sum_{k=0}^{3}\prod_{j=1}^{0}\left\{\frac{1}{\sqrt{2}}\left[|0_j\rangle_{1-j} + \exp\left(-\mathrm{i}\Delta_j\tau_j + \frac{2\pi\,\mathrm{i}2^{(1-j)}k}{2^2}\right)|1_j\rangle_{1-j}\right)\right\}_I \otimes |u_k\rangle_T \tag{20}$$

before the index register is measured by using the inverse QFT. Here, the unimportant global dynamical phase factor $\exp\left(-2\mathrm{i}E_j^0\tau_j\right)$ is neglected.

In the ideal case, i.e., $\tau_j^{(1)} = \tau_j^{(2)} = 0$, measuring the index register by the inverse QFT will, with a probability equal to $1/4$, produce the expected output state

$$|\Psi_{\text{out}}\rangle_I = |k_1\rangle_1 \otimes |k_0\rangle_0. \tag{21}$$

Simultaneously, the target register will 'collapse' into the state of the corresponding expected eigenvector $|u_k\rangle$. Once a measurement output, i.e., $k/2^2 = (2^1k_1 + 2^0k_0)/2^2$ is known, the order is efficiently verified by checking if $y^i \bmod N = 1$ for $i = 2^2/k, 2 \times 2^2/k, \ldots, r$. For example, if the output is $k = 3$, i.e., $|\Psi_{\text{out}}\rangle_I = |1_1\rangle_1 \otimes |1_0\rangle_0$, the order can be verified by testing $y^i \bmod N = 1$ for $i = \{2^2/3, 2 \times 2^2/3, 3 \times 2^2/3 = 4 = r\}$. Of course, the algorithm fails if the output is $k = 0$, i.e., the target register collapses into the corresponding eigenvector $|u_0\rangle$. However, these deductions may be modified in a realistic quantum computing process where the delays exist, i.e., $\tau_j^{(1)}, \tau_j^{(2)} \neq 0$. In fact, one can easily see from equation (18) that, after applying the inverse QFT, if the target register collapses into the state $|u_k\rangle$, the output in the index register reads

$$|\Psi_{\text{out}}\rangle_I = \prod_{j=1}^{0}\left[\frac{1}{2}(1 + \exp(-\mathrm{i}\Delta_j\tau_j + \pi\mathrm{i}k_j))|0_j\rangle_j + \frac{1}{2}(1 - \exp(-\mathrm{i}\Delta_j\tau_j + \pi\mathrm{i}k_j))|1_j\rangle_j\right]. \tag{22}$$

Therefore, the expected state $|k_1\rangle_1 \otimes |k_0\rangle_0$ is obtained, only if the delays are set up to satisfy the matching condition (14). Otherwise, some errors may appear in the index register. In particular, an undesirable bit flip error will be produced if equation (13) is satisfied. For example, if the target register collapses into the state $|u_3\rangle_T$, the index register generates a null $|0\rangle_I = |0_1\rangle_1 \otimes |0_0\rangle_0$, but not the expected output $|3\rangle_I = |1_1\rangle_1 \otimes |1_0\rangle_0$.

3.3. Quantum counting algorithm with operational delays

Quantum counting is an application of the phase estimation procedure to estimate the eigenvalues of the Grover iteration [17, 18],

$$\hat{G} = -\hat{A}\hat{U}_0\hat{A}^{-1}\hat{U}_f. \tag{23}$$

Here, $\hat{A}$ is any operator which maps $|0\rangle$ to $\sum_{x=0}^{N-1}|x\rangle/\sqrt{N}$, $\hat{U}_0$ maps $|0\rangle$ to $-|0\rangle$ and $\hat{U}_f$ maps $|x\rangle$ to $(-1)^{f(x)}|x\rangle$. This algorithm enables us to estimate the number of solutions to the search problem, as the Grover iterate is almost periodic with a period dependent on the number of solutions. Indeed, from the following equation,

$$\hat{G}|\Psi_\pm\rangle = \exp(\pm 2\pi\mathrm{i}\omega_l)|\Psi_\pm\rangle \qquad l = 0, 1, 2, \ldots, N \tag{24}$$

with $|\Psi_\pm\rangle = (|X_1\rangle \pm \mathrm{i}|X_0\rangle)/\sqrt{2}$, $\exp(\pm 2\pi\mathrm{i}\omega_l) = 1 - 2l/N \pm 2\mathrm{i}\sqrt{l/N - (l/N)^2}$, and $|X_1\rangle = \sum_{f(x)=1}|x\rangle/\sqrt{l}$, $|X_0\rangle = \sum_{f(x)=0}|x\rangle/\sqrt{N-l}$, we see that either ω_l or $-\omega_l$ can be estimated by using the phase estimation algorithm. This gives us an estimation of l, the number of solutions.

In order to explicitly demonstrate how the dynamical phase error reveals in quantum counting, we consider the simple case where $l = N/4$. The expected eigenvalues we want to estimate are $\exp(\pm\pi\mathrm{i}/3)$, corresponding to the target register being kept in the eigenstates $|\Psi_\pm\rangle$. However, in this case the expected output $\omega_1 = 1/6$ cannot be expressed exactly in an n-bit expansion. Following Jones *et al* [18] and Lee *et al* [19], we now adopt the ensemble measurement to approximately characterize the final state of the index register. The algorithm operates on two registers: a single-qubit index register and the target register with m qubits, which are initially prepared in their ground state: $|\psi(0)\rangle_I = |0\rangle$, $|\psi(0)\rangle_T = \prod_{j=m-1}^{0}|0\rangle_j$.

A quantum counting algorithm with delays can also be performed by three operational steps.

(1) Applying the Hadamard transform to two registers simultaneously, we have

$$|\Psi_1\rangle = |\psi_1\rangle_I \otimes |\psi_1\rangle_T \tag{25}$$

with $|\psi_1\rangle_I = \hat{H}|0\rangle_I = (|0\rangle + |1\rangle)/\sqrt{2}$, and $|\psi_1\rangle_T = c_+|\Psi_+\rangle_T + c_-|\Psi_-\rangle_T, c_\pm = \mp i \exp(\pm i\pi/6)/\sqrt{2}$.

(2) After the first finite-time delay $\tau^{(1)}$, we apply the controlled operation $c - \hat{G} = |1\rangle_{I\,I}\langle 1| \otimes \hat{G}_T + |0\rangle_{I\,I}\langle 0| \otimes \hat{I}_T$ to the state $|\Psi_1\rangle$, and have

$$|\Psi_2\rangle = \sum_{j=\pm} \frac{c_j}{\sqrt{2}}[|0\rangle_I + \exp(i(2\pi j\omega_l - \Delta\tau^{(1)}))|1\rangle_I] \otimes |\Psi_j\rangle_T. \tag{26}$$

After k repetitions of the above operations, the state of the system becomes

$$|\Psi_3\rangle = \sum_{j=\pm} \frac{c_j}{\sqrt{2}}[|0\rangle_I + \exp(i(2\pi jk\omega_l - \Delta(\tau^{(1)} + \tau^{(2)} + \cdots + \tau^{(k-1)}))|1\rangle_I] \otimes |\Psi_j\rangle_T. \tag{27}$$

Above, the controlled operation $c - \hat{G}$ means that the operation $\hat{G}$ is applied to the target register only when the control qubit is in state $|1\rangle_I$.

(3) After another finite-time delay $\tau^{(k)}$, we apply a second Hadamard transform to the control qubit, producing

$$|\Psi_4\rangle = \frac{1}{2}\sum_{j=\pm} c_j[(1 + \exp(i(2\pi kj\omega_l - \Delta\tau)))|0\rangle_I + (1 - \exp(i(2\pi kj\omega_l - \Delta\tau)))|1\rangle_I] \otimes |\Psi_j\rangle_T \tag{28}$$

$$\tau = \sum_{m=1}^{k} \tau^{(m)}$$

and then the expectation value of $\hat{\sigma}_z$ is measured to characterize the final state of the index register. This corresponds to determining the population difference between $|0\rangle_{I\,I}\langle 0|$ and $|1\rangle_{I\,I}\langle 1|$ in the state $|\Psi_4\rangle$, and the result can be expressed as

$$\langle\hat{\sigma}_z\rangle_I = \cos(2\pi k\omega_l - \Delta\tau). \tag{29}$$

The expected result for the ideal case, i.e., $\tau^{(m)} = 0$, is $\langle\hat{\sigma}_z\rangle_I(\tau) = \cos(2\pi k\omega_l)$, and the value ω_l is estimated by varying k in a manner based on a technique of Kitaev [11]. For the present problem, if the number of repetitions of the $c - \hat{G}$ operator is $k = 6$, the measurement result will be expected as $\langle\hat{\sigma}_z\rangle_I = 1$. This implies that before the measurement the control qubit is in state $|0\rangle$ with a high probability. However, in practice, operational delays always exist and thus the wavefunction of the control qubit acquires a nontrivial dynamical phase for each delay. As a consequence, the realistic result of the measurement is obviously dependent on the *total* delay time $\tau = \sum_{m=1}^{k} \tau^{(m)}$. We see again that the expected result is obtained only if the matching condition (14) is satisfied.

4. Conclusion and discussion

Ideal quantum algorithms usually assume that quantum computing can be performed by continuously applying a sequence of unitary transforms. In reality, when performing a practical quantum computations, there are finite time intervals between the sequential operations. During these delays, according to the Schrödinger equation, unwanted relative dynamical phases are acquired by the superposition wavefunction of the physical qubit in the quantum

register. In general, this phase modifies the desired quantum interference required for an ideal quantum computer and thus spoils the correct computational results. Note that any entanglement between qubits is caused during these delays, and thus resulting coherent phase errors can be avoided by simply setting up the total delay times to satisfy certain matching conditions. Under these conditions, the relative physical phases in the final state of the superposition wavefunction are deleted. Of course, the dynamical oscillations, due to delays, can also be suppressed by trivially setting up individual delays $\tau_j^{(m)}$, $m = 1, 2 \ldots$, as $\Delta_j \tau_j^{(m)} = 2n\pi$. The key observation here is that *only the total delay time*, instead of the duration for every delay, *needs to be set up accurately to avoid the coherent dynamical phase errors*. Therefore, only the proper setting up of the *total* delay is needed for avoiding coherent intrinsic errors. In these implementations, only the free evolution of the physical qubits in the index register is considered.

Compared to previous schemes [8–10] for studying similar problems, our scheme presents some advantages. First, it does not require that the Hamiltonian should be equal to zero during the quantum register in the idle state (as done in [9]). Second, operations to force the generation of additional phases to eliminate these phase errors (as done in [8]) are not needed. Finally, our approach does not need to use a pair of degenerate states, formed by using two or more physical qubits, to encode a logical qubit (as done in [10]) for transforming the relative phase into a global phase. Therefore, in principle, our proposal should allow the implementation of the expected ideal quantum phase estimation algorithm.

It is worthwhile to emphasize that only the delays between the sequential functional steps of quantum computing are considered in the present simplified scheme. The effective dynamical phases, acquired by superposition wavefunctions of physical qubits during the effective delays, may be added up, as the key operation $c - \hat{U}_j$ in the phase estimation algorithm is diagonal in the logical basis of index register. The applied non-diagonal Hadamard gate $\hat{H}$ and inverse QFT operation $\hat{F}^{-1}$ were assumed to be implemented exactly, and thus the coherent errors relating to the possible operational delays inside the initialization and measurements had been neglected. Indeed, the Hadamard gate had been performed exactly by using one-step operation [20], and the one-step operational approach had been proposed [21] to exactly implement the QFT. Furthermore, the present scheme for avoiding the coherent dynamical phase error is still robust, even if the operational delays inside the initialization and measurement are considered. Usually, only a non-diagonal σ_x-operation is included in a three-step process for realizing a Hadamard gate, and in the inverse QFT for measuring a physical qubit. Fortunately, it is not required to add up the dynamical phase before and after such a non-diagonal σ_x-operation in the quantum phase estimation algorithm. In fact, the qubit is not in superposition state before (after) the applied σ_x-operation in initialization (measurement). Therefore, in the framework of the quantum phase estimation algorithm, the present strategy for avoiding the coherent phase error is sufficiently robust. This approach can also be used for other quantum algorithms, e.g., Deutsch–Jozsa algorithm [1], wherein the key operation is diagonal and the possible non-diagonal operations are also only included in the initialization and measurement operations.

Acknowledgments

We acknowledge Drs Y X Liu and X Hu for discussions. This work was supported in part by the National Security Agency (NSA) and Advanced Research and Development Activity (ARDA) under Air Force Office of Research (AFOSR) contract no F49620-02-1-0334, and by the National Science Foundation grant no EIA-0130383.

References

[1] Nielsen M A and Chuang I L 2000 *Quantum computation and Quantum information* (Cambridge: Cambridge University Press)
[2] Mussinger M, Delgado A and Alber G 2000 *New J. Phys.* **2** 191
[3] Long G L *et al* 2000 *Phys. Rev.* **61** 042305
Long G L *et al* 2001 *J. Chin. Chem. Soc.* **48** 449
[4] Shor P W 1995 *Phys. Rev.* A **52** R2493
[5] Steane A 1998 *Phys. Rev. Lett.* **77** 793
Steane A 1996 *Rep. Prog. Phys.* **61** 117
[6] Lidar D A *et al* 1987 *Phys. Rev. Lett.* **81** 2594
[7] Zanardi P and Rasetti M 1997 *Phys. Rev. Lett.* **79** 3306
[8] Berman G B, Doolen G D and Tsifrinvovish V I 2000 *Phys. Rev. Lett.* **84** 1615
[9] Makhlin Y, Schön G and Shnirman A 1999 *Nature* **398** 305
[10] Feng M 2001 *Phys. Rev.* A **63** 052308
[11] Kitaev A Yu 1995 *Preprint* quant-ph/9511026
[12] Cleve R *et al* 1998 *Proc. R. Soc.* A **454** 339
[13] Abrams D S 1999 *Phys. Rev. Lett.* **83** 5162
[14] Travaglione B C *et al* 2001 *Phys. Rev.* A **63** 032301 (*Preprint* quant-ph/0203130)
[15] Shor P 1994 *Proc. 35th Annual Symposium on the Foundations of Computer Science* ed S Goldwasser (New York: IEEE Computer Society Press) p 124
[16] Vandersypen L M K *et al* 2001 *Nature* **414** 883
Vandersypen L M K *et al* 2000 *Phys. Rev. Lett.* **85** 5452
[17] Grover L K 1998 *Phys. Rev. Lett.* **80** 4329
Grover L K 1997 *Phys. Rev. Lett.* **79** 325
[18] Jones J A and Mosca M 1999 *Phys. Rev. Lett.* **83** 1050
[19] Lee J S *et al* 2002 *Phys. Rev.* A **66** 042316
[20] Nakamura Y, Pashkin Yu A and Tsai J S 1999 *Nature* **398** 786
[21] Niskanen A O, Vartiainen J J and Salomaa M M 2003 *Phys. Rev. Lett.* **90** 197901

EUROPHYSICS LETTERS 1 January 2004

Europhys. Lett., **65** (1), pp. 1–6 (2004)
DOI: 10.1209/epl/i2003-10053-y

Coherently manipulating two-qubit quantum information using a pair of simultaneous laser pulses

L. F. WEI[1,2] and F. NORI[1,3]

[1] *Frontier Research System, The Institute of Physical and Chemical Research (RIKEN) - Wako-shi, Saitama, 351-0198, Japan*
[2] *Institute of Quantum Optics and Quantum Information, Department of Physics Shanghai Jiaotong University - Shanghai 200030, PRC*
[3] *Center for Theoretical Physics, Physics Department Center for the Study of Complex Systems, The University of Michigan Ann Arbor, MI 48109-1120, USA*

(received 6 May 2003; accepted in final form 28 October 2003)

PACS. 03.67.Lx – Quantum computation.
PACS. 32.80.Pj – Optical cooling of atoms; trapping.

Abstract. – Several sequential operations are usually needed for implementing controlled quantum gates and generating entanglement between a pair of quantum bits. Based on the conditional quantum dynamics for a two-ion system beyond the Lamb-Dicke limit, here we propose a theoretical scheme for manipulating two-qubit quantum information, *i.e.*, implementing a universal two-qubit quantum gate and generating a two-qubit entangled state, by using a pair of simultaneous laser pulses. Neither the Lamb-Dicke approximation nor the auxiliary atomic level are required. The experimental realizability of this simple approach is also discussed.

As first suggested in [1], one of the most promising scenarios for implementing a practical quantum information processor is a system of laser-cooled trapped ions, due to its long coherence time [2]. In this system the qubit (*i.e.*, the elementary unit of quantum information) is encoded by two internal levels of each trapped cold ion and can be manipulated individually by using laser pulses. As explained below, a third auxiliary internal level of the ion is also required. Several key features of the proposal in [1], including the production of entangled states and the implementation of quantum controlled operations between a pair of trapped ions, have already been experimentally demonstrated (*e.g.*, [3–6]). Meanwhile, several alternative theoretical schemes (*e.g.*, [7–12]) have also been developed for overcoming various difficulties in realizing a practical ion-trap quantum information processor.

Auxiliary transitions between the encoded atomic levels and the auxiliary ones [1,3,5] and a series of laser pulses [1,9–11] are usually required in various previous schemes for manipulating two-qubit quantum information. For example, a *three*-step operation is required in [13], *five* laser pulses in [1,9], *six* pulses in ref. [10], and *seven* pulses are needed in ref. [11] in order to perform a quantum controlled-NOT (CNOT) logic gate. The first aim of the present work is to propose an efficient scheme for realizing quantum logic operations between a pair of trapped cold ions by *a single-step operation*. The Lamb-Dicke (LD) approximation, which requires that the coupling between the external and internal degrees of freedom of the ion be very weak, is made in *almost all* of the previous schemes (*e.g.*, [4,6,8,11,12]) in order to simplify the laser-ion interaction Hamiltonian. However, the quantum motion of the trapped ions is *not* limited to the LD regime [14]. Therefore, it is important to manipulate quantum information stored in trapped ions outside the LD limit.

The entanglement between different particles is a growing focus of activity in quantum physics [15], because of experiments on non-local features of quantum mechanics and the development of quantum information physics. Especially, entanglement plays a central role in quantum parallelism. The quantum entanglement of two and four trapped cold ions have been generated experimentally [5,6] in the LD limit. The second aim of the present work is to show how to deterministically produce the entangled states of two trapped ions outside the LD regime. The third aim is to achieve this without auxiliary internal levels.

In summary, here we propose a scheme for manipulating quantum information (*i.e.*, realizing quantum controlled operations and generating entanglement) of two trapped ions: i) *beyond* the LD limit, ii) *without* needing any auxiliary atomic level, and iii) by using a *single-step operation.*

We consider an array of N two-level cold ions of mass M confined to move in the z-direction of a Paul trap of frequency ν. The ions are cooled down to very low temperatures and may perform small oscillations around their equilibrium position z_{i0} ($i = 1, 2, \ldots, N$), due to their mutual repulsive Coulomb force. Each ion is assumed to be individually addressed by a separate laser beam. Similarly to ref. [16], we consider the case where an arbitrary pair (labeled by $j = 1, 2$) of the N trapped cold ions are illuminated independently by two weak travelling laser fields with frequencies ω_j. The Hamiltonian corresponding to this situation is

$$\begin{aligned}\hat{H}(t) &= \hbar\omega_0 \sum_{j=1}^{2} \frac{\hat{\sigma}_j^z}{2} + \sum_{l=0}^{N-1} \hbar\nu_l \left(\hat{b}_l^\dagger \hat{b}_l + \frac{1}{2}\right) + \\ &+ \frac{\hbar}{2} \sum_{j=1}^{2} \left\{ \Omega_j \hat{\sigma}_j^+ \exp\left[\sum_{l=0}^{N-1} i\eta_j^l (\hat{b}_l^\dagger + \hat{b}_l) - i\omega_j t - i\phi_j \right] + \text{H.c.} \right\}. \end{aligned} \tag{1}$$

Here, ν_l ($l = 0, 1, \ldots, N-1$) is the frequency of the l-th mode collective vibrational motion, and the LD parameter η_j^l accounts for the coupling strength between the internal state of the j-th ion and the l-th mode of the collective vibration. $\hat{b}_l^\dagger$ and $\hat{b}_l$ are the relevant ladder operators. Ω_j is the carrier Rabi frequency, which describes the coupling strength between the laser and the j-th ion and is proportional to the strength of the applied laser. $\hat{\sigma}_j^z$ and $\hat{\sigma}_j^\pm$ are Pauli operators, $\hbar\omega_0$ is the energy separation of two internal states $|g\rangle$ and $|e\rangle$ of the ion, and ϕ_j is the initial phase of the applied laser beam. Expanding the above Hamiltonian in terms of creation and annihilation operators of the normal modes, we have

$$\begin{aligned}\hat{H} &= \frac{\hbar}{2} \sum_{j=1,2} \left\{ \Omega_j \hat{\sigma}_j^+ \prod_{l=0}^{N-1} \times \right. \\ &\left. \times \left[e^{-(\eta_j^l)^2/2} \sum_{m,n=0}^{\infty} \frac{(i\eta_j^l)^{m+n}}{m!n!} \hat{b}_l^{\dagger m} \hat{b}_l^n \exp\left[i(m-n)\nu_l t + i(\delta_j t - \phi_j) \right] \right] + \text{H.c.} \right\} \end{aligned} \tag{2}$$

in the interaction picture. Here, $\delta_j = \omega_j - \omega_0$ is the detuning between the laser and the ion. Without any loss of generality, we set the frequencies of the applied laser beams as $\omega_j = \omega_0 - k_j\nu$ with $\nu = \nu_0$ being the frequency of the center-of-mass (CM) vibrational mode, $k_2 = 0$, and $k_1 = 1, 2, \ldots$. Like the procedure described in [16,17], we then make the usual rotating wave approximation (RWA). For small values of k_1, the excitations of the higher l-th ($l \geq 1$) vibrational modes can be safely neglected and the following effective Hamiltonian:

$$\hat{H} = \frac{\hbar}{2} \sum_{j=1,2} \left\{ \Omega_j \hat{F}_j \hat{\sigma}_j^+ \exp\left[-\frac{\eta_j^2}{2} - i\phi_j \right] \sum_{n=0}^{\infty} \frac{(i\eta_j)^{2n+k_j} \hat{a}^{\dagger n} \hat{a}^{n+k_j}}{n!(n+k_j)!} + \text{H.c.} \right\} \tag{3}$$

can be obtained. Here, $\hat{a} = \hat{b}_0$, $\hat{a}^\dagger = \hat{b}_0^\dagger$ and $\eta_j = \eta_j^0$ are the boson operators and the LD parameter related to the CM mode, respectively. The operator function $\hat{F}_j = \prod_{l=1}^{N-1} \exp[-(\eta_j^l)^2/2] \times \sum_{n=0}^{\infty} (i\eta_j^l)^{2n} \hat{b}_l^{\dagger n} \hat{b}_l^n / (n!)^2$ is irrelevant [16, 17, 19] in the weak-excitation regime ($\Omega_j \ll \nu$). Therefore, we may let $\hat{F}_j = \hat{I}$ and only label the CM mode excitations.

It is very important to stress that, to the lowest order of the LD parameter η_j, the effective Hamiltonian (3) reduces to that in previous works [4, 6, 8, 12, 17] under the usual LD approximation: $(m + 1/2)\eta_j^2 \ll 1$. Here, m is the occupation number of the Fock state of the CM vibrational quanta. We now analytically solve the quantum dynamical problem associated with the Hamiltonian (3) *without* performing the LD approximation. For simplicity, the information bus (*i.e.*, the CM vibrational mode of the ions) is assumed to be prepared beforehand in an arbitrary pure quantum state, *e.g.*, the Fock state $|m\rangle$. The Hamiltonian (3) implies that the laser pulse applied to the second ion does not excite the CM vibrational state but only rotates the atomic state of the second ion. If the condition $k_1 > m$ is satisfied, then the ground state $|g_1\rangle$ of the first ion will not evolve. Therefore, $\{|m\rangle|g_1\rangle|g_2\rangle, |m\rangle|g_1\rangle|e_2\rangle\}$ and $\{|m\rangle|e_1\rangle|g_2\rangle, |m\rangle|e_1\rangle|e_2\rangle, |m + k_1\rangle|g_1\rangle|g_2\rangle, |m + k_1\rangle|g_1\rangle|e_2\rangle\}$ form two different invariant subspaces of the dynamics ruled by the Hamiltonian (3) with $k_2 = 0$, $k_1 > m$. After a direct derivation, we obtain the exact time evolutions in these subspaces:

$$
\begin{cases}
|m\rangle|g_1\rangle|g_2\rangle \longrightarrow \cos(\tilde{\alpha}_2 t)|m\rangle|g_1\rangle|g_2\rangle - ie^{-i\phi_2}\sin(\tilde{\alpha}_2 t)|m\rangle|g_1\rangle|e_2\rangle, \\
|m\rangle|g_1\rangle|e_2\rangle \longrightarrow \cos(\tilde{\alpha}_2 t)|m\rangle|g_1\rangle|e_2\rangle - ie^{i\phi_2}\sin(\tilde{\alpha}_2 t)|m\rangle|g_1\rangle|g_2\rangle, \\
|m\rangle|e_1\rangle|g_2\rangle \longrightarrow E_1(t)|m + k_1\rangle|g_1\rangle|g_2\rangle + E_2(t)|m + k_1\rangle|g_1\rangle|e_2\rangle + \\
\qquad\qquad +E_3(t)|m\rangle|e_1\rangle|g_2\rangle + E_4(t)|m\rangle|e_1\rangle|e_2\rangle, \\
|m\rangle|e_1\rangle|e_2\rangle \longrightarrow F_1(t)|m + k_1\rangle|g_1\rangle|g_2\rangle + F_2(t)|m + k_1\rangle|g_1\rangle|e_2\rangle + \\
\qquad\qquad +F_3(t)|m\rangle|e_1\rangle|g_2\rangle + F_4(t)|m\rangle|e_1\rangle|e_2\rangle,
\end{cases}
\tag{4}
$$

with

$$
\begin{aligned}
E_1(t) &= (-i)^{k_1+1}\frac{e^{i\phi_1}}{\Delta}[\sin(\lambda_+ t) - \sin(\lambda_- t)], \\
E_4(t) &= -ie^{-i\phi_2}\frac{\rho^2}{\Delta}\left[\frac{\sin(\lambda_+ t)}{\zeta_+} - \frac{\sin(\lambda_- t)}{\zeta_-}\right], \\
E_2(t) &= (-i)^{k_1} e^{i(\phi_1 - \phi_2)}\left(\frac{\alpha_1\rho^2 + \tilde{\gamma}_2\zeta_+\rho}{\lambda_+\zeta_+\Delta}\right)[\cos(\lambda_+ t) - \cos(\lambda_- t)], \\
E_3(t) &= \frac{\rho^2}{\Delta}\left[\frac{\cos(\lambda_+ t)}{\zeta_+} - \frac{\cos(\lambda_- t)}{\zeta_-}\right]; \\
F_1(t) &= (-i)^{k_1} e^{i(\phi_1 + \phi_2)}\frac{\rho}{\Delta}[\cos(\lambda_+ t) - \cos(\lambda_- t)], \\
F_4(t) &= \frac{\rho^2}{\Delta}\left[\frac{\cos(\lambda_+ t)}{\zeta_+} - \frac{\cos(\lambda_- t)}{\zeta_-}\right], \\
F_2(t) &= (-i)^{k_1+1} e^{i\phi_1}\left(\frac{\alpha_1\rho^2 + \tilde{\gamma}_2\zeta_+\rho}{\lambda_+\zeta_+\Delta}\right)[\sin(\lambda_+ t) - \sin(\lambda_- t)], \\
F_3(t) &= -ie^{i\phi_2}\frac{\rho^2}{\Delta}\left[\frac{\sin(\lambda_+ t)}{\zeta_+} - \frac{\sin(\lambda_- t)}{\zeta_-}\right].
\end{aligned}
$$

Here,

$$\rho = \alpha_1(\tilde{\alpha}_2+\tilde{\gamma}_2), \qquad \lambda_\pm = \sqrt{\frac{\Lambda\pm\Delta}{2}}, \qquad \Lambda = \tilde{\alpha}_2^2+\tilde{\gamma}_2^2+2\alpha_1^2,$$

$$\Delta^2 = \Lambda^2-4\left(\tilde{\alpha}_2\tilde{\gamma}_2-\alpha_1^2\right)^2, \qquad \zeta_\pm = \lambda_\pm^2-\tilde{\alpha}_2^2-\alpha_1^2;$$

$$\alpha_j = \Omega_m^{(k_j)}, \qquad \Omega_m^{(k_j)} = \frac{\Omega_j\left(\eta_j\right)^{k_j}\exp\left[-\eta_j^2/2\right]}{2}\sqrt{\frac{(m+k_j)!}{m!}}\sum_{n=0}^{m}\frac{\left(-i\eta_j\right)^{2n}}{(n+k_j)!}\binom{n}{m},$$

$$\tilde{\alpha}_j = \Omega_m^{(0)}, \qquad \tilde{\gamma}_j = \Omega_{m+k_l}^{(0)}, \qquad j,l=1,2,\ j\neq l.$$

Note that the above evolutions are performed by a single-step operation by applying, separately to two ions, a pair of simultaneous laser pulses with different frequencies. The exact dynamical evolution for other cases can also be derived exactly in a similar way. For example, for the case where $k_1<0$ and $|k_1|>m$ (*i.e.*, the CM mode is excited by blue-sideband laser beam applied to the first ion), the relevant evolution equations can be easily obtained from eq. (4) by making the replacements $|e_j\rangle \leftrightarrow |g_j\rangle$ in the third and fourth formulas.

Based on the conditional quantum dynamics derived above, we now show how to simultaneously manipulate quantum information stored in two ions by *a single* operation, *i.e.*, implementing the universal two-qubit gate and engineering two-qubit entanglement, beyond the LD limit. This is achieved by properly controlling the initial phases, wave vectors, and the duration of the applied simultaneous beams.

First, the two-qubit controlled gate implies that the effect of the operation on the second qubit (target one) depends on what state the first qubit (control one) is in. It is easily seen from eq. (4) that, if the following conditions:

$$\cos(\tilde{\alpha}_2\tau)=\sin(\lambda_+\tau)=\sin(\lambda_-\tau)=1, \tag{5}$$

are satisfied, the two-qubit controlled operation

$$\tilde{C}_{12}^X = |g_1\rangle|g_2\rangle\langle g_1|\langle g_2| + |g_1\rangle|e_2\rangle\langle g_1|\langle e_2| - ie^{-i\phi_2}|e_1\rangle|g_2\rangle\langle e_1|\langle e_2| - ie^{i\phi_2}|e_1\rangle|e_2\rangle\langle e_1|\langle g_2| \tag{6}$$

can be realized directly. Here τ is the duration of the two simultaneously applied pulses. The state of the information bus is unchanged during this operation. Physically, by coupling to the common information bus, *i.e.*, the CM vibrational quanta, two ions may entangle. In fact, eqs. (4) clearly show that the rotation of the atomic states of the second ion depend on the quantum state of the bus, although the bus quanta is not excited by the applied resonant laser beam on the second ion ($\omega_2=\omega_0$). Therefore, the evolving quantum state of the bus, due to evolution of the first ion driven by a non-resonant laser beam, correlates two separate ions. Once the relevant experimental parameters are set to satisfy the conditions (5), the two-qubit entangled gate (6) is implemented. This controlled operation is equivalent [18] to the exact CNOT gate: $\hat{C}_{12}^X = |g_1\rangle|g_2\rangle\langle g_1|\langle g_2| + |g_1\rangle|e_2\rangle\langle g_1|\langle e_2| + |e_1\rangle|g_2\rangle\langle e_1|\langle e_2| + |e_1\rangle|e_2\rangle\langle e_1|\langle g_2|$, except for a local rotation. One can easily check that both the small and large, as well as negative and positive values of the LD parameters may be chosen to satisfy the condition (5) for realizing the desired two-qubit controlled gate. Our approach does not assume the LD approximation. Thus, the present scheme operates outside the LD regime and η_j can be large.

Second, we show below that the entangled states of two trapped ions can also be produced deterministically outside the LD regime. In fact, it is seen from the dynamical evolution eq. (4) that the entanglement between two ions can also be easily engineered outside the LD limit. Beginning with the non-entangled initial state $|\psi_0\rangle = |m\rangle|g_1\rangle|g_2\rangle$, we now describe a convenient approach to do this engineering.

We now first apply a laser beam with frequency $\omega_1 = \omega_0$, initial phase ϕ_1, and duration t_1 to ion 1, and realize the following evolution:

$$|\psi_0\rangle \xrightarrow{\hat{R}_1(m,t_1)} \cos(\tilde{\alpha}_1 t_1)|m\rangle|g_1\rangle|g_2\rangle - ie^{-i\phi_1}\sin(\tilde{\alpha}_1 t_1)|m\rangle|e_1\rangle|g_2\rangle = |\psi_1\rangle, \tag{7}$$

with $\hat{R}_1(m,t_1)$ being a simple operation of rotating the spin state of the ion 1. The CM mode quanta is not excited and the spin state of ion 2 is unchanged during this process. Obviously, this evolution may also be implemented by using a pair of simultaneous laser beams with frequencies $\omega_1 = \omega_0$ and $\omega_2 = \omega_0 - k_2\nu$ ($k_2 > m$), respectively.

We then apply another pair of simultaneous laser beams with frequencies $\omega_2 = \omega_0$ and $\omega_1 = \omega_0 - k_1\nu$ ($k_1 > m$) to realize the two-qubit controlled operation $\tilde{C}_{12}^X$ introduced above. This lets the non-entangled state $|\psi_1\rangle$ evolve in the desired entangled state $|\psi_{12}(t)\rangle$:

$$|\psi_1\rangle \xrightarrow{\tilde{C}_{12}^X} U(t)|g_1\rangle|g_2\rangle + V(t)|e_1\rangle|e_2\rangle = |\psi_{12}(t)\rangle, \tag{8}$$

with $U(t_1) = \cos(\tilde{\alpha}_1 t_1)$, $V(t_1) = -e^{i(\phi_2-\phi_1)}\sin(\tilde{\alpha}_1 t_1)$. Interestingly, the generated entangled state reduces to the two-qubit maximally entangled states; *i.e.*, the corresponding EPR states: $|\Psi_{12}^{\pm}\rangle = (|g_1\rangle|g_2\rangle \pm |e_1\rangle|e_2\rangle)/\sqrt{2}$, if the experimental parameters, such as the duration t_1 and wave vector $\vec{\kappa}_1$ of the applied laser beam for realizing the single-qubit rotation $\hat{R}_1(m,t_1)$, are further set properly.

We now briefly discuss the experimental realizability of this proposal. Indeed, it is not difficult to properly set the relevant parameters for satisfying the condition (5). For example, the desired LD parameter [19] defined by

$$\eta_j = \sqrt{\hbar\kappa_j^2/(2MN\nu)}\cos\theta_j, \qquad \theta_j = \arccos\left(\vec{\kappa}_j \cdot \vec{z}_j/\kappa_j\right), \tag{9}$$

can be reached by conveniently controlling the wave vector $\vec{\kappa}_j$ of the applied laser beams. It might seem at first, from the condition (5), that the present scheme for realizing the desired gate operation cannot be easily implemented, as the relevant experimental parameters should be set accurately. For example, if the Rabi frequencies and LD parameters are set as $\Omega_1 = \Omega_2 = \Omega$, $\eta_1 = \pm 2.18403$, $\eta_2 = \pm 1.73205$, then the duration τ of the two applied simultaneous pulses should be set up accurately as $\Omega\tau = 56.3186$. A simple numerical analysis shows that the lowest probability of realizing the desired operation is still very high, even if the relevant parameters cannot be set exactly. For example, even if the duration of the applied laser pulses is set roughly such that $\Omega\tau \approx 56.3$ (56.0), which is 0.03% (0.57%) away from the exact solution of condition (5), one can realize the operation $\tilde{C}_{12}^X$ with a very high probability, *i.e.*, 99.998% (99.36%), via a single-step operation. Indeed, by testing other values we have proven that our predictions are very robust.

Finally, we note that the duration of the applied simultaneous pulses for realizing the above quantum controlled operation is not much longer than that for other schemes [4,6,8,12] operating in the LD regime. The duration for implementing the above operation is estimated as $\sim 10^{-4}$ seconds, of the same order of the gate speed operating in the LD regime [3], for $\Omega/2\pi \approx 225\,\mathrm{kHz}$ and $\nu = \omega_z \approx 7\,\mathrm{MHz}$ [5]. To excite only the chosen sidebands of the CM mode, the spectral width of the applied laser pulse has to be small. However, it is not so small as to affect the speed of the operations, since the separation between the CM mode and the other ones is sufficiently large, *e.g.*, $\nu_1 - \nu = (\sqrt{3}-1)\nu \sim \nu$. In particular, it is not difficult for the current laser-cooling technologies to cool the trapped ions to their motional ground state. In our proposal, the ions must be cold. However, in principle, the heating effect may

be suppressed by atom interferometry [13]. Therefore, the present scheme might be realizable in the near future.

In summary, we have proposed an efficient theoretical scheme for simultaneously manipulating two-qubit quantum information stored in the chosen two ions. Under certain conditions a universal two-qubit gate can be exactly realized by a *single-step* pulse process performed by simultaneously applying a pair of laser beams with different frequencies. By using this quantum operation, one may engineer the entanglement state between the two chosen ions. All operations proposed here operate *outside* the LD regime and do *not* involve quantum transitions to auxiliary atomic levels. It is expected that the present scheme may be extended to simultaneously manipulate three-, four- or multi-qubit quantum information and may be also extended to other systems besides trapped ions, *e.g.*, quantum dots on quantum linear supports [20], for quantum information processing.

* * *

We thank X. HU and C. MONROE for useful comments and acknowledge the support of NSA and ARDA under AFOSR contract No. F49620-02-1-0334, and by the NSF grant No. EIA-0130383.

REFERENCES

[1] CIRAC J. I. and ZOLLER P., *Phys. Rev. Lett.*, **74** (1995) 4091.
[2] KIELPINSKI D. *et al.*, *Science*, **291** (2001) 1013; SCHMIDT-KALER F. *et al.*, *J. Mod. Opt.*, **47** (2000) 2573.
[3] MONROE C. *et al.*, *Phys. Rev. Lett.*, **75** (1995) 4714; ROOS CH. *et al.*, *Phys. Rev. Lett.*, **83** (1999) 4713.
[4] KING B. E. *et al.*, *Phys. Rev. Lett.*, **81** (1998) 1525.
[5] TURCHETTE Q. A. *et al.*, *Phys. Rev. Lett.*, **81** (1998) 3631; MORIGI G. *et al.*, *Phys. Rev. A*, **59** (1999) 3797.
[6] NGERL H. C. *et al.*, *Phys. Rev. A*, **60** (1999) 145; SCKETT C. A. *et al.*, *Nature (London)*, **404** (2000) 256.
[7] DUAN L. M., CIRAC J. I. and ZOLLER P., *Science*, **292** (2001) 1695; LI L. X. and GUO G. C., *Phys. Rev. A*, **60** (1999) 696.
[8] JONATHAN D. and PLENIO M. B., *Phys. Rev. Lett.*, **87** (2001) 127901.
[9] WEI L. F., LIU S. Y. and LEI X. L., *Phys. Rev. A*, **65** (2002) 062316.
[10] JONATHAN D. *et al.*, *Phys. Rev. A*, **62** (2000) 042307.
[11] CHILDS A. M. and CHUANG I. L., *Phys. Rev. A*, **63** (2000) 012306.
[12] MØLMER K. and SØRENSEN A., *Phys. Rev. Lett.*, **82** (1999) 1835; SØRENSEN A. and MØLMER K., *Phys. Rev. Lett.*, **82** (1999) 1971; SVANDAL A. and HANSEN J. P., *Phys. Rev. A*, **65** (2002) 033406; SØRENSEN A. and MØLMER K., *Phys. Rev. A*, **62** (1999) 022311.
[13] POYATOS J. F., CIRAC J. I. and ZOLLER P., *Phys. Rev. Lett.*, **81** (1998) 1322.
[14] WINELAND D. J. and ITANO W. M., *Phys. Rev. A*, **20** (1979) 1521; STEVENS D., BROCHARD J. and STEANE A. M., *Phys. Rev. A*, **58** (1998) 2750; STEANE A., *Appl. Phys. B*, **64** (1997) 623; JAMES D. F. V., *Appl. Phys. B*, **66** (1998) 181.
[15] See, *e.g.*, the following reviews: BENNETT C. H. and DIVINCENZO D. P., *Nature*, **44** (2000) 247; EKERT A. and JOSZA R., *Rev. Mod. Phys.*, **68** (1996) 733; STEANE A. M., *Rep. Prog. Phys.*, **61** (1998) 117.
[16] SOLANO E. *et al.*, *Phys. Rev. A*, **62** (2000) 021401; **59** (1999) R2539; **64** (2001) 024304.
[17] SOLANO E., DE MATOS FIHO R. L. and ZAGURY N., *Phys. Rev. Lett.*, **87** (2001) 060402.
[18] MONROE C. *et al.*, *Phys. Rev. A*, **55** (2001) R2489.
[19] ŠAŠURA M. and BUŽEK V., *J. Mod. Opt.*, **49** (2002) 1593.
[20] BROWN K. R., LIDAR D. A. and WHALEY K. B., *Phys. Rev. A*, **65** (2001) 012307.

Available online at www.sciencedirect.com
SCIENCE DIRECT
ELSEVIER
Physics Letters A 320 (2003) 131–139
PHYSICS LETTERS A
www.elsevier.com/locate/pla

An efficient single-step scheme for manipulating quantum information of two trapped ions beyond the Lamb–Dicke limit

L.F. Wei [a,b,*], Franco Nori [a,c]

[a] *Frontier Research System, The Institute of Physical and Chemical Research (RIKEN), Wako-shi, Saitama 351-0198, Japan*
[b] *Department of Physics, Institute of Quantum Optics and Quantum Information, Shanghai Jiaotong University, Shanghai 200030, PR China*
[c] *Physics Department, Center of Theoretical Physics, Center for the Study of Complex Systems, University of Michigan, Ann Arbor, MI 48109-1120, USA* [1]

Received 21 June 2003; received in revised form 6 November 2003; accepted 11 November 2003

Communicated by P.R. Holland

Abstract

Based on the exact conditional quantum dynamics for a two-ion system, we propose an efficient *single-step* scheme for coherently manipulating quantum information of two trapped cold ions by using a pair of synchronous laser pulses. Neither the auxiliary atomic level nor the Lamb–Dicke approximation are needed.

PACS: 03.65.Bz; 32.80.Pj; 89.70.+c

Keywords: Quantum information; Trapped cold ions; Lamb–Dicke limit

1. Introduction

The entanglement between different particles has recently become a focus of activity in quantum physics (see, e.g., [1]), because of experiments on non-local features of quantum mechanics and the development of quantum information physics. Einstein–Podolsky–Rosen (EPR) entangled states with two particles have been employed not only to test Bell's inequality [2], but also to realize quantum cryptography and quantum teleportation [1]. Also, entanglement plays a central quantitative role in quantum parallelism [3]. The demonstrations of quantum entanglement to date are usually based on various probabilistic processes, e.g., the generation of photon pairs in parametric down conversion [4]. However, it is very difficult to generate the entanglement of larger numbers of particles, as the probability of randomly generating the appropriate conditions decreases exponentially with the number of particles. Intense activities are now focused on generating an entanglement of particles in a deterministic

* Corresponding author.
E-mail addresses: lfwei@riken.jp (L.F. Wei), fnori@riken.jp (F. Nori).
[1] Permanent address.

0375-9601/$ – see front matter
doi:10.1016/j.physleta.2003.11.013

way, i.e., to produce a desired entangled state. For example, the entanglements of two and four trapped ions have been produced experimentally [5,6].

As first suggested by Cirac and Zoller [7], a very promising scenario for implementing a practical quantum information processor is the system of laser-cooled trapped ions, due to its long coherence time [8]. Information in this system is stored in the spin states of an array of trapped cold ions and manipulated by using laser pulses. The ions are held apart from one another by their mutual Coulomb repulsion. Each ion can be individually addressed by focusing laser beams on the selected ion. The collective normal modes of oscillation shared by all of the ions form the information bus, through which all gate operations can be performed. In the past few years, several key features of the proposal in [7], including the production of entangled states and the implementation of quantum controlled operations between a pair of trapped ions, have already been experimentally demonstrated [5,9–11]. Also, several alternative theoretical schemes (see, e.g., [12–19]) have been developed for overcoming various difficulties in realizing a practical ion-trap quantum information processor.

The Lamb–Dicke (LD) approximation is made in *almost all* of previous schemes (see, e.g., [5,10,13,18,19]), wherein the interaction between the internal states $|s\rangle = \{|g\rangle, |e\rangle\}$ and the external motional harmonic oscillator states $\{|n\rangle; n = 0, 1, 2, \ldots\}$ of the ion is usually expanded to the lowest order of the LD parameter η_L. This approximation requires that the coupling between the external and internal degrees of freedom of the ion is very weak, i.e., the spatial dimension of the motion of the ground state of the trapped ion should be much smaller than the effective wavelength of the applied laser field (see, e.g., [7,20]). However, the quantum motion of the trapped ions is *not* limited to the LD regime [21,22]. Inversely, utilizing the laser-ion interaction beyond this limit could be helpful for reducing the noise in the trap and improving the cooling rate (see, e.g., [22]). Therefore, it would be useful to implement the trapped-ion quantum information processing outside the LD regime. Experimentally, the cooling of the motional ground state of two trapped ions has been achieved in a Paul trap in the LD limit [10]. Recently, Morigi et al. has given a proposal for cooling the collective motional states of two trapped ions outside the LD regime [23]. This is a further step towards realizing the ion trap quantum computer operating outside the LD regime. In fact, several schemes [14–16] have been proposed to implement the quantum computation with trapped ions beyond the LD limit by sequently applying a series of pulses.

In this Letter, we propose an alternative scheme for manipulating quantum information, e.g., realizing quantum controlled operations and generating entanglement, of two trapped ions *beyond* the LD limit by using a pair of synchronous laser pulses. The information bus, i.e., the center-of-mass (CM) vibrational quanta of the ions, for communicating different ions, may be either in its ground or an arbitrary excitation state. Neither the auxiliary atomic level nor the Lamb–Dicke approximation are needed in this Letter. The experimental realization of this simple approach is discussed.

2. Conditional quantum dynamics for two trapped ions driven by two synchronous classical laser beams beyond the Lamb–Dicke limit

The ion trap quantum information processor consists of a string of ions stored in a very cold linear radio-frequency trap. The motion of the ions, which are coupled together due to the Coulomb force between them, is quantum mechanical in nature. The ions are sufficiently separated apart (see, e.g., [22,24]) to be easily addressed by different laser beams, i.e., each ion can be illuminated individually by a separate leaser beam. The communication and logic operations between qubits are usually performed by exciting or de-exciting quanta of the collective vibration (i.e., the shared phonon) modes, which act as the information bus (see, e.g., [7,14,17]).

We consider an array of N two-level cold ions of mass M trapped in a one-dimensional harmonic potential of frequency ν. The ions are able to perform small oscillations around their equilibrium position z_{i0} $(i = 1, 2, \ldots, N)$, due to the repulsive Coulomb force between them. Each one of the ions is assumed to be individually addressed by a separate laser beam. We consider the case where an arbitrary pair (labeled by $j = 1, 2$) of trapped cold ions from the chain of N trapped cold ions are illuminated independently by two weak classical laser beams. This is different

from the scheme proposed in [25,26] of using Raman lasers to drive the ions. The Hamiltonian corresponding to our situation is

$$\hat{H}(t) = \hbar\omega_0 \sum_{j=1}^{2} \frac{\hat{\sigma}_{z,j}}{2} + \hbar\nu\left(\hat{a}^\dagger\hat{a} + \frac{1}{2}\right) + \sum_{l=1}^{N-1} \hbar\nu_l\left(\hat{b}_l^\dagger\hat{b}_l + \frac{1}{2}\right)$$
$$+ \frac{\hbar}{2}\sum_{j=1}^{2}\left\{\Omega_j\hat{\sigma}_{+,j}\exp\left\{i\left[\eta_j(\hat{a}^\dagger + \hat{a}) + \sum_{l=1}^{N-1}\eta_{j,l}(\hat{b}_l^\dagger + \hat{b}_l) - \omega_j t - \phi_j\right]\right\} + \text{H.c.}\right\}. \quad (1)$$

Here, ν and ν_l $(l = 1, \ldots, N-1)$ are the frequencies of the collective center-of-mass (CM) vibrational motion $(l = 0)$ and the higher normal modes $(l \geqslant 1)$ of the trapped ions, respectively; $\hat{a}^\dagger$ and $\hat{a}$ are the ladder operators of CM mode, while $\hat{b}_l^\dagger$ and $\hat{b}_l$ are the ladder operators of the higher normal modes. Ω_j $(j = 1, 2)$ is the carrier Rabi frequency, which describes the coupling strength between the laser and the jth ion and is proportional to the strength of the applied laser. $\hat{\sigma}_{z,j}$ and $\hat{\sigma}_{\pm,j}$ are Pauli operators, $\hbar\omega_0$ is the energy separation of the two internal states $|g\rangle$ and $|e\rangle$ of the ion, and ϕ_j is the initial phase of the applied laser beam. The LD parameters η_j and $\eta_{j,l}$ account for the coupling strength between the internal state of the jth ion and the vibrational states of the CM mode and the higher frequency modes, respectively. Expanding Eq. (1) in terms of creation and annihilation operators of the normal modes, we can rewrite the Hamiltonian of system in the interaction picture as

$$\hat{H} = \frac{\hbar}{2}\sum_{j=1,2}\left\{\Omega_j\hat{\sigma}_{+,j}\hat{G}_j\left[\exp\left(-\frac{\eta_j^2}{2} - i\phi_j\right)\sum_{m,n=0}^{\infty}\frac{(i\eta_j)^{m+n}\hat{a}^{\dagger m}\hat{a}^n}{m!n!}\exp\left[i(m-n)\nu t + i\delta_j t\right]\right] + \text{H.c.}\right\}, \quad (2)$$

with

$$\hat{G}_j = \prod_{l=1}^{N-1}\exp\left(-\frac{(\eta_{j,l})^2}{2}\right)\sum_{m',n'=0}^{\infty}\frac{(i\eta_{j,l})^{m'+n'}\hat{b}_l^{\dagger m'}\hat{b}_l^{n'}}{m'!n'!}\exp\left[i(m'-n')\nu_l t\right].$$

We assume that the frequencies of the applied lasers to be tuned resonantly on the same lower red-sidebands of the center-of-mass (CM) vibrational mode, i.e., the frequencies ω_j of the applied lasers are chosen to be $\omega_j = \omega_0 - k_j\nu, k_j = k = 1, 2, \ldots$. Then, like the procedure described in [25,27,28], we make the usual rotating wave approximation (RWA) and have the following effective Hamiltonian

$$\hat{H}_{\text{eff}} = \frac{\hbar}{2}\sum_{j=1,2}\left\{\tilde{\Omega}_j\hat{\sigma}_{+,j}\exp\left(-\frac{\eta_j^2}{2} - i\phi_j\right)\sum_{n=0}^{\infty}\frac{(i\eta_j)^{2n+k}\hat{a}^{\dagger n}\hat{a}^{n+k}}{n!(n+k)!} + \text{H.c.}\right\}, \quad (3)$$

for small k values. Here, we are considering the weak excitation regime ($\Omega_j \ll \nu$, i.e., the intensity of the applied laser beams is assumed to be sufficiently weak) [25,27,28]. In this regime, the excitations of the higher-l normal modes $(l \geqslant 1)$ is irrelevant and can be renormalized to the effective Rabi frequencies $\tilde{\Omega}_j$. We stress the following important fact: the effective Hamiltonian (3) reduces to that in previous works (e.g., [5,10,13,19] under the usual LD approximation: $(m+1)\eta_j^2 \ll 1$), to the lowest order of the LD parameter η_j. Here m is the occupation number of the Fock state of the CM vibrational quanta. Also, the Hamiltonian (3) reduces to that in [27] for $k = 1$.

In order to manipulate a pair of trapped ions outside the LD regime, we now wish to solve the quantum dynamical problem associated with the above Hamiltonian (3) *without* using the LD approximation. All operations presented below are based on this solution and do not involve quantum transitions to auxiliary atomic levels. Without loss of generality, the information bus (i.e., the CM vibrational mode of the ions) is assumed to be prepared beforehand in a pure quantum state, e.g., the Fock state $|m\rangle$ with $m < k$. During the time-evolution $\hat{U}(t) = \exp(-it\hat{H}_{\text{eff}}/\hbar)$, the initial state $|m\rangle|g_1\rangle|g_2\rangle$ is unchanged, i.e.,

$$|m\rangle|g_1\rangle|g_2\rangle \xrightarrow{\hat{U}(t)} |m\rangle|g_1\rangle|g_2\rangle, \quad (4)$$

since $\hat{H}_{\rm eff}|m\rangle|g_1\rangle|g_2\rangle = 0$. Using the relations

$$\hat{H}_{\rm eff}|m\rangle|e_1\rangle|g_2\rangle = (-i)^k\hbar e^{i\phi_1}\alpha_1|m+k\rangle|g_1\rangle|g_2\rangle, \qquad \hat{H}_{\rm eff}|m\rangle|g_1\rangle|e_2\rangle = (-i)^k\hbar e^{i\phi_2}\alpha_2|m+k\rangle|g_1\rangle|g_2\rangle,$$

and

$$\hat{H}_{\rm eff}|m+k\rangle|g_1\rangle|g_2\rangle = i^k\hbar\big(e^{-i\phi_1}\alpha_1|m\rangle|e_1\rangle|g_2\rangle + e^{-i\phi_2}\alpha_2|m\rangle|g_1\rangle|e_2\rangle\big),$$

we have the evolutions

$$\begin{cases} |m\rangle|g_1\rangle|e_2\rangle \xrightarrow{\hat{U}(t)} B_1(t)|m+k\rangle|g_1\rangle|g_2\rangle + B_2(t)|m\rangle|g_1\rangle|e_2\rangle + B_3(t)|m\rangle|e_1\rangle|g_2\rangle, \\ |m\rangle|e_1\rangle|g_2\rangle \xrightarrow{\hat{U}(t)} C_1(t)|m+k\rangle|g_1\rangle|g_2\rangle + C_2(t)|m\rangle|g_1\rangle|e_2\rangle + C_3(t)|m\rangle|e_1\rangle|g_2\rangle, \end{cases} \tag{5}$$

with

$$B_1(t) = (-i)^{k+1}e^{i\phi_2}\frac{\alpha_2\sin(\chi t)}{\chi}, \qquad B_2(t) = \frac{\alpha_1^2+\alpha_2^2\cos(\chi t)}{\chi^2}, \qquad B_3(t) = e^{-i(\phi_1-\phi_2)}\frac{\alpha_1\alpha_2[\cos(\chi t)-1]}{\chi^2};$$
$$C_1(t) = (-i)^{k+1}e^{i\phi_1}\frac{\alpha_1\sin(\chi t)}{\chi}, \qquad C_3(t) = \frac{\alpha_2^2+\alpha_1^2\cos(\chi t)}{\chi^2}, \qquad C_2(t) = e^{i(\phi_1-\phi_2)}\frac{\alpha_1\alpha_2[\cos(\chi t)-1]}{\chi^2}.$$

Here, $j = 1, 2$, and

$$\chi = \sqrt{\alpha_1^2+\alpha_2^2}, \quad \alpha_j = \tilde{\Omega}^j_{m,k}, \qquad \beta_j = \tilde{\Omega}^j_{m+k,k}, \quad \tilde{\Omega}^j_{m,k} = \frac{\tilde{\Omega}_j e^{-\eta_j^2/2}}{2}\sqrt{\frac{(m+k)!}{m!}}\sum_{n=0}^{m}\frac{(-i\eta_j)^{2n+k}}{(n+k)!}\binom{n}{m}.$$

Finally, in order to obtain the time-evolution of the initial state $|m\rangle|e_1\rangle|e_2\rangle$, we solve the Schrödinger equation $i\hbar\partial|\psi(t)\rangle/\partial t = \hat{H}_{\rm eff}|\psi(t)\rangle$ in the invariant subspace $\{|m+2k\rangle|g_1\rangle|g_2\rangle, |m+k\rangle|e_1\rangle|g_2\rangle, |m+k\rangle|g_1\rangle|e_2\rangle, |m\rangle|e_1\rangle \times |e_2\rangle\}$,

$$i\frac{\partial}{\partial t}\begin{pmatrix} D_1(t) \\ D_2(t) \\ D_3(t) \\ D_4(t) \end{pmatrix} = \begin{pmatrix} 0 & (-i)^k\alpha_1 e^{i\phi_1} & (-i)^k\alpha_2 e^{i\phi_2} & 0 \\ i^k\alpha_1 e^{-i\phi_1} & 0 & 0 & (-i)^k\beta_2 e^{i\phi_2} \\ i^k\alpha_2 e^{-i\phi_2} & 0 & 0 & (-i)^k\beta_1 e^{i\phi_1} \\ 0 & i^k\beta_2 e^{-i\phi_2} & i^k\beta_1 e^{-i\phi_1} & 0 \end{pmatrix}\begin{pmatrix} D_1(t) \\ D_2(t) \\ D_3(t) \\ D_4(t) \end{pmatrix},$$

with initial conditions: $D_1(0) = D_2(0) = D_3(0) = 0$, $D_4(0) = 1$. Here, $|\psi(t)\rangle = D_1(t)|m+2k\rangle|g_1\rangle|g_2\rangle + D_2(t)|m+k\rangle|e_1\rangle|g_2\rangle + D_3(t)|m+k\rangle|g_1\rangle|e_2\rangle + D_4(t)|m\rangle|e_1\rangle|e_2\rangle$. After a long but direct algebraic derivation, we obtain the exact time-evolution

$$\begin{aligned} |m\rangle|e_1\rangle|e_2\rangle \xrightarrow{\hat{U}(t)} & D_1(t)|m+2k\rangle|g_1\rangle|g_2\rangle + D_2(t)|m+k\rangle|e_1\rangle|g_2\rangle + D_3(t)|m+k\rangle|g_1\rangle|e_2\rangle \\ & + D_4(t)|m\rangle|e_1\rangle|e_2\rangle, \end{aligned} \tag{6}$$

with

$$D_1(t) = i^{(2k)}e^{i(\phi_1+\phi_2)}\frac{\rho}{\Delta}\big[\cos(\lambda_+ t) - \cos(\lambda_- t)\big], \qquad D_4(t) = \frac{1}{\Delta}\big[\zeta_+\cos(\lambda_- t) - \zeta_-\cos(\lambda_+ t)\big],$$
$$D_2(t) = (-i)^{k+1}e^{i\phi_2}\frac{\rho}{\Delta}\left[\frac{\alpha_2\rho+\beta_1\zeta_+}{\lambda_+\zeta_+}\sin(\lambda_+ t) - \frac{\alpha_2\rho+\beta_1\zeta_-}{\lambda_-\zeta_-}\sin(\lambda_- t)\right],$$

and

$$D_3(t) = (-i)^{k+1}e^{i\phi_1}\frac{\rho}{\Delta}\left[\frac{\alpha_1\rho+\beta_2\zeta_+}{\lambda_+\zeta_+}\sin(\lambda_+ t) - \frac{\alpha_1\rho+\beta_2\zeta_-}{\lambda_-\zeta_-}\sin(\lambda_- t)\right].$$

Here,

$$\rho = \alpha_1\beta_2 + \alpha_2\beta_1,$$
$$\zeta_\pm = \lambda_\pm^2 - \sum_{j=1}^{2}\alpha_j^2, \quad \lambda_\pm = \sqrt{\frac{\Lambda \pm \Delta}{2}}, \quad \Lambda = \sum_{j=1}^{2}(\alpha_j^2 + \beta_j^2), \quad \Delta^2 = \Lambda^2 - 4(\alpha_1\beta_1 - \alpha_2\beta_2)^2.$$

Analogously, the effective Hamiltonian and the relevant dynamical evolutions for other driving cases can also be derived exactly. For example, for the case where $k_1 = k_2 = k' < 0$ and $|k'| = k > m$ (i.e., the ions are excited by blue-sideband laser beams with equal frequencies instead of red-sideband ones), the effective Hamiltonian and the relevant dynamics of the system can be easily obtained from Eq. (3) and Eqs. (4)–(6) by making the replacements: $\hat{a} \leftrightarrow \hat{a}^\dagger$ and $|e_j\rangle \leftrightarrow |g_j\rangle$, respectively.

3. Manipulation of quantum information in two trapped cold ions

Based on the conditional quantum dynamics for the two-qubit system derived in the previous section, we now show how to effectively manipulate two-qubit quantum information stored in two ions by applying a pair of simultaneous laser pulses. Generally, the motion state entangles with the spin states during the dynamical evolution. We afterwards focus on how to decouple them and realize *in one step* and beyond the LD limit: either a two-qubit controlled operation or an entanglement between the trapped ions. The state of the information bus (CM mode) remains in its initial state, which is not entangled with the qubits after the operations. This is achieved by properly setting up the controllable experimental parameters, e.g., the Lamb–Dicke parameters η_j, the effective Rabi frequencies $\tilde{\Omega}_j$, the frequencies ω_j ($j = 1, 2$) and the duration of the applied synchronous pulses.

3.1. Two-qubit controlled operations

As one of the simplest universal two-qubit quantum gates, the C^Z logic operation between the 1st and the 2nd ions

$$\hat{C}_{12}^Z = |g_1\rangle|g_2\rangle\langle g_1|\langle g_2| + |g_1\rangle|e_2\rangle\langle g_1|\langle e_2| + |e_1\rangle|g_2\rangle\langle e_1|\langle g_2| - |e_1\rangle|e_2\rangle\langle e_1|\langle e_2|, \tag{7}$$

means that if the first ion is in the state $|g_1\rangle$, the operation has no effect, whereas if the control qubit (first ion) is in the state $|e_1\rangle$, the state of the second ion is rotated by the Pauli operator $\hat{\sigma}_z$. The first qubit is the control qubit and the second one is the target qubit. The C^Z operation is also known as controlled-rotation (CROT). It is seen from Eqs. (4)–(6) that the $\hat{C}_{12}^Z$ gate can be implemented exactly by a *one-step* operation, if the experimental parameters are set up so that the following conditions are simultaneously satisfied,

$$\cos(\chi\tau_z) = 1, \qquad \cos(\lambda_+\tau_z) = \cos(\lambda_-\tau_z) = -1. \tag{8}$$

Here τ_z is the duration of the two applied synchronous pulses. Notice that the second condition in (8), on $\lambda_\pm$, is equivalent to requiring $|D_4(t)|^2 = 1$, which forces $|D_1(t)|^2 = |D_2(t)|^2 = |D_3(t)|^2 = 0$ due to normalization. The information bus remains in its initial state after the operation. Without loss of generality, we give some solutions of the conditional equations (8) for $m = 0$ in Table 1.

We see from the Table 1 that both the small and large, both the negative and positive, values of the LD parameters may be chosen to satisfy the conditions (8) for realizing the desired two-qubit controlled gate. Our approach does not assume the LD approximation where $\eta_j \ll 1$ for $m = 0$. Thus, the present scheme can operate outside the LD regime and η_j can be large. According to previous works (see, e.g., [7,14]), it is known that an exact two-qubit gate $\hat{C}^Z$ surrounded by two one-qubit rotations on the target qubit can give rise to an exact two-qubit CNOT gate $\hat{C}^X$. The present Letter shows that the CNOT gate between different ions can be realized by using a *three-step* pulse process.

Table 1
A few solutions of Eq. (8) for $m = 0$. These parameters realize a C^Z or CROT gate between two trapped ions. Here, τ_z is the duration of the applied pulses, $\tilde{\Omega}_j$ and η_j ($j = 1, 2$) are the effective Rabi frequencies and the Lamb–Dicke parameters, respectively. The frequencies of the applied pulses are equal, i.e., $k_1 = k_2 = k = 1, 2, 3$

$\tilde{\Omega}_2/\tilde{\Omega}_1$	k	$\eta_1 = \eta_2 = \eta$	$\tilde{\Omega}_1\tau_z$	$\tilde{\Omega}_2/\tilde{\Omega}_1$	k	$\eta_1 = \eta_2 = \eta$	$\tilde{\Omega}_1\tau_z$
2.03951	1	1.93185	18.5069	1.81182	1	2.30578	37.5859
		0.517638	12.2197		2	±0.253727	137.757
	2	±0.915272	14.1979			±2.81702	57.2117
		±2.67624	39.2315		3	0.859544	33.8887
	3	1.12532	17.9115			3.40669	124.419
		2.69702	26.2324	4.02791	1	1.87083	18.6274
		3.34152	96.5506			0.707107	10.9967
0.658331	1	1.76579	56.5182		2	±0.983608	14.3592
		0.939131	34.7414			±2.65189	40.9890
	2	±1.09276	45.1673		3	1.16543	18.4811
		±2.60881	131.088			2.63899	26.2548
	3	1.23348	58.6299			3.11088	62.2365
		2.55336	80.4486			3.33069	102.936

3.2. *Two-qubit entangled states*

Recently, the quantum entanglement of two and four trapped ions have been generated experimentally (see, e.g., [5,11]), although the operations are limited to the weak-coupling LD regime. We now show that the entangled states of two trapped ions can also be produced outside the LD limit. Indeed, the dynamical evolutions (4)–(6) clearly reveal that there are many ways to produce various deterministic entangled states of two trapped ions. For example, if the conditions

$$\alpha_j = \beta_j, \qquad \phi_1 = \phi_2, \qquad \alpha_1 \neq \alpha_2, \qquad \cos(\chi\tau_e) = -1, \tag{9}$$

are satisfied, then two equal red-sideband pulses (i.e., $k_1 = k_2 = k > 0$) with frequencies $\omega_1 = \omega_2 = \omega_0 + k\nu$, applied to two ions individually and simultaneously, yield the following dynamical evolutions:

$$\begin{cases} |m\rangle|g_1\rangle|e_2\rangle \longrightarrow |m\rangle \otimes |\psi_{12}^-\rangle, & |\psi_{12}^-\rangle = U|g_1\rangle|e_2\rangle - V|e_1\rangle|g_2\rangle, \\ |m\rangle|e_1\rangle|g_2\rangle \longrightarrow |m\rangle \otimes |\psi_{12}^+\rangle, & |\psi_{12}^+\rangle = -V|g_1\rangle|e_2\rangle - U|e_1\rangle|g_2\rangle, \end{cases} \tag{10}$$

with

$$U = \frac{\alpha_1^2 - \alpha_2^2}{\alpha_1^2 + \alpha_2^2}, \qquad V = \frac{2\alpha_1\alpha_2}{\alpha_1^2 + \alpha_2^2}.$$

Therefore, entangled states $|\psi_{12}^{\pm}\rangle$ can be generated, in a *single-step* process, by the dynamical evolution of the initial non-entangled states $|g_1\rangle|e_2\rangle$ or $|e_1\rangle|g_2\rangle$. We note that the degrees of entanglement for the above entangled states $|\psi_{12}^{\pm}\rangle$ are equivalent. They are

$$E = -U^2 \log_2 U^2 - V^2 \log_2 V^2. \tag{11}$$

Here E is the degree of entanglement defined [29] as $E[\psi] = -\sum_i C_i^2 \log_2 C_i^2$, for an general two-particle entangled pure state $|\psi(A, B)\rangle = \sum_i C_i|\alpha_i\rangle_A \otimes |\beta_i\rangle_B$, $\sum_i |C_i|^2 = 1$. The entangled state of two trapped ions realized experimentally in [11] is not the maximally entangled state. Its degree of entanglement E is 0.94. However, in principle, maximally entangled states with $E = 1$ can be generated deterministically in the present scheme.

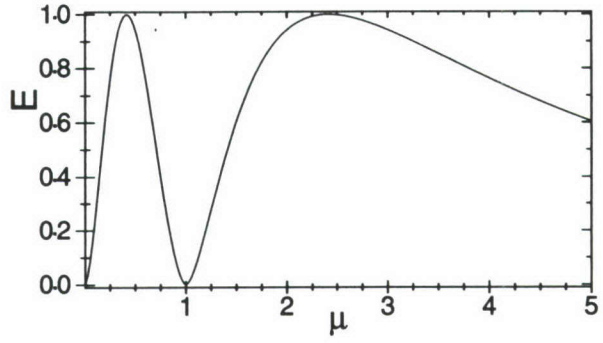

Fig. 1. The degree of entanglement E for the states $|\psi_{12}^{\pm}\rangle$ versus $\mu = \alpha_2/\alpha_1$, which is a function of the LD parameters η_j, effective Rabi frequencies $\tilde{\Omega}_j$, and the laser frequencies ω_j ($j = 1, 2$). Note that $E = 1$ for $\alpha_2/\alpha_1 = \sqrt{2} \pm 1$, and $E = 0$ for $\alpha_2/\alpha_1 = 1$. For $\alpha_2/\alpha_1 > \sqrt{2} + 1$ the degree of entanglement E decreases when α_2/α_1 increases.

Indeed, it is seen from Fig. 1 that, if the experimental parameters further satisfy the following conditions

$$\frac{\alpha_2}{\alpha_1} = \sqrt{2} \pm 1, \qquad \alpha_1 \tau_e = \frac{(2l-1)\pi}{\sqrt{4 \pm 2\sqrt{2}}}, \quad l = 1, 2, 3, \ldots, \tag{12}$$

the above entangled states $|\psi_{12}^{\pm}\rangle$ become the maximally entangled two-qubit (i.e., EPR) states

$$|\Psi_{12}^{\pm}\rangle = \frac{1}{\sqrt{2}}\big(|g_1\rangle|e_2\rangle \pm |e_1\rangle|g_2\rangle\big). \tag{13}$$

In Fig. 1, we plot the degree of entanglement E for the above entangled states versus the ratio α_2/α_1, which is a function of the LD parameters η_j, effective Rabi frequencies $\tilde{\Omega}_j$, and the laser frequencies ω_j ($j = 1, 2$). Explicitly,

$$\frac{\alpha_2}{\alpha_1} = \frac{\tilde{\Omega}_2}{\tilde{\Omega}_1}\left(\frac{\eta_2}{\eta_1}\right)^{|k|} \exp\left(-\frac{\eta_2^2 - \eta_1^2}{2}\right) \times \frac{\sum_{n=0}^{m}(-i\eta_2)^{2n} C_m^n/(n+|k|)!}{\sum_{n=0}^{m}(-i\eta_1)^{2n} C_m^n/(n+|k|)!}, \tag{14}$$

for the processes (10). Especially, for the commonly considered case, $m = 0$, the above equation becomes

$$\frac{\alpha_2}{\alpha_1} = \frac{\tilde{\Omega}_2}{\tilde{\Omega}_1}\left(\frac{\eta_2}{\eta_1}\right)^{|k|} \exp\left(-\frac{\eta_2^2 - \eta_1^2}{2}\right). \tag{15}$$

Obviously, the values of E depend on the choice of the experimental parameters $\tilde{\Omega}_j$, η_j and k (thus ω_j) ($j = 1, 2$). For $\alpha_2/\alpha_2 = 1$ the condition (9) is violated and thus $E = 0$. Similarly,

$$\lim_{\alpha_2/\alpha_1 \to \infty} U = 1, \qquad \lim_{\alpha_2/\alpha_1 \to \infty} V = 0, \quad \text{thus} \quad \lim_{\alpha_2/\alpha_1 \to \infty} E = 0. \tag{16}$$

Inversely, it is seen from Eqs. (12)–(15) that $E = 1$ for $\alpha_2/\alpha_1 = \sqrt{2} \pm 1$. This implies that two-qubit maximally entangled states can be generated deterministically by using a *single-step* operation beyond the LD limit. For example, if the experimental parameters are set up simply as $\eta_1 = \eta_2$, $\tilde{\Omega}_2/\tilde{\Omega}_1 = \sqrt{2} \pm 1$, the EPR state $|\Psi_{12}^{-}\rangle$ can be generated by using a *single-step* synchronous red-sideband π pulses with frequencies $\omega_1 = \omega_2 = \omega_0 + \nu$ and duration $\tau_e = \pi/(\alpha_1\sqrt{4 \pm 2\sqrt{2}})$.

4. Conclusions and discussions

Based on the conditional quantum dynamics for two-qubit system, we have shown that, under certain conditions, the quantum controlled gate or entanglement between a pair of trapped ions can be realized deterministically by

only a single-step operation, performed by simultaneously applying two laser pulses to two ions. Each of the laser beams interacts with a single ion. Neither auxiliary atomic level nor Lamb–Dicke approximation are required during the operation. The CM mode of the ions always remains in its initial quantum state after the operation.

We now give a brief discussion on the experimental realization of the present scheme. For ion-trap quantum information processing, the information bus, i.e., the usual collective CM vibrational mode, must first be initialized in a pure quantum state, e.g., its ground state. Recently, the collective motion of two and four $^9Be^+$ ions has been successfully cooled to its ground state in the LD regime [5,10]. This is a further step towards realizing the ion trap quantum computer. Once the collective mode of motion of the ions is successfully cooled to the ground state outside the LD regime, the present theoretical scheme may be realized by properly setting up the controllable parameters (e.g., η_j, $\tilde{\Omega}_j$, ω_j) and the durations of the applied laser pulses. Indeed, it is seen from the formulae (see, e.g., [22,28])

$$\eta_j = \cos\theta_j \sqrt{\frac{\hbar\kappa_j^2}{2MN\nu}}, \quad \theta_j = \arccos\left(\frac{\vec{\kappa}_j \cdot \vec{z}_j}{\kappa_j}\right), \tag{17}$$

that the LD parameter η_j can be controlled by adjusting the wave vector $\vec{\kappa}_j$ of the applied laser pulse. Obviously, η_j can be positive or negative, depending on the values of θ_j. Here, MN is the total mass of the ion chain and θ_j is the angle between the laser beam and the z-axis. The effective Rabi frequency $\tilde{\Omega}_j$ of the jth ion can be controlled properly by applying a static electric field [11,30].

Finally, we note that the duration of the two applied simultaneous pulses for realizing the above quantum controlled operation is not much longer than that for other schemes (see, e.g., [5,10,13,19]) operating in the LD regime. The shortest duration of the applied synchronous pulses for realizing the above manipulations of two trapped ions is about 10^{-4} seconds, of the same order of the gate speed operating in the LD regime [31], for $\tilde{\Omega}_1/2\pi \approx 225$ kHz [11]. Of course, to excite only the chosen sidebands of the CM mode, the spectral width of the applied laser pulse has to be sufficiently small. It might seem at first, from the above numerical results, that the present scheme for realizing the desired gate operation cannot be easily implemented, as the relevant experimental parameters should be set up accurately. However, this is not the case. Simple numerical analysis shows that the lowest probability of realizing the desired operation is still very high, even if the relevant parameters cannot be set up exactly. For example, the lowest probability of realizing the two-qubit $\hat{C}^z$ operation is up to 99.97% (99.49%), if the rate of the two effective Rabi frequencies $\tilde{\Omega}_2/\tilde{\Omega}_1$ is roughly set up as 2.03 (2.0), which is 0.5% (1.9%) away from the exact solution of condition (8), see Table 1. Therefore, the proposed scheme may be realizable in the near future.

Acknowledgements

We acknowledge X. Hu for useful discussions, C. Monroe for comments on the manuscript, and the partial support of ARDA, AFOSR, and the US National Science Foundation Grant No. EIA-0130383.

References

[1] M.A. Nielsen, I.L. Chuang, Quantum Computation and Quantum Information, Cambridge Univ. Press, Cambridge, 2000.
[2] A. Einstein, B. Podolsky, N. Rosen, Phys. Rev. 47 (1935) 777.
[3] P. Shor, in: S. Goldwasser (Ed.), Proceedings of the 35th Annual Symposium on the Foundations of Computer Science, IEEE Computer Society Press, New York, 1994, p. 124.
[4] P.G. Kwiat, et al., Phys. Rev. Lett. 75 (1995) 4337.
[5] C.A. Sackett, et al., Nature (London) 404 (2000) 256.
[6] D. Leibfried, et al., Nature 422 (2003) 412.

[7] J.I. Cirac, P. Zoller, Phys. Rev. Lett. 74 (1995) 4091.
[8] D. Kielpinski, et al., Science 291 (2001) 1013.
[9] Ch. Roos, et al., Phys. Rev. Lett. 83 (1999) 4713.
[10] B.E. King, et al., Phys. Rev. Lett. 81 (1998) 1525.
[11] Q.A. Turchette, et al., Phys. Rev. Lett. 81 (1998) 3631.
[12] L.M. Duan, J.I. Cirac, P. Zoller, Science 292 (2001) 1695.
[13] D. Jonathan, M.B. Plenio, Phys. Rev. Lett. 87 (2001) 127901.
[14] L.F. Wei, S.Y. Liu, X.L. Lei, Phys. Rev. A 65 (2002) 062316.
[15] L.F. Wei, S.Y. Liu, X.L. Lei, Opt. Commun. 208 (2002) 131.
[16] S.S. Sharma, A. Vidiella-Barranco, Phys. Lett. A 309 (2003) 345.
[17] D. Jonathan, M.B. Plenio, P.L. Knight, Phys. Rev. A 62 (2000) 042307.
[18] A.M. Childs, I.L. Chuang, Phys. Rev. A 63 (2000) 012306.
[19] K. Mølmer, A. Sørensen, Phys. Rev. Lett. 82 (1999) 1835.
[20] D.M. Meekhof, et al., Phys. Rev. Lett. 76 (1996) 1796.
[21] D.J. Wineland, W.M. Itano, Phys. Rev. A 20 (1979) 1521.
[22] D. Stevens, J. Brochard, A.M. Steane, Phys. Rev. A 58 (1998) 2750.
[23] G. Morigi, J. Eschner, J.I. Cirac, P. Zoller, Phys. Rev. A 59 (1999) 3797.
[24] D. Leibfried, Phys. Rev. A 60 (1999) R3335.
[25] E. Solano, et al., Phys. Rev. A 62 (2000) 021401.
[26] E. Solano, et al., Phys. Rev. A 59 (1999) R2539.
[27] L.X. Li, G.C. Guo, Phys. Rev. A 60 (1999) 696.
[28] M. Šašura, V. Bužek, J. Mod. Opt. 49 (2002) 1593.
[29] C.H. Bennett, H.J. Bernstein, S. Popescu, B. Schumacher, Phys. Rev. A 53 (1996) 2046.
[30] S.R. Jefferts, C. Monroe, E.W. Bell, D.J. Wineland, Phys. Rev. A 51 (1995) 3112.
[31] C. Monroe, et al., Phys. Rev. Lett. 75 (1995) 4714.

Engineering quantum pure states of a trapped cold ion beyond the Lamb-Dicke limit

L.F. Wei,[1,2] Yu-xi Liu,[1] and Franco Nori[1,3]

[1] *Frontier Research System, The Institute of Physical and Chemical Research (RIKEN), Wako-shi, Saitama, 351-0198, Japan*
[2] *Institute of Quantum Optics and Quantum Information, Department of Physics, Shanghai Jiaotong University, Shanghai 200030, P.R. China*
[3] *Center for Theoretical Physics, Physics Department, Center for the Study of Complex Systems, The University of Michigan, Ann Arbor, Michigan 48109-1120*

(Dated: August 4, 2004)

Based on the conditional quantum dynamics of laser-ion interactions, we propose an efficient theoretical scheme to deterministically generate quantum pure states of a single trapped cold ion without performing the Lamb-Dicke approximation. An arbitrary quantum state can be created by sequentially using a series of classical laser pulses with selected frequencies, initial phases and durations. As special examples, we further show how to create or approximate several typical macroscopic quantum states, such as the phase state and the even/odd coherent states. Unlike previous schemes operating in the Lamb-Dicke regime, the present one does well for an arbitrary-strength coupling between the internal and external degrees of freedom of the ion. The experimental realizability of this approach is also discussed.

PACS numbers: 42.50.Dv, 42.50.Vk.

I. INTRODUCTION

The engineering of quantum states has attracted considerable attention in recent years. This in order to test fundamental quantum concepts, e.g. non-locality, and for implementing various potential applications, including sensitive detection and quantum information processing. Recent advances in quantum optics (e.g., micromasers, cavity QED) (see, e.g., [1]) and atomic physics (ion traps) (see, for instance [2]) have allowed a better control of quantum states.

Laser-cooled ions confined in an electromagnetic trap are good candidates for various quantum-state engineering processes. First, the trapped ion system possesses relatively long decoherence times. Second, various interactions including the usual one-quantum transition Jaynes-Cummings (JC) model and also higher order non-linear models can be implemented in this system by simply choosing the applied laser tunings (see, e.g., [3, 4]). Therefore, a trapped ion driven by a classical laser field provides the possibility of conveniently generating various quantum pure states. Indeed, various engineered quantum states of trapped cold ions have been studied. The thermal, Fock, coherent, squeezed, and arbitrary quantum superposition states of motion of a harmonically bound ion have been investigated [5, 6]. The manipulation of the entanglement between the external and internal degrees of freedom of the ion and the realization of a fundamental quantum logic gate between them has also been demonstrated experimentally (see, e.g., [7]).

Most of the previous proposals for engineering the quantum state of a single trapped cold ion operate in various extreme experimental conditions, such as the strong Raman excitation or the weak-coupling Lamb-Dicke (LD) approximations. The former (see, e.g., [8]) requires that the Rabi frequency Ω characterizing the laser-ion interaction is much larger than the trap frequency. While the later (see, e.g., [5, 6, 9]), requires that the coupling between the external and internal degrees of freedom of the ion is very weak, i.e., the spatial dimension of the motion of the ground state of the trapped ion should be much smaller than the effective wavelength of the applied laser field (see, e.g., [6]). These approximations can simplify the laser-ion interaction Hamiltonian to certain solvable models. For example, in the LD limit the interaction between the internal states $|s\rangle = \{|g\rangle, |e\rangle\}$ and the external motional harmonic oscillator states $\{|n\rangle;\ n = 0, 1, 2, ...\}$ of the ion can be expanded to the lowest order of the LD parameter η_L, then the usual JC or anti-JC-type model can be derived. In addition, the coherent state of the motion of the ion can be easily generated in those limits. Therefore, an arbitrary quantum state may be prepared via an atomic interference method by superimposing a finite number of generated coherent states along a line. Almost all the quantum-state engineering implementations in recent ion trap experiments were operated in these limits. Some meaningful second-order modifications of the these approximations to the above experimental conditions have been analyzed theoretically [10]. However, in general, these limits are not rigorously satisfied, and higher-order powers of the LD parameter must be taken into account [4]. Indeed, using the laser-ion interaction outside the LD regime could be helpful to reduce the noise in the trap and improve the cooling rate (see, e.g., [11]). Thus, efficiently engineering the quantum state of the trapped cold ion beyond these limits would be useful. Arbitrary Fock states can, in principle, be prepared as a dark motional state of a trapped ion, if the relevant LD parameters can be set with extreme precision [13]. More realistically, reference [14] showed that any pure state, including the Fock state, can be effectively approximated by the nonlinear coherent states of the trapped ion. Since these nonlinear coherent states are one of the motional dark states and are insensitive to some motional kick effects, the generation of highly excited Fock states is possible. Recently, a narrow quadrupole $S_{1/2}$ to $D_{5/2}$ transition at 729 nm of a single trapped $^{40}Ca^{+}$ ion has been successfully manipulated by accurately resolving its vibrational sidebands [12]. The measured lifetime of the excited level $D_{5/2}$ is long enough ($\approx$ 1 second) to allow for a hundred or more quantum operations. Note that the experiments in [12] do not strictly operate in the LD regime (with $\eta \ll 1$),

because the corresponding LD parameter is $\eta \approx 0.25$. Therefore, engineering quantum states of a single trapped cold ion by exciting various vibrational sidebands outside the Lamb-Dicke regime is possible to achieve with current technology.

Based on the exact conditional quantum dynamics for the laser-ion interaction, including all orders of the LD parameter, in this paper we propose an efficient scheme for exactly engineering arbitrary motional and entangled states of a single trapped ion beyond the LD limit. In this case, all of the target quantum states are generated deterministically, as any measurement is not required during the quantum state production or manipulations.

This paper is organized as follows. In Sec. II, we solve exactly the quantum dynamics for a trapped cold ion driven by a travelling classical laser beam beyond the LD limit and then introduce some fundamental unitary operations. By repeatedly using these quantum operations, in Sec. III we show how to deterministically generate an arbitrary motional state of a single trapped cold ion. The preparations of arbitrary entangled states between the external and internal degrees of freedom are given in Sec. IV. Conclusions and discussions are given in Sec. V.

II. DYNAMICS OF A TRAPPED COLD ION BEYOND THE LAMB-DICKE LIMIT

We assume that a single two-level ion is stored in a coaxial resonator RF-ion trap [15], which provides pseudopotential oscillation frequencies satisfying the condition $\omega_x \ll \omega_{y,z}$ along the principal axes of the trap. Only the quantized vibrational motion along the x direction is considered for the cooled ion [15]. The dynamics for such an ion, driven by a classical travelling-wave light-field of frequency ω_L and initial phase ϕ_L, can be described by the following Hamiltonian [3, 16]

$$\hat{H}(t) = \hbar\omega\left(\hat{a}^\dagger\hat{a} + \frac{1}{2}\right) + \frac{1}{2}\hbar\omega_0\hat{\sigma}_z + \frac{\hbar\Omega}{2}\left\{\hat{\sigma}_+ \exp\left[i\eta_L(\hat{a} + \hat{a}^\dagger) - i(\omega_L t + \phi_L)\right] + H.c.\right\}. \quad (1)$$

The first two terms describe the free motion of the external and internal degrees of freedom of the ion. Here $\hat{a}^\dagger$ and $\hat{a}$ are bosonic creation and annihilation operators of the atomic vibrational quanta with frequency ω. The Pauli operators $\hat{\sigma}_z$ and $\hat{\sigma}_\pm$ are defined by the internal ground state $|g\rangle$ and excited state $|e\rangle$ of the ion as $\sigma_z = |e\rangle\langle e| - |g\rangle\langle g|$, $\sigma_+ = |e\rangle\langle g|$, and $\sigma_- = |g\rangle\langle e|$. These operate on the internal degrees of freedom of the ion of mass M. The final term of $\hat{H}(t)$ describes the interaction between the ion and the light field with wave vector $\vec{\kappa}_L$, and initial phase ϕ_L. Ω is the carrier Rabi frequency, which describes the coupling between the laser and the ion, and is proportional to the intensity of the applied laser. The frequency ω_L and initial phase ϕ_L of the applied laser beam are experimentally controllable [16]. Usually, the atomic transition frequency ω_0 between two internal energy levels is much larger than the trap frequency ω (e.g., in the experiments in [12], $\omega_0 = 2\pi \times 4.11 \times 10^{11}$kHz and $\omega = 2\pi \times 135$kHz). Therefore, for lasers exciting at different vibrational sidebands with small k values, the LD parameters

$$\eta = \sqrt{\frac{\hbar\kappa_L^2}{2M\omega}} = \frac{(\omega_0 \pm k\omega)}{c}\sqrt{\frac{\hbar}{2M\omega}}, \quad k = 0, 1, 2, \ldots, \quad (2)$$

do not change significantly. Here, the Hamiltonian (1) reduces to different forms [4]

$$\hat{H}_{int} = \frac{\hbar\Omega}{2} \times \begin{cases} \left\{(i\eta)^k \exp[-\frac{(\eta)^2}{2} - i\phi^r]\,\hat{\sigma}_+ \left(\sum_{j=0}^{\infty} \frac{(i\eta)^{2j}\hat{a}^{\dagger j}\hat{a}^{j+k}}{j!(j+k)!}\right) + H.c.\right\}, & \omega_L = \omega_0 - k\omega, \\ \left\{(i\eta)^k \exp[-\frac{(\eta)^2}{2} - i\phi^b]\,\hat{\sigma}_+ \left(\sum_{j=0}^{\infty} \frac{(i\eta)^{2j}\hat{a}^{\dagger(j+k)}\hat{a}^{j}}{j!(j+k)!}\right) + H.c.\right\}, & \omega_L = \omega_0 + k\omega, \\ \left\{\exp\left(-\frac{\eta^2}{2} - i\phi^c\right)\hat{\sigma}_+ \left(\sum_{j=0}^{\infty} \frac{(i\eta)^{2j}\hat{a}^{\dagger j}\hat{a}^{j}}{j!j!}\right) + H.c.\right\}, & \omega_L = \omega_0, \end{cases} \quad (3)$$

in the interaction picture. The usual rotating-wave approximation has been made and all off-resonant transitions have been neglected by assuming a sufficiently weak applied laser field. The applied laser beam tuned at the frequency $\omega_L = \omega_0 - k\omega$ ($\omega_L = \omega_0 + k\omega$) with nonzero integer k being denoted as the kth red (blue) sideband line, because it is red (or blue) detuned from the atomic frequency ω_0. The line for $k = 0$ (i.e. $\omega_L = \omega_0$) is called the carrier. So, we rewrite the initial

phase ϕ_L as ϕ^r (ϕ^b, ϕ^c) for a transition process driven by the red-sideband (blue-sideband, carrier) laser beam respectively.

Previous discussions (see, e.g., [9]) are usually based on the LD perturbation approximation to first order in the LD parameter by assuming η to be very small. However, outside the LD regime the Hamiltonian (3) may provide various quantum transitions between the internal and external states of the ion. The dynamics for the trapped cold ion governed by the Hamiltonian (3) is exactly solvable [4, 17]. For example, if the external state of the system is initially in $|m\rangle$ and the internal state is initially in $|e\rangle$ or $|g\rangle$, then the dynamical evolution of an ion driven by a red-sideband laser beam with frequency $\omega_L = \omega_0 - k\omega$ can be exactly expressed as

$$\begin{cases} |m\rangle \otimes |g\rangle \longrightarrow \begin{cases} |m\rangle \otimes |g\rangle, & m < k, \\ \cos(\Omega_{m-k,k} t_l^r)|m\rangle \otimes |g\rangle + i^{k-1} e^{-i\phi_l^r} \sin(\Omega_{m-k,k} t_l^r)|m-k\rangle \otimes |e\rangle, & m \geq k, \end{cases} \\ |m\rangle \otimes |e\rangle \longrightarrow \cos(\Omega_{m,k} t_l^r)|m\rangle \otimes |e\rangle - (-i)^{k-1} e^{i\phi_l^r} \sin(\Omega_{m,k} t_l^r)|m+k\rangle \otimes |g\rangle, \end{cases} \tag{4}$$

with Rabi frequency

$$\Omega_{m,k} = \frac{\Omega \eta^k}{2} \sqrt{\frac{(m+k)!}{(m)!}} e^{-\eta^2/2} \sum_{j=0}^{m} \frac{(i\eta)^{2j}}{(j+k)!} \binom{j}{m}.$$

Where m is the occupation number of the initial Fock state of the external vibrational motion of the ion, t_l^r and ϕ_l^r are the duration and initial phase of the applied red-sideband laser beam, respectively. The above dynamical evolution can be equivalently defined as the kth red-sideband "exciting" quantum operator

$$\hat{R}_k^r(t_l^r) = \begin{cases} |m\rangle|g\rangle\langle m|\langle g| + \left[\left(1 - |\tilde{C}_m^{r_l}|^2\right)^{\frac{1}{2}} |m\rangle|e\rangle + \tilde{C}_m^{r_l} |m+k\rangle|g\rangle\right] \langle m|\langle e|, & m < k, \\ \left[(1 - |C_{m-k}^{r_l}|^2)^{\frac{1}{2}} |m\rangle|g\rangle + C_{m-k}^{r_l} |m-k\rangle|e\rangle\right] \langle m|\langle g| \\ \qquad + \left[\left(1 - |\tilde{C}_m^{r_l}|^2\right)^{\frac{1}{2}} |m\rangle|e\rangle + \tilde{C}_m^{r_l} |m+k\rangle|g\rangle\right] \langle m|\langle e|, & m \geq k, \end{cases} \tag{5}$$

with

$$C_m^{r_l} = i^{k-1} e^{-i\phi_l^r} \sin(\Omega_{m,k} t_l^r), \quad \tilde{C}_m^{r_l} = -(C_m^{r_l})^*.$$

The use of $\hat{R}_k^r$ is advantageous because it is compact, symmetric, and it is simple to iterate. This operator is quite useful for the generation of quantum states. Analogously, exciting the motional state of the ion to the kth blue-sideband, by applying a laser of frequency $\omega_L = \omega_0 + k\omega$, yields a unitary blue-sideband "exciting" quantum operation,

$$\hat{R}_k^b(t_l^b) = \begin{cases} \left[(1 - |C_m^{b_l}|^2)^{\frac{1}{2}} |m\rangle|g\rangle + C_m^{b_l} |m+k\rangle|e\rangle\right] \langle m|\langle g| + |m\rangle|e\rangle\langle m|\langle e|, & m < k, \\ \left[(1 - |C_m^{b_l}|^2)^{\frac{1}{2}} |m\rangle|g\rangle + C_m^{b_l} |m+k\rangle|e\rangle\right] \langle m|\langle g| \\ \qquad + \left[\left(1 - |\tilde{C}_{m-k}^{b_l}|^2\right)^{\frac{1}{2}} |m\rangle|e\rangle + \tilde{C}_{m-k}^{b_l} |m-k\rangle|g\rangle\right] \langle m|\langle e|, & m \geq k, \end{cases} \tag{6}$$

with

$$C_m^{b_l} = i^{k-1} e^{-i\phi_l^b} \sin(\Omega_{m,k} t_l^b), \quad \tilde{C}_m^{b_l} = -(C_m^{b_l})^*,$$

Here, t_l^b and ϕ_l^b are the duration and initial phase of the applied blue-sideband laser beam, respectively.

Finally, applying a carrier laser pulse with frequency $\omega_L = \omega_0$, a conditional rotation

$$\hat{R}_0^c(t_l^c) = \left[(1-|C_m^{c_l}|^2)^{\frac{1}{2}}\ \hat{I} + C_m^{c_l}\,|e\rangle\langle g| + \tilde{C}_m^{c_l}\,|g\rangle\langle e|\right] \otimes |m\rangle\langle m| \tag{7}$$

on the internal states of the ion can be implemented. Here, $\hat{I} = |g\rangle\langle g| + |e\rangle\langle e|$ is the identity operator, t_l^c is the duration of the applied carrier laser beam, and

$$C_m^{c_l} = -ie^{-i\phi_l^c}\sin(\Omega_{m,0}t_l^c), \qquad \tilde{C}_m^{c_l} = -(C_m^{c_l})^*,$$

with

$$\Omega_{m,0} = \frac{\Omega}{2}\exp\left(-\frac{\eta^2}{2}\right)\sum_{j=0}^{m}\frac{(i\eta)^{2j}}{j!}\begin{pmatrix} j \\ m \end{pmatrix}.$$

The quantum dynamics of the laser-ion system beyond the LD limit is conditional. This means that the internal and motional degrees of freedom are always coupled. The ion states of two degrees of freedom cannot be operated separately, even if the ion is driven by the carrier line laser. Of course, for a given carrier Rabi frequency Ω (which depends on the intensity/power of the applied laser beam) and the LD parameter, the Rabi frequencies $\Omega_{m,k}$ are sensitive to values of k. See, e.g., Fig. 1 for the same laser power but different LD parameters: $\eta = 0.202$ [5], 0.25 [12], 0.35, 0.5, and 0.9. As seen in Figure 1, a smaller η corresponds to a larger reduction of the Rabi frequency for certain k values (e.g., in Fig. 1, $\Omega_{0,20}/\Omega \sim 10^{-4}$ for $\eta = 0.202$). However, for any fixed value of k, larger values of η correspond to larger values of the reduced Rabi frequencies $2\Omega_{0,k}/\Omega$. Therefore, fast quantum operations can be obtained outside the LD regime, where η is not small.

In general, any quantum process for the laser-ion system can be realized by repeatedly applying the above three kinds of fundamental operations showed in Eqs. (5-7). Which operation is applied depends on the laser with the chosen frequency. Below we will use these fundamental unitary operations (5-7) to produce or engineer an arbitrary quantum state of a single trapped cold ion beyond the LD limit. The tunable experimental parameters in this process are the frequency ω_L, wave vector $\vec{\kappa}_L$, and the duration of the applied laser pulse. The generation of quantum states described below will start with a common non-entangled initial state $|\psi_0\rangle = |0\rangle \otimes |g\rangle$; that is, the trapped ion has been cooled to its motional ground state and the internal degree of the ion is initially in the low-energy state $|g\rangle$.

III. PREPARATION OF AN ARBITRARY MOTIONAL STATE OF A TRAPPED COLD ION

The first significant quantum state which we want to prepare is the Fock state of the external vibrational quanta of the ion

$$|\psi_1\rangle = |n\rangle, \tag{8}$$

with an arbitrary occupation number $n > 0$. The previous schemes (e.g. [5, 6, 7, 9]) operated in the LD limit only allowed one-quantum transition process (exciting and absorbing a single phonon process, respectively). Thus, at least $(n+1)$ transitions are required between $|j\rangle \otimes |g\rangle \longleftrightarrow |j \pm 1\rangle \otimes |e\rangle$ to generate the desired state (8). However, for larger values of the LD parameters, the LD approximation is no longer valid and multi-quantum transitions must be considered. One can obtain the different phonon transitions, beyond the LD limit, by choosing an appropriate driving laser frequency. For example, the quantum transition: $|0\rangle \otimes |g\rangle \rightarrow |n\rangle \otimes |e\rangle$, can be realized by choosing a blue-sideband driven laser beam with frequency $\omega_L = \omega_0 + n\omega$. So the desired Fock state $|n\rangle$ can be easily obtained by using a single blue-sideband exciting unitary operation $\hat{R}_n^b(t_0^b)$ with the duration t_0^b satisfying the condition: $\sin(\Omega_{0,n}t_0^b) = 1$. In other words, $\Omega_{0,n}t_0^b = p\pi/2$ with p an odd integer. Note that the resulting atomic state evolves to its excited state $|e\rangle$ which may transit to the ground state $|g\rangle$ via spontaneous emission. In order to avoid the additional excitation of the desired Fock state due to this emission, an additional operation $\hat{R}_0^c(t_n^c)$ is required to evolve the state $|e\rangle$ into the state $|g\rangle$ keeping the motional state unchanged, with the duration t_n^c satisfying the condition $\sin(\Omega_{n,0}t_n^c) = 1$. Therefore, by sequentially performing a $\pi/2$ blue-sideband

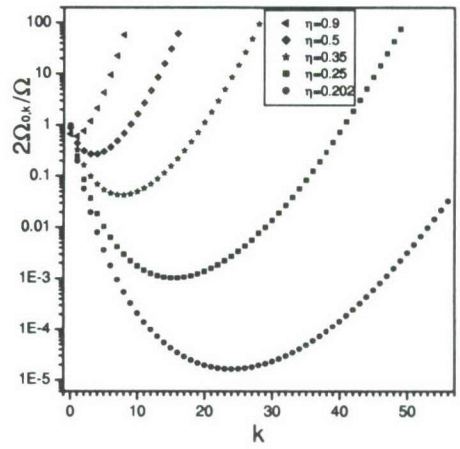

FIG. 1: The k-dependent Rabi frequency $\Omega_{0,k}$ for different LD parameters: $\eta = 0.202$ [5], 0.25 [12], 0.35, 0.5, and 0.9.

laser pulse and a $\pi/2$ carrier line laser pulse with initial phases ϕ_0^b and ϕ_n^c, respectively, a relatively steady target Fock state $|\psi_1\rangle$ is generated from the vacuum state $|0\rangle$ as follows

$$|0\rangle\otimes|g\rangle \xrightarrow{\hat{R}_n^b(t_0^b)} i^{n-1}e^{-i\phi_0^b}|n\rangle\otimes|e\rangle \xrightarrow{\hat{R}_0^c(t_n^c)} -i^n e^{i(\phi_n^c-\phi_0^b)}|n\rangle\otimes|g\rangle. \tag{9}$$

After these unitary operations, the internal electric state returns to its initial ground state $|g\rangle$. The target state $|n\rangle$ can also be prepared by continuously applying a carrier line operation $\hat{R}_0^c(t_0^c)$ and an nth red-sideband exciting operator $\hat{R}_n^r(t_n^r)$, i.e.,

$$|0\rangle\otimes|g\rangle \xrightarrow{\hat{R}_0^c(t_0^c)} -ie^{-i\phi_0^c}|0\rangle\otimes|e\rangle \xrightarrow{\hat{R}_n^r(t_n^r)} -(-i)^n e^{i(\phi_n^r-\phi_0^c)}|n\rangle\otimes|g\rangle, \tag{10}$$

with the durations t_0^c and t_n^r satisfying conditions $\sin(\Omega_{0,0}t_0^c) = 1$, $\sin(\Omega_{0,n}t_n^r) = 1$. Therefore, two unitary operations are sufficient to deterministically generate an arbitrary Fock state $|n\rangle$ from the initial ground state $|0\rangle$, if the laser-ion interaction is operated outside the LD regime by using the chosen laser beams with desired frequencies.

The more general motional state of the ion which we want to prepare is the following finite superposition of number states

$$|\psi_2\rangle = \sum_{j=0}^{N} c_j\,|j\rangle, \qquad \sum_{n=0}^{N}|\,c_j\,|^2 = 1, \tag{11}$$

with N being a finite integer. For a single-mode light field, this state can be probabilistically generated [18] by physically truncating the photon coherent state. The efficiency of generating a quantum state by the quantum truncation may be quite low due to the necessity of quantum measurements. In the present quantum-state generation the motional vacuum state $|0\rangle$, instead of the motional coherent states $|\alpha\rangle$, is given initially. A quantum-state production scheme, in the LD regime, for generating the desired state (11) has been proposed in [19]. We now extend this scheme to generate the target state $|\psi_2\rangle$ beyond the LD limit. Indeed, sequentially using $N+1$ laser pulses with frequencies $\omega_L = \omega_0, \omega_0-\omega, \cdots, \omega_0 - l\omega, \cdots, \omega_0 - N\omega$ and durations $t_0^c, t_1^r, \cdots, t_l^r, \cdots, t_N^r$, respectively, the desired state is obtained from the initial state $|\psi_0\rangle$ by a series of dynamical evolutions showed as follows:

$$\begin{aligned}
|\psi_0\rangle &\xrightarrow{\hat{R}_0^c(t_0^c)} c_0|0\rangle\otimes|g\rangle - ie^{-i\phi_0^c}\left(1-c_0^2\right)^{\frac{1}{2}}|0\rangle\otimes|e\rangle \\
&\xrightarrow{\hat{R}_1^r(t_1^r)} \left(\sum_{j=0}^{1}c_j\,|j\rangle\right)\otimes|g\rangle - ie^{-i\phi_0^c}\left(1-\sum_{j=0}^{1}|c_j|^2\right)^{\frac{1}{2}}|0\rangle\otimes|e\rangle \\
&\cdots \xrightarrow{\hat{R}_l^r(t_l^r)} \left(\sum_{j=0}^{l}c_j|j\rangle\right)\otimes|g\rangle - ie^{-i\phi_0^c}\left(1-\sum_{j=0}^{l}|c_j|^2\right)^{\frac{1}{2}}|0\rangle\otimes|e\rangle \\
&\cdots \xrightarrow{\hat{R}_N^r(t_N^r)} \left(\sum_{j=0}^{N}c_j|j\rangle\right)\otimes|g\rangle = |\psi_2\rangle\otimes|g\rangle.
\end{aligned} \tag{12}$$

The duration of the final unitary operations $\hat{R}_N^r(t_N^r)$ has been set to satisfy the condition: $\sin(\Omega_{0,N}t_N^r) = 1$. While, the durations and the initial phases of other applied laser beams can be used to arbitrarily prescribe the weights c_j of the su-

perposed Fock states $\{|j\rangle;\ j=0,1,...,N\}$, such as

$$c_j=\begin{cases}(1-|C_0^{c_0}|^2)^{\frac{1}{2}}=\cos(\Omega_{0,0}t_0^c), & j=0,\\ C_0^{c_0}\left[\prod_{l=1}^{j-1}(1-|\tilde{C}_0^{r_l}|^2)\right]^{\frac{1}{2}}\tilde{C}_0^{r_j}=-(-i)^j e^{i(\phi_j^r-\phi_0^c)}\sin(\Omega_{0,0}t_0^c)\prod_{l=1}^{j-1}\cos(\Omega_{0,l}t_l^r)\sin(\Omega_{0,j}t_j^r), & \\ \qquad\qquad 1\le j\le N-1,\\ C_0^{c_0}\left[\prod_{l=1}^{j-1}(1-|\tilde{C}_0^{r_l}|^2)\right]^{\frac{1}{2}}=-(-i)^j e^{i(\phi_N^r-\phi_0^c)}\sin(\Omega_{0,0}t_0^c)\prod_{l=1}^{N-1}\cos(\Omega_{0,l}t_l^r), & j=N.\end{cases} \tag{13}$$

Similarly, by sequentially applying a series of blue-sideband exciting operators $\hat{R}_j^b(t_j^b)$ with durations t_j^b, $j=1,2,...,N$, after a carrier line operation $\hat{R}_0^c(t_0^c)$, we can implement the following deterministic quantum state generation

$$|\psi_0\rangle\xrightarrow{\hat{R}_N^b(t_N^b)\cdots\hat{R}_1^b(t_1^b)\hat{R}_0^c(t_0^c)}\left(\sum_{j=0}^{N}c_j'|j\rangle\right)\otimes|e\rangle=|\psi_2'\rangle\otimes|e\rangle, \tag{14}$$

with

$$c_j'=\begin{cases}-ie^{-i\phi_0^c}\sin(\Omega_{0,0}t_0^c), & j=0,\\ i^{j-1}e^{-i\phi_j^b}\cos(\Omega_{0,0}t_0^c)\prod_{l=1}^{j-1}\cos(\Omega_{0,l}t_l^b)\sin(\Omega_{0,j}t_j^b), & \\ \qquad\qquad 1\le j\le N-1,\\ i^{N-1}e^{-i\phi_N^b}\cos(\Omega_{0,0}t_0^c)\prod_{l=1}^{N-1}\cos(\Omega_{0,l}t_l^b), & j=N.\end{cases}$$

Here, the duration t_N^b of the last operation $\hat{R}_N^b(t_N^b)$ is set as $\sin(\Omega_{0,N}t_N^b)=1$.

So far, we have shown that the desired superposition of a finite set of motional Fock states $\{|j\rangle;\ j=0,1,...,N\}$ of the ion can be generated deterministically from the ground state $|0\rangle$ by using $N+1$ unitary operations, i.e, a carrier line operation $\hat{R}_0^c$ and N red-sideband $\hat{R}_j^r$ (or blue-sideband $\hat{R}_j^b$) exciting operations performed by using the laser beams with frequencies $\omega_L=\omega_0-j\omega$ (or $\omega_L=\omega_0+j\omega$). It is worth pointing out that the motional state generated above in Eq.(11) or (13) may be reduced to an arbitrary quantum pure state of the external vibration of the trapped cold ion, as any weight c_j in Eq.(12) for the Fock state $|j\rangle$ can be prescribed arbitrarily. For example, the Pegg-Barnett phase state [20]

$$|\theta\rangle_N=\frac{1}{\sqrt{N+1}}\sum_{j=0}^{N}e^{ij\theta}\,|j\rangle \tag{15}$$

can be obtained from Eqs. (12-13) by setting the initial phases and the durations of the applied laser beams to satisfy the following conditions

$$\phi_0^c=\frac{\pi}{2},\quad e^{i\phi_j^r}=i^{j-1}e^{ij\theta}, \tag{16}$$

and

$$\begin{aligned}c_0 &= \cos(\Omega_{0,0}t_0^c)=\cdots\\ &= \sin(\Omega_{0,0}t_0^c)\prod_{l=1}^{j-1}\cos(\Omega_{0,l}t_l^r)\sin(\Omega_{0,j}t_j^r)=\cdots\\ &= \frac{1}{\sqrt{N+1}},\end{aligned} \tag{17}$$

which implies that $t_0^c=2\exp(\eta^2/2)[2n_0\pi+\arccos(1/\sqrt{N+1})]/\Omega$, and $t_j^r=2\exp(\eta^2/2)[2n_j\pi+\arcsin(1/\sqrt{N-j+1})]/(\Omega\eta^j)$, $j\neq 0$, with $n_0,n_j=0,1,2,....$ For example, in the typical experimental system [12] where $\omega_0=2\pi\times 4.11\times 10^{11}\,\mathrm{kHz}, \omega=2\pi\times 135\,\mathrm{kHz}, \Omega=50\,\mathrm{kHz}$, and $\eta=0.25$, the simplest phase state $|\theta\rangle_1=(|0\rangle+e^{i\theta}|1\rangle)/\sqrt{2}$ can be prepared by sequentially applying a resonant laser beam (with frequency $\omega_L=\omega_0$ and initial phase $\phi_0^c=\pi/2$) of the shortest duration $t_0^c\approx 3.24\times 10^{-5}\,\mathrm{s}$ and a red-sideband line (with frequency $\omega_L=\omega_0-\omega$ and initial phase $\phi_1^r=\theta$) of the shortest duration $t_1^r\approx 2.6\times 10^{-4}\,\mathrm{s}$.

The superposition state generated above may approach some macroscopic motional quantum states of the ion, if the number N of Fock states $|j\rangle$ is sufficiently large. For example, if the durations of the applied unitary operations are set to

satisfy the conditions

$$c_0 = \cos(\Omega_{0,0}t_0^c) = e^{-|\alpha|^2/2},\ c_1 = \alpha c_0,$$
$$c_2 = \alpha^2 c_0/\sqrt{2!},\ \cdots,\ c_j = \alpha^j c_0/\sqrt{j!}\,,\cdots, \quad (18)$$

the motional superposition state $\sum_{j=0}^{N} c_j|j\rangle$ in the limit $N \to \infty$ approaches the usual coherent state

$$|\alpha\rangle = e^{-|\alpha|^2/2}\sum_{j=0}^{\infty}\frac{\alpha^j}{\sqrt{j!}}|j\rangle. \quad (19)$$

Similarly, the usual even or odd coherent states may also be approached by the superposition motional states generated by sequentially applying the laser beams with frequencies $\omega_L = \omega-(2l)\omega$, $l = 0, 1, 2, \ldots$ or $\omega_L = \omega-(2l+1)\omega$, respectively.

IV. PRODUCING ENTANGLED STATES OF A TRAPPED COLD ION BEYOND THE LAMB-DICKE LIMIT

Before, we discussed how to generate a motional quantum state of the ion. Now, we turn our attention to the problem of how to control the entanglement between these degrees of freedom. It is well known that entanglement is one of the most striking aspects of quantum mechanics and plays an important role in quantum computation [7]. A laser-ion system provides an example for clearly showing how to produce an entanglement between two different quantum degrees of freedom (see, e.g., [21]). Therefore, the third target state which we want to prepare is the general entangled state of the internal and external motion degrees of freedom of the ion

$$|\Psi\rangle = \sum_{j=0}^{N_g} d_j^g\,|j\rangle\otimes|g\rangle + \sum_{j=0}^{N_e} d_j^e\,|j\rangle\otimes|e\rangle, \quad (20)$$

where $\sum_{j=0}^{N_g} d_j^g|j\rangle$ ($\sum_{j=0}^{N_e} d_j^e|j\rangle$) is the external state associated with the internal ground (excited) state. Notice that the coefficients c_j in the state $|\psi_2\rangle$ generated above are prescribed arbitrarily. Thus, applying an additional conditional operation $\hat{R}_0^c(t_{N+1}^c)$, with duration t_{N+1}^c, to the state $|\psi_2\rangle\otimes|g\rangle$, one may prepare an entangled state with $N_g = N_e = N$; i.e.,

$$|\psi_2\rangle\otimes|g\rangle \xrightarrow{\hat{R}_0^c} \sum_{j=0}^{N}\left(d_j^g|j\rangle\otimes|g\rangle + d_j^e|j\rangle\otimes|e\rangle\right), \quad (21)$$

with

$$d_j^g = c_j\cos(\Omega_{j,0}t_{N+1}^c), \qquad d_j^e = -ic_j e^{-i\phi_{N+1}^c}\sin(\Omega_{j,0}t_{N+1}^c).$$

In the sequence of operations shown above, $N+1$ laser-ion interactions (a carrier line and N red-sideband/blue-sideband excitations) are used. We now consider a relatively simple method to generate the entangled quantum states of the ion. That is, by alternatively switching the lasers on the first blue-sideband and the first red-sideband N times, one can generate a typical entangled state [21]

$$|\Psi'\rangle = \sum_{j=0}^{N_g} d_{2j+1}^g|2j+1\rangle\otimes|g\rangle + \sum_{j=0}^{N_e} d_{2j}^e|2j\rangle\otimes|e\rangle, \quad (22)$$

with the odd (even) -number motional states entangled with the ground (excited) internal spin states of the ion. Without any loss of generality, we assume that the ion has been prepared beforehand in a general non-entangled state

$$|\Psi_0\rangle = \hat{R}_0^c(t_0^c)\,|0\rangle\otimes|g\rangle = d_0^{g_0}\,|0\rangle\otimes|g\rangle + d_0^{e_0}\,|0\rangle\otimes|e\rangle, \quad (23)$$

with $d_0^{g_0} = \left(1-|C_0^{c_0}|^2\right)^{\frac{1}{2}}$, $d_0^{e_0} = C_0^{c_0}$.

We now first tune the laser beam to the first red-sideband and thus realize the following operation

$$|\Psi_0\rangle \xrightarrow{\hat{R}_1^r(t_1^r)} (d_0^{g_1}\,|0\rangle + d_1^{g_1}\,|1\rangle)\otimes|g\rangle + d_0^{e_1}|0\rangle\otimes|e\rangle = |\Psi_1\rangle. \quad (24)$$

Here,

$$d_0^{g_1} = d_0^{g_0}, \quad d_1^{g_1} = d_0^{e_0}\tilde{C}_0^{r_1}, \quad d_0^{e_1} = d_0^{e_0}\left(1-|\tilde{C}_0^{r_1}|^2\right)^{\frac{1}{2}}.$$

Obviously, the state $|\Psi_1\rangle$ is an entangled state. It reduces to the Bell-type state

$$|\psi_B\rangle = \frac{1}{\sqrt{2}}(|0\rangle\otimes|e\rangle + |1\rangle\otimes|g\rangle), \quad (25)$$

if $\phi_1^r = 3\pi/2$ and the durations of the operations $\hat{R}_0^c(t_0^c)$ and $\hat{R}_1^r(t_1^c)$ are set up properly such that $d_0^{e_0} = 1$ and $\tilde{C}_0^{r_1} = 1/\sqrt{2}$, corresponding to the shortest durations $t_0^c \approx 6.48\times10^{-5}$ s and $t_1^r \approx 2.6\times10^{-4}$ s.

We then tune the laser beam to the first blue-sideband and implement the evolution

$$|\Psi_1\rangle \xrightarrow{\hat{R}_1^b(t_2^b)} \sum_{j=0}^{1} d_j^{g_2}\,|j\rangle\otimes|g\rangle + \sum_{j=0}^{2} d_j^{e_2}\,|j\rangle\otimes|e\rangle = |\Psi_2\rangle, \quad (26)$$

with

$$d_0^{g_2} = d_0^{g_1}\left(1-|C_0^{b_2}|^2\right)^{\frac{1}{2}}, \qquad d_1^{g_2} = d_1^{g_1}\left(1-|C_1^{b_2}|^2\right)^{\frac{1}{2}},$$

and

$$d_0^{e_2} = d_0^{e_1}, \quad d_1^{e_2} = d_0^{g_1}C_0^{b_2}, \quad d_2^{e_2} = d_1^{g_1}C_1^{b_2}.$$

Repeating the above-mentioned procedure, we realize the following series of evolutions

$$|\Psi_2\rangle \xrightarrow{\hat{R}_1^r(t_3^r)} |\Psi_3\rangle \cdots \xrightarrow{\hat{R}_1^r(t_{2l}^b)} |\Psi_{2l}\rangle \xrightarrow{\hat{R}_1^r(t_{2l+1}^r)} |\Psi_{2l+1}\rangle \cdots \xrightarrow{\hat{R}_1^r(t_N^b)} |\psi_N\rangle, \tag{27}$$

with

$$\begin{cases} |\Psi_{2l}\rangle = \sum_{j=0}^{2l-1} d_j^{g_{2l}} |j\rangle \otimes |g\rangle + \sum_{j=0}^{2l} d_j^{e_{2l}} |j\rangle \otimes |e\rangle, \\ |\Psi_{2l+1}\rangle = \sum_{j=0}^{2l+1} d_j^{g_{2l+1}} |j\rangle \otimes |g\rangle + \sum_{j=0}^{2l} d_j^{e_{2l+1}} |j\rangle \otimes |e\rangle. \end{cases}$$

Here,

$$d_j^{g_{2l}} = \begin{cases} d_j^{g_{2l-1}} \left(1 - |C_j^{b_{2l}}|^2\right)^{\frac{1}{2}} + d_j^{e_{2l-1}} \tilde{C}_{j+1}^{b_{2l}}, \\ \qquad\qquad 0 \le j \le 2l-2, \\ d_j^{g_{2l-1}} \left(1 - |C_j^{b_{2l}}|^2\right)^{\frac{1}{2}}, \quad j = 2l-1, 2l, \end{cases}, \quad d_j^{e_{2l}} = \begin{cases} d_j^{e_{2l-1}}, \qquad j = 0 \\ d_j^{e_{2l-1}} \left(1 - |\tilde{C}_{j-1}^{b_{2l}}|^2\right)^{\frac{1}{2}} + d_{j-1}^{e_{2l-1}} C_{j-1}^{b_{2l}}, \\ \qquad\qquad 1 \le j \le 2l-2, \\ d_j^{g_{2l-1}} C_j^{b_{2l}}, \qquad j = 2l-1, 2l, \end{cases}$$

and

$$d_j^{g_{2l+1}} = \begin{cases} d_j^{g_{2l}}, \quad j = 0, \\ d_j^{g_{2l}} \left(1 - |C_{j-1}^{r_{2l+1}}|^2\right)^{\frac{1}{2}} + d_{j-1}^{e_{2l}} \tilde{C}_{j-11}^{r_{2l+1}}, \\ \qquad\qquad 1 \le j \le 2l-1, \\ d_j^{e_{2l}} \tilde{C}_j^{r_{2l+1}}, \quad j = 2l, 2l+1, \end{cases}, \quad d_j^{e_{2l+1}} = \begin{cases} d_j^{e_{2l}} \left(1 - |\tilde{C}_j^{r_{2l+1}}|^2\right)^{\frac{1}{2}} + d_{j-1}^{g_{2l}} C_{j-1}^{r_{2l+1}}, \\ \qquad\qquad 0 \le j \le 2l-1, \\ d_j^{e_{2l}} \left(1 - |\tilde{C}_j^{r_{2l+1}}|^2\right)^{\frac{1}{2}}, \; j = 2l, 2l+1. \end{cases}$$

Therefore, applying N ($N > 0$) pairs of the first red-sideband and blue-sideband laser beams may generate the desired entangled state

$$|\psi_N\rangle = \sum_{j=0}^{N-1} d_j^{g_N} |j\rangle \otimes |g\rangle + \sum_{j=0}^{N} d_j^{e_N} |j\rangle \otimes |e\rangle. \tag{28}$$

If the initial state of the above process of quantum state manipulation is prepared in $|0\rangle \otimes |e\rangle$ by setting the duration of the applied carrier line laser to satisfy condition $|C_0^{c_0}|^2 = 1$, then the desired entangled state (22), rewritten as

$$|\psi_N'\rangle = \sum_{j=0}^{[\frac{N-1}{2}]} d_{2j+1}^{g_N} |2j+1\rangle \otimes |g\rangle + \sum_{j=0}^{[\frac{N}{2}]} d_{2j}^{e_N} |2j\rangle \otimes |e\rangle, \tag{29}$$

is obtained by the above process. Here $[x]$ is the largest integer less than x.

V. DISCUSSIONS AND CONCLUSIONS

Based on the conditional quantum dynamics for laser-ion interactions beyond the Lamb-Dicke limit, we have introduced three kinds of unitary operations: the simple rotations of the internal states of the ion, the arbitrary red-sideband, and blue-sideband exciting operations. These unitary operations can be performed separately by applying the chosen laser beams with the relevant tunings. In general, any quantum state of the trapped cold ion can be generated deterministically by making use of these unitary operations selectively. Like some of the other schemes presented previously, several laser beams with different frequencies are also required in the present scheme. Tunable lasers provide the tool to create several types of quantum states of trapped ions.

Compared with previous approaches (see, e.g., [7, 9]) operated in the LD regime, the most important advantage of the present scheme is that the operations are relatively simple, since various laser-ion interactions may be easily used by

choosing the tunings of the applied laser beams. For example, at least n operations are required in the previous schemes to generate the state $|n\rangle\otimes|g\rangle$ from the initial state $|0\rangle\otimes|g\rangle$, as the dynamical process of the multiquantum motional excitation is negligible in the LD regime. However, we have shown here that only two unitary operations beyond the LD limit are sufficient to engineer the same quantum state. In addition, the generated superposition motional states and the entangled states of the ion are universal and thus may reduce to the various desired special quantum states. The reason is that the weights of the superposed Fock states can be adjusted independently by controlling the relevant experimental parameters; e.g., the durations, initial phases and frequencies of the applied laser beams. Several typical macroscopic quantum states of the motion of the ion, e.g., the Pegg-Barnett phase state, the coherent state, and the even and odd coherent states, etc. can be created or well-approximated, if the number of the superposition Fock states is sufficient large.

We now give a brief discussion for the realizability of our approach.

First, the present quantum manipulations need to resolve the vibrational sidebands of the ion trap. In fact, it is not difficult to generate the desired laser pulse with sufficiently narrow line-width with current experimental technology. For example, the line-width (1 kHz) of the laser beams (at 729 nm) used in Ref. [12] to drive the trapped ion $^{40}Ca^{+}$ is very small, corresponding to a resolution of better than $\Delta\nu/\nu = 2.5\times10^{-12}$. This line-width is also much smaller than the frequency of the applied trap (138 kHz). Thus, the vibrational sidebands can be well resolved. The expected initial phases of the applied laser beams can be controlled by switching different signal paths [22]. During the very short durations (e.g., $\lesssim 10^{-4}$ s) for implementing the expected quantum operations, the applied laser beams (generated by the Ti: sapphire laser) are sufficient stabile (e.g., the corresponding initial phase-diffusion and frequency-drift times may reach to, e.g., 10 ms [23] and bandwidth $\lesssim 1kHz$ in 1 s averaging time [24], respectively.). In fact, the proposed engineering scheme could also, in principle, be used for Raman excitation, where the phases of the applied laser beams can be well controlled (see, e.g., [2, 5, 6]).

Second, in the present scheme, an arbitrary Fock state can be prepared by using only two operations (see, e.g., Eqs. (9) and (10)). The duration of operation depends on the value of k, once the LD parameter and the intensity of the applied laser beam are given. The Rabi frequency does not significantly reduce for large LD parameters (e.g., $\eta \gtrsim 0.5$). However, for small values of η (e.g., $\eta \lesssim 0.25$), the Rabi frequency decreases fast for sufficiently small values of k. Small values of the Rabi frequency correspond to a long duration of quantum operations, and the allowed number of operations will be reduced. For example, if $\eta = 0.25$, $\Omega = 2\pi \times 50$ kHz, then the duration of the transition $|g\rangle \longrightarrow |e\rangle$ is $t_0^c \approx 10\,\mu$s. Adding a $\pi/2$ pulse with duration $t_1^r \approx 40\,\mu$s ($t_{10}^r \approx 3$ ms, or $t_{30}^r = 0.3$ ms), the Fock state: $|1\rangle$ ($|10\rangle$, or $|30\rangle$) can be generated. Note that, compared to the t_1^r, t_0^c, the durations of operations $\hat{R}_{10}^r$, $\hat{R}_{30}^r$ are relatively long, as the Rabi frequencies are relatively small; $\Omega_{0,10}/\Omega \approx 2\times10^{-3}$ and $\Omega_{0,30}/\Omega \approx 2\times10^{-2}$ for the same laser intensity (see, Fig. 1). In principle, these decreased Rabi frequencies can be effectively compensated by enhancing the powers (i.e., intensities) of the applied laser beams. In fact, the power of the laser applied to drive the trapped cold ion is generally controllable (e.g., the Ti: sapphire laser used in experiment [12] is adjustable in the range from a few μW to a few hundred mW). Therefore, the corresponding durations can be shorter by $2 \sim 5$ orders of magnitude. For example, for $\eta = 0.25$, if the power of the applied laser beam is adjusted from a few μW to a few mW, the Rabi frequency $\Omega_{0,10}$ of the transition $|0\rangle \otimes |e\rangle \rightarrow |10\rangle|g\rangle$ can be enhanced to the same order of magnitude of the carrier Rabi frequency $\Omega\,(= 2\pi \times 50)$ kHz. The duration of the corresponding quantum operation is then shortened to 10^{-5}s. The smaller LD parameters η correspond to lasers with larger adjustable power ranges; e.g., for $\eta = 0.202$, the adjustable power range should be five orders of magnitude larger. Therefore, it is difficult to realize transitions with higher k in the LD regime, where $\eta \ll 1$.

Finally, the generation of the macroscopic superposed Fock states is limited in practice by the existing decays of the vibrational and atomic states. The lifetime of the atomic excited state $|e\rangle$ reaches up to 1 s [12] allows, in principle, to perform $10^3 \sim 10^4$ manipulations. Also, the recent experiment [24] showed that coherence for the superposition of $|n = 0\rangle$ and $|n = 1\rangle$ was maintained for up to 1 ms. Usually, the lifetime (i.e., relaxation time) of the state $|1\rangle$ should be longer than this dephasing time. Therefore, roughly say, preparing a superposition (e.g., phase state) from ground state $|n = 0\rangle$ to the excited motional Fock states $|n\rangle$ with $n > 10$ is experimentally possible, as the durations of quantum operation are sufficiently short, e.g., $< 10^{-4}$s. Improvements might be expected by considering the more realistic dynamics [14] that includes the decays of the excited atomic and motional states.

Acknowledgments

This work was supported in part by the National Security Agency (NSA) and Advanced Research and Development Activity (ARDA) under Air Force Office of Research (AFOSR) contract number F49620-02-1-0334, and by the National Science Foundation grant No. EIA-0130383.

[1] K. Vogel, V.M. Akulin, and W.P. Schleich, Phys. Rev. Lett. **71**, 1816 (1993); A.S. Parkins, P. Marte, P. Zoller and H.J. Kimble, Phys. Rev. Lett. **71**, 3095 (1993); Phys. Rev. A **51**, 1578 (1995).

[2] C. A. Sackett, D. Kielpinski, B.E. King, C. Langer, V. Meyer, C.J. Myatt, M. Rowe, Q.A. Turchette, W.M. Itano, D.J. Wineland, C. Monroe, Nature (London) **404**, 256 (2000); D.J. Wineland, C.R. Monroe, W.M. Itano, D. Leibfried, B.E. King, and D.M. Meekhof, J. Res. NIST, **103**, 259 (1998); C. Monroe,

D. M. Meekhof, B. E. King, and D. J. Wineland, Science **272**, 1131 (1996); D.J. Wineland and W.M. Itano, Phys. Rev. A **20**, 1521 (1979).

[3] C.A. Blockley, D.F. Walls and H. Kisken, Europhys. Lett. **17**, 509 (1992).

[4] W. Vogel and R.L.de Matos Filho, Phys. Rev. A **52**, 4214 (1995); W. Vogel and D.-G. Welsch, *ibid.* **40**, 7113 (1989); A. Steane, C.F. Roos, D. Stevens, A. Mundt, D. Leibfried, F. Schmidt-Kaler, and R. Blatt, *ibid.* **62**, 042305 (2000).

[5] D.M. Meekhof, C.R. Monroe, B.E. King, W.M. Itano, and D.J. Wineland, Phys. Rev. Lett. **76**, 1796 (1996).

[6] D. Leibfried, D.M. Meekhof, B.E. King, C.R. Monroe, W.M. Itano, and D.J. Wineland, *ibid*, **77**, 4281 (1996); **89**, 247901 (2002); J.I. Cirac, R. Blatt, A.S. Parkins, and P. Zoller, *ibid.* **70**, 762 (1993); **70**, 556 (1993); Ch. Roos, Th. Zeiger, H. Rohde, H. C. Nägerl, J. Eschner, D. Leibfried, F. Schmidt-Kaler, and R. Blatt, *ibid.* **83**, 4713 (1999); A. Ben-Kish, B. DeMarco, V. Meyer, M. Rowe, J. Britton, W.M. Itano, B.M. Jelenkovi, C. Langer, D. Leibfried, T. Rosenband, and D. J. Wineland, *ibid*, **90**, 037902(2003).

[7] C.R. Monroe, D.M. Meekhof, B.E. King, W.M. Itano, and D.J. Wineland, Phys. Rev. Lett. **75**, 4714 (1995); V. Meyer, M.A. Rowe, D. Kielpinski, C.A. Sackett, W.M. Itano, C. Monroe, and D. J. Wineland, *ibid.* **86**, 5870 (2001).

[8] J.F. Poyatos, J.I. Cirac, R. Blatt and P. Zoller, Phys. Rev. A **54**, 1532(1996); S.B. Zheng, X.W. Zhu, and M. Feng, *ibid.* **62**, 033807 (2000); H.P. Zeng, *ibid.* **57**, 388 (1998).

[9] R.L. de Matos Filho and W. Vogel, Phys. Rev. Lett. **76**, 608 (1996); C.C. Gerry, Phys. Rev. A **55**, 2478 (1997); S.A. Gardiner, J.I. Cirac, and P. Zoller, *ibid* **55**, 1683(1997); S.B. Zheng, *ibid*, **58**, 761 (1998); H. Moya-Cessa, S. Wallentowitz and W. Vogel, *ibid*, **59**, 2920 (1999).

[10] H.P. Zeng, Y.Z. Wang, and Y. Segawa, Phys. Rev. A **59**, 02174 (2000).

[11] D. Stevens, J. Brochard and A.M. Steane, Phys. Rev. A **58**, 2750 (1998); A. Steane, App. Phys. B **64**, 623 (1997); D.F.V. James, *ibid.* **66**, 181 (1998); G. Morigi, J.I. Cirac, M. Lewenstein and P. Zoller, Europhys. Lett. **39** (1), 13 (1997).

[12] P. A. Barton, C. J. S. Donald, D. M. Lucas, D. A. Stevens, A. M. Steane, and D. N. Stacey, Phys. Rev. A **62**, 032503 (2000); H. C. Nägerl, Ch. Roos, D. Leibfried, H. Rohde, G. Thalhammer, J. Eschner, F. Schmidt-Kaler, and R. Blatt, Phys. Rev. A **61**, 023405 (2000).

[13] H. Moya-Cessa and P. Tombesi, Phys. Rev. A **61**, 025401 (2000).

[14] Z. Kis, W. Vogel, and L. Davidovich, Phys. Rev. A **64**, 033401 (2001).

[15] S.R. Jefferts, C. Monroe, E.W. Bell, and D.J. Wineland, Phys. Rev. A **51**, 3112 (1995).

[16] J.I. Cirac, A.S. Parkins, R. Blatt, and P. Zoller, Adv. Atom. Molec. and Opt. Phys. **37**, 237 (1996).

[17] L.F. Wei, S.Y. Liu and X.L. Lei, Phys. Rev. A **65**, 062316 (2002); Opt. Commun. **208**, 131 (2002).

[18] M. Dakna, J. Clausen, L. Knöll, and D.-G. Welsch, Phys. Rev. A **59**, 1658 (1999); D.T. Pegg, L.S. Phillips, and S.M. Barnett, Phys. Rev. Lett. **81**, 1604 (1998).

[19] S.B. Zheng, Phys. Rev. A **63**, 015801 (2001); Phys. Lett. A **248**, 25 (1998).

[20] D.T. Pegg and S.M. Barnett, Europhys. Lett. **6**, 483 (1988); Phys. Rev. A**39**, 1665 (1989).

[21] B. Kneer and C.K. Law, Phys. Rev. A **57**, 2096 (1998).

[22] S. Gulde, M. Riebe, G.P.T. Lancaster, C. Becher, J. Eschner, H. Häffner, F. Schmidt-Kaler, I.L. Chuang, R. Blatt, Nature **421**, 48 (2003); http://heart-c704.uibk.ac.at/papers.html.

[23] Y.-F. Chou, J. Wang, H.-H. Liu, and N.-P. Kuo, Opt. Lett. **19**, 566 (1994).

[24] Ch. Roos, Th. Zeiger, H. Rohde, H.C. Nägerl, J. Eschner, D. Leibfried, F. Schmidt-Kaler, R. Blatt, Phys. Rev. Lett. **83**, 4713 (1999).

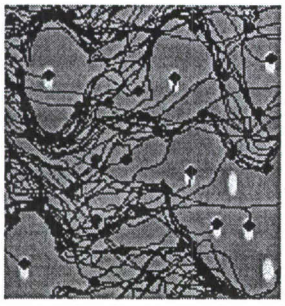

Franco Nori

Quantum Computing, Nanoscience, Condensed Matter Theory, and Complex Systems.

Permanent Address: Physics Department, The University of Michigan, Ann Arbor, MI 48109-1120

Also with the Center for Theoretical Physics, Applied Physics Program, and the Center for the Study of Complex Systems, University of Michigan.

Also with the Digital Materials Laboratory, Frontier Research System, RIKEN, Saitama, Japan.

Click the above image for details.

- List of Publications
- Access to several of out E-prints (very incomplete list)
  (abstracts, RevTeX, Postscript, and other formats)

- Scientific Outreach (Our research results featured in the news)
- Abbreviated Curriculum Vitae
- Student Awards

Quantum Computing (more links and preprints to be added later)

- Scalable quantum computing with Josephson charge qubits
- PRL Nov. 2002 on "Scalable quantum computing with Josephson charge qubits"
- A few non-technical summaries are in Technology Review News, EE Times, UM Press release, and Supercomputing Online, among others.

Collective Transport in Disordered Systems

- Vortex Dynamics and Collective Transport in Disordered Systems
  - Vortex Dynamics:
    - Brief Overview
    - non-technical summaries from the APS News and The University Record

  - Seminar on Vortex Dynamics. (including an introduction)
    This seminar is a slide presentation with simultaneous voice.

    - Microscopic Derivation of the Kim and Bean States in Superconductors
    - Vortex Plastic Flow in Superconductors
    - Plastic Motion in Twinned Superconductors
    - Periodic Arrays of Pinning Sites
    - Dynamic Phases in Superconductors with Periodic Pinning
    - Vortex Avalanches
    - Fractal Networks, Braiding Channels, and Voltage Noise in Vortex Rivers [Phys. Rev. Lett. 80, 2197, (1998)]
      and here for a brief nontechnical summary. Further information appears here
    - Nonequilibrium Dynamic Phase Diagram for Vortex Lattices

Click here for a link to the article [Phys. Rev. Lett. 81, 3757 (1998)]

- Phase Locking, Devil's Staircases, Farey Trees, and Arnold's Tongues in Driven Vortex Lattices [Phys. Rev. Lett. 82, 414 (1999)].
- Topological Invariants in Microscopic Transport on Rough Landscapes: Hierarchical Structure, Morphology, and Horton Analysis of River-like Networks of Vortices. [Phys. Rev. Lett. 82, 3641 (1999)].
- Vortex Motion in Channels [PRB 2003]
- Vortex Optics: fluxon convex/concave lenses, pumps, diodes, and stochastic rectification. [Phys. Rev. Lett. 83, 5106 (1999)].
  A very different approach to the same problem appears in Phys. Rev. Lett. 87, 177002 (2001).

- V I D E O S of Vortex Dynamics in Superconductors (JAVA format)

- Additional VIDEO CLIPS of Vortex Dynamics (Quicktime format)
- "Science" Perspective: Intermittently Flowing Rivers of Quantized Magnetic Flux
  - Videos in "Science"

- Avalanches in Granular Materials: Mean Field Theory and Experiments
- Instabilities in Systems with Threshold Dynamics: Experiments and Theory
- Water Droplet Avalanches

- Instabilities and Chaos in Falling Objects: From Maxwell to Bar Tricks (Nature, 1997)

- Sound-Producing Sand Avalanches (Scientific American, 1997)

Suppressing Quantum Noise in Solids: Squeezed Phonons

- Link to the URL of Phys. Rev. Lett. Dec. 8, 1997
  Phonon Squeezed States Generated by Second-Order Raman Scattering.

- Squeezed Phonons: Manipulating Quantum Fluctuations of Atomic Displacements.
- Controlling Quantum Noise in Condensed Matter:
  Squeezed Phonon States and Squeezed States in Superconducting Junctions

- Acoustic Interference and Phonon Localization

Feynman Path-Integral Analytical Studies of Quantum Interference: Superconducting Networks, Josephson junction Arrays, and Electron Motion in Magnetic Fields

- Analytical Studies of Quantum Interference Effects due to Electron Motion in Magnetic Fields

- Superconducting Micronetworks and Josephson-Junction Arrays: Feynman Path-Integral and Multiloop Aharonov-Bohm Approches.

- Course for Fall 2001 (Physics 510): Statistical Mechanics and Thermodynamics

- Course for Winter 2000: Rackham Interdisciplinary Seminar on Spatio-Temporal Complexity in Science and Engineering.

Last Update: 06/99. Initial version prepared by: Bartholomew Hsu and Jared Groth.
Return to the U of M Physics Department Homepage

Publications in Refereed Journals

1. Loop-Space Quantum Formulation of Free Electromagnetism,
C. Di Bartolo, F. Nori, R. Gambini, and A. Trias,
Lett. Nuov. Cim. **38**, 497 (1983).

2. Acoustic and Electronic Properties of One-dimensional Quasicrystals,
F. Nori and J.P. Rodriguez,
Phys. Rev. B **34**, 2207 (1986).

3. Renormalization Group Study of One-dimensional Quasiperiodic Systems,
Q. Niu and F. Nori,
Phys. Rev. Lett. **57**, 2057 (1986).

4. Superconducting-Normal Phase Boundary of Quasicrystalline Arrays,
F. Nori, Q. Niu, E. Fradkin, and S.-J. Chang,
Phys. Rev. B **36**, 8338 (1987).

5. Aperiodic Superconducting Phase Boundary of Periodic Micronetworks in a Magnetic Field,
F. Nori and Q. Niu,
Phys. Rev. B (Rapid Communications) **37**, 2364 (1988).

6. Superconducting $T_c(H)$ for Micronetworks: Analytical and Numerical Results,
F. Nori and Q. Niu,
Physica **152B**, 105 (1988).

7. Strain Accumulation in Quasicrystalline Solids,
F. Nori, M. Ronchetti and V. Elser,
Phys. Rev. Lett. **61**, 2774 (1988).

8. Theory of Superconducting Wire Networks and Josephson Junction Arrays in Magnetic Fields,
Q. Niu and F. Nori,
Phys. Rev. B **39**, 2134 (1989).

9. Thue-Morse Quantum Ising Model, M. Doria, F. Nori, and I. Satija,
Phys. Rev. B **39**, 6802 (1989).

10. Quasicrystalline Diffraction Pattern: Exact Expression in terms of Elementary Functions, S.-J. Chang and F. Nori, (invited paper) Chinese Journal of Physics **26**, No. 4 (1989).

11. Transmission and Frequency Spectra of Acoustic Phonons in Thue–Morse Superlattices,
S. Tamura and F. Nori,
Phys. Rev. B **40**, 9790 (1989).

12. Generalized Flux States of the $t - J$ Model,
F. Nori, E. Abrahams and G.T. Zimanyi,
Phys. Rev. B (Rapid Communications) **41**, 7277 (1990).

13. Acoustic Interference in Random Superlattices,
S. Tamura and F. Nori,
Phys. Rev. B (Rapid Communications) **41**, 7941 (1990).

14. Trace Maps for Aperiodic Chains,
M. Kolář and F. Nori
Phys. Rev. B (Rapid Communications) **42**, 1062 (1990).

15. Spectral-Splitting and Wave Function Scaling in Quasicrystalline and Hierarchical Structures,
Q. Niu and F. Nori,
Phys. Rev. B **42**, 10329 (1990).

16. Generalized Thue-Morse Chains and their Properties,
M. Kolář, M.K. Ali and F. Nori,
Phys. Rev. B **43**, 1034 (1991).

17. Systematic Study of Generalized Flux Phases,
F. Nori, B. Doucot, and R. Rammal,
Phys. Rev. B **44**, 7637 (1991).

18. Theoretical Analysis of the Thermal Conductivity of $YBa_2Cu_3O_{7-\delta}$ Single Crystals,
S.D. Peacor, R.A. Richardson, F. Nori, and C. Uher,
Phys. Rev. B **44**, 9508 (1991).

19. Comparison of Frustration and Doping Effects in Generalized Flux Phases,
F. Nori and G.T. Zimanyi,
Europhys. Lett. **16**, 397 (1991).

20. Self-Organized Critical Behavior in Pinned Flux Lattices,
O. Pla and F. Nori,
Phys. Rev. Lett. **67**, 919 (1991).

21. Thermal Conductivity of $YBa_2Cu_3O_{7-\delta}$ in a Magnetic Field: Can $k(H)$ Probe the Vortex State?,
R.A. Richardson, S.D. Peacor, F. Nori, and C. Uher,
Phys. Rev. Lett. **67**, 3856 (1991).

22. Does Frustration Describe Doping in Models for High-Temperature Superconductors?,
F. Nori, S. Bacci, and E. Gagliano,
Phys. Rev. Lett. **68**, 240 (1992).

23. Imaging of Avalanches in Granular Materials,
M. Bretz, J. Cunningham, P. Kurczynski, and F. Nori.
Phys. Rev. Lett. **69**, 2431 (1992).

24. $YBa_2Cu_3O_{7-\delta}$ Films: Calculation of the Thermal Conductivity and Phonon Mean-Free Path, S.D. Peacor, R.A. Richardson, C. Uher, and F. Nori,
J. Appl. Phys. **72**, 4788 (1992).

25. Water Droplet Avalanches, B. Plourde, F. Nori, and M. Bretz,
Phys. Rev. Lett. **71**, 2741 (1993).

26. Mean Field Theory of Sandpile Avalanches: from the Intermittent to the Continuous Flow Regime,
V.G. Benza, F. Nori, and O. Pla,
Phys. Rev. E **48**, 4095 (1993).

27. Phonon Transmission Rate, Fluctuations, and Localization in Random Semiconductor Superlattices: Green's Function Approach,
N. Nishiguchi, S. Tamura, and F. Nori,
Phys. Rev. B **48**, 2515 (1993).

28. Phonon Universal Transmission Fluctuations and Localization in Semiconductor Superlattices with a Controlled Degree of Order,
N. Nishiguchi, S. Tamura, and F. Nori,
Phys. Rev. B **48**, 14426 (1993).

29. Effective Carrier Mean-Free Path in Confined Geometries,
R. Richardson and F. Nori,
Appl. Phys. Lett. **63**, 2076 (1993).

30. Transport and Boundary Scattering in Confined Geometries: Analytical Results,
R. Richardson and F. Nori,
Phys. Rev. B **48**, 15209 (1993).

31. Analytical Approaches for the Electronic Structure of C_{60},
Y.-L. Lin and F. Nori,
Phys. Lett. **183A**, 214 (1993).

32. The Real-Space Renormalization Group and Generating Function for Penrose Lattices,
J.Q. You and F. Nori,
J. Physics: Condensed Matter **5**, 9431 (1993).

33. Exact Renormalization-Group Approach to the Generating Function of a Vicsek Fractal, J.Q. You, C.-H. Lam, F. Nori, and L. Sander
Phys. Rev. E (Rapid Communications) **48**, R4183 (1993).

34. Electronic Structure of C_{60} and C_{70} molecules: Generating Functional Approach,
J.Q. You, F. Nori, and Y.-L. Lin,
Solid State Comm. **91**, 117 (1994).

35. Electronic Structure of Single- and Multiple–Shell Carbon Fullerenes,
Y.-L. Lin and F. Nori,
Phys. Rev. B **49**, 5020 (1994).

36. Analytical Solution for the Fermi-Sea Energy of two-dimensional Electrons in a Magnetic Field: Lattice Path Integral Approach and Quantum Interference,
F. Nori and Y.-L. Lin,
Phys. Rev. B **49**, 4131 (1994).

37. Quantum Interference on the Kagomé Lattice,
Y.-L. Lin and F. Nori,
Phys. Rev. B, **50**, 15953 (1994).

38. Raman Spectra in two-dimensional Spin-1/2 Heisenberg Antiferromagnets,
S. Haas, E. Dagotto, J. Riera, R. Merlin, and F. Nori,
Journal of Applied Physics **75**, 6340 (1994).

39. Confirmation of the Modified Bean Model from Simulations of Superconducting Vortices,
R. Richardson, O. Pla, and F. Nori,
Phys. Rev. Lett. **72**, 1268 (1994).

40. Marginal Stability and Chaos in a Stick-Slip Electronic Circuit Modeling Coupled Faults,
S. Field, N. Venturi, and F. Nori,
Phys. Rev. Lett. **74**, 74 (1995).

41. Superconducting Vortex Avalanches,
S. Field, J. Witt, F. Nori, and X. Lin,
Phys. Rev. Lett. **74**, 1206 (1995).

42. Droplet Avalanches; Comment. F. Nori, B. Plourde, and M. Bretz,
Phys. Rev. Lett. **74**, 3498 (1995).

43. Magnetic Raman Scattering in Two-Dimensional Spin-1/2 Heisenberg Antiferromagnets: Spectral Shape Anomaly and Magnetostrictive Effects,
F. Nori, R. Merlin, S. Haas, A. Sandvik, and E. Dagotto,
Phys. Rev. Lett. **75**, 553 (1995).

44. Microscopic Derivation of Magnetic Flux Density Profiles, Magnetization Hysteresis Loops, and Critical Currents in Strongly Pinned Superconductors,
C. Reichhardt, J. Groth, C.J. Olson, S. Field, and F. Nori.
Phys. Rev. B **52**, 10441 (1995).

45. Vortex Plastic Flow, Local Flux Density, Magnetization Hysteresis Loops, and Critical Currents Deep in the Bose Glass and Mott-Insulator Regimes,
C. Reichhardt, C.J. Olson, J. Groth, S. Field, and F. Nori,
Phys. Rev. B (Rapid Communications) **53**, R8898 (1996).

46. Spatio-Temporal Dynamics and Plastic Flow of Vortices in Superconductors with Periodic Arrays of Pinning Sites,
C. Reichhardt, J. Groth, C.J. Olson, S. Field, and F. Nori,
Phys. Rev. B **54**, 16108 (1996); Enhanced-clarity grey-scale figures were published in **56**, 14196 (1997).

47. Vortex Plastic Motion in Twinned Superconductors,
J. Groth, C. Reichhardt, C.J. Olson, S. Field, and F. Nori,
Phys. Rev. Lett. **77**, 3625 (1996).

48. Intermittently Flowing Rivers of Quantized Magnetic Flux,
F. Nori,
Science **276**, 1373 (1996).

49. Exact Solutions for the Electronic Structure of C_{60}: Recursion and Path-Integral Approaches,
Y.-L. Lin and F. Nori,
Phys. Rev. B, **53**, 1641 (1996).

50. Quantum Interference from Sums over Closed Paths for Electrons on a Three-Dimensional Lattice in a Magnetic Field: Total Energy, Magnetic Moment, and Orbital Susceptibility,
Y.-L. Lin and F. Nori,
Phys. Rev. B **53**, 13374 (1996).

51. Analytical Results on Quantum Interference and Magnetoconductance for Strongly Localized Electrons in a Magnetic Field: Exact Summation of Forward-Scattering paths,
Y.-L. Lin and F. Nori,
Phys. Rev. B **53**, 15543 (1996).

52. Strongly Localized Electrons in a Magnetic Field: Quantum Interference and Exact Summation of Forward-Scattering Paths in Two and Three Dimensions,
Y.-L. Lin and F. Nori,
Phys. Rev. Lett. **76**, 4580 (1996).

53. Squeezed Phonon States: Modulating Quantum Fluctuations of Atomic Displacements,
X. Hu and F. Nori,
Phys. Rev. Lett. **76**, 2294 (1996).

54. Quantum Phonon Optics: Coherent and Squeezed Atomic Displacements,
X. Hu and F. Nori,
Phys. Rev. B **53**, 2419 (1996).

55. Phonon Squeezed States Generated by Second Order Raman Scattering,
X. Hu and F. Nori,
Phys. Rev. Lett. **79**, 4605 (1997).

56. Plastic Flow, Voltage Noise, and Vortex Avalanches in Superconductors,
C.J. Olson, C. Reichhardt, J. Groth, S. Field, and F. Nori,
Physica C **290**, 89 (1997).

57. Superconducting Vortex Avalanches, Voltage Bursts, and Vortex Plastic Flow: Effect of the Microscopic Pinning Landscape on the Macroscopic Properties,
C.J. Olson, C. Reichhardt, and F. Nori,
Phys. Rev. B **56**, 6175 (1997).

58. Dynamical Phases of Vortices in Superconductors with Periodic Pinning,
C. Reichhardt, C.J. Olson, and F. Nori,
Phys. Rev. Lett. **78**, 2648 (1997).

59. Chaotic Dynamics of Falling Disks,
S. Field, M. Klaus, M.G. Moore, and F. Nori,
Nature **387**, 252 (July 17, 1997) .

60. BOOMING SAND,
F. Nori, P. Sholtz, and M. Bretz,
Scientific American **277**, No. 3, 84 (September 1997).

61. SOUND-PRODUCING SAND AVALANCHES,
P. Sholtz, M. Bretz, and F. Nori,
Contemporary Physics **38**, No. 5, 329 (1997).

62. COMMENSURATE VORTEX STATES IN SUPERCONDUCTORS WITH PERIODIC PINNING ARRAYS,
C. Reichhardt, C.J. Olson, and F. Nori,
Phys. Rev. B **57**, 7937 (1998).

63. NONEQUILIBRIUM DYNAMICAL PHASES AND PLASTIC FLOW OF DRIVEN VORTEX LATTICES IN SUPERCONDUCTORS WITH PERIODIC ARRAYS OF PINNING SITES,
C. Reichhardt, C.J. Olson, and F. Nori,
Phys. Rev. B **58**, 6534—6564 (1998).

64. FRACTAL NETWORKS, BRAIDING CHANNELS, AND VOLTAGE NOISE IN INTERMITTENTLY FLOWING RIVERS OF QUANTIZED MAGNETIC FLUX,
C.J. Olson, C. Reichhardt, and F. Nori,
Phys. Rev. Lett. **80**, 2197 (1998).

65. NONEQUILIBRIUM DYNAMIC PHASE DIAGRAM FOR VORTEX LATTICES,
C.J. Olson, C. Reichhardt, and F. Nori,
Phys. Rev. Lett. **81**, 3757 (1998).

66. PHASE LOCKING, DEVIL'S STAIRCASES, AND ARNOLD'S TONGUES IN DRIVEN VORTEX LATTICES WITH PERIODIC PINNING,
C. Reichhardt and F. Nori,
Phys. Rev. Lett., **82**, 414 (1999).

67. TOPOLOGICAL INVARIANTS IN MICROSCOPIC TRANSPORT ON ROUGH LANDSCAPES: MORPHOLOGY AND HORTON ANALYSIS OF RIVER–LIKE NETWORKS OF VORTICES,
A. Mehta, C. Reichhardt, C.J. Olson, and F. Nori,
Phys. Rev. Lett., **82**, 3641 (1999).

68. SUPERCONDUCTOR FLUXON PUMP AND LENSES,
J.W. Wambaugh, C. Reichhardt, C.J. Olson, F. Marchesoni, and F. Nori,
Phys. Rev. Lett., **83**, 5106 (1999).

69. PHONON SQUEEZED STATES: QUANTUM NOISE REDUCTION IN SOLIDS,
X. Hu and F. Nori,
Physica B, **263**, 16 (1999).

70. DYNAMIC VORTEX PHASES AND PINNING IN SUPERCONDUCTORS WITH TWIN BOUNDARIES,
C. Reichhardt, C.J. Olson, F. Nori,
Phys. Rev. B, **61**, 3665 (2000).

71. DYNAMIC PHASE DIAGRAM AND ORIENTATIONAL DEPENDENCE FOR VORTICES IN SUPERCONDUCTORS WITH PERIODIC ARRAYS OF PINNING SITES
F. Nori and C. Reichhardt,
Physica C **332**, 40 (2000).

72. CRITICAL DYNAMICS OF BURST INSTABILITIES IN THE PORTEVIN-LE CHATELIER EFFECT
G. D'Anna and F. Nori,
Phys. Rev. Lett., **85**, 4096 (2000).

73. MOVING WIGNER GLASSES AND SMECTICS: DYNAMICS OF DISORDERED WIGNER CRYSTALS
C. Reichhardt, C.J. Olson, N. Grombech-Jensen, and F. Nori,
Phys. Rev. Lett., **86**, 4354 (2001).

74. COLLECTIVE INTERACTION-DRIVEN RATCHET FOR TRANSPORTING FLUX QUANTA
C.J. Olson, C. Reichhardt, B. Janko, F. Nori,
Phys. Rev. Lett., **87**, 177002 (2001).

75. Effects of Columnar and Point Defects on Magnetic Hysteresis Curves Produced by 3-dimensional Vortices in Layered Superconductors
C.J. Olson and F. Nori,
Physica C, **363**, 67 (2001).

76. Vortex structure and dynamics in kagome and triangular pinning potentials
M.F. Laguna, C.A. Balseiro, D. Dominguez, F. Nori,
Phys. Rev. B, **64**, 104505 (2001).

77. Quantum Interference in Superconducting Wire Networks and Josephson Junction Arrays: Analytical Approach based on Multiple-Loop Aharonov-Bohm Feynman Path-Integrals
Yeong-Lieh Lin and Franco Nori,
Phys. Rev. B, **65**, 214504 (2002).

78. Experimentally-realizable devices for controlling the motion of magnetic flux quanta in anisotropic superconductors
S. Savelev and F. Nori,
Nature Materials, **1**, 179 (2002).
Listed in the cover of the November issue, and also featured in a nice two-pages "News and Views", "Controlling the motion of quanta" *Nature Materials* **1**, 143 (2002).

79. Scalable Quantum Computing with Josephson junction Qubits
J.Q. You, J.S. Tsai, and F. Nori,
Phys. Rev. Lett., **89**, 179 (2002).

80. Controllable manipulation of macroscopic quantum states in coupled charge qubits,
J.Q. You, J.S. Tsai, and F. Nori,
Phys. Rev. B **68**, 024510 (2003).

81. Quantum information processing with superconducting qubits in a microwave field,
J.Q. You and F. Nori,
Phys. Rev. B, **68**, 64509 (2003).

82. Shear and Loading in Channels: Oscillatory shearing and Leapfrogging Edge Currents of Superconducting Vortices,
J. Wambaugh, F. Marchesoni, and F. Nori,
Phys. Rev. B **67**, 144515 (2003).

83. Force-free current-induced "inverse" melting of the vortex-lattice in superconductors,
S. Savel'ev, C. Catutto, and F. Nori,
Phys. Rev. B, Rapid Communications, **67**, 180509 (2003).

84. Controllable stepmotors and rectifiers of magnetic flux quanta using periodic arrays of asymmetric pinning defects,
B.Y. Zhu, F. Marchesoni, V.V. Moshchalkov, and F. Nori,
Phys. Rev. B **65**, 14514 (2003).

85. Anomalous interstitial dynamics, Stokes' drift, and current inversion in AC-driven vortex lattices in superconductors with arrays of asymmetric double-well traps,
F. Marchesoni, B.Y. Zhu, and F. Nori,
Physica A, **325**, 78 (2003).

86. Controlling transport in mixtures of interacting particles using Brownian motors,
S. Savel'ev, F. Marchesoni, and F. Nori,
Phys. Rev. Lett. **91**, 10601 (2003).

87. Observing Brownian motion in vibro-fluidized granular matter,
G. D'Anna, P. Mayor, A. Barrat, V. Loreto, and F. Nori,
Nature, **424**, 909-912 (August 21, 2003).
This article (featured all over via press, newswires, radio, and TV) is the *Cover Story* of the 21 August, 2003, issue of Nature. Also featured in that issue in the table of contents and via a companion "News and Views". A month later, featured again in Nature (October. 2003).

88. REVERSIBLE RECTIFIER THAT CONTROLS THE MOTION OF MAGNETIC FLUX QUANTA IN SUPERCONDUCTORS,
J.E. Villegas, S. Savel'ev, F. Nori, E.M. Gonzalez, J.V. Anguita, R. Garcia, and J.L. Vicent, *Science* **302** 1188 (2003). Also featured in an "Enhanced Perspectives" *Science* **302** 1159 (2003)), the only one for that issue, and one of about three for all of Physics during 2003. Also featured in the "This week in Science" page of that issue of *Science.*

89. AN EFFICIENT SINGLE-STEP SCHEME FOR MANIPULATING QUANTUM INFORMATION OF TWO TRAPPED IONS BEYOND THE LAMB-DICKE LIMIT,
L.F. Wei and F. Nori, *Phys. Lett. A*, **320**, 131-139 (2003).

90. COHERENTLY MANIPULATING TWO-QUBIT QUANTUM INFORMATION USING A PAIR OF SIMULTANEOUS LASER PULSES,
L.F. Wei and F. Nori, *Europhysics Letters*, **65**, 1-6 (2004).

91. CONTROLLING THE MOTION OF MAGNETIC FLUX QUANTA,
B.Y. Zhu, F. Marchesoni, and F. Nori, *Phys. Rev. Lett.*, in press (2004).

92. MANIPULATING SMALL PARTICLES IN MIXTURES FAR FROM EQUILIBRIUM,
S. Savel'ev, F. Marchesoni, and F. Nori, *Phys. Rev. Lett.*, in press (2004).

Submitted manuscripts (preprints available upon request):

93. INTERACTING PARTICLES ON A ROCKED RATCHET: RECTIFICATION BY CONDENSATION,
S. Savelev, F. Marchesoni, and F. Nori, submitted.

94. TRANSPORT VIA NONLINEAR SIGNAL MIXING IN A RATCHET DEVICE,
S. Savel'ev, F. Marchesoni, P. Hanggi, and F. Nori, submitted (2004).

95. CORRELATION-INDUCED COHERENCE-PRESERVING MACROSCOPIC QUANTUM STATES,
J.Q. You, X. Hu, and F. Nori, submitted.

96. FAST TWO-BIT OPERATIONS IN INDUCTIVELY COUPLED FLUX QUBITS,
J.Q. You, Y. Nakamura, and F. Nori, submitted.

97. COHERENTLY MANIPULATING TWO-QUBIT QUANTUM INFORMATION BY A SINGLE-STEP OPERATION,
L.F. Wei and F. Nori, submitted.

98. ENGINEERING QUANTUM PURE STATES OF A TRAPPED COLD ION BEYOND THE LAMB-DICKE LIMIT,
L.F. Wei, Y.X. Liu, and F. Nori, submitted.

99. QUANTUM PHASE ESTIMATION ALGORITHMS WITH DELAYS: HOW TO AVOID DYNAMICAL PHASE ERRORS,
L.F. Wei and F. Nori, submitted.

100. PHASE-MATCHING APPROACH TO ELIMINATE THE DYNAMICAL PHASE ERROR IN SHOR'S FACTORING ALGORITHM ,
L.F. Wei, X. Li, X. Hu, and F. Nori, submitted.

101. COUPLING JOSEPHSON QUBITS VIA A CURRENT-BIASED INFORMATION BUS,
L.F. Wei, Y.X. Liu, and F. Nori, submitted.

102. QUBIT TOMOGRAPHY FOR SOLID-STATE SYSTEMS,
Y.X. Liu, L.F. Wei, and F. Nori, submitted.

103. QUANTUM TOMOGRAPHY FOR SUPERCONDUCTING QUBITS,
Y.X. Liu, L.F. Wei, and F. Nori, submitted.

104. GENERATION OF NON-CLASSICAL PHOTON STATES USING A SUPERCONDUCTING QUBIT IN A QUANTUM ELECTRODYNAMIC MICROCAVITY,
Y.X. Liu, L.F. Wei, and F. Nori, submitted.

105. ENTANGLEMENT OF TWO COUPLED CHARGE QUBITS,
Y.A. Pashkin, et al., submitted.

Articles Reprinted in Books (Reprint Collections)

STRAIN ACCUMULATION IN QUASICRYSTALLINE SOLIDS, originally published in Phys. Rev. Lett. **66**, 2774 (1988), has been reprinted in the book *Simulation Approach to Solids*, M. Ronchetti and J. Jacucci, eds. (Kluwer Academic Publishers, 1991)

Publications in Books: Refereed Conference Proceedings

106. STRAIN ACCUMULATION IN TWO-DIMENSIONAL QUASICRYSTALS,
M. Ronchetti, F. Nori and V. Elser,
Quasicrystalline Materials, Ch. Janot and J.M. Dubois (eds.), p. 299,
(World Scientific Publishing Co., Singapore, 1988).

107. ANGULAR MOMENTUM IRREDUCIBLE REPRESENTATION AND DESTRUCTIVE QUANTUM INTERFERENCE FOR PENROSE LATTICE HAMILTONIANS,
F. Nori and Q. Niu,
Quasicrystals and Incommensurate Structures in Condensed Matter E. Gomez *et al*, eds., p. 434
(World Scientific Publishing Co., Singapore, 1990).

108. EXACT EXPRESSION IN TERMS OF ELEMENTARY FUNCTIONS FOR A QUASICRYSTALLINE DIFFRACTION PATTERN, S.-J. Chang and F. Nori,
Quasicrystals and Incommensurate Structures in Condensed Matter E. Gomez *et al*, eds., p. 79
(World Scientific Publishing Co., Singapore, 1990).

109. PEAK BROADENING IN QUASICRYSTALLINE SOLIDS, F. Nori, M. Ronchetti and V. Elser,
Quasicrystals and Incommensurate Structures in Condensed Matter E. Gomez *et al*, eds., p. 420
(World Scientific Publishing Co., Singapore, 1990).

110. BAND-SPLITTING AND WAVE FUNCTION SCALING IN QUASICRYSTALLINE STRUCTURES,
Q. Niu and F. Nori,
Quasicrystals and Incommensurate Structures in Condensed Matter E. Gomez *et al*, eds., p. 426
(World Scientific Publishing Co., Singapore, 1990).

111. DIAMAGNETISM IN QUASICRYSTALLINE SUPERCONDUCTING NETWORKS, Q. Niu and F. Nori, *Quasicrystals* M. V. Jaric and S. Lundqvist, eds., p. 425 (World Scientific Publishing Co., Singapore, 1990).

112. LONG-RANGE ORDER IN ONE-DIMENSIONAL QUASIPERIODIC MAGNETIC CHAINS,
I. Satija, M. Doria, and F. Nori, *Magnetic Properties of Low Dimensional Systems: New Developments.* L.M. Falicov et al, eds., (Springer-Verlag, New York, 1990).

113. DYNAMICS AND MACROSCOPIC RIGIDITY IN GLASSY THIN FILMS, F. Nori,
Nonlinear Structures in Physical Systems, L. Lam and H.C. Morris, eds., p. 247
(Springer-Verlag, New York, 1990).

114. HOLE DYNAMICS IN A QUANTUM ANTIFERROMAGNET: SLAVE-BOSON GENERALIZED FLUX STATES,
F. Nori and G.T. Zimany,
Nonlinear Structures in Physical Systems, L. Lam and H.C. Morris, eds., p. 261
(Springer-Verlag, New York, 1990).

115. FRUSTRATED SPIN (J-J') SYSTEMS DO NOT MODEL THE MAGNETIC PROPERTIES OF HIGH-TEMPERATURE SUPERCONDUCTORS,
S. Bacci, E. Gagliano, and F. Nori,
High-Temperature Superconductors and Strongly Correlated Electron Systems II
G. Baskaran et al eds., p. 325 (World Scientific Publishing Co., Singapore, 1991).

116. HARD-CORE SLAVE-BOSON GENERALIZED FLUX STATES OF THE T-J MODEL,
F. Nori, G.T. Zimanyi, and E. Abrahams,
High-Temperature Superconductors and Strongly Correlated Electron Systems II
G. Baskaran et al eds., p. 119 (World Scientific Publishing Co., Singapore, 1991).

117. QUANTUM INTERFERENCE IN SUPERCONDUCTING WIRE NETWORKS AND JOSEPHSON JUNCTION ARRAYS IN MAGNETIC FIELDS, F. Nori and Q. Niu,
Physical Phenomena at High Magnetic Fields
E. Manousakis et al eds., p. 334 (Addison-Wesley, 1991).

118. FILLING LANDAU LEVELS: FERMI SEA GROUND-STATE ENERGY, COMPETING INTERACTIONS AND MARGINAL DISPERSIONS IN GENERALIZED FLUX PHASES,
B. Doucot, F. Nori, and R. Rammal,
High-Temperature Superconductors and Strongly Correlated Electron Systems III
G. Baskaran et al eds., p. 115 (World Scientific Publishing Co., Singapore, 1992).

119. ELECTRONIC DENSITY OF STATES FOR PENROSE TILINGS AND VICSEK FRACTAL,
J.Q. You, F. Nori, and C.-H. Lam,
Materials Science Forum, **150-151**, 435 (1994).

120. SIMULATION OF VORTEX DYNAMICS IN NANOSTRUCTURED PINNING ARRAYS,
M.F. Laguna, C.A. Balseiro, D. Dominguez, and F. Nori,
Phys. Status Solidi B **230** (2): 499-503 (2002).

121. COOPER-PAIR-BOX QUBITS IN A QUANTUM ELECTRODYNAMIC CAVITY,
J.Q. You, J.S. Tsai, and F. Nori.
Physica E **18**, 33 (2003).

122. EXPERIMENTALLY REALIZABLE SCALABLE QUANTUM COMPUTING USING SUPERCONDUCTING QUBITS,
J.Q. You, J.S. Tsai, and F. Nori,
Physica E **18**, 35 (2003).

123. FLUCTUATIONS IN THE JOSEPHSON-PANCAKE COMBINED VORTEX LATTICE,
S. Savel'ev, J. Mirković, and F. Nori,
Physica C **388**, 653 (2003).

124. CONTROLLING THE COLLECTIVE MOTION OF INTERACTING PARTICLES: ANALYTICAL STUDY VIA THE NONLINEAR FOKKER-PLANCK EQUATION,
S. Savel'ev, F. Marchesoni, and F. Nori.
Physica C **388**, 661 (2003).

125. EASILY-CONTROLLABLE COLLECTIVE STEPMOTOR OF MAGNETIC FLUX QUANTA,
B.Y. Zhu, F. Marchesoni, V.V. Moshchalkov, and F. Nori,
Physica C **388**, 665 (2003).

126. VORTEX LATTICE MELTING IN VERY ANISOTROPIC SUPERCONDUCTORS INFLUENCED BY THE FORCE-FREE CURRENT,
S. Savel'ev, F. Nori, J. Mirković, and K. Kadowaki.
Physica C **388**, 685 (2003).

127. BIOLOGICALLY-INSPIRED DEVICES FOR EASILY CONTROLLING THE MOTION OF MAGNETIC FLUX QUANTA,
B.Y. Zhu, F. Marchesoni, and F. Nori,
Physica E **18**, 318 (2003).

128. VORTEX DYNAMICS IN SUPERCONDUCTORS WITH A TRIANGULAR ARRAYS OF TRIANGULAR BLIND ANTIDOTS,
B.Y. Zhu, L. Van Look, V.V. Moshchalkov, F. Marchesoni, and F. Nori,
Physica E **18**, 322 (2003).

129. MANIPULATING QUANTUM INFORMATION OF TWO TRAPPED IONS BY A SINGLE-STEP OPERATION,
L.F. Wei and F. Nori, Submitted.

130. QUANTUM COMPUTING WITH MANY SUPERCONDUCTING QUBITS,
J.Q. You, J.S. Tsai, and F. Nori,
New Directions in Mesoscopic Physics, 351-360 (2003).

131. ENTANGLEMENT OF TWO COUPLED CHARGE QUBITS,
Y.A. Pashkin, et al., *Int. J. Quantum Information*, **1**, 1 (2003).

Science Outreach.

The press is communicating some of our results (as well as their importance and significance) to the general public. This is a role that the American Physical Society, American Institute for Physics, American Association for the Advancement of Science, the National Science Foundation, etc. are strongly urging scientists to fill.

Outreach efforts to the general public have been repeatedly described by policymakers as crucial to the survival of support for science.

Recent work (about ten year's period: circa 1992—2003) by our group has been featured in:

- *Science News* **142**, 231 (Oct. 92)
- *Science News* **144**, 261 (Oct. 93)
- *Physics World* **6**, 42 (Dec. 93)
- *Science* **264**, 200 (April 94)
- *New Scientist*, p. 36 (12 March 1994)
- *Science News* **147**, 198 (April 95)
- *American Physical Society News* **4**, 8 (June 95)
- *American Institute of Physics: Physics News* **261** (March 6, 96)
- *Science* **271**, 1373 (March 8, 96)
- *American Physical Society News* **5**, 9 (June 96)
- *Physics Today* ("Search and Discovery" section) **50**, No. 6, 19 (June 97)
- *Science News* **152**, No. 3, 37 (July 97)
- *Science On-Line: ScienceNow* (July 17, 1997)
- *American Institute of Physics: Physics News* **331** (July 24, 97)
- *Scientific American* (August, 1997)
- 1998: translations into Japanese, Chinese, Spanish, German, French, Polish, Arabic, etc. of our *Scientific American* article.
- *American Institute of Physics:* Science Report Radio (Physics News broadcasted by Radio Stations) (1998). (Note: For over 25 years, Science Report Radio has been played regularly on 181 stations nationwide. It is the nation's longest running radio science feature. Each program reaches approximately four million listeners. At least one radio station in 19 of the top 20 markets broadcasts the show. In 1997, Science Report also became available via the Public Radio Satellite System).
- *American Physical Society:* Division of Materials Physics' Webpage (1996–present).
- *New Scientist*, No. 2140, p. 16 (June 27, 1998).

- *Science News*, No. 155 (October 31, 1998). Coverstory, and the only featured long article of the issue.
- *New Scientist*, Vol. 161, No. 2179, P. 40 (27 March 1999). Also listed in the cover.
- *Physics World*, **12**, No. 4, p. 24 (April 1999); coverstory.
- 1999 *American Physical Society:* Centennial Exhibit celebrating the 100 years of the APS. Very large posters and also videos on our theory work on vortex dynamics were featured right next to the "history of superconductivity" exhibit. Only another group, Argonne National Laboratory, was featured (experiments on vortex dynamics).
- Featured in the book *How Nature Works*, by Per Bak (Springer-Verlag, 1996). A full page with color photos and text, plus additional mentions elsewhere in the book.
- Newspapers in the US (e.g., *Dallas Morning News*, Oct. 20, 1997, Discovery Section, Cover Story); also in newspapers in Michigan and Colorado.
- Newspapers abroad (e.g., Swiss *Die Weltwoche*, Oct. 2 1997, Science Section, Full page article; and also in Germany).
- Science Magazines abroad. For instance, the December 1997 issue of the European science magazine *Focus* (with a circulation of over 300,000 copies per issue) devoted five pages (p. 32-36), including an interview, and also in the cover; the weekly *Panorama* (page 165; May 14, 1994) also featured our work.
- German Television Program on Science *Programmbereich Kultur und Wissenschaft*, MDR, Leipzig, Nov. 10, 1997.
- 1998: Featured in the book *Impossibility: The Limits of Science and the Science of Limits*, (Oxford University Press, Oxford, 1998).
- 1998: Several of our results are very prominently featured and described in some detail in Chapter 2 of the book: *Self-organized Criticality: Emergent Complex Behavior in Physical and Biological Systems*, by H. Jensen (Cambridge, 1998). This book is used in several specialized graduate courses and is considered one of the best introductions to the area of emergent complex behavior in physical systems, viewing self-organization as a critical phenomenon (i.e., applying ideas of critical phenomena to jammed systems like granular assemblies, vortices in superconductors, dislocations in materials, charge density waves, fault dynamics, etc.).
- 1999: Michigan Daily (2-12-1999). Ann Arbor News (2000). Both on sand avalanches.
- 1999: 10-minutes Television program broadcasted by The Learning Channel (part of the Discovery Channel Network). It was first broadcasted on February 15, 16, and 17 of 1999, and replayed many times later. The Discovery Channel is broadcasted in 18 languages over eight networks by 13 satellites worldwide, reaching over 39 million homes internationally in 144 countries and 71 million households in the United States.
- 2000: The Discovery Channel: Television program first broadcasted in the summer of 2000, and rebroadcasted many times since then. In early October of 1999, the TV filming crew (from Europe) and myself spent several days in Sand Mountain, Nevada. There, I explained the mechanism of acoustic emissions of sand avalanches. In the previous TV program, in 1999, a different TV director flew from Los Angeles and filmed here on campus, filming some lab demonstrations and an interview. I helped with the initial versions of the script and as an advisor to both programs. The 1999 program was centered in our research. The 2000 program was more general and briefly mentioned it (in this one our input was mostly as an advisor to the program, and as an on-site guide in Nevada while measurements were taken with a group from the University of Nevada).

- 2002: Our publication on novel quantum nano-circuitry: "Scalable Quantum Computing with Josephson junction Qubits", J.Q. You, J.S. Tsai, and F. Nori, in *Physical Review Letters*, **89**, 179 (November 2002) (available on line from http://link.aps.org/abstract/PRL/v89/e197902) has been featured in several places, including:

  - The December 11 to 18, 2002, issue of the *Technology Review News*, Page 1. Available at http://www.trnmag.com/. It features our results, and also four other stories for that week. The article, titled "Design links quantum bits", is relatively long (for a news piece).
  - November 22, 2002: United Business Media's *Electrical Engineering Times*, described as "The Industry Source for Engineers and Technical Managers Worldwide", has an article describing our results (titled: "Superconducting junctions eyed for quantum computing" and available at http://www.eetimes.com/story/OEG20021122S0013).
  - *Electronics Weekly*, November 06, 2002, News; Pg. 5, on our results on "Quantum qubits".
  - October 23, 2002. "Paper Discusses Circuitry for Quantum Computing", in *Supercomputing online.* Available at http://www.supercomputingonline.com/article.php?sid=2756
  - Our work motivated the long article "Thoughtful about uploading", Bill Tammeus, Kansas City Star, November 2, 2002.
  - October 2002: Featured in *Innovations Report, Forum für Wissenschaft, Industrie und Wirtschaft*, a technical news site in Germany.
  - October 23, 2002, featured in *AScribe* - The Public Interest Newswire. October 24, 2002, featured in *NewsWise*, that covers new science and technology developments.
  - The December 2002 issue of *Science and Technology Trends* (number 21, Dec. 2002) has a one-page article featuring our November 2002 PRL results. This is a publication of the "Science and Technology Foresight Center" of the National Institute of Science and Technology Policy (NISTEP). The latter is part of the Ministry of Education, Culture, Science and Technology. Japan. It is available on-line in English at http://www-personal.engin.umich.edu/~nori/scalable/

  Newspaper articles overseas include the following ones:

  - *Japan Industry News* of the "Japan Industrial Journal", page 2, Thursday, October 24, 2002.
  - *Daily Industrial Newspaper* (the Nikkan Kogyo Shinbun), page 4, Thursday, October 24, 2002.
  - *Nikkei* (this important newspaper is the Japanese version of the "Wall Street Journal"), Friday, October 25, 2002.
  - *Science News* (in Japan), November 8, 2002.

- 2002: Our publication "Experimentally-realizable devices for controlling the motion of magnetic flux quanta in anisotropic superconductors", S. Savelev and F. Nori, published in *Nature Materials*, **1**, 179 (November 2002), has been:

  - Listed on the cover of the November issue of *Nature Materials.*
  - also featured in a pedagogical two-pages "News and Views", *Nature Materials* **1**, 143 (2002), titled: "Controlling the Motion of Quanta".
  - *Nikkei* (this newspaper is the Japanese version of the "Wall Street Journal"), Monday, January 6, 2003. An article on Page 23 describing these results.
  - November 6, 2002. "Stories of modern science, from UPI", By Ellen Beck. (UPI = United Press International).
  - November 13, 2002. *Electronics Weekly*, Pg. 6. "US and Japanese scientists control magnetic flux quanta".
  - The UM press release in http://www.umich.edu/%7Enewsinfo/Releases/2002/Nov02/r110402c.html was covered by news agencies and newswire services, including: (*) *Innovations Report, Forum für Wissenschaft, Industrie und Wirtschaft*, a technical news site in Germany); (*) *AScribe*, The Public Interest Newswire; (*) *NewsWise*, that covers new science and technology developments.

- 2002: Our 1999 work on "Biologically-inspired solid-state devices for the control of the motion of quanta" is nicely highlighted in the *Molecular Motors* first feature article of the November, 2002, Physics Today, page 38.

- 2003: Our work OBSERVING BROWNIAN MOTION IN VIBRO-FLUIDIZED GRANULAR MATTER, by G. D'Anna, et al. *Nature*, **424**, 909-912 (August 21, 2003), available on-line at http://www.nature.com/nature/links/030821/030821-1.html has been featured in (the list below is very incomplete):

  - *Cover Story of Nature* (August 21st 2003 issue of Nature). The text accompanying the cover photo was: "Against the Grain. Brownian motion in a non-equilibrium system".
  - A companion "News and Views" in that issue of Nature.
  - it Science Letter, September 15, 2003. http://www.NewsRX.net.
  - TV programs. Three examples (of about five minutes each) were broadcasted in Europe (one on the German "Fokus" (by MTW: Menschen Technik Wissenschaft), a different program in Italian, and a quite different one in French). Also in radio programs (e.g., Radio Swiss International).
  - Featured (in all languages of the European Union) in the High-Tech News of "Euronews".
  - Long Newspaper articles include *Il Secolo XIX*, Agosto 27, 2003, page 31, (in Italian) in the section on "Research and Science". Also, *Sole 24 Ore*, Settembre 11, 2003, the most important Italian newspaper on finances and the economy.
  - Featured in the long article: "Nel Mondo dei Granelli di Sabbia", *Scienza e Conoscenza*, 9-12-2003.
  - News coverage in French include: *L'Hebdo, Le Temps, 24 Heures.*
  - News coverage in German include: *Tages-Anzeiger, Neue Zürcher Zeitung, St. Galler Tagblatt Gesamtausgabe, Basler Zeitung.*
  - Interviewed by Nikkei, the most important Japanese newspaper on finances and the economy.
  - the University of Michigan press release in
    http://www.umich.edu/news/index.html?Releases/2003/Aug03/r082003
    http://ipumich.temppublish.com/cgi-bin/print.cgi?Releases/2003/Aug03/r082003
    was covered by news agencies and newswire services, including:
    * *The Resource for Science Information* (BrightSurf.com). One of the few "Today's Science News" for August, 25, 2003.
    * *Innovations Report* (Forum fur Wissenschaft, Industrie und Wirtschaft, Germany). August, 25, 2003.
    * *Global Technology Market Place* (GlobalTechnoScan.com). Weekly Magazine on New Technology. Issue 27th Aug to 2nd Sept. 2003.
    * *EurekAlert! Public News.* A Service of the American Association for the Advancement of Science, with support from the US Department of Energy and the US National Institutes of Health. Eurekalert.org is described as the premier web site for science news since 1996. Public release date: 22-Aug-2003.
    * *Science News.* 8/22/2003. http://sciguy.com/News/Article.asp?ArticleID=5410
    * *Headline News.* NewsHub.com. 22-Aug-2003.
    * *Knowledge Science.* http://www.kenkyu40.net/index.php
    * World Wide News Headliner.

- 2003: Our work on vortex dynamics in superconductors will be featured in part of a television program, prepared by the Danish Broadcast Corporation, about the study of superconducting materials.

- 2003: Our recent publication "Controlling Transport in Mixtures of Interacting Particles using Brownian Motors", by S. Savel'ev, F. Marchesoni, and F. Nori, Phys. Rev. Lett. **91**, 10601 (2003), available on-line at http://link.aps.org/abstract/PRL/v91/e010601, has been featured:
  - for several weeks as the top-listed research news in the front page of the University of Michigan web site (www.umich.edu). This web site gets a lot of traffic everyday. The actual press release is in http://www.umich.edu/news/Releases/2003/Jun03/r061903.html.
    A very nontechnical and brief graphical summary is in
    http://www.umich.edu/news/Releases/2003/May03/img/ratchets.jpg
  - Newswise/Science News also appeared in Small Times magazine (presenting technological advances in nano-science). http://www.smalltimes.com
  - *Le Scienze*, the Italian version of Scientific American, among other science news outlets.
  - "Conveyor Belt on a nanometer scale", *Machine Design*, No. 19. Vol. 75, Pg. 35; October 9, 2003.

- 2003: Our recent publication "Reversible Rectifier that Controls the Motion of Magnetic Flux Quanta in Superconductors", by J.E. Villegas, S. Savel'ev, F. Nori, E.M. Gonzalez, J.V. Anguita, R. Garcia, and J.L. Vicent, *Science* **302** 1188 (2003) has been featured in several venues including:
  - an "Enhanced Perspectives" in *Science* **302** 1159 (2003). It is available on-line at
    http://www.sciencemag.org/cgi/content/full/302/5648/1159 . This is the only "Enhanced Perspectives" of that issue of *Science*, with dozens of links with further information on the subject, and one of three "Enhanced Perspectives" covering all of physics for 2003.
  - prominently featured in the page "This week in Science" of that issue of *Science* (Nov. 14, 2003).
  - High-Tc Update (November 2003).
  - Newspapers in Europe (e.g., El Pais, Madrid), Japan, and the USA.